

Third Edition

# COMPUTATIONAL CONTINUUM MECHANICS

Ahmed A. Shabana

$$\mathbf{Q}_g = \int_V \mathbf{S}^T \begin{bmatrix} 0 & -g & 0 \end{bmatrix}^T dV \quad \varepsilon = \frac{1}{2}(\mathbf{J}^T \mathbf{J} - \mathbf{I}) = \frac{1}{2}(\mathbf{J}_o^{-1T} (\mathbf{J}_e^T \mathbf{J}_e) \mathbf{J}_o^{-1} - \mathbf{I}) \quad \mathbf{J} = \frac{\partial \mathbf{r}}{\partial \mathbf{X}} = \left( \frac{\partial \mathbf{r}}{\partial \mathbf{x}} \right) \left( \frac{\partial \mathbf{x}}{\partial \mathbf{X}} \right) = \mathbf{J}_e \mathbf{J}_o^{-1}$$



$$s_{ij} = \sum_{k=1}^3 t_{ijk} b_k = t_{ij1} b_1 + t_{ij2} b_2 + t_{ij3} b_3$$

$$t_{ijk} = \sum_{l=1}^3 f_{ijkl} v_l = f_{ijk1} v_1 + f_{ijk2} v_2 + f_{ijk3} v_3$$

WILEY

# COMPUTATIONAL CONTINUUM MECHANICS



---

# COMPUTATIONAL CONTINUUM MECHANICS

## THIRD EDITION

---

**AHMED A. SHABANA**

Richard and Loan Hill Professor of Engineering  
University of Illinois at Chicago  
Chicago, Illinois, USA

**WILEY**

This edition first published 2018  
© 2018 John Wiley & Sons Ltd  
First edition published 2008 by Cambridge University Press  
Second edition published 2012 by Cambridge University Press

All rights reserved. No part of this publication may be reproduced, stored in a retrieval system, or transmitted, in any form or by any means, electronic, mechanical, photocopying, recording or otherwise, except as permitted by law. Advice on how to obtain permission to reuse material from this title is available at <http://www.wiley.com/go/permissions>.

The right of Ahmed A. Shabana to be identified as the author of this work has been asserted in accordance with law.

*Registered Office(s)*

John Wiley & Sons, Inc., 111 River Street, Hoboken, NJ 07030, USA  
John Wiley & Sons Ltd, The Atrium, Southern Gate, Chichester, West Sussex, PO19 8SQ, UK

*Editorial Office*

The Atrium, Southern Gate, Chichester, West Sussex, PO19 8SQ, UK

For details of our global editorial offices, customer services, and more information about Wiley products visit us at [www.wiley.com](http://www.wiley.com).

Wiley also publishes its books in a variety of electronic formats and by print-on-demand. Some content that appears in standard print versions of this book may not be available in other formats.

*Limit of Liability/Disclaimer of Warranty*

While the publisher and authors have used their best efforts in preparing this work, they make no representations or warranties with respect to the accuracy or completeness of the contents of this work and specifically disclaim all warranties, including without limitation any implied warranties of merchantability or fitness for a particular purpose. No warranty may be created or extended by sales representatives, written sales materials or promotional statements for this work. The fact that an organization, website, or product is referred to in this work as a citation and/or potential source of further information does not mean that the publisher and authors endorse the information or services the organization, website, or product may provide or recommendations it may make. This work is sold with the understanding that the publisher is not engaged in rendering professional services. The advice and strategies contained herein may not be suitable for your situation. You should consult with a specialist where appropriate. Further, readers should be aware that websites listed in this work may have changed or disappeared between when this work was written and when it is read. Neither the publisher nor authors shall be liable for any loss of profit or any other commercial damages, including but not limited to special, incidental, consequential, or other damages.

*Library of Congress Cataloging-in-Publication Data:*

Names: Shabana, Ahmed A., 1951- author.  
Title: Computational continuum mechanics / by Ahmed A. Shabana.  
Description: Third edition. | Hoboken, NJ, USA : Wiley, [2018] | Includes bibliographical references and index. |  
Identifiers: LCCN 2017032713 (print) | LCCN 2017035575 (ebook) | ISBN 9781119293231 (ePDF) | ISBN 9781119293200 (ePUB) | ISBN 9781119293217 (cloth)  
Subjects: LCSH: Continuum mechanics. | Engineering mathematics.  
Classification: LCC QA808.2 (ebook) | LCC QA808.2 .S46 2018 (print) | DDC 531-dc23  
LC record available at <https://lcn.loc.gov/2017032713>

Cover design by Wiley

Cover Images: (Gas Tank) © scanrail/Gettyimages; (Tire) © Rellas/Gettyimages; (Water) © molotovcocketail/Gettyimages; (Wave) © Shannon Stent/iStockphoto; (Leaf Springs) © ABBPhoto/Gettyimages

Typeset in 10/12pt TimesLTStd by SPi Global, Chennai, India

# CONTENTS

---

<b>PREFACE</b>	<b>ix</b>
<b>1 INTRODUCTION</b>	<b>1</b>
1.1 Matrices / 2	
1.2 Vectors / 6	
1.3 Summation Convention / 11	
1.4 Cartesian Tensors / 12	
1.5 Polar Decomposition Theorem / 21	
1.6 D'Alembert's Principle / 23	
1.7 Virtual Work Principle / 29	
1.8 Approximation Methods / 32	
1.9 Discrete Equations / 34	
1.10 Momentum, Work, and Energy / 37	
1.11 Parameter Change and Coordinate Transformation / 39	
Problems / 44	
<b>2 KINEMATICS</b>	<b>47</b>
2.1 Motion Description / 48	
2.2 Strain Components / 55	
2.3 Other Deformation Measures / 60	

- 2.4 Decomposition of Displacement / 62
- 2.5 Velocity and Acceleration / 64
- 2.6 Coordinate Transformation / 68
- 2.7 Objectivity / 74
- 2.8 Change of Volume and Area / 77
- 2.9 Continuity Equation / 81
- 2.10 Reynolds' Transport Theorem / 82
- 2.11 Examples of Deformation / 84
- 2.12 Geometry Concepts / 92
- Problems / 94

### 3 FORCES AND STRESSES

97

- 3.1 Equilibrium of Forces / 97
- 3.2 Transformation of Stresses / 100
- 3.3 Equations of Equilibrium / 100
- 3.4 Symmetry of the cauchy Stress Tensor / 102
- 3.5 Virtual Work of the Forces / 103
- 3.6 Deviatoric Stresses / 113
- 3.7 Stress Objectivity / 115
- 3.8 Energy Balance / 119
- Problems / 120

### 4 CONSTITUTIVE EQUATIONS

123

- 4.1 Generalized Hooke's Law / 124
- 4.2 Anisotropic Linearly Elastic Materials / 126
- 4.3 Material Symmetry / 127
- 4.4 Homogeneous Isotropic Material / 129
- 4.5 Principal Strain Invariants / 136
- 4.6 Special Material Models for Large Deformations / 137
- 4.7 Linear Viscoelasticity / 141
- 4.8 Nonlinear Viscoelasticity / 155
- 4.9 A Simple Viscoelastic Model for Isotropic Materials / 161
- 4.10 Fluid Constitutive Equations / 162
- 4.11 Navier–Stokes Equations / 164
- Problems / 164

### 5 FINITE ELEMENT FORMULATION: LARGE-DEFORMATION, LARGE-ROTATION PROBLEM

167

- 5.1 Displacement Field / 169

5.2	Element Connectivity /	176
5.3	Inertia and Elastic Forces /	178
5.4	Equations of Motion /	180
5.5	Numerical Evaluation of The Elastic Forces /	188
5.6	Finite Elements and Geometry /	193
5.7	Two-Dimensional Euler–Bernoulli Beam Element /	199
5.8	Two-Dimensional Shear Deformable Beam Element /	203
5.9	Three-Dimensional Cable Element /	205
5.10	Three-Dimensional Beam Element /	206
5.11	Thin-Plate Element /	208
5.12	Higher-Order Plate Element /	210
5.13	Brick Element /	211
5.14	Element Performance /	212
5.15	Other Finite Element Formulations /	216
5.16	Updated Lagrangian and Eulerian Formulations /	218
5.17	Concluding Remarks /	221
	Problems /	223

## **6 FINITE ELEMENT FORMULATION: SMALL-DEFORMATION, LARGE-ROTATION PROBLEM**

**225**

6.1	Background /	226
6.2	Rotation and Angular Velocity /	229
6.3	Floating Frame of Reference (FFR) /	234
6.4	Intermediate Element Coordinate System /	236
6.5	Connectivity and Reference Conditions /	238
6.6	Kinematic Equations /	243
6.7	Formulation of The Inertia Forces /	245
6.8	Elastic Forces /	248
6.9	Equations of Motion /	250
6.10	Coordinate Reduction /	251
6.11	Integration of Finite Element and Multibody System Algorithms /	253
	Problems /	258

## **7 COMPUTATIONAL GEOMETRY AND FINITE ELEMENT ANALYSIS**

**261**

7.1	Geometry and Finite Element Method /	262
7.2	ANCF Geometry /	264
7.3	Bezier Geometry /	266
7.4	B-Spline Curve Representation /	267
7.5	Conversion of B-Spline Geometry to ANCF Geometry /	271



- 7.6 ANCF and B-Spline Surfaces / 273
- 7.7 Structural and Nonstructural Discontinuities / 275
- Problems / 277

## **8 PLASTICITY FORMULATIONS 279**

- 8.1 One-Dimensional Problem / 281
- 8.2 Loading and Unloading Conditions / 282
- 8.3 Solution of the Plasticity Equations / 283
- 8.4 Generalization of The Plasticity Theory: Small Strains / 291
- 8.5  $J_2$  Flow Theory with Isotropic/Kinematic Hardening / 298
- 8.6 Nonlinear Formulation for Hyperelastic–Plastic Materials / 312
- 8.7 Hyperelastic–Plastic  $J_2$  Flow Theory / 322
- Problems / 326

## **REFERENCES 329**

## **INDEX 339**

# PREFACE

---

Nonlinear continuum mechanics is one of the fundamental subjects that form the foundation of modern computational mechanics. The study of the motion and behavior of materials under different loading conditions requires understanding of basic, general, and nonlinear kinematic and dynamic relationships that are covered in continuum mechanics courses. The finite element method, on the other hand, has emerged as a powerful tool for solving many problems in engineering and physics. The finite element method became a popular and widely used computational approach because of its versatility and generality in solving large-scale and complex physics and engineering problems. Nonetheless, the success of using the continuum-mechanics-based finite element method in the analysis of the motion of bodies that experience general displacements, including arbitrary large rotations, has been limited. The solution to this problem requires resorting to some of the basic concepts in continuum mechanics and putting the emphasis on developing sound formulations that satisfy the principles of mechanics. Some researchers, however, have tried to solve fundamental formulation problems using numerical techniques that lead to approximations. Although numerical methods are an integral part of modern computational algorithms and can be effectively used in some applications to obtain efficient and accurate solutions, it is the opinion of many researchers that numerical methods should only be used as a last resort to fix formulation problems. Sound formulations must be first developed and tested to make sure that these formulations satisfy the basic principles of mechanics. The equations that result from the use of the analytically correct formulations can then be solved using numerical methods.

This book is focused on presenting the nonlinear theory of continuum mechanics and demonstrating its use in developing nonlinear computer formulations that can be used in the large displacement dynamic analysis. To this end, the basic concepts used in continuum mechanics are first presented and then used to develop nonlinear general finite element

formulations for the large displacement analysis. Two nonlinear finite element dynamic formulations will be considered in this book. The first is a general large-deformation finite element formulation, whereas the second is a formulation that can be used efficiently to solve small-deformation problems that characterize very and moderately stiff structures. In this latter case, an elaborate method for eliminating the unnecessary degrees of freedom must be used in order to be able to efficiently obtain a numerical solution. An attempt has been made to present the materials in a clear and systematic manner with the assumption that the reader has only basic knowledge in matrix and vector algebra as well as basic knowledge of dynamics. The book is designed for a course at the senior undergraduate and first-year graduate level. It can also be used as a reference for researchers and practicing engineers and scientists who are working in the areas of computational mechanics, biomechanics, computational biology, multibody system dynamics, and other fields of science and engineering that are based on the general continuum mechanics theory.

In **Chapter 1**, matrix, vector, and tensor notations are introduced. These notations will be repeatedly used in all chapters of the book, and therefore, it is necessary that the reader reviews this chapter in order to be able to follow the presentation in subsequent chapters. The polar decomposition theorem, which is fundamental in continuum and computational mechanics, is also presented in this chapter. D'Alembert's principle and the principle of virtual work can be used to systematically derive the equations of motion of physical systems. These two important principles are discussed and the relationship between them is explained. The use of a finite dimensional model to describe the continuum motion is also discussed and the procedure for developing the discrete equations of motion is outlined. The principles of momentum and principle of work and energy are presented, and the problems associated with some of the finite element formulations that violate these analytical mechanics principles are discussed. Chapter 1 also provides a discussion on the definitions of the gradient vectors that are used in continuum mechanics to define the strain components.

In **Chapter 2**, the general kinematic displacement equations of a continuum are developed and used to define the strain components. The Green–Lagrange strains and the Almansi or Eulerian strains are introduced. The Green–Lagrange strains are defined in the reference configuration, whereas the Almansi or Eulerian strains are defined in the current deformed configuration. The relationships between these strain components are established and used to shed light on the physical meaning of the strain components. Other deformation measures as well as the velocity and acceleration equations are also defined in this chapter. The important issue of objectivity that must be considered when large deformations and inelastic formulations are used is discussed. The equations that govern the change of volume and area, the conservation of mass, and examples of deformation modes are also presented in this chapter.

Forces and stresses are discussed in **Chapter 3**. Equilibrium of forces acting on an infinitesimal material element is used to define the Cauchy stresses, which are used to develop the partial differential equations of equilibrium. The transformation of the stress components and the symmetry of the Cauchy stress tensor are among the topics discussed in this chapter. The virtual work of the forces due to the change of the shape of the continuum is defined. The deviatoric stresses, stress objectivity, and energy balance equations are also discussed in Chapter 3.

The definition of the strain and stress components is not sufficient to describe the motion of a continuum. One must define the relationship between the stresses and strains using the constitutive equations that are discussed in **Chapter 4**. In Chapter 4, the generalized Hooke's law

is introduced and the assumptions used in the definition of homogeneous isotropic materials are outlined. The principal strain invariants and special large-deformation material models are discussed. The linear and nonlinear viscoelastic material behavior is also discussed in Chapter 4.

Nonlinear finite element formulations are discussed in **Chapters 5 and 6**. Two formulations are discussed in these two chapters. The first is a large-deformation finite element formulation, which is discussed in **Chapter 5**. This formulation, called the absolute nodal coordinate formulation (ANCF), is based on a continuum mechanics theory and employs position gradients as coordinates. It leads to a unique displacement and rotation fields and imposes no restrictions on the amount of rotation or deformation within the finite element. The absolute nodal coordinate formulation has some unique features that distinguish it from other existing large-deformation finite element formulations: it leads to a constant mass matrix; it leads to zero centrifugal and Coriolis forces; it automatically satisfies the principles of mechanics; it correctly describes an arbitrary rigid-body motion including finite rotations; and it can be used to develop several beam, plate, and shell elements that relax many of the assumptions used in classical theorems. When using ANCF finite elements, no distinction is made between plate and shell elements since shell geometry can be systematically obtained using the nodal coordinates in the reference configuration.

Clearly, large-deformation finite element formulations can also be used to solve small-deformation problems. However, it is not recommended to use a large-deformation finite element formulation to solve a small-deformation problem. Large-deformation formulations do not exploit some particular features of small-deformation problems, and therefore, such formulations can be very inefficient in the solution of stiff and moderately stiff systems. The development of an efficient small-deformation finite element formulation that correctly describes an arbitrary rigid-body motion requires the use of more elaborate techniques in order to define a local linear problem without compromising the ability of the method to describe large-displacement, small-deformation behavior. The finite element floating frame of reference (FFR) formulation, widely used in the analysis of small deformations, is discussed in **Chapter 6**. This formulation allows eliminating high-frequency modes that do not have a significant effect on the solution, thereby leading to a lower-dimension dynamic model that can be efficiently solved using numerical and computer methods.

Although finite element (FE) formulations are based on polynomial representations, the polynomial-based geometric representation used in computer-aided design (CAD) methods cannot be converted exactly to the kinematic description used in many existing FE formulations. For this reason, converting a CAD model to an FE mesh can be costly and time-consuming. CAD software systems use computational geometry methods such as B-spline and Non-Uniform Rational B-Splines (NURBS). These methods can describe accurately complex geometry. The relationship between these CAD geometry methods and the FE formulations presented in this book are discussed in **Chapter 7**. As explained in Chapter 7, modeling modern engineering and physics systems requires the successful integration of computer-aided design and analysis (I-CAD-A) by developing an efficient interface between CAD systems and analysis tools or by developing a new mechanics based CAD/analysis system.

In many engineering applications, plastic deformations occur due to excessive forces and impact as well as thermal loads. Several plasticity formulations are presented in **Chapter 8**. First, a one-dimensional theory is used in order to discuss the main concepts

and solution procedures used in the plasticity analysis. The theory is then generalized to the three-dimensional analysis for the case of small strains. Large strain nonlinear plasticity formulations as well as the  $J_2$  flow theory are among the topics discussed in Chapter 8.

I would like to thank many students and colleagues with whom I worked for several years on the subject of flexible body dynamics. I was fortunate to collaborate with excellent students and colleagues who educated me in this important field of computational mechanics. In particular, I would like to thank my doctorate students, Bassam Hussein, Luis Maqueda, Mohil Patel, Brian Tinsley, and Liang Wang, who provided solutions for several of examples and figures presented in several chapters of the book. I would also like to thank my family for their help, patience, and understanding during the time of preparing this book.

AHMED A. SHABANA  
Chicago, IL  
2016

# CHAPTER 1

---

## INTRODUCTION

---

Matrix, vector, and tensor algebras are often used in the theory of continuum mechanics in order to have a simpler and more tractable presentation of the subject. In this chapter, the mathematical preliminaries required to understand the matrix, vector, and tensor operations used repeatedly in this book are presented. Principles of mechanics and approximation methods that represent the basis for the formulation of the kinematic and dynamic equations developed in this book are also reviewed in this chapter. In the first two sections of this chapter, matrix and vector notations are introduced and some of their important identities are presented. Some of the vector and matrix results are presented without proofs with the assumption that the reader has some familiarity with matrix and vector notations. In Section 3, the summation convention, which is widely used in continuum mechanics texts, is introduced. This introduction is made despite the fact that the summation convention is rarely used in this book. Tensor notations, on the other hand, are frequently used in this book and, for this reason, tensors are discussed in Section 4. In Section 5, the *polar decomposition theorem*, which is fundamental in continuum mechanics, is presented. This theorem states that any nonsingular square matrix can be decomposed as the product of an orthogonal matrix and a symmetric matrix. Other matrix decompositions that are used in computational mechanics are also discussed. In Section 6, D'Alembert's principle is introduced, while Section 7 discusses the virtual work principle. The finite element method is often used to obtain finite dimensional models of continuous systems that in reality have infinite number of degrees of freedom. To introduce the reader to some of the basic concepts used to obtain finite dimensional models, discussions of approximation methods are included in Section 8. The procedure for developing the discrete equations of motion is outlined in Section 9, while the principle of conservation of momentum and the principle of work and energy are discussed in Section 10. In continuum mechanics,

the gradients of the position vectors can be determined by differentiation with respect to different parameters. The change of parameters can lead to the definitions of strain components in different directions. This change of parameters, however, does not change the coordinate system in which the gradient vectors are defined. The effect of the change of parameters on the definitions of the gradients is discussed in Section 11.

## 1.1 MATRICES

In this section, some identities, results, and properties from matrix algebra that are used repeatedly in this book are presented. Some proofs are omitted, with the assumption that the reader is familiar with the subject of linear algebra.

### Definitions

An  $m \times n$  matrix  $\mathbf{A}$  is an ordered rectangular array, which can be written in the following form:

$$\mathbf{A} = (a_{ij}) = \begin{bmatrix} a_{11} & a_{12} & \cdots & a_{1n} \\ a_{21} & a_{22} & \cdots & a_{2n} \\ \vdots & \vdots & \ddots & \vdots \\ a_{m1} & a_{m2} & \cdots & a_{mn} \end{bmatrix} \quad (1.1)$$

where  $a_{ij}$  is the  $ij$ th element that lies in the  $i$ th row and  $j$ th column of the matrix. Therefore, the first subscript  $i$  refers to the row number and the second subscript  $j$  refers to the column number. The arrangement of Equation 1 shows that the matrix  $\mathbf{A}$  has  $m$  rows and  $n$  columns. If  $m = n$ , the matrix is said to be *square*; otherwise, the matrix is said to be *rectangular*. The *transpose* of an  $m \times n$  matrix  $\mathbf{A}$  is an  $n \times m$  matrix, denoted as  $\mathbf{A}^T$ , which is obtained from  $\mathbf{A}$  by exchanging the rows and columns, that is,  $\mathbf{A}^T = (a_{ji})$ .

A *diagonal matrix* is a square matrix whose only nonzero elements are the diagonal elements, that is,  $a_{ij} = 0$  if  $i \neq j$ . An *identity* or *unit matrix*, denoted as  $\mathbf{I}$ , is a diagonal matrix that has all its diagonal elements equal to one. The *null* or *zero matrix* is a matrix that has all its elements equal to zero. The *trace* of a square matrix  $\mathbf{A}$  is the sum of all its diagonal elements, that is,

$$\text{tr}(\mathbf{A}) = \sum_{i=1}^n a_{ii} \quad (1.2)$$

This equation shows that  $\text{tr}(\mathbf{I}) = n$ , where  $\mathbf{I}$  is the identity matrix and  $n$  is the dimension of the matrix.

A square matrix  $\mathbf{A}$  is said to be *symmetric* if

$$\mathbf{A} = \mathbf{A}^T, \quad a_{ij} = a_{ji} \quad (1.3)$$

A square matrix is said to be *skew symmetric* if

$$\mathbf{A} = -\mathbf{A}^T, \quad a_{ij} = -a_{ji} \quad (1.4)$$

This equation shows that all the diagonal elements of a skew-symmetric matrix must be equal to zero. That is, if  $\mathbf{A}$  is a skew-symmetric matrix with dimension  $n$ , then  $a_{ii} = 0$  for  $i = 1, 2, \dots, n$ . Any square matrix can be written as the sum of a symmetric matrix and a skew-symmetric matrix. For example, if  $\mathbf{B}$  is a square matrix,  $\mathbf{B}$  can be written as

$$\mathbf{B} = \bar{\mathbf{B}} + \tilde{\mathbf{B}} \quad (1.5)$$

where  $\bar{\mathbf{B}}$  and  $\tilde{\mathbf{B}}$  are, respectively, symmetric and skew-symmetric matrices defined as

$$\bar{\mathbf{B}} = \frac{1}{2}(\mathbf{B} + \mathbf{B}^T), \quad \tilde{\mathbf{B}} = \frac{1}{2}(\mathbf{B} - \mathbf{B}^T) \quad (1.6)$$

Skew-symmetric matrices are used in continuum mechanics to characterize the rotations of the material elements.

## Determinant

The *determinant* of an  $n \times n$  square matrix  $\mathbf{A}$ , denoted as  $|\mathbf{A}|$  or  $\det(\mathbf{A})$ , is a scalar quantity. In order to be able to define the unique value of the determinant, some basic definitions have to be introduced. The *minor*  $M_{ij}$  corresponding to the element  $a_{ij}$  is the determinant of a matrix obtained by deleting the  $i$ th row and  $j$ th column from the original matrix  $\mathbf{A}$ . The *cofactor*  $C_{ij}$  of the element  $a_{ij}$  is defined as

$$C_{ij} = (-1)^{i+j} M_{ij} \quad (1.7)$$

Using this definition, the determinant of the matrix  $\mathbf{A}$  can be obtained in terms of the cofactors of the elements of an arbitrary row  $j$  as follows:

$$|\mathbf{A}| = \sum_{k=1}^n a_{jk} C_{jk} \quad (1.8)$$

One can show that the determinant of a diagonal matrix is equal to the product of the diagonal elements, and the determinant of a matrix is equal to the determinant of its transpose; that is, if  $\mathbf{A}$  is a square matrix, then  $|\mathbf{A}| = |\mathbf{A}^T|$ . Furthermore, the interchange of any two columns or rows only changes the sign of the determinant. It can also be shown that if the matrix has linearly dependent rows or linearly dependent columns, the determinant is equal to zero. A matrix whose determinant is equal to zero is called a *singular matrix*. For an arbitrary square matrix, singular or nonsingular, it can be shown that the value of the determinant does not change if any row or column is added or subtracted from another. It can be also shown that the determinant of the product of two matrices is equal to the product of their determinants. That is, if  $\mathbf{A}$  and  $\mathbf{B}$  are two square matrices, then  $|\mathbf{AB}| = |\mathbf{A}||\mathbf{B}|$ .

As will be shown in this book, the determinants of some of the deformation measures used in continuum mechanics are used in the formulation of the energy expressions. Furthermore, the relationship between the volumes of a continuum in the undeformed state and the deformed state is expressed in terms of the determinant of the matrix of position vector gradients. Therefore, if the elements of a square matrix depend on a parameter, it is important to be able to



determine the derivatives of the determinant with respect to this parameter. Using Equation 8, one can show that if the elements of the matrix  $\mathbf{A}$  depend on a parameter  $t$ , then

$$\frac{d}{dt} |\mathbf{A}| = \sum_{k=1}^n \dot{a}_{1k} C_{1k} + \sum_{k=1}^n \dot{a}_{2k} C_{2k} + \cdots + \sum_{k=1}^n \dot{a}_{nk} C_{nk} \quad (1.9)$$

where  $\dot{a}_{ij} = da_{ij}/dt$ . The use of this equation is demonstrated by the following example.

### Example 1.1

Consider the matrix  $\mathbf{J}$  defined as

$$\mathbf{J} = \begin{bmatrix} J_{11} & J_{12} & J_{13} \\ J_{21} & J_{22} & J_{23} \\ J_{31} & J_{32} & J_{33} \end{bmatrix}$$

where  $J_{ij} = \partial r_i / \partial x_j$ , and  $\mathbf{r}$  and  $\mathbf{x}$  are the vectors

$$\mathbf{r}(x_1, x_2, x_3, t) = [r_1 \quad r_2 \quad r_3]^T, \quad \mathbf{x} = [x_1 \quad x_2 \quad x_3]^T$$

That is, the elements of the vector  $\mathbf{r}$  are functions of the coordinates  $x_1$ ,  $x_2$ , and  $x_3$  and the parameter  $t$ . If  $J = |\mathbf{J}|$  is the determinant of  $\mathbf{J}$ , prove that

$$\frac{dJ}{dt} = \left( \frac{\partial \dot{r}_1}{\partial r_1} + \frac{\partial \dot{r}_2}{\partial r_2} + \frac{\partial \dot{r}_3}{\partial r_3} \right) J$$

where  $\partial \dot{r}_i / \partial r_j = (\partial / \partial r_j)(dr_i / dt)$ ,  $i, j = 1, 2, 3$ .

*Solution:* Using Equation 9, one can write

$$\frac{dJ}{dt} = \sum_{k=1}^3 \dot{J}_{1k} C_{1k} + \sum_{k=1}^3 \dot{J}_{2k} C_{2k} + \sum_{k=1}^3 \dot{J}_{3k} C_{3k}$$

where  $C_{ij}$  is the cofactor associated with element  $J_{ij}$ . Note that the preceding equation can be written as

$$\frac{dJ}{dt} = \begin{vmatrix} \dot{J}_{11} & \dot{J}_{12} & \dot{J}_{13} \\ J_{21} & J_{22} & J_{23} \\ J_{31} & J_{32} & J_{33} \end{vmatrix} + \begin{vmatrix} J_{11} & J_{12} & J_{13} \\ \dot{J}_{21} & \dot{J}_{22} & \dot{J}_{23} \\ J_{31} & J_{32} & J_{33} \end{vmatrix} + \begin{vmatrix} J_{11} & J_{12} & J_{13} \\ J_{21} & J_{22} & J_{23} \\ \dot{J}_{31} & \dot{J}_{32} & \dot{J}_{33} \end{vmatrix}$$

In this equation,

$$\dot{J}_{ij} = \frac{\partial \dot{r}_i}{\partial x_j} = \frac{\partial \dot{r}_i}{\partial r_1} \frac{\partial r_1}{\partial x_j} + \frac{\partial \dot{r}_i}{\partial r_2} \frac{\partial r_2}{\partial x_j} + \frac{\partial \dot{r}_i}{\partial r_3} \frac{\partial r_3}{\partial x_j} = \sum_{k=1}^3 \frac{\partial \dot{r}_i}{\partial r_k} J_{kj}$$

Using this expansion, one can show that

$$\begin{vmatrix} \dot{J}_{11} & \dot{J}_{12} & \dot{J}_{13} \\ J_{21} & J_{22} & J_{23} \\ J_{31} & J_{32} & J_{33} \end{vmatrix} = \left( \frac{\partial \dot{r}_1}{\partial r_1} \right) J$$

Similarly, one can show that

$$\begin{vmatrix} J_{11} & J_{12} & J_{13} \\ \dot{J}_{21} & \dot{J}_{22} & \dot{J}_{23} \\ J_{31} & J_{32} & J_{33} \end{vmatrix} = \left( \frac{\partial \dot{r}_2}{\partial r_2} \right) J, \quad \begin{vmatrix} J_{11} & J_{12} & J_{13} \\ J_{21} & J_{22} & J_{23} \\ \dot{J}_{31} & \dot{J}_{32} & \dot{J}_{33} \end{vmatrix} = \left( \frac{\partial \dot{r}_3}{\partial r_3} \right) J$$

Using the preceding equations, it is clear that

$$\frac{dJ}{dt} = \left( \frac{\partial \dot{r}_1}{\partial r_1} + \frac{\partial \dot{r}_2}{\partial r_2} + \frac{\partial \dot{r}_3}{\partial r_3} \right) J$$

This matrix identity is important and is used in this book to evaluate the rate of change of the determinant of the matrix of position vector gradients in terms of important deformation measures.

## Inverse and Orthogonality

A square matrix  $\mathbf{A}^{-1}$  that satisfies the relationship

$$\mathbf{A}^{-1} \mathbf{A} = \mathbf{A} \mathbf{A}^{-1} = \mathbf{I} \quad (1.10)$$

where  $\mathbf{I}$  is the identity matrix, is called the *inverse* of the matrix  $\mathbf{A}$ . The inverse of the matrix  $\mathbf{A}$  is defined as

$$\mathbf{A}^{-1} = \frac{\mathbf{C}_t}{|\mathbf{A}|} \quad (1.11)$$

where  $\mathbf{C}_t$  is the *adjoint* of the matrix  $\mathbf{A}$ . The adjoint matrix  $\mathbf{C}_t$  is the transpose of the matrix of the cofactors ( $C_{ij}$ ) of the matrix  $\mathbf{A}$ . One can show that the determinant of the inverse  $|\mathbf{A}^{-1}|$  is equal to  $1/|\mathbf{A}|$ .

A square matrix is said to be *orthogonal* if

$$\mathbf{A}^T \mathbf{A} = \mathbf{A} \mathbf{A}^T = \mathbf{I} \quad (1.12)$$

Note that in the case of an orthogonal matrix  $\mathbf{A}$ , one has

$$\mathbf{A}^T = \mathbf{A}^{-1} \quad (1.13)$$

That is, the inverse of an orthogonal matrix is equal to its transpose. One can also show that if  $\mathbf{A}$  is an orthogonal matrix, then  $|\mathbf{A}| = \pm 1$ ; and if  $\mathbf{A}_1$  and  $\mathbf{A}_2$  are two orthogonal matrices that have the same dimensions, then their product  $\mathbf{A}_1 \mathbf{A}_2$  is also an orthogonal matrix.

Examples of orthogonal matrices are the  $3 \times 3$  transformation matrices that define the orientation of coordinate systems. In the case of a right-handed coordinate system, one can show that the determinant of the transformation matrix is  $+1$ ; this is a *proper orthogonal transformation*. If the right-hand rule is not followed, the determinant of the resulting orthogonal transformation is equal to  $-1$ , which is an *improper orthogonal transformation*, such as in the case of a reflection.

## Matrix Operations

The sum of two matrices  $\mathbf{A} = (a_{ij})$  and  $\mathbf{B} = (b_{ij})$  is defined as

$$\mathbf{A} + \mathbf{B} = (a_{ij} + b_{ij}) \quad (1.14)$$

In order to add two matrices, they must have the same dimensions. That is, the two matrices  $\mathbf{A}$  and  $\mathbf{B}$  must have the same number of rows and same number of columns in order to apply Equation 14.

The product of two matrices  $\mathbf{A}$  and  $\mathbf{B}$  is another matrix  $\mathbf{C}$  defined as

$$\mathbf{C} = \mathbf{AB} \quad (1.15)$$

The element  $c_{ij}$  of the matrix  $\mathbf{C}$  is defined by multiplying the elements of the  $i$ th row in  $\mathbf{A}$  by the elements of the  $j$ th column in  $\mathbf{B}$  according to the rule

$$c_{ij} = a_{i1}b_{1j} + a_{i2}b_{2j} + \cdots + a_{in}b_{nj} = \sum_k a_{ik}b_{kj} \quad (1.16)$$

Therefore, the number of columns in  $\mathbf{A}$  must be equal to the number of rows in  $\mathbf{B}$ . If  $\mathbf{A}$  is an  $m \times n$  matrix and  $\mathbf{B}$  is an  $n \times p$  matrix, then  $\mathbf{C}$  is an  $m \times p$  matrix. In general,  $\mathbf{AB} \neq \mathbf{BA}$ . That is, matrix multiplication is not commutative. The *associative law* for matrix multiplication, however, is valid; that is,  $(\mathbf{AB})\mathbf{C} = \mathbf{A}(\mathbf{BC}) = \mathbf{ABC}$ , provided consistent dimensions of the matrices  $\mathbf{A}$ ,  $\mathbf{B}$ , and  $\mathbf{C}$  are used.

## 1.2 VECTORS

Vectors can be considered special cases of matrices. An  $n$ -dimensional vector  $\mathbf{a}$  can be written as

$$\mathbf{a} = (a_i) = \begin{bmatrix} a_1 \\ a_2 \\ \vdots \\ a_n \end{bmatrix} = [a_1 \quad a_2 \quad \cdots \quad a_n]^T \quad (1.17)$$

Therefore, it is assumed that the vector is a column, unless it is transposed to make it a row.

Because vectors can be treated as columns of matrices, the addition of vectors is the same as the addition of column matrices. That is, if  $\mathbf{a} = (a_i)$  and  $\mathbf{b} = (b_i)$  are two  $n$ -dimensional vectors, then  $\mathbf{a} + \mathbf{b} = (a_i + b_i)$ . Three different types of products, however, can be used with vectors.

These are the *dot product*, the *cross product*, and the *outer* or *dyadic product*. The result of the dot product of two vectors is a scalar, the result of the cross product is a vector, and the result of the dyadic product is a matrix. These three different types of products are discussed in the following sections.

## Dot Product

The *dot*, *inner*, or *scalar product* of two vectors  $\mathbf{a}$  and  $\mathbf{b}$  is defined as

$$\mathbf{a} \cdot \mathbf{b} = \mathbf{a}^T \mathbf{b} = a_1 b_1 + a_2 b_2 + \cdots + a_n b_n = \sum_{i=1}^n a_i b_i \quad (1.18)$$

Note that the two vectors  $\mathbf{a}$  and  $\mathbf{b}$  must have the same dimension. The two vectors  $\mathbf{a}$  and  $\mathbf{b}$  are said to be *orthogonal* if  $\mathbf{a} \cdot \mathbf{b} = \mathbf{a}^T \mathbf{b} = 0$ . The *norm*, *magnitude*, or *length* of an  $n$ -dimensional vector is defined as

$$|\mathbf{a}| = \sqrt{\mathbf{a} \cdot \mathbf{a}} = \sqrt{\mathbf{a}^T \mathbf{a}} = \sqrt{\sum_{i=1}^n (a_i)^2} \quad (1.19)$$

It is clear from this definition that the norm is always a positive number, and it is equal to zero only when  $\mathbf{a}$  is the zero vector, that is, all the components of  $\mathbf{a}$  are equal to zero.

In the special case of three-dimensional vectors, the dot product of two arbitrary three-dimensional vectors  $\mathbf{a}$  and  $\mathbf{b}$  can be written in terms of their norms as  $\mathbf{a} \cdot \mathbf{b} = |\mathbf{a}| |\mathbf{b}| \cos \alpha$ , where  $\alpha$  is the angle between the two vectors. A vector is said to be a *unit vector* if its norm is equal to one. It is clear from the definition of the norm given by Equation 19 that the absolute value of any element of a unit vector must not exceed one. A unit vector  $\hat{\mathbf{a}}$  along the vector  $\mathbf{a}$  can be simply obtained by dividing the vector by its norm. That is,  $\hat{\mathbf{a}} = \mathbf{a}/|\mathbf{a}|$ . The dot product  $\mathbf{b} \cdot \hat{\mathbf{a}} = |\mathbf{b}| \cos \alpha$  defines the component of the vector  $\mathbf{b}$  along the unit vector  $\hat{\mathbf{a}}$ , where  $\alpha$  is the angle between the two vectors. The projection of the vector  $\mathbf{b}$  on a plane perpendicular to the unit vector  $\hat{\mathbf{a}}$  is defined by the equation  $\mathbf{b} - (\mathbf{b} \cdot \hat{\mathbf{a}}) \hat{\mathbf{a}}$ , or equivalently by  $\mathbf{b} - (|\mathbf{b}| \cos \alpha) \hat{\mathbf{a}}$ .

## Cross Product

The vector cross product is defined for three-dimensional vectors only. Let  $\mathbf{a}$  and  $\mathbf{b}$  be two three-dimensional vectors defined in the same coordinate system. Unit vectors along the axes of the coordinate system are denoted by the vectors  $\mathbf{i}_1$ ,  $\mathbf{i}_2$ , and  $\mathbf{i}_3$ . These base vectors are *orthonormal*, that is,

$$\mathbf{i}_i \cdot \mathbf{i}_j = \delta_{ij} \quad (1.20)$$

where  $\delta_{ij}$  is the *Kronecker delta* defined as

$$\delta_{ij} = \begin{cases} 1 & i = j \\ 0 & i \neq j \end{cases} \quad (1.21)$$

The *cross product* of the two vectors  $\mathbf{a}$  and  $\mathbf{b}$  is defined as

$$\begin{aligned}\mathbf{c} = \mathbf{a} \times \mathbf{b} &= \begin{vmatrix} \mathbf{i}_1 & \mathbf{i}_2 & \mathbf{i}_3 \\ a_1 & a_2 & a_3 \\ b_1 & b_2 & b_3 \end{vmatrix} \\ &= (a_2 b_3 - a_3 b_2) \mathbf{i}_1 + (a_3 b_1 - a_1 b_3) \mathbf{i}_2 + (a_1 b_2 - a_2 b_1) \mathbf{i}_3\end{aligned}\quad (1.22)$$

which can be written as

$$\mathbf{c} = \mathbf{a} \times \mathbf{b} = \begin{bmatrix} c_1 \\ c_2 \\ c_3 \end{bmatrix} = \begin{bmatrix} a_2 b_3 - a_3 b_2 \\ a_3 b_1 - a_1 b_3 \\ a_1 b_2 - a_2 b_1 \end{bmatrix} = \begin{bmatrix} 0 & -a_3 & a_2 \\ a_3 & 0 & -a_1 \\ -a_2 & a_1 & 0 \end{bmatrix} \begin{bmatrix} b_1 \\ b_2 \\ b_3 \end{bmatrix}\quad (1.23)$$

This equation can be written as

$$\mathbf{c} = \mathbf{a} \times \mathbf{b} = \tilde{\mathbf{a}} \mathbf{b}\quad (1.24)$$

where  $\tilde{\mathbf{a}}$  is the skew-symmetric matrix associated with the vector  $\mathbf{a}$  and is defined as

$$\tilde{\mathbf{a}} = \begin{bmatrix} 0 & -a_3 & a_2 \\ a_3 & 0 & -a_1 \\ -a_2 & a_1 & 0 \end{bmatrix}\quad (1.25)$$

One can show that the determinant of the skew-symmetric matrix  $\tilde{\mathbf{a}}$  is equal to zero. That is,  $|\tilde{\mathbf{a}}| = 0$ . One can also show that

$$\mathbf{c} = \mathbf{a} \times \mathbf{b} = -\mathbf{b} \times \mathbf{a} = -\tilde{\mathbf{b}} \mathbf{a}\quad (1.26)$$

In this equation,  $\tilde{\mathbf{b}}$  is the skew-symmetric matrix associated with the vector  $\mathbf{b}$ . If  $\mathbf{a}$  and  $\mathbf{b}$  are two parallel vectors, it can be shown that  $\mathbf{a} \times \mathbf{b} = \mathbf{0}$ . That is, the cross product of two parallel vectors is equal to zero.

## Dyadic Product

Another form of vector product used in this book is the *dyadic* or *outer product*. Whereas the dot product leads to a scalar and the cross product leads to a vector, the dyadic product leads to a matrix. The dyadic product of two vectors  $\mathbf{a}$  and  $\mathbf{b}$  is written as  $\mathbf{a} \otimes \mathbf{b}$  and is defined as

$$\mathbf{a} \otimes \mathbf{b} = \mathbf{a} \mathbf{b}^T\quad (1.27)$$

Note that, in general,  $\mathbf{a} \otimes \mathbf{b} \neq \mathbf{b} \otimes \mathbf{a}$ . One can show that the dyadic product of two vectors satisfies the following identities:

$$(\mathbf{a} \otimes \mathbf{b}) \mathbf{c} = \mathbf{a} (\mathbf{b} \cdot \mathbf{c}), \quad \mathbf{a} \cdot (\mathbf{b} \otimes \mathbf{c}) = (\mathbf{a} \cdot \mathbf{b}) \mathbf{c}^T\quad (1.28)$$

In Equation 28, it is assumed that the vectors have the appropriate dimensions. The dyadic product satisfies the following additional properties for any arbitrary vectors  $\mathbf{u}$ ,  $\mathbf{v}$ ,  $\mathbf{v}_1$ , and  $\mathbf{v}_2$  and a square matrix  $\mathbf{A}$ :

$$\left. \begin{aligned} (\mathbf{u} \otimes \mathbf{v})^T &= \mathbf{v} \otimes \mathbf{u} \\ \mathbf{A}(\mathbf{u} \otimes \mathbf{v}) &= (\mathbf{A}\mathbf{u} \otimes \mathbf{v}) \\ (\mathbf{u} \otimes \mathbf{v})\mathbf{A} &= (\mathbf{u} \otimes \mathbf{A}^T \mathbf{v}) \\ \mathbf{u} \otimes (\mathbf{v}_1 + \mathbf{v}_2) &= \mathbf{u} \otimes \mathbf{v}_1 + \mathbf{u} \otimes \mathbf{v}_2 \end{aligned} \right\} \quad (1.29)$$

The second and third identities of Equation 29 show that  $(\mathbf{A}\mathbf{u} \otimes \mathbf{A}\mathbf{v}) = \mathbf{A}(\mathbf{u} \otimes \mathbf{v})\mathbf{A}^T$ . This result is important in understanding the rule of transformation of the second-order tensors that will be used repeatedly in this book. It is left to the reader as an exercise to verify the identities of Equation 29.

### Example 1.2

Consider the two vectors  $\mathbf{a} = [a_1 \ a_2]^T$  and  $\mathbf{b} = [b_1 \ b_2 \ b_3]^T$ . The dyadic product of these two vectors is given by

$$\mathbf{a} \otimes \mathbf{b} = \begin{bmatrix} a_1 \\ a_2 \end{bmatrix} \begin{bmatrix} b_1 & b_2 & b_3 \end{bmatrix} = \begin{bmatrix} a_1 b_1 & a_1 b_2 & a_1 b_3 \\ a_2 b_1 & a_2 b_2 & a_2 b_3 \end{bmatrix}$$

For a given vector  $\mathbf{c} = [c_1 \ c_2 \ c_3]^T$ , one has

$$\begin{aligned} (\mathbf{a} \otimes \mathbf{b})\mathbf{c} &= \begin{bmatrix} a_1 b_1 & a_1 b_2 & a_1 b_3 \\ a_2 b_1 & a_2 b_2 & a_2 b_3 \end{bmatrix} \begin{bmatrix} c_1 \\ c_2 \\ c_3 \end{bmatrix} \\ &= \begin{bmatrix} a_1 b_1 \\ a_2 b_1 \end{bmatrix} c_1 + \begin{bmatrix} a_1 b_2 \\ a_2 b_2 \end{bmatrix} c_2 + \begin{bmatrix} a_1 b_3 \\ a_2 b_3 \end{bmatrix} c_3 \\ &= \begin{bmatrix} a_1 \\ a_2 \end{bmatrix} b_1 c_1 + \begin{bmatrix} a_1 \\ a_2 \end{bmatrix} b_2 c_2 + \begin{bmatrix} a_1 \\ a_2 \end{bmatrix} b_3 c_3 = \mathbf{a}(\mathbf{b} \cdot \mathbf{c}) \end{aligned}$$

Also note that the dyadic product  $\mathbf{a} \otimes \mathbf{b}$  can be written as

$$\mathbf{a} \otimes \mathbf{b} = \begin{bmatrix} a_1 \\ a_2 \end{bmatrix} b_1 \begin{bmatrix} a_1 \\ a_2 \end{bmatrix} b_2 \begin{bmatrix} a_1 \\ a_2 \end{bmatrix} b_3 = [\mathbf{a}b_1 \ \mathbf{a}b_2 \ \mathbf{a}b_3]$$

It follows that if  $\mathbf{R}$  is a  $2 \times 2$  matrix, one has

$$\begin{aligned} \mathbf{R}(\mathbf{a} \otimes \mathbf{b}) &= \mathbf{R}[\mathbf{a}b_1 \ \mathbf{a}b_2 \ \mathbf{a}b_3] = [(\mathbf{R}\mathbf{a})b_1 \ (\mathbf{R}\mathbf{a})b_2 \ (\mathbf{R}\mathbf{a})b_3] \\ &= (\mathbf{R}\mathbf{a} \otimes \mathbf{b}) \end{aligned}$$

Several important identities can be written in terms of the dyadic product. Some of these identities are valuable in the computer implementation of the dynamic formulations presented in this book because the use of these identities can lead to significant simplification of the computational algorithms. By using these identities, one can avoid rewriting codes that perform the same mathematical operations, thereby saving effort and time by producing a manageable computer code. One of these identities that can be written in terms of the dyadic product is obtained in the following example.

### Example 1.3

In the computer implementation of the formulations presented in this book, one may require differentiating a unit vector  $\hat{\mathbf{r}}$  along the vector  $\mathbf{r}$  with respect to the components of the vector  $\mathbf{r}$ . Such a differentiation can be written in terms of the dyadic product. To demonstrate this, we write

$$\hat{\mathbf{r}} = \frac{1}{\sqrt{\mathbf{r}^T \mathbf{r}}} \mathbf{r} = \frac{1}{|\mathbf{r}|} \mathbf{r}$$

where  $|\mathbf{r}| = \sqrt{\mathbf{r}^T \mathbf{r}}$ . It follows that

$$\frac{\partial \hat{\mathbf{r}}}{\partial \mathbf{r}} = \frac{1}{\sqrt{\mathbf{r}^T \mathbf{r}}} \left( \mathbf{I} - \frac{1}{\mathbf{r}^T \mathbf{r}} \mathbf{r} \mathbf{r}^T \right)$$

This equation can be written in terms of the dyadic product as

$$\frac{\partial \hat{\mathbf{r}}}{\partial \mathbf{r}} = \frac{1}{\sqrt{\mathbf{r}^T \mathbf{r}}} \left( \mathbf{I} - \frac{1}{\mathbf{r}^T \mathbf{r}} \mathbf{r} \otimes \mathbf{r} \right) = \frac{1}{|\mathbf{r}|} (\mathbf{I} - \hat{\mathbf{r}} \otimes \hat{\mathbf{r}})$$

## Projection

If  $\hat{\mathbf{a}}$  is a unit vector, the component of a vector  $\mathbf{b}$  along the unit vector  $\hat{\mathbf{a}}$  is defined by the dot product  $\mathbf{b} \cdot \hat{\mathbf{a}}$ . The projection of  $\mathbf{b}$  along  $\hat{\mathbf{a}}$  is then defined as  $(\mathbf{b} \cdot \hat{\mathbf{a}})\hat{\mathbf{a}}$ , which can be written using Equation 28 as  $(\mathbf{b} \cdot \hat{\mathbf{a}})\hat{\mathbf{a}} = (\hat{\mathbf{a}} \otimes \hat{\mathbf{a}})\mathbf{b}$ . The matrix  $\mathbf{P} = \hat{\mathbf{a}} \otimes \hat{\mathbf{a}}$  defines a *projection matrix*. For an arbitrary integer  $n$ , one can show that the projection matrix  $\mathbf{P}$  satisfies the identity  $\mathbf{P}^n = \mathbf{P}$ . This is an expected result because the vector  $(\hat{\mathbf{a}} \otimes \hat{\mathbf{a}})\mathbf{b} = \mathbf{P}\mathbf{b}$  is defined along  $\hat{\mathbf{a}}$  and has no components in other directions. Other projections should not change this result.

The projection of the vector  $\mathbf{b}$  on a plane perpendicular to the unit vector  $\hat{\mathbf{a}}$  is defined as  $\mathbf{b} - (\mathbf{b} \cdot \hat{\mathbf{a}})\hat{\mathbf{a}}$ , which can be written using the dyadic product as  $(\mathbf{I} - \hat{\mathbf{a}} \otimes \hat{\mathbf{a}})\mathbf{b}$ . This equation defines another projection matrix  $\mathbf{P}_p = \mathbf{I} - \hat{\mathbf{a}} \otimes \hat{\mathbf{a}}$ , or simply  $\mathbf{P}_p = \mathbf{I} - \mathbf{P}$ . For an arbitrary integer  $n$ , one can show that the projection matrix  $\mathbf{P}_p$  satisfies the identity  $\mathbf{P}_p^n = \mathbf{P}_p$ . Furthermore,  $\mathbf{P}\mathbf{P}_p = \mathbf{0}$  and  $\mathbf{P} + \mathbf{P}_p = \mathbf{I}$ .

**Example 1.4**

Consider the vector  $\mathbf{a} = [1 \ 2 \ 0]^T$ . A unit vector along  $\mathbf{a}$  is defined as

$$\hat{\mathbf{a}} = \frac{1}{\sqrt{5}} [1 \ 2 \ 0]^T$$

The projection matrix  $\mathbf{P}$  associated with this unit vector can be written as

$$\mathbf{P} = \hat{\mathbf{a}} \otimes \hat{\mathbf{a}} = \frac{1}{5} \begin{bmatrix} 1 & 2 & 0 \\ 2 & 4 & 0 \\ 0 & 0 & 0 \end{bmatrix}$$

It follows that

$$\mathbf{P}^2 = \frac{1}{25} \begin{bmatrix} 5 & 10 & 0 \\ 10 & 20 & 0 \\ 0 & 0 & 0 \end{bmatrix} = \frac{1}{5} \begin{bmatrix} 1 & 2 & 0 \\ 2 & 4 & 0 \\ 0 & 0 & 0 \end{bmatrix} = \mathbf{P}$$

The projection matrix  $\mathbf{P}_p$  is defined in this example as

$$\mathbf{P}_p = \mathbf{I} - \hat{\mathbf{a}} \otimes \hat{\mathbf{a}} = \mathbf{I} - \mathbf{P} = \frac{1}{5} \begin{bmatrix} 4 & -2 & 0 \\ -2 & 1 & 0 \\ 0 & 0 & 5 \end{bmatrix}$$

Note that  $\mathbf{P}_p^2 = (\mathbf{I} - \mathbf{P})^2 = \mathbf{I} - 2\mathbf{P} + \mathbf{P}^2 = \mathbf{I} - \mathbf{P} = \mathbf{P}_p$ . Successive application of this equation shows that  $\mathbf{P}_p^n = \mathbf{P}_p$ . The reader can verify this fact by the data given in this example.

**1.3 SUMMATION CONVENTION**

In this section, another convenient notational method, the *summation convention*, is discussed. The summation convention is used in most books on the subject of continuum mechanics. According to this convention, summation over the values of the indices is automatically assumed if an index is repeated in an expression. For example, if an index  $j$  takes the values from 1 to  $n$ , then in the summation convention, one has

$$a_{jj} = a_{11} + a_{22} + \cdots + a_{nn} \quad (1.30)$$

and

$$a_{ijj} = a_{i11} + a_{i22} + \cdots + a_{inn} \quad (1.31)$$

The repeated index used in the summation is called the *dummy index*, an example of which is the index  $j$  used in the preceding equation. If the index is not a dummy index, it is called a *free index*, an example of which is the index  $i$  used in Equation 31. It follows that the trace of a matrix  $\mathbf{A}$  can be written using the summation convention as  $\text{tr}(\mathbf{A}) = a_{ii}$ . The dot product between two  $n$ -dimensional vectors  $\mathbf{a}$  and  $\mathbf{b}$  can be written using the summation convention as  $\mathbf{a} \cdot \mathbf{b} = \mathbf{a}^T \mathbf{b} = a_i b_i$ . The product of a matrix  $\mathbf{A}$  and a vector  $\mathbf{b}$  is another vector  $\mathbf{c} = \mathbf{A}\mathbf{b}$  whose



components can be written using the summation convention as  $c_i = a_{ij}b_j$ . Here,  $i$  is the free index and  $j$  is the dummy index.

### Unit Dyads

The dyadic product between two vectors can also be written using the summation convention. For example, in the case of three-dimensional vectors, one can define the base vectors  $\mathbf{i}_k$ ,  $k = 1, 2, 3$ . Any three-dimensional vector can be written in terms of these base vectors using the summation convention as  $\mathbf{a} = a_i \mathbf{i}_i = a_1 \mathbf{i}_1 + a_2 \mathbf{i}_2 + a_3 \mathbf{i}_3$ . The dyadic product of two vectors  $\mathbf{a}$  and  $\mathbf{b}$  can then be written as

$$\mathbf{a} \otimes \mathbf{b} = (a_i \mathbf{i}_i) \otimes (b_j \mathbf{i}_j) = a_i b_j (\mathbf{i}_i \otimes \mathbf{i}_j) \quad (1.32)$$

For example, if  $\mathbf{i}_i = \mathbf{i}_1 = [1 \ 0 \ 0]^T$ ,  $\mathbf{i}_j = \mathbf{i}_2 = [0 \ 1 \ 0]^T$ , and  $\mathbf{a}$  and  $\mathbf{b}$  are arbitrary three-dimensional vectors, one can show that the dyadic product of the preceding equation can be written in the following matrix form:

$$\mathbf{a} \otimes \mathbf{b} = a_i b_j (\mathbf{i}_i \otimes \mathbf{i}_j) = \begin{bmatrix} a_1 b_1 & a_1 b_2 & a_1 b_3 \\ a_2 b_1 & a_2 b_2 & a_2 b_3 \\ a_3 b_1 & a_3 b_2 & a_3 b_3 \end{bmatrix} \quad (1.33)$$

The dyadic products of the base vectors  $\mathbf{i}_i \otimes \mathbf{i}_j$  are called the *unit dyads*. Using this notation, the dyadic product can be generalized to the products of three or more vectors. For example, the *triadic product* of the vectors  $\mathbf{a}$ ,  $\mathbf{b}$ , and  $\mathbf{c}$  can be written as  $\mathbf{a} \otimes \mathbf{b} \otimes \mathbf{c} = (a_i \mathbf{i}_i) \otimes (b_j \mathbf{i}_j) \otimes (c_k \mathbf{i}_k) = a_i b_j c_k (\mathbf{i}_i \otimes \mathbf{i}_j \otimes \mathbf{i}_k)$ . In this book, the familiar summation sign  $\sum$  will be used for the most part, instead of the summation convention.

## 1.4 CARTESIAN TENSORS

It is clear from the preceding section that a dyadic product is a linear combination of unit dyads. The *second-order Cartesian tensor* is defined as a linear combination of dyadic products. A second-order Cartesian tensor  $\mathbf{A}$  takes the following form:

$$\mathbf{A} = \sum_{i,j=1}^3 a_{ij} (\mathbf{i}_i \otimes \mathbf{i}_j) \quad (1.34)$$

where  $a_{ij}$  are called the components of  $\mathbf{A}$ . Using the analysis presented in the preceding section, one can show that the second-order tensor can be written in the matrix form of Equation 33. Nonetheless, for a given second-order tensor  $\mathbf{A}$ , one cannot in general find two vectors  $\mathbf{a}$  and  $\mathbf{b}$  such that  $\mathbf{A} = \mathbf{a} \otimes \mathbf{b}$ .

The *unit* or *identity tensor* can be written in terms of the base vectors as

$$\mathbf{I} = \sum_{i=1}^3 \mathbf{i}_i \otimes \mathbf{i}_i \quad (1.35)$$

Using the definition of the second-order tensor as a linear combination of dyadic products, one can show, as previously mentioned, that the components of any second-order tensor can be arranged in the form of a  $3 \times 3$  matrix. In continuum mechanics, the elements of tensors represent physical quantities such as moments of inertia, strains, and stresses. These elements can be defined in any coordinate system. The coordinate systems used depend on the formulation used to obtain the equilibrium equations. It is, therefore, important that the reader understands the rule of the coordinate transformation of tensors and recognizes that such a transformation leads to the definition of the same physical quantities in different frames of reference or different directions. One must also distinguish between the transformation of vectors and the change of parameters. The latter does not change the coordinate system in which the vectors are defined. This important difference will be discussed in more detail before concluding this chapter.

A tensor that has the same components in any coordinate system is called an *isotropic tensor*. An example of isotropic tensors is the unit tensor. It can be shown that second-order isotropic tensors take only one form and can be written as  $\alpha \mathbf{I}$ , where  $\alpha$  is a scalar and  $\mathbf{I}$  is the unit or the identity tensor. Second-order isotropic tensors are sometimes called *spherical tensors*.

### Double Product or Double Contraction

If  $\mathbf{A}$  is a second-order tensor, the *contraction* of this tensor to a scalar is defined as  $\sum_{i=1}^3 a_{ii} = a_{11} + a_{22} + a_{33} = \text{tr}(\mathbf{A})$ , where  $\text{tr}$  denotes the trace of the matrix (sum of the diagonal elements) (Aris 1962). It can be shown that the trace of a second-order tensor is invariant under orthogonal coordinate transformations. In addition to the trace, the determinant of  $\mathbf{A}$  is invariant under orthogonal coordinate transformation. This important result can also be obtained in the case of second-order tensors using the facts that the determinant of an orthogonal matrix is equal to  $\pm 1$  and the determinant of the product of matrices is equal to the product of the determinants of these matrices.

If  $\mathbf{A}$  and  $\mathbf{B}$  are second-order tensors, the *double product* or *double contraction* is defined as

$$\mathbf{A} : \mathbf{B} = \text{tr}(\mathbf{A}^T \mathbf{B}) \quad (1.36)$$

Using the properties of the trace, one can show that

$$\mathbf{A} : \mathbf{B} = \text{tr}(\mathbf{A}^T \mathbf{B}) = \text{tr}(\mathbf{B} \mathbf{A}^T) = \text{tr}(\mathbf{B}^T \mathbf{A}) = \text{tr}(\mathbf{A} \mathbf{B}^T) = \sum_{i,j=1}^3 a_{ij} b_{ij} \quad (1.37)$$

where  $a_{ij}$  and  $b_{ij}$  are, respectively, the elements of the tensors  $\mathbf{A}$  and  $\mathbf{B}$ . If  $\mathbf{a}$ ,  $\mathbf{b}$ ,  $\mathbf{u}$ , and  $\mathbf{v}$  are arbitrary vectors and  $\mathbf{A}$  is a second-order tensor, one can show that the double contraction has the following properties:

$$\left. \begin{aligned} \text{tr}(\mathbf{A}) &= \mathbf{I} : \mathbf{A} \\ \mathbf{A} : (\mathbf{u} \otimes \mathbf{v}) &= \mathbf{u} \cdot (\mathbf{A} \mathbf{v}) \\ (\mathbf{a} \otimes \mathbf{b}) : (\mathbf{u} \otimes \mathbf{v}) &= (\mathbf{a} \cdot \mathbf{u})(\mathbf{b} \cdot \mathbf{v}) \end{aligned} \right\} \quad (1.38)$$

It can also be shown that if  $\mathbf{A}$  is a symmetric tensor and  $\mathbf{B}$  is a skew-symmetric tensor, then  $\mathbf{A}:\mathbf{B}=0$ . It follows that if  $\mathbf{A}$  is a symmetric tensor and  $\mathbf{B}$  is an arbitrary tensor, the definition of the double product can be used to show that  $\mathbf{A}:\mathbf{B}=\mathbf{A}:\mathbf{B}^T=\mathbf{A}:(\mathbf{B}+\mathbf{B}^T)/2$ .

If  $\mathbf{A}$  and  $\mathbf{B}$  are two symmetric tensors, one can show that

$$\mathbf{A}:\mathbf{B} = a_{11}b_{11} + a_{22}b_{22} + a_{33}b_{33} + 2(a_{12}b_{12} + a_{13}b_{13} + a_{23}b_{23}) \quad (1.39)$$

The preceding equation will be used in this book in the formulation of the elastic forces of continuous bodies. These forces are expressed in terms of the strain and stress tensors. As will be shown in Chapters 2 and 3, the strain and stress tensors are symmetric and are given, respectively, in the following form:

$$\boldsymbol{\varepsilon} = \begin{bmatrix} \varepsilon_{11} & \varepsilon_{12} & \varepsilon_{13} \\ \varepsilon_{12} & \varepsilon_{22} & \varepsilon_{23} \\ \varepsilon_{13} & \varepsilon_{23} & \varepsilon_{33} \end{bmatrix}, \quad \boldsymbol{\sigma} = \begin{bmatrix} \sigma_{11} & \sigma_{12} & \sigma_{13} \\ \sigma_{12} & \sigma_{22} & \sigma_{23} \\ \sigma_{13} & \sigma_{23} & \sigma_{33} \end{bmatrix} \quad (1.40)$$

Using Equation 39, one can write the double contraction of the strain and stress tensors as

$$\boldsymbol{\varepsilon}:\boldsymbol{\sigma} = \varepsilon_{11}\sigma_{11} + \varepsilon_{22}\sigma_{22} + \varepsilon_{33}\sigma_{33} + 2(\varepsilon_{12}\sigma_{12} + \varepsilon_{13}\sigma_{13} + \varepsilon_{23}\sigma_{23}) \quad (1.41)$$

Because a second-order symmetric tensor has six independent elements, vector notations, instead of tensor notations, can also be used to define the strain and stress components of the preceding two equations. In this case, six-dimensional strain and stress vectors can be introduced as follows:

$$\left. \begin{aligned} \boldsymbol{\varepsilon}_v &= [\varepsilon_{11} \ \varepsilon_{22} \ \varepsilon_{33} \ \varepsilon_{12} \ \varepsilon_{13} \ \varepsilon_{23}]^T \\ \boldsymbol{\sigma}_v &= [\sigma_{11} \ \sigma_{22} \ \sigma_{33} \ \sigma_{12} \ \sigma_{13} \ \sigma_{23}]^T \end{aligned} \right\} \quad (1.42)$$

where subscript  $v$  is used to denote a vector. The dot product of the strain and stress vectors is given by

$$\boldsymbol{\varepsilon} \cdot \boldsymbol{\sigma} = \boldsymbol{\varepsilon}^T \boldsymbol{\sigma} = \varepsilon_{11}\sigma_{11} + \varepsilon_{22}\sigma_{22} + \varepsilon_{33}\sigma_{33} + \varepsilon_{12}\sigma_{12} + \varepsilon_{13}\sigma_{13} + \varepsilon_{23}\sigma_{23} \quad (1.43)$$

Note the difference between the results of the double contraction and the dot product of Equations 41 and 43, respectively. There is a factor of 2 multiplied by the term that includes the off-diagonal elements in the double contraction of Equation 41. Equation 41 arises naturally when the elastic forces are formulated, as will be shown in Chapter 3. Therefore, it is important to distinguish between the double contraction and the dot product despite the fact that both products lead to scalar quantities.

## Invariants of the Second-Order Tensor

Under an orthogonal transformation that represents rotation of the axes of the coordinate systems, the components of the vectors and second-order tensors change. Nonetheless, certain vector and tensor quantities do not change and remain invariant under such an orthogonal transformation. For example, the norm of a vector and the dot product of two three-dimensional vectors remain invariant under a rigid-body rotation.

For a second-order tensor  $\mathbf{A}$ , one has the following three invariants that do not change under an orthogonal coordinate transformation:

$$\left. \begin{aligned} I_1 &= \text{tr}(\mathbf{A}) \\ I_2 &= \frac{1}{2} \{ (\text{tr}(\mathbf{A}))^2 - \text{tr}(\mathbf{A}^2) \} \\ I_3 &= \det(\mathbf{A}) = |\mathbf{A}| \end{aligned} \right\} \quad (1.44)$$

These three invariants can also be written in terms of the *eigenvalues* of the tensor  $\mathbf{A}$ . For a given tensor or a matrix  $\mathbf{A}$ , the eigenvalue problem is defined as

$$\mathbf{A}\mathbf{y} = \lambda\mathbf{y} \quad (1.45)$$

where  $\lambda$  is called the eigenvalue and  $\mathbf{y}$  is the *eigenvector* of  $\mathbf{A}$ . Equation 45 shows that the direction of the vector  $\mathbf{y}$  is not affected by multiplication with the tensor  $\mathbf{A}$ . That is,  $\mathbf{A}\mathbf{y}$  can change the length of  $\mathbf{y}$ , but such a multiplication does not change the direction of  $\mathbf{y}$ . For this reason,  $\mathbf{y}$  is called a principal direction of the tensor  $\mathbf{A}$ . The preceding eigenvalue equation can be written as

$$(\mathbf{A} - \lambda\mathbf{I})\mathbf{y} = \mathbf{0} \quad (1.46)$$

For this equation to have a nontrivial solution, the determinant of the coefficient matrix must be equal to zero, that is,

$$\det(\mathbf{A} - \lambda\mathbf{I}) = 0 \quad (1.47)$$

This equation is called the *characteristic equation*, and in the case of a second-order tensor it has three roots  $\lambda_1$ ,  $\lambda_2$ , and  $\lambda_3$ . Associated with these three roots, there are three corresponding eigenvectors  $\mathbf{y}_1$ ,  $\mathbf{y}_2$ , and  $\mathbf{y}_3$  that can be determined to within an arbitrary constant using Equation 46. That is, for a root  $\lambda_i$ ,  $i = 1, 2, 3$ , one can solve the system of homogeneous equations  $(\mathbf{A} - \lambda_i\mathbf{I})\mathbf{y}_i = \mathbf{0}$  for the eigenvector  $\mathbf{y}_i$  to within an arbitrary constant, as demonstrated by the following example.

### Example 1.5

Consider the matrix

$$\mathbf{A} = \begin{bmatrix} 1 & -1 & 2 \\ 0 & 3 & 1 \\ 0 & 0 & 2 \end{bmatrix}$$

The characteristic equation of this matrix can be obtained using Equation 47 as

$$\det(\mathbf{A} - \lambda\mathbf{I}) = (1 - \lambda)(3 - \lambda)(2 - \lambda) = 0$$

The roots of this characteristic equation define the following three eigenvalues of the matrix  $\mathbf{A}$ :

$$\lambda_1 = 1, \quad \lambda_2 = 2, \quad \lambda_3 = 3$$

Associated with these three eigenvalues, there are three eigenvectors, which can be determined using Equation 46 as

$$(\mathbf{A} - \lambda_i \mathbf{I})\mathbf{y}_i = \mathbf{0}, \quad i = 1, 2, 3$$

or

$$\begin{bmatrix} 1 - \lambda_i & -1 & 2 \\ 0 & 3 - \lambda_i & 1 \\ 0 & 0 & 2 - \lambda_i \end{bmatrix} \begin{bmatrix} y_{i1} \\ y_{i2} \\ y_{i3} \end{bmatrix} = \mathbf{0}, \quad i = 1, 2, 3$$

This equation can be used to solve for the eigenvectors associated with the three eigenvalues  $\lambda_1$ ,  $\lambda_2$ , and  $\lambda_3$ . For  $\lambda_1 = 1$ , the preceding equation yields the following system of algebraic equations:

$$\begin{bmatrix} 0 & -1 & 2 \\ 0 & 2 & 1 \\ 0 & 0 & 1 \end{bmatrix} \begin{bmatrix} y_{11} \\ y_{12} \\ y_{13} \end{bmatrix} = \mathbf{0}$$

This system of algebraic equations defines the first eigenvector to within an arbitrary constant as

$$\mathbf{y}_1 = \begin{bmatrix} y_{11} \\ y_{12} \\ y_{13} \end{bmatrix} = \begin{bmatrix} 1 \\ 0 \\ 0 \end{bmatrix}$$

For  $\lambda_2 = 2$ , one has

$$\mathbf{y}_2 = \begin{bmatrix} y_{21} \\ y_{22} \\ y_{23} \end{bmatrix} = \begin{bmatrix} -3 \\ 1 \\ -1 \end{bmatrix}$$

The eigenvector associated with  $\lambda_3 = 3$  can also be determined as

$$\mathbf{y}_3 = \begin{bmatrix} y_{31} \\ y_{32} \\ y_{33} \end{bmatrix} = \begin{bmatrix} 1 \\ -2 \\ 0 \end{bmatrix}$$

## Symmetric Tensors

In the special case of a *symmetric tensor*, one can show that the eigenvalues are real and the eigenvectors are orthogonal. Because the eigenvectors can be determined to within an arbitrary constant, the eigenvectors can be normalized as unit vectors. For a symmetric tensor, one can then write

$$\left. \begin{aligned} \mathbf{A}\mathbf{y}_i &= \lambda_i \mathbf{y}_i, \quad i = 1, 2, 3 \\ \mathbf{y}_i^T \mathbf{y}_j &= \delta_{ij}, \quad i, j = 1, 2, 3 \end{aligned} \right\} \quad (1.48)$$

If  $\mathbf{y}_i$ ,  $i = 1, 2, 3$ , are selected as orthogonal unit vectors, one can form the orthogonal matrix  $\Phi$  whose columns are the orthonormal eigenvectors, that is,

$$\Phi = [\mathbf{y}_1 \quad \mathbf{y}_2 \quad \mathbf{y}_3] \quad (1.49)$$

It follows that

$$\mathbf{A}\Phi = \Phi\lambda \quad (1.50)$$

where

$$\lambda = \begin{bmatrix} \lambda_1 & 0 & 0 \\ 0 & \lambda_2 & 0 \\ 0 & 0 & \lambda_3 \end{bmatrix} \quad (1.51)$$

Using the orthogonality property of  $\Phi$ , one has

$$\mathbf{A} = \Phi\lambda\Phi^T = \sum_{i=1}^3 \lambda_i(\mathbf{y}_i \otimes \mathbf{y}_i) \quad (1.52)$$

This equation, which defines the *spectral decomposition* of  $\mathbf{A}$ , shows that the orthogonal transformation  $\Phi$  can be used to transform the tensor  $\mathbf{A}$  to a diagonal matrix as

$$\Phi^T \mathbf{A} \Phi = \lambda = \begin{bmatrix} \lambda_1 & 0 & 0 \\ 0 & \lambda_2 & 0 \\ 0 & 0 & \lambda_3 \end{bmatrix} \quad (1.53)$$

That is, the matrices  $\mathbf{A}$  and  $\lambda$  have the same determinant and the same trace. This important result is often used in continuum mechanics to study the invariant properties of different tensors.

Let  $\mathbf{R}$  be an orthogonal transformation matrix. Using the transformation  $\mathbf{y} = \mathbf{R}\mathbf{z}$  in Equation 46 and premultiplying by  $\mathbf{R}^T$ , one obtains

$$(\mathbf{R}^T \mathbf{A} \mathbf{R} - \lambda \mathbf{I})\mathbf{z} = \mathbf{0} \quad (1.54)$$

This equation shows that the eigenvalues of a tensor or a matrix do not change under an orthogonal coordinate transformation. Furthermore, as previously discussed, the determinant and trace of the tensor or the matrix do not change under such a coordinate transformation. One then concludes that the invariants of a symmetric second-order tensor can be expressed in terms of its eigenvalues as follows:

$$\left. \begin{aligned} I_1 &= \text{tr}(\mathbf{A}) = \lambda_1 + \lambda_2 + \lambda_3 \\ I_2 &= \frac{1}{2} \{(\text{tr}(\mathbf{A}))^2 - \text{tr}(\mathbf{A}^2)\} = \lambda_1 \lambda_2 + \lambda_1 \lambda_3 + \lambda_2 \lambda_3 \\ I_3 &= \det(\mathbf{A}) = \lambda_1 \lambda_2 \lambda_3 \end{aligned} \right\} \quad (1.55)$$

Some of the material constitutive equations used in continuum mechanics are formulated in terms of the invariants of the strain tensor. Therefore, Equation 55 will be used in later chapters of this book.

For a general second-order tensor  $\mathbf{A}$  (symmetric or nonsymmetric), the invariants are  $I_1 = \text{tr}(\mathbf{A})$ ,  $I_2 = \frac{1}{2} \{(\text{tr}(\mathbf{A}))^2 - \text{tr}(\mathbf{A}^2)\}$ , and  $I_3 = \det(\mathbf{A})$ , as previously presented. One can show that the characteristic equation of a second-order tensor can be written in terms of these invariants as  $\lambda^3 - I_1 \lambda^2 + I_2 \lambda - I_3 = 0$ . Furthermore, by repeatedly multiplying Equation 45  $n$  times by  $\mathbf{A}$ , one obtains  $\mathbf{A}^n \mathbf{y} = \lambda^n \mathbf{y}$ . Using this identity after multiplying the characteristic equation  $\lambda^3 - I_1 \lambda^2 + I_2 \lambda - I_3 = 0$  by  $\mathbf{y}$ , one obtains  $\mathbf{A}^3 - I_1 \mathbf{A}^2 + I_2 \mathbf{A} - I_3 \mathbf{I} = \mathbf{0}$ , which is the mathematical statement of the *Cayley–Hamilton theorem*, which states that a second-order tensor satisfies its characteristic equation. The simple proof provided here for the Cayley–Hamilton theorem is based on the assumption that the eigenvectors are linearly independent. A more general proof can be found in the literature.

For a second-order skew-symmetric tensor  $\mathbf{W}$ , one can show that the invariants are given by  $I_1 = I_3 = 0$  and  $I_2 = w_{12}^2 + w_{13}^2 + w_{23}^2$ , where  $w_{ij}$  is the  $ij$ th element of the tensor  $\mathbf{W}$ . Using these results, the characteristic equation of a second-order tensor  $\mathbf{W}$  can be written as  $\lambda^3 + I_2 \lambda = 0$ . This equation shows that  $\mathbf{W}$  has only one real eigenvalue,  $\lambda = 0$ , whereas the other two eigenvalues are imaginary.

## Higher-Order Tensors

In continuum mechanics, the stress and strain tensors are related using the constitutive equations that define the material behavior. This relationship can be expressed in terms of a fourth-order tensor whose components are material coefficients. In general, a tensor  $\mathbf{A}$  of order  $n$  is defined by  $3^n$  elements, which can be written as  $a_{ijk\dots n}$ . A lower-order tensor can be obtained as a special case by reducing the number of indices. A zero-order tensor is represented by a scalar, a first-order tensor is represented by a vector, and a second-order tensor is represented by a matrix. A tensor of order  $n$  is said to be *symmetric* with respect to two indices if the interchange of these two indices does not change the value of the elements of the tensor. The tensor is said to be *antisymmetric* or *skew symmetric* with respect to two indices if the interchange of these two indices changes only the sign of the elements of the tensor.

As in the case of the second-order tensors, higher-order tensors can be defined using outer products. For example, a third-order tensor  $\mathbf{T}$  can be defined as the outer product of three vectors  $\mathbf{u}$ ,  $\mathbf{v}$ , and  $\mathbf{w}$  as follows:

$$\mathbf{T} = (\mathbf{u} \otimes \mathbf{v} \otimes \mathbf{w}) = (t_{ijk}) \quad (1.56)$$

An element of the tensor  $\mathbf{T}$  takes the form  $u_i v_j w_k$ . Roughly speaking, in the case of three-dimensional vectors, one may consider the third-order tensor a linear combination of a new set of unit dyads that consist of 27 elements (3 layers, each of which has 9 elements). Recall that the multiplication  $\mathbf{S}\mathbf{b}$  of a second-order tensor  $\mathbf{S} = (s_{ij})$  and a vector  $\mathbf{b} = (b_i)$  defines a vector  $\mathbf{c} = (c_i)$  according to  $c_i = \sum_{j=1}^3 s_{ij} b_j = s_{i1} b_1 + s_{i2} b_2 + s_{i3} b_3$ , which represents a *single contraction*. Similarly, the multiplication  $\mathbf{T}\mathbf{b}$  of a third-order tensor  $\mathbf{T} = (t_{ijk})$  with a vector  $\mathbf{b} = (b_i)$  is a single contraction that defines a second-order tensor  $\mathbf{S} = (s_{ij})$  such

that

$$s_{ij} = \sum_{k=1}^3 t_{ijk} b_k = t_{ij1} b_1 + t_{ij2} b_2 + t_{ij3} b_3 \quad (1.57)$$

Using this definition, it follows that the elements of layer or matrix  $l$ ,  $l = 1, 2, 3$  are given by  $w_l(\mathbf{u} \otimes \mathbf{v}) = \mathbf{T} \mathbf{i}_l$ . Using this definition of the product or following a procedure similar to the one used to define the elements of the second-order tensor, one can show that the elements of the third-order tensor are defined as

$$t_{ijk} = (\mathbf{i}_i \otimes \mathbf{i}_j) : \mathbf{T} \mathbf{i}_k \quad (1.58)$$

In this equation, the third-order tensor is defined such that it maps an arbitrary vector  $\mathbf{b}$  according to  $(\mathbf{u} \otimes \mathbf{v} \otimes \mathbf{w})\mathbf{b} = (\mathbf{w} \cdot \mathbf{b})(\mathbf{u} \otimes \mathbf{v})$ . Note that whereas a third-order tensor can in general be written as  $\mathbf{T} = (t_{ijk})$ , one cannot always, as in the case of second-order tensors, find vectors  $\mathbf{u}$ ,  $\mathbf{v}$ , and  $\mathbf{w}$  such that  $\mathbf{T} = (\mathbf{u} \otimes \mathbf{v} \otimes \mathbf{w})$ .

### Example 1.6

Let  $\mathbf{T} = (t_{ijk}) = (\mathbf{u} \otimes \mathbf{v} \otimes \mathbf{w})$  be a third-order tensor and  $\mathbf{u}$ ,  $\mathbf{v}$ , and  $\mathbf{w}$  be three-dimensional vectors. The third-order tensor  $\mathbf{T}$  has 27 elements defined by the products  $w_1(\mathbf{u} \otimes \mathbf{v})$ ,  $w_2(\mathbf{u} \otimes \mathbf{v})$ , and  $w_3(\mathbf{u} \otimes \mathbf{v})$ . It follows that

$$\mathbf{T} \mathbf{i}_k = w_k(\mathbf{u} \otimes \mathbf{v}) = w_k \begin{bmatrix} u_1 v_1 & u_1 v_2 & u_1 v_3 \\ u_2 v_1 & u_2 v_2 & u_2 v_3 \\ u_3 v_1 & u_3 v_2 & u_3 v_3 \end{bmatrix}$$

The element  $t_{13k}$  of the tensor  $\mathbf{T}$  can be defined as

$$t_{13k} = (\mathbf{i}_1 \otimes \mathbf{i}_3) : \mathbf{T} \mathbf{i}_k = \text{tr}\{(\mathbf{i}_1 \otimes \mathbf{i}_3)^T \mathbf{T} \mathbf{i}_k\}$$

where

$$(\mathbf{i}_1 \otimes \mathbf{i}_3) = \begin{bmatrix} 0 & 0 & 1 \\ 0 & 0 & 0 \\ 0 & 0 & 0 \end{bmatrix}$$

Using the preceding three equations, one obtains

$$t_{13k} = (\mathbf{i}_1 \otimes \mathbf{i}_3) : \mathbf{T} \mathbf{i}_k = \text{tr}\{(\mathbf{i}_1 \otimes \mathbf{i}_3)^T \mathbf{T} \mathbf{i}_k\} = u_1 v_3 w_k$$

Other elements of the tensor  $\mathbf{T}$  can be determined in a similar manner.

The *double product or double contraction* can also be applied to third-order tensors. Let  $\mathbf{T}$  and  $\mathbf{S}$  be, respectively, third- and second-order tensors and  $\mathbf{a}$ ,  $\mathbf{b}$ ,  $\mathbf{c}$ ,  $\mathbf{u}$ , and  $\mathbf{v}$  be arbitrary vectors. For such tensors, one can verify the following properties based on the double contraction



(Bonet and Wood, 1997):

$$\left. \begin{aligned} \mathbf{T} : (\mathbf{a} \otimes \mathbf{b}) &= (\mathbf{T}\mathbf{b})\mathbf{a} \\ (\mathbf{a} \otimes \mathbf{b} \otimes \mathbf{c}) : (\mathbf{u} \otimes \mathbf{v}) &= (\mathbf{u} \cdot \mathbf{b})(\mathbf{v} \cdot \mathbf{c})\mathbf{a} \\ (\mathbf{a} \otimes \mathbf{S}) : \mathbf{T} &= (\mathbf{S} : \mathbf{T}) \otimes \mathbf{a} \\ (\mathbf{S} \otimes \mathbf{a}) : \mathbf{T} &= \mathbf{S}(\mathbf{T}\mathbf{a}) \end{aligned} \right\} \quad (1.59)$$

Using the first of these equations, one can show that the double contraction of a third-order tensor  $\mathbf{T}$  by a second-order tensor  $\mathbf{S}$  can be evaluated in terms of their components as

$$\mathbf{T} : \mathbf{S} = \sum_{i,j,k=1}^3 t_{ijk} s_{jk} \mathbf{i}_i \quad (1.60)$$

An important example of a third-order tensor is the *alternating tensor*  $\mathbf{\Gamma}$ , which, when applied to a vector  $\mathbf{v} = [v_1 \ v_2 \ v_3]^T$ , maps this vector to a skew-symmetric matrix associated with this vector, that is,

$$\mathbf{\Gamma} \mathbf{v} = -\tilde{\mathbf{v}} \quad (1.61)$$

where

$$\tilde{\mathbf{v}} = \begin{bmatrix} 0 & -v_3 & v_2 \\ v_3 & 0 & -v_1 \\ -v_2 & v_1 & 0 \end{bmatrix} \quad (1.62)$$

The components  $\Gamma_{ijk}$  of  $\mathbf{\Gamma}$  are defined as

$$\Gamma_{ijk} = \mathbf{i}_i \cdot (\mathbf{i}_j \times \mathbf{i}_k) \quad (1.63)$$

From this equation, it is clear that  $\Gamma_{ijk} = 0$  if any indices are repeated;  $\Gamma_{ijk} = 1$  for an even permutation of  $i, j$ , and  $k$ ;  $\{(i, j, k), (j, k, i), (k, i, j)\}$ ; and  $\Gamma_{ijk} = -1$  for any other permutation. Using the first equation in Equation 59, one can show that, for any two arbitrary vectors  $\mathbf{u}$  and  $\mathbf{v}$ , the alternating tensor  $\mathbf{\Gamma}$  can be introduced using another definition as

$$\mathbf{\Gamma} : (\mathbf{u} \otimes \mathbf{v}) = (\mathbf{\Gamma}\mathbf{v})\mathbf{u} = -\tilde{\mathbf{v}}\mathbf{u} = \mathbf{u} \times \mathbf{v} \quad (1.64)$$

Equation 61 can also be written in component form as  $\tilde{v}_{ij} = \sum_{k=1}^3 \Gamma_{ijk} v_k$  because for a fixed  $k$ , only terms that do not have repeated indices will appear. For example, if the summation convention is used,  $\Gamma_{ij2} \tilde{v}_{ij} = \Gamma_{132} \tilde{v}_{13} + \Gamma_{312} \tilde{v}_{31} = -\tilde{v}_{13} + \tilde{v}_{31} = 2v_2$ . One can follow the same procedure for the other two components for the vector  $\mathbf{v}$  and show that  $v_k = -\frac{1}{2} \sum_{i,j=1}^3 \Gamma_{ijk} \tilde{v}_{ij} = -\frac{1}{2} \sum_{i,j=1}^3 \Gamma_{kij} \tilde{v}_{ij} = \frac{1}{2} \sum_{i,j=1}^3 \Gamma_{ikj} \tilde{v}_{ij}$  (Aris, 1962). The alternating tensor  $\mathbf{\Gamma}$  is another example of an isotropic tensor. Furthermore, one can show that the cross product between the two vectors in Equation 64 can be written as  $\mathbf{u} \times \mathbf{v} = \sum_{i,j=1}^3 u_i v_j (\mathbf{i}_i \times \mathbf{i}_j) = \sum_{i,j,k=1}^3 \Gamma_{ijk} u_i v_j \mathbf{i}_k$ .

In a similar manner to the third-order tensor, a *fourth-order tensor*  $\mathbf{F}$  can be defined as

$$\mathbf{F} = (\mathbf{u}_1 \otimes \mathbf{u}_2 \otimes \mathbf{u}_3 \otimes \mathbf{u}_4) = (f_{ijkl}) \quad (1.65)$$

where  $\mathbf{u}_m$ ,  $m = 1, 2, 3, 4$ , is an arbitrary vector. As in the case of third-order tensors, one can write  $u_{4m}(\mathbf{u}_1 \otimes \mathbf{u}_2 \otimes \mathbf{u}_3) = \mathbf{F}\mathbf{i}_m$ , where  $u_{4m}$  is the  $m$ th component of the vector  $\mathbf{u}_4$ . It can then be shown that the coefficients  $f_{ijkl}$  can be written as

$$f_{ijkl} = (\mathbf{i}_i \otimes \mathbf{i}_j) : \mathbf{F} : (\mathbf{i}_k \otimes \mathbf{i}_l) \quad (1.66)$$

More generally, if  $\mathbf{F} = (f_{ijkl})$  is a fourth-order tensor and  $\mathbf{v} = (v_i)$  is a vector, one has the single contraction,  $\mathbf{F}\mathbf{v} = \mathbf{T}$ , where  $\mathbf{T} = (t_{ijk})$  is a third-order tensor whose elements are defined as

$$t_{ijk} = \sum_{l=1}^3 f_{ijkl} v_l = f_{ijk1} v_1 + f_{ijk2} v_2 + f_{ijk3} v_3 \quad (1.67)$$

Similarly, the double contraction  $\mathbf{F} : \mathbf{S} = \mathbf{B}$  of the fourth-order tensor  $\mathbf{F} = (f_{ijkl})$  and a second-order tensor  $\mathbf{S} = (s_{ij})$  defines a second-order tensor  $\mathbf{B} = (b_{ij})$  whose elements are defined as  $b_{ij} = \sum_{k,l=1}^3 f_{ijkl} b_{kl}$ . Using this definition, one can show that

$$\mathbf{F} : (\mathbf{u}_1 \otimes \mathbf{u}_2) = (\mathbf{F}\mathbf{u}_2)\mathbf{u}_1 \quad (1.68)$$

which results in a second-order tensor. The double product of fourth- and second-order tensors is important because it will be used to define the product that appears in the constitutive equations of the materials.

Alternatively, a fourth-order tensor  $\mathbf{F}$  can be defined as the outer product of two second-order tensors  $\mathbf{A}$  and  $\mathbf{B}$  as  $\mathbf{F} = \mathbf{A} \otimes \mathbf{B}$ . In this case, the elements of the tensor  $\mathbf{F}$  can be defined in terms of the elements of the tensors  $\mathbf{A}$  and  $\mathbf{B}$  as  $f_{ijkl} = A_{ij}B_{kl}$ . Furthermore,  $\mathbf{F}^T = (\mathbf{A} \otimes \mathbf{B})^T = (\mathbf{B} \otimes \mathbf{A})$ , and for arbitrary second-order tensors  $\mathbf{S}_1$  and  $\mathbf{S}_2$ , one has the following identity:  $\mathbf{S}_1 : \mathbf{F}^T : \mathbf{S}_2 = \mathbf{S}_2 : \mathbf{F} : \mathbf{S}_1 = (\mathbf{F} : \mathbf{S}_1) : \mathbf{S}_2$ .

## 1.5 POLAR DECOMPOSITION THEOREM

The *polar decomposition* theorem states that any square nonsingular matrix can be decomposed as the product of an orthogonal matrix and a symmetric matrix. According to this theorem, the square matrix  $\mathbf{J}$  can have one of the following two decompositions:

$$\mathbf{J} = \mathbf{R}\mathbf{U}, \quad \mathbf{J} = \mathbf{V}\mathbf{R} \quad (1.69)$$

where  $\mathbf{R}$  is an orthogonal matrix and  $\mathbf{U}$  and  $\mathbf{V}$  are nonsingular symmetric matrices. Note that if the decomposition in the first equation is proved, the proof of the decomposition of the second equation follows because  $\mathbf{V} = \mathbf{J}\mathbf{R}^T = \mathbf{R}\mathbf{U}\mathbf{R}^T$ . Therefore, it is sufficient to prove the first decomposition.

Although the proof of the polar decomposition theorem is outlined in this section for  $3 \times 3$  matrices, the generalization to square matrices with higher dimensions is straightforward. In order to prove the polar decomposition theorem, we define the following symmetric matrix:

$$\mathbf{C} = \mathbf{J}^T \mathbf{J} \quad (1.70)$$

Because  $\mathbf{C}$  is symmetric, its eigenvalues are real and its eigenvectors are orthogonal. Furthermore, in addition to the symmetry property, the property of *positive definiteness* of  $\mathbf{C}$  is required. The matrix  $\mathbf{C}$  is said to be positive definite if for all nonzero vectors  $\mathbf{a}$ ,  $\mathbf{a}^T \mathbf{C} \mathbf{a}$  is positive. It can be shown that the eigenvalues of a positive definite matrix are positive. Let  $\lambda_1$ ,  $\lambda_2$ , and  $\lambda_3$  be the eigenvalues of the symmetric positive definite matrix  $\mathbf{C}$  and let  $\Phi$  be the matrix whose columns are the eigenvectors of  $\mathbf{C}$  associated with the eigenvalues  $\lambda_1$ ,  $\lambda_2$ , and  $\lambda_3$ . Using the orthogonality property of the eigenvectors, one has

$$\Phi^T \mathbf{C} \Phi = \begin{bmatrix} \lambda_1 & 0 & 0 \\ 0 & \lambda_2 & 0 \\ 0 & 0 & \lambda_3 \end{bmatrix} \quad (1.71)$$

One can define the following matrix:

$$\mathbf{U} = \Phi \begin{bmatrix} \sqrt{\lambda_1} & 0 & 0 \\ 0 & \sqrt{\lambda_2} & 0 \\ 0 & 0 & \sqrt{\lambda_3} \end{bmatrix} \Phi^T \quad (1.72)$$

Again using the orthogonality of the eigenvectors, one can show that

$$\mathbf{U}^2 = \Phi \begin{bmatrix} \lambda_1 & 0 & 0 \\ 0 & \lambda_2 & 0 \\ 0 & 0 & \lambda_3 \end{bmatrix} \Phi^T = \mathbf{C}, \quad \mathbf{U}^{-1} = \Phi \begin{bmatrix} \frac{1}{\sqrt{\lambda_1}} & 0 & 0 \\ 0 & \frac{1}{\sqrt{\lambda_2}} & 0 \\ 0 & 0 & \frac{1}{\sqrt{\lambda_3}} \end{bmatrix} \Phi^T \quad (1.73)$$

The matrix  $\mathbf{R}$  that appears in the polar decomposition theorem can now be defined as

$$\mathbf{R} = \mathbf{J} \mathbf{U}^{-1} \quad (1.74)$$

One can show that this matrix is an orthogonal matrix. To this end, we write

$$\mathbf{R}^T \mathbf{R} = \mathbf{U}^{-1} \mathbf{J}^T \mathbf{J} \mathbf{U}^{-1} = \mathbf{U}^{-1} \mathbf{C} \mathbf{U}^{-1} = \mathbf{U}^{-1} \mathbf{U}^2 \mathbf{U}^{-1} = \mathbf{I} \quad (1.75)$$

which shows that  $\mathbf{R}$  is indeed an orthogonal matrix. Using the positive definiteness property, one can show that the matrices  $\mathbf{R}$ ,  $\mathbf{U}$ , and  $\mathbf{V}$  that appear in the polar decomposition theorem are unique.

The result of the polar decomposition theorem, which states that a matrix can be written as the product of an orthogonal matrix and a symmetric matrix, can be used to explain some of the fundamental problems associated with some finite element formulations. In continuum mechanics, as will be discussed, the position field can be used to define the matrix of *position vector gradients*. This matrix can be written as the product of an orthogonal matrix and a symmetric matrix. The orthogonal matrix defines the rotation of the material elements. That is, the

*rotation field* can be defined using the matrix of position vector gradients, which is determined from the displacement or position field. In some finite element formulations, the displacement and rotation fields are interpolated independently, and as a consequence, the geometry is not uniquely defined (Ding et al., 2014). The result of the polar decomposition theorem shows that the use of such independent interpolations for the displacements and rotations can lead to a redundancy problem. In computational mechanics, such a redundancy can lead to serious fundamental and numerical problems. In Chapters 5 and 6, two nonlinear finite element formulations are introduced. The two formulations define unique displacement and rotation fields, and therefore, the problem of coordinate redundancy is not an issue when these two nonlinear formulations are used.

### Other Decompositions

There are several other techniques that can be used in the decomposition of matrices. One of these techniques is the **QR** decomposition, which is based on the *Householder transformation*. Using this technique, a square matrix  $\mathbf{A}$  can be written as  $\mathbf{A} = \mathbf{QR}$ , where  $\mathbf{Q}$  is an orthogonal matrix and  $\mathbf{R}$  is an upper triangular matrix. The Householder transformation operates on the columns of the matrix  $\mathbf{A}$  to produce a set of orthonormal vectors. For example, if  $\mathbf{A}$  is a  $3 \times 3$  matrix, one can make the first column a unit vector and use this unit vector with the other two columns to produce an orthogonal triad that consists of three orthonormal vectors. This triad defines a coordinate system and the orthogonal matrix  $\mathbf{Q}$ . One can show that the use of this procedure leads to the upper triangular matrix  $\mathbf{R}$  defined as  $\mathbf{R} = \mathbf{Q}^T \mathbf{A}$ . The way the orthogonal matrix  $\mathbf{Q}$  is defined here gives a physical interpretation for the **QR** decomposition of  $3 \times 3$  matrices. In the next chapter, it will be shown that the matrix of *position vector gradients* plays an important role in the formulation of the kinematic and strain equations. One can show that the matrix  $\mathbf{Q}$ , which results from the **QR** decomposition of the matrix of position vector gradients, is associated with a coordinate system, called the *tangent frame*, frequently used in computational mechanics (Sugiyama et al., 2006). Furthermore, the triangular matrix  $\mathbf{R}$ , whose diagonal elements define the principal values, provides an alternate upper triangular form instead of the symmetric matrix  $\mathbf{U}$  that results from the polar decomposition theorem. The matrix  $\mathbf{U}$  in continuum mechanics, when obtained from the decomposition of the matrix of position vector gradients, describes the deformations of the continuum and can be used to determine the strain components because such strain components are not affected by the orthogonal matrix that results from the polar decomposition or the **QR** decomposition. The **QR** decomposition and the Householder transformation have been used in other areas of computational mechanics as reported in the literature (Kim and Vanderploeg, 1986; Shabana, 2001).

## 1.6 D'ALEMBERT'S PRINCIPLE

The virtual work method represents a powerful technique that can be used to formulate the equations of motion of the continuum. This method is based on *D'Alembert's principle*, which is the foundation for the skillful approaches developed by Lagrange. In this section, we review the particle and rigid-body mechanics to demonstrate the use of D'Alembert's principle in formulating the dynamic equations of motion.

## Particle Mechanics

A continuum consists of an infinite number of particles or material points that can move relative to each other if the rigid-body assumptions cannot be applied. The dynamic equations of particles can be obtained using *Newton's second law of motion*, which states that the force acting on a particle is equal to the rate of change of momentum. Newton's second law can be written in vector form as  $\mathbf{F} = \dot{\mathbf{p}}$ . In this equation,  $\mathbf{F}$  is the resultant of the forces acting on the particle and  $\mathbf{p}$  is the particle momentum defined as  $\mathbf{p} = m\mathbf{v}$ , where  $m$  and  $\mathbf{v}$  are, respectively, the mass and the absolute velocity vector of the particle. If the mass  $m$  is assumed to be constant, the preceding two equations lead to

$$\mathbf{F} = \dot{\mathbf{p}} = m \frac{d\mathbf{v}}{dt} = m\mathbf{a} \quad (1.76)$$

In this equation,  $\mathbf{a}$  is the absolute acceleration vector of the particle. In general, three scalar equations are required to describe the particle dynamics. This is mainly due to the fact that, in the case of unconstrained motion, the particle has three degrees of freedom in the spatial analysis because it is represented by a point that has no dimensions. In the case of planar motion, only two equations are required because, in this case, the particle has only two degrees of freedom.

## Rigid-Body Kinematics

Rigid bodies are assumed to have dimensions, and therefore, they differ from particles. Nonetheless, a rigid body can be assumed to consist of an infinite number of particles. In this special case of continuum, the distances between the particles of the rigid body remain constant. As a consequence, the displacements of the points on the rigid body are constrained such that there is no relative motion between two points along the line joining them. Using this condition of rigidity, the number of degrees of freedom of a continuum can be significantly reduced. In the case of spatial analysis, a rigid body has six degrees of freedom that describe three independent translations and three independent rotations. In the case of planar motion, the rigid body has only three degrees of freedom: two describe the body translation and one describes the rotation of the body. For instance, as shown in Figure 1, the configuration of the rigid body in planar motion can be described using the vector  $\mathbf{r}_O$  and the angle  $\theta$ . The vector  $\mathbf{r}_O$  defines the location of the reference point that represents the origin of a selected body coordinate system, whereas the angle  $\theta$  defines the body rotation. Using these three coordinates, one can show that the global position vector of an arbitrary point on the body can be written as

$$\mathbf{r} = \mathbf{r}_O + \mathbf{u} \quad (1.77)$$

In this equation,  $\mathbf{u}$  is the vector that defines the position of the point with respect to the reference point  $\bar{O}$ . Because the coordinates of the arbitrary point in the body coordinate system remain constant by virtue of the rigidity assumption, the vector  $\mathbf{u}$  can be expressed in terms of these constant coordinates as

$$\mathbf{u} = \begin{bmatrix} \bar{x}_1 \cos \theta - \bar{x}_2 \sin \theta \\ \bar{x}_1 \sin \theta + \bar{x}_2 \cos \theta \end{bmatrix} \quad (1.78)$$

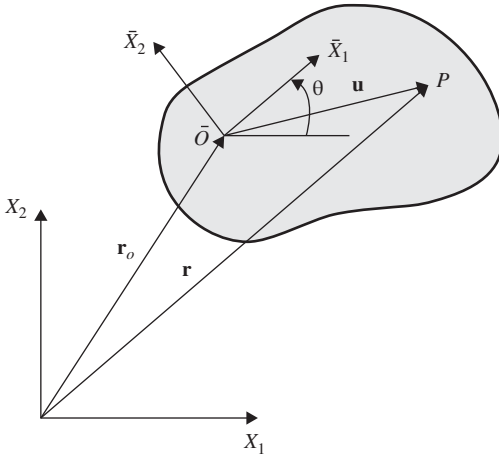


**Figure 1.1** Rigid-body coordinates

where  $\bar{x}_1$  and  $\bar{x}_2$  are the constant coordinates of the arbitrary point defined in the body coordinate system. The preceding equation can be written in matrix form as

$$\mathbf{u} = \mathbf{A}\bar{\mathbf{u}} \quad (1.79)$$

where

$$\mathbf{A} = \begin{bmatrix} \cos \theta & -\sin \theta \\ \sin \theta & \cos \theta \end{bmatrix}, \quad \bar{\mathbf{u}} = \begin{bmatrix} \bar{x}_1 \\ \bar{x}_2 \end{bmatrix} \quad (1.80)$$

Substituting Equation 79 into Equation 77 one obtains

$$\mathbf{r} = \mathbf{r}_O + \mathbf{A}\bar{\mathbf{u}} \quad (1.81)$$

In this equation,  $\mathbf{A}$  represents the transformation matrix that defines the orientation of the selected body coordinate system. This transformation matrix is orthogonal, that is,  $\mathbf{A}\mathbf{A}^T = \mathbf{A}^T\mathbf{A} = \mathbf{I}$ . Equation 81 shows that the position vector of an arbitrary point on the body is a function of the three coordinates  $\mathbf{r}_O$  and  $\theta$  that can change throughout the body motion. Therefore, these coordinates depend on time. If these coordinates are determined, the global position of any point on the body, or equivalently the body configuration, can be determined using the preceding equation. An equation in the same form as Equation 81 can be obtained in the case of spatial motion of rigid bodies, as will be demonstrated in Chapter 6. In the case of spatial motion, three-dimensional vectors instead of two-dimensional vectors are used, and the transformation matrix  $\mathbf{A}$  is expressed in terms of three independent rotation parameters instead of one parameter.

The absolute velocity of an arbitrary point on the rigid body can be obtained by differentiating Equation 81 with respect to time. This leads to

$$\dot{\mathbf{r}} = \dot{\mathbf{r}}_O + \dot{\theta}\mathbf{A}_\theta\bar{\mathbf{u}} \quad (1.82)$$

where  $\mathbf{A}_\theta = \partial \mathbf{A} / \partial \theta$  is the partial derivative of the transformation matrix  $\mathbf{A}$  with respect to the angle  $\theta$ . In deriving Equation 82,  $\dot{\mathbf{u}}$  is assumed to be zero because the case of a rigid body is considered. One can define the following *angular velocity vector*:

$$\bar{\boldsymbol{\omega}} = [0 \quad 0 \quad \dot{\theta}]^T \quad (1.83)$$

Using this definition, the absolute velocity vector of Equation 82 can be written, after extending the vectors to three-dimensional form by adding zeros, as

$$\dot{\mathbf{r}} = \dot{\mathbf{r}}_O + \mathbf{A}(\bar{\boldsymbol{\omega}} \times \bar{\mathbf{u}}) \quad (1.84)$$

The planar transformation matrix is defined when the preceding equation is used as

$$\mathbf{A} = \begin{bmatrix} \cos \theta & -\sin \theta & 0 \\ \sin \theta & \cos \theta & 0 \\ 0 & 0 & 1 \end{bmatrix} \quad (1.85)$$

Equation 84 can also be rewritten using vectors defined in the global coordinate system as

$$\dot{\mathbf{r}} = \dot{\mathbf{r}}_O + \boldsymbol{\omega} \times \mathbf{u} \quad (1.86)$$

In this equation,  $\boldsymbol{\omega} = \mathbf{A}\bar{\boldsymbol{\omega}}$ , and  $\mathbf{u} = \mathbf{A}\bar{\mathbf{u}}$ . In the case of the simple planar motion,  $\boldsymbol{\omega} = \bar{\boldsymbol{\omega}}$ . In the more general case of spatial rigid-body motion, the absolute velocity vector takes the same form as Equations 84 and 86 except for the definition of the transformation matrix  $\mathbf{A}$  and the angular velocity vectors  $\boldsymbol{\omega}$  and  $\bar{\boldsymbol{\omega}}$ , which must be formulated using three rotation parameters instead of one, as described in Chapter 6.

The absolute acceleration of an arbitrary point on a rigid body in a planar motion can be obtained by differentiating Equation 82 with respect to time. This leads to

$$\ddot{\mathbf{r}} = \ddot{\mathbf{r}}_O + \ddot{\theta} \mathbf{A}_\theta \bar{\mathbf{u}} - \dot{\theta}^2 \mathbf{A} \bar{\mathbf{u}} \quad (1.87)$$

In deriving this equation, the fact that  $\mathbf{A}_{\theta\theta} = \partial^2 \mathbf{A} / \partial \theta^2 = -\mathbf{A}$  is utilized. This identity applies only to planar transformation; it is a special case of a more general identity that applies to spatial transformation matrices (Roberson and Schwertassek, 1988; Shabana, 2013). Using three-dimensional vectors to represent this planar motion and introducing the following definition for the *angular acceleration*:

$$\bar{\boldsymbol{\alpha}} = [0 \quad 0 \quad \ddot{\theta}]^T, \quad (1.88)$$

one can show that the absolute acceleration vector of Equation 87 can be written as

$$\ddot{\mathbf{r}} = \ddot{\mathbf{r}}_O + \mathbf{A}(\bar{\boldsymbol{\alpha}} \times \bar{\mathbf{u}}) + \mathbf{A}\{\bar{\boldsymbol{\omega}} \times (\bar{\boldsymbol{\omega}} \times \bar{\mathbf{u}})\} \quad (1.89)$$

Alternatively, this equation can be written using vectors defined in the global coordinate system as

$$\ddot{\mathbf{r}} = \ddot{\mathbf{r}}_O + \boldsymbol{\alpha} \times \mathbf{u} + \boldsymbol{\omega} \times (\boldsymbol{\omega} \times \mathbf{u}) \quad (1.90)$$

In this equation,  $\boldsymbol{\alpha} = \mathbf{A}\ddot{\boldsymbol{\alpha}}$ , and other vectors are as defined previously in this section. Again, Equations 89 and 90 are also applicable to the spatial rigid-body motion. The only difference is in the definition of the transformation matrix and the angular velocity and angular acceleration vectors, which depend on three rotation parameters instead of one as will be discussed in Chapter 6.

### Application of D'Alembert's Principle

D'Alembert's principle is the foundation for the skillful development of the principle of virtual work made by Lagrange. D'Alembert's principle states that the inertia forces can be treated as the applied external forces. This principle can be used to conveniently derive the equations of motion of rigid bodies by invoking Newton's second law and assuming that the rigid body consists of a large number of particles. To demonstrate the use of this principle, we consider the planar motion of a rigid body. Assuming that the body consists of a large number of particles, the equations of motion of an infinitesimal material volume on the rigid body can be written as

$$(\rho dV)\ddot{\mathbf{r}} = d\mathbf{F} \quad (1.91)$$

In this equation,  $dm = \rho dV$  is the mass of the infinitesimal volume  $dV$ ,  $\rho$  is the mass density of the body,  $\ddot{\mathbf{r}}$  is the absolute acceleration vector defined by Equation 87, and  $d\mathbf{F}$  is the body force per unit volume. In the *Newton–Euler formulation* of the equations of motion, the origin of the body coordinate system (reference point) is assumed to be attached to the body center of mass. In this case, the vector  $\mathbf{u}$  defines the position of the arbitrary point with respect to the body center of mass. It follows that

$$\int_V \rho \mathbf{u} dV = \mathbf{0} \quad (1.92)$$

Using this identity and the fact that the angular velocity and angular acceleration do not depend on the spatial coordinates, substitution of Equation 87 into Equation 91, and integration leads to

$$m\ddot{\mathbf{r}}_O = \mathbf{F} \quad (1.93)$$

where  $m$  is the total mass of the body, and  $\mathbf{F}$  is the vector of resultant forces acting on the body. Both are defined as

$$m = \int_V \rho dV, \quad \mathbf{F} = \int_V d\mathbf{F} \quad (1.94)$$

Equation 93 is the *Newton equation* for the rigid body. The vector of resultant forces  $\mathbf{F}$  also includes the effect of other concentrated forces. Equation 93 for the planar motion includes two scalar equations. Because the unconstrained body in planar motion has three degrees of freedom, an additional moment equation is needed. Because D'Alembert's principle states that the inertia forces can be treated as the external forces, one can equate the moment of the inertia force  $\rho dV\ddot{\mathbf{r}}$  with the moment of the applied forces  $d\mathbf{F}$  about any point, we select to be the center of mass. Following this procedure and integrating, one obtains

$$\int_V \mathbf{u} \times (\rho dV\ddot{\mathbf{r}}) = \int_V \mathbf{u} \times d\mathbf{F} + \mathbf{M} \quad (1.95)$$



In this equation,  $\mathbf{M}$  is the external moment applied to the body. Using Equations 87 and 92, one can show that the preceding equation reduces to one nontrivial equation associated with the rotation about the  $X_3$ -axis and is given by

$$I_O \ddot{\theta} = M_O \quad (1.96)$$

In this equation,  $I_O = \int_V \rho(\bar{x}_1^2 + \bar{x}_2^2) dV$  defines the *mass moment of inertia* of the body about its center of mass, and  $M_O$  is the third component of the vector  $\int_V \mathbf{u} \times d\mathbf{F} + \mathbf{M}$ . Equation 96 is called *Euler equation*. Equations 93 and 96 are the two equations that govern the planar motion of the rigid body.

A similar procedure based on D'Alembert's principle can be used to obtain the equations that govern the spatial motion of rigid bodies. These equations are called the *Newton–Euler equations* and are given by

$$\begin{bmatrix} m\mathbf{I} & \mathbf{0} \\ \mathbf{0} & \bar{\mathbf{I}}_{\theta\theta} \end{bmatrix} \begin{bmatrix} \ddot{\mathbf{r}}_O \\ \ddot{\boldsymbol{\alpha}} \end{bmatrix} = \begin{bmatrix} \mathbf{F} \\ \bar{\mathbf{M}}_O - \bar{\boldsymbol{\omega}} \times (\bar{\mathbf{I}}_{\theta\theta} \bar{\boldsymbol{\omega}}) \end{bmatrix} \quad (1.97)$$

In this equation,  $m$  is the total mass of the body,  $\mathbf{I}$  is the identity matrix,  $\mathbf{F}$  is the vector of the resultant forces defined in the global coordinate system,  $\bar{\mathbf{M}}_O$  is the vector of the resultant moments defined in the body coordinate system, and  $\bar{\mathbf{I}}_{\theta\theta}$  is the constant symmetric inertia tensor defined in the body coordinate system. The inertia tensor  $\bar{\mathbf{I}}_{\theta\theta}$  is defined as

$$\bar{\mathbf{I}}_{\theta\theta} = \begin{bmatrix} \int_V \rho(\bar{x}_2^2 + \bar{x}_3^2) dV & \text{Symmetric} \\ -\int_V \rho \bar{x}_1 \bar{x}_2 dV & \int_V \rho(\bar{x}_1^2 + \bar{x}_3^2) dV \\ -\int_V \rho \bar{x}_1 \bar{x}_3 dV & -\int_V \rho \bar{x}_2 \bar{x}_3 dV & \int_V \rho(\bar{x}_1^2 + \bar{x}_2^2) dV \end{bmatrix} \quad (1.98)$$

where  $\bar{x}_1$ ,  $\bar{x}_2$ , and  $\bar{x}_3$  are the components of the vector  $\bar{\mathbf{u}}$  that defines the position of the arbitrary point with respect to the origin of the body coordinate system. Equation 97 shows that Newton–Euler equations do not include inertia coupling between the body translation and rotation. This is mainly due to the use of the body center of mass as the reference point.

The analysis presented in this section shows that starting with Newton's second law, D'Alembert's principle can be used to obtain Euler equations of motion of the rigid body by equating the moments of the inertia forces to the moments of the applied forces. The application of D'Alembert's principle also allows for systematically eliminating the constraint forces, thereby obtaining a minimum number of motion equations equal to the number of degrees of freedom of the system. This subject is covered in more detail in books on computational and analytical dynamics.

The analysis presented in this section also shows that in the special case of rigid-body motion, precise description of the finite rotation of the body is important in the formulation of the dynamic equations. This description of the finite rotation becomes even more important when the body undergoes deformation coupled with a rigid-body motion. Therefore, in the case of deformable bodies, it is important to select a set of coordinates that correctly describe the rigid-body motion when computational methods are used to develop finite dimensional

models. The coordinates selected must define a unique displacement and rotation field and must lead to zero strain under an arbitrary rigid-body displacement. This subject will be discussed in more detail when large displacement finite element formulations are introduced in later chapters.

## Continuum Forces

In the case of rigid bodies, the mass density and volume remain constant. However, in the case of a continuum subjected to arbitrary displacements, the mass density and volume change. For this reason, in continuum mechanics, it is important to distinguish between the mass density  $\rho_o$  and the volume  $V$  in the reference undeformed configuration and the mass density  $\rho$  and the volume  $v$  in the current deformed configuration. Nevertheless, the definitions and basic principles used in rigid-body dynamics can be generalized to the case of a general continuum by considering the continuum to consist of an infinite number of points that can move relative to each other. For example, the inertia force of a material point of an infinitesimal mass  $\rho dv$  on the continuum in the current configuration can be written as  $(\rho dv)\ddot{\mathbf{r}}$ , where  $\ddot{\mathbf{r}}$  is the absolute acceleration vector of the material point. Using this expression for the inertia force of the material point, the inertia force for the continuum can be defined as  $\int_v \rho \ddot{\mathbf{r}} dv$ . Using a similar procedure, the kinetic energy of the continuum can be written as  $(1/2) \int_v \rho \dot{\mathbf{r}}^T \dot{\mathbf{r}} dv$ . In the next chapter, the relationship between the mass density and volume in the reference configuration and in the current configuration will be defined. This relationship will allow us to carry out the integration using the known properties and dimensions in the undeformed reference configuration. For instance, the use of the *principle of conservation of mass* obtained in the next chapter allows one to write the inertia force as  $\int_V \rho_o \ddot{\mathbf{r}} dV$ , where  $\rho_o$  and  $V$  are, respectively, the mass density and volume in the undeformed reference configuration.

In a similar manner, one can define the body forces acting on the continuum. Let  $\mathbf{f}_b$  be the distributed body force per unit volume acting on the continuum at the material points. Examples of these forces are gravity and magnetic forces. The sum of the body forces acting on the continuum can be defined as  $\int_v \mathbf{f}_b dv$ . The effect of the traction forces that include tangential friction forces and normal reaction and pressure can be obtained by integration over the area. If  $\mathbf{f}_s$  is the vector of distributed surface forces that act on a surface area  $s$ , the surface forces acting on the continuum can be defined using the integral  $\int_s \mathbf{f}_s ds$ .

Expressions for the internal elastic forces due to the continuum deformations will be developed in this book. These expressions will be written in terms of the strain and stress components, which are introduced in Chapters 2 and 3, respectively. As will be shown, D'Alembert's principle and Lagrange's techniques can still be used to obtain the equations of motion of the continuum. Nonetheless, the internal elastic forces can be expressed using different deformation and stress measures. It is important, however, that the resulting work of the elastic forces and the strain energy remain constant under an arbitrary rigid-body transformation. For this reason, the important concept of the *objectivity* will be a subject of discussion in this book.

## 1.7 VIRTUAL WORK PRINCIPLE

As previously mentioned, D'Alembert's principle represents the foundation for the skillful virtual work method developed by Lagrange. The virtual work principle can be used to

systematically derive the equations of motion of complex systems. In this principle, the concept of the virtual displacement, which represents an infinitesimal change in coordinates that is consistent with the constraints imposed on the motion of the system, is important. During this virtual change, time is assumed to be frozen. For a vector  $\mathbf{r}$ , the virtual change is denoted as  $\delta\mathbf{r}$ . Given a system that consists of  $n_p$  particles, the equations of motion of a particle  $i$  in the system can be written using Newton's second law as

$$m^i \ddot{\mathbf{r}}^i = \mathbf{F}_e^i + \mathbf{F}_c^i, \quad i = 1, 2, \dots, n_p \quad (1.99)$$

In this equation,  $m^i$  is the mass of the particle,  $\mathbf{r}^i$  is the global position vector,  $\mathbf{F}_e^i$  is the vector of applied forces acting on the particle, and  $\mathbf{F}_c^i$  is the vector of constraint forces. Multiplying the preceding equation by the virtual change in the position vector of the particle, one obtains

$$m^i \ddot{\mathbf{r}}^i \cdot \delta\mathbf{r}^i = \mathbf{F}_e^i \cdot \delta\mathbf{r}^i + \mathbf{F}_c^i \cdot \delta\mathbf{r}^i, \quad i = 1, 2, \dots, n_p \quad (1.100)$$

This equation, which is called the *Lagrange–D'Alembert equation*, can be written as

$$\delta W_i^i = \delta W_e^i + \delta W_c^i \quad (1.101)$$

where  $\delta W_i^i$  is the virtual work of the inertia forces,  $\delta W_e^i$  is the virtual work of the applied forces, and  $\delta W_c^i$  is the virtual work of the constraint forces. These expressions for the virtual work are defined for particle  $i$  as

$$\delta W_i^i = m^i \ddot{\mathbf{r}}^i \cdot \delta\mathbf{r}^i, \quad \delta W_e^i = \mathbf{F}_e^i \cdot \delta\mathbf{r}^i, \quad \delta W_c^i = \mathbf{F}_c^i \cdot \delta\mathbf{r}^i \quad (1.102)$$

Using Equation 101, one can write

$$\sum_{i=1}^{n_p} \delta W_i^i = \sum_{i=1}^{n_p} \delta W_e^i + \sum_{i=1}^{n_p} \delta W_c^i \quad (1.103)$$

which can be written as

$$\delta W_i = \delta W_e + \delta W_c \quad (1.104)$$

where

$$\delta W_i = \sum_{i=1}^{n_p} \delta W_i^i, \quad \delta W_e = \sum_{i=1}^{n_p} \delta W_e^i, \quad \delta W_c = \sum_{i=1}^{n_p} \delta W_c^i \quad (1.105)$$

represent, respectively, the virtual work of the system inertia forces, the virtual work of the system applied forces, and the virtual work of the system constraint forces. Because the constraint forces acting on two particles are equal in magnitude and opposite in direction and because the virtual change in a specified (prescribed) coordinate is equal to zero, one must have  $\delta W_c = 0$ . This equation and Equation 104 lead to the principle of virtual work, which can be stated mathematically as

$$\delta W_i = \delta W_e \quad (1.106)$$

This principle states that the virtual work of the system inertia forces must be equal to the virtual work of the system applied forces. Note that in Equation 106, the constraint forces are systematically eliminated. Note also that although  $\delta W_c = 0$ ,  $\delta W_c^i \neq 0$  if the particle  $i$  is subjected to constraints.

### Relationship with D'Alembert's Principle

A simple example can be used to demonstrate the relationship between the principle of virtual work and D'Alembert's principle. To this end, we consider the derivation of the equations of motion of a planar rigid body. The virtual work of the inertia forces of the rigid body can be written as

$$\delta W_i = \int_V \rho \ddot{\mathbf{r}} \cdot \delta \mathbf{r} dV \quad (1.107)$$

where  $\mathbf{r}$  and  $\ddot{\mathbf{r}}$  are given, respectively, by Equations 81 and 87. The virtual change  $\delta \mathbf{r}$  can be written as

$$\delta \mathbf{r} = \delta \mathbf{r}_O + \mathbf{A}_\theta \bar{\mathbf{u}} \delta \theta \quad (1.108)$$

This equation can be written using matrix notation as

$$\delta \mathbf{r} = \begin{bmatrix} \mathbf{I} & \mathbf{A}_\theta \bar{\mathbf{u}} \end{bmatrix} \begin{bmatrix} \delta \mathbf{r}_O \\ \delta \theta \end{bmatrix} \quad (1.109)$$

where  $\mathbf{I}$  is the  $2 \times 2$  identity matrix. The acceleration vector of Equation 87 can also be written as

$$\ddot{\mathbf{r}} = \begin{bmatrix} \mathbf{I} & \mathbf{A}_\theta \bar{\mathbf{u}} \end{bmatrix} \begin{bmatrix} \ddot{\mathbf{r}}_O \\ \ddot{\theta} \end{bmatrix} - \dot{\theta}^2 \mathbf{A} \bar{\mathbf{u}} \quad (1.110)$$

Substituting Equations 109 and 110 into Equation 107 and using Equation 92, which is the result of using the center of mass as the reference point, one obtains

$$\delta W_i = \begin{bmatrix} \delta \mathbf{r}_O^T & \delta \theta \end{bmatrix} \begin{bmatrix} m\mathbf{I} & \mathbf{0} \\ \mathbf{0} & I_O \end{bmatrix} \begin{bmatrix} \ddot{\mathbf{r}}_O \\ \ddot{\theta} \end{bmatrix} \quad (1.111)$$

where  $m$  is the mass of the rigid body and  $I_O$  is the mass moment of inertia about the center of mass that was used in Equation 96.

The virtual work of all the applied forces and moments acting on the body can be written as

$$\delta W_e = \mathbf{F}^T \delta \mathbf{r}_O + M_O \delta \theta = \begin{bmatrix} \delta \mathbf{r}_O^T & \delta \theta \end{bmatrix} \begin{bmatrix} \mathbf{F} \\ M_O \end{bmatrix} \quad (1.112)$$

Substituting Equations 111 and 112 into the principle of virtual work of Equation 106, one obtains

$$\begin{bmatrix} \delta \mathbf{r}_O^T & \delta \theta \end{bmatrix} \left\{ \begin{bmatrix} m\mathbf{I} & \mathbf{0} \\ \mathbf{0} & I_O \end{bmatrix} \begin{bmatrix} \ddot{\mathbf{r}}_O \\ \ddot{\theta} \end{bmatrix} - \begin{bmatrix} \mathbf{F} \\ M_O \end{bmatrix} \right\} = 0 \quad (1.113)$$

In the case of unconstrained motion of the planar rigid body,  $\mathbf{r}_O$  and  $\theta$  represent three independent coordinates, and therefore, the coefficients of their virtual change in the preceding

equation must be identically equal to zero. This leads to the following system of equations of motion:

$$\begin{bmatrix} m\mathbf{I} & \mathbf{0} \\ \mathbf{0} & I_O \end{bmatrix} \begin{bmatrix} \ddot{\mathbf{r}}_O \\ \ddot{\theta} \end{bmatrix} - \begin{bmatrix} \mathbf{F} \\ M_O \end{bmatrix} = \begin{bmatrix} \mathbf{0} \\ 0 \end{bmatrix} \quad (1.114)$$

This matrix equation has three scalar equations, which are the planar Newton–Euler equations previously obtained in this chapter (see Equations 93 and 96) using D’Alembert’s principle.

Although D’Alembert’s principle and the virtual work principle lead to the same equations, it is important to note that in the virtual work principle, scalar quantities are used and there is no need to use cross products to define moments. The forces and moments are defined using the scalar virtual work expressions. In the case of constrained motion, D’Alembert’s principle and the virtual work principle also lead to the same results. Both principles can be used to systematically eliminate the constraint forces and obtain a number of equations equal to the number of degrees of freedom of the system. Nonetheless, the principle of virtual work is much easier to use, particularly when complex systems are considered.

## 1.8 APPROXIMATION METHODS

Solids and fluids have an infinite number of degrees of freedom because their particles can have arbitrary displacements with respect to each other. The dynamics of such systems is described using partial differential equations that depend on time and the spatial coordinates. These general partial differential equations, which are applicable to any solid or fluid material, are derived in Chapter 3. Only for very simple problems, one can find a closed-form solution for these partial differential equations. For most problems, however, one resorts to numerical methods to obtain the solution of the partial differential equations. Approximation methods such as the *finite difference* and *finite element methods* are often used to solve the partial differential equations by transforming these equations into a finite set of ordinary differential or algebraic equations that can be solved using computer and numerical methods. In some of the numerical techniques based on the *Rayleigh–Ritz method*, physical variables such as position, displacement, velocity, and/or acceleration are approximated using interpolation functions that have finite order. The coefficients of the interpolating functions in the case of dynamics can be expressed in terms of coordinates that depend on time. In order to demonstrate the use of this procedure, the two-dimensional beam shown in Figure 2 is considered. It is assumed that the position of the material points on the beam can be described using the following polynomials:

$$\mathbf{r} = \begin{bmatrix} r_1 \\ r_2 \end{bmatrix} = \begin{bmatrix} a_0 + a_1x_1 + a_2x_2 + a_3x_1x_2 + a_4(x_1)^2 + a_5(x_1)^3 \\ b_0 + b_1x_1 + b_2x_2 + b_3x_1x_2 + b_4(x_1)^2 + b_5(x_1)^3 \end{bmatrix} \quad (1.115)$$

where  $x_1$  and  $x_2$  are the beam local coordinates defined in the beam coordinate system shown in Figure 2 and  $a_i$  and  $b_i$ ,  $i=0, 1, 2, \dots, 5$ , are the polynomial coefficients. The procedure used in computational methods such as the finite element method is to replace the polynomial coefficients with a set of coordinates that have physical meaning. This can be accomplished by developing a set of algebraic equations that relate the polynomial coefficients to the new set of coordinates. These algebraic equations can be solved to determine the polynomial coefficients in terms of the new coordinates. In the beam example considered in this section, there are

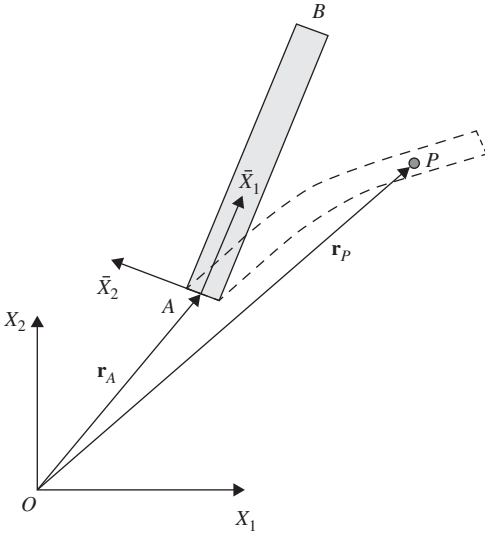


**Figure 1.2** Two-dimensional beam

12 polynomial coefficients, and therefore, 12 coordinates can be used to replace the coefficients  $a_i$  and  $b_i$  in Equation 1.15. To this end, the preceding equation can be written as

$$\mathbf{r} = \begin{bmatrix} r_1 \\ r_2 \end{bmatrix} = \begin{bmatrix} 1 & x_1 & x_2 & x_1 x_2 & (x_1)^2 & (x_1)^3 & 0 & 0 & 0 & 0 & 0 & 0 \\ 0 & 0 & 0 & 0 & 0 & 0 & 1 & x_1 & x_2 & x_1 x_2 & (x_1)^2 & (x_1)^3 \end{bmatrix} \begin{bmatrix} a_0 \\ a_1 \\ a_2 \\ a_3 \\ a_4 \\ a_5 \\ b_0 \\ b_1 \\ b_2 \\ b_3 \\ b_4 \\ b_5 \end{bmatrix} \quad (1.116)$$

The coefficients  $a_i$  and  $b_i$ ,  $i=0, 1, 2, \dots, 5$ , can be replaced by coefficients that represent position and gradient coordinates. To this end, we choose a set of coordinates associated with the position and gradient coordinates of the two endpoints of the beam. For the first endpoint at A, we use

$$\mathbf{r}^1 = \mathbf{r}(0, 0) = \begin{bmatrix} e_1 \\ e_2 \end{bmatrix}, \quad \mathbf{r}_{x_1}^1 = \mathbf{r}_{x_1}(0, 0) = \begin{bmatrix} e_3 \\ e_4 \end{bmatrix}, \quad \mathbf{r}_{x_2}^1 = \mathbf{r}_{x_2}(0, 0) = \begin{bmatrix} e_5 \\ e_6 \end{bmatrix} \quad (1.117)$$

and for the second endpoint at B, we use

$$\mathbf{r}^2 = \mathbf{r}(l, 0) = \begin{bmatrix} e_7 \\ e_8 \end{bmatrix}, \quad \mathbf{r}_{x_1}^2 = \mathbf{r}_{x_1}(l, 0) = \begin{bmatrix} e_9 \\ e_{10} \end{bmatrix}, \quad \mathbf{r}_{x_2}^2 = \mathbf{r}_{x_2}(l, 0) = \begin{bmatrix} e_{11} \\ e_{12} \end{bmatrix} \quad (1.118)$$

In this equation,  $l$  is the length of the beam and  $\mathbf{r}_{,x_k} = \partial \mathbf{r} / \partial x_k$ ,  $k = 1, 2$ . There are 12 coordinates in Equations 117 and 118, and therefore, these coordinates, which have physical meaning, can be used to replace the coefficients  $a_i$  and  $b_i$ ,  $i = 0, 1, 2, \dots, 5$ , in Equation 116. Using Equations 116–118, one can show that the position vector  $\mathbf{r}$  can be written in terms of the coordinates of Equations 117 and 118 as (Omar and Shabana, 2001):

$$\mathbf{r} = \mathbf{S}(\mathbf{x})\mathbf{e}(t) \quad (1.119)$$

where  $\mathbf{e} = \mathbf{e}(t) = [e_1 \ e_2 \ \dots \ e_{12}]^T$  is a vector of time-dependent coefficients or coordinates, which consist of position and gradient coordinates,  $t$  is time,  $\mathbf{x} = [x_1 \ x_2]^T$ , and  $\mathbf{S} = \mathbf{S}(\mathbf{x})$  is a matrix called the *shape function matrix* that depends on the local coordinates  $x_1$  and  $x_2$  and is given by

$$\mathbf{S} = \begin{bmatrix} s_1 & 0 & s_2 & 0 & s_3 & 0 & s_4 & 0 & s_5 & 0 & s_6 & 0 \\ 0 & s_1 & 0 & s_2 & 0 & s_3 & 0 & s_4 & 0 & s_5 & 0 & s_6 \end{bmatrix} \quad (1.120)$$

The elements  $s_i$ ,  $i = 1, 2, \dots, 6$ , which appear in this equation, are given by

$$\left. \begin{aligned} s_1 &= 1 - 3\xi^2 + 2\xi^3, & s_2 &= l(\xi - 2\xi^2 + \xi^3), & s_3 &= l\eta(1 - \xi) \\ s_4 &= 3\xi^2 - 2\xi^3, & s_5 &= l(-\xi^2 + \xi^3), & s_6 &= l\xi\eta \end{aligned} \right\} \quad (1.121)$$

where  $\xi = x_1/l$  and  $\eta = x_2/l$ .

The procedure described in this section to approximate a field using polynomials and replace the polynomial coefficients using coordinates that can have physical meaning is a fundamental step in the finite element formulation. The choice of the coordinates to consist of absolute position and gradient coordinates is the basis of a finite element formulation called the *absolute nodal coordinate formulation* (ANCF). This formulation, which is discussed in Chapter 5, can be used to correctly describe an arbitrary rigid-body displacement including arbitrary rotations. Using the absolute position and gradient coordinates, ANCF does not impose any restriction on the amount of rotation or deformation within the element, and therefore, it is suited for the large-deformation analysis. Efficient solution of small-deformation problems, on the other hand, requires the use of a more elaborate procedure in order to eliminate displacement modes, which have a negligible effect on the solution. In the literature, small-deformation problems are often solved using the *floating frame of reference* (FFR) formulation, which is discussed in Chapter 6. In the FFR formulation, which can be considered a generalization of the Newton–Euler equations used in rigid-body dynamics, a different set of coordinates is used to define a local linear deformation problem that allows reducing systematically the number of degrees of freedom.

## 1.9 DISCRETE EQUATIONS

The principle of virtual work and approximation techniques can be used to determine a set of discrete ordinary differential equations that govern the dynamics of the continuum. As will be shown in Chapter 3, the motion of the continuum is governed by partial differential equations that depend on the spatial coordinates  $\mathbf{x}$  and time  $t$ . The principle of virtual work

and the approximation techniques can be used to systematically convert the partial differential equations to a set of discrete ordinary differential equations. To demonstrate this standard procedure, consider a deformable body that may undergo arbitrary displacements. The global position vector of an arbitrary point on the body is defined by the vector  $\mathbf{r}$ . The mass of an infinitesimal volume  $dv$  of the body is  $\rho dv$ , where  $\rho$  is the mass density in the current configuration. It follows that the inertia force of this infinitesimal volume is  $(\rho dv)\ddot{\mathbf{r}}$ , where  $\ddot{\mathbf{r}}$  is the absolute acceleration vector. Therefore, the virtual work of the inertia forces of the body can be written as follows:

$$\delta W_i = \int_v \rho \ddot{\mathbf{r}}^T \delta \mathbf{r} dv \quad (1.122)$$

Using the approximation techniques, the virtual displacement  $\delta \mathbf{r}$  can be expressed in terms of the virtual changes of a finite set of coordinates  $\mathbf{q}$ , as previously demonstrated in the case of rigid bodies. That is,

$$\delta \mathbf{r} = \mathbf{S} \delta \mathbf{q} \quad (1.123)$$

In this equation,  $\mathbf{S}$  is an appropriate matrix that relates the virtual change of  $\mathbf{r}(\mathbf{x}, t)$  to the virtual change in the coordinates  $\mathbf{q}(t)$ . Note that, whereas  $\mathbf{r}(\mathbf{x}, t)$  depends on both coordinates  $\mathbf{x}$  and time  $t$ , the coordinates  $\mathbf{q}(t)$  depend only on time. As will be shown in this book, the matrix  $\mathbf{S}$  depends, in general, on both  $\mathbf{x}$  and  $\mathbf{q}$ , as in the case of the small-deformation FFR formulation discussed in Chapter 6. That is, one can write  $\mathbf{S} = \mathbf{S}(\mathbf{x}, \mathbf{q}(t))$ . However, in other formulations, such as ANCF discussed in Chapter 5, one can write  $\mathbf{S}$  as a function of  $\mathbf{x}$  only, as demonstrated in the preceding section. Therefore, in large displacement formulations, one can in general write the absolute velocity and acceleration vectors as

$$\dot{\mathbf{r}} = \mathbf{S}\dot{\mathbf{q}}, \quad \ddot{\mathbf{r}} = \mathbf{S}\ddot{\mathbf{q}} + \boldsymbol{\gamma} \quad (1.124)$$

In this equation,  $\boldsymbol{\gamma} = \dot{\mathbf{S}}\dot{\mathbf{q}}$  is a vector, which is quadratic in the first derivatives of the coordinates. If the matrix  $\mathbf{S}$  is only a function of  $\mathbf{x}$ , the vector  $\boldsymbol{\gamma}$  is identically zero. Substituting Equations 123 and 124 into Equation 122, one obtains

$$\delta W_i = \int_v \rho (\mathbf{S}\ddot{\mathbf{q}} + \boldsymbol{\gamma})^T (\mathbf{S}\delta \mathbf{q}) dv \quad (1.125)$$

The terms in this equation can be rearranged. This leads to

$$\delta W_i = \int_v \rho \{ \ddot{\mathbf{q}}^T (\mathbf{S}^T \mathbf{S}) + \boldsymbol{\gamma}^T \mathbf{S} \} dv \delta \mathbf{q} \quad (1.126)$$

This equation can be written as

$$\delta W_i = (\mathbf{M}\ddot{\mathbf{q}} - \mathbf{Q}_v)^T \delta \mathbf{q} \quad (1.127)$$

where

$$\mathbf{M} = \int_v \rho \mathbf{S}^T \mathbf{S} dv, \quad \mathbf{Q}_v = - \int_v \rho \mathbf{S}^T \boldsymbol{\gamma} dv \quad (1.128)$$



In this equation,  $\mathbf{M}$  is the symmetric mass matrix, and  $\mathbf{Q}_v$  is the vector of Coriolis and centrifugal forces. Depending on the set of coordinates selected, some nonlinear finite element formulations, as will be discussed in this book, lead to a constant mass matrix and zero centrifugal and Coriolis forces, while other formulations lead to a nonlinear mass matrix and nonzero centrifugal and Coriolis forces. The use of Equation 128 to evaluate the inertia forces leads to what is known in the literature as a *consistent mass formulation*. In some structural finite element formulations, *lumped mass techniques* are used to formulate the inertia forces by representing the inertia of the body using discrete bodies or masses instead of using the distributed inertia representation of Equation 128. In the finite element formulations discussed in this book, the mass matrix cannot, in general, be diagonal, even in the case in which lumped mass techniques are used. Furthermore, in the large-deformation finite element formulation presented in Chapter 5, one cannot use lumped masses, because the use of such a lumping scheme does not lead to correct modeling of the rigid-body dynamics.

Similarly, by using Equation 123, the virtual work of the applied forces can be written as

$$\delta W_e = \mathbf{Q}_e^T \delta \mathbf{q} \quad (1.129)$$

Using Equations 127 and 129 and the principle of virtual work, which states that  $\delta W_i = \delta W_e$ , one obtains the following equation:

$$(\mathbf{M}\ddot{\mathbf{q}} - \mathbf{Q}_e - \mathbf{Q}_v)^T \delta \mathbf{q} = 0 \quad (1.130)$$

If the elements of the vector  $\mathbf{q}$  are independent, the preceding equation leads to the discrete ordinary differential equations of the system given as

$$\mathbf{M}\ddot{\mathbf{q}} = \mathbf{Q}_e + \mathbf{Q}_v \quad (1.131)$$

However, if the elements of the vector  $\mathbf{q}$  are not totally independent because of kinematic relationships between the coordinates, one can always write the coordinates  $\mathbf{q}$  in terms of a reduced set of independent coordinates  $\mathbf{q}_i$ . In this case, one can write the following relationship between the virtual changes of the system coordinates and the virtual changes of the independent coordinates:

$$\delta \mathbf{q} = \mathbf{B} \delta \mathbf{q}_i \quad (1.132)$$

In this equation,  $\mathbf{B}$  is a velocity transformation matrix that can be defined using the kinematic relationship between the coordinates. Substituting the preceding equation into Equation 130 and using the argument that the elements of the vector  $\mathbf{q}_i$  are independent, one obtains the following reduced system of ordinary differential equations:

$$\mathbf{B}^T (\mathbf{M}\ddot{\mathbf{q}} - \mathbf{Q}_e - \mathbf{Q}_v) = \mathbf{0} \quad (1.133)$$

The vector of accelerations can also be expressed in terms of the independent accelerations, leading to a number of equations equal to the number of independent coordinates (degrees of freedom). To this end, one can use Equation 132 to write

$$\dot{\mathbf{q}} = \mathbf{B}\dot{\mathbf{q}}_i, \quad \ddot{\mathbf{q}} = \mathbf{B}\ddot{\mathbf{q}}_i + \dot{\mathbf{B}}\dot{\mathbf{q}}_i \quad (1.134)$$

Substituting these equations into Equation 133, one obtains a set of equations solely expressed in terms of the independent accelerations. These equations are given as

$$(\mathbf{B}^T \mathbf{M} \mathbf{B}) \ddot{\mathbf{q}}_i = \mathbf{B}^T (\mathbf{Q}_e + \mathbf{Q}_v - \mathbf{M} \dot{\mathbf{B}} \dot{\mathbf{q}}_i) \quad (1.135)$$

In this equation,  $(\mathbf{B}^T \mathbf{M} \mathbf{B})$  is the generalized inertia matrix associated with the independent coordinates and  $\mathbf{B}^T (\mathbf{Q}_e + \mathbf{Q}_v - \mathbf{M} \dot{\mathbf{B}} \dot{\mathbf{q}}_i)$  is the vector of generalized forces that include applied, centrifugal, and Coriolis forces.

The procedure described in this section for writing the dynamic equations in terms of the independent coordinates or the degrees of freedom is called the *embedding technique*. The dynamic equations can also be formulated in terms of *redundant coordinates* using the technique of *Lagrange multipliers*. The subject of constrained dynamics is discussed in more detail in the multibody system dynamics literature (Roberson and Schwertassek, 1988; Shabana, 2013).

## 1.10 MOMENTUM, WORK, AND ENERGY

The study of the computational finite element method requires a sound understanding of the basic analytical mechanics principles. If correctly derived, the equations of motion must satisfy these principles. Violations of these mechanics principles are a clear indication of inconsistencies in formulating the dynamic equations of motion. Among the principles of mechanics that will be discussed in this section are the principle of linear and angular momentum and the principle of work and energy. Correct and consistent formulations of the finite element equations of motion must automatically satisfy these principles. When these equations of motion are numerically solved, the violations in these principles must be within the range of the error tolerance of the numerical integration method used. Nonetheless, some finite element formulations lead to energy drift as a result of being inconsistent. For example, the use of a nonunique rotation field can lead to violations of the principle of work and energy as evident by many of the results presented in the finite element literature.

### Linear and Angular Momentum

The *linear momentum* of a body is defined as

$$\mathbf{M}_l = \int_v \rho \mathbf{r} dv \quad (1.136)$$

where  $\mathbf{M}_l$  is the vector of linear momentum,  $\rho$  and  $v$  are, respectively, the mass density and volume of the body in the current configuration, and  $\mathbf{r}$  is the position vector of an arbitrary point on the body. Newton's second law states that the rate of change of the linear momentum is equal to the resultant of the forces acting on the body, that is,

$$\dot{\mathbf{M}}_l = \frac{d}{dt} \left( \int_v \rho \mathbf{r} dv \right) = \mathbf{F} \quad (1.137)$$

where  $\mathbf{F}$  is the resultant of the forces acting on the body. In the case of rigid bodies, the volume is assumed to remain constant; as a result, the preceding equation, when a centroidal body coordinate system is used, defines the Newton equation,  $m\ddot{\mathbf{r}}_O = \mathbf{F}$ , where  $m$  is the total mass of the body and  $\ddot{\mathbf{r}}_O$  is the acceleration of the body center of mass. If the resultant of the forces acting on the body is equal to zero, one obtains the *principle of conservation of the linear momentum*, which is written as

$$\mathbf{M}_l = \mathbf{c}_l \quad (1.138)$$

In this equation,  $\mathbf{c}_l$  is a constant vector.

The vector of the *angular momentum* of the body is defined as

$$\mathbf{M}_a = \int_v \rho(\mathbf{r} \times \dot{\mathbf{r}}) dv \quad (1.139)$$

In the case of rigid bodies, the rate of change of the angular momentum is given by

$$\dot{\mathbf{M}}_a = \frac{d}{dt} \left( \int_v \rho(\mathbf{r} \times \dot{\mathbf{r}}) dv \right) = \int_v \rho(\mathbf{r} \times \ddot{\mathbf{r}}) dv \quad (1.140)$$

Using Newton's equation and D'Alembert's principle, one can show that, in the case of rigid bodies, the rate of change of angular momentum is equal to the resultant of the moment applied to the body. If the resultant of the moments is equal to zero, one obtains the *principle of conservation of angular momentum*, which is expressed mathematically as

$$\mathbf{M}_a = \mathbf{c}_a \quad (1.141)$$

where  $\mathbf{c}_a$  is a constant vector.

## Work and Energy

According to D'Alembert's principle, the work of the inertia forces is equal to the work of the applied forces. This statement can be written mathematically in the following form:

$$\int_v \rho(\ddot{\mathbf{r}} \cdot d\mathbf{r}) dv = \mathbf{F} \cdot d\mathbf{r} \quad (1.142)$$

Using the identity  $\ddot{r}_k = \dot{r}_k(d\dot{r}_k/dr_k)$ ,  $k = 1, 2, 3$ , one can show that

$$\ddot{\mathbf{r}} \cdot d\mathbf{r} = \dot{\mathbf{r}} \cdot d\dot{\mathbf{r}} \quad (1.143)$$

Substituting this equation into Equation 142 one obtains

$$\int_v \rho(\dot{\mathbf{r}} \cdot d\dot{\mathbf{r}}) dv = \mathbf{F} \cdot d\mathbf{r} \quad (1.144)$$

Integrating this equation from  $t_0$  to  $t$  and using the rigid-body assumption, one can show that

$$\frac{1}{2} \int_v \rho(\dot{\mathbf{r}} \cdot \dot{\mathbf{r}}) dv - T_0 = \int_{t_0}^t \mathbf{F} \cdot d\mathbf{r} \quad (1.145)$$

where  $T_0$  is the kinetic energy of the body at the initial configuration. The preceding equation is a statement of the *principle of work and energy*. This equation shows that the change in the body kinetic energy is equal to the work done by the applied forces. This principle is derived using the equations of motion of the body. Therefore, any set of equations of motion, if correctly and consistently derived, must satisfy the principle of work and energy. As previously mentioned, some of the nonlinear finite element formulations proposed in the literature for the large displacement analysis fail to automatically satisfy this principle. The nonlinear finite element formulations presented in later chapters of this book automatically satisfy the principle of work and energy, and their use does not require taking special measures when the equations of motion are integrated numerically.

## 1.11 PARAMETER CHANGE AND COORDINATE TRANSFORMATION

In continuum mechanics, it is important to differentiate between two different transformations. The first is the *change of parameters* and the second is the *coordinate transformation of vectors*. Understanding the difference between these two transformations is crucial in understanding the definitions of the strain components that will be introduced in the next chapter. This subject is also important in the large-deformation finite element formulation discussed in this book.

### Change of Parameters

In order to explain the difference between the change of parameters and the coordinate transformation of vectors, we consider the vector  $\mathbf{r}$ , which is expressed in terms of three coordinates  $x_1$ ,  $x_2$ , and  $x_3$ . The vector  $\mathbf{r}$  can then be written as

$$\mathbf{r} = [r_1 \quad r_2 \quad r_3]^T = \mathbf{r}(x_1, x_2, x_3) \quad (1.146)$$

Assume that the components of this vector are defined in the coordinate system  $X_1X_2X_3$ . The matrix of gradients of this vector obtained by differentiation with respect to the parameters  $x_1$ ,  $x_2$ , and  $x_3$  is given by

$$\mathbf{J} = [\mathbf{r}_{x_1} \quad \mathbf{r}_{x_2} \quad \mathbf{r}_{x_3}] = \begin{bmatrix} \frac{\partial r_1}{\partial x_1} & \frac{\partial r_1}{\partial x_2} & \frac{\partial r_1}{\partial x_3} \\ \frac{\partial r_2}{\partial x_1} & \frac{\partial r_2}{\partial x_2} & \frac{\partial r_2}{\partial x_3} \\ \frac{\partial r_3}{\partial x_1} & \frac{\partial r_3}{\partial x_2} & \frac{\partial r_3}{\partial x_3} \end{bmatrix} \quad (1.147)$$

It is important to realize that  $x_1$ ,  $x_2$ , and  $x_3$  represent coordinate lines, and the vector  $\mathbf{r}_{x_i}$ ,  $i = 1, 2, 3$ , which is a gradient vector defined by differentiation with respect to the coordinate  $x_i$ ,

represents the change in the vector  $\mathbf{r}$  as a result of a small change in the coordinate  $x_i$ . The vector  $\mathbf{r}_{x_i}$  is not necessarily a unit vector, and a measure of the deviation from a unit vector is defined as  $(\mathbf{r}_{x_i}^T \mathbf{r}_{x_i} - 1)$ . A measure of the angle between two gradient vectors can be obtained using the dot product  $\mathbf{r}_{x_i}^T \mathbf{r}_{x_j}$ ,  $i \neq j$ . Therefore, equations such as  $(\mathbf{r}_{x_i}^T \mathbf{r}_{x_i} - 1)$  and  $\mathbf{r}_{x_i}^T \mathbf{r}_{x_j}$ ,  $i \neq j$ , can be used to measure the deformation and shear effects at material points of the continuum.

The vector  $\mathbf{r}$  defined in the same coordinate system  $X_1X_2X_3$  can be written in terms of another set of parameters  $\bar{x}_1$ ,  $\bar{x}_2$ , and  $\bar{x}_3$ , which are related to the parameters  $x_1$ ,  $x_2$ , and  $x_3$  by the relation

$$\mathbf{x} = \bar{\mathbf{x}}(x_1, x_2, x_3) \quad (1.148)$$

where  $\mathbf{x} = [x_1 \ x_2 \ x_3]^T$  and  $\bar{\mathbf{x}} = [\bar{x}_1 \ \bar{x}_2 \ \bar{x}_3]^T$ . Using differentiation with respect to the parameters  $\bar{x}_1$ ,  $\bar{x}_2$ , and  $\bar{x}_3$ , the matrix of gradients can be written as

$$\bar{\mathbf{J}} = [\mathbf{r}_{\bar{x}_1} \ \mathbf{r}_{\bar{x}_2} \ \mathbf{r}_{\bar{x}_3}] = \begin{bmatrix} \frac{\partial r_1}{\partial \bar{x}_1} & \frac{\partial r_1}{\partial \bar{x}_2} & \frac{\partial r_1}{\partial \bar{x}_3} \\ \frac{\partial r_2}{\partial \bar{x}_1} & \frac{\partial r_2}{\partial \bar{x}_2} & \frac{\partial r_2}{\partial \bar{x}_3} \\ \frac{\partial r_3}{\partial \bar{x}_1} & \frac{\partial r_3}{\partial \bar{x}_2} & \frac{\partial r_3}{\partial \bar{x}_3} \end{bmatrix} \quad (1.149)$$

In this case, the vector  $\mathbf{r}_{\bar{x}_i}$ ,  $i = 1, 2, 3$ , represents a gradient vector obtained by differentiation with respect to the coordinate  $\bar{x}_i$ . Again, the vector  $\mathbf{r}_{\bar{x}_i}$  is not necessarily a unit vector, and a measure of the deviation from a unit vector is given by  $(\mathbf{r}_{\bar{x}_i}^T \mathbf{r}_{\bar{x}_i} - 1)$ . A measure of the angle between two gradient vectors can be obtained using the dot product  $\mathbf{r}_{\bar{x}_i}^T \mathbf{r}_{\bar{x}_j}$ ,  $i \neq j$ . Note that the relationship between  $\mathbf{J}$  and  $\bar{\mathbf{J}}$  is given by

$$\bar{\mathbf{J}} = \frac{\partial \mathbf{r}}{\partial \bar{\mathbf{x}}} = \frac{\partial \mathbf{r}}{\partial \mathbf{x}} \frac{\partial \mathbf{x}}{\partial \bar{\mathbf{x}}} = \mathbf{J} \frac{\partial \mathbf{x}}{\partial \bar{\mathbf{x}}} \quad (1.150)$$

Although we assume in this section that parameters are defined along the orthogonal axes of coordinate systems, the relationship of Equation 150 is general and governs the definition of the gradients when defined using different parameters, including the case of curvilinear coordinates. It is important, however, to point out that the use of different sets of parameters leads to the definition of different gradient vectors. Nonetheless, these gradient vectors, regardless of what set of parameters is used, are defined in the same coordinate system in which the vector  $\mathbf{r}$  is defined. That is, the differentiation of a vector does not change the coordinate system in which this vector is defined.

As a special case, the curve shown in Figure 3 is considered. The position of points on this curve can be defined in the coordinate system  $X_1X_2X_3$  and can be written in terms of one parameter  $s$  as  $\mathbf{r} = \mathbf{r}(s)$ . Because there is only one parameter, there is only one gradient vector, defined as

$$\mathbf{r}_s = \frac{\partial \mathbf{r}}{\partial s} \quad (1.151)$$

This gradient vector defines the tangent vector, as shown in Figure 3, and if  $s$  is selected as the arc length,  $\mathbf{r}_s$  is a unit vector. One may choose other parameters, such as  $\alpha_1$  and  $\alpha_2$ , and define

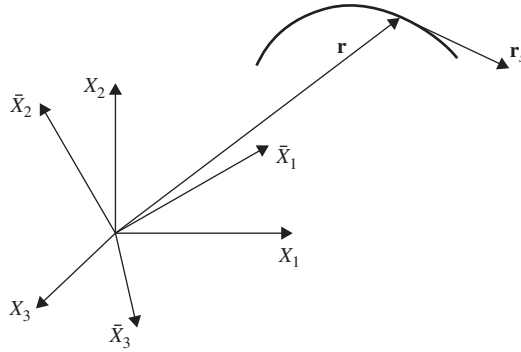


**Figure 1.3** Space curve

the gradient vector by differentiation with respect to these new parameters. This leads to other definitions of the gradient vector as

$$\mathbf{r}_{\alpha_1} = \frac{\partial \mathbf{r}}{\partial \alpha_1}, \quad \mathbf{r}_{\alpha_2} = \frac{\partial \mathbf{r}}{\partial \alpha_2} \quad (1.152)$$

Clearly, the three gradient vectors defined in Equations 151 and 152 are different expressions for the tangent vector, for example,

$$\mathbf{r}_{\alpha_1} = \frac{\partial \mathbf{r}}{\partial \alpha_1} = \frac{\partial \mathbf{r}}{\partial s} \frac{\partial s}{\partial \alpha_1} \quad (1.153)$$

which shows that  $\mathbf{r}_{\alpha_1}$  and  $\mathbf{r}_s$  are two parallel vectors that differ by a scalar multiplier that depends on the relationship between the two parameters  $\alpha_1$  and  $s$ . This simple example shows that the change of parameters does not lead to a change in the coordinate system because the resulting gradient vectors are defined in the  $X_1X_2X_3$  coordinate system in which the vector  $\mathbf{r}$  is defined.

Although in the simple one-dimensional example the change of parameters does not change the orientation of the gradient vector, when two or more parameters are used, the change of parameters can lead to a change of the orientation of the gradient vectors but does not change the coordinate system in which these gradient vectors are defined. This is clear from Equation 150, which shows that the columns of the gradient matrix  $\bar{\mathbf{J}}$  are linear combinations of the columns of the gradient matrix  $\mathbf{J}$ .

## Coordinate Transformation

The analysis presented thus far in this section shows that the change of parameters does not imply a change of the coordinate system in which the gradient vectors are defined. That is, if  $x_1, x_2$ , and  $x_3$  are coordinates along the orthogonal axes of the coordinate system  $X_1X_2X_3$  and  $\bar{x}_1, \bar{x}_2$ , and  $\bar{x}_3$  are the coordinates along the axes of another coordinate system  $\bar{X}_1\bar{X}_2\bar{X}_3$ , then, in general,  $\mathbf{r}_{x_i} = \partial \mathbf{r} / \partial x_i \neq \mathbf{R} \mathbf{r}_{\bar{x}_i}, i = 1, 2, 3$ , where  $\mathbf{R}$  is the matrix that defines the orientation

of the coordinate system  $\bar{X}_1\bar{X}_2\bar{X}_3$  with respect to the coordinate system  $X_1X_2X_3$ . The gradient vector  $\mathbf{r}_{x_i}$  can be written in terms of components defined in the coordinate system  $\bar{X}_1\bar{X}_2\bar{X}_3$  as

$$\bar{\mathbf{r}}_{x_i} = \mathbf{R}^T \mathbf{r}_{x_i}, \quad i = 1, 2, 3 \quad (1.154)$$

In the analysis presented in this book, it is important to understand the difference between the change of parameters and the transformation between two coordinate systems, particularly when the large-deformation ANCF finite elements presented in Chapter 5 are discussed.

## Deformation and Strains

In continuum mechanics, strains are used as measure of the deformation. The strains at a point on the continuum are defined using dot products of gradient vectors, and therefore, their values in a certain direction are independent of the coordinate system used. As will be shown in the following chapter, the strain components are used as measure of the stretch and shear. For example, a stretch strain component is defined as  $(\mathbf{r}_{x_i} \cdot \mathbf{r}_{x_i} - 1)/2$ , where  $\mathbf{r}_{x_i} = \partial \mathbf{r} / \partial x_i$  is the gradient vector in the direction of the parameter  $x_i$ . Clearly, the strain measure  $(\mathbf{r}_{x_i} \cdot \mathbf{r}_{x_i} - 1)/2$  is independent of the coordinate system as well as of a rigid-body coordinate transformation; this is clear from the dot product definition. Furthermore, this definition of the strain is unique since it measures the change at a point on the continuum in a specific direction defined by the coordinate line  $x_i$ , which can represent a straight or curved line.

The deformation on the other hand is not unique and depends on the choice of the coordinate system. For this reason, deformations are not often used in the general continuum mechanics developments. In order to provide an explanation, one can consider the slider crank mechanism shown in Figure 4. This mechanism is widely used in many applications including engines. As the crankshaft of the mechanism rotates and the piston moves, the connecting rod can be subjected to excessive forces that will produce deformation. A magnification of the deformation of the connecting is shown in Figure 4b. Regardless of the coordinate system used, the strains at an arbitrary point on the connecting rod have unique values since they are defined in terms of the dot product of gradient vectors. The deformation definition, however, is not unique. As shown in Figure 5, different coordinate systems can be used to measure the deformation. The figure shows the deformation  $\delta$  of the mid-point defined in different coordinate systems. It is clear that these deformation measures have very different values. In fact, the deformation of some points, such as the end points of the connecting rod, can be zero in some coordinate

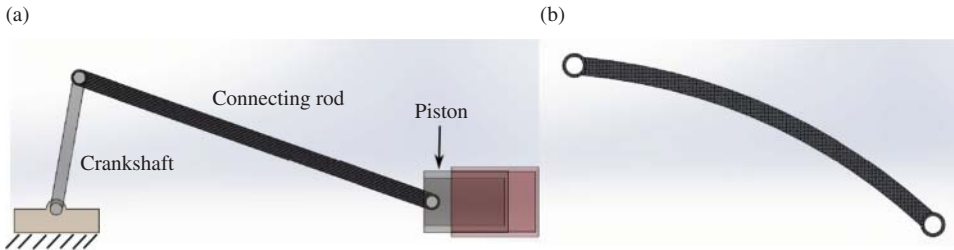


**Figure 1.4** Slider crank mechanism

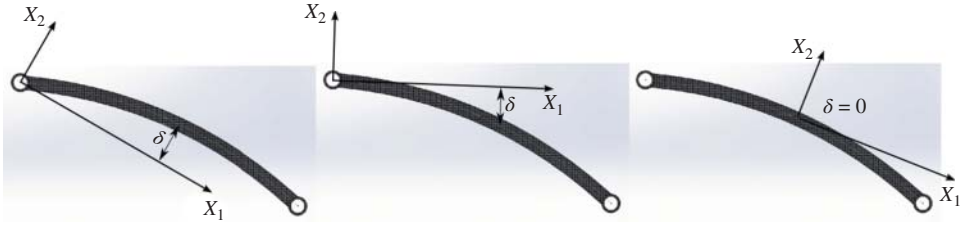


**Figure 1.5** Deformation measurement.

systems and can assume a very large value in other coordinate systems. The strain measures, on the other hand, are absolute and do not depend on the choice of the coordinate systems.

### Position Vector Gradients and Rigid Body Kinematics

It can be shown that the rigid body kinematic equations can be written as a linear polynomial in the spatial coordinates if the concept of the position vector gradients is used. That is, a polynomial similar to Equation 115 with a lower order can be used to describe the rigid body motion provided appropriate constraints are imposed on the position vector gradients. Using Equations 81 and 85, one can show that Equation 81 can be written as

$$\mathbf{r} = \mathbf{r}_O + \mathbf{A}\bar{\mathbf{u}} = \begin{bmatrix} a_0 + a_1x_1 + a_2x_2 \\ b_0 + b_1x_1 + b_2x_2 \end{bmatrix} \quad (1.155)$$

In this equation,

$$\mathbf{r}_O = \begin{bmatrix} a_0 \\ b_0 \end{bmatrix}, \quad \begin{bmatrix} \bar{x}_1 \\ \bar{x}_2 \end{bmatrix} = \begin{bmatrix} x_1 \\ x_2 \end{bmatrix}, \quad \mathbf{r}_{x_1} = \begin{bmatrix} a_1 \\ b_1 \end{bmatrix} = \begin{bmatrix} \cos \theta \\ \sin \theta \end{bmatrix}, \quad \mathbf{r}_{x_2} = \begin{bmatrix} a_2 \\ b_2 \end{bmatrix} = \begin{bmatrix} -\sin \theta \\ \cos \theta \end{bmatrix} \quad (1.156)$$

This equation shows that the rigid body kinematic equations can be written in the form of the linear polynomials of Equation 115. Since in the case of unconstrained planar motion the rigid body has three degrees of freedom, the six coefficients  $a_0, a_1, a_2, b_0, b_1,$  and  $b_2$  must be related by three algebraic equations. It is clear from Equation 156 that these three algebraic constraint equations imposed on the gradient vectors are

$$\mathbf{r}_{x_1}^T \mathbf{r}_{x_1} = 1, \quad \mathbf{r}_{x_2}^T \mathbf{r}_{x_2} = 1, \quad \mathbf{r}_{x_1}^T \mathbf{r}_{x_2} = 0 \quad (1.157)$$

These constraint equations imply that in the case of rigid body motion, the position vector gradients remain orthogonal unit vectors, and in this special case, the transformation matrix that defines the orientation of the body coordinate system can be written as  $\mathbf{A} = [\mathbf{r}_{x_1} \ \mathbf{r}_{x_2}]$ . A similar procedure can be used in the spatial analysis to show that the three-dimensional rigid body kinematic equations can be written in the form of linear polynomials in the spatial coordinates. It is important to note that the spatial coordinates  $x_1$  and  $x_2$  are defined with respect to the body coordinate system and assume their constant initial values regardless of the amount of displacement and rotation of the rigid body. That is, when the polynomial representation is used, the spatial coordinates always assume constant values and the motion of the body



or the finite element is defined by the time dependent coefficients of the polynomial used, or alternatively, by the element nodal coordinates used to replace the polynomial coefficients. It is also clear from Equations 155 and 156 that the rigid body kinematics can be expressed as linear functions of the angles. Furthermore, the position vector gradients in Equation 156 are written in terms of trigonometric functions which have infinite orders. Therefore, finite elements, in which the element displacement field is written as linear functions of angles, cannot correctly describe rigid body motion and such finite elements cannot be used with the nonincremental solution procedures often used in multibody system dynamics.

## PROBLEMS

1. Find the sum of the following two matrices:

$$\mathbf{A} = \begin{bmatrix} -3 & 4 & -1 \\ 2 & 0 & 5 \\ -4 & 1 & 3 \end{bmatrix}, \quad \mathbf{B} = \begin{bmatrix} 2 & 1 & 0 \\ 2 & 3 & 4 \\ -4 & -2 & -3 \end{bmatrix}$$

Find also the trace of these two matrices as well as the trace of their product.

2. Find the product of the following three matrices:

$$\mathbf{A}_1 = \begin{bmatrix} 1 & 0 & 0 \\ 0 & \cos \phi & -\sin \phi \\ 0 & \sin \phi & \cos \phi \end{bmatrix}, \quad \mathbf{A}_2 = \begin{bmatrix} \cos \theta & 0 & \sin \theta \\ 0 & 1 & 0 \\ -\sin \theta & 0 & \cos \theta \end{bmatrix},$$

$$\mathbf{A}_3 = \begin{bmatrix} \cos \psi & -\sin \psi & 0 \\ \sin \psi & \cos \psi & 0 \\ 0 & 0 & 1 \end{bmatrix}$$

3. Find the determinant and the inverse of the following two matrices:

$$\mathbf{A} = \begin{bmatrix} -3 & 4 & -1 \\ 0 & 1 & 2 \\ 0 & 0 & 3 \end{bmatrix}, \quad \mathbf{B} = \begin{bmatrix} 1 & 0 & 0 \\ 1 & 1 & 0 \\ 1 & 1 & 1 \end{bmatrix}$$

4. Show that the following two matrices are orthogonal:

$$\mathbf{A}_1 = \begin{bmatrix} \cos \theta & 0 & \sin \theta \\ 0 & 1 & 0 \\ -\sin \theta & 0 & \cos \theta \end{bmatrix}, \quad \mathbf{A}_2 = \mathbf{I} + \tilde{\mathbf{v}} \sin \theta + 2\tilde{\mathbf{v}}^2 \sin^2 \left( \frac{\theta}{2} \right)$$

where  $\theta$  is an angle,  $\mathbf{v}$  is a three-dimensional unit vector,  $\tilde{\mathbf{v}}$  is the skew-symmetric matrix associated with the unit vector  $\mathbf{v}$ , and  $\mathbf{I}$  is the identity matrix.

5. Show that the determinant of a  $3 \times 3$  matrix does not change if a row or a column is subtracted or added to another.

6. Show that the matrices in Problem 2 are orthogonal and that their product is an orthogonal matrix.
7. Find the norm of the columns of the matrices of Problem 3.
8. Prove the identities given in Equations 28 and 29 for three-dimensional vectors.
9. Prove Equation 32 for three-dimensional vectors.
10. Show that if  $\mathbf{A}$  is a symmetric tensor and  $\mathbf{B}$  is a skew-symmetric tensor, then  $\mathbf{A} : \mathbf{B} = 0$ .
11. If  $\mathbf{A}$ ,  $\mathbf{B}$ , and  $\mathbf{C}$  are second-order tensors, show that the double product satisfies the identity  $\mathbf{A} : (\mathbf{BC}) = (\mathbf{AC}^T) : \mathbf{B} = (\mathbf{B}^T \mathbf{A}) : \mathbf{C}$ .
12. If  $\mathbf{A}$  and  $\mathbf{B}$  are two symmetric tensors, show that

$$\mathbf{A} : \mathbf{B} = A_{11}B_{11} + A_{22}B_{22} + A_{33}B_{33} + 2(A_{12}B_{12} + A_{13}B_{13} + A_{23}B_{23})$$

13. Find the invariants, eigenvalues, and eigenvectors of the following two matrices:

$$\mathbf{A} = \begin{bmatrix} -3 & 4 & -1 \\ 4 & 0 & 5 \\ -1 & 5 & 3 \end{bmatrix}, \quad \mathbf{B} = \begin{bmatrix} 2 & 1 & 0 \\ 1 & 3 & -2 \\ 0 & -2 & -3 \end{bmatrix}$$

Verify that the three invariants of each of these matrices can be written in terms of the eigenvalues.

14. Find the projection matrices  $\mathbf{P}$  and  $\mathbf{P}_p$  associated with the unit vector  $\hat{\mathbf{a}} = [1/\sqrt{3} \ 1/\sqrt{3} \ 1/\sqrt{3}]^T$ .
15. Show that the components of a third-order tensor  $\mathbf{T}$  can be written as  $t_{ijk} = (\mathbf{i}_i \otimes \mathbf{i}_j) : \mathbf{T} \mathbf{i}_k$ , where  $\mathbf{i}_i$ ,  $\mathbf{i}_j$ , and  $\mathbf{i}_k$  are base vectors.
16. Prove the properties of Equation 59.
17. Show that the component  $v_k$  of any vector  $\mathbf{v}$  can be written as  $v_k = -(1/2)\Gamma_{ijk}\tilde{v}_{ij} = -(1/2)\Gamma_{kij}\tilde{v}_{ij} = (1/2)\Gamma_{ikj}\tilde{v}_{ij}$ , where  $\Gamma = (\Gamma_{ijk})$  is the third-order alternating tensor and  $\tilde{\mathbf{v}} = (\tilde{v}_{ij})$  is the skew-symmetric matrix associated with the vector  $\mathbf{v}$ .
18. Show that the cross product between the two vectors  $\mathbf{u}$  and  $\mathbf{v}$  can be written as  $\mathbf{u} \times \mathbf{v} = \sum_{i,j=1}^3 u_i v_j (\mathbf{i}_i \times \mathbf{i}_j) = \sum_{i,j,k=1}^3 \Gamma_{ijk} u_i v_j \mathbf{i}_k$ , where  $\mathbf{i}_i$ ,  $\mathbf{i}_j$ , and  $\mathbf{i}_k$  are base vectors and  $\Gamma = (\Gamma_{ijk})$  is the third-order alternating tensor.
19. Show that the components of a fourth-order tensor  $\mathbf{F}$  can be written as  $f_{ijkl} = (\mathbf{i}_i \otimes \mathbf{i}_j) : \mathbf{F} : (\mathbf{i}_k \otimes \mathbf{i}_l)$ , where  $\mathbf{i}_i$ ,  $\mathbf{i}_j$ ,  $\mathbf{i}_k$ , and  $\mathbf{i}_l$  are base vectors.
20. Find the polar decomposition of the matrix

$$\mathbf{A} = \begin{bmatrix} 2 & 1 & 3 \\ 0 & 1 & -2 \\ 0 & 0 & 2 \end{bmatrix}$$

21. Derive Euler equation of motion using Equation 95.
22. Using D'Alembert's principle, derive the equation of motion of a pendulum connected to the ground at one of its ends by a pin joint. Assume that the pendulum rod has length  $l$ , mass  $m$ , and mass moment of inertia about the center of mass  $I_O$ . The pendulum is subjected to an external moment  $M$ . Consider the effect of gravity. Explain how D'Alembert's principle can be used to systematically eliminate the reaction forces in this problem.
23. Solve Problem 22 using the principle of virtual work. Discuss the relationship between D'Alembert's principle and the principle of virtual work.
24. Verify the shape functions of Equation 121.

## CHAPTER 2

---

# KINEMATICS

---

In this chapter, the general kinematic equations for the continuum are developed. The kinematic analysis presented in this chapter is purely geometric and does not involve any force analysis. The continuum is assumed to undergo an arbitrary displacement and no simplifying assumptions are made except when special cases are discussed. Recall that in the special case of an unconstrained three-dimensional rigid-body motion, six independent coordinates are required in order to describe arbitrary rigid-body translation and rotation displacements. The general displacement of an infinitesimal material volume on a deformable body, on the other hand, can be described in terms of 12 independent variables: 3 translation parameters, 3 rigid-body rotation parameters, and 6 deformation parameters. One can visualize these modes of displacements by considering an infinitesimal cube that may undergo an arbitrary displacement. The cube can be translated in three independent orthogonal directions (translation degrees of freedom), rotated as a rigid body about three orthogonal axes, and subjected to six independent modes of deformation. These deformation modes are elongations or contractions in three different directions and three shear deformation modes.

It is shown in this chapter that the rotations and the deformations can be completely described using the matrix of the position vector gradients, which in general has nine independent elements. This fact can be mathematically proven using the *polar decomposition theorem* discussed in the preceding chapter. The deformation at the material points on the body can be described in terms of six independent *strain components*. These strain components can be defined in the undeformed reference configuration leading to the *Green–Lagrange strains* or can be defined using the current deformed configuration leading to the *Eulerian* or *Almansi strains*. The *velocity gradients* and the *rate of deformation tensor* also play a fundamental

role in the theory of nonlinear continuum mechanics and for this reason they are discussed in detail in this chapter.

The concept of *objectivity* or *frame indifference*, which is important in the analysis of large deformations, particularly in formulations that involve the strain rates, is also introduced and will be discussed in more detail in the following chapter. In order to correctly formulate the dynamic equations of the continuum, one needs to develop the relationships between the volume and area of the body in the reference configuration and its volume and area in the current configuration. These relationships as well as the continuity equation derived from the conservation of mass are presented in Sections 8 and 9. *Reynolds' transport theorem*, which is used in fluid mechanics, is discussed in Section 10. In Section 11, several examples of simple deformations are presented.

Whereas a continuum has an infinite number of degrees of freedom, for simplicity, concepts and definitions are explained in the examples throughout this book using models that have a finite number of degrees of freedom. This provides the reader with a natural introduction to the finite element formulations that will be discussed in later chapters.

## 2.1 MOTION DESCRIPTION

Figure 1 shows a body in the reference and current configurations. The position vector of an arbitrary material point on the body in the reference configuration is defined by the vector  $\mathbf{x} = [x_1 \ x_2 \ x_3]^T$ , whereas the position vector of this arbitrary material point in the current configuration after displacement is defined by the vector  $\mathbf{r} = [r_1 \ r_2 \ r_3]^T$ . One can then write the following relationship:

$$\mathbf{r} = \mathbf{x} + \mathbf{u} \quad (2.1)$$

where  $\mathbf{u} = [u_1 \ u_2 \ u_3]^T$  is the displacement vector, and the three vectors  $\mathbf{r}$ ,  $\mathbf{x}$ , and  $\mathbf{u}$  are defined in the same global coordinate system as shown in Figure 1. In the preceding equation, it is assumed that both the position and displacement vectors  $\mathbf{r}$  and  $\mathbf{u}$  are functions of the components of the position vector  $\mathbf{x}$  in the reference configuration. That is, given a material point defined by the position  $\mathbf{x}$  in the reference configuration, one should be able to define the position vector  $\mathbf{r}$  of this point in the current configuration as well as the displacement vector  $\mathbf{u}$ . In general, the position vector  $\mathbf{r}$  and the displacement vector  $\mathbf{u}$  can be written as functions of  $\mathbf{x}$  and time  $t$ , that is

$$\mathbf{r} = \mathbf{r}(\mathbf{x}, t), \quad \mathbf{u} = \mathbf{u}(\mathbf{x}, t) \quad (2.2)$$

The coordinates  $\mathbf{x}$  are called the *material* or *Lagrangian coordinates*, whereas the coordinates  $\mathbf{r}$  are called the *spatial* or *Eulerian coordinates*. Both sets of coordinates can be used in the formulation of the kinematic and dynamic equations. If the Lagrangian coordinates are used to formulate the dynamic equations, one obtains the *Lagrangian description*, which is often used in solid mechanics. If the Eulerian coordinates are used, on the other hand, one obtains the *Eulerian description*, which is often used in the study of the motion of the fluids. In the case of a *fluid*, it is sometimes inconvenient to describe the motion with respect to the reference configuration, as in the case of a flow around an airfoil. In the case of solids, on the other hand, the history of the deformation is important, and for this reason, the Lagrangian description is more suited.

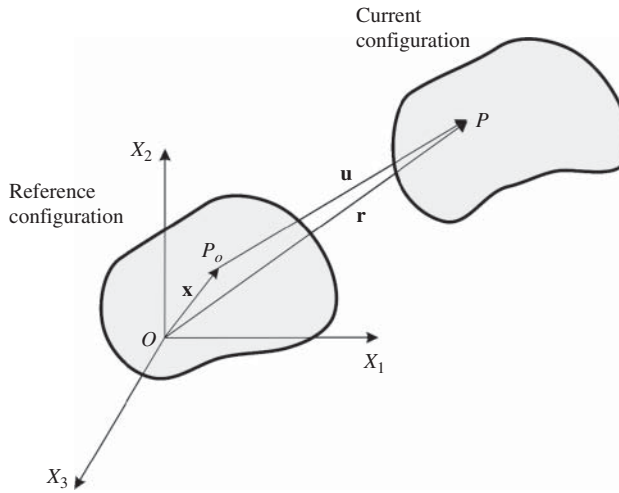


**Figure 2.1** Reference and current configurations

### Example 2.1

As shown in Chapter 1, the general motion of a two-dimensional beamlike structure, depicted in Figure 2, can be described using the following position vector field (Omar and Shabana, 2001):

$$\mathbf{r} = \mathbf{S}\mathbf{e} \quad (2.3)$$

where  $\mathbf{e} = \mathbf{e}(t) = [e_1 \ e_2 \ \dots \ e_{12}]^T$  is a vector of time-dependent coefficients or coordinates, which consist of absolute position and slope coordinates as described in Chapter 1, and  $\mathbf{S} = \mathbf{S}(\mathbf{x})$  is a

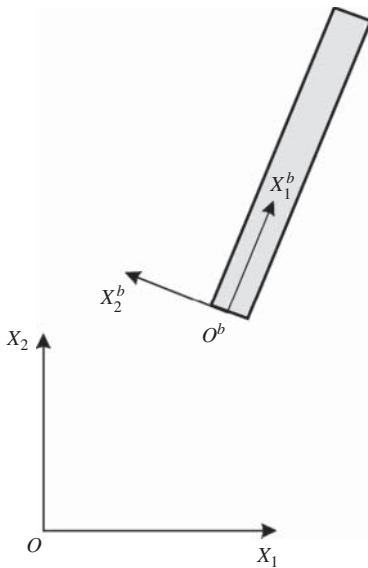


**Figure 2.2** Planar beam

matrix that depends on the Lagrangian coordinates and is given by

$$\mathbf{S} = \begin{bmatrix} s_1 & 0 & s_2 & 0 & s_3 & 0 & s_4 & 0 & s_5 & 0 & s_6 & 0 \\ 0 & s_1 & 0 & s_2 & 0 & s_3 & 0 & s_4 & 0 & s_5 & 0 & s_6 \end{bmatrix} \quad (2.4)$$

The elements  $s_i$  that appear in this equation are given by

$$\left. \begin{aligned} s_1 &= 1 - 3\xi^2 + 2\xi^3, & s_2 &= l(\xi - 2\xi^2 + \xi^3), & s_3 &= l\eta(1 - \xi) \\ s_4 &= 3\xi^2 - 2\xi^3, & s_5 &= l(-\xi^2 + \xi^3), & s_6 &= l\xi\eta \end{aligned} \right\} \quad (2.5)$$

where  $\xi = x_1/l$  and  $\eta = x_2/l$ ; and  $l$  is the length of the beam in the reference configuration. A reference configuration of the beam in which the beam axis is parallel to the global  $X_1$  axis is given for the following values of the coefficients or coordinates:

$$\mathbf{e} = \mathbf{e}(0) = [0 \ 0 \ 1 \ 0 \ 0 \ 1 \ l \ 0 \ 1 \ 0 \ 0 \ 1]^T$$

Using these values of the coordinates, one can verify that

$$\mathbf{r}(\mathbf{x}, 0) = \mathbf{S}(\mathbf{x})\mathbf{e}(0) = \begin{bmatrix} x_1 \\ x_2 \end{bmatrix} = \mathbf{x}$$

This equation defines the position of the material points on the beam in the undeformed reference configuration. That is, the position vector field of Equation 3 correctly describes the position of the beam material points in the undeformed reference configuration.

## Line Elements

In the study of deformation, the change of the length of a line element is used to define the basic strain variables used in continuum mechanics. It is clear that if the change of the distance between two arbitrary points as the result of deformation is known, changes of areas and volumes can be determined. A differential line element  $d\mathbf{r}$  in the current configuration can be written as

$$d\mathbf{r} = \frac{\partial \mathbf{r}}{\partial \mathbf{x}} d\mathbf{x} = \mathbf{J} d\mathbf{x} \quad (2.6)$$

where  $\mathbf{J}$  is the *matrix of position vector gradients*, also called the *Jacobian matrix*. This matrix is defined as follows:

$$\mathbf{J} = \frac{\partial \mathbf{r}}{\partial \mathbf{x}} = \begin{bmatrix} \frac{\partial r_1}{\partial x_1} & \frac{\partial r_1}{\partial x_2} & \frac{\partial r_1}{\partial x_3} \\ \frac{\partial r_2}{\partial x_1} & \frac{\partial r_2}{\partial x_2} & \frac{\partial r_2}{\partial x_3} \\ \frac{\partial r_3}{\partial x_1} & \frac{\partial r_3}{\partial x_2} & \frac{\partial r_3}{\partial x_3} \end{bmatrix} = [\mathbf{r}_{x_1} \ \mathbf{r}_{x_2} \ \mathbf{r}_{x_3}] \quad (2.7)$$

In this equation,  $\mathbf{r}_{x_i} = \partial \mathbf{r} / \partial x_i$ ,  $i = 1, 2, 3$ . If there are no displacements of the particles of the body, the vector  $d\mathbf{r}$  is equal to the vector  $d\mathbf{x}$ . In this case,  $\mathbf{J}$  is the identity matrix and has a

positive determinant that is equal to one. Because the Jacobian matrix  $\mathbf{J}$  cannot be singular and the displacement is assumed to be continuous function, the determinant of  $\mathbf{J}$  must be positive. Therefore, a necessary and sufficient condition for a continuous displacement to be physically possible is that the determinant of  $\mathbf{J}$  be greater than zero, that is,  $\mathbf{J}$  is always positive definite. This requirement of continuous displacement allows transformation from the current configuration to the reference configuration and vice versa. It is therefore assumed that the transformation is one-to-one and the function  $\mathbf{r} = \mathbf{r}(\mathbf{x}, t)$  is single-valued, continuous, and has the following unique inverse:

$$\mathbf{x} = \mathbf{x}(\mathbf{r}, t) \quad (2.8)$$

This property, when guaranteed for every material point on the body, allows for the transformation between the Eulerian and Lagrangian descriptions.

### Rigid-Body Motion

Recall that in the special case of *rigid-body motion*, the length of a line segment remains constant. This implies that

$$d\mathbf{r}^T d\mathbf{r} = d\mathbf{x}^T d\mathbf{x} \quad (2.9)$$

In this special case of rigid-body motion, one has  $\mathbf{J}^T \mathbf{J} = \mathbf{J} \mathbf{J}^T = \mathbf{I}$ . That is,  $\mathbf{J}$  is an orthogonal matrix that describes the relationship between the line element  $d\mathbf{x}$  before the displacement and the line element  $d\mathbf{r}$  after the displacement. Equation 9 shows that in the case of rigid-body motion, the *stretch* of the line element defined as  $|d\mathbf{r}| - |d\mathbf{x}|$  is equal to zero everywhere. Because the components of the line elements are not affected by the translation, the matrix  $\mathbf{J}$  in the case of rigid-body motion describes pure rotation, and it is the matrix that can be used to define the orientation of the rigid body in space. In this special case of rigid-body motion, the elements of the Jacobian matrix  $\mathbf{J}$  are the direction cosines of unit vectors that define the axes of a selected body coordinate system whose origin is attached to the rigid body (Goldstein, 1950; Greenwood, 1988; Shabana, 2013).

In the case of a rigid-body motion, as shown in Figure 3, one can always select a *body coordinate system*,  $X_1^b X_2^b X_3^b$ , that moves with the body. Line segments or locations of the material points can be measured with respect to the origin of the body coordinate system. Without any loss of generality, one can assume that before displacement, the axes of the body coordinate system  $X_1^b X_2^b X_3^b$  coincide with the axes of the global coordinate system  $X_1 X_2 X_3$ . In this case, the location of an arbitrary material point on the rigid body can be defined after the displacement using the following equation:

$$\mathbf{r} = \mathbf{r}_O(t) + \mathbf{J} \mathbf{x}^b \quad (2.10)$$

where  $\mathbf{r}_O$  is the vector that defines the location of the origin of the body coordinate system;  $\mathbf{J}$ , in this case of a rigid-body motion, is an orthogonal matrix that can be expressed in terms of three independent orientation coordinates (Goldstein, 1950; Greenwood, 1988; Shabana, 2013); and  $\mathbf{x}^b$  is the vector that defines the position of the material points in the moving coordinate system. Note that if an assumption is made that the moving reference coordinate system coincides with the global coordinate system before displacement, one has  $\mathbf{x} = \mathbf{x}^b$ .



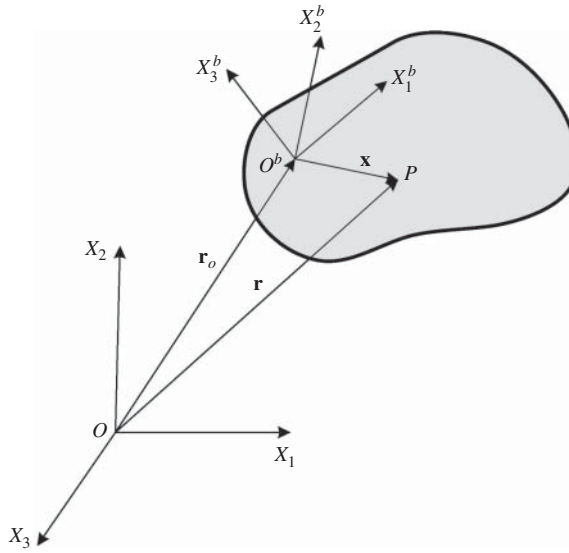
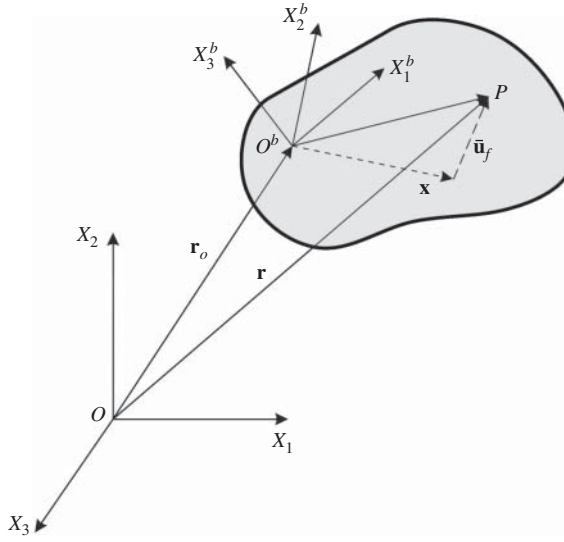


Figure 2.3 Rigid-body motion

### Floating Frame of Reference (FFR)

In this book, two different, yet equivalent, motion descriptions are frequently used to define the absolute position vector  $\mathbf{r}$ . In the first motion description, the vector  $\mathbf{r}$  is defined using absolute coordinates based on a description similar to the one used in Equation 3. In the second motion description, a coordinate system that follows the motion of the body is introduced. The position vector  $\mathbf{r}$  can be defined in terms of the motion of this reference plus the motion of the body with respect to the reference. This description is referred to in this book as the *floating frame of reference (FFR) approach*. It is important to recognize that these two different descriptions are equivalent and are consistent with the general continuum mechanics description. That is, the FFR approach does not lead to a separation between the rigid-body motion and the elastic deformation. Whereas the reference motion is a rigid-body motion, this motion is not the rigid-body motion of the continuum because different references can be selected for the same continuum.

In the case of general displacement, the floating frame of reference follows the motion of the body but does not have to be rigidly attached to a point on the body. Nonetheless, it is required that there is no relative rigid-body displacement between the body and its coordinate system. Using the FFR formulation kinematic description, the global position vector of an arbitrary point, as shown in Fig. 4, can in general be written as  $\mathbf{r}(\mathbf{x}, t) = \mathbf{r}_O(t) + \mathbf{A}(t)(\mathbf{x} + \bar{\mathbf{u}}_f(\mathbf{x}, t))$ , where  $\mathbf{A}$  is the transformation matrix that defines the orientation of the body coordinate system, and  $\bar{\mathbf{u}}_f(\mathbf{x}, t)$  measures the deformation of the body with respect to the selected body reference. Since the choice of  $\mathbf{A}$  is arbitrary; one can have infinite number of arrangements for the body coordinate system, and consequently infinite ways for measuring the deformation. Because the deformation is considered a relative measure, strains are used to describe the body kinematics when developing a general continuum mechanics theory. While coordinate systems are imaginary, strains are defined using the gradients of position vectors, which have a clear physical



**Figure 2.4** Floating frame of reference

meaning. Nonetheless, the relationship  $\mathbf{r}(\mathbf{x}, t) = \mathbf{r}_O(t) + \mathbf{A}(t)(\mathbf{x} + \bar{\mathbf{u}}_f(\mathbf{x}, t))$  is general, does not imply any approximation, and is the starting point in the development of the FFR formulation discussed in Chapter 6. This formulation is widely used in the multibody system (MBS) dynamics literature and allows for obtaining an efficient formulation for flexible bodies that undergo large rigid-body displacements as well as deformations that can be described using simple shapes. The FFR formulation was introduced many decades before the finite element (FE) method was introduced. The *corotational frame* used in the FE literature is not in general equivalent to the floating frame used in MBS dynamics. The configuration of the corotational frame is defined by the FE nodal coordinates, while the configuration of the floating frame is defined by a set of absolute Cartesian coordinates. If the FE nodal coordinates cannot correctly describe finite rigid-body displacements, as in the case of conventional beam, plate and shell elements that employ infinitesimal rotations as nodal coordinates; the corotational frame does not lead to zero strains under an arbitrary rigid-body displacement. On the other hand, the FFR formulation always leads to zero strains under an arbitrary rigid-body displacement regardless of the finite element used to describe the deformation. Furthermore, using the FFR kinematic description  $\mathbf{r}(\mathbf{x}, t) = \mathbf{r}_O(t) + \mathbf{A}(t)(\mathbf{x} + \bar{\mathbf{u}}_f(\mathbf{x}, t))$ , one can show that the matrix of position vector gradients  $\mathbf{J}$  can always be written as  $\mathbf{J} = \mathbf{A}(\mathbf{I} + (\partial \bar{\mathbf{u}}_f / \partial \mathbf{x}))$ , where  $\mathbf{I}$  is the identity matrix.

The basic kinematic description used in the FFR formulation is based on the general kinematic equations used in the nonlinear continuum mechanics. Nonetheless, it is not necessary in computational continuum mechanics to write the displacement as the sum of reference motion plus the displacement with respect to the reference coordinate system. One can always use the expression  $\mathbf{r} = \mathbf{r}(\mathbf{x})$  with a proper definition of  $\mathbf{r}$  in terms of  $\mathbf{x}$  to correctly describe the general displacement of the continuum, as discussed in Chapter 5. This fact is also demonstrated by the following simple example.

**Example 2.2**

The displacement field of the two-dimensional beamlike structure, discussed in Example 1, can describe an arbitrary rigid-body motion. Such a general rigid-body motion can be described if the element time-dependent coordinates take the following form:

$$\mathbf{e} = [e_1 \ e_2 \ \cos \theta \ \sin \theta \ -\sin \theta \ \cos \theta \\ (e_1 + l \cos \theta) \ (e_2 + l \sin \theta) \ \cos \theta \ \sin \theta \ -\sin \theta \ \cos \theta]^T$$

Using these values of the coordinates, one can verify that

$$\mathbf{r}(\mathbf{x}, t) = \mathbf{S}(\mathbf{x})\mathbf{e}(t) = \begin{bmatrix} e_1 \\ e_2 \end{bmatrix} + \begin{bmatrix} \cos \theta & -\sin \theta \\ \sin \theta & \cos \theta \end{bmatrix} \begin{bmatrix} x_1 \\ x_2 \end{bmatrix} = \mathbf{r}_O + \mathbf{J}\mathbf{x}$$

where  $\mathbf{r}_O$ ,  $\mathbf{J}$ , and  $\mathbf{x}$  can be recognized in this case as

$$\mathbf{r}_O = \begin{bmatrix} e_1 \\ e_2 \end{bmatrix}, \quad \mathbf{J} = \begin{bmatrix} \cos \theta & -\sin \theta \\ \sin \theta & \cos \theta \end{bmatrix}, \quad \mathbf{x} = \begin{bmatrix} x_1 \\ x_2 \end{bmatrix}$$

Note that, in this case of rigid-body motion,  $\mathbf{J}$  is an orthogonal matrix.

**Displacement Vector Gradients**

As previously mentioned, in the case of general displacement,  $\mathbf{J}$  is not an orthogonal matrix because the lengths of the line segments do not remain constant. There are, however, motion types in which the determinant of  $\mathbf{J}$  remains constant, but  $\mathbf{J}$  is not an orthogonal matrix. As will be shown later in this book, the determinant of  $\mathbf{J}$  remains constant if the volume does not change as in the case of incompressible materials. This type of motion is called *isochoric*. Rigid-body motion is a special case of *isochoric motion*.

In the case of general displacement, the matrix of position vector gradients can also be written in terms of the displacement gradients by writing  $d\mathbf{r}$  using Equation 1 as follows:

$$d\mathbf{r} = \left( \mathbf{I} + \frac{\partial \mathbf{u}}{\partial \mathbf{x}} \right) d\mathbf{x} = (\mathbf{I} + \mathbf{J}_d) d\mathbf{x} \quad (2.11)$$

where  $\mathbf{J}_d = (\mathbf{J} - \mathbf{I})$  is the *matrix of the displacement vector gradients* defined as

$$\mathbf{J}_d = \frac{\partial \mathbf{u}}{\partial \mathbf{x}} = \begin{bmatrix} \frac{\partial u_1}{\partial x_1} & \frac{\partial u_1}{\partial x_2} & \frac{\partial u_1}{\partial x_3} \\ \frac{\partial u_2}{\partial x_1} & \frac{\partial u_2}{\partial x_2} & \frac{\partial u_2}{\partial x_3} \\ \frac{\partial u_3}{\partial x_1} & \frac{\partial u_3}{\partial x_2} & \frac{\partial u_3}{\partial x_3} \end{bmatrix} \quad (2.12)$$

In the analysis presented in this book, it is important to distinguish between the matrix of the position vector gradients and the matrix of the displacement vector gradients.

## 2.2 STRAIN COMPONENTS

The strain components defined in this section arise naturally when the equations of motion are formulated as will be shown in later chapters of this book. The strain components can be introduced by considering the elongation of a line element. The square of the length of the line element in the reference configuration is defined as

$$(l_o)^2 = d\mathbf{x}^T d\mathbf{x} \quad (2.13)$$

The square of the length of the line element in the current configuration can be defined using Equation 6 as

$$(l_d)^2 = d\mathbf{r}^T d\mathbf{r} = d\mathbf{x}^T \mathbf{J}^T \mathbf{J} d\mathbf{x} \quad (2.14)$$

One measure of the elongation of the line element can be written using the preceding two equations as

$$(l_d)^2 - (l_o)^2 = d\mathbf{r}^T d\mathbf{r} - d\mathbf{x}^T d\mathbf{x} = d\mathbf{x}^T (\mathbf{J}^T \mathbf{J} - \mathbf{I}) d\mathbf{x} \quad (2.15)$$

which can be written as

$$(l_d)^2 - (l_o)^2 = 2d\mathbf{x}^T \boldsymbol{\varepsilon} d\mathbf{x} \quad (2.16)$$

where  $\boldsymbol{\varepsilon}$  is the symmetric *Green–Lagrange strain tensor* defined as

$$\boldsymbol{\varepsilon} = \frac{1}{2}(\mathbf{J}^T \mathbf{J} - \mathbf{I}) \quad (2.17)$$

Using the definition of the matrix of position vector gradients, the Green–Lagrange strain tensor  $\boldsymbol{\varepsilon}$  can be written more explicitly as follows:

$$\boldsymbol{\varepsilon} = \frac{1}{2}(\mathbf{J}^T \mathbf{J} - \mathbf{I}) = \frac{1}{2} \begin{bmatrix} (\mathbf{r}_{x_1}^T \mathbf{r}_{x_1} - 1) & \mathbf{r}_{x_1}^T \mathbf{r}_{x_2} & \mathbf{r}_{x_1}^T \mathbf{r}_{x_3} \\ \mathbf{r}_{x_1}^T \mathbf{r}_{x_2} & (\mathbf{r}_{x_2}^T \mathbf{r}_{x_2} - 1) & \mathbf{r}_{x_2}^T \mathbf{r}_{x_3} \\ \mathbf{r}_{x_1}^T \mathbf{r}_{x_3} & \mathbf{r}_{x_2}^T \mathbf{r}_{x_3} & (\mathbf{r}_{x_3}^T \mathbf{r}_{x_3} - 1) \end{bmatrix} \quad (2.18)$$

One can also write the Green–Lagrange strain tensor  $\boldsymbol{\varepsilon}$  in terms of the elements of the matrix of the displacement vector gradients  $\mathbf{J}_d$ . Recall that  $\mathbf{J} = \mathbf{J}_d + \mathbf{I}$  and substituting in the definition of  $\boldsymbol{\varepsilon}$ , one obtains the following definition of the elements of the strain tensor:

$$\varepsilon_{ij} = \frac{1}{2} \left( u_{i,j} + u_{j,i} + \sum_{k=1}^3 u_{k,i} u_{k,j} \right), \quad i, j = 1, 2, 3 \quad (2.19)$$

In this equation,  $\varepsilon_{ij}$  are the elements of the tensor  $\boldsymbol{\varepsilon}$  and  $u_{i,j} = \partial u_i / \partial x_j$ ;  $i, j = 1, 2, 3$ . It is clear from the preceding two equations that the Green–Lagrange strains are nonlinear functions of the position vector and displacement vector gradients.

Because the strain tensor is symmetric, one can identify six independent strain components that can be used to define the following *strain vector*:

$$\boldsymbol{\varepsilon}_v = [\varepsilon_{11} \ \varepsilon_{22} \ \varepsilon_{33} \ \varepsilon_{12} \ \varepsilon_{13} \ \varepsilon_{23}]^T \quad (2.20)$$

In this vector,  $\varepsilon_{ij}$  for  $i=j$  are called *normal strains* and  $\varepsilon_{ij}$  for  $i \neq j$  are called the *shear strains*.

In the case of rigid-body motion,  $\mathbf{J}$  is an orthogonal matrix, and as a consequence,  $\boldsymbol{\varepsilon} = \mathbf{0}$ . This demonstrates that  $\boldsymbol{\varepsilon}$  can be used as a measure of the deformation, whereas  $\mathbf{J}$  cannot be used as deformation measure because it changes under an arbitrary rigid-body motion. In the case of rigid-body motion, the strains are identically zero. It is left to the reader as an exercise to show that if the nonlinear displacement gradient terms in Equation 19 are neglected, the Green–Lagrange strain tensor will not lead to zero strains under an arbitrary rigid-body motion.

### Geometric Interpretation of the Strains

The gradient vectors  $\mathbf{r}_{x_i}$ ,  $i = 1, 2, 3$ , define the rate of change of the position vector  $\mathbf{r}$  with respect to the coordinate  $x_i$ . Therefore, the normal strains,  $(\mathbf{r}_{x_i}^T \mathbf{r}_{x_i} - 1)$ , measure the change of the length of the gradient vectors. On the other hand, the shear strains,  $\mathbf{r}_{x_i}^T \mathbf{r}_{x_j}$ ,  $i \neq j$  measure the change of the relative orientation between the gradient vectors.

Another geometric interpretation of the strains can be provided for simple cases. To this end, the extension of the line element per unit length can be defined as

$$\varepsilon = \frac{l_d - l_o}{l_o} \quad (2.21)$$

This equation defines what is called *engineering strain* because the extension is divided by the length in the reference configuration. Another measure that can be used is the *logarithmic* or *natural strain* defined as  $\int_{l_o}^{l_d} dl/l = \ln(l_d/l_o)$ . Equation 21 leads to

$$l_d = (1 + \varepsilon)l_o \quad (2.22)$$

Using Equations 16 and 22, one can write the following quadratic equation for the strain  $\varepsilon$ :

$$\varepsilon^2 + 2\varepsilon - \alpha = 0 \quad (2.23)$$

where  $\alpha = 2\mathbf{t}^T \boldsymbol{\varepsilon} \mathbf{t}$ , and  $\mathbf{t} = d\mathbf{x}/l_o$ . Equation 23, which is a quadratic equation, has two solutions,  $\varepsilon = -1 \pm (1 + \alpha)^{1/2}$ . The second solution is not physically possible because it does not represent a rigid-body motion. Therefore, the strain  $\varepsilon$  can be evaluated using the components of the Green–Lagrange strain tensor as

$$\varepsilon = -1 + (1 + \alpha)^{1/2} \quad (2.24)$$

This equation can be used to provide a measure of the elongation of a line element.

Consider the special case in which  $d\mathbf{x} = [dx_1 \ 0 \ 0]^T$ ; one obtains in this special case from the definition of the Green–Lagrange strain tensor, the following equation:

$$(l_d)^2 - (l_o)^2 = 2\varepsilon_{11}(l_o)^2 \quad (2.25)$$

Using this equation, one has  $\varepsilon_{11} = \frac{1}{2} \{(1 + \varepsilon)^2 - 1\}$ , or  $\varepsilon = \sqrt{1 + 2\varepsilon_{11}} - 1$ . In the case of small strains, it can be shown that  $\varepsilon = \varepsilon_{11}$ . Because shear strains can be defined using the

dot product of vectors, these strains can always be defined in terms of angles or rotations. Therefore, a geometric interpretation of the shear strains can also be obtained.

### Example 2.3

For the beam defined in Example 1, the displacement field is given by

$$\mathbf{r} = s_1 \begin{bmatrix} e_1 \\ e_2 \end{bmatrix} + s_2 \begin{bmatrix} e_3 \\ e_4 \end{bmatrix} + s_3 \begin{bmatrix} e_5 \\ e_6 \end{bmatrix} + s_4 \begin{bmatrix} e_7 \\ e_8 \end{bmatrix} + s_5 \begin{bmatrix} e_9 \\ e_{10} \end{bmatrix} + s_6 \begin{bmatrix} e_{11} \\ e_{12} \end{bmatrix}$$

where the shape functions  $s_i$ ,  $i = 1, 2, \dots, 6$ , are defined in Example 1. Using the definitions of these shape functions, the vectors of gradients are

$$\mathbf{r}_{x_1} = \frac{\partial \mathbf{r}}{\partial x_1} = s_{1,1} \begin{bmatrix} e_1 \\ e_2 \end{bmatrix} + s_{2,1} \begin{bmatrix} e_3 \\ e_4 \end{bmatrix} + s_{3,1} \begin{bmatrix} e_5 \\ e_6 \end{bmatrix} + s_{4,1} \begin{bmatrix} e_7 \\ e_8 \end{bmatrix} + s_{5,1} \begin{bmatrix} e_9 \\ e_{10} \end{bmatrix} + s_{6,1} \begin{bmatrix} e_{11} \\ e_{12} \end{bmatrix}$$

and

$$\mathbf{r}_{x_2} = \frac{\partial \mathbf{r}}{\partial x_2} = s_{3,2} \begin{bmatrix} e_5 \\ e_6 \end{bmatrix} + s_{6,2} \begin{bmatrix} e_{11} \\ e_{12} \end{bmatrix}$$

where  $s_{i,j} = \partial s_i / \partial x_j$ , and  $i = 1, 2, \dots, 6$ ,  $j = 1, 2$ . Using these notations and the definitions given in Example 1, one has

$$\begin{aligned} s_{1,1} &= \frac{6}{l}(-\xi + \xi^2), & s_{2,1} &= (1 - 4\xi + 3\xi^2), & s_{3,1} &= -\eta, \\ s_{4,1} &= \frac{6}{l}(\xi - \xi^2), & s_{5,1} &= (-2\xi + 3\xi^2), & s_{6,1} &= \eta, \\ s_{3,2} &= (1 - \xi), & s_{6,2} &= \xi \end{aligned}$$

It is clear from these equations that

$$\begin{aligned} \begin{bmatrix} e_1 \\ e_2 \end{bmatrix} &= \mathbf{r}(\xi = 0), & \begin{bmatrix} e_3 \\ e_4 \end{bmatrix} &= \mathbf{r}_{x_1}(\xi = 0), & \begin{bmatrix} e_5 \\ e_6 \end{bmatrix} &= \mathbf{r}_{x_2}(\xi = 0) \\ \begin{bmatrix} e_7 \\ e_8 \end{bmatrix} &= \mathbf{r}(\xi = 1), & \begin{bmatrix} e_9 \\ e_{10} \end{bmatrix} &= \mathbf{r}_{x_1}(\xi = 1), & \begin{bmatrix} e_{11} \\ e_{12} \end{bmatrix} &= \mathbf{r}_{x_2}(\xi = 1) \end{aligned}$$

Consider the case in which the vector of coordinates is defined as

$$\mathbf{e} = [0 \ 0 \ 1 \ 0 \ 0 \ 1 \ l + \delta \ 0 \ 1 \ 0 \ 0 \ 1]^T$$

Here,  $l$  is the initial length of the beam, and  $\delta$  is the elongation at the end. Substituting this vector in the displacement field  $\mathbf{r} = \mathbf{S}\mathbf{e}$ , one obtains

$$\begin{aligned} \mathbf{r} &= \begin{bmatrix} x_1 + s_4 \delta \\ l \eta \end{bmatrix} = \begin{bmatrix} x_1 + \delta (3\xi^2 - 2\xi^3) \\ x_2 \end{bmatrix}, \\ \mathbf{r}_{x_1} &= \begin{bmatrix} 1 + \frac{6\delta}{l}(\xi - \xi^2) \\ 0 \end{bmatrix}, & \mathbf{r}_{x_2} &= \begin{bmatrix} 0 \\ 1 \end{bmatrix} \end{aligned}$$

These equations show that the maximum elongation occurs at  $\xi = 1$  and it is equal to  $\delta$ . The maximum gradient is at  $\xi = 0.5$  and is equal to  $1 + 1.5 (\delta/l)$ . The matrix of position vector gradients is

$$\mathbf{J} = \begin{bmatrix} 1 + \frac{6\delta}{l}\xi(1-\xi) & 0 \\ 0 & 1 \end{bmatrix}$$

The Green–Lagrange strain tensor can then be defined as

$$\boldsymbol{\varepsilon} = \frac{1}{2}(\mathbf{J}^T \mathbf{J} - \mathbf{I}) = \frac{1}{2} \begin{bmatrix} \frac{12\delta}{l}\xi(1-\xi) \left\{ 1 + 3 \left( \frac{\delta}{l} \right) \xi(1-\xi) \right\} & 0 \\ 0 & 0 \end{bmatrix}$$

This equation shows that the shear strains and the transverse normal strain are equal to zero, and the maximum normal strain in the axial direction occurs at  $\xi = 0.5$  and is equal to

$$(\varepsilon_{11})_{\max} = 1.5 \left( \frac{\delta}{l} \right) \left\{ 1 + 0.75 \left( \frac{\delta}{l} \right) \right\}$$

As will be discussed in later chapters of this book, elongation of a beam, as the one given in this example, leads to a change of the dimensions of the beam cross section and results in transverse normal stresses. This is due to the Poisson effect, which cannot be captured based on purely kinematic considerations.

A different strain distribution can be obtained if the vector of coordinates takes the following form:

$$\mathbf{e} = \begin{bmatrix} 0 & 0 & \left(1 + \frac{\delta}{l}\right) & 0 & 0 & 1 & l + \delta & 0 & \left(1 + \frac{\delta}{l}\right) & 0 & 0 & 1 \end{bmatrix}^T$$

In this case, one can show that

$$\mathbf{r} = \begin{bmatrix} (1 + \delta)\xi \\ l\eta \end{bmatrix}, \quad \mathbf{r}_{x_1} = \begin{bmatrix} 1 + \frac{\delta}{l} \\ 0 \end{bmatrix}, \quad \mathbf{r}_{x_2} = \begin{bmatrix} 0 \\ 1 \end{bmatrix}$$

Note that in this case the deformation at  $x_1 = 0$  is zero, and the deformation at  $x_1 = l$  is maximum and is equal to  $\delta$ . The Green–Lagrange strain tensor is defined in this case as

$$\boldsymbol{\varepsilon} = \frac{1}{2}(\mathbf{J}^T \mathbf{J} - \mathbf{I}) = \begin{bmatrix} \frac{\delta}{l} \left(1 + \frac{\delta}{2l}\right) & 0 \\ 0 & 0 \end{bmatrix}$$

This equation shows that the strain is constant everywhere. If  $\delta$  is small such that second-order terms in  $\delta$  can be neglected, the axial strain reduces to  $\delta/l$ , which defines the engineering strain.

## Eulerian Strain Tensor

Because  $d\mathbf{x}$  can be written as

$$d\mathbf{x} = \mathbf{J}^{-1} d\mathbf{r} = \frac{\partial \mathbf{x}}{\partial \mathbf{r}} d\mathbf{r}, \quad (2.26)$$

one can write

$$(l_d)^2 - (l_0)^2 = d\mathbf{r}^T d\mathbf{r} - d\mathbf{x}^T d\mathbf{x} = d\mathbf{r}^T (\mathbf{I} - \mathbf{J}^{-1T} \mathbf{J}^{-1}) d\mathbf{r} \quad (2.27)$$

Using this equation, the *Eulerian* or *Almansi strain tensor* is defined as

$$\boldsymbol{\varepsilon}_e = \frac{1}{2}(\mathbf{I} - \mathbf{J}^{-1\text{T}} \mathbf{J}^{-1}) \quad (2.28)$$

This tensor is also a symmetric tensor. It is important to note that the components of the Eulerian (Almansi) strain tensor are defined using the current configuration, whereas the components of the Green–Lagrange strain tensor are defined using the reference configuration. Such definitions are important when the expressions of the elastic forces due to deformation are developed. Clearly, the relationship between the Green–Lagrange strain tensor and the Eulerian strain tensor can be written as

$$\boldsymbol{\varepsilon} = \mathbf{J}^{\text{T}} \boldsymbol{\varepsilon}_e \mathbf{J} \quad (2.29)$$

This equation can be interpreted as  $\boldsymbol{\varepsilon}$  is the *pullback* of  $\boldsymbol{\varepsilon}_e$  by  $\mathbf{J}$ , or  $\boldsymbol{\varepsilon}_e$  is the *push-forward*, of  $\boldsymbol{\varepsilon}$  in the equation  $\boldsymbol{\varepsilon}_e = \mathbf{J}^{-1\text{T}} \boldsymbol{\varepsilon} \mathbf{J}^{-1}$ . In the case of *infinitesimal strains*, the Eulerian strain tensor is called *Cauchy strain tensor*. One can show that in the case of infinitesimal strains (small displacement gradients), one has

$$\boldsymbol{\varepsilon}_e = \boldsymbol{\varepsilon} = \frac{1}{2}(\mathbf{J}_d + \mathbf{J}_d^{\text{T}}) \quad (2.30)$$

That is, the Eulerian and Lagrangian strain tensors are equal in the case of infinitesimal strains.

#### Example 2.4

Consider again the displacement field defined in Example 1. Assume that the position vector of an arbitrary point on the beam is defined by the vector

$$\mathbf{r} = \begin{bmatrix} (l + \delta)\xi \cos \theta - l\eta \sin \theta \\ (l + \delta)\xi \sin \theta + l\eta \cos \theta \end{bmatrix}$$

where  $\delta$  is assumed to be the axial displacement of the beam at the end  $x_1 = l$  and  $\theta$  is an angle that defines the orientation of the beam. One can show that the values of the coordinates that lead to the position vector defined in the preceding equation are

$$\mathbf{e} = \begin{bmatrix} 0 & 0 & \left(1 + \frac{\delta}{l}\right) \cos \theta & \left(1 + \frac{\delta}{l}\right) \sin \theta & -\sin \theta & \cos \theta & (l + \delta) \cos \theta \\ (l + \delta) \sin \theta & \left(1 + \frac{\delta}{l}\right) \cos \theta & \left(1 + \frac{\delta}{l}\right) \sin \theta & -\sin \theta & \cos \theta \end{bmatrix}^{\text{T}}$$

The matrix of position vector gradients is given by

$$\mathbf{J} = \begin{bmatrix} \left(1 + \frac{\delta}{l}\right) \cos \theta & -\sin \theta \\ \left(1 + \frac{\delta}{l}\right) \sin \theta & \cos \theta \end{bmatrix}$$



Note that this matrix of position vector gradients can be written as the product of two matrices as

$$\mathbf{J} = \begin{bmatrix} \cos \theta & -\sin \theta \\ \sin \theta & \cos \theta \end{bmatrix} \begin{bmatrix} \left(1 + \frac{\delta}{l}\right) & 0 \\ 0 & 1 \end{bmatrix}$$

The inverse of the matrix of the position vector gradients is given by

$$\mathbf{J}^{-1} = \begin{bmatrix} \frac{l}{l + \delta} & 0 \\ 0 & 1 \end{bmatrix} \mathbf{R}^T$$

where  $\mathbf{R}$  is the orthogonal matrix

$$\mathbf{R} = \begin{bmatrix} \cos \theta & -\sin \theta \\ \sin \theta & \cos \theta \end{bmatrix}$$

The Green–Lagrange strain tensor is

$$\boldsymbol{\varepsilon} = \frac{1}{2}(\mathbf{J}^T \mathbf{J} - \mathbf{I}) = \begin{bmatrix} \frac{\delta}{l} \left( \frac{\delta}{2l} + 1 \right) & 0 \\ 0 & 0 \end{bmatrix}$$

This equation shows that the Green–Lagrange strain tensor does not depend on the orthogonal matrix  $\mathbf{R}$ .

The Eulerian strain tensor is

$$\boldsymbol{\varepsilon}_e = \frac{1}{2}(\mathbf{I} - \mathbf{J}^{-1T} \mathbf{J}^{-1}) = \frac{1}{2} \mathbf{R} \begin{bmatrix} 1 - \frac{1}{\left(1 + \frac{\delta}{l}\right)^2} & 0 \\ 0 & 0 \end{bmatrix} \mathbf{R}^T$$

It can be shown that when  $\delta$  and  $\theta$  are small, the Lagrangian and Eulerian strains are the same.

Let  $\mathbf{U}$  be the matrix

$$\mathbf{U} = \begin{bmatrix} \left(1 + \frac{\delta}{l}\right) & 0 \\ 0 & 1 \end{bmatrix}$$

With this definition, one can write  $d\mathbf{r} = \mathbf{J}d\mathbf{x} = \mathbf{R}\mathbf{U}d\mathbf{x}$ . Using the definition  $\mathbf{J} = \mathbf{R}\mathbf{U}$  and Equation 29, one can derive the expression for Green–Lagrange strain tensor previously obtained in this example from the Almansi strain tensor. Note that, in this simple example, the two tensors are not related by orthogonal transformation because the matrix  $\mathbf{U}$  enters into the relationship between the two tensors.

## 2.3 OTHER DEFORMATION MEASURES

Other deformation measures that are invariant under an arbitrary rigid-body motion can be used as alternatives to the Lagrangian and Eulerian strain tensors. In this section, some of these deformation measures are defined.

## Right and Left Cauchy–Green Deformation Tensors

In order to introduce alternate strain measures, a unit vector  $\mathbf{t}$  is defined as

$$\mathbf{t} = \frac{d\mathbf{x}}{l_0} = \frac{1}{l_0} [dx_1 \ dx_2 \ dx_3]^T \quad (2.31)$$

Using this definition, one can write

$$\left(\frac{l_d}{l_0}\right)^2 = \mathbf{t}^T \mathbf{J}^T \mathbf{J} \mathbf{t} = \mathbf{t}^T \mathbf{C}_r \mathbf{t} \quad (2.32)$$

where  $\mathbf{C}_r$  is a symmetric tensor called the *right Cauchy–Green deformation tensor* and is defined as

$$\mathbf{C}_r = \mathbf{J}^T \mathbf{J} \quad (2.33)$$

This tensor can be used as a measure of the deformation because in the case of an arbitrary rigid-body displacement  $\mathbf{C}_r = \mathbf{I}$ , and it remains constant throughout the rigid-body motion. The Green–Lagrange strain tensor can be expressed in terms of  $\mathbf{C}_r$  as

$$\boldsymbol{\varepsilon} = \frac{1}{2}(\mathbf{C}_r - \mathbf{I}) \quad (2.34)$$

That is, the tensors  $\mathbf{C}_r$  and  $\boldsymbol{\varepsilon}$  have a linear relationship. It follows that the derivatives of one tensor with respect to a set of coordinates can be used to define the derivatives of the other tensor with respect to the same coordinates. This linear relationship can be conveniently used when different constitutive models are used. Some of these constitutive models are expressed in terms of  $\boldsymbol{\varepsilon}$ , whereas the others are expressed in terms of  $\mathbf{C}_r$ .

Another deformation measure is the *left Cauchy–Green deformation tensor*  $\mathbf{C}_l$  defined as

$$\mathbf{C}_l = \mathbf{J} \mathbf{J}^T \quad (2.35)$$

This tensor also remains constant and is equal to the identity matrix in the case of rigid-body motion. The Eulerian strain tensor can be written in terms of  $\mathbf{C}_l$  as

$$\boldsymbol{\varepsilon}_e = \frac{1}{2}(\mathbf{I} - \mathbf{C}_l^{-1}) \quad (2.36)$$

## Infinitesimal Strain Tensor

It was previously mentioned that in the case of small strains, the Lagrangian and Eulerian strain tensors are the same and both are defined by the equation  $\boldsymbol{\varepsilon}_e = \boldsymbol{\varepsilon} = (1/2)(\mathbf{J}_d + \mathbf{J}_d^T)$ . In this equation,  $\mathbf{J}_d$  is the matrix of displacement vector gradients. It is important, however, to point out at this point that the *infinitesimal strain tensor* is not an exact measure of the deformation because it does not remain constant in the case of an arbitrary rigid-body motion. Recall that in the case of a rigid-body motion  $\mathbf{J} = \mathbf{J}_d + \mathbf{I}$  is an orthogonal matrix. It follows that in the case of infinitesimal strains,

$$\boldsymbol{\varepsilon}_e = \boldsymbol{\varepsilon} = \frac{1}{2}(\mathbf{J}_d + \mathbf{J}_d^T) = \frac{1}{2}(\mathbf{J} + \mathbf{J}^T - 2\mathbf{I}) \quad (2.37)$$

This equation shows that the linear form of the strain tensors does not remain constant under an arbitrary rigid-body motion because  $\mathbf{J}$  changes, as previously discussed. In order to provide

an estimate of the errors as the result of using the infinitesimal strain tensor in the case of general rigid-body motion, we use the expression of the rotation matrix defined by *Rodriguez formula*. In the case of a rigid-body motion,  $\mathbf{J}$  is the rotation matrix that can be defined using Rodriguez formula as follows:

$$\mathbf{J} = \mathbf{I} + \tilde{\mathbf{a}} \sin \theta + 2(\tilde{\mathbf{a}})^2 \sin^2 \frac{\theta}{2} \quad (2.38)$$

where  $\tilde{\mathbf{a}}$  is the skew-symmetric matrix associated with a unit vector  $\mathbf{a}$  along the axis of rotation and  $\theta$  is the angle of rotation (Shabana, 2013). Substituting the preceding equation into the expression of the infinitesimal strain tensor and considering the fact that  $\tilde{\mathbf{a}}$  is a skew-symmetric matrix and  $(\tilde{\mathbf{a}})^2$  is a symmetric matrix, one has

$$\boldsymbol{\varepsilon}_e = \boldsymbol{\varepsilon} = 2(\tilde{\mathbf{a}})^2 \sin^2 \frac{\theta}{2} \quad (2.39)$$

Because the components of the unit vector  $\mathbf{a}$  can be equal to or less than one, the preceding equation shows that in the case of infinitesimal rotations, the error in the infinitesimal strain tensor is of second order in the rotation  $\theta$ .

## 2.4 DECOMPOSITION OF DISPLACEMENT

Using the *polar decomposition theorem* discussed in Chapter 1, any nonsingular square matrix can be written as the product of two matrices; one is an orthogonal matrix, whereas the other is a symmetric matrix. Applying this decomposition to the matrix of position vector gradients  $\mathbf{J}$ , one obtains

$$\mathbf{J} = \mathbf{A}_J \mathbf{J}_r = \mathbf{J}_l \mathbf{A}_J \quad (2.40)$$

where  $\mathbf{A}_J$  is an orthogonal *rotation matrix*, and  $\mathbf{J}_r$  and  $\mathbf{J}_l$  are symmetric positive definite matrices called, respectively, the *right stretch* and *left stretch tensors*. It follows from the preceding equation that

$$\mathbf{J}_r = \mathbf{A}_J^T \mathbf{J}_l \mathbf{A}_J, \quad \mathbf{J}_l = \mathbf{A}_J \mathbf{J}_r \mathbf{A}_J^T \quad (2.41)$$

The right and left Cauchy–Green strain tensors  $\mathbf{C}_r$  and  $\mathbf{C}_l$  can be expressed, respectively, in terms of  $\mathbf{J}_r$  and  $\mathbf{J}_l$  as follows:

$$\left. \begin{aligned} \mathbf{C}_r &= \mathbf{J}^T \mathbf{J} = \mathbf{J}_r \mathbf{A}_J^T \mathbf{A}_J \mathbf{J}_r = \mathbf{J}_r^2 \\ \mathbf{C}_l &= \mathbf{J} \mathbf{J}^T = \mathbf{J}_l \mathbf{A}_J \mathbf{A}_J^T \mathbf{J}_l = \mathbf{J}_l^2 \end{aligned} \right\} \quad (2.42)$$

Therefore,  $\mathbf{C}_r$  is equivalent to  $\mathbf{J}_r$ , whereas  $\mathbf{C}_l$  is equivalent to  $\mathbf{J}_l$ . It is, however, easier and more efficient to calculate  $\mathbf{C}_r$  and  $\mathbf{C}_l$  for a given  $\mathbf{J}$  than to evaluate  $\mathbf{J}_r$  and  $\mathbf{J}_l$  from the polar decomposition theorem.

Equation 42 shows that the deformation measures  $\mathbf{C}_r$  and  $\mathbf{C}_l$  do not depend on the orthogonal matrix  $\mathbf{A}_J$ . The expression of  $\mathbf{C}_r$  in the preceding equation with Equation 34 also shows that the Green–Lagrange strain tensor  $\boldsymbol{\varepsilon}$  does not depend on the orthogonal matrix  $\mathbf{A}_J$  because it can be written as  $\boldsymbol{\varepsilon} = (1/2)(\mathbf{J}_r^2 - \mathbf{I})$ . Similarly, the Eulerian strain tensor of Equation 36 can be written as  $\boldsymbol{\varepsilon}_e = (1/2)(\mathbf{I} - (\mathbf{J}_l^{-1})^2)$ .

## Homogeneous Motion

In the special case of *homogeneous motion*, the matrix of position vector gradients  $\mathbf{J}$  is assumed to be independent of the coordinates  $\mathbf{x}$ . In this special case, one can write  $\mathbf{r} = \mathbf{J}\mathbf{x}$ . The motion of the body from the initial configuration  $\mathbf{x}$  to the final configuration  $\mathbf{r}$  can be viewed as two successive homogeneous motions. In the first motion, the coordinate vector  $\mathbf{x}$  changes to  $\mathbf{x}_i$ , and in the second motion, the coordinate vector  $\mathbf{x}_i$  changes to  $\mathbf{r}$ . These two displacements can be described using the two equations  $\mathbf{x}_i = \mathbf{J}_r \mathbf{x}$ , and  $\mathbf{r} = \mathbf{A}_J \mathbf{x}_i$ . Clearly, these two equations lead to  $\mathbf{r} = \mathbf{A}_J \mathbf{x}_i = \mathbf{A}_J \mathbf{J}_r \mathbf{x} = \mathbf{J} \mathbf{x}$ . Therefore, any homogeneous displacement can be decomposed into a deformation described by the tensor  $\mathbf{J}_r$  followed by a rotation described by the orthogonal tensor  $\mathbf{A}_J$ . Similarly, if  $\mathbf{J}_l$  is used instead of  $\mathbf{J}_r$ , the displacement of the body can be considered as a rotation described by the orthogonal tensor  $\mathbf{A}_J$  followed by a deformation defined by the tensor  $\mathbf{J}_l$ .

## Nonhomogeneous Motion

In the case of *nonhomogeneous motion*, the relationship between the coordinates can be written as  $d\mathbf{r} = \mathbf{J}d\mathbf{x}$ . Although  $\mathbf{J}$  in this case is a function of the reference coordinates  $\mathbf{x}$ , the polar decomposition theorem can still be applied. Different material points in this case have different decompositions and different stretch and rotation tensors.

### Example 2.5

For the model used in Example 4, the matrix of position vector gradients was defined as

$$\mathbf{J} = \begin{bmatrix} \left(1 + \frac{\delta}{l}\right) \cos \theta & -\sin \theta \\ \left(1 + \frac{\delta}{l}\right) \sin \theta & \cos \theta \end{bmatrix}$$

This matrix can be written as

$$\mathbf{J} = \mathbf{A}_J \mathbf{J}_r = \begin{bmatrix} \cos \theta & -\sin \theta \\ \sin \theta & \cos \theta \end{bmatrix} \begin{bmatrix} \left(1 + \frac{\delta}{l}\right) & 0 \\ 0 & 1 \end{bmatrix}$$

where

$$\mathbf{A}_J = \begin{bmatrix} \cos \theta & -\sin \theta \\ \sin \theta & \cos \theta \end{bmatrix}, \quad \mathbf{J}_r = \begin{bmatrix} \left(1 + \frac{\delta}{l}\right) & 0 \\ 0 & 1 \end{bmatrix}$$

The matrix  $\mathbf{J}_l$  is defined as

$$\mathbf{J}_l = \mathbf{A}_J \mathbf{J}_r \mathbf{A}_J^T = \begin{bmatrix} \left(1 + \frac{\delta}{l} \cos^2 \theta\right) & \frac{\delta}{2l} \sin 2\theta \\ \frac{\delta}{2l} \sin 2\theta & \left(1 + \frac{\delta}{l} \sin^2 \theta\right) \end{bmatrix}$$

It follows that the right Cauchy–Green strain tensor is

$$\mathbf{C}_r = \mathbf{J}_r^2 = \begin{bmatrix} \left(1 + \frac{\delta}{l}\right)^2 & 0 \\ 0 & 1 \end{bmatrix}$$

The left Cauchy–Green strain tensor is

$$\mathbf{C}_l = \mathbf{J}_l^2 = \begin{bmatrix} \left(1 + \frac{\delta}{l}\right)^2 \cos^2 \theta + \sin^2 \theta & \frac{\delta}{2l} \left(2 + \frac{\delta}{l}\right) \sin 2\theta \\ \frac{\delta}{2l} \left(2 + \frac{\delta}{l}\right) \sin 2\theta & \left(1 + \frac{\delta}{l}\right)^2 \sin^2 \theta + \cos^2 \theta \end{bmatrix}$$

## 2.5 VELOCITY AND ACCELERATION

The absolute velocity vector can be obtained by differentiation of  $\mathbf{r} = \mathbf{r}(\mathbf{x}, t)$  with respect to time. This leads to

$$\mathbf{v} = \dot{\mathbf{r}} = \frac{d\mathbf{r}(\mathbf{x}, t)}{dt} = \frac{d\mathbf{u}(\mathbf{x}, t)}{dt} = \dot{\mathbf{u}} \quad (2.43)$$

In developing this equation for the velocity, the vector  $\mathbf{x}$  is assumed to be independent of time because it defines the position of the material points in the reference configuration. In fluid mechanics, the curl of the velocity given by  $\nabla \times \mathbf{v}$  is called the *vorticity*. In this definition,  $\nabla = [\partial/\partial r_1 \quad \partial/\partial r_2 \quad \partial/\partial r_3]^T$ . In the case of *irrotational flow*, the vorticity is equal to zero everywhere.

The absolute acceleration vector  $\mathbf{a}(\mathbf{x}, t)$  is the rate of change of the velocity of the material points with respect to time. The acceleration vector can then be written as

$$\mathbf{a}(\mathbf{x}, t) = \dot{\mathbf{v}} = \frac{d\mathbf{v}(\mathbf{x}, t)}{dt} = \frac{d^2\mathbf{u}(\mathbf{x}, t)}{dt^2} = \ddot{\mathbf{u}} \quad (2.44)$$

In deriving this equation, it is assumed again that the vector  $\mathbf{x}$  is not a function of time.

As previously mentioned in this chapter, one can, without any loss of generality, select a coordinate system, the *floating frame of reference*, that follows the motion of the body. In this case, the position of an arbitrary point on the body is described by the global position of the origin of the floating frame plus the position of the arbitrary point with respect to the floating frame. In this case, as previously explained, the global position of a point on the body can be written as  $\mathbf{r} = \mathbf{r}_O(t) + \mathbf{A}(\mathbf{x} + \bar{\mathbf{u}}_f(\mathbf{x}, t))$ , where  $\mathbf{r}_O(t)$  is the global position of the body reference,  $\mathbf{A}$  is the orthogonal transformation matrix that defines the orientation of the body coordinate system in the global system, and  $\bar{\mathbf{u}}_f(\mathbf{x}, t)$  is the vector of deformation with respect to the body coordinate system. Differentiating the vector  $\mathbf{r}$  once and twice with respect to time, one obtains, respectively, the absolute velocity and acceleration vectors of the arbitrary point. Using this motion description, the velocity and acceleration vectors include terms that represent the rate of change of the motion of the arbitrary point with respect to the origin of the floating frame. These terms include the *Coriolis acceleration*, as discussed in more detail in Chapter 6.

## Eulerian Description

The velocity vector can also be expressed in terms of the spatial (Eulerian) coordinates as  $\mathbf{v} = \mathbf{v}(\mathbf{r}, t)$ . In this case,  $\mathbf{r}$  is a function of time. The total derivative of this expression of the velocity is given by

$$\frac{d\mathbf{v}}{dt} = \frac{\partial \mathbf{v}}{\partial \mathbf{r}} \frac{d\mathbf{r}}{dt} + \frac{\partial \mathbf{v}}{\partial t} = \frac{\partial \mathbf{v}}{\partial \mathbf{r}} \mathbf{v} + \frac{\partial \mathbf{v}}{\partial t} \quad (2.45)$$

The term  $(\partial \mathbf{v} / \partial \mathbf{r}) \mathbf{v}$  is called the *convective* or *transport term*, while  $\partial \mathbf{v} / \partial t$  is called the spatial time derivative. The preceding equation can also be written as

$$\frac{d\mathbf{v}}{dt} = \mathbf{L} \mathbf{v} + \frac{\partial \mathbf{v}}{\partial t} \quad (2.46)$$

where  $\mathbf{L}$  is called the *velocity gradient tensor* and is defined as

$$\mathbf{L} = \frac{\partial \mathbf{v}}{\partial \mathbf{r}} \quad (2.47)$$

Note that the velocity gradient tensor is obtained by differentiation with respect to the spatial coordinates.

## Rate of Deformation and Spin Tensors

Another strain measure considered in this section is called the *rate of deformation tensor*. The rate of deformation tensor  $\mathbf{D}$ , which is also called the *velocity strain* and is used in the formulation of some material constitutive laws, differs from Green–Lagrange strain tensor, which is a measure of the deformation and not the rate of deformation. In order to define the rate of deformation tensor, the velocity gradient tensor is written as the sum of a symmetric tensor and a skew-symmetric tensor as follows:

$$\mathbf{L} = \frac{1}{2} (\mathbf{L} + \mathbf{L}^T) + \frac{1}{2} (\mathbf{L} - \mathbf{L}^T) \quad (2.48)$$

The first matrix on the right-hand side of this equation is symmetric and is called the *rate of deformation tensor*  $\mathbf{D}$ , whereas the second matrix is a skew-symmetric matrix called the *spin tensor*  $\mathbf{W}$ . The preceding equation can then be written as

$$\mathbf{L} = \mathbf{D} + \mathbf{W} \quad (2.49)$$

where

$$\mathbf{D} = \frac{1}{2} (\mathbf{L} + \mathbf{L}^T), \quad \mathbf{W} = \frac{1}{2} (\mathbf{L} - \mathbf{L}^T) \quad (2.50)$$

The rate of deformation tensor  $\mathbf{D}$  can be used as a measure of the deformation because it vanishes in the case of a rigid-body motion. In order to demonstrate this fact, the rate of change of the square of the length of the line segment is considered. This change can be written as

$$\frac{d}{dt} (l_d)^2 = \frac{d}{dt} (d\mathbf{r}^T d\mathbf{r}) = 2d\mathbf{r}^T d\mathbf{v} = 2d\mathbf{r}^T \frac{\partial \mathbf{v}}{\partial \mathbf{r}} d\mathbf{r} = 2d\mathbf{r}^T \mathbf{L} d\mathbf{r} \quad (2.51)$$

Using the definition of the matrix of the velocity gradients in terms of the rate of deformation and spin tensors, one obtains

$$\frac{d}{dt}(l_d)^2 = 2d\mathbf{r}^T(\mathbf{D} + \mathbf{W})d\mathbf{r} \quad (2.52)$$

Because  $\mathbf{W}$  is a skew-symmetric matrix,  $d\mathbf{r}^T\mathbf{W}d\mathbf{r} = 0$ , and as a result, the preceding equation reduces to

$$\frac{d}{dt}(l_d)^2 = 2d\mathbf{r}^T\mathbf{D}d\mathbf{r} \quad (2.53)$$

Because  $d\mathbf{r}$  is arbitrary, the preceding equation shows that in the case of rigid-body motion the rate of deformation tensor  $\mathbf{D}$  is identically zero and such a tensor can indeed be used as a measure of the rate of deformation. The preceding equation also shows that

$$(\dot{l}_d/l_d) = \mathbf{t}_c^T\mathbf{D}\mathbf{t}_c \quad (2.54)$$

where  $\mathbf{t}_c = d\mathbf{r}/l_d$  defines a unit vector.

### Rate of Change of the Green–Lagrange Strain

A relationship between the rate of deformation tensor and the rate of change of the Green–Lagrange strain tensor can be obtained. To obtain this relationship, the tensor of velocity vector gradients is written as

$$\mathbf{L} = \frac{\partial \mathbf{v}}{\partial \mathbf{r}} = \frac{\partial \mathbf{v}}{\partial \mathbf{x}} \frac{\partial \mathbf{x}}{\partial \mathbf{r}} = \mathbf{J}\mathbf{J}^{-1} \quad (2.55)$$

Using this equation, the rate of deformation tensor can be written as

$$\mathbf{D} = \frac{1}{2}(\mathbf{L} + \mathbf{L}^T) = \frac{1}{2}(\mathbf{J}\mathbf{J}^{-1} + \mathbf{J}^{-1^T}\mathbf{J}^T) \quad (2.56)$$

Differentiation of the Green–Lagrange strain tensor leads to

$$\dot{\boldsymbol{\epsilon}} = \frac{d}{dt} \left\{ \frac{1}{2}(\mathbf{J}^T\mathbf{J} - \mathbf{I}) \right\} = \frac{1}{2}(\mathbf{J}^T\dot{\mathbf{J}} - \dot{\mathbf{J}}^T\mathbf{J}) \quad (2.57)$$

The preceding two equations show that

$$\dot{\boldsymbol{\epsilon}} = \mathbf{J}^T\mathbf{D}\mathbf{J} \quad (2.58)$$

This equation is another example of a pullback operation in which a tensor associated with the undeformed configuration is defined using a tensor associated with the deformed or current configuration. The preceding equation also leads to  $\mathbf{D} = \mathbf{J}^{-1^T}\dot{\boldsymbol{\epsilon}}\mathbf{J}^{-1}$ , which is an example of a push-forward operation in which a tensor in the deformed (current) configuration is obtained using a tensor associated with the undeformed (reference) configuration. Here, the push-forward operation is simply the result of pushing forward the Lagrangian vector  $d\mathbf{x}$  to the Eulerian vector  $d\mathbf{r}$  using the Jacobian matrix  $\mathbf{J}$  as shown in Equation 6. On the other

hand, the pullback of the Eulerian vector  $d\mathbf{r}$  to the reference configuration using  $\mathbf{J}^{-1}$  defines the Lagrangian vector  $d\mathbf{x}$  as  $d\mathbf{x} = \mathbf{J}^{-1}d\mathbf{r}$ . The relationship between the rate of deformation tensor and the Green–Lagrange strain tensor is an example of the push-forward and pullback operations. Other examples are presented in the literature (Belytschko et al., 2000).

Another way of defining the relationship between the rate of deformation tensor and the rate of change of the Green–Lagrange strain tensor is to use the function relationship between  $\mathbf{r}$  and  $\mathbf{x}$ . To this end, we write

$$\dot{\epsilon} = \frac{d}{dt} \left\{ \frac{1}{2} (\mathbf{J}^T \mathbf{J} - \mathbf{I}) \right\} = \frac{1}{2} (\mathbf{J}^T \dot{\mathbf{J}} + \dot{\mathbf{J}}^T \mathbf{J}) = \frac{1}{2} \left( \mathbf{J}^T \frac{\partial \mathbf{v}}{\partial \mathbf{x}} + \left( \frac{\partial \mathbf{v}}{\partial \mathbf{x}} \right)^T \mathbf{J} \right) \quad (2.59)$$

Because

$$\frac{\partial \mathbf{v}}{\partial \mathbf{x}} = \frac{\partial \mathbf{v}}{\partial \mathbf{r}} \frac{\partial \mathbf{r}}{\partial \mathbf{x}} = \mathbf{L} \mathbf{J}, \quad (2.60)$$

one has

$$\dot{\epsilon} = \frac{1}{2} (\mathbf{J}^T \mathbf{L} \mathbf{J} + (\mathbf{L} \mathbf{J})^T \mathbf{J}) = \frac{1}{2} (\mathbf{J}^T \mathbf{L} \mathbf{J} + \mathbf{J}^T \mathbf{L}^T \mathbf{J}) = \frac{1}{2} \mathbf{J}^T (\mathbf{L} + \mathbf{L}^T) \mathbf{J} = \mathbf{J}^T \mathbf{D} \mathbf{J} \quad (2.61)$$

as previously obtained. Note that  $\dot{\epsilon}$  and  $\mathbf{D}$  are not related by orthogonal tensor transformation and, therefore, they do not represent the same physical variables. Furthermore, it is important to point out that the time integral of  $\dot{\epsilon}$  is path independent, whereas the time integral of  $\mathbf{D}$  is path dependent. It is also important to keep in mind that the rate of deformation tensor is not the time derivative of the Eulerian (Almansi) strain tensor.

### Example 2.6

One can show that the position vector given in Example 4 can be written as

$$\mathbf{r} = \mathbf{r}(\mathbf{x}, t) = \mathbf{R} \mathbf{C}_1 \begin{bmatrix} x_1 \\ x_2 \end{bmatrix} = \mathbf{R} \mathbf{C}_1 \mathbf{x}$$

where the diagonal matrix  $\mathbf{C}_1 = \mathbf{J}_r$  and the orthogonal matrix  $\mathbf{R} = \mathbf{A}_r$  are given by

$$\mathbf{C}_1 = \begin{bmatrix} \left(1 + \frac{\delta}{l}\right) & 0 \\ 0 & 1 \end{bmatrix}, \quad \mathbf{R} = \begin{bmatrix} \cos \theta & -\sin \theta \\ \sin \theta & \cos \theta \end{bmatrix}$$

It is clear that the matrix of position vector gradients is given in this example as

$$\mathbf{J} = \mathbf{R} \mathbf{C}_1$$

Using these equations, one can write the material (Lagrangian) coordinates  $\mathbf{x}$  in terms of the spatial (Eulerian) coordinates as

$$\mathbf{x} = \mathbf{x}(\mathbf{r}, t) = \mathbf{C}_1^{-1} \mathbf{R}^T \begin{bmatrix} r_1 \\ r_2 \end{bmatrix} = \mathbf{C}_1^{-1} \mathbf{R}^T \mathbf{r}$$



Assuming that the deformation  $\delta$  remains constant (constant strain), the velocity vector  $\mathbf{v}$  is given by

$$\mathbf{v} = \dot{\mathbf{r}}(\mathbf{x}, t) = \dot{\mathbf{R}}\mathbf{C}_1\mathbf{x}$$

The acceleration vector is

$$\mathbf{a} = \ddot{\mathbf{r}}(\mathbf{x}, t) = \ddot{\mathbf{R}}\mathbf{C}_1\mathbf{x}$$

where

$$\dot{\mathbf{R}} = \dot{\theta} \left( \frac{\partial \mathbf{R}}{\partial \theta} \right) = \dot{\theta} \mathbf{R}_\theta, \quad \ddot{\mathbf{R}} = \ddot{\theta} \mathbf{R}_\theta - \dot{\theta}^2 \mathbf{R}$$

Clearly, the velocity vector can be written in terms of the Eulerian coordinate vector  $\mathbf{r}$  as

$$\mathbf{v} = \dot{\mathbf{r}}(\mathbf{x}, t) = \dot{\mathbf{R}}\mathbf{R}^T\mathbf{r}$$

The tensor of velocity vector gradients  $\mathbf{L}$  can then be defined as

$$\mathbf{L} = \dot{\mathbf{R}}\mathbf{R}^T$$

The symmetric rate of deformation tensor and the skew-symmetric spin tensor are given by

$$\mathbf{D} = \frac{1}{2} (\dot{\mathbf{R}}\mathbf{R}^T + \mathbf{R}\dot{\mathbf{R}}^T), \quad \mathbf{W} = \frac{1}{2} (\dot{\mathbf{R}}\mathbf{R}^T - \mathbf{R}\dot{\mathbf{R}}^T)$$

Direct matrix multiplication shows that

$$\dot{\mathbf{R}}\mathbf{R}^T = \dot{\theta} \begin{bmatrix} 0 & -1 \\ 1 & 0 \end{bmatrix}$$

Because  $\dot{\mathbf{R}}\mathbf{R}^T$  is a skew-symmetric matrix, one has  $\dot{\mathbf{R}}\mathbf{R}^T = -(\dot{\mathbf{R}}\mathbf{R}^T)^T = -\mathbf{R}\dot{\mathbf{R}}^T$ . It follows that

$$\mathbf{D} = \mathbf{0}, \quad \mathbf{W} = \dot{\mathbf{R}}\mathbf{R}^T = \dot{\theta} \begin{bmatrix} 0 & -1 \\ 1 & 0 \end{bmatrix}$$

The results that  $\mathbf{D} = \mathbf{0}$  is expected because the Green–Lagrange strain tensor is considered constant in time as the result of the assumption made in this example that the elongation of the beam remains constant during the beam rotation. Clearly, if the elongation is time dependent,  $\mathbf{D}$  will be different from zero. This more general case is left to the reader as an exercise.

## 2.6 COORDINATE TRANSFORMATION

As discussed in Chapter 1, the gradients defined by differentiation with respect to a set of coordinates  $x_1, x_2$ , and  $x_3$  represent changes of the position vector along these coordinate lines. The rate of change of the position vector with respect to one set of coordinates differs from the rate of change of this vector with respect to another set of coordinates. Although the two sets of coordinates can be related by a transformation, the change of the set of coordinates does not

change the coordinate system in which the position vector or the gradient vectors are defined. In fact, the gradient vectors obtained by differentiation of the vector  $\mathbf{r}$  with respect to one set of coordinates can be written as a linear combination of the gradient vectors obtained by differentiation of  $\mathbf{r}$  with respect to another set of coordinates, as discussed in Chapter 1. That is, the two sets of gradient vectors are defined in the same coordinate system. Nonetheless, the strain components defined by the two different sets of gradients give measures of deformations along two different sets of directions.

In one-dimensional problems, as in the case of Euler–Bernoulli beams, there is one gradient vector that defines the tangent to a space curve. Change of the scalar coordinate  $\alpha$  used to define the gradient vector  $\mathbf{r}_\alpha$  does not change the orientation of this tangent vector because any selected coordinate  $\alpha$  differs from another coordinate  $\beta$  by a scalar multiplier. It follows that  $\mathbf{r}_\alpha = \mathbf{r}_\beta (\partial\beta/\partial\alpha)$  which implies that  $\mathbf{r}_\alpha$  and  $\mathbf{r}_\beta$  are parallel vectors. In this case of a one-dimensional problem,  $(\mathbf{r}_\alpha^T \mathbf{r}_\alpha - 1)$  will always define the strain along the tangent to the centerline of the beam regardless of what the coordinate  $\alpha$  represents. Furthermore, this tangent remains defined in the same coordinate system in which the vector  $\mathbf{r}$  is defined. In two-dimensional problems, as in the case of plates, change of the coordinates can lead to a change in the direction of the two resulting gradient vectors. Nonetheless, the two gradient vectors remain tangent to the surface at the point they are evaluated regardless of the coordinates used to define these gradient vectors. In the three-dimensional case, the change of coordinates can lead to a more general change in the orientation of the gradient vectors, as discussed in Chapter 1.

In continuum mechanics, it is important to understand the rules that govern the coordinate (parameter) transformation because this transformation defines the coordinate lines along which the strain components are measured. In order to develop this transformation, we consider two sets of coordinates  $\mathbf{x} = [x_1 \ x_2 \ x_3]^T$  and  $\bar{\mathbf{x}} = [\bar{x}_1 \ \bar{x}_2 \ \bar{x}_3]^T$  associated with two coordinate systems  $X_1 X_2 X_3$  and  $\bar{X}_1 \bar{X}_2 \bar{X}_3$ , respectively. These two sets of coordinate lines are used for the same configuration of the continuum. The relationship between these two sets of coordinates can be written as  $\mathbf{x} = \mathbf{A}\bar{\mathbf{x}}$ , where  $\mathbf{A}$  is the transformation matrix that defines the relationship between the two sets of coordinate lines. The absolute position vector  $\mathbf{r}$  can be written in terms of  $\mathbf{x}$  or in terms of  $\bar{\mathbf{x}}$ . That is,  $\mathbf{r} = \mathbf{r}(x_1 \ x_2 \ x_3) = \mathbf{r}(\bar{x}_1 \ \bar{x}_2 \ \bar{x}_3)$ . The matrix of the position vector gradients (Jacobian matrix) can then be written by differentiation of the vector  $\mathbf{r}$  with respect to  $\mathbf{x}$  or with respect to  $\bar{\mathbf{x}}$ . One can therefore write the following equation:

$$\mathbf{J} = \frac{\partial \mathbf{r}}{\partial \mathbf{x}} = \frac{\partial \mathbf{r}}{\partial \bar{\mathbf{x}}} \frac{\partial \bar{\mathbf{x}}}{\partial \mathbf{x}} = \frac{\partial \mathbf{r}}{\partial \bar{\mathbf{x}}} \mathbf{A}^T \quad (2.62)$$

That is, the gradients of the vectors  $\mathbf{r}$  defined by differentiation with respect to coordinate lines along the axes of the coordinate system  $\bar{X}_1 \bar{X}_2 \bar{X}_3$  are defined as

$$\bar{\mathbf{J}} = \frac{\partial \mathbf{r}}{\partial \bar{\mathbf{x}}} = \mathbf{J} \mathbf{A} = \frac{\partial \mathbf{r}}{\partial \mathbf{x}} \mathbf{A} \quad (2.63)$$

This rule of position vector gradient transformation is crucial in developing the finite element formulation presented in Chapter 5. Note that in the preceding equation,  $\mathbf{r}$  is still the vector that defines the position vector of the material points, say in the  $X_1 X_2 X_3$  coordinate system. It follows that the columns of the matrices  $\mathbf{r}_x = \partial \mathbf{r} / \partial \mathbf{x}$  and  $\mathbf{r}_{\bar{x}} = \partial \mathbf{r} / \partial \bar{\mathbf{x}}$  are vectors defined

in the  $X_1X_2X_3$  coordinate system. In Chapter 5, finite elements that do not have a complete set of gradient vectors are considered. These finite elements are referred to as *gradient deficient*.

### Strain Transformation

Using the gradient transformation developed in this section and the definition of the strains in terms of the gradients, one can show that the Green–Lagrange strains along the coordinate lines  $\bar{x}_1$ ,  $\bar{x}_2$ , and  $\bar{x}_3$  can be written as

$$\bar{\epsilon} = \frac{1}{2} (\bar{\mathbf{J}}^T \bar{\mathbf{J}} - \mathbf{I}) = \mathbf{A}^T \epsilon \mathbf{A} \quad (2.64)$$

where  $\mathbf{A}$  is again the matrix that defines the relationship between the coordinates  $\bar{x}_1$ ,  $\bar{x}_2$ , and  $\bar{x}_3$  and  $x_1$ ,  $x_2$ , and  $x_3$ . The same results can be obtained by using the transformation for the line element,  $d\mathbf{x} = \mathbf{A} d\bar{\mathbf{x}}$ . Substituting this equation into the equation that defines the square of the length of the line element, one obtains the expressions for the transformed strains given by Equation 64.

### Gradients and Strains

By definition,  $\mathbf{r}_{x_i} = \{\mathbf{r}(x_i + \Delta x_i) - \mathbf{r}(x_i)\} / \Delta x_i$ ,  $i = 1, 2, 3$ . This equation shows again that  $\mathbf{r}_{x_i}$ , which measures the change of the vector  $\mathbf{r}$  along the coordinate line  $x_i$ , is defined in the same reference frame as the one used to define the vector  $\mathbf{r}$ , as previously stated. Nonetheless, the change of the coordinates from  $\mathbf{x}$  to  $\bar{\mathbf{x}}$  can lead to another set of gradient vectors  $\mathbf{r}_{\bar{x}}$  because the vector  $\{\mathbf{r}(\bar{x}_i + \Delta \bar{x}_i) - \mathbf{r}(\bar{x}_i)\}$  can have different length and/or orientation from the vector  $\{\mathbf{r}(x_i + \Delta x_i) - \mathbf{r}(x_i)\}$ . It follows that the normal strain components  $\epsilon_{ii} = (\mathbf{r}_{x_i}^T \mathbf{r}_{x_i} - 1)/2$ ,  $i = 1, 2, 3$ , measure the magnitude of the change of the vector  $\mathbf{r}$  along the coordinate line  $x_i$ , whereas the normal strain components  $\bar{\epsilon}_{ii} = (\mathbf{r}_{\bar{x}_i}^T \mathbf{r}_{\bar{x}_i} - 1)/2$ ,  $i = 1, 2, 3$ , measure the magnitude of this change along the coordinate line  $\bar{x}_i$ . These two measures are, in general, different because they represent the variations of vectors in different directions. Similar comments apply to the shear strain components.

#### Example 2.7

In Example 4, it was shown that the Green–Lagrange strain tensor for a beam whose axis is parallel to the reference  $X_1$  axis and subjected to an elongation  $\delta$  is given by

$$\epsilon = \frac{1}{2} (\mathbf{J}^T \mathbf{J} - \mathbf{I}) = \begin{bmatrix} \frac{\delta}{l} \left( \frac{\delta}{2l} + 1 \right) & 0 \\ 0 & 0 \end{bmatrix}$$

In this case,  $\epsilon_{11}$  represents the axial normal strain, and all other strain components including the shear strains are equal to zero. The strain components in another coordinate system  $\bar{X}_1\bar{X}_2$  that is rotated by an angle  $\beta$  with respect to the coordinate system  $X_1X_2$  can be written as

$$\bar{\epsilon} = \mathbf{A}^T \epsilon \mathbf{A}$$

where  $\mathbf{A}$  is the transformation matrix defined as

$$\mathbf{A} = \begin{bmatrix} \cos \beta & -\sin \beta \\ \sin \beta & \cos \beta \end{bmatrix}$$

Using this transformation, it can be shown that

$$\bar{\epsilon} = \mathbf{A}^T \epsilon \mathbf{A} = \begin{bmatrix} \epsilon_{11} \cos^2 \beta & -\epsilon_{11} \sin \beta \cos \beta \\ -\epsilon_{11} \sin \beta \cos \beta & \epsilon_{11} \sin^2 \beta \end{bmatrix}$$

where

$$\epsilon_{11} = \frac{\delta}{l} \left( \frac{\delta}{2l} + 1 \right)$$

For the special case in which  $\beta = \pi/2$ , one has

$$\bar{\epsilon} = \begin{bmatrix} 0 & 0 \\ 0 & \epsilon_{11} \end{bmatrix}$$

This equation shows that  $\bar{\epsilon}_{22} = \epsilon_{11}$ , and all other strains, including shear strains, are equal to zero. One can show by examining the general expression of  $\bar{\epsilon}$  in terms of the angle  $\beta$  that a maximum value for a strain component in this example is obtained when  $\sin \beta = 0$  or  $\cos \beta = 0$ . For these values of  $\beta$ , the shear strains are equal to zero. One can show that there are always directions along which the shear strains are equal to zero. These directions are called the *principal directions* and can be determined in a systematic manner as explained in this section.

## Principal Strains

The principal directions of the strain tensor  $\epsilon$  can be obtained by defining the following *eigenvalue problem*:

$$(\epsilon - \lambda \mathbf{I})\mathbf{Y} = \mathbf{0} \quad (2.65)$$

In this equation,  $\lambda$  is the eigenvalue and  $\mathbf{Y}$  is the eigenvector of the matrix  $\epsilon$ . In order to have a nontrivial solution, the determinant of the coefficient matrix in the preceding equation must be equal to zero. This defines the following characteristic equation:

$$|\epsilon - \lambda \mathbf{I}| = 0 \quad (2.66)$$

This equation, which is cubic in  $\lambda$  in the three-dimensional case, has three roots  $\lambda_1$ ,  $\lambda_2$ , and  $\lambda_3$  called the *eigenvalues* or the *principal values*. Because  $\epsilon$  is symmetric, the three roots  $\lambda_1$ ,  $\lambda_2$ , and  $\lambda_3$  are real. Associated with these three roots, one can define three eigenvectors  $\mathbf{Y}_1$ ,  $\mathbf{Y}_2$ , and  $\mathbf{Y}_3$  to within an arbitrary constant using the following equation:

$$(\epsilon - \lambda_i \mathbf{I})\mathbf{Y}_i = \mathbf{0}, \quad i = 1, 2, 3 \quad (2.67)$$

As discussed in Chapter 1, because the strain tensor is symmetric, one can show that the eigenvectors  $\mathbf{Y}_i$  are orthogonal and if they are normalized such that they are orthonormal

(orthogonal unit vectors), one can show that

$$\mathbf{Y}_i^T \boldsymbol{\varepsilon} \mathbf{Y}_i = \lambda_i, \quad i = 1, 2, 3 \quad (2.68)$$

That is, the orthonormal eigenvectors can define an orthogonal matrix  $\mathbf{Y}_m = [\mathbf{Y}_1 \ \mathbf{Y}_2 \ \mathbf{Y}_3]$  such that

$$\mathbf{Y}_m^T \boldsymbol{\varepsilon} \mathbf{Y}_m = \begin{bmatrix} \lambda_1 & 0 & 0 \\ 0 & \lambda_2 & 0 \\ 0 & 0 & \lambda_3 \end{bmatrix} \quad (2.69)$$

Because  $\mathbf{Y}_m$  is an orthogonal matrix, its columns define directions of three orthogonal axes called the *principal axes* or *principal directions*. The roots  $\lambda_1$ ,  $\lambda_2$ , and  $\lambda_3$  are called the *principal normal strains*. Note that in the principal directions, the shear strains are identically equal to zero. Therefore, one can always select coordinate lines  $\bar{\mathbf{x}}$  along which the shear strains vanish by using the coordinate transformation  $d\mathbf{x} = \mathbf{Y}_m d\bar{\mathbf{x}}$ . Equation 69 also shows that the strain tensor  $\boldsymbol{\varepsilon}$  can be written as  $\boldsymbol{\varepsilon} = \sum_{i=1}^3 \lambda_i \mathbf{Y}_i \otimes \mathbf{Y}_i$ , which is the *spectral decomposition* of the strain tensor  $\boldsymbol{\varepsilon}$ .

### Strain Invariants

The following quantities associated with the strain tensor  $\boldsymbol{\varepsilon}$  are called the *principal strain invariants*:

$$I_1 = \text{tr}(\boldsymbol{\varepsilon}), \quad I_2 = \frac{1}{2} \{ (\text{tr}(\boldsymbol{\varepsilon}))^2 - \text{tr}(\boldsymbol{\varepsilon}^2) \}, \quad I_3 = \det(\boldsymbol{\varepsilon}) = |\boldsymbol{\varepsilon}| \quad (2.70)$$

For the symmetric strain tensor  $\boldsymbol{\varepsilon}$ , one can show that

$$\left. \begin{aligned} I_1 &= \lambda_1 + \lambda_2 + \lambda_3 \\ I_2 &= \lambda_1 \lambda_2 + \lambda_1 \lambda_3 + \lambda_2 \lambda_3 \\ I_3 &= \lambda_1 \lambda_2 \lambda_3 \end{aligned} \right\} \quad (2.71)$$

The first strain invariant  $I_1 = \varepsilon_{11} + \varepsilon_{22} + \varepsilon_{33}$  is called the *dilatation* or the *volumetric strain*.

Relationships between the principal values of different strain measures can be established. For example, the relationship between the principal values of the Green–Lagrange strain tensor and the principal values of the right Cauchy–Green deformation tensor can be developed using Equation 34, which when substituted into Equation 65 yields  $\{(\mathbf{C}_r - \mathbf{I})/2\} - \lambda \mathbf{I} \mathbf{Y} = \mathbf{0}$ . This equation shows that the principal values and principal directions of the deformation tensor  $\mathbf{C}_r$  can be determined using the equation  $(\mathbf{C}_r - (2\lambda + 1)\mathbf{I})\mathbf{Y} = \mathbf{0}$ , which shows that  $\boldsymbol{\varepsilon}$  and  $\mathbf{C}_r$  have the same principal directions and also shows the difference between the principal values of the two deformation tensors. As will be shown in Chapter 4, there are material constitutive models, which are expressed in terms of the principal values and invariants of the deformation measures.

#### Example 2.8

In Example 7, it was shown that the strain tensor for the beam considered in this chapter can be defined in an arbitrary coordinate system that differs from the reference coordinate system by

an angle  $\beta$  using the following equation:

$$\bar{\epsilon} = \mathbf{A}^T \epsilon \mathbf{A} = \begin{bmatrix} \epsilon_{11} \cos^2 \beta & -\epsilon_{11} \sin \beta \cos \beta \\ -\epsilon_{11} \sin \beta \cos \beta & \epsilon_{11} \sin^2 \beta \end{bmatrix}$$

The strain invariants of this tensor are

$$I_1 = \text{tr}(\epsilon) = \epsilon_{11},$$

$$I_2 = \frac{1}{2} \{ (\text{tr}(\epsilon))^2 - \text{tr}(\epsilon^2) \} = 0,$$

$$I_3 = \det(\epsilon) = |\epsilon| = 0$$

Note that these invariants do not depend on the angle  $\beta$  that defines the orientation of the coordinate system.

The principal values or eigenvalues can be determined using the following characteristic equation:

$$(\epsilon_{11} \cos^2 \beta - \lambda) (\epsilon_{11} \sin^2 \beta - \lambda) - \epsilon_{11}^2 \sin^2 \beta \cos^2 \beta = 0$$

This equation leads to the following quadratic equation in  $\lambda$ :

$$\lambda^2 - \lambda \epsilon_{11} = 0$$

This characteristic equation defines the following eigenvalues or principal strains:

$$\lambda_1 = \epsilon_{11}, \quad \lambda_2 = 0$$

Using these principal values, the strain invariants can be recalculated as

$$I_1 = \lambda_1 + \lambda_2 = \epsilon_{11},$$

$$I_2 = \lambda_1 \lambda_2 = 0,$$

$$I_3 = \lambda_1 \lambda_2 = 0$$

These results are consistent with the results previously obtained in this example. Using the eigenvalues, one can show that the ratio between the elements of the eigenvectors or principal directions can be written as follows:

$$\frac{y_{i2}}{y_{i1}} = \frac{(\epsilon_{11} \cos^2 \beta - \lambda_i)}{\epsilon_{11} \sin \beta \cos \beta} = \frac{\epsilon_{11} \sin \beta \cos \beta}{(\epsilon_{11} \sin^2 \beta - \lambda_i)}$$

That is, the principal directions determined to be within an arbitrary constant are given by

$$\mathbf{Y}_1 = \begin{bmatrix} \cos \beta \\ -\sin \beta \end{bmatrix}, \quad \mathbf{Y}_2 = \begin{bmatrix} \sin \beta \\ \cos \beta \end{bmatrix}$$

Using these vectors, one can show that  $\mathbf{Y}_i^T \bar{\epsilon} \mathbf{Y}_i = \lambda_i$ . The matrix of eigenvectors  $\mathbf{Y}_m$  can then be defined as

$$\mathbf{Y}_m = [\mathbf{Y}_1 \quad \mathbf{Y}_2] = \begin{bmatrix} \cos \beta & \sin \beta \\ -\sin \beta & \cos \beta \end{bmatrix}$$

Using this matrix, one can show that

$$\mathbf{Y}_m^T \boldsymbol{\varepsilon} \mathbf{Y}_m = \begin{bmatrix} \varepsilon_{11} & 0 \\ 0 & 0 \end{bmatrix} = \begin{bmatrix} \frac{\delta}{l} \left( \frac{\delta}{2l} + 1 \right) & 0 \\ 0 & 0 \end{bmatrix}$$

This transformation defines the strain tensor in the original configuration. That is, the original reference configuration is defined by the principal directions, and the normal strains along these directions define the principal values. The shear strains are equal to zero.

## 2.7 OBJECTIVITY

The concept of *objectivity* is important in solid mechanics and is associated with the study of the effect of the rigid-body motion. Quantities, such as strains, stresses, inertia, and distances between points, should satisfy certain requirements when the continuum experiences a rigid-body rotation. Stresses and deformation measures as well as their rate enter into the formulation of the material constitutive equations. It is important to make sure that the work of the resulting elastic forces and strain energy are not affected under pure rigid-body coordinate transformation. In particular, the stress and deformation measures used to define the elastic forces must be chosen such that the work of these forces and the strain energy remain constant when the continuum experiences a rigid-body rotation. In this case, the stresses and deformation measures are said to satisfy the *objectivity requirement*. In this book, we will not speak of objective variables, vectors, or tensors; instead we will speak of sets of variables that satisfy the objectivity requirement when used together in the formulation of the elastic forces. This is an approach slightly different from the one used in most continuum mechanics books to introduce the concept of objectivity.

In order to provide an introduction to the concept of objectivity, let  $\mathbf{A}$  be the matrix that describes an arbitrary rigid-body rotation, and let  $\mathbf{a}_o$  and  $\mathbf{a}$  be three-dimensional vectors on the continuous body before and after the rigid-body rotation, respectively. The relationship between the components of the vectors  $\mathbf{a}_o$  and  $\mathbf{a}$  can be written as  $\mathbf{a} = \mathbf{A}\mathbf{a}_o$ . Note that in this case, despite the fact that  $\mathbf{a}_o$  and  $\mathbf{a}$  have different components, they have the same length because  $\mathbf{A}$  is an orthogonal matrix, and as a consequence,  $\mathbf{a}^T \mathbf{a} = \mathbf{a}_o^T \mathbf{a}_o$ . Examples of vectors that satisfy this requirement are the vector  $d\mathbf{r}$  that defines the line segment on the continuous body. For example, consider the two-step motion of a continuum. The first step is a general displacement defined by the reference coordinates  $\mathbf{x}$  and current spatial coordinates  $\mathbf{r}_o$ . For this step, one can write  $d\mathbf{r}_o = \mathbf{J}_o d\mathbf{x}$ , and as a result  $d\mathbf{r}_o^T d\mathbf{r}_o = d\mathbf{x}^T \mathbf{J}_o^T \mathbf{J}_o d\mathbf{x}$ , where in this equation,  $\mathbf{J}_o$  is the matrix of position vector gradients. In the second step, the continuum undergoes a rigid-body rotation defined by the orthogonal transformation matrix  $\mathbf{A}$ . If the spatial coordinates at the end of this step are defined by the vector  $\mathbf{r}$ , one has  $d\mathbf{r} = \mathbf{A}d\mathbf{r}_o = \mathbf{A}\mathbf{J}_o d\mathbf{x}$ . Using the fact that  $\mathbf{A}$  is an orthogonal transformation matrix, one has  $d\mathbf{r}^T d\mathbf{r} = d\mathbf{x}^T \mathbf{J}_o^T \mathbf{J}_o d\mathbf{x} = d\mathbf{r}_o^T d\mathbf{r}_o$ . That is, the length of the line segment does not change under an arbitrary rigid-body rotation.

The analysis presented in this section shows that if a vector is defined on the continuum at any configuration, and the continuum experiences a pure rigid-body rotation from this configuration, the components of the vector defined in a selected global coordinate system will change as the result of this rigid-body rotation. Nonetheless, the length of the vector

will not change. As will be discussed in this book, the elastic and dissipative forces due to the continuum displacements are expressed in terms of stress and deformation measures. Whereas some of these measures can change as the result of a rigid-body motion, it is required as previously stated that the work of the elastic forces and strain energy remain constant. It is, therefore, important to understand how different measures change as the result of the rigid-body rotation in order to be able to check the objectivity requirement.

In order to examine the change in the Green–Lagrange strain tensor as the result of the rigid-body rotation, we consider again a continuum at a certain configuration defined by the matrix of position vector gradients  $\mathbf{J}_o$ . At this configuration, the Green–Lagrange strain tensor is defined as

$$\boldsymbol{\varepsilon}_o = \frac{1}{2} (\mathbf{J}_o^T \mathbf{J}_o - \mathbf{I}) \quad (2.72)$$

Assume that the continuum experiences a rigid-body rotation from this configuration defined by the transformation matrix  $\mathbf{A}$ . The new matrix of the position vector gradients can be written as  $\mathbf{J} = \mathbf{A} \mathbf{J}_o$ . It follows that the Green–Lagrange strain tensor for the final configuration is defined as

$$\boldsymbol{\varepsilon} = \frac{1}{2} (\mathbf{J}^T \mathbf{J} - \mathbf{I}) = \frac{1}{2} (\mathbf{J}_o^T \mathbf{A}^T \mathbf{A} \mathbf{J}_o - \mathbf{I}) = \frac{1}{2} (\mathbf{J}_o^T \mathbf{J}_o - \mathbf{I}) = \boldsymbol{\varepsilon}_o \quad (2.73)$$

That is, Green–Lagrange strain tensor is not affected by the rigid-body rotation, an expected result based on the analysis previously presented in this chapter. It will be shown in the following chapter that the Green–Lagrange strain tensor is used with a stress tensor called the *second Piola–Kirchhoff stress tensor* to formulate the elastic forces. Because the Green–Lagrange strain tensor remains constant under an arbitrary rigid-body rotation, the second Piola–Kirchhoff stress tensor is also expected to remain constant in order to satisfy the objectivity requirement, and ensure that the work of the elastic forces and strain energy are not influenced by an arbitrary rigid-body coordinate transformation.

Next, we examine the effect of the rigid-body rotation on the velocity gradient tensor  $\mathbf{L} = \dot{\mathbf{J}} \mathbf{J}^{-1}$ . Let again  $\mathbf{J}_o$  and  $\mathbf{J}$  be, respectively, the matrices of position vector gradients before and after the rigid-body rotation defined by the matrix  $\mathbf{A}$ . Both  $\mathbf{J}_o$  and  $\mathbf{J}$  are defined by differentiation with respect to the same material coordinates  $\mathbf{x}$ . As the result of the rigid-body rotation,  $\mathbf{J}$  can be written in terms of  $\mathbf{J}_o$ , as previously shown in this section, as  $\mathbf{J} = \mathbf{A} \mathbf{J}_o$ . Differentiating this equation with respect to time, one obtains

$$\dot{\mathbf{J}} = \mathbf{A} \dot{\mathbf{J}}_o + \dot{\mathbf{A}} \mathbf{J}_o \quad (2.74)$$

The velocity gradient tensor  $\mathbf{L}$  is then defined as

$$\mathbf{L} = \dot{\mathbf{J}} \mathbf{J}^{-1} = (\mathbf{A} \dot{\mathbf{J}}_o + \dot{\mathbf{A}} \mathbf{J}_o) \mathbf{J}_o^{-1} \mathbf{A}^T = \mathbf{A} \dot{\mathbf{J}}_o \mathbf{J}_o^{-1} \mathbf{A}^T + \dot{\mathbf{A}} \mathbf{A}^T \quad (2.75)$$

which can be written using the fact that  $\mathbf{L}_o = \dot{\mathbf{J}}_o \mathbf{J}_o^{-1}$  as

$$\mathbf{L} = \mathbf{A} \mathbf{L}_o \mathbf{A}^T + \dot{\mathbf{A}} \mathbf{A}^T \quad (2.76)$$

The second term on the right-hand side of this equation makes the velocity gradient tensor  $\mathbf{L}$  unsuitable for use with a Lagrangian stress measure in the definition of the elastic forces,



because when it is used with such Lagrangian stress measures, the objectivity requirement is not satisfied. Nonetheless, other stress measures, as discussed in Chapter 3, can be used with the velocity gradient tensor to formulate the energy balance equations.

The rate of deformation tensor, on the other hand, is often used with known stress measures to satisfy the objectivity requirement. In order to show the effect of the rigid-body rotation on the rate of deformation tensor  $\mathbf{D}$ , one can write

$$\mathbf{D} = \frac{1}{2} (\mathbf{L} + \mathbf{L}^T) = \frac{1}{2} \mathbf{A} (\mathbf{L}_o + \mathbf{L}_o^T) \mathbf{A}^T + (\dot{\mathbf{A}} \mathbf{A}^T + \mathbf{A} \dot{\mathbf{A}}^T) \quad (2.77)$$

Because  $(d/dt)(\mathbf{A} \mathbf{A}^T) = \mathbf{0} = (\dot{\mathbf{A}} \mathbf{A}^T + \mathbf{A} \dot{\mathbf{A}}^T)$ , the preceding equation reduces to

$$\mathbf{D} = \mathbf{A} \mathbf{D}_o \mathbf{A}^T \quad (2.78)$$

This equation shows that the rate of deformation tensor is affected by the rigid-body rotation in a manner similar to some known stress measures. For this reason,  $\mathbf{D}$  is used in several large deformation and plasticity constitutive models to account for the energy dissipation and at the same time to satisfy the objectivity requirement.

When studying the objectivity, it is important to distinguish between the change of the coordinate lines (parameters) and the change of the current configuration due to a rigid-body rotation. The change of the parameters does not lead to a change of the current configuration. Consider the change of the parameters from  $x_1 x_2 x_3$  to a new set of parameters along the axis of the coordinate system  $\bar{x}_1 \bar{x}_2 \bar{x}_3$ , as shown in Figure 5. Both coordinate systems are used with the same current configuration. Let  $\mathbf{A}$  be the transformation matrix that defines the relationship between the two set of parameters. As previously discussed, the matrix of position vector gradients  $\bar{\mathbf{J}}$  associated with the coordinate system  $\bar{x}_1 \bar{x}_2 \bar{x}_3$  can be written in terms of the matrix of position vector gradients  $\mathbf{J}$  associated with the coordinate system  $x_1 x_2 x_3$  using the equation  $\bar{\mathbf{J}} = \mathbf{J} \mathbf{A}$ . This gradient transformation does not change the vector  $\mathbf{r}$  or the components of the line segment  $d\mathbf{r}$ ; it changes the definition of the reference coordinates (parameters) from  $\mathbf{x}$  to  $\bar{\mathbf{x}}$ .

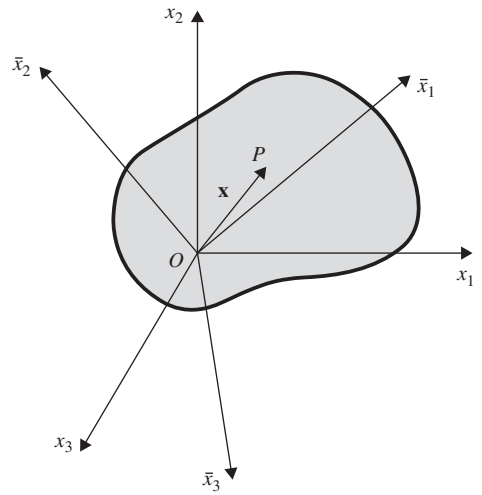


**Figure 2.5** One current configuration and two reference coordinate systems (strain transformation)

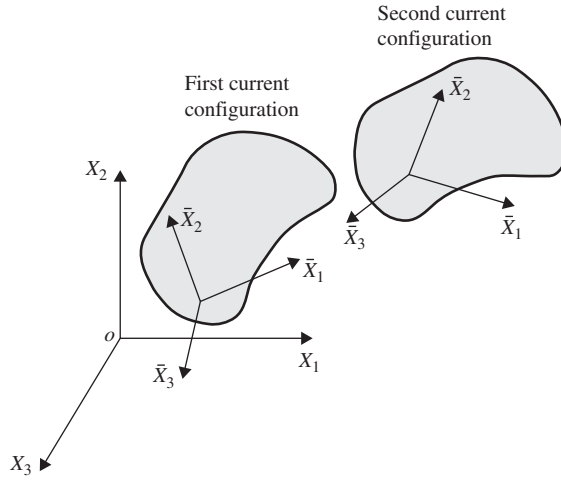


**Figure 2.6** Two current configurations and one reference coordinate system (objectivity)

On the other hand, a rigid-body rotation of the continuum from a given current configuration defines a new current configuration, as shown in Figure 6. If the rigid-body rotation is defined by the transformation matrix  $\mathbf{A}$ , then the relationship between the new matrix of position vector gradients  $\bar{\mathbf{J}}$  and the matrix of position vector gradients  $\mathbf{J}$  associated with the previous current configuration is defined as  $\bar{\mathbf{J}} = \mathbf{A}\mathbf{J}$ . Note that this change of the current configuration changes the definition of the components of the vectors  $\mathbf{r}$  and  $d\mathbf{r}$ , whereas the coordinate lines (parameters) remain the same.

## 2.8 CHANGE OF VOLUME AND AREA

The relationships between the areas and volumes in the reference and current configurations are important in formulating the equations that define the effect of the inertia and elastic forces of the continuum. These relationships, which will be used in later chapters of this book, are obtained in this section. First, the relationship between the volumes is obtained and used to define the relationship between the areas.

### Volume

The volume of an element can be obtained using the *scalar triple product*. Consider an element whose base is defined by the two vectors  $\mathbf{b}$  and  $\mathbf{c}$ , while another side is defined by the vector  $\mathbf{a}$ . The volume of the element is defined as  $V = \mathbf{a} \cdot (\mathbf{b} \times \mathbf{c})$ . The term  $(\mathbf{b} \times \mathbf{c})$  defines a vector whose magnitude is the area of the base and its direction is along a vector perpendicular to both  $\mathbf{b}$  and  $\mathbf{c}$ . In fact, the volume can be written using any cyclic permutation of the vectors  $\mathbf{a}$ ,  $\mathbf{b}$ , and  $\mathbf{c}$ , that is,

$$V = \mathbf{a} \cdot (\mathbf{b} \times \mathbf{c}) = \mathbf{c} \cdot (\mathbf{a} \times \mathbf{b}) = \mathbf{b} \cdot (\mathbf{c} \times \mathbf{a}) \quad (2.79)$$

Now consider a volume element that has sides of length  $dx_1$ ,  $dx_2$ , and  $dx_3$  in the reference configuration. The lengths of these line elements in the current configuration are given

by  $dr_1$ ,  $dr_2$ , and  $dr_3$ , where

$$dr_k = \frac{\partial r_k}{\partial x_1} dx_1 + \frac{\partial r_k}{\partial x_2} dx_2 + \frac{\partial r_k}{\partial x_3} dx_3 = \sum_{i=1}^3 \frac{\partial r_k}{\partial x_i} dx_i, \quad k = 1, 2, 3 \quad (2.80)$$

The length of the side of the volume element in the current configuration can then be defined in the direction of the parameters  $x_1$ ,  $x_2$ , and  $x_3$  using the following three vectors:

$$\mathbf{j}_1 = \frac{\partial \mathbf{r}}{\partial x_1} dx_1, \quad \mathbf{j}_2 = \frac{\partial \mathbf{r}}{\partial x_2} dx_2, \quad \mathbf{j}_3 = \frac{\partial \mathbf{r}}{\partial x_3} dx_3 \quad (2.81)$$

The current volume of the element can then be written as

$$dv = \mathbf{j}_1 \cdot (\mathbf{j}_2 \times \mathbf{j}_3) = \mathbf{r}_{x_1} dx_1 \cdot (\mathbf{r}_{x_2} dx_2 \times \mathbf{r}_{x_3} dx_3) = \{\mathbf{r}_{x_1} \cdot (\mathbf{r}_{x_2} \times \mathbf{r}_{x_3})\} dx_1 dx_2 dx_3 \quad (2.82)$$

Because  $|\mathbf{J}| = \mathbf{r}_{x_1} \cdot (\mathbf{r}_{x_2} \times \mathbf{r}_{x_3})$ , and  $x_1$ ,  $x_2$ , and  $x_3$  are defined along the orthogonal axes of a Cartesian coordinate system, that is,  $dx_1 dx_2 dx_3 = dV$  is the volume of the element in the reference configuration, one has from the preceding equation, the following relationship between the volumes in the current and reference configurations:

$$dv = J dV \quad (2.83)$$

where  $J = |\mathbf{J}|$ . In the case of small deformation, the determinant of  $\mathbf{J}$  remains approximately equal to one, and the volume in the current configuration can be assumed to be equal to the volume in the reference configuration. Furthermore, if the determinant of  $\mathbf{J}$  remains constant, the volume of the continuous body does not change. In this case, the displacement is called *isochoric*. The deformation of an incompressible material is isochoric because the volume does not change. Note also that if  $\mathbf{A}$  is an orthogonal matrix, then  $|\mathbf{A}\mathbf{J}| = |\mathbf{J}| = J$ , which shows that the volume does not change under an arbitrary rigid-body motion.

## Area

The relationship between the volumes in the reference and current configurations can be used to obtain the relationship between the areas. To this end, consider an area element defined in the reference and current configurations, respectively, by

$$d\mathbf{S} = \mathbf{N} dS, \quad d\mathbf{s} = \mathbf{n} ds \quad (2.84)$$

where  $\mathbf{N}$  and  $\mathbf{n}$  are unit vectors normal to the areas in the reference and current configurations, respectively. Consider an arbitrary line element  $d\mathbf{x}$ , which in the current configuration is defined by  $d\mathbf{r}$ , where  $d\mathbf{r} = \mathbf{J} d\mathbf{x}$ . The corresponding volumes in the reference and current configurations are given by

$$dV = d\mathbf{x} \cdot d\mathbf{S} = d\mathbf{x} \cdot \mathbf{N} dS, \quad dv = d\mathbf{r} \cdot d\mathbf{s} = d\mathbf{r} \cdot \mathbf{n} ds \quad (2.85)$$

Using Equation 83, it follows that

$$d\mathbf{r} \cdot \mathbf{n} ds = J d\mathbf{x} \cdot \mathbf{N} dS \quad (2.86)$$

which upon using the fact that  $d\mathbf{r} = \mathbf{J}d\mathbf{x}$ , one obtains

$$(\mathbf{J}d\mathbf{x}) \cdot \mathbf{n}ds = Jd\mathbf{x} \cdot \mathbf{N}dS \quad (2.87)$$

Because  $d\mathbf{x}$  is arbitrary, one has

$$\mathbf{N} = \frac{1}{J} \mathbf{J}^T \mathbf{n} \frac{ds}{dS} \quad (2.88)$$

In some references, this equation is called *Nanson's formula* (Ogden, 1984). Because  $\mathbf{N}$  is a unit vector, it follows from Equation 88 that

$$\left( \frac{ds}{dS} \right)^2 = \frac{J^2}{(\mathbf{n}^T \mathbf{J} \mathbf{J}^T \mathbf{n})} \quad (2.89)$$

or equivalently,

$$ds = \frac{J}{(\mathbf{n}^T \mathbf{J} \mathbf{J}^T \mathbf{n})^{\frac{1}{2}}} dS \quad (2.90)$$

This equation defines the relationship between the area in the current configuration and the area in the reference configuration. Recall that the left Cauchy–Green deformation tensor  $\mathbf{C}_l$  is defined as  $\mathbf{C}_l = \mathbf{J} \mathbf{J}^T$ . It follows that  $(ds/dS) = J / \sqrt{\mathbf{n}^T \mathbf{C}_l \mathbf{n}}$ .

### Example 2.9

Consider the beam model of Example 3. Assume that the beam deformation defined by the following equation:

$$\mathbf{r} = [x_1 \quad x_2 + \xi \eta \delta]^T$$

where  $\delta$  is a constant,  $x_1$  and  $x_2$  are the beam local coordinates, and  $\xi = x_1/l$  and  $\eta = x_2/l$ , where  $l$  is the length of the beam in the undeformed configuration. The displacement defined by the preceding equation corresponds to the following vector of beam coordinates:

$$\mathbf{e} = \left[ 0 \quad 0 \quad 1 \quad 0 \quad 0 \quad 1 \quad l \quad 0 \quad 1 \quad 0 \quad 0 \quad 1 + \frac{\delta}{l} \right]^T$$

This shows that the displacement considered in this example can be produced by a change of the length of the gradient vector  $\mathbf{r}_{x_2}$  at  $\xi = 1$ . The direction of this vector remains the same. The matrix of position vector gradients is defined as

$$\mathbf{J} = \begin{bmatrix} 1 & 0 \\ \eta \left( \frac{\delta}{l} \right) & 1 + \xi \left( \frac{\delta}{l} \right) \end{bmatrix}$$

The determinant of this matrix is

$$J = 1 + \xi \left( \frac{\delta}{l} \right)$$

Note that  $J$  is always positive at an arbitrary material point for a positive  $\delta$ , and the maximum value of the determinant for a positive  $\delta$  occurs at  $\xi = 1$ . Also note that, for  $\eta \neq 0$ , the gradient vector  $\mathbf{r}_{x_1}$  is no longer a unit vector, and its orientation depends on  $\eta$ . The relationship between the volumes in the current and reference configurations at an arbitrary material point can then be written as

$$dv = JdV = \left\{ 1 + \xi \left( \frac{\delta}{l} \right) \right\} dV$$

That is, as the length of the gradient vector  $\mathbf{r}_{x_2}$  ( $\xi = 1$ ) increases, the volume in the current configuration increases according to the linear relationship in  $\xi$  given by the preceding equation.

In order to evaluate the ratio between the areas in the current and reference configurations, the left Cauchy–Green deformation tensor is evaluated as

$$\mathbf{C}_l = \mathbf{J}\mathbf{J}^T = \begin{bmatrix} 1 & \eta \left( \frac{\delta}{l} \right) \\ \eta \left( \frac{\delta}{l} \right) & \eta^2 \left( \frac{\delta}{l} \right)^2 + \left( 1 + \xi \left( \frac{\delta}{l} \right) \right)^2 \end{bmatrix}$$

Consider an area defined by the normal  $\mathbf{n} = [1 \ 0]^T$ . Using this vector and the definition of  $\mathbf{C}_l$ , one can show that

$$\mathbf{n}^T \mathbf{C}_l \mathbf{n} = 1$$

The ratio between the areas in the current and reference configurations can then be written as

$$(ds/dS) = J / \sqrt{\mathbf{n}^T \mathbf{C}_l \mathbf{n}} = J = 1 + \xi \left( \frac{\delta}{l} \right)$$

This equation shows that, in this example, the ratio between the areas is the same as the ratio between the volumes because deformation along the  $x_3$  axis of the beam is not considered in this planar case.

In order to demonstrate the use of Nanson's formula to evaluate the area, consider the same displacement field given in this example written as the three-dimensional vector  $\mathbf{r} = [x_1 \ (x_2 + \xi\eta\delta) \ x_3]^T$ . This displacement field defines the shape shown in Figure 7a, which has the reference configuration shown in Figure 7b. In this reference configuration, the beam has length  $l$  and height  $h$ . Using the displacement field, one can show that the height of the beam at the second node is  $h(1 + \delta/l)$ . Therefore, the height above the beam centerline

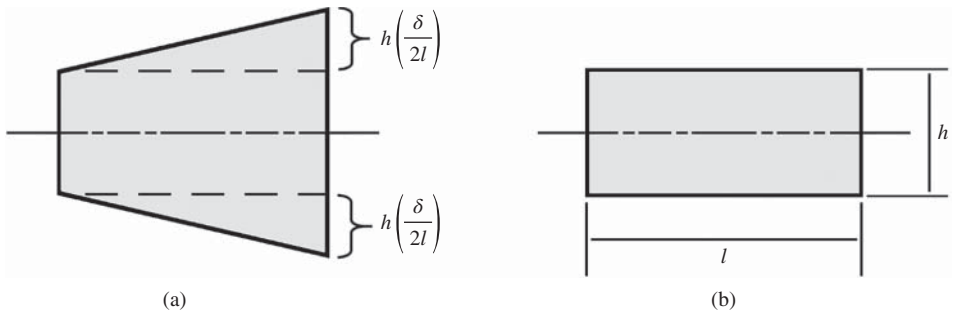


**Figure 2.7** Nanson's formula

is increased by  $h\delta/2l$  and the height below the centerline is extended by  $h\delta/2l$ . Using the three-dimensional displacement field vector, the matrix of position vector gradients can be written as

$$\mathbf{J} = \begin{bmatrix} 1 & 0 & 0 \\ \eta \left( \frac{\delta}{l} \right) & 1 + \xi \left( \frac{\delta}{l} \right) & 0 \\ 0 & 0 & 1 \end{bmatrix}$$

Using the area whose normal is defined by the vector  $\mathbf{n} = [0 \ 0 \ 1]^T$ , one can show that  $\mathbf{n}\mathbf{J}\mathbf{J}^T\mathbf{n} = 1$ , therefore,  $ds = JdS = (1 + \xi(\delta/l))dS$ . It follows that

$$s = \int_S (1 + \xi(\delta/l))dS = \int_0^l \int_{-h/2}^{h/2} (1 + \xi(\delta/l))dx_1 dx_2 = hl + \frac{1}{2}h\delta,$$

which gives the correct area that can be evaluated directly using Figure 7a. This result clearly shows that a finite dimensional model based on the interpolation used in the examples presented in this chapter can correctly describe the geometry in case of structural elements such as beams and plates. More detailed discussion of the nature of this interpolation will be discussed in Chapter 5. One can also show that horizontal straight line segment  $d\mathbf{x}$  at a distance  $b$  above the element centerline will have two endpoints defined by the coordinates  $(x_1 = 0, x_2 = b)$  and  $(x_1 = l, x_2 = b)$ . In writing these definitions of the endpoints, one can make  $l$  arbitrarily small. The equation of the straight line segment  $d\mathbf{x}$  is then  $x_2 = b$ . Using the assumed displacement field, one can show that the line segment remains a straight line with endpoints defined by  $(r_1 = 0, r_2 = b)$  and  $(r_1 = l, r_2 = b(1 + \delta/l))$ . The equation that defines the straight line  $d\mathbf{r}$  can then be written as  $r_2 = (b\delta/l^2)r_1 + b$ . One can show that in this case  $d\mathbf{x} = [l \ 0]^T$  and  $d\mathbf{r} = [l \ b\delta/l]^T$  which show that  $d\mathbf{r} = \mathbf{J}d\mathbf{x}$ . In the case of an arbitrarily oriented line segment  $d\mathbf{x}$ , the equation of this segment can be function of  $\xi$  and  $\eta$ . To better understand some of the kinematics concepts introduced in this chapter, the reader can take different line segments and use the assumed displacement field presented in this example to obtain the definitions of  $d\mathbf{x}$  and  $d\mathbf{r}$ .

## 2.9 CONTINUITY EQUATION

If the mass is conserved, an element of mass  $dm$  can be written using the volumes and densities in the initial and current configurations as

$$dm = \rho_0 dV = \rho dv \quad (2.91)$$

In this equation,  $\rho_0$  and  $\rho$  are, respectively, the mass density in the initial and current configurations. Using the preceding equation and Equation 83, it is clear that

$$\rho_0 = \rho J \quad (2.92)$$

This equation, which is obtained using the *principle of conservation of mass*, is called the *continuity equation*. In the case of incompressible materials, the volume does not change and  $J = 1$ . In this case, the mass density remains constant; that is,  $\rho_0 = \rho$ .

The continuity equation can be written in another form by considering the rates of the mass flow. If the mass is conserved, the rate at which an element mass increases must be equal to the rate at which the mass flows out of the element. Using the concept of a *control volume*, the element volume  $dv$  and the element area  $ds$  can be used to write the following conservation of mass equation:

$$\int_v \frac{\partial \rho}{\partial t} dv = - \int_s \rho \mathbf{v} \cdot \mathbf{n} ds \quad (2.93)$$

In this equation,  $\mathbf{v}$  is the velocity vector and  $\mathbf{n}$  is the normal to the surface. Because  $\mathbf{n}$  is used here to denote the outward normal, the negative sign is used. Furthermore, the partial derivative  $\partial \rho / \partial t$  is used because the rate of change of the mass density  $\rho$  is assumed to be evaluated at a fixed point in the control volume. Using the *divergence theorem*, the surface integral can be written in terms of volume integral leading to

$$\int_v \left\{ \frac{\partial \rho}{\partial t} + \text{div}(\rho \mathbf{v}) \right\} dv = 0 \quad (2.94)$$

Because this equation must be satisfied everywhere in the continuum, one has

$$\frac{\partial \rho}{\partial t} + \text{div}(\rho \mathbf{v}) = 0 \quad (2.95)$$

This is another form of the continuity equation, which can also be written as

$$\frac{\partial \rho}{\partial t} + \frac{\partial \rho}{\partial \mathbf{r}} \mathbf{v} + \rho \sum_{i=1}^3 \frac{\partial v_i}{\partial r_i} = 0 \quad (2.96)$$

or equivalently

$$\frac{\partial \rho}{\partial t} + \rho \sum_{i=1}^3 \frac{\partial v_i}{\partial r_i} = 0 \quad (2.97)$$

In the case of *incompressible materials*, the mass density remains constant, that is,  $d\rho/dt = 0$ . It then follows from the preceding equation that  $\sum_{i=1}^3 \partial v_i / \partial r_i = 0$  for incompressible materials. This implies that the trace of the rate of deformation tensor must be equal to zero if the incompressibility condition is imposed, that is,  $\text{tr}(\mathbf{D}) = 0$ . This result will be used in Chapter 4 when the constitutive equations of the fluids are discussed.

From the identities presented in the preceding chapter, one can write  $\dot{J} = J \text{tr}(\mathbf{D}) = J \text{tr}(\mathbf{L}) = J \text{div}(\mathbf{v})$ , where  $\mathbf{D}$  and  $\mathbf{L}$  are, respectively, the rate of deformation tensor and the velocity gradient tensor, and  $\mathbf{v}$  is the velocity vector. Because  $\rho_0 = \rho J$ , one has  $\dot{\rho} J + \rho \dot{J} = 0$ . It follows that  $\dot{\rho} + \rho \text{div}(\mathbf{v}) = 0$ . This provides another simple derivation of the continuity equation (Ogden, 1984).

## 2.10 REYNOLDS' TRANSPORT THEOREM

In the preceding chapter, it was shown that the time rate of the change of the determinant of the Jacobian matrix  $\mathbf{J}$  can be written as

$$\frac{dJ}{dt} = \left( \frac{\partial \dot{r}_1}{\partial r_1} + \frac{\partial \dot{r}_2}{\partial r_2} + \frac{\partial \dot{r}_3}{\partial r_3} \right) J = (\nabla \mathbf{v}) J \quad (2.98)$$

In this equation,  $\nabla \mathbf{v} = \text{div}(\mathbf{v})$ . The preceding equation can also be written as

$$\frac{dJ}{dt} = \text{tr}(\mathbf{L})J = \text{tr}(\mathbf{D})J \quad (2.99)$$

This equation can be used to obtain *Reynolds' transport theorem*, which defines the rate of change of a volume integral. Let  $\Psi(\mathbf{r}, t)$  be any function defined in terms of the current configuration. The volume integral of this function is given as

$$\Pi(t) = \int_v \Psi(\mathbf{r}, t) dv \quad (2.100)$$

Because the volume  $v$  is time varying, when evaluating the time rate of change of  $\Pi(t)$ , one cannot take the differentiation through the integral sign. Using Equation 83, which relates the volumes in the current and reference configurations, Equation 100 can be written as

$$\Pi(t) = \int_V \Psi(\mathbf{r}, t) J dV \quad (2.101)$$

It follows that

$$\frac{d}{dt} \Pi(t) = \frac{d}{dt} \int_V \Psi(\mathbf{r}, t) J dV = \int_V \frac{d}{dt} \{ \Psi(\mathbf{r}, t) J \} dV \quad (2.102)$$

This equation can be written as

$$\frac{d}{dt} \Pi(t) = \int_V \left\{ \frac{d\Psi(\mathbf{r}, t)}{dt} J + \Psi(\mathbf{r}, t) \frac{dJ}{dt} \right\} dV \quad (2.103)$$

Substituting Equation 98 into Equation 103, one obtains

$$\frac{d}{dt} \Pi(t) = \int_V \left\{ \frac{d\Psi(\mathbf{r}, t)}{dt} + \Psi(\mathbf{r}, t) (\nabla \mathbf{v}) \right\} J dV \quad (2.104)$$

This equation upon the use of Equation 83 can be written again in terms of the volume defined in the current configuration as

$$\frac{d}{dt} \Pi(t) = \int_v \left\{ \frac{d\Psi(\mathbf{r}, t)}{dt} + \Psi(\mathbf{r}, t) (\nabla \mathbf{v}) \right\} dv \quad (2.105)$$

Because  $d/dt = (\partial/\partial t) + \mathbf{v} \cdot \nabla$ , the preceding equation can be rewritten as

$$\frac{d}{dt} \Pi(t) = \int_v \left\{ \frac{\partial \Psi(\mathbf{r}, t)}{\partial t} + \nabla(\Psi \mathbf{v}) \right\} dv \quad (2.106)$$

This equation, upon the use of the divergence theorem, can be written as

$$\frac{d}{dt} \Pi(t) = \int_v \frac{\partial \Psi(\mathbf{r}, t)}{\partial t} dv + \int_s \Psi \mathbf{v} \cdot \mathbf{n} ds \quad (2.107)$$



In this equation,  $s$  is the surface area in the current configuration, and  $\mathbf{n}$  is the outward normal. The preceding equation, which is a statement of the *Reynolds' transport theorem*, shows that the rate of the change of the volume integral of the function  $\Psi(\mathbf{r}, t)$  is the integral of the rate of change at the material points plus the net flow of  $\Psi(\mathbf{r}, t)$  over the surface. In Reynolds' transport theorem,  $\Psi(\mathbf{r}, t)$  can be a scalar, vector, or tensor function.

The principle of conservation of mass can be easily derived using the analysis presented in this section. To this end, the mass  $m$  of any volume can be written as

$$m(t) = \int_v \rho(\mathbf{r}, t) dv \quad (2.108)$$

where  $\rho$  is the mass density in the current configuration. Letting  $\Pi = m$  and  $\Psi = \rho$  in Equation 106, one obtains in the case of conservation of mass

$$\frac{dm}{dt} = \int_v \left\{ \frac{\partial \rho(\mathbf{r}, t)}{\partial t} + \nabla(\rho \mathbf{v}) \right\} dv = 0 \quad (2.109)$$

Because this equation is valid for an arbitrary volume, the integrand in this equation must be equal to zero everywhere. This leads to

$$\frac{\partial \rho(\mathbf{r}, t)}{\partial t} + \nabla(\rho \mathbf{v}) = 0 \quad (2.110)$$

which is the equation of continuity previously obtained in this chapter.

## 2.11 EXAMPLES OF DEFORMATION

In this section, several deformation examples are presented in order to shed light on some of the important concepts and definitions introduced in this chapter. Among these examples are the special case of planar deformation, extension and dilatational deformations, and shear deformation. The example of the two-dimensional beam used throughout this chapter will be used to demonstrate several deformation modes. The assumed displacement field used in this example is one of the displacement fields used in finite elements based on the *absolute nodal coordinate formulation* discussed in Chapter 5. This finite element formulation relaxes many of the assumptions used in classical beam and plate theories and, therefore, it can be conveniently used to demonstrate some of the general concepts discussed in this chapter.

### Planar Displacement

In the case of planar displacement, the matrix of position vector gradients and its inverse take the following form:

$$\mathbf{J} = \begin{bmatrix} J_{11} & J_{12} & 0 \\ J_{21} & J_{22} & 0 \\ 0 & 0 & 1 \end{bmatrix}, \quad \mathbf{J}^{-1} = \frac{1}{J} \begin{bmatrix} J_{22} & -J_{12} & 0 \\ -J_{21} & J_{11} & 0 \\ 0 & 0 & J \end{bmatrix} \quad (2.111)$$

In this equation,  $J = J_{11}J_{22} - J_{12}J_{21}$ . In this special case,  $\mathbf{r}_{x_3}$  does not change because the displacement is assumed to be planar. The Green–Lagrange strain tensor is defined as

$$\boldsymbol{\varepsilon} = \begin{bmatrix} \varepsilon_{11} & \varepsilon_{12} & 0 \\ \varepsilon_{21} & \varepsilon_{22} & 0 \\ 0 & 0 & 0 \end{bmatrix} = \frac{1}{2} \begin{bmatrix} (J_{11}^2 + J_{21}^2) - 1 & (J_{11}J_{12} + J_{21}J_{22}) & 0 \\ (J_{11}J_{12} + J_{21}J_{22}) & (J_{12}^2 + J_{22}^2) - 1 & 0 \\ 0 & 0 & 0 \end{bmatrix} \quad (2.112)$$

This equation shows that  $\varepsilon_{13}$ ,  $\varepsilon_{23}$ , and  $\varepsilon_{33}$  are identically equal to zero. The velocity gradient tensor is

$$\mathbf{L} = \dot{\mathbf{J}}\mathbf{J}^{-1} = \frac{1}{J} \begin{bmatrix} \dot{J}_{11}J_{22} - \dot{J}_{12}J_{21} & \dot{J}_{12}J_{11} - \dot{J}_{11}J_{12} & 0 \\ \dot{J}_{21}J_{22} - \dot{J}_{22}J_{21} & \dot{J}_{22}J_{11} - \dot{J}_{21}J_{12} & 0 \\ 0 & 0 & 0 \end{bmatrix} \quad (2.113)$$

For such a planar motion, one can show that the rate of deformation and spin tensors are given, respectively, by

$$\mathbf{D} = \frac{1}{2} (\mathbf{L} + \mathbf{L}^T) = \frac{1}{2J} \begin{bmatrix} 2(\dot{J}_{11}J_{22} - \dot{J}_{12}J_{21}) & \text{symmetric} & \\ (\dot{J}_{21}J_{22} - \dot{J}_{22}J_{21} + \dot{J}_{12}J_{11} - \dot{J}_{11}J_{12}) & 2(\dot{J}_{22}J_{11} - \dot{J}_{21}J_{12}) & \\ 0 & 0 & 0 \end{bmatrix} \quad (2.114)$$

and

$$\mathbf{W} = \frac{1}{2} (\mathbf{L} - \mathbf{L}^T) = \frac{1}{2J} \begin{bmatrix} 0 & -\omega & 0 \\ \omega & 0 & 0 \\ 0 & 0 & 0 \end{bmatrix} \quad (2.115)$$

In this equation,  $\omega = (\dot{J}_{21}J_{22} - \dot{J}_{22}J_{21} - \dot{J}_{12}J_{11} + \dot{J}_{11}J_{12})$ . Note that the skew-symmetric spin tensor in the special case of planar rigid-body motion can be written as a function of the rate of one variable only. In the case of rigid-body motion,  $J = 1$ ,  $J_{11} = J_{22} = \cos \theta$ , and  $J_{21} = -J_{12} = \sin \theta$ , where  $\theta$  is the angle of the rigid-body rotation. It follows in this case that the rate of deformation tensor  $\mathbf{D}$  is identically zero, and the spin tensor  $\mathbf{W}$  is

$$\mathbf{W} = \begin{bmatrix} 0 & -\dot{\theta} & 0 \\ \dot{\theta} & 0 & 0 \\ 0 & 0 & 0 \end{bmatrix} \quad (2.116)$$

## Extension and Stretch

If the gradient vectors change their lengths but remain orthogonal, one obtains pure extension or stretch; the most general case of which is the dilatational deformation. In this case, the matrix of position vector gradients can be written as  $\mathbf{J} = \mathbf{R}\mathbf{U}$ , where  $\mathbf{R}$  is an orthogonal matrix and  $\mathbf{U}$  is a diagonal stretch matrix given as

$$\mathbf{U} = \begin{bmatrix} \alpha_1 & 0 & 0 \\ 0 & \alpha_2 & 0 \\ 0 & 0 & \alpha_3 \end{bmatrix} \quad (2.117)$$

where  $\alpha_i$  is the stretch in the  $i$ th direction. That is,  $\alpha_i = |\mathbf{r}_{x_i}|$ . The Green–Lagrange strain tensor can be written as

$$\boldsymbol{\varepsilon} = \begin{bmatrix} \varepsilon_{11} & 0 & 0 \\ 0 & \varepsilon_{22} & 0 \\ 0 & 0 & \varepsilon_{33} \end{bmatrix} = \frac{1}{2} \begin{bmatrix} (\alpha_1^2 - 1) & 0 & 0 \\ 0 & (\alpha_2^2 - 1) & 0 \\ 0 & 0 & (\alpha_3^2 - 1) \end{bmatrix} \quad (2.118)$$

This equation shows that all the shear strain components are identically equal to zero and the motion is a *dilatational deformation*. Because  $\mathbf{U}$  and  $\dot{\mathbf{U}}$  are diagonal, one can show that the rate of deformation tensor can be written as

$$\mathbf{D} = \mathbf{R}\dot{\mathbf{U}}\mathbf{U}^{-1}\mathbf{R}^T = \dot{\mathbf{U}}\mathbf{U}^{-1} \quad (2.119)$$

Because both  $\mathbf{U}$  and  $\dot{\mathbf{U}}$  are diagonal, the rate of deformation tensor  $\mathbf{D}$  is also a diagonal tensor with diagonal elements  $D_{ii} = \dot{\alpha}_i/\alpha_i$ .

For this mode of purely extension deformations, the diagonal elements of the Green–Lagrange strains of Equation 118 are the principal values, and the coordinate axes define the principal directions because the shear stresses are identically equal to zero. Because the trace and determinant are among the invariants of a second-order tensor, one can show that an orthogonal coordinate transformation does not change the values of these diagonal elements. Extensions in only one or two directions can be obtained as special cases of the model presented in this section.

Several classical formulations used in the small- and large-deformation analysis of beams and plates do not capture some stretch modes. For example, classical beam theories assume that the beam cross section remains rigid. That is, when the beam experiences bending, for example, the dimensions of the beam cross section do not change. Although such an assumption can be acceptable for small-deformation problems, the theories based on this assumption cannot be used to correctly predict the behavior of beams when they are subjected to large and inelastic deformations. Such simplified theories cannot also be used to fully capture *Poisson effect*, which results in change of the cross-sectional dimensions when the beam is subjected to elongation or bending. The material constitutive equations couple the normal strains, leading to normal stresses (positive or negative) in the plane of the cross section. With some of the existing nonlinear formulations, such a Poisson effect cannot be captured. This represents a serious limitation when considering applications related to mechanical, aerospace, biomedical, and biological systems in which the deformations of the cross sections can have a significant effect. Modeling the structural stiffness of ligaments, muscles, and DNA as well as many other engineering and biomedical applications are among the examples that require a more general approach that allows implementing more general constitutive models. In Chapter 5, a nonlinear formulation that captures the Poisson effect and other coupled modes of deformation is discussed in more detail. The displacement field used in the following example is one of the displacement fields used for the finite element absolute nodal coordinate formulation discussed in Chapter 5.

**Example 2.10**

Consider the beam model described in Example 3. The displacement field is given by

$$\mathbf{r} = s_1 \begin{bmatrix} e_1 \\ e_2 \end{bmatrix} + s_2 \begin{bmatrix} e_3 \\ e_4 \end{bmatrix} + s_3 \begin{bmatrix} e_5 \\ e_6 \end{bmatrix} + s_4 \begin{bmatrix} e_7 \\ e_8 \end{bmatrix} + s_5 \begin{bmatrix} e_9 \\ e_{10} \end{bmatrix} + s_6 \begin{bmatrix} e_{11} \\ e_{12} \end{bmatrix}$$

The vectors of gradients are

$$\mathbf{r}_{x_1} = \frac{\partial \mathbf{r}}{\partial x_1} = s_{1,1} \begin{bmatrix} e_1 \\ e_2 \end{bmatrix} + s_{2,1} \begin{bmatrix} e_3 \\ e_4 \end{bmatrix} + s_{3,1} \begin{bmatrix} e_5 \\ e_6 \end{bmatrix} + s_{4,1} \begin{bmatrix} e_7 \\ e_8 \end{bmatrix} + s_{5,1} \begin{bmatrix} e_9 \\ e_{10} \end{bmatrix} + s_{6,1} \begin{bmatrix} e_{11} \\ e_{12} \end{bmatrix}$$

and

$$\mathbf{r}_{x_2} = \frac{\partial \mathbf{r}}{\partial x_2} = s_{3,2} \begin{bmatrix} e_5 \\ e_6 \end{bmatrix} + s_{6,2} \begin{bmatrix} e_{11} \\ e_{12} \end{bmatrix}$$

where  $s_{i,j} = \partial s_i / \partial x_j$  and  $i = 1, 2, \dots, 6, j = 1, 2$ . Using these notations and the definitions given in Example 1, one has

$$\begin{aligned} s_{1,1} &= \frac{6}{l}(-\xi + \xi^2), & s_{2,1} &= (1 - 4\xi + 3\xi^2), & s_{3,1} &= -\eta, \\ s_{4,1} &= \frac{6}{l}(\xi - \xi^2), & s_{5,1} &= (-2\xi + 3\xi^2), & s_{6,1} &= \eta, \\ s_{3,2} &= (1 - \xi), & s_{6,2} &= \xi \end{aligned}$$

The coordinates at the two ends of the beam are defined as

$$\begin{aligned} \begin{bmatrix} e_1 \\ e_2 \end{bmatrix} &= \mathbf{r}(\xi = 0), & \begin{bmatrix} e_3 \\ e_4 \end{bmatrix} &= \mathbf{r}_{x_1}(\xi = 0), & \begin{bmatrix} e_5 \\ e_6 \end{bmatrix} &= \mathbf{r}_{x_2}(\xi = 0) \\ \begin{bmatrix} e_7 \\ e_8 \end{bmatrix} &= \mathbf{r}(\xi = 1), & \begin{bmatrix} e_9 \\ e_{10} \end{bmatrix} &= \mathbf{r}_{x_1}(\xi = 1), & \begin{bmatrix} e_{11} \\ e_{12} \end{bmatrix} &= \mathbf{r}_{x_2}(\xi = 1) \end{aligned}$$

Consider the case in which the vector of coordinates is defined as

$$\mathbf{e} = [0 \ 0 \ 1 \ 0 \ 0 \ 1 \ l \ 0 \ \alpha_1 \ 0 \ 0 \ 1]^T$$

where  $l$  is the initial length of the beam and  $\alpha_1$  is a stretch factor. Substituting this vector in the displacement field  $\mathbf{r} = \mathbf{S}\mathbf{e}$  and using the shape functions given in Example 1, one can show that the position vector of an arbitrary point on the beam can be written as

$$\mathbf{r} = [cx_1 \ x_2]^T$$

where

$$c = 1 + (1 - \alpha_1)\xi(1 - \xi)$$

The preceding two equations describe an interesting kinematic mode of displacement. These equations show that if  $\alpha_1 > 1$ , all points on the beam will move toward the end  $\xi = 0$ , while the two ends of the beam remain fixed. The maximum displacement occurs at  $\xi = 0.5$ . When the Poisson effect is considered in formulating the stress–strain relationship, such a displacement will lead, in general, to a change in the dimension of the beam cross section and changes in the volume and density at the material points, an effect that cannot be captured using only kinematic analysis based on the simple displacement mode presented in this example. Nonetheless, because bending is not captured by this mode, the length of the beam centerline does not change because a unit vector tangent to the beam centerline, is given by

$$\mathbf{t} = \frac{\mathbf{r}_{x_1}}{|\mathbf{r}_{x_1}|} = [1 \ 0]^T$$

This equation shows that  $\int_0^{l_d} |\mathbf{t}| ds = l_d$ , where  $s$  is the arc length. More discussion on the differential geometry relevant to the large deformation of beams and plates is presented in Chapter 5.

The matrix of position vector gradients can be defined for the beam discussed in this example as

$$\mathbf{J} = \begin{bmatrix} \beta & 0 \\ 0 & 1 \end{bmatrix}$$

where

$$\beta = 1 + (1 - \alpha_1)\xi(2 - 3\xi)$$

Note that, in this example, the gradient vectors remain orthogonal and, therefore, the deformation will be stretch with no shear strains. This can be confirmed by evaluating the Green–Lagrange strain tensor as

$$\boldsymbol{\epsilon} = \frac{1}{2} \begin{bmatrix} \beta^2 - 1 & 0 \\ 0 & 0 \end{bmatrix}$$

In this simple example, the rate of deformation tensor takes the following simple form:

$$\mathbf{D} = \begin{bmatrix} \dot{\beta}/\beta & 0 \\ 0 & 0 \end{bmatrix}$$

The beam model used in this example, which is based on the large-deformation absolute nodal coordinate formulation discussed in more detail in Chapter 5 allows for the stretch of the beam cross section. This mode of deformation, as previously mentioned, cannot be captured by many of the existing beam models that assume that the cross section of the beam remains rigid. The reader can verify that the following vector of coordinates will lead to a stretch of the beam cross section:

$$\mathbf{e} = [0 \ 0 \ 1 \ 0 \ 0 \ 1 \ l \ 0 \ 1 \ 0 \ 0 \ \alpha_2]^T$$

where  $\alpha_2$  is an assumed stretch coefficient. As in the case of elongation, when general constitutive equations are used, the assumed beam displacement field used in this example captures the Poisson effect as well as the coupling between the bending and deformation of the cross section. More general three-dimensional beam and plate models are presented in Chapter 5.

## Shear Deformation

If the lengths of all the gradient vectors remain constant, the normal strains in the defined configuration will not change as is clear from the definition of the Green–Lagrange strain tensor. If the motion is the result of only the change of the relative orientation between the gradient vectors, one obtains the case of shear deformations. In this case, the Green–Lagrange strain tensor can be written as

$$\boldsymbol{\varepsilon} = \frac{1}{2} (\mathbf{J}^T \mathbf{J} - \mathbf{I}) = \begin{bmatrix} 0 & \varepsilon_{12} & \varepsilon_{13} \\ \varepsilon_{12} & 0 & \varepsilon_{23} \\ \varepsilon_{13} & \varepsilon_{23} & 0 \end{bmatrix} = \frac{1}{2} \begin{bmatrix} 0 & \mathbf{r}_{x_1}^T \mathbf{r}_{x_2} & \mathbf{r}_{x_1}^T \mathbf{r}_{x_3} \\ \mathbf{r}_{x_1}^T \mathbf{r}_{x_2} & 0 & \mathbf{r}_{x_2}^T \mathbf{r}_{x_3} \\ \mathbf{r}_{x_1}^T \mathbf{r}_{x_3} & \mathbf{r}_{x_2}^T \mathbf{r}_{x_3} & 0 \end{bmatrix} \quad (2.120)$$

That is, the normal strains are zeros; however, the shear strains are functions of the angles between the gradient vectors. It is left to the reader to examine the effect of the coordinate transformation on the form of the Green–Lagrange strain tensor when the lengths of the gradient vectors remain constant.

### Example 2.11

Consider the beam model described in Example 10. Assume that the vector of coordinates is defined as

$$\mathbf{e} = [0 \quad 0 \quad 1 \quad 0 \quad -\sin \gamma \quad \cos \gamma \quad l \quad 0 \quad 1 \quad 0 \quad -\sin \gamma \quad \cos \gamma]^T$$

where  $l$  is the initial length of the beam and  $\gamma$  is a constant that represents an angle. The vector of coordinates shows that the gradient vectors at the endpoints of the beam are defined as

$$\mathbf{r}_{x_2}(\xi = 0) = \mathbf{r}_{x_2}(\xi = 1) = [-\sin \gamma \quad \cos \gamma]^T$$

That is, these two gradient vectors at the endpoints remain unit vectors. Substituting this vector in the displacement field  $\mathbf{r} = \mathbf{S}\mathbf{e}$ , one can show that the position vector of an arbitrary point on the beam is given by

$$\mathbf{r} = [x_1 - x_2 \sin \gamma \quad x_2 \cos \gamma]^T$$

This equation shows that points on the centerline of the beam are not displaced. One can then define the matrix of position vector gradients as

$$\mathbf{J} = \begin{bmatrix} 1 & -\sin \gamma \\ 0 & \cos \gamma \end{bmatrix}$$

In this example, the gradient vectors are no longer orthogonal, and this leads to shear strains. This can be confirmed by evaluating the Green–Lagrange strain tensor as

$$\boldsymbol{\varepsilon} = \begin{bmatrix} 0 & \varepsilon_{12} \\ \varepsilon_{12} & 0 \end{bmatrix} = \frac{1}{2} \begin{bmatrix} 0 & -\sin \gamma \\ -\sin \gamma & 0 \end{bmatrix}$$

This equation shows that  $2\varepsilon_{12} = -\sin \gamma = \cos(\gamma + \pi/2)$ , where  $(\gamma + \pi/2)$  is the angle between the gradient vectors  $\mathbf{r}_{x_1}$  and  $\mathbf{r}_{x_2}$  at the two endpoints. If  $\gamma$  is a small angle, then  $2\varepsilon_{12} \approx -\gamma$ .

In this example, one can show

$$\mathbf{J}^{-1} = \frac{1}{\cos \gamma} \begin{bmatrix} \cos \gamma & \sin \gamma \\ 0 & 1 \end{bmatrix}, \quad \dot{\mathbf{J}} = \dot{\gamma} \begin{bmatrix} 0 & -\cos \gamma \\ 0 & -\sin \gamma \end{bmatrix}$$

The velocity gradient tensor is then defined as

$$\mathbf{L} = \dot{\mathbf{J}}\mathbf{J}^{-1} = \frac{\dot{\gamma}}{\cos \gamma} \begin{bmatrix} 0 & -\cos \gamma \\ 0 & -\sin \gamma \end{bmatrix}$$

Note that there is a singularity encountered when  $\gamma = \pi/2$ . At this singular configuration, the matrix of position vector gradients has linearly dependent columns, and as a consequence, its determinant is equal to zero. The rate of deformation tensor is defined as follows:

$$\mathbf{D} = \frac{1}{2} (\mathbf{L} + \mathbf{L}^T) = \frac{\dot{\gamma}}{2 \cos \gamma} \begin{bmatrix} 0 & -\cos \gamma \\ -\cos \gamma & -2 \sin \gamma \end{bmatrix}$$

The skew-symmetric spin tensor is defined as

$$\mathbf{W} = \frac{1}{2} (\mathbf{L} - \mathbf{L}^T) = \frac{\dot{\gamma}}{2} \begin{bmatrix} 0 & -1 \\ 1 & 0 \end{bmatrix}$$

This equation shows that the spin tensor is function of  $\dot{\gamma}$  only.

In this example, one can show that the principal values of the Green-Lagrange strain tensor are

$$\lambda_1 = \varepsilon_{12} = -\frac{\sin \gamma}{2}, \quad \lambda_2 = -\varepsilon_{12} = \frac{\sin \gamma}{2}$$

The associated orthonormal principal directions are

$$\mathbf{Y}_1 = \frac{1}{\sqrt{2}} \begin{bmatrix} 1 \\ 1 \end{bmatrix}, \quad \mathbf{Y}_2 = \frac{1}{\sqrt{2}} \begin{bmatrix} 1 \\ -1 \end{bmatrix}$$

The matrix of eigenvectors  $\mathbf{Y}_m$  can then be written as

$$\mathbf{Y}_m = \frac{1}{\sqrt{2}} \begin{bmatrix} 1 & 1 \\ 1 & -1 \end{bmatrix}$$

This matrix defines a coordinate system that makes an angle  $\pi/4$  with the original coordinate system. It follows that

$$\mathbf{Y}_m^T \boldsymbol{\varepsilon} \mathbf{Y}_m = \begin{bmatrix} \varepsilon_{12} & 0 \\ 0 & -\varepsilon_{12} \end{bmatrix} = \frac{1}{2} \begin{bmatrix} -\sin \gamma & 0 \\ 0 & \sin \gamma \end{bmatrix}$$

The reader can show that the strain components in the direction of the axes of a coordinate system that makes an angle  $\pi/2$  with the original coordinate system are defined by  $-\epsilon$ . That is, in the direction of the axes of this new coordinate system, the normal strains remain equal to zero, and the shear strain changes its sign.

The preceding example sheds light on the strain transformation and the change of the strain definitions in different planes and coordinate systems. Note that in the special planar case, the general form of the symmetric strain tensor can be written as

$$\epsilon = \begin{bmatrix} \epsilon_{11} & \epsilon_{12} \\ \epsilon_{12} & \epsilon_{22} \end{bmatrix} \quad (2.121)$$

The definition of this strain tensor in another coordinate system whose orientation is defined by the transformation matrix  $\mathbf{A}$  is given as previously mentioned by the equation  $\bar{\epsilon} = \mathbf{A}^T \epsilon \mathbf{A}$ . Let the matrix  $\mathbf{A}$  be defined using the general planar transformation

$$\mathbf{A} = \begin{bmatrix} \cos \theta & -\sin \theta \\ \sin \theta & \cos \theta \end{bmatrix} \quad (2.122)$$

Then the components of the symmetric strain tensor are defined as

$$\left. \begin{aligned} \bar{\epsilon}_{11} &= \epsilon_{11} \cos^2 \theta + 2\epsilon_{12} \sin \theta \cos \theta + \epsilon_{22} \sin^2 \theta \\ \bar{\epsilon}_{22} &= \epsilon_{11} \sin^2 \theta - 2\epsilon_{12} \sin \theta \cos \theta + \epsilon_{22} \cos^2 \theta \\ \bar{\epsilon}_{12} &= (\epsilon_{22} - \epsilon_{11}) \sin \theta \cos \theta + \epsilon_{12} (\cos^2 \theta - \sin^2 \theta) \end{aligned} \right\} \quad (2.123)$$

This equation can also be written in the following form:

$$\left. \begin{aligned} \bar{\epsilon}_{11} &= \frac{(\epsilon_{11} + \epsilon_{22})}{2} + \frac{(\epsilon_{11} - \epsilon_{22})}{2} \cos 2\theta + \epsilon_{12} \sin 2\theta \\ \bar{\epsilon}_{22} &= \frac{(\epsilon_{11} + \epsilon_{22})}{2} - \frac{(\epsilon_{11} - \epsilon_{22})}{2} \cos 2\theta - \epsilon_{12} \sin 2\theta \\ \bar{\epsilon}_{12} &= \frac{(\epsilon_{22} - \epsilon_{11})}{2} \sin 2\theta + \epsilon_{12} \cos 2\theta \end{aligned} \right\} \quad (2.124)$$

This equation is the basis for a graphical representation known as *Mohr's circle* (Ugural and Fenster, 1979). The orientation of the coordinate system in which the maximum normal strains are defined can be obtained by differentiating one of the first two equations in Equation 124 with respect to  $\theta$ . This defines the angle  $\theta$  that can be substituted back into the first two equations to determine the principal strains. This procedure for determining the principal normal strains and principal directions is equivalent to the use of the eigenvalue analysis previously discussed in this chapter.

If the coordinate system is selected such that the normal strains are zero, as in the case of the preceding example, one has  $\epsilon_{11} = \epsilon_{22} = 0$ . In this case, Equation 124 leads to

$$\bar{\epsilon}_{11} = \epsilon_{12} \sin 2\theta, \quad \bar{\epsilon}_{22} = -\epsilon_{12} \sin 2\theta, \quad \bar{\epsilon}_{12} = \epsilon_{12} \cos 2\theta \quad (2.125)$$



The orientation of a coordinate system, which gives the maximum normal strains, can be determined using the preceding equation as

$$\frac{\partial \bar{\epsilon}_{11}}{\partial \theta} = \frac{\partial}{\partial \theta}(\epsilon_{12} \sin 2\theta) = 0, \quad \frac{\partial \bar{\epsilon}_{22}}{\partial \theta} = \frac{\partial}{\partial \theta}(-\epsilon_{12} \sin 2\theta) = 0 \quad (2.126)$$

which have solution  $\theta = \pi/4$ , an angle that defines the coordinate system in which the normal strains are maximum or minimum. Equation 125 shows that in this new coordinate system,  $\bar{\epsilon}_{12}$  is identically equal to zero. This result was obtained in the preceding example using the eigenvalue analysis.

Alternatively, if one starts with a coordinate system in which the shear strains are equal to zero, Equation 124 yields

$$\left. \begin{aligned} \bar{\epsilon}_{11} &= \frac{(\epsilon_{11} + \epsilon_{22})}{2} + \frac{(\epsilon_{11} - \epsilon_{22})}{2} \cos 2\theta \\ \bar{\epsilon}_{22} &= \frac{(\epsilon_{11} + \epsilon_{22})}{2} - \frac{(\epsilon_{11} - \epsilon_{22})}{2} \cos 2\theta \\ \bar{\epsilon}_{12} &= \frac{(\epsilon_{22} - \epsilon_{11})}{2} \sin 2\theta \end{aligned} \right\} \quad (2.127)$$

The orientation of the coordinate system in which the shear strain is maximum can be determined from the following equation:

$$\frac{\partial \bar{\epsilon}_{12}}{\partial \theta} = \frac{\partial}{\partial \theta} \left\{ \frac{(\epsilon_{22} - \epsilon_{11})}{2} \sin 2\theta \right\} = 0 \quad (2.128)$$

This equation defines again  $\theta = \pi/4$ . Substituting this value of  $\theta$  in the first two equations of Equation 127, one does not obtain zero normal strains.

## 2.12 GEOMETRY CONCEPTS

In many applications, the position vector gradients in the undeformed reference configuration are not orthogonal unit vectors because of the continuum initial geometry. Examples of these applications, which include tires, belt drives, and tank cars, are shown in Figure 8. In these cases, the strains evaluated using the matrix of position vector gradients in the initial configuration must be identically equal to zero. In order to explain how the strains are formulated in these cases of initial curved geometry, the three different configurations shown in Figure 9 are considered in this section. Complex geometries can always be obtained by changing the shape of simple objects; the first configuration in Figure 9 depicts the simple geometry, which can represent straight metal sheets. In this simple geometry configuration, the location of the material points is defined using the position vector  $\mathbf{x}$ . The second configuration is the reference configuration, which defines the initial undeformed geometry. In this undeformed reference configuration, the position of the material points is defined by the vector  $\mathbf{X}$ . One can write  $d\mathbf{X} = \mathbf{J}_o d\mathbf{x}$ , where  $\mathbf{J}_o = \partial \mathbf{X} / \partial \mathbf{x}$ . The third configuration shown in Figure 9 defines the current deformed configuration. In this configuration, the position of the material points



Figure 2.8 Initial geometry

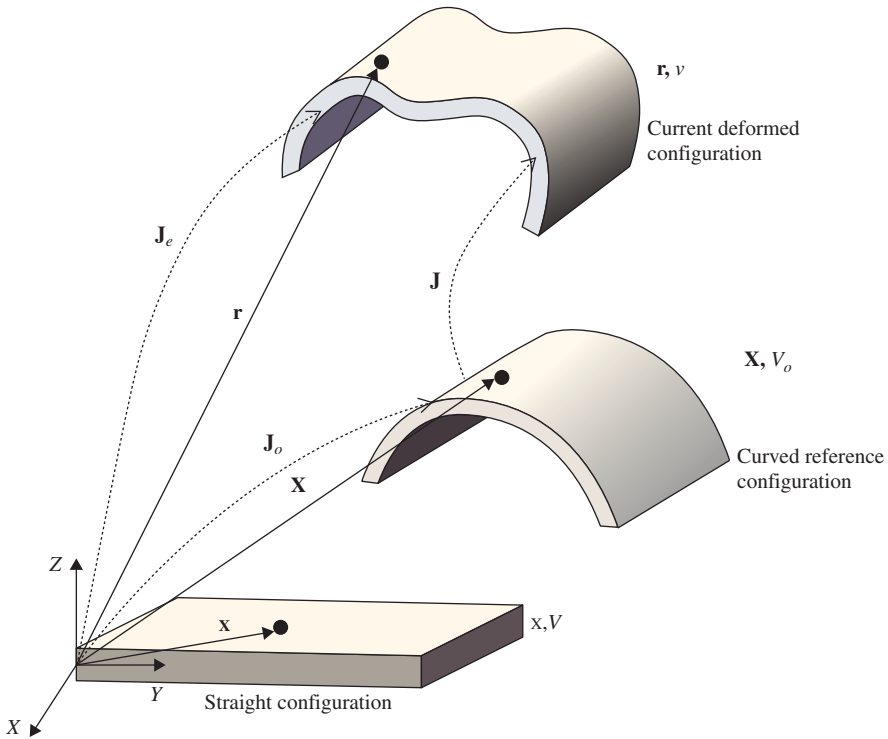


Figure 2.9 Geometry description

is defined by the vector  $\mathbf{r}$ . One can then write  $d\mathbf{r} = \mathbf{J}d\mathbf{X}$ , with  $\mathbf{J} = \partial\mathbf{r}/\partial\mathbf{X}$ . It follows that  $\mathbf{J} = \partial\mathbf{r}/\partial\mathbf{X} = (\partial\mathbf{r}/\partial\mathbf{x})(\partial\mathbf{x}/\partial\mathbf{X}) = \mathbf{J}_e\mathbf{J}_o^{-1}$ , where  $\mathbf{J}_e = \partial\mathbf{r}/\partial\mathbf{x}$ .

The volume of the curved structure  $V_o$  is related to the volume of the straight structure  $V$  (Figure 9) using the relationship  $dV_o = J_o dV$ , where  $J_o = |\mathbf{J}_o|$  is the determinant of the matrix of position vector gradients  $\mathbf{J}_o = \partial\mathbf{X}/\partial\mathbf{x}$ . Therefore, integration with respect to the domain  $V_o$  can be converted to integration with respect to the straight domain  $V$  by using the transformation  $dV_o = J_o dV$ . This allows for using the original dimensions of the simpler geometry to carry out the integrations associated with the initially curved configuration. Note that the matrix  $\mathbf{J}_o = \partial\mathbf{X}/\partial\mathbf{x}$  is constant.

The matrix of position vector gradients  $\mathbf{J} = \partial \mathbf{r} / \partial \mathbf{X}$  is the matrix, used to determine the Lagrangian strain tensor  $\boldsymbol{\epsilon}$  as  $\boldsymbol{\epsilon} = (\mathbf{J}^T \mathbf{J} - \mathbf{I})/2$ . This matrix can be defined using the ANCF description introduced in Chapter 5 as

$$\mathbf{J} = \frac{\partial \mathbf{r}}{\partial \mathbf{X}} = \left( \frac{\partial \mathbf{r}}{\partial \mathbf{x}} \right) \left( \frac{\partial \mathbf{x}}{\partial \mathbf{X}} \right) = \mathbf{J}_e \mathbf{J}_o^{-1} \quad (2.129)$$

where, as previously defined,  $\mathbf{J}_e = \partial \mathbf{r} / \partial \mathbf{x}$ . Therefore, the Lagrangian strain tensor can be written as

$$\boldsymbol{\epsilon} = \frac{1}{2} (\mathbf{J}^T \mathbf{J} - \mathbf{I}) = \frac{1}{2} (\mathbf{J}_o^{-1T} (\mathbf{J}_e^T \mathbf{J}_e) \mathbf{J}_o^{-1} - \mathbf{I}) \quad (2.130)$$

Recall that the relationship between the volume in the current deformed configuration  $v$  and the volume in the curved reference configuration  $V$  can be written as  $dv = J dV_o$ , where  $J = |\mathbf{J}|$  is the determinant of the matrix of position gradients  $\mathbf{J}$ . It follows that  $dv = J dV_o = |\mathbf{J}_e| |\mathbf{J}_o^{-1}| dV_o$ . Using the relationship  $dV_o = J_o dV$ , one has  $dv = |\mathbf{J}_e| dV$ .

The procedure described in this section to model the initial curvature, which is the same as the one used in the literature for modeling the initially curved configuration of belt drives and rubber chains (Dufva et al., 2007; and Maqueda et al., 2010), will lead to zero strains for an arbitrary initially curved geometry. Using the ANCF finite elements discussed later in this book, the constant matrix of position vector gradients  $\mathbf{J}_o = \partial \mathbf{X} / \partial \mathbf{x}$  can be determined in a straightforward manner.

## PROBLEMS

1. The assumed displacement field of a two-dimensional beam is given by  $\mathbf{r} = \mathbf{S}\mathbf{e}$ , where  $\mathbf{S}$  is a  $2 \times 8$  shape function matrix defined as

$$\mathbf{S} = [s_1 \mathbf{I} \quad s_2 \mathbf{I} \quad s_3 \mathbf{I} \quad s_4 \mathbf{I}]$$

In this equation,  $\mathbf{I}$  is a  $2 \times 2$  identity matrix and

$$\begin{aligned} s_1 &= 1 - 3\xi^2 + 2\xi^3, & s_2 &= l(\xi - 2\xi^2 + \xi^3), \\ s_3 &= 3\xi^2 - 2\xi^3, & s_4 &= l(-\xi^2 + \xi^3), \end{aligned}$$

where  $\xi = x_1/l$  and  $l$  is the length of the beam. The vector of time-dependent coordinates  $\mathbf{e}$  is defined as

$$\mathbf{e} = [\mathbf{r}^T(x_1 = 0) \quad \mathbf{r}_{x_1}^T(x_1 = 0) \quad \mathbf{r}^T(x_1 = l) \quad \mathbf{r}_{x_1}^T(x_1 = l)]^T$$

Show that this displacement field can describe an arbitrary planar rigid-body motion.

2. Show that the Green–Lagrange strain tensor does not lead to zero strains under an arbitrary rigid-body motion if nonlinear terms of the displacement gradients that appear in the definition of this strain tensor are neglected.

3. Let  $\varepsilon = (l_d - l_o)/l_o$  (see Equation 21). For the problem in Example 3, determine  $\varepsilon$  using Equation 24 at  $x_1 = 0.5l$  and  $x_1 = l$  for the following two cases of nodal coordinates assuming that  $\mathbf{t} = [1 \ 0]^T$ :

$$\mathbf{e} = [0 \ 0 \ 1 \ 0 \ 0 \ 1 \ l + \delta \ 0 \ 1 \ 0 \ 0 \ 1]^T$$

$$\mathbf{e} = \left[ 0 \ 0 \ \left(1 + \frac{\delta}{l}\right) \ 0 \ 0 \ 1 \ l + \delta \ 0 \ \left(1 + \frac{\delta}{l}\right) \ 0 \ 0 \ 1 \right]^T$$

4. Instead of the definition of  $\varepsilon$  given by Equation 21, define  $\varepsilon = (l_d - l_o)/l_d$ . Using this definition, determine an expression of  $\varepsilon$  (similar to Equation 24) in terms of the Eulerian strain tensor.
5. Using the definition of  $\varepsilon$  in the preceding problem, determine the Eulerian strain tensor and  $\varepsilon$  at  $x_1 = 0.5l$  and  $x_1 = l$  for the two cases of Problem 3.
6. For the problem in Example 3, discuss the differences between the Green–Lagrange and Eulerian strain tensors in the case of arbitrary deflection  $\delta$ .
7. For the problem in Example 3, determine the right and left Cauchy–Green deformation tensors for the two different sets of nodal coordinates.
8. For the problem in Example 4, show whether or not the right and left Cauchy–Green strain tensors depend on the rotation angle  $\theta$ .
9. For the problem in Example 3, determine the polar decomposition of the matrix of position vector gradients for  $(\delta/l) = 0.1$  at  $x_1 = 0.5l$  and  $x_1 = l$  for the two different sets of nodal coordinates. Determine both the right and left symmetric stretch matrices.
10. In the problem of Example 3, determine the rate of deformation tensor assuming that  $\dot{\delta}$  is known.
11. Repeat Example 6, assuming that the elongation  $\delta$  is not constant.
12. The Green–Lagrange strain tensor at a given point on the continuous body is defined as

$$\boldsymbol{\varepsilon} = \begin{bmatrix} 0.1 & -0.01 & 0.02 \\ -0.01 & 0.15 & 0 \\ 0.02 & 0 & 0.1 \end{bmatrix}$$

Determine the principal values, principal directions, and the strain invariants.

13. Discuss the difference between the change of the reference coordinate system and the change of the current configuration.
14. Show that  $|\mathbf{J}| = \mathbf{r}_{x_1} \cdot (\mathbf{r}_{x_2} \times \mathbf{r}_{x_3})$ , where  $|\mathbf{J}|$  is the determinant of the matrix of position vector gradients.



## CHAPTER 3

---

# FORCES AND STRESSES

---

In the theory of continuum mechanics, stresses are used as measures of the forces and pressures. As in the case of strains, different definitions can be used for the stresses; some of these definitions are associated with the reference configuration, whereas the others are associated with the current deformed configuration. The effect of the forces on the body dynamics can only be taken into consideration by using both stresses and strains. These stress and strain components must be defined in the same coordinate system in order to have a consistent formulation. In this chapter, several stress measures are introduced and the relationship between them is discussed. The *Cauchy stress formula* is presented and used to develop the partial differential equations of equilibrium of the continuous body. The equations of equilibrium are used to develop an expression for the virtual work of the stress forces expressed in terms of the stress and strain components. The objectivity of the stress rate and the energy balance equations are also among the topics discussed in this chapter.

### 3.1 EQUILIBRIUM OF FORCES

In this section, the equilibrium of forces acting in the interior of a continuous body is considered. Let  $P$  be a point on the surface of the body,  $\mathbf{n}$  be a unit vector directed along the outward normal to the surface at  $P$ , and  $ds$  be the area of an element of the surface that contains  $P$  in the current configuration. It is assumed that on the surface element with area  $ds$ , the material outside the region under consideration exerts, as shown in Figure 1, a force  $\mathbf{f}$  on the material in the region under consideration given by

$$\mathbf{f} = \boldsymbol{\sigma}_n ds \quad (3.1)$$

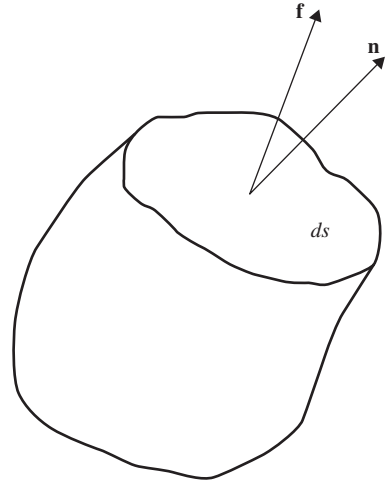


**Figure 3.1** Surface traction

The force vector  $\mathbf{f}$  is called the *surface force*, and the vector  $\boldsymbol{\sigma}_n$  is called the *mean surface traction* transmitted across the element of area  $ds$  from the outside to the inside of the region under consideration. All the variables that appear in Equation 1 are defined in the current configuration. A surface traction equal in magnitude and opposite in direction to  $\boldsymbol{\sigma}_n$  is transmitted across the element with area  $ds$  from the inside to the outside of the part of the body under consideration. It is assumed that as  $ds$  tends to zero,  $\boldsymbol{\sigma}_n$  tends to a finite limit that is independent of the shape of the element with area  $ds$ .

The mean surface traction  $\boldsymbol{\sigma}_n$  has a component along the normal to the surface defined by the dot product  $\boldsymbol{\sigma}_n \cdot \mathbf{n}$  and has components tangent to the surface defined by the vector  $\boldsymbol{\sigma}_n - (\boldsymbol{\sigma}_n \cdot \mathbf{n})\mathbf{n}$ . The tangent components introduce shear effect and define what are called shear stresses, whereas the normal component  $\boldsymbol{\sigma}_n \cdot \mathbf{n}$  defines the normal stress.

The stress force on an arbitrary surface through point  $P$  can be written in terms of the stress forces acting on three perpendicular surfaces of an infinitesimal volume containing  $P$ . In this case, as shown in Figure 2, the application of Newton's second law leads to

$$\rho \mathbf{a} dv = \mathbf{f}_b dv + \boldsymbol{\sigma}_n ds - (\boldsymbol{\sigma}_1 d\bar{s}_1 + \boldsymbol{\sigma}_2 d\bar{s}_2 + \boldsymbol{\sigma}_3 d\bar{s}_3) \quad (3.2)$$

where  $\rho$  and  $dv$  are, respectively, the mass density and volume in the current configuration;  $\mathbf{a}$  is the acceleration vector;  $\mathbf{f}_b$  is the vector of the *body forces*; and  $\boldsymbol{\sigma}_1$ ,  $\boldsymbol{\sigma}_2$ , and  $\boldsymbol{\sigma}_3$  are the mean surface tractions on the three perpendicular surfaces of the tetrahedral whose areas are  $d\bar{s}_1$ ,  $d\bar{s}_2$ , and  $d\bar{s}_3$ , respectively. Examples of the body forces are the gravitational and magnetic forces. Note that the areas  $d\bar{s}_1$ ,  $d\bar{s}_2$ , and  $d\bar{s}_3$  can be written as

$$d\bar{s}_1 = n_1 ds, \quad d\bar{s}_2 = n_2 ds, \quad d\bar{s}_3 = n_3 ds \quad (3.3)$$

where  $n_1$ ,  $n_2$ , and  $n_3$  are the components of the normal vector  $\mathbf{n}$ . Substituting the preceding area identities of Equation 3 into Newton's second law of Equation 2 and rearranging terms, one obtains

$$(\rho \mathbf{a} - \mathbf{f}_b) dv = \boldsymbol{\sigma}_n ds - (\boldsymbol{\sigma}_1 n_1 + \boldsymbol{\sigma}_2 n_2 + \boldsymbol{\sigma}_3 n_3) ds \quad (3.4)$$

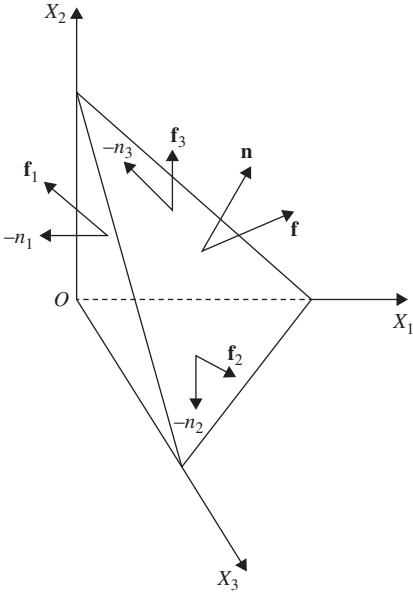


**Figure 3.2** Tetrahedral surface forces

Rearranging terms again and dividing by  $ds$ , one has

$$\sigma_n = (\sigma_1 n_1 + \sigma_2 n_2 + \sigma_3 n_3) + (\rho a - f_b) \frac{dv}{ds} \quad (3.5)$$

Because  $dv$  is proportional to the cube of the length and  $ds$  is proportional to the square of the length, as the dimensions of the tetrahedron approach zero in the limit, one has  $dv/ds$  approaching zero. Therefore, in the limit, the preceding equation leads to

$$\sigma_n = \sigma_1 n_1 + \sigma_2 n_2 + \sigma_3 n_3 \quad (3.6)$$

where  $\sigma_1$ ,  $\sigma_2$ , and  $\sigma_3$  are evaluated at point  $P$ . The preceding equation can be written using matrix notation as

$$\sigma_n = \begin{bmatrix} \sigma_1 & \sigma_2 & \sigma_3 \end{bmatrix} \begin{bmatrix} n_1 \\ n_2 \\ n_3 \end{bmatrix} = \sigma \mathbf{n} \quad (3.7)$$

Writing  $\sigma_1$ ,  $\sigma_2$ , and  $\sigma_3$  in terms of their Cartesian components, the matrix  $\sigma$  can be written as

$$\sigma = \begin{bmatrix} \sigma_1 & \sigma_2 & \sigma_3 \end{bmatrix} = \begin{bmatrix} \sigma_{11} & \sigma_{21} & \sigma_{31} \\ \sigma_{12} & \sigma_{22} & \sigma_{32} \\ \sigma_{13} & \sigma_{23} & \sigma_{33} \end{bmatrix} \quad (3.8)$$

Equation 6 or 7 is called the *Cauchy stress formula*, and the elements  $\sigma_{ij}$  of the matrix  $\sigma$  are called *Cauchy stresses*. The elements  $\sigma_{ij}$  for  $i=j$  are called the *normal stresses*, whereas  $\sigma_{ij}$  for



$i \neq j$  are called the *shear stresses*. Therefore, the vector of forces exerted on the region under consideration can be written in terms of the Cauchy stresses as

$$\mathbf{f} = \boldsymbol{\sigma} \mathbf{n} ds \quad (3.9)$$

It is important to emphasize again that all the variables in this equation, unlike the definition of the Green–Lagrange strains, are defined using the current configuration.

### 3.2 TRANSFORMATION OF STRESSES

In order to be able to develop the expressions for the components of the stress tensor  $\boldsymbol{\sigma}$  in different coordinate systems, consider a coordinate system  $\tilde{X}_1\tilde{X}_2\tilde{X}_3$  whose orientation with respect to the coordinate system  $X_1X_2X_3$  is defined by the orthogonal transformation matrix  $\mathbf{A}$ . The vector  $\boldsymbol{\sigma}_n = \boldsymbol{\sigma} \mathbf{n}$  can be defined in the  $\tilde{X}_1\tilde{X}_2\tilde{X}_3$  as

$$\bar{\boldsymbol{\sigma}}_n = \mathbf{A}^T \boldsymbol{\sigma}_n = \mathbf{A}^T \boldsymbol{\sigma} \mathbf{n} = \mathbf{A}^T \boldsymbol{\sigma} \mathbf{A} \bar{\mathbf{n}} \quad (3.10)$$

where  $\mathbf{n} = \mathbf{A} \bar{\mathbf{n}}$ . The preceding equation can be written as  $\bar{\boldsymbol{\sigma}}_n = \bar{\boldsymbol{\sigma}} \bar{\mathbf{n}}$  where

$$\bar{\boldsymbol{\sigma}} = \mathbf{A}^T \boldsymbol{\sigma} \mathbf{A} \quad (3.11)$$

This equation, which shows the rule of transformation of the stress tensor  $\boldsymbol{\sigma}$ , can be used to define the stress components in different coordinate systems. As in the case of the strain tensor, one can define directions, called *principal directions*, along which the normal stresses take maximum or minimum values and the shear stresses vanish.

### 3.3 EQUATIONS OF EQUILIBRIUM

The equations of equilibrium of the continuous body can be obtained by summing the integrals of all the forces acting on the body material points. The formulation of the *body forces* such as gravitational, magnetic, and inertia forces can be obtained from integration over the volume, whereas surface forces such as contact forces and hydrostatic pressure can be formulated in terms of surface integrals. Thus, the condition for the dynamic equilibrium can be written as

$$\int_s \boldsymbol{\sigma}_n ds + \int_v \mathbf{f}_b dv = \int_v \rho \mathbf{a} dv \quad (3.12)$$

where  $s$  and  $v$  are, respectively, the area and volume of the continuous body in the current configuration, and  $\rho$  is the mass density. The first integral in the preceding equation can be written as a volume integral using the *divergence theorem* as follows:

$$\int_s \boldsymbol{\sigma}_n ds = \int_s \boldsymbol{\sigma} \mathbf{n} ds = \int_v (\nabla \boldsymbol{\sigma}^T)^T dv \quad (3.13)$$

Because the integrals in this equation are defined with respect to the current configuration, the *divergence operator* is defined as

$$\nabla = \frac{\partial}{\partial \mathbf{r}} = \left[ \frac{\partial}{\partial r_1} \quad \frac{\partial}{\partial r_2} \quad \frac{\partial}{\partial r_3} \right] \quad (3.14)$$

Using the preceding relationships, the dynamic equations of equilibrium can be written as follows:

$$\int_v \left\{ (\nabla \boldsymbol{\sigma}^T)^T + \mathbf{f}_b - \rho \mathbf{a} \right\} dv = \mathbf{0} \quad (3.15)$$

This equation must hold in every region in the body and, therefore, the integrand must be equal to zero. This leads to

$$(\nabla \boldsymbol{\sigma}^T)^T + \mathbf{f}_b - \rho \mathbf{a} = \mathbf{0} \quad (3.16)$$

These equations are known as the *equations of equilibrium*. In some texts, Equation 16 is called *Cauchy's first law of motion* (Ogden, 1984). In a more explicit form, the equations of equilibrium can be written as

$$\left. \begin{aligned} \sigma_{11,1} + \sigma_{21,2} + \sigma_{31,3} + f_{b1} &= \rho a_1 \\ \sigma_{12,1} + \sigma_{22,2} + \sigma_{32,3} + f_{b2} &= \rho a_2 \\ \sigma_{13,1} + \sigma_{23,2} + \sigma_{33,3} + f_{b3} &= \rho a_3 \end{aligned} \right\} \quad (3.17)$$

where subscript  $(,i)$  denotes differentiation with respect to  $r_i$ ;  $a_1, a_2$ , and  $a_3$  are the components of the absolute acceleration vector; and  $f_{b1}, f_{b2}$ , and  $f_{b3}$  are the components of the vector of the body forces. Note that the equations of equilibrium are partial differential equations that are space- and time dependent. These equations are general and are applicable to any solid or fluid materials because no assumptions are made in their derivation. Furthermore, the partial differential equations of equilibrium impose no restrictions on the amount of deformation or rotation at the material points of the continuum and, therefore, these equations can be used for the linear as well as the nonlinear analyses. Nonetheless, special forms of motion can be systematically obtained from the partial differential equations of equilibrium by employing the appropriate assumptions. For example, the Newton–Euler equations used in rigid-body dynamics can be systematically obtained from Equation 17 by recognizing that the rigid body has a finite number of degrees of freedom instead of an infinite number. In this case, as discussed in the preceding chapters, the global position vector of an arbitrary point on the rigid body can be written as  $\mathbf{r} = \mathbf{r}_O + \mathbf{A}\mathbf{x}$ , where  $\mathbf{r}_O$  is the global position vector of the origin of the selected body coordinate system,  $\mathbf{A}$  is the orthogonal transformation matrix that defines the orientation of the body coordinate system with respect to the global coordinate system, and  $\mathbf{x}$  is the position vector of the arbitrary point in the reference configuration. The transformation matrix  $\mathbf{A}$  can be expressed in terms of a set of orientation parameters  $\boldsymbol{\theta}$ . Using this motion description, the acceleration vector  $\mathbf{a}$  can be obtained as  $\mathbf{a} = \ddot{\mathbf{r}}$ . Multiplying Equation 17 by the virtual change  $\delta \mathbf{r}$ , assuming the stresses are zero due to the rigid-body assumption, integrating over the volume, and grouping the coefficients of  $\delta \mathbf{r}_O$  and  $\delta \boldsymbol{\theta}$ ; one can systematically obtain the ordinary differential equations that govern the motion of the rigid bodies (Roberson and Schwertassek, 1988; Shabana, 2001). Applying this systematic procedure to derive the Newton–Euler equations of

planar rigid bodies is left to the reader as an exercise. It is important, however, to realize that when the Newton–Euler formulation is used, the origin of the body coordinate system is assumed to be attached to the body center of mass. If this assumption is not considered, the principle of virtual work leads to a more general form of the equations of motion, which include dynamic coupling between the translation and rotation of the rigid body.

In the general case of a continuum, the stresses can be expressed in terms of the strains and their derivatives using the *constitutive equations*, which distinguish one material from another and will be discussed in the following chapter. The strain variables can be written in terms of the displacements, as explained in Chapter 2. That is, one can always, for a given material, write the stresses in terms of the displacements. When these relationships are substituted into Equation 17, the partial differential equations of equilibrium can be expressed in terms of the displacements and their spatial and time derivatives. The resulting partial differential equations can have a closed-form solution only under strict simplifying assumptions and in the case of simple structural elements such as rods and beams. These simplified formulations that are the result of linearization assumptions lead to the linear wave equations, which can be solved for given sets of initial and boundary conditions. The wave equations are covered in texts on the subjects of vibration and wave propagation. For more general nonlinear systems, the principle of virtual work and the finite element method can always be used to obtain a set of ordinary differential equations that govern the motion of the continuum. These ordinary differential equations can be solved numerically to determine the behavior of the continuum in response to arbitrary loading conditions.

### 3.4 SYMMETRY OF THE CAUCHY STRESS TENSOR

In developing the partial differential equations of motion, the equilibrium of the forces was considered. The condition that the resultant of the moments of all forces, including the inertia forces, about the origin must be equal to zero can be used to prove the symmetry of the stress tensor. This condition can be written as

$$\int_s \mathbf{r} \times \boldsymbol{\sigma}_n ds + \int_v \mathbf{r} \times \mathbf{f}_b dv = \int_v \rho \mathbf{r} \times \mathbf{a} dv \quad (3.18)$$

The first integral of this equation can be written as

$$\int_s \mathbf{r} \times \boldsymbol{\sigma}_n ds = \int_s \mathbf{r} \times (\boldsymbol{\sigma} \mathbf{n}) ds = \int_s (\tilde{\mathbf{r}} \boldsymbol{\sigma}) \mathbf{n} ds = \int_v \{ \nabla (\tilde{\mathbf{r}} \boldsymbol{\sigma})^T \}^T dv \quad (3.19)$$

It can be shown that this equation can be written as

$$\int_s \mathbf{r} \times \boldsymbol{\sigma}_n ds = \int_v \{ \nabla (\tilde{\mathbf{r}} \boldsymbol{\sigma})^T \}^T dv = \int_v \{ (\nabla \boldsymbol{\sigma}^T) \tilde{\mathbf{r}}^T + \mathbf{b}_s^T \}^T dv \quad (3.20)$$

where the vector  $\mathbf{b}_s$  is defined as

$$\mathbf{b}_s = \begin{bmatrix} \sigma_{23} - \sigma_{32} \\ \sigma_{31} - \sigma_{13} \\ \sigma_{12} - \sigma_{21} \end{bmatrix} \quad (3.21)$$

Substituting Equation 20 into Equation 18 yields

$$\int_v \left\{ \mathbf{r} \times \left( (\nabla \boldsymbol{\sigma}^T)^T + \mathbf{f}_b - \rho \mathbf{a} \right) \right\} dv + \int_v \mathbf{b}_s dv = \mathbf{0} \quad (3.22)$$

It is clear that the first integral in this equation vanishes by the virtue of the equation of equilibrium. Therefore, one has  $\int_v \mathbf{b}_s dv = \mathbf{0}$ . Because this equation must hold in every region in the body, the integrand must be equal to zero, that is,

$$\mathbf{b}_s = \begin{bmatrix} \sigma_{23} - \sigma_{32} \\ \sigma_{31} - \sigma_{13} \\ \sigma_{12} - \sigma_{21} \end{bmatrix} = \mathbf{0} \quad (3.23)$$

which shows that

$$\sigma_{23} = \sigma_{32}, \quad \sigma_{31} = \sigma_{13}, \quad \sigma_{12} = \sigma_{21} \quad (3.24)$$

that is,  $\sigma_{ij} = \sigma_{ji}$  for  $i \neq j$ . This proves that the Cauchy stress tensor is indeed a symmetric tensor. Some authors refer to Equation 23, or equivalently Equation 24 as *Cauchy's second law of motion* (Ogden, 1984).

### Principal Stresses

Because the Cauchy stress tensor  $\boldsymbol{\sigma}$  is symmetric, it has three real principal values that can be determined by solving the following eigenvalue problem:

$$(\boldsymbol{\sigma} - \tau \mathbf{I})\mathbf{c} = \mathbf{0} \quad (3.25)$$

where  $\tau$  is the eigenvalue or principal value, and  $\mathbf{c}$  is the eigenvector. As in the case of the strain tensor, the preceding equation can be used to determine three principal values  $\tau_1$ ,  $\tau_2$ , and  $\tau_3$  called the *principal stresses*. Associated with these three eigenvalues, there are three eigenvectors  $\mathbf{c}_1$ ,  $\mathbf{c}_2$ , and  $\mathbf{c}_3$ , which define the *principal directions*. If the coordinate axes coincide with the principal directions, shear stresses are identically equal to zeros.

The three principal values  $\tau_1$ ,  $\tau_2$ , and  $\tau_3$  are invariants and do not depend on the choice of the coordinate system. Clearly, any quantity that is expressed in terms of these invariants only is also an invariant. Because of the symmetry of the Cauchy stress tensor  $\boldsymbol{\sigma}$ , one can define the following three independent stress invariants:

$$\left. \begin{aligned} J_1 &= \tau_1 + \tau_2 + \tau_3 = \text{tr}(\boldsymbol{\sigma}) \\ J_2 &= \tau_1 \tau_2 + \tau_1 \tau_3 + \tau_2 \tau_3 = \frac{1}{2} \{ (\text{tr}(\boldsymbol{\sigma}))^2 - \text{tr}(\boldsymbol{\sigma}^2) \} \\ J_3 &= \tau_1 \tau_2 \tau_3 = \det(\boldsymbol{\sigma}) = |\boldsymbol{\sigma}| \end{aligned} \right\} \quad (3.26)$$

Some of these definitions are used later in this chapter when the deviatoric stresses are introduced.

### 3.5 VIRTUAL WORK OF THE FORCES

The definitions of the forces and stresses presented in the preceding sections are based on the current configuration; areas and volumes in the current configuration instead of the reference configuration are used. For this reason, Cauchy stress is called the *physical* or *true stress*.

In the preceding chapter, on the other hand, the reference configuration is used to define the Green–Lagrange strains. In the case of large deformations, the Cauchy stress tensor is not associated with the Green–Lagrange strain tensor because Cauchy stress tensor is defined in the current (deformed) configuration, whereas the Green–Lagrange strain tensor is defined in the reference configuration.

In this section, the partial differential equations of equilibrium are used to derive the virtual work of the forces. The principle of virtual work and the approximation of the displacement field are the two main building blocks that form the foundation of the finite element method. Approximation methods, as discussed in Chapter 1, lead to a finite dimensional model; whereas the principle of virtual work, which has its roots in D’Alembert’s principle, can be used to systematically eliminate the connection forces and obtain a set of discrete equations that govern the motion of the continuum.

The analysis presented in this section shows that the stresses and strains arise naturally in the formulation of the elastic forces of the continuum. It is important, however, to use consistent stress and strain definitions, particularly in the analysis of large-deformation problems. The development in this section will show that another symmetric stress tensor, the *second Piola–Kirchhoff stress tensor*, is associated with the Green–Lagrange strain tensor  $\epsilon$ . In order to simplify the derivation presented in this section, the *tensor double product* and the change of the volume of a material element, which are used in the derivation presented in this section, are first reviewed.

### Tensor Double Product (Contraction)

As discussed in Chapter 1, if  $\mathbf{A}$  and  $\mathbf{B}$  are second-order tensors, the double product or double contraction is defined as

$$\mathbf{A} : \mathbf{B} = \text{tr}(\mathbf{A}^T \mathbf{B}) \quad (3.27)$$

where  $\text{tr}$  denotes the trace of the matrix (sum of the diagonal elements). Using the properties of the trace, one can show that

$$\left. \begin{aligned} \mathbf{A} : \mathbf{B} &= \text{tr}(\mathbf{A}^T \mathbf{B}) = \text{tr}(\mathbf{B} \mathbf{A}^T) = \text{tr}(\mathbf{B}^T \mathbf{A}) = \text{tr}(\mathbf{A} \mathbf{B}^T) = \sum_{i,j=1}^3 A_{ij} B_{ij} \\ \mathbf{A} : (\mathbf{B} \mathbf{C}) &= (\mathbf{A} \mathbf{C}^T) : \mathbf{B} = (\mathbf{B}^T \mathbf{A}) : \mathbf{C} \end{aligned} \right\} \quad (3.28)$$

where  $A_{ij}$  and  $B_{ij}$  are, respectively, the elements of the tensors  $\mathbf{A}$  and  $\mathbf{B}$ , and  $\mathbf{C}$  is a second-order tensor.

### Volume Change

It was shown in the preceding chapter that  $dV$  and  $dv$ , which represent the volumes of a material element in the reference and current configurations, respectively, are related by

$$dv = J dV \quad (3.29)$$

where  $J = |\mathbf{J}|$  is the determinant of the matrix of position vector gradients  $\mathbf{J}$ .

## Virtual Work

In this section, the principle of virtual work in dynamics is used to define the virtual work of the elastic forces in terms of the stress and strain components. To this end, the equations of equilibrium (Equation 16 or 17) are multiplied by  $\delta \mathbf{r}$  and integrated over the current volume to obtain

$$\int_v \{(\nabla \boldsymbol{\sigma})^T + \mathbf{f}_b - \rho \mathbf{a}\}^T \delta \mathbf{r} dv = 0 \quad (3.30)$$

In this equation,  $\nabla = \left[ \frac{\partial}{\partial r_1} \frac{\partial}{\partial r_2} \frac{\partial}{\partial r_3} \right]$  is considered as a row vector. The form of the equation of motion defined by Equation 30 is called in the literature the *weak form* and is used with approximation methods as the basis for computational techniques such as the finite element method. One can show that

$$\nabla(\boldsymbol{\sigma} \delta \mathbf{r}) = (\nabla \boldsymbol{\sigma}) \delta \mathbf{r} + \boldsymbol{\sigma} : \frac{\partial}{\partial \mathbf{r}}(\delta \mathbf{r}) \quad (3.31)$$

where

$$\frac{\partial}{\partial \mathbf{r}}(\delta \mathbf{r}) = \frac{\partial(\delta \mathbf{r})}{\partial \mathbf{x}} \frac{\partial \mathbf{x}}{\partial \mathbf{r}} = (\delta \mathbf{J}) \mathbf{J}^{-1} \quad (3.32)$$

Substituting the preceding two equations into the virtual work of the forces and using *Gauss theorem*, one obtains

$$\int_s \mathbf{n}^T \boldsymbol{\sigma} \delta \mathbf{r} ds - \int_v \boldsymbol{\sigma} : (\delta \mathbf{J}) \mathbf{J}^{-1} dv + \int_v (\mathbf{f}_b - \rho \mathbf{a})^T \delta \mathbf{r} dv = 0 \quad (3.33)$$

where  $s$  is the current surface area, and  $\mathbf{n}$  is a unit normal to the surface. The first integral in the preceding equation represents the virtual work of the surface traction forces, the second integral is the virtual work of the internal elastic forces, and the third integral is the virtual work of the body and inertia forces. If the principle of *conservation of mass* or *continuity condition* ( $\rho dv = \rho_o dV$ ) is assumed, the virtual work of the inertia forces can be written as

$$\delta W_i = \int_v \rho \mathbf{a}^T \delta \mathbf{r} dv = \int_V \rho_o \mathbf{a}^T \delta \mathbf{r} dV \quad (3.34)$$

This equation is important in developing the inertia forces of the continuous bodies when computational techniques such as the finite element method are used.

## Other Stress Measures

The virtual work of the internal elastic forces defined by the second term of Equation 33 is

$$\delta W_s = - \int_v \boldsymbol{\sigma} : (\delta \mathbf{J}) \mathbf{J}^{-1} dv \quad (3.35)$$

Using Equation 29, the integration can be performed using the volume at the reference configuration. The preceding equation can then be written as

$$\delta W_s = - \int_V \mathbf{J} \boldsymbol{\sigma} : (\delta \mathbf{J}) \mathbf{J}^{-1} dV \quad (3.36)$$

where as previously defined  $J = |\mathbf{J}|$ . The tensor  $\boldsymbol{\sigma}_K = J\boldsymbol{\sigma}$  is called the *Kirchhoff stress tensor*, which is a symmetric tensor and differs from Cauchy stress tensor by a scalar multiplier equal to the determinant of the matrix of the position vector gradients. In the case of small deformations, this determinant remains approximately equal to one, and Cauchy and Kirchhoff stress tensors do not differ significantly. Note also that  $(\delta\mathbf{J})\mathbf{J}^{-1}$  is the virtual change in the deformation measure associated with Kirchhoff stress tensor  $\boldsymbol{\sigma}_K$ .

## First and Second Piola–Kirchhoff Stress Tensors

In deriving Nanson's formula presented in the preceding chapter, it was shown that the normal  $\mathbf{N}$  to a surface  $dS$  in the reference configuration can be written in terms of the normal  $\mathbf{n}$  to a surface  $ds$  in the current deformed configuration as  $\mathbf{N} = (1/J)\mathbf{J}^T\mathbf{n}(ds/dS)$ . Using this equation, one can write  $\mathbf{n}ds = J(\mathbf{J}^T)^{-1}\mathbf{N}dS$ . As previously shown in this chapter, the force acting on a surface with unit normal  $\mathbf{n}$  is defined as  $\mathbf{f} = \boldsymbol{\sigma}_n ds = \boldsymbol{\sigma}\mathbf{n}ds$ , where  $\boldsymbol{\sigma}_n$  is the pressure distribution on the surface and  $\boldsymbol{\sigma}$  is the Cauchy stress tensor or the true stress defined using the current deformed configuration. Substituting for  $\mathbf{n}ds$ , one can write the force  $\mathbf{f} = \boldsymbol{\sigma}\mathbf{n}ds$  in terms of the normal and area defined in the reference configuration as  $\mathbf{f} = (J\boldsymbol{\sigma}(\mathbf{J}^T)^{-1})\mathbf{N}dS$ , which defines another stress measure called the *first Piola–Kirchhoff stress*, which is associated with the reference configuration and is given by

$$\boldsymbol{\sigma}_{P1} = J\boldsymbol{\sigma}(\mathbf{J}^T)^{-1} \quad (3.37)$$

This equation shows that the first Piola–Kirchhoff stress tensor, which can be used to define the force in terms of the normal and area in the reference configuration, is not a symmetric tensor and it is not the tensor that is associated with the Green–Lagrange strain tensor in the formulation of the elastic forces. Nonetheless, since the Cauchy stress tensor  $\boldsymbol{\sigma}$  is symmetric, the preceding equation can be used to show that the first Piola–Kirchhoff stress tensor satisfies the identity  $\boldsymbol{\sigma}_{P1}\mathbf{J}^T = \mathbf{J}\boldsymbol{\sigma}_{P1}^T$ . Furthermore, it follows from Eq. 36 and the properties of the double product that the virtual work of the elastic forces can be written in terms of the first Piola–Kirchhoff stress tensor as  $\delta W_s = -\int_V \boldsymbol{\sigma}_{P1} : \delta\mathbf{J} dV$ , which shows that  $\boldsymbol{\sigma}_{P1}$  is associated with the matrix of the position vector gradients  $\mathbf{J}$ . Recall that the matrix of position vector gradients  $\mathbf{J}$  is not an appropriate measure of the deformation since this matrix does not remain constant under an arbitrary rigid-body motion.

Using the definition of the Green–Lagrange strain tensor defined in the preceding chapter,  $\boldsymbol{\varepsilon} = (1/2)(\mathbf{J}^T\mathbf{J} - \mathbf{I})$ , one can show that

$$\delta\boldsymbol{\varepsilon} = \frac{1}{2}(\mathbf{J}^T\delta\mathbf{J} + (\delta\mathbf{J}^T)\mathbf{J}) \quad (3.38)$$

Using this equation and the identities of Equation 28, the virtual work of the internal elastic forces of Equation 36 can be written in terms of the virtual changes of the components of the Green–Lagrange strain tensor as

$$\delta W_s = -\int_V J\boldsymbol{\sigma} : \mathbf{J}^{-1^T} \delta\boldsymbol{\varepsilon} \mathbf{J}^{-1} dV \quad (3.39)$$

This equation upon the use of the properties of the tensor double product (Equation 28) can be written as

$$\delta W_s = - \int_V (J\mathbf{J}^{-1}\boldsymbol{\sigma}\mathbf{J}^{-1T}) : \delta\boldsymbol{\varepsilon} dV \quad (3.40)$$

which can be written as follows:

$$\delta W_s = - \int_V \boldsymbol{\sigma}_{P2} : \delta\boldsymbol{\varepsilon} dV \quad (3.41)$$

where  $\boldsymbol{\sigma}_{P2}$  is the *second Piola–Kirchhoff stress tensor* defined as

$$\boldsymbol{\sigma}_{P2} = J\mathbf{J}^{-1}\boldsymbol{\sigma}\mathbf{J}^{-1T} \quad (3.42)$$

Clearly, the second Piola–Kirchhoff stress tensor is a symmetric tensor, and it is the stress tensor associated with the Green–Lagrange strain tensor because both are defined with respect to the reference configuration.

Another stress tensor that is used in continuum mechanics is the *Biot stress tensor*  $\boldsymbol{\sigma}_B$ . This stress tensor is defined in terms of the first Piola–Kirchhoff stress tensor as  $\boldsymbol{\sigma}_B = (\mathbf{R}\boldsymbol{\sigma}_{P1})^T$ , where  $\mathbf{R}$  is the orthogonal matrix that appears in the polar decomposition of the matrix of position vector gradients. That is,  $\mathbf{J} = \mathbf{R}\mathbf{U}$ , where  $\mathbf{U}$  is the symmetric stretch matrix. It can also be shown that the Biot stress tensor can be written in terms of the second Piola–Kirchhoff stress tensor as  $\boldsymbol{\sigma}_B = \mathbf{R}^T \mathbf{J} \boldsymbol{\sigma}_{P2}$ .

### Example 3.1

Consider the beam model used in the examples of the preceding chapter. Assume that the beam displacement is described by

$$\mathbf{r} = [(l + \delta)\xi \quad l\eta]^T$$

where  $\xi = x_1/l$ ,  $\eta = x_2/l$ ,  $l$  is the length of the beam, and  $\delta$  is a constant that defines the beam axial deformation. It was shown in Example 3 of the preceding chapter that this displacement can be produced using the following vector of beam coordinates:

$$\mathbf{e} = \left[ 0 \quad 0 \quad \left(1 + \frac{\delta}{l}\right) \quad 0 \quad 0 \quad 1 \quad l + \delta \quad 0 \quad \left(1 + \frac{\delta}{l}\right) \quad 0 \quad 0 \quad 1 \right]^T$$

The matrix of position vector gradients and its inverse are defined as

$$\mathbf{J} = \begin{bmatrix} 1 + \frac{\delta}{l} & 0 \\ 0 & 1 \end{bmatrix}, \quad \mathbf{J}^{-1} = \begin{bmatrix} \frac{l}{l + \delta} & 0 \\ 0 & 1 \end{bmatrix}$$

The determinant of the matrix of the position vector gradients

$$J = |\mathbf{J}| = 1 + \frac{\delta}{l}$$



Note that for large  $\delta$ ,  $J$  can differ significantly from one. The Green–Lagrange strain tensor is defined in this case as

$$\boldsymbol{\varepsilon} = \frac{1}{2}(\mathbf{J}^T \mathbf{J} - \mathbf{I}) = \begin{bmatrix} \varepsilon_{11} & \varepsilon_{12} \\ \varepsilon_{21} & \varepsilon_{22} \end{bmatrix} = \begin{bmatrix} \frac{\delta}{l} \left(1 + \frac{\delta}{2l}\right) & 0 \\ 0 & 0 \end{bmatrix} = \varepsilon_{11} \begin{bmatrix} 1 & 0 \\ 0 & 0 \end{bmatrix}$$

where  $\varepsilon_{11} = (\delta/l) (1 + (\delta/2l))$ .

Assume that the second Piola–Kirchhoff stress tensor is given for this strain state by the following linear relationship:

$$\boldsymbol{\sigma}_{P2} = \begin{bmatrix} \lambda_1 \varepsilon_{11} & 0 \\ 0 & \lambda_2 \varepsilon_{11} \end{bmatrix} = \varepsilon_{11} \begin{bmatrix} \lambda_1 & 0 \\ 0 & \lambda_2 \end{bmatrix}$$

where  $\lambda_1$  and  $\lambda_2$  are appropriate stiffness coefficients. The Cauchy stress tensor can be defined for this simple example as

$$\boldsymbol{\sigma} = \frac{1}{J} \mathbf{J} \boldsymbol{\sigma}_{P2} \mathbf{J}^T = \frac{l \varepsilon_{11}}{l + \delta} \begin{bmatrix} \lambda_1 \left(\frac{l + \delta}{l}\right)^2 & 0 \\ 0 & \lambda_2 \end{bmatrix}$$

It is clear from this equation and from the definition of  $\varepsilon_{11}$  that if  $\delta$  is small, then  $\boldsymbol{\sigma}_{P2} \approx \boldsymbol{\sigma}$ ; otherwise, there can be significant differences between the two stress measures.

## Notation and Procedure

As previously pointed out, if the displacement is small, the matrix of the position vector gradients (Jacobian)  $\mathbf{J}$  does not differ significantly from the identity matrix, and as a consequence, it is acceptable not to distinguish between Cauchy stress tensor, which is defined using the deformed configuration and the second Piola–Kirchhoff stress tensor associated with the reference undeformed configuration. In this book, unless stated otherwise, we will always use the Green–Lagrange strains with the understanding that the associated stress is the second Piola–Kirchhoff stress tensor. For the sake of simplicity of the notation in some of the general developments presented in the following chapters, we will occasionally use  $\boldsymbol{\sigma}$  to denote the stress measure. That is,  $\boldsymbol{\sigma}$  will be used to denote other stress measures such as the second Piola–Kirchhoff stress tensor  $\boldsymbol{\sigma}_{P2}$  instead of Cauchy stress tensor because whenever there is a difference between the two tensors (case of large deformation), it is with the understanding that the second Piola–Kirchhoff stress tensor is the one to be used with the Green–Lagrange strain tensor. Using the tensor double product, and the fact that both  $\boldsymbol{\sigma}_{P2}$  and  $\boldsymbol{\varepsilon}$  are symmetric tensors, one can show that Equation 41 can be written as follows:

$$\begin{aligned} \delta W_s &= - \int_V \boldsymbol{\sigma}_{P2} : \delta \boldsymbol{\varepsilon} dV \\ &= - \int_V (\sigma_{11} \delta \varepsilon_{11} + \sigma_{22} \delta \varepsilon_{22} + \sigma_{33} \delta \varepsilon_{33} + 2\sigma_{12} \delta \varepsilon_{12} + 2\sigma_{13} \delta \varepsilon_{13} + 2\sigma_{23} \delta \varepsilon_{23}) dV \quad (3.43) \end{aligned}$$

where  $\sigma_{ij}$  and  $\varepsilon_{ij}$  are, respectively, the elements of the second Piola–Kirchhoff stress tensor and the Green–Lagrange strain tensor. Using the preceding equation, one can show that the virtual work of the elastic forces can be written in terms of the virtual changes in the position vector gradients as  $\delta W_s = -\int_V ((\mathbf{r}_x \boldsymbol{\sigma}_{c1})^T \delta \mathbf{r}_{x_1} + (\mathbf{r}_x \boldsymbol{\sigma}_{c2})^T \delta \mathbf{r}_{x_2} + (\mathbf{r}_x \boldsymbol{\sigma}_{c3})^T \delta \mathbf{r}_{x_3}) dV$ , where  $\mathbf{r}_x = [\mathbf{r}_{x_1} \ \mathbf{r}_{x_2} \ \mathbf{r}_{x_3}]$  is the matrix of position vector gradients,  $\mathbf{x} = [x_1 \ x_2 \ x_3]^T$  is the vector of spatial coordinates, and  $\boldsymbol{\sigma}_{c1} = [\sigma_{11} \ \sigma_{12} \ \sigma_{13}]^T$ ,  $\boldsymbol{\sigma}_{c2} = [\sigma_{12} \ \sigma_{22} \ \sigma_{23}]^T$ , and  $\boldsymbol{\sigma}_{c3} = [\sigma_{13} \ \sigma_{23} \ \sigma_{33}]^T$  are the column of the stress tensor. When a finite dimensional model based on the kinematic description  $\mathbf{r} = \mathbf{S}(\mathbf{x})\mathbf{q}$  is used, one has  $\delta \mathbf{r}_{x_i} = \mathbf{S}_{x_i} \delta \mathbf{q}$ . It follows that the virtual work of the elastic forces can be written as  $\delta W_s = -(\int_V ((\mathbf{r}_x \boldsymbol{\sigma}_{c1})^T \mathbf{S}_{x_1} + (\mathbf{r}_x \boldsymbol{\sigma}_{c2})^T \mathbf{S}_{x_2} + (\mathbf{r}_x \boldsymbol{\sigma}_{c3})^T \mathbf{S}_{x_3}) dV) \delta \mathbf{q}$ , which can be written as  $\delta W_s = \mathbf{Q}_s^T \delta \mathbf{q}$ , where  $\mathbf{Q}_s = -\int_V ((\mathbf{S}_{x_1}^T \mathbf{r}_x) \boldsymbol{\sigma}_{c1} + (\mathbf{S}_{x_2}^T \mathbf{r}_x) \boldsymbol{\sigma}_{c2} + (\mathbf{S}_{x_3}^T \mathbf{r}_x) \boldsymbol{\sigma}_{c3}) dV$  is the vector of elastic generalized forces. This vector is, in general, a highly nonlinear function of the coordinates and, therefore, numerical integration is often required to calculate this force vector.

In addition to the virtual work of the elastic forces, the principle of virtual work also defines the virtual works of the inertia and applied forces. The virtual work of the inertia forces is defined as  $\delta W_i = \int_V \rho \mathbf{a}^T \delta \mathbf{r} dv$ , with  $\mathbf{a} = \ddot{\mathbf{r}}$  as the acceleration vector. The virtual work of the body forces is defined as  $\delta W_e = \int_V \mathbf{f}_b^T \delta \mathbf{r} dv$ . If the forces are defined in the reference configuration, the volume in the reference configuration should be used, instead of the volume in the current configuration, in evaluating the integration resulting from the use of the virtual work principle. If approximation methods are used to define  $\mathbf{r}$  and  $\delta \mathbf{r}$ , one can systematically obtain a finite dimensional model. The following example demonstrates the use of this procedure for the inertia forces. The same procedure can be applied for other forces, as will be discussed in more detail in Chapters 5 and 6.

### Example 3.2

As discussed previously in Chapter 1, in some of the nonlinear finite element formulations, the global position vector of an arbitrary point on the body can be written as  $\mathbf{r} = \mathbf{S}\mathbf{q}$ , where  $\mathbf{S} = \mathbf{S}(\mathbf{x})$  is the space-dependent shape function matrix,  $\mathbf{x} = [x_1 \ x_2 \ x_3]^T$  is the vector of reference coordinates, and  $\mathbf{q} = \mathbf{q}(t)$  is the vector of time-dependent coordinates. In this case, the virtual change in the position vector and the acceleration vector can be written, respectively, as

$$\delta \mathbf{r} = \mathbf{S} \delta \mathbf{q}, \quad \ddot{\mathbf{r}} = \mathbf{S} \ddot{\mathbf{q}}$$

The mass of an arbitrary infinitesimal volume is  $\rho dv$  and its acceleration is  $\ddot{\mathbf{r}}$ . That is, the inertia force of the infinitesimal volume is  $(\rho dv) \ddot{\mathbf{r}}$ . The virtual work of this force is  $(\rho dv) \ddot{\mathbf{r}}^T \delta \mathbf{r}$ . Integrating over the volume, one obtains the virtual work of the inertia forces of the continuum, previously obtained in this section from the partial differential equations of equilibrium, as

$$\delta W_i = \int_V \rho \ddot{\mathbf{r}}^T \delta \mathbf{r} dv = \int_V \rho_o \ddot{\mathbf{r}}^T \delta \mathbf{r} dV$$

where  $\rho_o$  and  $V$  are, respectively, the mass density and volume in the reference configuration. The preceding equation can be written, upon the use of  $\delta \mathbf{r}$  and  $\ddot{\mathbf{r}}$  as

$$\delta W_i = \ddot{\mathbf{q}}^T \left( \int_V \rho_o \mathbf{S}^T \mathbf{S} dV \right) \delta \mathbf{q}$$

This equation can be written as

$$\delta W_i = \dot{\mathbf{q}}^T \mathbf{M} \delta \mathbf{q}$$

where  $\mathbf{M}$  is the symmetric mass matrix of the continuum defined as

$$\mathbf{M} = \int_V \rho_o \mathbf{S}^T \mathbf{S} dV$$

This symmetric mass matrix has dimension equal to the dimension of the vector of coordinate vector  $\mathbf{q}$ . When the inertia forces are formulated using the shape function matrix and the procedure described in this example, one has what is called a *consistent mass formulation*. There is another technique that is used often in the finite element literature to approximate the inertia forces by assuming that the continuum consists of a number of concentrated masses or rigid bodies. This latter approach is called a *lumped mass formulation*. In the large rotation finite element formulations, it is important to recognize the fundamental problems that may arise as the result of using the lumped mass technique. This important topic is discussed in more detail in subsequent chapters.

As discussed in Chapter 1, in some nonlinear finite element formulations, as in the case of the floating frame of reference formulation discussed in Chapter 6. The simple description of  $\mathbf{r}$  as  $\mathbf{r} = \mathbf{S}(\mathbf{x})\mathbf{q}(t)$  is not used. Nonetheless, the same coordinate reduction procedure described in this example can still be used to obtain a finite dimensional model. In the floating frame of reference formulation, however, the mass matrix is not constant because it must account for the nonlinear dynamic coupling between the reference motion and the elastic deformation.

## Surface Forces

Taking into consideration the effects of the body forces, inertia forces, and stress forces requires integration over the volume. There are other forces that require integration over areas. Examples are forces that result from pressure distributions as in the case of the tire example shown in Figure 3. One approach to consider the effect of the air pressure in tire applications is to write an expression for the tire pressure as  $p_t = p_t(\mathbf{q}, t)$ , where  $\mathbf{q}$  is the vector of coordinates that can be used to define the tire deformations. The pressure is assumed to apply in a direction normal to the surface defined by the unit normal  $\mathbf{n}$ . One can, therefore, define the pressure vector  $\mathbf{p}_t = \mathbf{p}_t(\mathbf{q}, t) = p_t \mathbf{n}$ . The position vector of the material points on the surface can be written as  $\mathbf{r} = \mathbf{r}(\alpha_1, \alpha_2)$ , where  $\alpha_1$  and  $\alpha_2$  are the parameters that define the surface. In the finite element formulation presented in Chapter 5, one can, without any loss of generality, select  $\alpha_1$  and  $\alpha_2$  such that  $\alpha_1 = x_1$  and  $\alpha_2 = x_2$ . A unit normal to the surface  $\mathbf{n}$  can be defined as  $\mathbf{n} = \mathbf{r}_{\alpha_1} \times \mathbf{r}_{\alpha_2} / |\mathbf{r}_{\alpha_1} \times \mathbf{r}_{\alpha_2}|$ . The virtual work of the pressure force can then be written as  $\delta W_p = \int_s \mathbf{p}_t^T \delta \mathbf{r} ds$ , where  $s$  is the area in the current configuration. Using Nanson's formula introduced in the preceding chapter, one can write  $ds$  in terms of the area defined in the reference configuration as  $ds = (J / \sqrt{\mathbf{n}^T \mathbf{J} \mathbf{J}^T \mathbf{n}}) dS$ , where  $J$  is the determinant of the matrix of position vector gradients  $\mathbf{J}$  and  $S$  is the area in the reference configuration. It follows that  $\delta W_p = \int_s (J p_t \mathbf{n} / \sqrt{\mathbf{n}^T \mathbf{J} \mathbf{J}^T \mathbf{n}})^T \delta \mathbf{r} dS$ .

When approximation methods are used, the vector  $\mathbf{r}$  can be written as  $\mathbf{r} = \mathbf{S}(\mathbf{x})\mathbf{q}$ , where  $\mathbf{S}$  is an appropriate space-dependent shape function matrix, and  $\mathbf{q}$  is the vector of time-dependent

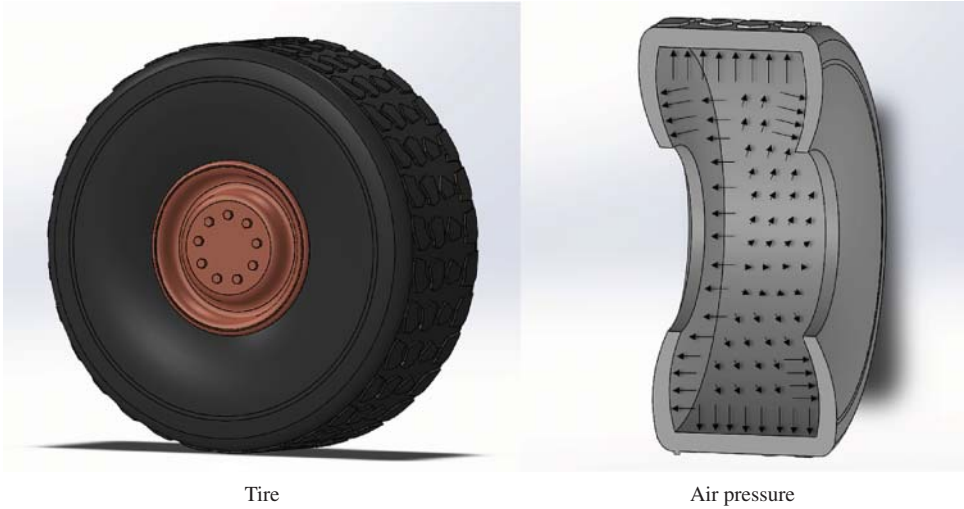


**Figure 3.3** Surface forces

generalized coordinates. One can then write the virtual work of the pressure force as  $\delta W_p = (\int_s (J p_t \mathbf{n} / \sqrt{\mathbf{n}^T \mathbf{J} \mathbf{J}^T \mathbf{n}})^T \mathbf{S}(\mathbf{x}) dS) \delta \mathbf{q}$ . This equation can be written as  $\delta W_p = \mathbf{Q}_p^T \delta \mathbf{q}$ , where the vector of generalized pressure forces is defined as  $\mathbf{Q}_p = \int_s \mathbf{S}^T (J p_t \mathbf{n} / \sqrt{\mathbf{n}^T \mathbf{J} \mathbf{J}^T \mathbf{n}}) dS$ . This vector has dimension equal to the dimension of the vector of generalized coordinates  $\mathbf{q}$ . Note that in the case of small deformation,  $J / \sqrt{\mathbf{n}^T \mathbf{J} \mathbf{J}^T \mathbf{n}} \approx 1$ , and the expression of the vector of generalized pressure force reduces to  $\mathbf{Q}_p = \int_s \mathbf{S}^T (p_t \mathbf{n}) dS$ . In both the cases of small and large deformations, it is difficult to obtain a closed form solution for the pressure forces and, therefore, the methods of numerical integration are often used.

### Total and Updated Lagrangian Formulations

The analysis presented in this section shows that the weak form of the equations of motion can be expressed in terms of variables defined in the original undeformed reference configuration or in terms of variables defined in the current deformed configuration. When the equations are expressed in terms of variables defined in the reference configuration and differentiations and integrations are carried out with respect to the Lagrangian coordinates  $\mathbf{x}$ , one has the *total Lagrangian formulation*. If the equations of motion, on the other hand, are expressed in terms of variables defined in the current configuration and differentiations and integrations are carried out with respect to the Eulerian coordinates  $\mathbf{r}$ , one has the *updated Lagrangian formulation*. It is important to realize that both formulations are equivalent and one formulation can be obtained from the other by simply using a coordinate transformation; this is despite the fact that different deformation and stress measures are used in these formulations. For example, the traction forces can be formulated in terms of the Cauchy stresses and the deformed geometry as  $\int_s \boldsymbol{\sigma} \mathbf{n} dS$ . Using Nanson's formula  $\mathbf{n} dS = \mathbf{J} \mathbf{J}^{-1^T} \mathbf{N} dS$ , which was derived in the preceding chapter, the traction forces can be written in terms of

the first Piola–Kirchhoff stress tensor and the surface area in the reference configuration as  $\int_S J \mathbf{J}^{-1} \boldsymbol{\sigma} \mathbf{N} dS = \int_S \boldsymbol{\sigma}_{P1}^T \mathbf{N} dS$ . Similarly, using the continuity condition  $\rho_o dV = \rho dv$ , where  $\rho_o$  and  $V$  are, respectively, the mass density and volume in the reference configuration, the inertia forces, as previously mentioned, can be written using integrals defined in the reference configuration as  $\int_V \rho_o \ddot{\mathbf{r}} dV$ . Similar comments apply to the body forces. Following this procedure, recognizing that  $\partial/\partial \mathbf{r} = (\partial/\partial \mathbf{x})(\partial \mathbf{x}/\partial \mathbf{r}) = (\partial/\partial \mathbf{x}) \mathbf{J}^{-1}$ , and using the divergence theorem, one can show that the partial differential equations of equilibrium can be written in terms of variables defined in the reference configuration as  $(\nabla \boldsymbol{\sigma}_{P1})^T + \mathbf{f}_{bo} = \rho_o \ddot{\mathbf{r}}$ , where  $\mathbf{f}_{bo}$  is the vector of body forces associated with the reference configuration. Therefore, the equations of motion can be expressed in terms of variables defined in the current configuration or alternatively in terms of variables defined in the reference configuration, and the total and updated Lagrangian formulations are in principle the same.

### Example 3.3

Assuming that the gravity forces act in the direction of the  $X_2$  global axis, the gravity forces acting on an infinitesimal volume of mass  $\rho dv$  in the current configuration can be written as  $[0 \ -g \ 0]^T \rho dv$ . The sum of the inertia forces acting on the body can be written as  $\int_V \rho [0 \ -g \ 0]^T dv$ , which upon using the continuity equation, can also be written in the reference configuration as  $\int_V \rho_o [0 \ -g \ 0]^T dV$ . The virtual work of the gravity forces can also be written in the current and reference configuration, respectively, as

$$\delta W_e = \int_V \rho [0 \ -g \ 0] \delta \mathbf{r} dv, \quad \delta W_e = \int_V \rho_o [0 \ -g \ 0] \delta \mathbf{r} dV$$

As previously mentioned, in the large deformation finite element formulation discussed in Chapter 5, the position vector can be written as  $\mathbf{r} = \mathbf{S} \mathbf{e}$ , where  $\mathbf{S}$  is the space-dependent shape function and  $\mathbf{e}$  is the vector of time-dependent coordinates. Using this motion description, the virtual work of the gravity forces in the current and reference configuration can be written as

$$\delta W_e = \left( \int_V \rho [0 \ -g \ 0] \mathbf{S} dv \right) \delta \mathbf{e}, \quad \delta W_e = \left( \int_V \rho_o [0 \ -g \ 0] \mathbf{S} dV \right) \delta \mathbf{e}$$

These equations can be used to define a finite dimensional vector of generalized gravity forces associated with the time-dependent generalized coordinates  $\mathbf{e}$  as  $\mathbf{Q}_g = \int_V \mathbf{S}^T [0 \ -g \ 0]^T dV$ .

In the total Lagrangian formulation, strain tensors such as the Green–Lagrange strain tensor are often used with the second Piola–Kirchhoff stress tensor; however, in the updated Lagrangian formulation, the rate of deformation tensor is often used with the Cauchy stress tensor. Furthermore, in the total Lagrangian formulation, the virtual displacement  $\delta \mathbf{r}$  is used to define the virtual work principle, whereas in the updated Lagrangian formulation the virtual velocity  $\delta \mathbf{v}$  is used to define a *virtual power principle*.

The total and updated Lagrangian formulations are used more often in the solution of solid mechanics problems and the motion description employed in both formulations is different from the *Eulerian formulation*, which is used more often in fluid mechanics. In the

Eulerian formulation, the material density, the Cauchy stress components, and the velocity are treated as the dependent variables. In order to solve for these dependent variables, three sets of equations are used: the continuity equation or conservation of mass in its differential form defined in the preceding chapter, the constitutive equations, which are defined in the following chapter, and the equations of motion that result from the use of the principle of virtual work or virtual power. Using these three sets of equations, one obtains a number of equations equal to the number of unknown dependent variables. In general, the continuity equation is a first-order partial differential equation, the constitutive equations can be in an algebraic, differential, or integral form depending on the type of problem solved as will be discussed later in this book, and the equations of motion are second-order partial differential equations. In the Eulerian formulation, these three sets of equations are solved simultaneously to determine the density, stresses, and velocities. When the finite element approximation is used with the Eulerian formulation, the finite element nodes are assumed to be fixed in space and do not deform as in the case of the Lagrangian formulations. Furthermore, independent interpolation functions are used for the density, stresses, and velocities.

### Physical Interpretation

The analysis presented in this chapter and the preceding chapter shows that different measures for the strains and stresses can be used. Some measures can be more suited for specific problems. Nonetheless, understanding the physical interpretations of these measures is important. For example, Cauchy stress is derived using forces and areas defined in the current configuration. This is the reason that Cauchy stress is called the true stress. The trace of the Cauchy stress tensor  $(1/3) \sum_{i=1}^3 \sigma_{ii} = p$  defines the true pressure  $p$  that is commonly used in fluid mechanics. On the other hand, it is difficult to give a physical meaning to the symmetric second Piola–Kirchhoff stress tensor. The lack of a clear physical meaning for the second Piola–Kirchhoff stress tensor makes its use difficult in some applications as in the case of plasticity theory where the yield functions must be formulated in terms of stresses that have physical meaning.

### 3.6 DEVIATORIC STRESSES

In some formulations based on the continuum mechanics theory, it is useful to write the Cauchy stress tensor in the following form:

$$\boldsymbol{\sigma} = \mathbf{S} + p\mathbf{I} \quad (3.44)$$

Here  $\mathbf{S}$  is called the *stress deviator tensor* and  $p$  is called the *hydrostatic pressure* defined as

$$p = \frac{1}{3}(\sigma_{11} + \sigma_{22} + \sigma_{33}) = \frac{1}{3} \sum_{i=1}^3 \sigma_{ii} \quad (3.45)$$

Note that  $\text{tr}(\mathbf{S}) = 0$ . Therefore, if  $s_1$ ,  $s_2$ , and  $s_3$  are the principal values of  $\mathbf{S}$ , then

$$s_1 + s_2 + s_3 = 0 \quad (3.46)$$

Furthermore, because  $(\boldsymbol{\sigma} - \tau \mathbf{I})\mathbf{c} = \mathbf{0}$  can also be written as  $\{\mathbf{S} - (\tau - p)\mathbf{I}\}\mathbf{c} = \mathbf{0}$  and  $p = \frac{1}{3}(\tau_1 + \tau_2 + \tau_3)$  where  $\tau_1$ ,  $\tau_2$ , and  $\tau_3$  are the principal values of  $\boldsymbol{\sigma}$ ; one can show that the principal values of  $\mathbf{S}$  can be written in terms of the principal values of  $\boldsymbol{\sigma}$  as follows:

$$\left. \begin{aligned} s_1 &= \frac{1}{3}(2\tau_1 - \tau_2 - \tau_3) \\ s_2 &= \frac{1}{3}(2\tau_2 - \tau_1 - \tau_3) \\ s_3 &= \frac{1}{3}(2\tau_3 - \tau_1 - \tau_2) \end{aligned} \right\} \quad (3.47)$$

Because  $\text{tr}(\mathbf{S}) = 0$ , the stress deviator tensor has only two independent invariants  $J'_2$  and  $J'_3$ , which can be written in terms of the principal values of  $\mathbf{S}$  as follows:

$$\left. \begin{aligned} J'_2 &= s_1 s_2 + s_1 s_3 + s_2 s_3 = -\frac{1}{2}\text{tr}(\mathbf{S}^2) \\ J'_3 &= s_1 s_2 s_3 = \det(\mathbf{S}) = -\frac{1}{3}\text{tr}(\mathbf{S}^3) \end{aligned} \right\} \quad (3.48)$$

Using the preceding two equations, it is clear that the invariants  $J'_2$  and  $J'_3$  of the stress deviator  $\mathbf{S}$  can be expressed in terms of the invariants  $J_1$ ,  $J_2$ , and  $J_3$  of the Cauchy stress tensor  $\boldsymbol{\sigma}$ . It is sometimes convenient to use  $J_1$ ,  $J'_2$ , and  $J'_3$  as the set of invariants of  $\boldsymbol{\sigma}$ . It is also important to mention that the isolation of the hydrostatic pressure component  $p$  from the components of the stress deviator  $\mathbf{S}$  is advantageous in many formulations in the field of plasticity and soil mechanics.

Similar decomposition can be developed for the first and second Piola–Kirchhoff stress tensors by substituting  $\boldsymbol{\sigma}$  in their expressions. For the first Piola–Kirchhoff stress tensor, one has

$$\boldsymbol{\sigma}_{P1} = J\boldsymbol{\sigma}\mathbf{J}^{-1T} = J(\mathbf{S} + p\mathbf{I})\mathbf{J}^{-1T} = \mathbf{S}_{P1} + pJ\mathbf{J}^{-1T} \quad (3.49)$$

where again  $J = |\mathbf{J}|$ , and

$$\mathbf{S}_{P1} = J\mathbf{S}\mathbf{J}^{-1T} \quad (3.50)$$

Similarly, for the second Piola–Kirchhoff stress tensor, one has

$$\boldsymbol{\sigma}_{P2} = J\mathbf{J}^{-1}\boldsymbol{\sigma}\mathbf{J}^{-1T} = J\mathbf{J}^{-1}(\mathbf{S} + p\mathbf{I})\mathbf{J}^{-1T} = \mathbf{S}_{P2} + pJ\mathbf{J}^{-1}\mathbf{J}^{-1T} \quad (3.51)$$

where

$$\boldsymbol{\sigma}_{P2} = J\mathbf{J}^{-1}\mathbf{S}\mathbf{J}^{-1T} \quad (3.52)$$

The tensors  $\mathbf{S}_{P1}$  and  $\mathbf{S}_{P2}$  are known as the deviatoric components of the first and second Piola–Kirchhoff stress tensors. Note that the traces of  $\mathbf{S}_{P1}$  and  $\mathbf{S}_{P2}$  are not necessarily equal to zero despite the fact that the trace of  $\mathbf{S}$  is equal to zero. It can, however, be shown that

$$\text{tr}(\mathbf{S}_{P2}\mathbf{J}^T\mathbf{J}) = \mathbf{S}_{P2}:\mathbf{C}_r = 0 \quad (3.53)$$

where  $\mathbf{C}_r = \mathbf{J}^T \mathbf{J}$  is the right Cauchy–Green deformation tensor. In order to prove the identity of Equation 53, the properties of the trace and double product are used. This leads to

$$\text{tr}(\mathbf{S}_{P2} \mathbf{J}^T \mathbf{J}) = \text{tr}(\mathbf{J} \mathbf{J}^{-1} \mathbf{S} \mathbf{J}^{-1T} \mathbf{J}^T \mathbf{J}) = \text{tr}(\mathbf{J} \mathbf{J}^{-1} \mathbf{S} \mathbf{J}) = J \text{tr}(\mathbf{S}) = 0 \quad (3.54)$$

This equation shows that indeed  $\text{tr}(\mathbf{S}_{P2} \mathbf{J}^T \mathbf{J}) = \mathbf{S}_{P2} : \mathbf{C}_r = 0$ . Using this identity after postmultiplying  $\boldsymbol{\sigma}_{P2}$  by  $\mathbf{C}_r$  shows that the hydrostatic pressure  $p$  can be obtained using the second Piola–Kirchhoff stress tensor as

$$p = \frac{1}{3J} \text{tr}(\boldsymbol{\sigma}_{P2} \mathbf{J}^T \mathbf{J}) = \frac{1}{3J} (\boldsymbol{\sigma}_{P2} : \mathbf{C}_r) \quad (3.55)$$

Therefore, the deviator tensor associated with the second Piola–Kirchhoff stress tensor can be written as

$$\mathbf{S}_{P2} = \boldsymbol{\sigma}_{P2} - \frac{1}{3} (\boldsymbol{\sigma}_{P2} : \mathbf{C}_r) \mathbf{C}_r^{-1} \quad (3.56)$$

Following a similar procedure, one can also show that the hydrostatic pressure  $p$  can be obtained using the first Piola–Kirchhoff stress tensor as

$$p = \frac{1}{3J} \text{tr}(\boldsymbol{\sigma}_{P1} \mathbf{J}) = \frac{1}{3J} (\boldsymbol{\sigma}_{P1}^T : \mathbf{J}) \quad (3.57)$$

Using this equation, an expression for the deviatoric part of the first Piola–Kirchhoff stress tensor can be obtained.

For the most part, particularly in the analysis of large deformation used in this book, the second Piola–Kirchhoff stress tensor will be used because this is the tensor associated with the Green–Lagrange strain tensor. In some plasticity and viscoelasticity formulations that require the use of true stress measures, the Cauchy stress or the Kirchhoff stress tensors are used. Furthermore, being able to identify the effect of the hydrostatic pressure is not only important in many large-deformation formulations, but it is also important in improving the numerical performance of the finite elements in some applications. Although in some nonlinear formulations such as the  $J_2$  plasticity formulations, the constitutive equations are formulated in terms of the deviatoric stresses because the hydrostatic pressure is of less significance; in some other linear and nonlinear applications, the performance of the finite elements can significantly deteriorate owing to *locking problems* associated with the volumetric changes, as in the case of incompressible or nearly incompressible materials. By understanding the contributions of the hydrostatic pressure to the elastic forces, one can propose solutions to these locking problems. Some of these locking problems are discussed in more detail in Chapter 5.

### 3.7 STRESS OBJECTIVITY

The Cauchy stress tensor is a key element in the formulation of the partial differential equations of equilibrium. It is, therefore, important to check whether or not this stress tensor satisfies the objectivity requirement as defined in the preceding chapter. To this end, the transformations of the normal and traction vectors as the result of a rigid-body motion are considered. The traction is defined using the Cauchy stress formula as  $\boldsymbol{\sigma}_n = \boldsymbol{\sigma} \mathbf{n}$ . If, from a given current configuration,



the continuous body undergoes a rigid-body rotation defined by the transformation matrix  $\mathbf{A}$  and because the Cauchy stresses are defined in the current configuration, the traction and normal vectors as the result of the rigid-body rotation can be defined as

$$\bar{\boldsymbol{\sigma}}_n = \mathbf{A}\boldsymbol{\sigma}_n, \quad \bar{\mathbf{n}} = \mathbf{A}\mathbf{n} \quad (3.58)$$

Using these two equations, one has

$$\bar{\boldsymbol{\sigma}}_n = \mathbf{A}\boldsymbol{\sigma}_n = \mathbf{A}\boldsymbol{\sigma}\mathbf{n} = \mathbf{A}\boldsymbol{\sigma}\mathbf{A}^T\bar{\mathbf{n}} \quad (3.59)$$

which can be written as  $\bar{\boldsymbol{\sigma}}_n = \bar{\boldsymbol{\sigma}}\bar{\mathbf{n}}$  where

$$\bar{\boldsymbol{\sigma}} = \mathbf{A}\boldsymbol{\sigma}\mathbf{A}^T \quad (3.60)$$

Note that this transformation is different from the transformation defined by Equation 11. Equation 11 can be used to define the stresses in different directions for a given current configuration. Equation 60 can be used to show that the Cauchy stress tensor satisfies the objectivity requirement as it is used in the principle of virtual work. For the Cauchy stress tensor to satisfy the objectivity requirement, one needs to show that the virtual work of the elastic forces and the strain energy are not affected by the rigid-body rotation. Recall that when the Cauchy stresses are used, the virtual work of the elastic forces is written in terms of  $\boldsymbol{\sigma}$ :  $(\delta\mathbf{J})\mathbf{J}^{-1}$ . In the case of a rigid-body rotation defined by the transformation matrix  $\mathbf{A}$ , one has  $\bar{\mathbf{J}} = \mathbf{A}\mathbf{J}$ ,  $\bar{\mathbf{J}}^{-1} = \mathbf{J}^{-1}\mathbf{A}^T$ , and  $\bar{\boldsymbol{\sigma}} = \mathbf{A}\boldsymbol{\sigma}\mathbf{A}^T$ . Here  $\bar{\mathbf{J}}$  remains the matrix of position vector gradients and not that of displacement gradients. It follows that  $\delta\bar{\mathbf{J}} = (\delta\mathbf{A})\mathbf{J} + \mathbf{A}(\delta\mathbf{J})$  and  $(\delta\bar{\mathbf{J}})\bar{\mathbf{J}}^{-1} = (\delta\mathbf{A})\mathbf{A}^T + \mathbf{A}(\delta\mathbf{J})\mathbf{J}^{-1}\mathbf{A}^T$ . Note that because  $(\delta\mathbf{A})\mathbf{A}^T$  is a skew-symmetric matrix because  $(\delta\mathbf{A}\mathbf{A}^T) = (\delta\mathbf{A})\mathbf{A}^T + \mathbf{A}(\delta\mathbf{A}^T) = \mathbf{0}$  and  $\mathbf{A}\boldsymbol{\sigma}\mathbf{A}^T$  is a symmetric tensor, then  $\mathbf{A}\boldsymbol{\sigma}\mathbf{A}^T : (\delta\mathbf{A})\mathbf{A}^T = 0$ . It follows that  $\bar{\boldsymbol{\sigma}} : (\delta\bar{\mathbf{J}})\bar{\mathbf{J}}^{-1} = \boldsymbol{\sigma} : (\delta\mathbf{J})\mathbf{J}^{-1}$ , which shows that the virtual work of the elastic forces remains the same and is not affected by the rigid-body rotation. That is, Cauchy stress tensor is indeed objective when it is used with  $(\delta\mathbf{J})\mathbf{J}^{-1}$  to evaluate the elastic forces. Furthermore, it is interesting to note the similarity between the tensor  $(\delta\mathbf{J})\mathbf{J}^{-1}$  and the velocity gradient tensor  $\mathbf{L} = \dot{\mathbf{J}}\mathbf{J}^{-1}$ , which is not in general an exact differential. As shown in Chapter 2,  $\bar{\mathbf{L}} = \mathbf{A}\mathbf{L}\mathbf{A}^T + \dot{\mathbf{A}}\mathbf{A}^T$ . Using this equation, one can also show that  $\bar{\boldsymbol{\sigma}} : \bar{\mathbf{L}} = \boldsymbol{\sigma} : \mathbf{L}$ , and  $\bar{\boldsymbol{\sigma}} : \bar{\mathbf{D}} = \boldsymbol{\sigma} : \mathbf{D}$ , where  $\mathbf{D}$  is the rate of deformation tensor.

The second Piola–Kirchhoff stress tensor, on the other hand, is independent of the superimposed rigid-body rotations. In order to demonstrate this fact, consider the rigid-body rotation defined by the transformation matrix  $\mathbf{A}$ . The matrix of position vector gradient  $\mathbf{J}$  as the result of this superimposed rigid-body rotation can be again written as  $\bar{\mathbf{J}} = \mathbf{A}\mathbf{J}$ , where  $\mathbf{J}$  is the matrix of position vector gradients before the rigid-body rotation. The matrix  $\mathbf{J}$  is premultiplied by  $\mathbf{A}$  because the gradients in both configurations are defined by differentiation with respect to the same parameters. It follows that

$$\bar{\boldsymbol{\sigma}}_{p2} = \bar{J}\bar{\mathbf{J}}^{-1} \bar{\boldsymbol{\sigma}}\bar{\mathbf{J}}^{-1T} = J\mathbf{J}^{-1}\mathbf{A}^T\mathbf{A}\boldsymbol{\sigma}\mathbf{A}^T\mathbf{A}\mathbf{J}^{-1T} = J\mathbf{J}^{-1}\boldsymbol{\sigma}\mathbf{J}^{-1T} = \boldsymbol{\sigma}_{p2} \quad (3.61)$$

In this equation,  $J = |\mathbf{J}|$ , and  $\bar{J} = |\bar{\mathbf{J}}| = |\mathbf{A}\mathbf{J}| = |\mathbf{J}|$  because  $\mathbf{A}$  is an orthogonal matrix. Recall that under the arbitrary rigid-body rotation defined by the matrix  $\mathbf{A}$ , Green–Lagrange strain tensor satisfies the identity  $\bar{\boldsymbol{\varepsilon}} = \boldsymbol{\varepsilon}$ , as was shown in the preceding chapter. It follows that

$\bar{\sigma}_{P2} : \delta \bar{\epsilon} = \sigma_{P2} : \delta \epsilon$ , which shows that the elastic forces and strain energy remain the same under an arbitrary rigid-body rotation. As a consequence, the second Piola–Kirchhoff stress tensor satisfies the objectivity requirement when it is used with the Green–Lagrange strain tensor.

### Stress Rate

Although Cauchy stress tensor satisfies the objectivity requirement, when it is used with  $(\delta \mathbf{J})\mathbf{J}^{-1}$  to formulate the elastic forces, it is important to define the rate of change of the Cauchy stress tensor as the result of an arbitrary rigid-body rotation defined by the transformation matrix  $\mathbf{A}$ . To this end, Equation 60 is differentiated with respect to time. This leads to

$$\dot{\bar{\sigma}} = \mathbf{A}\dot{\sigma}\mathbf{A}^T + \dot{\mathbf{A}}\sigma\mathbf{A}^T + \mathbf{A}\sigma\dot{\mathbf{A}}^T \quad (3.62)$$

This equation clearly shows that  $\dot{\bar{\sigma}} \neq \mathbf{A}\dot{\sigma}\mathbf{A}^T$  unless the rotation matrix  $\mathbf{A}$  does not depend on time. That is, the rate of Cauchy stress tensor  $\dot{\sigma}$  does not follow the same rule of transformation as the Cauchy stress tensor  $\sigma$  when the continuum is subjected to a rigid-body motion. Therefore, such a stress rate does not satisfy the objectivity requirement when used with the deformation measures used with Cauchy stress tensor. It is, therefore, important to define stress rate and deformation measures that satisfy the objectivity requirements. Among the stress rate measures used in the literature are the *Truesdell stress rate*, the *Oldroyd stress rate*, the *convective stress rate*, the *Green–Naghdi stress rate*, and the *Jaumann stress rate* (Bonet and Wood, 1997). These stress rate measures are discussed in the following paragraphs.

### Truesdell Stress Rate $\sigma^\circ$

The Truesdell stress rate is defined by applying a transformation, called *Piola transformation*, to the time derivative of the second Piola–Kirchhoff stress tensor as follows:

$$\sigma^\circ = \frac{1}{J}\mathbf{J}\dot{\sigma}_{P2}\mathbf{J}^T = \frac{1}{J}\mathbf{J}\left\{\frac{d}{dt}\left(\mathbf{J}\mathbf{J}^{-1}\sigma\mathbf{J}^{-1T}\right)\right\}\mathbf{J}^T \quad (3.63)$$

In this equation,  $J = |\mathbf{J}|$ . It was shown in the preceding chapter that  $(dJ/dt) = J\text{tr}(\mathbf{D})$ , where  $\mathbf{D}$  is the rate of deformation tensor. Because the tensor of velocity gradients  $\mathbf{L} = \dot{\mathbf{J}}\mathbf{J}^{-1} = \mathbf{D} + \mathbf{W}$ , where  $\mathbf{W}$  is the skew-symmetric spin tensor, that is  $|\mathbf{W}| = 0$ ; one has  $(dJ/dt) = J\text{tr}(\mathbf{L})$ . The Truesdell stress rate can then be written as

$$\sigma^\circ = \dot{\sigma} - \mathbf{L}\sigma - \sigma\mathbf{L}^T + \text{tr}(\mathbf{L})\sigma \quad (3.64)$$

Note that because  $\mathbf{J}\mathbf{J}^{-1} = \mathbf{I}$ , one has  $\dot{\mathbf{J}}\mathbf{J}^{-1} = -\mathbf{J}\dot{\mathbf{J}}^{-1}$ , an identity that is utilized in deriving the Truesdell stress rate measure presented in Equation 64.

In order to define the rule of transformation of Truesdell stress rate measure, a general rigid-body rotation defined by the transformation matrix  $\mathbf{A}$  is considered. As the result of this rotation, one has the following relationships between the tensors before and after the rigid-body rotation:

$$\left. \begin{aligned} \bar{\sigma} &= \mathbf{A}\sigma\mathbf{A}^T \\ \dot{\bar{\sigma}} &= \mathbf{A}\dot{\sigma}\mathbf{A}^T + \dot{\mathbf{A}}\sigma\mathbf{A}^T + \mathbf{A}\sigma\dot{\mathbf{A}}^T \\ \bar{\mathbf{L}} &= \dot{\mathbf{A}}\mathbf{A}^T + \mathbf{A}\mathbf{L}\mathbf{A}^T \end{aligned} \right\} \quad (3.65)$$

The Truesdell stress rate measure can be written in the current configuration after the rigid-body rotation as

$$\bar{\sigma}^o = \dot{\bar{\sigma}} - \bar{\mathbf{L}}\bar{\sigma} - \bar{\sigma}\bar{\mathbf{L}}^T + \text{tr}(\bar{\mathbf{L}})\bar{\sigma} \quad (3.66)$$

Substituting Equation 65 into this equation, one can show that

$$\bar{\sigma}^o = \mathbf{A}(\dot{\sigma} - \mathbf{L}\sigma - \sigma\mathbf{L}^T + \text{tr}(\mathbf{L})\sigma)\mathbf{A}^T = \mathbf{A}\sigma^o\mathbf{A}^T \quad (3.67)$$

which shows that Truesdell stress rate measure follows the rule of tensor transformation.

It is important to note that the Truesdell rate of the Kirchhoff stress  $\sigma_K^o = \mathbf{J}\sigma^o$  is the push-forward of the rate of the second Piola–Kirchhoff stress tensor  $\dot{\sigma}_{P2}$ . This observation is important when the constitutive equations of some hyperelastic–plastic models are formulated.

### Oldroyd and Convective Stress Rates $\sigma^\circ$ and $\sigma^\diamond$

The time derivative of the Cauchy stress tensor can be used to define the *Oldroyd stress rate*  $\sigma^\circ$  as follows:

$$\sigma^\circ = \mathbf{J} \left\{ \frac{d}{dt} \left( \mathbf{J}^{-1} \sigma \mathbf{J}^{-1T} \right) \right\} \mathbf{J}^T = \dot{\sigma} - \mathbf{L}\sigma - \sigma\mathbf{L}^T \quad (3.68)$$

If before the differentiation a pullback operation is used with  $\mathbf{J}^T$ , and after the differentiation, a push-forward operation is used with  $\mathbf{J}^{-1T}$ , one obtains the *convective stress rate*  $\sigma^\diamond$  defined as follows:

$$\sigma^\diamond = \mathbf{J}^{-1T} \left\{ \frac{d}{dt} (\mathbf{J}^T \sigma \mathbf{J}) \right\} \mathbf{J}^{-1} = \dot{\sigma} + \mathbf{L}^T \sigma + \sigma \mathbf{L} \quad (3.69)$$

In order to prove that the Oldroyd and the convective stress rates follow the rule of transformation as the Cauchy stress tensor, the identities of Equation 65 can be used again. This is left to the reader as an exercise.

### Green–Naghdi Stress Rate $\sigma^\Delta$

The Green–Naghdi stress rate  $\sigma^\Delta$  is defined using the rotation tensor  $\mathbf{R}$  instead of the tensor of the position vector gradients  $\mathbf{J}$ . Therefore, the effect of the stretch tensor is not considered in the pullback and push-forward operations. The Green–Naghdi stress rate is defined as

$$\sigma^\Delta = \mathbf{R} \left\{ \frac{d}{dt} (\mathbf{R}^T \sigma \mathbf{R}) \right\} \mathbf{R}^T = \dot{\sigma} + \sigma \dot{\mathbf{R}}\mathbf{R}^T - \dot{\mathbf{R}}\mathbf{R}^T \sigma \quad (3.70)$$

In obtaining this expression for the Green–Naghdi stress rate, the fact that  $\mathbf{R}\dot{\mathbf{R}}^T = -\dot{\mathbf{R}}\mathbf{R}^T$  is utilized. Note that the Green–Naghdi stress rate has the same form as Oldroyd stress rate by replacing  $\mathbf{J}$  by  $\mathbf{R}$ .

### Jaumann Stress Rate $\sigma^\nabla$

As discussed in Chapter 2, when the motion is not purely a rigid-body motion,  $\dot{\mathbf{R}}\mathbf{R}^T$  is not the spin tensor  $\mathbf{W}$  that accounts for the deformation. If in the expression of Green–Naghdi stress tensor,  $\dot{\mathbf{R}}\mathbf{R}^T$  is approximated by the spin tensor  $\mathbf{W} = (\mathbf{L} - \mathbf{L}^T)/2$ , where  $\mathbf{L}$  is the tensor of velocity gradients, one obtains the Jaumann stress rate  $\sigma^\nabla$  defined as

$$\sigma^\nabla = \dot{\sigma} + \sigma\mathbf{W} - \mathbf{W}\sigma \quad (3.71)$$

The proof that the Green–Naghdi and Jaumann stress rates follow a rule of transformation similar to the Cauchy stress tensor in the case of a rigid-body motion is left to the reader as an exercise.

## 3.8 ENERGY BALANCE

The partial differential equations of equilibrium can be used to define the rate of change of the energy of the continuum. In order to demonstrate that, Equation 16 or alternatively Equation 17 is multiplied by the absolute velocity vector  $\dot{\mathbf{r}}$ . This, upon the use of the symmetry of the Cauchy stress tensor, yields

$$(\nabla\sigma)^T \cdot \dot{\mathbf{r}} + \mathbf{f}_b \cdot \dot{\mathbf{r}} = \rho \ddot{\mathbf{r}} \cdot \dot{\mathbf{r}} \quad (3.72)$$

Note that

$$\nabla(\sigma\dot{\mathbf{r}}) = (\nabla\sigma)\dot{\mathbf{r}} + \sigma:\mathbf{L} \quad (3.73)$$

where  $\mathbf{L} = \mathbf{D} + \mathbf{W}$  is the velocity gradient tensor, and  $\mathbf{D}$  and  $\mathbf{W}$  are, respectively, the symmetric rate of deformation and the skew-symmetric spin tensors. Using the preceding two equations, one has

$$\nabla(\sigma\dot{\mathbf{r}}) - \text{tr}(\sigma\mathbf{L}) + \mathbf{f}_b \cdot \dot{\mathbf{r}} = \rho \ddot{\mathbf{r}} \cdot \dot{\mathbf{r}} \quad (3.74)$$

Integrating over the current volume, using the identity  $\text{tr}(\sigma\mathbf{L}) = \text{tr}(\sigma\mathbf{D})$ , and using the divergence theorem and the principle of conservation of mass, one obtains

$$\int_v \mathbf{f}_b \cdot \dot{\mathbf{r}} dv + \int_s (\sigma\mathbf{n}) \cdot \dot{\mathbf{r}} ds = \frac{d}{dt} \left( \frac{1}{2} \int_v \rho \dot{\mathbf{r}} \cdot \dot{\mathbf{r}} dv \right) + \int_v (\sigma:\mathbf{D}) dv \quad (3.75)$$

This is the *energy balance equation*, which shows that the rate of change of the kinetic energy  $\left( \frac{1}{2} \int_v \rho \dot{\mathbf{r}} \cdot \dot{\mathbf{r}} dv \right)$  plus the *elastic force power*  $\int_v (\sigma:\mathbf{D}) dv$  is equal to the power of the body and surface forces. The power of the elastic forces may include the effect of dissipative forces as in the case of viscoelastic materials. In this case, Equation 75 governs the behavior of *nonconservative systems*.

One can also define the energy balance equation in the reference configuration. This can be achieved by directly using Equation 16 or using Equation 75 and changing the variables used

to the reference configuration. It is left to the reader as an exercise to show that the energy balance equation can be defined in the reference configuration as

$$\int_V \mathbf{f}_{bo} \cdot \dot{\mathbf{r}} dV + \int_S (\boldsymbol{\sigma}_{P1}^T \mathbf{N}) \cdot \dot{\mathbf{r}} dS = \frac{d}{dt} \left( \frac{1}{2} \int_V \rho_o \dot{\mathbf{r}} \cdot \dot{\mathbf{r}} dV \right) + \int_V (\boldsymbol{\sigma}_{P1} : \dot{\mathbf{J}}) dV \quad (3.76)$$

where all the variables that appear in this equation are the same as previously defined in this chapter. Note the structural similarity between the principle of virtual work for the continuum and the energy balance equations if  $\delta \mathbf{r}$  is replaced by  $\dot{\mathbf{r}}$  in the virtual work principle.

As in the case of the virtual work, the energy and power equations developed in this section show that the Cauchy stress tensor  $\boldsymbol{\sigma}$  is directly associated with the tensor of velocity gradients or equivalently the rate of deformation tensor because  $\boldsymbol{\sigma} : \mathbf{L} = \boldsymbol{\sigma} : \mathbf{D}$ . Because the velocity gradient tensor is not an exact differential, the Cauchy stress tensor  $\boldsymbol{\sigma}$  is not directly associated with a strain measure in the virtual work or energy equations. One can show that other stress and strain measures can also be used in the formulation of the energy equations. For example, as shown by Equation 76, the stress power can be written, using an analogy similar to the virtual work, in terms of the first Piola–Kirchhoff stress tensor  $\boldsymbol{\sigma}_{P1}$  and the rate of the matrix of position gradients  $\dot{\mathbf{J}}$  using the double product  $\boldsymbol{\sigma}_{P1} : \dot{\mathbf{J}}$ . Similarly, the stress power can be written in terms of the second Piola–Kirchhoff stress tensor  $\boldsymbol{\sigma}_{P2}$  and the rate of the Green–Lagrange strain tensor  $\dot{\boldsymbol{\epsilon}}$  using the double product  $\boldsymbol{\sigma}_{P2} : \dot{\boldsymbol{\epsilon}}$ . Because  $\mathbf{J}$  is not a deformation measure, the analysis presented in this chapter shows that, among the stress measures considered, only the second Piola–Kirchhoff stress tensor is directly related to a deformation measure, which can be expressed in a nondifferential form. Nonetheless, it is important to recognize that all the stress measures are related, as shown in this chapter and, therefore, relationships between different stress and strain measures can always be obtained.

## PROBLEMS

1. The Cauchy stress tensor at a point  $P$  is defined as

$$\boldsymbol{\sigma} = \begin{bmatrix} 2 & 0 & 3 \\ 0 & 3 & 1 \\ 3 & 1 & 4 \end{bmatrix}$$

Find the surface traction at  $P$  on planes whose normals are defined by the vectors  $\mathbf{n} = (1/\sqrt{5})[1 \ 0 \ 2]^T$  and  $\mathbf{n} = (1/\sqrt{3})[1 \ -1 \ 1]^T$ .

2. Verify the results of Equations 31 and 32.
3. Use the partial differential equations of equilibrium to derive the Newton–Euler equations that govern the planar motion of rigid bodies.
4. Derive the partial differential equations of equilibrium in the reference configuration in terms of the first Piola–Kirchhoff stress tensor.
5. Find the principal stresses and principal directions of the stress tensor given in Problem 1. Define also the stress invariants.

6. Using the virtual strains  $\delta \mathbf{e} = (1/2)\{\mathbf{J}^T \delta \mathbf{J} + (\delta \mathbf{J}^T) \mathbf{J}\}$  and the identities of the double product, show that the virtual work of the elastic forces can be written as  $\delta W_s = -\int_V \mathbf{J} \boldsymbol{\sigma} : \mathbf{J}^{-1T} \delta \mathbf{e} \mathbf{J}^{-1} dV$ , where  $\boldsymbol{\sigma}$  is the Cauchy stress tensor.
7. Show that the virtual work of the stresses can be written in terms of the first Piola–Kirchhoff stress tensor as  $\delta W_s = -\int_V \boldsymbol{\sigma}_{P1} : \delta \mathbf{J} dV$ .
8. Show that the principal values  $s_1, s_2$ , and  $s_3$  of the stress deviator tensor  $\mathbf{S}$  can be written in terms of the principal values  $\tau_1, \tau_2$ , and  $\tau_3$  of the Cauchy stress tensor  $\boldsymbol{\sigma}$  as

$$s_1 = \frac{1}{3}(2\tau_1 - \tau_2 - \tau_3), \quad s_2 = \frac{1}{3}(2\tau_2 - \tau_1 - \tau_3), \quad s_3 = \frac{1}{3}(2\tau_3 - \tau_1 - \tau_2)$$

9. Determine the deviator stress tensor  $\mathbf{S}$  associated with the Cauchy stress tensor given in Problem 1. Determine also the principal values of the deviator stress tensor and the hydrostatic pressure.
10. Using Equations 47 and 48, show that the invariants  $J'_2$  and  $J'_3$  of the stress deviator  $\mathbf{S}$  can be expressed in terms of the invariants  $J_1, J_2$ , and  $J_3$  of the Cauchy stress tensor  $\boldsymbol{\sigma}$ .
11. Derive the expression for the hydrostatic pressure in terms of the first Piola–Kirchhoff stress tensor.
12. Derive the expression for the deviatoric part associated with the first Piola–Kirchhoff stress tensor.
13. Show that  $dJ/dt = J \text{tr}(\mathbf{L})$ , where  $\mathbf{J}$  is the matrix of position vector gradients,  $J = |\mathbf{J}|$  and  $\mathbf{L}$  is the matrix of velocity gradients.
14. Obtain the rule of transformation of the Oldroyd and the convective stress rates when the continuum is subjected to a rigid-body motion.
15. Obtain the rule of transformation of the Green–Naghdi stress rate  $\boldsymbol{\sigma}^\Delta$  when the continuum is subjected to a rigid-body motion.
16. Obtain the rule of transformation of the Jaumann stress rate  $\boldsymbol{\sigma}^\nabla$  when the continuum is subjected to a rigid-body motion.
17. Derive the energy balance equation in the reference configuration.



## CHAPTER 4

---

# CONSTITUTIVE EQUATIONS

---

The kinematic and force equations developed in the preceding two chapters are general and applicable to all types of materials. The mechanics of solids and fluids is governed by the same equations, which do not distinguish between different materials. The definitions of the strain and stress tensors, however, are not sufficient for describing the behavior of continuous bodies. The force–displacement relationship or equivalently the stress–strain relationship is required in order to be able to distinguish between different materials and solve the equilibrium equations. The continuum displacements depend on the applied forces, and the force–displacement relationship depends on the material of the continuum. To complete the specification of the mechanical properties of a material, one needs an additional set of equations called the *constitutive equations*, which serve to distinguish one material from another. The form of the constitutive equations of a material should not be altered in the case of a pure rigid-body motion. These equations, therefore, must be objective, and should not lead to change in the work and energy of the stresses under an arbitrary rigid-body motion. Using the constitutive equations, the partial differential equations of equilibrium obtained in the preceding chapter can be expressed in terms of the strains. Using the strain–displacement relationships, these equilibrium equations can be expressed in terms of displacements or position coordinates and their time and spatial derivatives. If the continuum density is considered as an unknown variable, as it is the case in some fluid applications, the continuity equations can be added to the resulting system of partial differential equations in order to have a number of equations equal to the number of unknowns.

If the constitutive equations of a material depend only on the current state of deformation, the behavior is said to be elastic. If the stresses can be derived from a stored energy function, the material is termed *hyperelastic* or called *Green elastic material*. A more general



class of materials, for which the stresses cannot be derived from a stored energy function, is called *Cauchy elastic material*. For hyperelastic materials, the work done by the stresses during a deformation process is path independent. That is, the work done depends only on the initial and final states. For such systems, the continuum returns to its original configuration after the load is released. For viscoelastic materials, on the other hand, the work done during a deformation process is path dependent due to the dissipation of energy during the deformation process. The constitutive equations of viscoelastic materials are formulated in terms of rate of deformation measures in order to account for the energy dissipation.

In this chapter, the general constitutive equations of the materials are presented and systematically simplified in order to obtain the important special case of isotropic materials. It is shown that for isotropic materials that satisfy certain homogeneity and symmetry properties, the constitutive equations depend only on two constants called *Lame's constants*. Materials described by this model are called *Hookean materials*. The Hookean material model can be used in the case of small deformations. Other models, which are more appropriate for large deformations, such as the *Neo-Hookean* and the *incompressible Mooney–Rivlin material models*, are discussed. These nonlinear material models can be more accurate and lead to more efficient solutions in some applications, particularly when the assumption of linearity can no longer be used. The constitutive equations for viscoelastic materials and fluids are also discussed in this chapter. The behavior of elastic–plastic materials is discussed in a later chapter of this book.

## 4.1 GENERALIZED HOOKE'S LAW

The analysis presented in the preceding chapter shows that the second Piola–Kirchhoff stress tensor is the only tensor considered so far in this book that is directly associated in the virtual work and energy equations to a strain measure that can be expressed in a nondifferential form. Therefore, in this chapter, for the most part, the constitutive equations are assumed to relate the second Piola–Kirchhoff stress tensor and the Green–Lagrange strain tensor. In many inelastic formulations, however, constitutive equations in rate form are often expressed in terms of other stress and strain measures.

In this section, the general linear relationship between the stress and strain components is developed. As discussed in the preceding chapter, it is important to use consistent stress and deformation measures in the definition of the elastic forces. In this section, the Green–Lagrange strain tensor is used with the second Piola–Kirchhoff stress tensor to define a linear constitutive model. Nonetheless, one can always develop constitutive relationship between different stress and strain measures because these measures are related as previously mentioned. In this section, unless stated otherwise,  $\boldsymbol{\sigma}$  is used for simplicity to denote the stress measure, which is assumed to be the second Piola–Kirchhoff stress measure, whereas  $\boldsymbol{\epsilon}$  is used to denote the Green–Lagrange strain measure. The goal is to develop the relationship  $\boldsymbol{\sigma} = \boldsymbol{\sigma}(\boldsymbol{\epsilon})$ . In developing this relationship, it is important to distinguish between *homogeneous* and *isotropic materials*. A material is said to be homogeneous if it has the same properties at every point. That is, the elastic properties are not function of the location of the material points. In the case of isotropic materials, on the other hand, the elastic properties are assumed to be the same in all directions. That is, a coordinate transformation does not affect the definition of the elastic constants.

It has been found experimentally that for most materials, the measured strains are functions of the applied forces. For most solids, the strains are proportional to the applied forces, provided that the load does not exceed a given value known as the *elastic limit*. This experimental observation can be stated as follows: the stress components at any point in the body are linear functions of the strain components. This statement is a generalization of *Hooke's law* and does not apply to viscoelastic, plastic, or viscoplastic materials. The generalization of Hooke's law may thus be written, using vector and matrix notation instead of tensor notation, as

$$\boldsymbol{\sigma}_v = \mathbf{E}_m \boldsymbol{\varepsilon}_v \quad (4.1)$$

where  $\mathbf{E}_m$  is the matrix of elastic coefficients, and  $\boldsymbol{\sigma}_v$  and  $\boldsymbol{\varepsilon}_v$  are, respectively, the stress and strain components written in a vector form and defined as

$$\left. \begin{aligned} \boldsymbol{\sigma}_v &= [\sigma_1 \ \sigma_2 \ \sigma_3 \ \sigma_4 \ \sigma_5 \ \sigma_6]^T = [\sigma_{11} \ \sigma_{22} \ \sigma_{33} \ \sigma_{12} \ \sigma_{13} \ \sigma_{23}]^T \\ \boldsymbol{\varepsilon}_v &= [\varepsilon_1 \ \varepsilon_2 \ \varepsilon_3 \ \varepsilon_4 \ \varepsilon_5 \ \varepsilon_6]^T = [\varepsilon_{11} \ \varepsilon_{22} \ \varepsilon_{33} \ \varepsilon_{12} \ \varepsilon_{13} \ \varepsilon_{23}]^T \end{aligned} \right\} \quad (4.2)$$

One may also write Equation 1 using tensor notation as

$$\boldsymbol{\sigma} = \mathbf{E} : \boldsymbol{\varepsilon} \quad (4.3)$$

In this equation,  $\boldsymbol{\sigma}$  and  $\boldsymbol{\varepsilon}$  are, respectively, the second-order stress and strain tensors and  $\mathbf{E}$  is the fourth-order tensor of the elastic coefficients. When tensor notations are used, the stresses are defined according to the rule of the double contraction as  $\sigma_{ij} = \sum_{k,l=1}^3 E_{ijkl} \varepsilon_{kl}$ , where in this equation  $E_{ijkl}$  are the elements of the fourth-order tensor  $\mathbf{E}$ , that is,  $\mathbf{E} = (E_{ijkl})$ . In this chapter, the vector and matrix form of Equations 1 and 2 are sometimes used in order to simplify the derivations and take advantage of the symmetry of the stress and strain tensors. It is important, however, to recognize that Equations 1 and 3 are equivalent.

It was shown in the preceding two chapters that the Green–Lagrange strain tensor and the second Piola–Kirchhoff stress tensor do not change under an arbitrary rigid-body motion and the product  $\boldsymbol{\sigma}_{P2} : \boldsymbol{\varepsilon}$  satisfies the objectivity requirement. It is important, therefore, that the constitutive law used satisfies the objectivity requirement, which is automatically satisfied for linear isotropic elastic materials since the tensor of elastic coefficients  $\mathbf{E}$  is constant, as demonstrated in this chapter.

In the case of a general material, the matrix of elastic coefficients  $\mathbf{E}_m$  has 36 coefficients. This matrix can be written in its general form as follows:

$$\mathbf{E}_m = \begin{bmatrix} e_{11} & e_{12} & e_{13} & e_{14} & e_{15} & e_{16} \\ e_{21} & e_{22} & e_{23} & e_{24} & e_{25} & e_{26} \\ e_{31} & e_{32} & e_{33} & e_{34} & e_{35} & e_{36} \\ e_{41} & e_{42} & e_{43} & e_{44} & e_{45} & e_{46} \\ e_{51} & e_{52} & e_{53} & e_{54} & e_{55} & e_{56} \\ e_{61} & e_{62} & e_{63} & e_{64} & e_{65} & e_{66} \end{bmatrix} \quad (4.4)$$

The coefficients  $e_{ij}$ ,  $i, j = 1, 2, \dots, 6$ , define the material elastic properties when the behavior is assumed to be linear. The number of independent coefficients can be reduced if the material exhibits special characteristics as discussed in the following sections.

## 4.2 ANISOTROPIC LINEARLY ELASTIC MATERIALS

Let  $U$  be the *strain energy*, per unit volume, that represents the work done by the internal stresses. Using the definition of the work presented in the preceding chapter, one then has

$$dU = \boldsymbol{\sigma} : d\boldsymbol{\varepsilon} \quad (4.5)$$

which implies that

$$\boldsymbol{\sigma} = \left( \frac{\partial U}{\partial \boldsymbol{\varepsilon}} \right)^T \quad (4.6)$$

This equation can be written more explicitly in terms of the stress and strain components as

$$\sigma_{ij} = \frac{\partial U}{\partial \varepsilon_{ij}}, \quad i, j = 1, 2, 3 \quad (4.7)$$

The preceding two equations when combined with the constitutive equations (Equation 3) imply

$$\boldsymbol{\sigma} = \left( \frac{\partial U}{\partial \boldsymbol{\varepsilon}} \right)^T = \mathbf{E} : \boldsymbol{\varepsilon} \quad (4.8)$$

Note that this relationship is valid only for linearly elastic materials in which the elastic coefficients are assumed to be independent of the strains. This equation shows that

$$\frac{\partial^2 U}{\partial \varepsilon_i \partial \varepsilon_j} = e_{ij} = \frac{\partial^2 U}{\partial \varepsilon_j \partial \varepsilon_i} = e_{ji} \quad (4.9)$$

Here, for simplicity, a single subscript is used for the strain components according to the definitions of Equation 2. Equation 9 implies that

$$e_{ij} = e_{ji}, \quad i, j = 1, 2, 3 \quad (4.10)$$

This equation shows that for linearly elastic materials, the matrix of elastic coefficients is symmetric and there are only 21 distinct elastic coefficients for a general *anisotropic linearly elastic material*. This result is obtained based on energy considerations using the basic definition of the work of the elastic forces obtained in the preceding chapter and as defined by Equation 5.

### Example 4.1

For hyperelastic materials, the work of the stresses depends on the initial and final configurations and is independent of the path. In order to prove this result, we consider Green–Lagrange strain tensor and the second Piola–Kirchhoff stress tensor. Let  $t$  be time, and let the initial and final configurations be defined at  $t_1$  and  $t_2$ . Then, the work of the stresses can be written as

$$W_s = \int_{t_1}^{t_2} \boldsymbol{\sigma} : d\boldsymbol{\varepsilon} = \int_{t_1}^{t_2} \boldsymbol{\sigma} : \dot{\boldsymbol{\varepsilon}} dt = \int_{t_1}^{t_2} \frac{\partial U}{\partial \boldsymbol{\varepsilon}} : \dot{\boldsymbol{\varepsilon}} dt$$

One can show that this equation can be written as

$$W_s = \int_{t_1}^{t_2} \frac{\partial U}{\partial \mathbf{e}} : \dot{\mathbf{e}} dt = \int_{t_1}^{t_2} \frac{dU}{dt} dt = U(t_2) - U(t_1)$$

This equation shows that for hyperelastic materials, in which the stresses can be obtained from a potential function, the work of the stresses does not depend on the path but only on the initial and final configurations. In the case of a closed cycle, the work is identically zero.

### 4.3 MATERIAL SYMMETRY

In some structural materials, special kinds of symmetry may exist. The elastic coefficients, for example, may remain invariant under coordinate transformations. In this section, a reflection transformation and a proper orthogonal transformation due to rotations are considered. The obtained transformation results are used to reduce the number of unknown elastic coefficients.

#### Reflection

Consider the *reflection* with respect to the  $X_1X_2$  plane given by the following transformation:

$$\mathbf{A} = \begin{bmatrix} 1 & 0 & 0 \\ 0 & 1 & 0 \\ 0 & 0 & -1 \end{bmatrix} \quad (4.11)$$

The transformed stress and strain tensors  $\bar{\sigma}$  and  $\bar{\epsilon}$  are given, respectively, by

$$\left. \begin{aligned} \bar{\sigma} &= \mathbf{A}^T \boldsymbol{\sigma} \mathbf{A} \\ \bar{\epsilon} &= \mathbf{A}^T \boldsymbol{\epsilon} \mathbf{A} \end{aligned} \right\} \quad (4.12)$$

Using this transformation for the stresses and strains, one obtains

$$\left. \begin{aligned} \bar{\sigma}_{11} &= \sigma_{11}, & \bar{\sigma}_{22} &= \sigma_{22}, & \bar{\sigma}_{33} &= \sigma_{33} \\ \bar{\sigma}_{12} &= \sigma_{12}, & \bar{\sigma}_{13} &= -\sigma_{13}, & \bar{\sigma}_{23} &= -\sigma_{23} \end{aligned} \right\} \quad (4.13)$$

and

$$\left. \begin{aligned} \bar{\epsilon}_{11} &= \epsilon_{11}, & \bar{\epsilon}_{22} &= \epsilon_{22}, & \bar{\epsilon}_{33} &= \epsilon_{33} \\ \bar{\epsilon}_{12} &= \epsilon_{12}, & \bar{\epsilon}_{13} &= -\epsilon_{13}, & \bar{\epsilon}_{23} &= -\epsilon_{23} \end{aligned} \right\} \quad (4.14)$$

If the elastic coefficients are assumed to be invariant under the reflection transformation, that is, the elastic properties at two material points on the opposite sides of the  $X_1X_2$  plane are the same, one can write, for example,  $\bar{\sigma}_{11}$  as

$$\bar{\sigma}_{11} = e_{11}\bar{\epsilon}_{11} + e_{12}\bar{\epsilon}_{22} + e_{13}\bar{\epsilon}_{33} + e_{14}\bar{\epsilon}_{12} + e_{15}\bar{\epsilon}_{13} + e_{16}\bar{\epsilon}_{23} \quad (4.15)$$

Using the result of the reflection transformation, one can write

$$\sigma_{11} = \bar{\sigma}_{11} = e_{11}\epsilon_{11} + e_{12}\epsilon_{22} + e_{13}\epsilon_{33} + e_{14}\epsilon_{12} - e_{15}\bar{\epsilon}_{13} - e_{16}\bar{\epsilon}_{23} \quad (4.16)$$

Comparing the preceding two equations, one obtains  $e_{15} = -e_{15}$ , and  $e_{16} = -e_{16}$ , or

$$e_{15} = e_{16} = 0 \quad (4.17)$$

In a similar manner by considering other stress components, one can show that

$$e_{25} = e_{26} = e_{35} = e_{36} = e_{45} = e_{46} = 0 \quad (4.18)$$

Therefore, the number of independent elastic coefficients for a material that possesses a plane of elastic symmetry reduces to 13. If this plane of symmetry is the  $X_1X_2$  plane, that is, the elastic properties are invariant under a reflection with respect to the  $X_1X_2$  plane, the matrix  $\mathbf{E}_m$  of elastic coefficients can be written as

$$\mathbf{E}_m = \begin{bmatrix} e_{11} & & & & & \\ e_{21} & e_{22} & & & & \\ & & \text{symmetric} & & & \\ e_{31} & e_{32} & e_{33} & & & \\ e_{41} & e_{42} & e_{43} & e_{44} & & \\ 0 & 0 & 0 & 0 & e_{55} & \\ 0 & 0 & 0 & 0 & e_{65} & e_{66} \end{bmatrix} \quad (4.19)$$

If the material has *two mutually orthogonal planes of symmetry*, one can show that  $e_{41} = e_{42} = e_{43} = e_{65} = 0$  and the matrix of elastic coefficients reduces to

$$\mathbf{E}_m = \begin{bmatrix} e_{11} & & & & & \\ e_{21} & e_{22} & & & & \\ & & \text{symmetric} & & & \\ e_{31} & e_{32} & e_{33} & & & \\ 0 & 0 & 0 & e_{44} & & \\ 0 & 0 & 0 & 0 & e_{55} & \\ 0 & 0 & 0 & 0 & 0 & e_{66} \end{bmatrix} \quad (4.20)$$

That is, the number of elastic coefficients is reduced to nine.

## Rotations

In some materials, the elastic coefficients  $e_{ij}$  remain invariant under a *rotation* through an angle  $\alpha$  about one of the axes, that is, the values of these coefficients are independent of the set of

the rectangular axes chosen. For example, the transformation matrix  $\mathbf{A}$  in the case of a rotation about the  $X_3$  axis is given by

$$\mathbf{A} = \begin{bmatrix} \cos \alpha & -\sin \alpha & 0 \\ \sin \alpha & \cos \alpha & 0 \\ 0 & 0 & 1 \end{bmatrix} \quad (4.21)$$

One may write expressions for the transformed stress and strain tensors for different values of  $\alpha$  and proceed as in the case of reflection to show that in the case of an *isotropic solid* there are only two independent constants, denoted by  $\lambda$  and  $\mu$ . One can show that in this case

$$\left. \begin{aligned} e_{12} = e_{13} = e_{21} = e_{23} = e_{31} = e_{32} &= \lambda \\ e_{44} = e_{55} = e_{66} &= 2\mu \\ e_{11} = e_{22} = e_{33} &= \lambda + 2\mu \end{aligned} \right\} \quad (4.22)$$

The two elastic constants  $\lambda$  and  $\mu$  are known as *Lame's constants*. These two constants do not have to take the same values at every point on the continuum unless the material is assumed to be homogeneous. The case of homogeneous isotropic materials is discussed in the following section.

#### 4.4 HOMOGENEOUS ISOTROPIC MATERIAL

If the material is homogeneous,  $\lambda$  and  $\mu$  are constants at all points. The matrix  $\mathbf{E}_m$  of elastic coefficients can be written in the case of an isotropic homogeneous material in terms of Lamé's constants as

$$\mathbf{E}_m = \begin{bmatrix} \lambda + 2\mu & & & & & \\ & \lambda & \lambda + 2\mu & & & \\ & \lambda & \lambda & \lambda + 2\mu & & \\ & 0 & 0 & 0 & 2\mu & \\ & 0 & 0 & 0 & 0 & 2\mu \\ & 0 & 0 & 0 & 0 & 0 & 2\mu \end{bmatrix} \quad (4.23)$$

In this case, the relationship between the stresses and strains can be written explicitly as

$$\left. \begin{aligned} \sigma_{ii} &= \lambda \epsilon_t + 2\mu \epsilon_{ii}, \quad i = 1, 2, 3 \\ \sigma_{ij} &= 2\mu \epsilon_{ij}, \quad i \neq j \end{aligned} \right\} \quad (4.24)$$

where

$$\epsilon_t = \epsilon_{11} + \epsilon_{22} + \epsilon_{33} \quad (4.25)$$

is called the *dilatation*. The strains can be written in terms of the stresses (inverse relationship) as follows:

$$\left. \begin{aligned} \epsilon_{ii} &= \frac{1}{E} \{ (1 + \gamma) \sigma_{ii} - \gamma \sigma_t \}, \quad i = 1, 2, 3 \\ \epsilon_{ij} &= \frac{1}{2\mu} \sigma_{ij} = \left\{ \left( \frac{1 + \gamma}{E} \right) \sigma_{ij} \right\}, \quad i \neq j \end{aligned} \right\} \quad (4.26)$$

where

$$\sigma_t = \sigma_{11} + \sigma_{22} + \sigma_{33} \quad (4.27)$$

and

$$E = \frac{(3\lambda + 2\mu)\mu}{\lambda + \mu}, \quad \gamma = \frac{\lambda}{2(\lambda + \mu)} \quad (4.28)$$

The constants  $\mu$ ,  $E$ , and  $\gamma$  are, respectively, called the *modulus of rigidity* or *shear modulus*, *Young's modulus* or *modulus of elasticity*, and *Poisson's ratio*. In terms of these elastic coefficients, Equation 24 can be written as

$$\left. \begin{aligned} \sigma_{ii} &= \frac{E}{(1 + \gamma)(1 - 2\gamma)} \{ \gamma \epsilon_t + (1 - 2\gamma) \epsilon_{ii} \}, \quad i = 1, 2, 3 \\ \sigma_{ij} &= \frac{E}{(1 + \gamma)} \epsilon_{ij}, \quad i \neq j \end{aligned} \right\} \quad (4.29)$$

### Poisson Effect and Locking

Lame's constants can also be written in terms of the modulus of elasticity and Poisson ratio as

$$\lambda = \frac{\gamma E}{(1 + \gamma)(1 - 2\gamma)}, \quad \mu = \frac{E}{2(1 + \gamma)} \quad (4.30)$$

Equations 26 and 29 show that the effect of the Poisson ratio is to produce stresses that couple the stretch deformations in different directions. That is, if the Poisson ratio is equal to zero, the normal stresses are related to the normal strains by the equation  $\sigma_{ii} = E \epsilon_{ii}$ ,  $i = 1, 2, 3$ , which shows that the normal stress in one direction is independent of the normal strains in the other two directions. Furthermore, the value of the Poisson ratio cannot exceed 0.5. If the Poisson ratio becomes close to 0.5, the elastic coefficient associated with the dilatation  $\epsilon_t$  becomes very large, producing high stiffness that tends to resist any volume change. When the continuum equations are solved numerically, this high stiffness can be a source of problems and introduces what is referred to as *locking*. In fact, there are several types of locking including volumetric, shear, and membrane locking associated with different materials and structural elements. For instance, the volumetric locking can be explained by using the first equation in Equation 24. Using this equation, one can show that  $\sigma_{11} + \sigma_{22} + \sigma_{33} = (3\lambda + 2\mu)\epsilon_t$ . This equation shows that the hydrostatic pressure  $p$ , in the case of small deformation, can be written as  $p = \{(3\lambda + 2\mu)\epsilon_t\}/3$ , which upon the use of Equation 30 can be written as  $p = K\epsilon_t$ , where  $K$  is the *Bulk modulus* defined as  $K = E/[3(1 - 2\gamma)]$ . The equation  $p = K\epsilon_t$ , defines the relationship between the hydrostatic pressure and the dilatation. If the Poisson ratio approaches 0.5, the bulk modulus becomes very large leading to a very large stiffness coefficient associated with the volumetric change.

The locking problem will be revisited in Chapter 5 when large-deformation finite element formulations are discussed. It is important, however, to point out that many of the existing finite element formulations for structural elements such as beams do not take into consideration *Poisson effects*. This is mainly due to the fact that the element cross sections in these formulations are assumed rigid and are not allowed to deform. The large-deformation finite element formulation discussed in Chapter 5 allows taking into consideration the Poisson effect

because the element cross section is allowed to deform. Such a formulation allows for the use of general constitutive models as the ones discussed in this chapter, and therefore, coupling between different displacement modes such as the bending deformation and the stretch of the cross section can be taken into account in the case of beam, plate, and shell problems.

### Stress and Strain Invariants

Using Equation 24 and the definitions of the symmetric strain and stress tensor invariants presented in the preceding two chapters, one can show that the stress invariants  $J_1$ ,  $J_2$ , and  $J_3$  are related to the strain invariants  $I_1$ ,  $I_2$ , and  $I_3$  by the following equations (Boresi and Chong, 2000):

$$\left. \begin{aligned} J_1 &= (3\lambda + 2\mu)I_1 \\ J_2 &= \lambda(3\lambda + 4\mu)I_1^2 + 4\mu^2 I_2 \\ J_3 &= \lambda^2(\lambda + 2\mu)I_1^3 + 4\lambda\mu^2 I_1 I_2 + 8\mu^3 I_3 \end{aligned} \right\} \quad (4.31)$$

Some material constitutive models are formulated in terms of the invariants of deformation measures as discussed later in this chapter.

Using Equation 24, the strain energy density function can be written in terms of Lamé's constants and the strain components as

$$U_d = \frac{1}{2} \boldsymbol{\sigma} : \boldsymbol{\varepsilon} = \frac{1}{2} \lambda \varepsilon_t^2 + \mu (\varepsilon_{11}^2 + \varepsilon_{22}^2 + \varepsilon_{33}^2) + 2\mu (\varepsilon_{12}^2 + \varepsilon_{13}^2 + \varepsilon_{23}^2) \quad (4.32)$$

Recall that the invariants of the symmetric strain tensor are defined in terms of the strain components as

$$\left. \begin{aligned} I_1 &= \varepsilon_t = \varepsilon_{11} + \varepsilon_{22} + \varepsilon_{33} \\ I_2 &= \varepsilon_{11}\varepsilon_{22} + \varepsilon_{11}\varepsilon_{33} + \varepsilon_{22}\varepsilon_{33} - \varepsilon_{12}^2 - \varepsilon_{13}^2 - \varepsilon_{23}^2 \\ I_3 &= \det(\boldsymbol{\varepsilon}) \end{aligned} \right\} \quad (4.33)$$

This equation shows that  $I_1$  is a function of the normal strains, whereas  $I_2$  depends on the normal and shear strain components. Using the preceding two equations, one can show that the strain energy density function for linearly elastic and isotropic materials can be written in terms of the invariants of the strain tensor as

$$U_d = \frac{1}{2} \{ (\lambda + 2\mu)I_1^2 - 4\mu I_2 \} = \left( \frac{1}{2} \lambda + \mu \right) I_1^2 - 2\mu I_2 \quad (4.34)$$

The coefficient of the square of the dilatation in this strain energy density expression can be written as

$$\left( \frac{1}{2} \lambda + \mu \right) = \frac{E(1 - \gamma)}{2(1 + \gamma)(1 - 2\gamma)} \quad (4.35)$$

This equation demonstrates once again the numerical problems that can be encountered when dealing with incompressible and nearly incompressible materials.

Invariants of the deformation measures can have a clear physical meaning that explains the stiffness coefficients that enter into the formulation of the material constitutive equations. For example,  $I_3$  is a measure of the change of volume, whereas the dilatation  $I_1$  can be a measure of



the stretch. For isotropic materials, it is sometimes more convenient to use directly the invariants of the deformation measure to develop the constitutive equations. For this reason, some identities related to these invariants are discussed in detail in the following section, whereas the use of these identities in developing constitutive models for other material types is discussed in Section 5.

### Plane-Stress and Plane-Strain Problems

If  $\sigma_{13}$ ,  $\sigma_{23}$ , and  $\sigma_{33}$  are equal to zero, that is,  $\sigma_{13} = \sigma_{23} = \sigma_{33} = 0$ , one has the case of *plane stress*. In this case, Equation 26 yields

$$\left. \begin{aligned} \varepsilon_{11} &= \frac{1}{E}(\sigma_{11} - \gamma\sigma_{22}), & \varepsilon_{22} &= \frac{1}{E}(\sigma_{22} - \gamma\sigma_{11}) \\ \varepsilon_{33} &= \frac{-\gamma}{E}(\sigma_{11} + \sigma_{22}), & \varepsilon_{12} &= \frac{1+\gamma}{E}\sigma_{12} \end{aligned} \right\} \quad (4.36)$$

Using these equations, one can show that the constitutive equations for linearly elastic isotropic materials can be written as

$$\begin{bmatrix} \sigma_{11} \\ \sigma_{22} \\ \sigma_{12} \end{bmatrix} = E \begin{bmatrix} \frac{1}{1-\gamma^2} & \frac{\gamma}{1-\gamma^2} & 0 \\ \frac{\gamma}{1-\gamma^2} & \frac{1}{1-\gamma^2} & 0 \\ 0 & 0 & \frac{1}{1+\gamma} \end{bmatrix} \begin{bmatrix} \varepsilon_{11} \\ \varepsilon_{22} \\ \varepsilon_{12} \end{bmatrix} \quad (4.37)$$

The assumptions of plane stress are made in several applications such as in the analysis of thin plates. If the interest is focused on the deformation of the plate midsurface in response to applied forces, the normal and shear stresses in the direction of the plate thickness can be neglected.

In the case of *plane strain*, one has  $\varepsilon_{13} = \varepsilon_{23} = \varepsilon_{33} = 0$ . Using Equation 24, one has

$$\left. \begin{aligned} \sigma_{11} &= (\lambda + 2\mu)\varepsilon_{11} + \lambda\varepsilon_{22} \\ \sigma_{22} &= (\lambda + 2\mu)\varepsilon_{22} + \lambda\varepsilon_{11} \\ \sigma_{33} &= \lambda(\varepsilon_{11} + \varepsilon_{22}) \\ \sigma_{12} &= 2\mu\varepsilon_{12} \end{aligned} \right\} \quad (4.38)$$

The constitutive equations can be written in this case as

$$\begin{bmatrix} \sigma_{11} \\ \sigma_{22} \\ \sigma_{12} \end{bmatrix} = \begin{bmatrix} (\lambda + 2\mu) & \lambda & 0 \\ \lambda & (\lambda + 2\mu) & 0 \\ 0 & 0 & 2\mu \end{bmatrix} \begin{bmatrix} \varepsilon_{11} \\ \varepsilon_{22} \\ \varepsilon_{12} \end{bmatrix} \quad (4.39)$$

Recall that the stress–strain relationships presented in this section are based on the assumption of linear behavior of the materials. These relationships, therefore, cannot be used directly in the case of materials that do not exhibit linear behavior based on the assumptions described in this chapter. Other constitutive relationships must be used for nonlinear materials, materials that have directional properties, or plastic and viscoelastic materials.

**Example 4.2**

Consider again the beam model used in several examples presented in the preceding chapters. Assume that the beam displacement is described by

$$\mathbf{r} = [(l + \delta)\xi \quad l\eta]^T$$

where  $\xi = x_1/l$ ,  $\eta = x_2/l$ ,  $l$  is the length of the beam, and  $\delta$  is a constant that defines the beam axial deformation. It was shown in Example 3 of Chapter 2 that this displacement can be produced using the following vector of beam coordinates:

$$\mathbf{e} = \left[ 0 \quad 0 \quad \left(1 + \frac{\delta}{l}\right) \quad 0 \quad 0 \quad 1 \quad l + \delta \quad 0 \quad \left(1 + \frac{\delta}{l}\right) \quad 0 \quad 0 \quad 1 \right]^T$$

One can show that the matrix of position vector gradients is defined as

$$\mathbf{J} = \begin{bmatrix} 1 + \frac{\delta}{l} & 0 \\ 0 & 1 \end{bmatrix}$$

The determinant of the matrix of the position vector gradients is

$$J = |\mathbf{J}| = 1 + \frac{\delta}{l}$$

The Green–Lagrange strain tensor is defined in this case as

$$\boldsymbol{\varepsilon} = \frac{1}{2}(\mathbf{J}^T \mathbf{J} - \mathbf{I}) = \begin{bmatrix} \varepsilon_{11} & \varepsilon_{12} \\ \varepsilon_{12} & \varepsilon_{22} \end{bmatrix} = \begin{bmatrix} \frac{\delta}{l} \left(1 + \frac{\delta}{2l}\right) & 0 \\ 0 & 0 \end{bmatrix} = \varepsilon_{11} \begin{bmatrix} 1 & 0 \\ 0 & 0 \end{bmatrix}$$

where  $\varepsilon_{11} = (\delta/l)(1 + (\delta/2l))$ .

If the case of plane strain is assumed, the relationship between the stresses and strains are given as

$$\begin{bmatrix} \sigma_{11} \\ \sigma_{22} \\ \sigma_{12} \end{bmatrix} = \begin{bmatrix} (\lambda + 2\mu) & \lambda & 0 \\ \lambda & (\lambda + 2\mu) & 0 \\ 0 & 0 & 2\mu \end{bmatrix} \begin{bmatrix} \varepsilon_{11} \\ \varepsilon_{22} \\ \varepsilon_{12} \end{bmatrix}$$

Assume that this constitutive equation governs the relationship between the second Piola–Kirchhoff stress and Green–Lagrange strain tensors. The second Piola–Kirchhoff stress tensor can then be written as

$$\boldsymbol{\sigma}_{P2} = \begin{bmatrix} \alpha_1 \varepsilon_{11} & 0 \\ 0 & \alpha_2 \varepsilon_{11} \end{bmatrix} = \varepsilon_{11} \begin{bmatrix} \alpha_1 & 0 \\ 0 & \alpha_2 \end{bmatrix}$$

where  $\alpha_1$  and  $\alpha_2$  are defined as

$$\alpha_1 = \lambda + 2\mu, \quad \alpha_2 = \lambda$$

Lame's constants  $\lambda$  and  $\mu$ , can be expressed in terms of the modulus of elasticity and Poisson ratio as shown in Equation 30. In the case of incompressible or nearly incompressible materials, some of the coefficients that appear in the stress–strain relationships of this simple example can take high values leading to a stiff behavior of the continuum.

### Finite Dimensional Model

As in the case of the inertia and body forces, one can systematically develop, using approximation methods, an expression of the stress forces of the infinite-dimension continuum in terms of a finite set of coordinates. To this end, the strain energy expression or the virtual work of the elastic forces can be used. The strains can be expressed in terms of the position vector gradients. The position vector gradients can be written in terms of the time-dependent coordinates. Using the constitutive equations, the virtual work or the strain energy can be expressed in terms of the coordinates used in the assumed displacement field. This systematic procedure is described by the following example.

#### Example 4.3

It was shown in the preceding chapter that the virtual work of the elastic forces can be written in terms of the Green–Lagrange strain tensor and the second Piola–Kirchhoff stress tensor as

$$\delta W_s = - \int_V \boldsymbol{\sigma}_{P2} : \delta \boldsymbol{\varepsilon} dV$$

In this equation, integration over the volume in the reference configuration is used because the stress and strain tensors used are associated with the reference configuration. The Green–Lagrange strain tensor and the virtual change in this tensor can be written, respectively, as

$$\boldsymbol{\varepsilon} = \frac{1}{2}(\mathbf{J}^T \mathbf{J} - \mathbf{I}), \quad \delta \boldsymbol{\varepsilon} = \frac{1}{2}(\mathbf{J}^T \delta \mathbf{J} + (\delta \mathbf{J})^T \mathbf{J})$$

where  $\mathbf{J}$  is the matrix of position vector gradients. Because the second Piola–Kirchhoff stress tensor  $\boldsymbol{\sigma}_{P2}$  is symmetric, one has

$$\delta W_s = - \int_V \boldsymbol{\sigma}_{P2} : \delta \boldsymbol{\varepsilon} dV = - \int_V \boldsymbol{\sigma}_{P2} : \mathbf{J}^T \delta \mathbf{J} dV$$

This equation, upon using the constitutive equations, can be expressed explicitly in terms of the position vector gradients, which in turn can be expressed in terms of the coordinate  $\mathbf{q}$ , which are used in the assumed displacement field. Recall that

$$\mathbf{r} = \mathbf{S}\mathbf{q}, \quad \delta \mathbf{r} = \mathbf{S}\delta \mathbf{q}$$

Using this assumed displacement field, one can write

$$\mathbf{r}_{x_i} = \mathbf{S}_{x_i} \mathbf{q}, \quad \delta \mathbf{r}_{x_i} = \mathbf{S}_{x_i} \delta \mathbf{q}, \quad i = 1, 2, 3$$

This equation shows that the virtual change of the position vector gradients can be expressed in terms of the virtual change in the coordinates  $\mathbf{q}$ . It follows that  $\delta \mathbf{J} = [\mathbf{S}_{x_1} \delta \mathbf{q} \ \mathbf{S}_{x_2} \delta \mathbf{q} \ \mathbf{S}_{x_3} \delta \mathbf{q}]$ . Therefore,

$$\mathbf{J}^T \delta \mathbf{J} = [(\mathbf{J}^T \mathbf{S}_{x_1}) \delta \mathbf{q} \ (\mathbf{J}^T \mathbf{S}_{x_2}) \delta \mathbf{q} \ (\mathbf{J}^T \mathbf{S}_{x_3}) \delta \mathbf{q}]$$

Equivalently, one can write

$$\begin{aligned} \delta W_s &= - \int_V \boldsymbol{\sigma}_{p2} : \delta \boldsymbol{\varepsilon} dV \\ &= - \int_V (\sigma_{11} \delta \varepsilon_{11} + \sigma_{22} \delta \varepsilon_{22} + \sigma_{33} \delta \varepsilon_{33} + 2\sigma_{12} \delta \varepsilon_{12} + 2\sigma_{13} \delta \varepsilon_{13} + 2\sigma_{23} \delta \varepsilon_{23}) dV \end{aligned}$$

In this equation,  $\sigma_{ij}$  are the components of the second Piola–Kirchhoff stress tensor. The constitutive equations and the expression for the position vector gradients can be directly substituted into this equation to obtain an expression of the virtual work expressed in terms of the components of the coordinate vector  $\mathbf{q}$  and their virtual changes.

## Generalized Elastic Forces

As explained in the preceding chapter, the last equation in the preceding example can be used to write the virtual work of the elastic forces in terms of the virtual changes in the position vector gradients as  $\delta W_s = - \int_V ((\mathbf{r}_x \boldsymbol{\sigma}_{c1})^T \delta \mathbf{r}_{x_1} + (\mathbf{r}_x \boldsymbol{\sigma}_{c2})^T \delta \mathbf{r}_{x_2} + (\mathbf{r}_x \boldsymbol{\sigma}_{c3})^T \delta \mathbf{r}_{x_3}) dV$ , where  $\mathbf{r}_x = [\mathbf{r}_{x_1} \ \mathbf{r}_{x_2} \ \mathbf{r}_{x_3}]$  is the matrix of position vector gradients,  $\mathbf{x} = [x_1 \ x_2 \ x_3]^T$  is the vector of spatial coordinates, and  $\boldsymbol{\sigma}_{c1} = [\sigma_{11} \ \sigma_{12} \ \sigma_{13}]^T$ ,  $\boldsymbol{\sigma}_{c2} = [\sigma_{12} \ \sigma_{22} \ \sigma_{23}]^T$ , and  $\boldsymbol{\sigma}_{c3} = [\sigma_{13} \ \sigma_{23} \ \sigma_{33}]^T$  are the columns of the stress tensor. When using the finite dimensional model based on the kinematic description  $\mathbf{r} = \mathbf{S}(\mathbf{x})\mathbf{q}$  used in the preceding example, one has  $\delta \mathbf{r}_{x_i} = \mathbf{S}_{x_i} \delta \mathbf{q}$ . It follows that the virtual work of the elastic forces can be written as  $\delta W_s = - \left( \int_V ((\mathbf{r}_x \boldsymbol{\sigma}_{c1})^T \mathbf{S}_{x_1} + (\mathbf{r}_x \boldsymbol{\sigma}_{c2})^T \mathbf{S}_{x_2} + (\mathbf{r}_x \boldsymbol{\sigma}_{c3})^T \mathbf{S}_{x_3}) dV \right) \delta \mathbf{q}$ , which can be written as  $\delta W_s = \mathbf{Q}_s^T \delta \mathbf{q}$ , where  $\mathbf{Q}_s = - \int_V ((\mathbf{S}_{x_1}^T \mathbf{r}_x) \boldsymbol{\sigma}_{c1} + (\mathbf{S}_{x_2}^T \mathbf{r}_x) \boldsymbol{\sigma}_{c2} + (\mathbf{S}_{x_3}^T \mathbf{r}_x) \boldsymbol{\sigma}_{c3}) dV$  is the vector of elastic generalized forces. As mentioned in the preceding chapter, this vector is, in general, a highly nonlinear function of the coordinates, and therefore, numerical integration is often required to calculate this force vector.

## Homogeneous Displacement

Some of the finite elements used in the literature yield constant strains. That is, the strain components are the same at every material point. These elements, which are defined using linear displacement field, are called *constant-strain* elements. As discussed in the preceding chapter, in the case of *homogeneous displacements*, the matrix of position vector gradients  $\mathbf{J}$  is the same everywhere throughout the continuum. A special example of this motion is the rigid-body motion, in which  $\mathbf{J}$  represents an orthogonal matrix. Because in the case of

homogeneous displacements, the strain components are the same at all material points, the stress tensor is independent of the location at which this tensor is evaluated if the matrix of the elastic coefficients is independent of the location, as in the case of isotropic materials. One, therefore, has  $\nabla \boldsymbol{\sigma} = \mathbf{0}$ .

#### 4.5 PRINCIPAL STRAIN INVARIANTS

In the case of isotropic materials, the constitutive behavior must be the same in any material direction. This means that the relationship between the potential function  $U$  and the Green–Lagrange strain tensor  $\boldsymbol{\varepsilon}$ , or equivalently the right Cauchy–Green deformation tensor  $\mathbf{C}_r$ , is independent of the chosen material axes. As a consequence, the potential function  $U$  must depend only on the invariants of  $\boldsymbol{\varepsilon}$ , as demonstrated in the preceding section or equivalently on the invariants of the right Cauchy–Green deformation tensor  $\mathbf{C}_r$ . In this case, one can write the potential function as

$$U = U(I_1, I_2, I_3) \quad (4.40)$$

where  $I_1$ ,  $I_2$ , and  $I_3$  are considered here to be the invariants of  $\mathbf{C}_r$  defined as

$$I_1 = \text{tr}(\mathbf{C}_r), \quad I_2 = \frac{1}{2} \{(\text{tr}(\mathbf{C}_r))^2 - \text{tr}(\mathbf{C}_r^2)\}, \quad I_3 = \det(\mathbf{C}_r) = |\mathbf{C}_r| \quad (4.41)$$

These invariants can be written in terms of the eigenvalues  $\lambda_1$ ,  $\lambda_2$ , and  $\lambda_3$  of  $\mathbf{C}_r$  as

$$\left. \begin{aligned} I_1 &= \lambda_1 + \lambda_2 + \lambda_3 \\ I_2 &= \lambda_1 \lambda_2 + \lambda_1 \lambda_3 + \lambda_2 \lambda_3 \\ I_3 &= \lambda_1 \lambda_2 \lambda_3 \end{aligned} \right\} \quad (4.42)$$

In the analysis of the large deformation, the second Piola–Kirchhoff stress tensor can be obtained from the potential function  $U$ . Recall that the right Cauchy–Green deformation tensor can be written in terms of the Green–Lagrange strain tensor as  $\mathbf{C}_r = 2\boldsymbol{\varepsilon} + \mathbf{I}$ . Because  $\boldsymbol{\varepsilon}$  and  $\boldsymbol{\sigma}_{P2}$  are symmetric, the second Piola–Kirchhoff stress tensor can then be written as

$$\boldsymbol{\sigma}_{P2} = \frac{\partial U}{\partial \boldsymbol{\varepsilon}} = 2 \frac{\partial U}{\partial \mathbf{C}_r} = 2 \frac{\partial U}{\partial I_1} \frac{\partial I_1}{\partial \mathbf{C}_r} + 2 \frac{\partial U}{\partial I_2} \frac{\partial I_2}{\partial \mathbf{C}_r} + 2 \frac{\partial U}{\partial I_3} \frac{\partial I_3}{\partial \mathbf{C}_r} \quad (4.43)$$

The derivatives of the principal invariants of a second-order tensor with respect to the tensor itself are known in a closed form. For the right Cauchy–Green deformation tensor, one has

$$\frac{\partial I_1}{\partial \mathbf{C}_r} = \mathbf{I}, \quad \frac{\partial I_2}{\partial \mathbf{C}_r} = I_1 \mathbf{I} - \mathbf{C}_r, \quad \frac{\partial I_3}{\partial \mathbf{C}_r} = I_3 \mathbf{C}_r^{-1} \quad (4.44)$$

Using these results and the fact that  $\mathbf{C}_r$  is symmetric, the second Piola–Kirchhoff stress tensor can be written as

$$\boldsymbol{\sigma}_{P2} = 2 \frac{\partial U}{\partial \mathbf{C}_r} = 2 \left( \frac{\partial U}{\partial I_1} + I_1 \frac{\partial U}{\partial I_2} \right) \mathbf{I} - 2 \frac{\partial U}{\partial I_2} \mathbf{C}_r + 2 I_3 \frac{\partial U}{\partial I_3} \mathbf{C}_r^{-1} \quad (4.45)$$

The Kirchhoff stress tensor  $\boldsymbol{\sigma}_K$  can also be written as

$$\boldsymbol{\sigma}_K = \mathbf{J} \boldsymbol{\sigma}_{P2} \mathbf{J}^T = 2 \left( \frac{\partial U}{\partial I_1} + I_1 \frac{\partial U}{\partial I_2} \right) \mathbf{C}_l - 2 \frac{\partial U}{\partial I_2} \mathbf{C}_l^2 + 2 I_3 \frac{\partial U}{\partial I_3} \mathbf{I} \quad (4.46)$$

where  $\mathbf{J}$  is the matrix of position vector gradients, and  $\mathbf{C}_l = \mathbf{J} \mathbf{J}^T$  is the left Cauchy–Green deformation tensor. Recall that Cauchy stress tensor, which is of practical significance, differs from Kirchhoff stress tensor  $\boldsymbol{\sigma}_K$  by only a scalar multiplier that is equal to the determinant of the matrix of the position vector gradients. Therefore, an expression of the Cauchy stress tensor in terms of the invariants of the right Cauchy–Green deformation tensor can be easily obtained using the preceding equation.

## 4.6 SPECIAL MATERIAL MODELS FOR LARGE DEFORMATIONS

Hooke's law describes linear elastic materials in which the stresses are proportional to the strains. In the case of one-dimensional problem, the stress–strain relationship can be described by a straight line. Some materials such as metals behave in this manner up to a certain limit for the applied stress called the *proportional limit*. After this point, the material remains elastic, but it exhibits nonlinear behavior, up to a stress limit known as the *elastic limit*. The proportional and elastic limits can be different for some materials such as steel. After the elastic limit, the stress reaches a local maximum called the *yield stress*, after which the stress drops to a local minimum and plastic deformation starts. In the plastic region, a small increase in the stress can lead to significant increase in the strain.

Not all materials follow the deformation sequence described earlier. Some materials exhibit nonlinear behavior from the start, and some other materials can be brittle and do not exhibit any significant elastic deformation. In this section, other material models that can be used in the analysis of *large-deformation problems* are discussed. The first is the *Neo–Hookean material model*, which is an extension of Hooke's law for isotropic linear material to large deformation. The second model is the *Modified Mooney–Rivlin material model*, which can be used in the large-deformation analysis of incompressible materials such as rubbers.

### Compressible Neo–Hookean Material Models

The Neo–Hookean material model is developed for the large deformation analysis. The constitutive equations are obtained using the following expression for the energy density function (Bonet and Wood, 1997):

$$U = \frac{\mu}{2} (I_1 - 3) - \mu \ln J + \frac{\lambda}{2} (\ln J)^2 \quad (4.47)$$

In this equation,  $\mu$  and  $\lambda$  are Lamé's constants used in the linear theory,  $I_1$  is the first invariant of the right Cauchy–Green deformation tensor  $\mathbf{C}_r$ , and  $J = \det(\mathbf{J})$  is the determinant of the matrix of position vector gradients. It is clear from the preceding equation that if there is no deformation, that is,  $\mathbf{C}_r = \mathbf{I}$  (rigid-body motion),  $I_1 = 3$ , and  $J = 1$ ;  $U$  is identically equal to zero and there is no energy stored as expected.

The second Piola–Kirchhoff stress tensor can now be obtained using the results presented in the preceding section as

$$\begin{aligned}\boldsymbol{\sigma}_{P2} &= 2 \left( \frac{\partial U}{\partial I_1} + I_1 \frac{\partial U}{\partial I_2} \right) \mathbf{I} - 2 \frac{\partial U}{\partial I_2} \mathbf{C}_r + 2 I_3 \frac{\partial U}{\partial I_3} \mathbf{C}_r^{-1} \\ &= \mu(\mathbf{I} - \mathbf{C}_r^{-1}) + \lambda(\ln J) \mathbf{C}_r^{-1}\end{aligned}\quad (4.48)$$

Similarly, the Kirchhoff stress tensor can be obtained for the Neo–Hookean material as

$$\begin{aligned}\boldsymbol{\sigma}_K &= 2 \left\{ \left( \frac{\partial U}{\partial I_1} + I_1 \frac{\partial U}{\partial I_2} \right) \mathbf{C}_l - \frac{\partial U}{\partial I_2} \mathbf{C}_l^2 + I_3 \frac{\partial U}{\partial I_3} \mathbf{I} \right\} \\ &= \mu(\mathbf{C}_l - \mathbf{I}) + \lambda(\ln J) \mathbf{I}\end{aligned}\quad (4.49)$$

The fourth-order Lagrangian tensor of the elastic coefficients for the Neo–Hookean material can be obtained by differentiating the expression for the second Piola–Kirchhoff stress tensor with respect to the components of the Green–Lagrange strain tensor. That is,

$$e_{ijkl} = \frac{\partial(\boldsymbol{\sigma}_{P2})_{ij}}{\partial \epsilon_{kl}} = \frac{\partial\{\mu(\mathbf{I} - \mathbf{C}_r^{-1}) + \lambda(\ln J) \mathbf{C}_r^{-1}\}_{ij}}{\partial \epsilon_{kl}} \quad (4.50)$$

Note that  $\partial(\boldsymbol{\sigma}_{P2})_{ij}/\partial \epsilon_{kl} = (\partial(\boldsymbol{\sigma}_{P2})_{ij}/\partial c_{kl}) (\partial c_{kl}/\partial \epsilon_{kl})$ , and  $(\partial c_{kl}/\partial \epsilon_{kl}) = 2$ , where  $c_{kl}$  here is the  $kl$ th element of the right Cauchy–Green deformation tensor  $\mathbf{C}_r$ . The preceding equation can be used to define the fourth-order tensor of elastic coefficients as

$$\mathbf{E} = \lambda_h \mathbf{C}_r^{-1} \otimes \mathbf{C}_r^{-1} - 2\mu_h \frac{\partial \mathbf{C}_r^{-1}}{\partial \mathbf{C}_r} \quad (4.51)$$

In this equation,

$$\lambda_h = \lambda, \quad \mu_h = \mu - \lambda \ln J \quad (4.52)$$

are the effective coefficients for the Neo–Hookean material. It is clear from Equation 51 that the elastic coefficients of the Neo–Hookean material model are not constants. These coefficients depend on the position vector gradients, which are functions of the continuum displacements. While the material is still considered homogeneous because it has the same properties ( $\lambda$  and  $\mu$ ) in the reference configuration, the elastic coefficients  $e_{ijkl}$  will have values that depend on the location of the material points as it is clear from Equation 51, which shows the dependency on the right Cauchy–Green deformation tensor  $\mathbf{C}_r$ .

Alternatively, one can obtain the elastic coefficients  $e_{ij}$  used in the vector and matrix notation instead of the tensor notation using the following equation:

$$e_{ij} = \frac{\partial^2 U}{\partial \varepsilon_i \partial \varepsilon_j} = \frac{\partial^2 \left\{ \frac{\mu}{2}(I_1 - 3) - \mu \ln J + \frac{\lambda}{2}(\ln J)^2 \right\}}{\partial \varepsilon_i \partial \varepsilon_j} \quad (4.53)$$

The special case of nearly incompressible material can be obtained from the general Neo–Hookean model by choosing Lamé's constants such that  $\lambda \gg \mu$ . In this case, the third term in the strain energy density function  $\lambda (\ln J)^2/2$  can be considered as a penalty term, which makes the deviation of  $J$  from 1 very small, and as a consequence, enforces the incompressibility condition.

#### Example 4.4

In order to prove Equation 51, one can write

$$\begin{aligned} e_{ijkl} &= \frac{\partial(\sigma_{p2})_{ij}}{\partial(\varepsilon)_{kl}} = 2 \frac{\partial(\sigma_{p2})_{ij}}{\partial(\mathbf{C}_r)_{kl}} = 2 \frac{\partial\{\mu(\mathbf{I} - \mathbf{C}_r^{-1}) + \lambda(\ln J)\mathbf{C}_r^{-1}\}_{ij}}{\partial(\mathbf{C}_r)_{kl}} \\ &= 2 \left\{ -\mu \frac{\partial(\mathbf{C}_r^{-1})_{ij}}{\partial(\mathbf{C}_r)_{kl}} + \lambda(\ln J) \frac{\partial(\mathbf{C}_r^{-1})_{ij}}{\partial(\mathbf{C}_r)_{kl}} + \lambda \frac{\partial(\ln J)}{\partial(\mathbf{C}_r)_{kl}} (\mathbf{C}_r^{-1})_{ij} \right\} \end{aligned}$$

Note that

$$J = \det(\mathbf{J}) = \sqrt{\det(\mathbf{C}_r)} = \sqrt{I_3}$$

Using this identity and Equation 44, one obtains

$$\frac{\partial(\ln J)}{\partial(\mathbf{C}_r)_{kl}} = \frac{\partial(\ln \sqrt{I_3})}{\partial I_3} \frac{\partial I_3}{\partial(\mathbf{C}_r)_{kl}} = \frac{1}{2\sqrt{I_3}} I_3 (\mathbf{C}_r^{-1})_{kl} = \frac{1}{2} (\mathbf{C}_r^{-1})_{kl}$$

Substituting this equation into the expression for  $e_{ijkl}$ , one obtains

$$e_{ijkl} = \lambda (\mathbf{C}_r^{-1})_{ij} (\mathbf{C}_r^{-1})_{kl} - 2(\mu - \lambda(\ln J)) \frac{\partial(\mathbf{C}_r^{-1})_{ij}}{\partial(\mathbf{C}_r)_{kl}}$$

which can be written as

$$\mathbf{E} = \lambda_h \mathbf{C}_r^{-1} \otimes \mathbf{C}_r^{-1} - 2\mu_h \frac{\partial \mathbf{C}_r^{-1}}{\partial \mathbf{C}_r}$$

where  $\lambda_h$  and  $\mu_h$  are defined by Equation 52.

### Incompressible Mooney–Rivlin Materials

A general form of the strain energy function for incompressible rubber materials is based on Mooney–Rivlin model. For incompressible materials,  $J = \det(\mathbf{J}) = 1$ , and therefore,



the third invariant of  $\mathbf{C}_r$  is equal to one because  $I_3 = \det(\mathbf{C}_r) = J^2 = 1$ . Therefore, the strain energy function for such incompressible materials depends on  $I_1$  and  $I_2$  only and is given by (Bonet and Wood, 1997)

$$U = U(I_1, I_2) = \sum_{r=0}^{\infty} \sum_{s=0}^{\infty} \mu_{rs} (I_1 - 3)^r (I_2 - 3)^s, \quad \mu_{00} = 0 \quad (4.54)$$

In this equation, the coefficients  $\mu_{rs}$  are constants. A special case of the preceding equation that was shown to match experimental results by Mooney and Rivlin is when  $\mu_{01}$  and  $\mu_{10}$  only are different from zero. In this particular case, one has

$$U = U(I_1, I_2) = \mu_{10}(I_1 - 3) + \mu_{01}(I_2 - 3) \quad (4.55)$$

The incompressibility condition that  $J = 1$ , or equivalently  $I_3 = 1$ , must be imposed. In order to impose this constraint, one can use the *technique of Lagrange* multipliers or the *penalty method*. The method of Lagrange multipliers introduces additional algebraic equations and unknown constraint forces, which enter into the formulation of the dynamic equations (Roberston and Schwertassek, 1988; Shabana, 2013). If the dependent variables that result from introducing the algebraic equations are not systematically eliminated, one must solve a system of differential and algebraic equations. The use of Lagrange multipliers requires a more sophisticated numerical procedure in order to be able to accurately solve the resulting dynamic equations.

On the other hand, if the penalty method is used, the preceding equation for the strain energy density function can be modified to include the penalty terms. There are several forms that can be used to introduce a penalty energy function  $U_p$ . One example is to use an energy function that produces a restoring force if the determinant of the matrix of position vector gradients deviates from one. In this case, the penalty function takes the form  $U_p = k(J - 1)^2/2$ , where  $k$  is a stiffness coefficient that must be selected high enough to enforce the incompressibility condition. In this case, the modified strain energy density function can be written as  $\bar{U} = U + U_p$ . Another example is to use the following modified strain energy density function (Belytschko et al., 2000).

$$\begin{aligned} \bar{U} &= U + k_1 \ln I_3 + k_2 (\ln I_3)^2 \\ &= \mu_{10}(I_1 - 3) + \mu_{01}(I_2 - 3) + k_1 \ln I_3 + k_2 (\ln I_3)^2 \end{aligned} \quad (4.56)$$

In this equation,  $U_p = k_1 \ln I_3 + k_2 (\ln I_3)^2$  is the penalty energy term, and  $k_1$  and  $k_2$  are constants. The constant  $k_1$  is selected such that the components of the second Piola–Kirchhoff stress tensor are zero in the initial configuration. This condition is satisfied if  $k_1 = -(\mu_{10} + 2\mu_{01})$  (Belytschko et al., 2000). The penalty constant  $k_2$  must be chosen large enough such that the compressibility error is small. The value of such constant must not be selected extremely large in order to avoid numerical problems associated with high-stiffness coefficients. The value recommended by Belytschko et al. (2000) is  $k_2 = 10^3 \times \max(\mu_{01}, \mu_{10})$  to  $k_2 = 10^7 \times \max(\mu_{01}, \mu_{10})$ . The components of the second Piola–Kirchhoff stress tensor can be obtained from the modified strain energy density function as

$$\sigma_{p2} = 2 \frac{\partial \bar{U}}{\partial \mathbf{C}_r} = 2 \frac{\partial U}{\partial \mathbf{C}_r} + 2 \{k_1 + k_2 (\ln I_3)\} \mathbf{C}_r^{-1} \quad (4.57)$$

The penalty method has two main drawbacks. First, it requires making assumptions for the penalty coefficients because there is no standard formula for determining these coefficients. Second, if the penalty coefficients required to satisfy the incompressibility condition are very high, the system becomes very stiff and numerical problems can be encountered as previously discussed. On the other hand, although the use of Lagrange multipliers leads to a more sound analytical approach, one must develop a procedure for solving the resulting differential and algebraic equations, as previously mentioned. The algebraic constraint equations reduce the number of the system degrees of freedom and lead to a more robust, yet more complex numerical algorithm. The use of the penalty method, on the other hand, does not require introducing algebraic constraint equations.

### Objectivity

In the literature, there are different constitutive models that are used to characterize the behavior of different materials. These constitutive models, however, must satisfy the objectivity requirement or the principle of material frame indifference. Any form of the constitutive equations leads to a functional relationship that can be written in the form  $\boldsymbol{\sigma} = \boldsymbol{\Phi}(\mathbf{J})$ . Using this functional relationship, one can, in a straightforward manner, obtain the conditions that must be met in order to satisfy the objectivity requirement. For example, consider  $\boldsymbol{\sigma}$  to be the Cauchy stress tensor. If the continuum is subjected from its current configuration to a rigid-body rotation defined by the transformation matrix  $\mathbf{A}$ , the new matrix of position vector gradients is defined as  $\tilde{\mathbf{J}} = \mathbf{A}\mathbf{J}$ , whereas the new Cauchy stress tensor is defined as  $\tilde{\boldsymbol{\sigma}} = \mathbf{A}\boldsymbol{\sigma}\mathbf{A}^T$ . It follows that  $\tilde{\boldsymbol{\sigma}} = \boldsymbol{\Phi}(\mathbf{A}\mathbf{J}) = \mathbf{A}\boldsymbol{\sigma}\mathbf{A}^T = \mathbf{A}\boldsymbol{\Phi}(\mathbf{J})\mathbf{A}^T$ . That is, the constitutive equations must satisfy the condition  $\boldsymbol{\Phi}(\mathbf{A}\mathbf{J}) = \mathbf{A}\boldsymbol{\Phi}(\mathbf{J})\mathbf{A}^T$  in order to meet the objectivity requirement.

Recall that the second Piola–Kirchhoff stress tensor does not change under an arbitrary rigid-body rotation. If this stress tensor is used, the constitutive model can in general be written in the form  $\boldsymbol{\sigma}_{P2} = \boldsymbol{\Phi}_{P2}(\mathbf{J})$ . In the case of a rigid-body rotation defined by the transformation matrix  $\mathbf{A}$ , one has  $\tilde{\mathbf{J}} = \mathbf{A}\mathbf{J}$  and  $\tilde{\boldsymbol{\sigma}}_{P2} = \boldsymbol{\sigma}_{P2}$ . It follows that  $\tilde{\boldsymbol{\sigma}}_{P2} = \boldsymbol{\Phi}_{P2}(\mathbf{A}\mathbf{J}) = \boldsymbol{\sigma}_{P2} = \boldsymbol{\Phi}_{P2}(\mathbf{J})$ , which leads to the condition  $\boldsymbol{\Phi}_{P2}(\mathbf{A}\mathbf{J}) = \boldsymbol{\Phi}_{P2}(\mathbf{J})$ .

## 4.7 LINEAR VISCOELASTICITY

In this section, viscoelastic materials that are dissipative in nature are considered. Such materials, which are not hyperelastic, can have permanent deformation when the loads are released. The constitutive equations for viscoelastic models are written in terms of derivatives of strains or stresses. These constitutive equations, as will be demonstrated, can be given in the form of differential or integral equations. For this reason, unlike the case of purely elastic model, the full history of the strains and stresses is required. First, the case of one-dimensional linear viscoelastic models is discussed. Generalization of the one-dimensional theory to three-dimensional models is demonstrated next. In the case of linear viscoelasticity, one does not need to distinguish between different stress and strain measures because the linear theory is applicable, for the most part, to small-deformation problems.

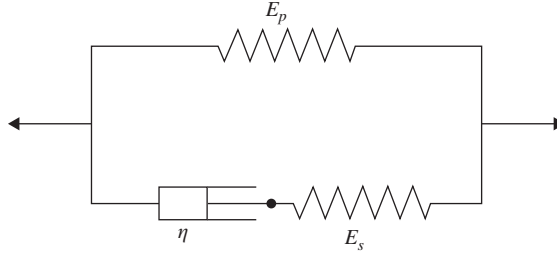


Figure 4.1 Standard model

### One-Dimensional Model

Several models are used in the analysis of viscoelastic materials. First, the *standard model* shown in Figure 1 is considered. This model consists of two springs and a dashpot that are arranged as shown in the figure. The spring constants are  $E_p$  and  $E_s$  and the dashpot constant is  $\eta$ . The total strain can be written as the sum of the elastic strain due to the deformation of the spring  $E_s$  and the inelastic strain due to the motion of the dashpot (assumption of series connection), that is,

$$\epsilon = \epsilon_{se} + \epsilon_v \quad (4.58)$$

where  $\epsilon$  is the total strain,  $\epsilon_{se}$  is the elastic strain in the spring  $E_s$ , and  $\epsilon_v$  is the strain due to the viscosity of the material. Equation 58 is an example of the *strain additive decomposition* which can be assumed in the case of linear viscoelasticity. Differentiating the preceding equation with respect to time, one obtains

$$\dot{\epsilon} = \dot{\epsilon}_{se} + \dot{\epsilon}_v \quad (4.59)$$

Using the arrangement of the standard model and small strain assumptions, the stresses in the spring and the dashpot are assumed equal, that is

$$\sigma_s = E_s \epsilon_{se} = E_s (\epsilon - \epsilon_v) = \eta \dot{\epsilon}_v \quad (4.60)$$

The total stress can then be written as

$$\sigma = E_p \epsilon + \sigma_s = E_p \epsilon + E_s (\epsilon - \epsilon_v) \quad (4.61)$$

Equation 60 shows that

$$\dot{\epsilon}_v + \frac{E_s}{\eta} \epsilon_v = \frac{E_s}{\eta} \epsilon(t) \quad (4.62)$$

or

$$\dot{\epsilon}_v + \frac{1}{\tau_r} \epsilon_v = \frac{1}{\tau_r} \epsilon(t) \quad (4.63)$$

where  $\tau_r = \eta/E_s$  is called the *relaxation time*.

Equation 63 can be considered as a first-order nonhomogeneous ordinary differential equation in the strain  $\dot{\epsilon}_v$ . The solution of this equation can be obtained, as shown in Example 5, using the *convolution* or the *Duhamel integral* as (Weaver et al., 1990; Shabana, 1996c)

$$\epsilon_v(t) = \frac{1}{\tau_r} \int_{-\infty}^t H(t - \tau) \epsilon(\tau) d\tau \quad (4.64)$$

where  $H(t - \tau)$  is the *impulse response function* defined as

$$H(t - \tau) = e^{-\frac{(t-\tau)}{\tau_r}} \quad (4.65)$$

Integrating Equation 64 by parts and using the condition that  $\epsilon(t) \rightarrow 0$  as  $t \rightarrow -\infty$ , one obtains

$$\epsilon_v(t) = \epsilon(t) - \int_{-\infty}^t H(t - \tau) \dot{\epsilon}(\tau) d\tau \quad (4.66)$$

Substituting this equation into the expression for the stress of Equation 61 in order to eliminate  $\epsilon_v$  and writing  $\epsilon$  in terms of the integral of  $\dot{\epsilon}$ , one obtains

$$\sigma(t) = \int_{-\infty}^t G(t - \tau) \dot{\epsilon}(\tau) d\tau \quad (4.67)$$

where the kernel  $G(t)$  is called the *relaxation function* associated with the standard model and is defined as

$$G(t) = E_p + E_s H(t) \quad (4.68)$$

Equation 67 is the constitutive equation in the case of one-dimensional linear viscoelastic material models. This equation is based on the assumptions of the standard model of viscoelasticity.

#### Example 4.5

In order to provide a proof of some of the equations presented in this section, Equation 63 is used as the starting point. This equation can be written as

$$\dot{\epsilon}_v + \frac{1}{\tau_r} \epsilon_v = \frac{1}{\tau_r} \epsilon(t)$$

The homogeneous form of this equation, which can be used to obtain the response due to initial conditions, can be written as

$$\dot{\epsilon}_v + \frac{1}{\tau_r} \epsilon_v = 0$$

This equation can be written as

$$\frac{d\varepsilon_v}{dt} = -\frac{1}{\tau_r}\varepsilon_v$$

That is,

$$\frac{d\varepsilon_v}{\varepsilon_v} = -\frac{1}{\tau_r}dt$$

This equation, upon integration and using the assumption that  $\varepsilon(t) \rightarrow 0$  as  $t \rightarrow -\infty$ , can be written as

$$\varepsilon_v = E_v e^{-t/\tau_r}$$

where  $E_v$  is a constant that depends on the initial conditions. Using this equation, the impulse response function can be defined as

$$H(t) = e^{-t/\tau_r}$$

Using the right-hand side of Equation 63, one can write

$$d\varepsilon_v = \frac{1}{\tau_r}\varepsilon(\tau)H(t-\tau)d\tau$$

which leads to the convolution or the Duhamel integral

$$\varepsilon_v = \frac{1}{\tau_r} \int_{-\infty}^t H(t-\tau)\varepsilon(\tau)d\tau$$

Integrating this equation by parts and using the definition of  $H(t)$  and the assumption that  $\varepsilon(t) \rightarrow 0$  as  $t \rightarrow -\infty$ , one obtains

$$\begin{aligned} \varepsilon_v(t) &= \frac{1}{\tau_r} \int_{-\infty}^t e^{-\frac{(t-\tau)}{\tau_r}} \varepsilon(\tau)d\tau = \frac{1}{\tau_r} \left\{ \left[ \varepsilon(\tau)\tau_r e^{-\frac{(t-\tau)}{\tau_r}} \right]_{\tau=-\infty}^{\tau=t} - \int_{-\infty}^t \tau_r e^{-\frac{(t-\tau)}{\tau_r}} \dot{\varepsilon}(\tau)d\tau \right\} \\ &= \frac{1}{\tau_r} \left\{ \varepsilon(t)\tau_r - \int_{-\infty}^t \tau_r e^{-\frac{(t-\tau)}{\tau_r}} \dot{\varepsilon}(\tau)d\tau \right\} = \varepsilon(t) - \int_{-\infty}^t e^{-\frac{(t-\tau)}{\tau_r}} \dot{\varepsilon}(\tau)d\tau \end{aligned}$$

Substituting this result into Equation 61, one obtains

$$\sigma(t) = E_p \varepsilon(t) + E_s \int_{-\infty}^t e^{-\frac{(t-\tau)}{\tau_r}} \dot{\varepsilon}(\tau)d\tau$$

One can also write

$$\varepsilon(t) = \int_{-\infty}^t \dot{\varepsilon}(\tau) d\tau$$

where the condition that  $\varepsilon(t) \rightarrow 0$  when  $t \rightarrow -\infty$  is utilized again. Using the preceding two equations, one obtains

$$\begin{aligned} \sigma(t) &= \int_{-\infty}^t \left( E_p + E_s e^{-\frac{(t-\tau)}{\tau_r}} \right) \dot{\varepsilon}(\tau) d\tau \\ &= \int_{-\infty}^t (E_p + E_s H(t-\tau)) \dot{\varepsilon}(\tau) d\tau = \int_{-\infty}^t G(t-\tau) \dot{\varepsilon}(\tau) d\tau \end{aligned}$$

where  $G(t)$  is defined by Equation 68.

For the standard model, the stress response can be inverted to obtain an expression for the strain history in terms of the stress history using the following convolution integral:

$$\varepsilon(t) = \int_{-\infty}^t K(t-\tau) \frac{d\sigma(\tau)}{d\tau} d\tau \quad (4.69)$$

where  $K$  is the *creep function*, which is defined for the standard model by the following equation:

$$K(t) = \frac{1}{E_p} \left( 1 - \frac{E_s}{E_t} e^{-\frac{E_p}{\tau_r E_t} t} \right) \quad (4.70)$$

In this equation,

$$E_t = E_p + E_s \quad (4.71)$$

It is important to point out that the use of the convolution integral as the solution of ordinary differential equations implies the use of the principle of superposition. Therefore, the convolution integral can only be used to obtain the solution of linear ordinary differential equations.

#### Example 4.6

As in the case of the relaxation function, a proof of the definition of the creep function of Equation 70 can be provided. To this end, Equation 61 can be used to obtain the following expression for the strain:

$$\varepsilon(t) = \frac{\sigma(t) + E_s \varepsilon_v}{E_t}$$

where  $E_t$  is defined by Equation 71. Substituting the preceding equation into Equation 60, one obtains

$$\dot{\varepsilon}_v(t) + \frac{1}{\tau_r} \left( 1 - \frac{E_s}{E_t} \right) \varepsilon_v(t) = \frac{1}{\tau_r E_t} \sigma(t)$$

This is a first-order nonhomogeneous ordinary differential equation, which can be solved again using the convolution integral. Alternatively, one can try to find a function  $\alpha(t)$  such that

$$\alpha(t) \dot{\varepsilon}_v(t) + \alpha(t) \frac{1}{\tau_r} \left( 1 - \frac{E_s}{E_t} \right) \varepsilon_v(t) = \alpha(t) \frac{1}{\tau_r E_t} \sigma(t)$$

One may also write

$$\frac{d}{dt} \{ \alpha(t) \varepsilon_v(t) \} = \alpha(t) \frac{1}{\tau_r E_t} \sigma(t)$$

This equation yields

$$\alpha(t) \dot{\varepsilon}_v(t) + \dot{\alpha}(t) \varepsilon_v(t) = \alpha(t) \frac{1}{\tau_r E_t} \sigma(t)$$

Comparing the preceding three equations, one obtains

$$\dot{\alpha}(t) = \alpha(t) \frac{1}{\tau_r} \left( 1 - \frac{E_s}{E_t} \right) = \alpha(t) \frac{1}{\tau_r} \frac{E_p}{E_t}$$

This equation shows that

$$\alpha(t) = e^{\left( \frac{E_p}{E_t} \right) \frac{t}{\tau_r}}$$

Substituting this equation into the equation  $d\{\alpha(t)\varepsilon_v(t)\}/dt = \alpha(t)\sigma(t)/\tau_r E_t$ , previously obtained in this example and integrating, one obtains

$$\int_{-\infty}^t \frac{d}{d\tau} \{ \alpha(\tau) \varepsilon_v(\tau) \} d\tau = \frac{1}{\tau_r E_t} \int_{-\infty}^t \alpha(\tau) \sigma(\tau) d\tau$$

Using the preceding two equations, one obtains

$$\alpha(t) \varepsilon_v(t) = \frac{1}{\tau_r E_t} \int_{-\infty}^t \alpha(\tau) \sigma(\tau) d\tau$$

which can be written as

$$\varepsilon_v(t) = \frac{1}{\tau_r E_t} \int_{-\infty}^t e^{-\left( \frac{E_p}{E_t} \right) \frac{(t-\tau)}{\tau_r}} \sigma(\tau) d\tau$$

Integrating this equation by parts, one obtains

$$\begin{aligned}
 \epsilon_v(t) &= \frac{1}{\tau_r E_t} \int_{-\infty}^t e^{-\left(\frac{E_p}{E_t}\right)\left(\frac{t-\tau}{\tau_r}\right)} \sigma(\tau) d\tau \\
 &= \frac{1}{\tau_r E_t} \left\{ \frac{\tau_r E_t}{E_p} \left[ \sigma(\tau) e^{-\left(\frac{E_p}{E_t}\right)\left(\frac{t-\tau}{\tau_r}\right)} \right]_{\tau=-\infty}^{\tau=t} - \frac{\tau_r E_t}{E_p} \int_{-\infty}^t e^{-\left(\frac{E_p}{E_t}\right)\left(\frac{t-\tau}{\tau_r}\right)} \dot{\sigma}(\tau) d\tau \right\} \\
 &= \frac{1}{\tau_r E_t} \left\{ \frac{\tau_r E_t}{E_p} \sigma(t) - \frac{\tau_r E_t}{E_p} \int_{-\infty}^t e^{-\left(\frac{E_p}{E_t}\right)\left(\frac{t-\tau}{\tau_r}\right)} \dot{\sigma}(\tau) d\tau \right\} \\
 &= \frac{1}{E_p} \left\{ \sigma(t) - \int_{-\infty}^t e^{-\left(\frac{E_p}{E_t}\right)\left(\frac{t-\tau}{\tau_r}\right)} \dot{\sigma}(\tau) d\tau \right\}
 \end{aligned}$$

Substituting this equation into the expression  $\epsilon(t) = (\sigma(t) + E_s \epsilon_v(t))/E_t$ , one obtains

$$\begin{aligned}
 \epsilon(t) &= \frac{\sigma(t) + \frac{E_s}{E_p} \left\{ \sigma(t) - \int_{-\infty}^t e^{-\left(\frac{E_p}{E_t}\right)\left(\frac{t-\tau}{\tau_r}\right)} \dot{\sigma}(\tau) d\tau \right\}}{E_t} \\
 &= \frac{1}{E_p} \sigma(t) - \frac{\frac{E_s}{E_p} \int_{-\infty}^t e^{-\left(\frac{E_p}{E_t}\right)\left(\frac{t-\tau}{\tau_r}\right)} \dot{\sigma}(\tau) d\tau}{E_t}
 \end{aligned}$$

One can also write

$$\sigma(t) = \int_{-\infty}^t \dot{\sigma}(\tau) d\tau$$

where the condition that  $\sigma(t) \rightarrow 0$  when  $t \rightarrow -\infty$  is utilized. Using the preceding two equations, one obtains

$$\begin{aligned}
 \epsilon(t) &= \frac{1}{E_p} \int_{-\infty}^t \dot{\sigma}(\tau) d\tau - \frac{E_s}{E_t E_p} \int_{-\infty}^t e^{-\left(\frac{E_p}{E_t}\right)\left(\frac{t-\tau}{\tau_r}\right)} \dot{\sigma}(\tau) d\tau \\
 &= \int_{-\infty}^t \frac{1}{E_p} \left( 1 - \frac{E_s}{E_t} e^{-\left(\frac{E_p}{E_t}\right)\left(\frac{t-\tau}{\tau_r}\right)} \right) \dot{\sigma}(\tau) d\tau = \int_{-\infty}^t K(t-\tau) \dot{\sigma}(\tau) d\tau
 \end{aligned}$$

where  $K(t)$  is defined by Equation 70.



## Other Viscoelastic Models

Although in this section, only the standard model is considered, it is important to mention that two other models are often used in the analysis of the viscoelastic behavior of materials. These are the *Maxwell model* and the *Kelvin (Voigt) model* (Fung, 1977). In the Maxwell model, only series connection is used, whereas the Voigt model has elements that are connected in parallel. Both models (Maxwell and Voigt) can be obtained as special cases of the standard model previously discussed in this section. The Maxwell model is a special case in which  $E_p = 0$ . It is important to note, however, that for the Maxwell model it is impossible to write the strain in terms of the stress because the creep function is not defined as it is clear from Equation 70. On the other hand, the Voigt model can be obtained from the standard model in case  $E_s = 0$ . In this case, one has

$$\sigma = E_p(\epsilon + \tau_r \dot{\epsilon}) = E_p \epsilon + \eta \dot{\epsilon}, \quad \tau_r = \frac{\eta}{E_p} \quad (4.72)$$

For the Voigt model, one can obtain a convolution integral in which the history of the strain is written in terms of the history of the stress. The inverse representation in which the history of the stress is written in terms of the history of the strain cannot be defined for the Voigt model.

## Generalization

The standard model can be generalized to include an arbitrary number of series spring-dashpot elements connected in parallel in addition to the spring  $E_p$  as shown in Figure 2. In this case, Equation 61 can be generalized and written as (Simo and Hughes, 1998)

$$\sigma = E_p \epsilon + \sum_{i=1}^N \sigma_{si} = E_p \epsilon + \sum_{i=1}^N E_{si}(\epsilon - \epsilon_{vi}) \quad (4.73)$$

In this equation,  $N$  is the total number of spring-dashpot elements connected in parallel. One can define

$$E_t = E_p + \sum_{i=1}^N E_{si} \quad (4.74)$$

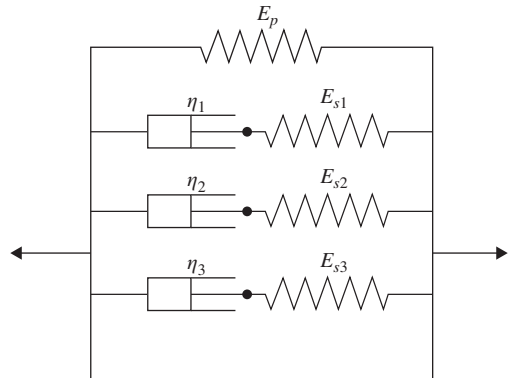


**Figure 4.2** Generalization

and use this equation to write Equation 73 as

$$\sigma = E_t \varepsilon - \sum_{i=1}^N E_{si} \varepsilon_{vi} \quad (4.75)$$

For each series connection, an equation similar to Equation 60 can be obtained. Therefore, the viscous strains  $\varepsilon_{vi}$  are governed by the following equations:

$$\dot{\varepsilon}_{vi} + \frac{1}{\tau_{ri}} \varepsilon_{vi} = \frac{1}{\tau_{ri}} \varepsilon, \quad i = 1, 2, \dots, N \quad (4.76)$$

where  $\tau_{ri} = \eta_i / E_{si}$ . In this case, one can use a procedure similar to the one described previously in this section to obtain the following convolution integral for the stress:

$$\sigma(t) = \int_{-\infty}^t G(t - \tau) \dot{\varepsilon}(\tau) d\tau \quad (4.77)$$

with the relaxation function  $G(t)$  defined as

$$G(t) = E_p + \sum_{i=1}^N E_{si} e^{-\frac{t}{\tau_{ri}}} \quad (4.78)$$

Note that Equation 77 is in the same form as Equation 67 with a different definition of the relaxation function.

### Elastic Energy and Dissipation

The stored strain energy density function in the springs of the generalized standard model can be written as

$$U(\varepsilon, \varepsilon_{vi}) = \frac{1}{2} E_p \varepsilon^2 + \frac{1}{2} \sum_{i=1}^N E_{si} (\varepsilon - \varepsilon_{vi})^2 \quad (4.79)$$

Differentiation of this equation with respect to the strain yields

$$\frac{\partial U(\varepsilon, \varepsilon_{vi})}{\partial \varepsilon} = E_p \varepsilon + \sum_{i=1}^N E_{si} (\varepsilon - \varepsilon_{vi}) \quad (4.80)$$

This equation shows that

$$\sigma = E_p \varepsilon + \sum_{i=1}^N E_{si} (\varepsilon - \varepsilon_{vi}) = \frac{\partial U(\varepsilon, \varepsilon_{vi})}{\partial \varepsilon} \quad (4.81)$$

Recall that

$$\sigma_{si} = E_{si} (\varepsilon - \varepsilon_{vi}) = \eta_i \dot{\varepsilon}_{vi}, \quad i = 1, 2, \dots, N \quad (4.82)$$

The energy dissipated, assuming a linear force–strain rate relationship, can be written as

$$D(\epsilon, \epsilon_{vi}, \dot{\epsilon}_{vi}) = \frac{1}{2} \sum_{i=1}^N \sigma_{si} \dot{\epsilon}_{vi} = \frac{1}{2} \sum_{i=1}^N \frac{E_{si}^2}{\eta_i} (\epsilon - \epsilon_{vi})^2 = \frac{1}{2} \sum_{i=1}^N \eta_i (\dot{\epsilon}_{vi})^2 \quad (4.83)$$

This dissipated energy is greater than zero for positive viscous damping coefficients. It is clear that the viscous stress can be obtained from the energy dissipation function as

$$\sigma_{si} = \frac{\partial D}{\partial \dot{\epsilon}_{vi}} = \eta_i \dot{\epsilon}_{vi} = E_{si} (\epsilon - \epsilon_{vi}) \quad (4.84)$$

This equation bears a similarity to the equations used to define the elastic stresses in the case of hyperelastic materials. Here the dissipation function replaces the strain energy function.

### Another Form of the Viscoelastic Equations

The elementary model discussed in this section can be presented in a different form, which can be extended in a straightforward manner to include nonlinear elastic response (Simo and Hughes, 1998). To this end, one can introduce a new set of stress-like variables called *partial stresses*:

$$q_i = E_{si} \epsilon_{vi}, \quad i = 1, 2, \dots, N \quad (4.85)$$

It follows that

$$\sigma = E_t \epsilon - \sum_{i=1}^N q_i, \quad (4.86)$$

and

$$\dot{q}_i + \frac{1}{\tau_{ri}} q_i = \frac{E_{si}}{\tau_{ri}} \epsilon, \quad i = 1, 2, \dots, N \quad (4.87)$$

Let

$$\left. \begin{aligned} \gamma_p &= \frac{E_p}{E_t} \\ \gamma_i &= \frac{E_{si}}{E_t}, \quad i = 1, 2, \dots, N \end{aligned} \right\} \quad (4.88)$$

Using the definition of  $E_p$  of Equation 74, one can show that the coefficient in the preceding equation must satisfy the following relationship:

$$\gamma_p + \sum_{i=1}^N \gamma_i = 1 \quad (4.89)$$

Therefore, the first-order differential equations for the partial stresses can be written as

$$\dot{q}_i + \frac{1}{\tau_{ri}} q_i = \frac{\gamma_i E_t}{\tau_{ri}} \epsilon, \quad i = 1, 2, \dots, N \quad (4.90)$$

The solution of this equation must satisfy  $\lim_{t \rightarrow -\infty} q_i(t) = 0$ .

It is clear from Equation 86 that one can introduce an *auxiliary strain energy density function*  $U_v$  such that  $U_v = E_t \epsilon^2 / 2$ . Using this definition and Equation 86, the stress  $\sigma$  can be defined as  $\sigma = (\partial U_v / \partial \epsilon) - \sum_{i=1}^N q_i$ . This form of the stress can be generalized and used in the case of the three-dimensional analysis.

### Three-Dimensional Linear Viscoelasticity

The one-dimensional model discussed in this section can be further generalized to the case of three-dimensional analysis. If  $U_v$  is the strain energy density function, one can write the following model previously presented in this section (Simo and Hughes, 1998)

$$\boldsymbol{\sigma} = \frac{\partial U_v}{\partial \boldsymbol{\epsilon}} - \sum_{i=1}^N \mathbf{q}_i \quad (4.91)$$

Viscoelastic constitutive models are often used for modeling the response of polymer materials. For these materials, the bulk response is elastic and appears to be much stiffer than the deviatoric response. For this reason, the assumption of incompressibility is often used. Using this assumption, the strain tensor can be written as

$$\boldsymbol{\epsilon} = \boldsymbol{\epsilon}_d + \boldsymbol{\epsilon}_t \quad (4.92)$$

where  $\boldsymbol{\epsilon}_d$  is the deviatoric strain tensor and  $\boldsymbol{\epsilon}_t$  is the volumetric strain tensor, defined as

$$\boldsymbol{\epsilon}_d = \boldsymbol{\epsilon} - \boldsymbol{\epsilon}_t, \quad \boldsymbol{\epsilon}_t = \frac{1}{3} \text{tr}(\boldsymbol{\epsilon}) \mathbf{I} \quad (4.93)$$

The stored strain energy density function can also be written as

$$U_v = U_d(\boldsymbol{\epsilon}_d) + U_t(\boldsymbol{\epsilon}_t) \quad (4.94)$$

In this equation,  $U_d$  and  $U_t$  are, respectively, the strain energy density functions due to the deviatoric and volumetric strains. It can be shown that  $\partial U_v / \partial \boldsymbol{\epsilon}$  in the definition of  $\boldsymbol{\sigma}$  in Equation 91 can be written using chain rule of differentiation as

$$\frac{\partial U_v}{\partial \boldsymbol{\epsilon}} = \text{dev} \left( \frac{\partial U_d}{\partial \boldsymbol{\epsilon}_d} \right) + \frac{\partial U_t}{\partial \boldsymbol{\epsilon}} \quad (4.95)$$

The evolution equations for the partial stresses can be written as

$$\dot{\mathbf{q}}_i + \frac{1}{\tau_{ri}} \mathbf{q}_i = \frac{\gamma_i}{\tau_{ri}} \text{dev} \left( \frac{\partial U_d}{\partial \boldsymbol{\epsilon}_d} \right), \quad i = 1, 2, \dots, N \quad (4.96)$$

As in the one-dimensional theory, the material parameters must satisfy the following condition:

$$\gamma_p + \sum_{i=1}^N \gamma_i = 1, \quad (4.97)$$

and the solutions for the partial stresses must satisfy  $\lim_{t \rightarrow -\infty} \mathbf{q}_i(t) = \mathbf{0}$ . Using the convolution integrals, the solution for the partial stresses can be obtained as

$$\mathbf{q}_i = \frac{\gamma_i}{\tau_{ri}} \int_{-\infty}^t e^{-\frac{(t-\tau)}{\tau_{ri}}} \text{dev} \left( \frac{\partial U_d}{\partial \boldsymbol{\varepsilon}_d} \right) d\tau, \quad i = 1, 2, \dots, N \quad (4.98)$$

Substituting this equation into the expression for  $\boldsymbol{\sigma}$ , one obtains the constitutive equations in the convolution integral form as

$$\boldsymbol{\sigma} = \frac{\partial U_t}{\partial \boldsymbol{\varepsilon}} + \int_{-\infty}^t G(t-\tau) \frac{d}{d\tau} \left\{ \text{dev} \left( \frac{\partial U_d}{\partial \boldsymbol{\varepsilon}_d} \right) \right\} d\tau \quad (4.99)$$

In this equation,

$$G(t) = \gamma_p + \sum_{i=1}^N \gamma_i e^{-\left(\frac{t}{\tau_{ri}}\right)} \quad (4.100)$$

The function  $G(t)$  is called the *normalized relaxation function*. Other forms of the relaxation function  $G(t)$  can also be considered. One can also consider the bulk response to be viscoelastic by simply making the following substitution in the convolution form of the constitutive equation:

$$\frac{\partial U_t}{\partial \boldsymbol{\varepsilon}} = \int_{-\infty}^t G_b(t-\tau) \frac{d}{d\tau} \left\{ \text{dev} \left( \frac{\partial U_t}{\partial \boldsymbol{\varepsilon}} \right) \right\} d\tau \quad (4.101)$$

where  $G_b(t)$  is a suitable relaxation function associated with the bulk response (Simo and Hughes, 1998). Note that if  $U_t$  is a linear function of  $\boldsymbol{\varepsilon}_t$ , the term  $\text{dev}(\partial U_t / \partial \boldsymbol{\varepsilon})$  is the null tensor.

A Kelvin–Voigt model that distinguishes between the bulk and deviatoric responses can also be developed. For this model, one can write the following constitutive equations (Garcia-Vallejo et al., 2005):

$$\left. \begin{aligned} \mathbf{S} &= \mathbf{E}_d : \boldsymbol{\varepsilon}_d + \mathbf{D}_d : \dot{\boldsymbol{\varepsilon}}_d \\ p &= E_t \varepsilon_t + D_t \dot{\varepsilon}_t \end{aligned} \right\} \quad (4.102)$$

In this equation,  $\mathbf{S}$  and  $\boldsymbol{\varepsilon}_d$  are, respectively, the deviatoric stress and strain tensors;  $\mathbf{E}_d$  and  $\mathbf{D}_d$  are, respectively, the tensors of elastic and damping coefficients;  $p$  is the hydrostatic pressure;  $\varepsilon_t$  is the dilatational strain; and  $E_t$  and  $D_t$  are elastic and damping coefficients. In the case of linear elastic materials,  $\mathbf{E}_d = 2\mu \mathbf{I}$  and  $E_t = 3K$ , where  $\mu$  is the shear modulus or modulus of rigidity,  $K = E/3(1-2\gamma)$  is the bulk modulus,  $E$  is the modulus of elasticity, and  $\gamma$  is the Poisson ratio. In the literature (Garcia-Vallejo et al., 2005), the damping coefficients are assumed to be  $\mathbf{D}_d = 2\mu \xi_d$ ,  $D_d = 3K \xi_t$  where  $\xi_d$  and  $\xi_t$  are the dissipation coefficients associated with the deviatoric and volumetric strains. Using the preceding equation and the fact that  $\boldsymbol{\sigma} = p\mathbf{I} + \mathbf{S}$  and  $\boldsymbol{\varepsilon} = \varepsilon_t \mathbf{I} + \boldsymbol{\varepsilon}_d$ , the constitutive equations based on the Kelvin–Voigt model can be written as

$$\boldsymbol{\sigma} = \mathbf{E} : \boldsymbol{\varepsilon} + \mathbf{D}_v : \dot{\boldsymbol{\varepsilon}} \quad (4.103)$$

In this equation,  $\mathbf{D}_v$ , is an appropriate damping matrix.

**Example 4.7**

Equation 95 can be written in the following form:

$$\frac{\partial U_v}{\partial \mathbf{\epsilon}} = \frac{\partial U_d}{\partial \mathbf{\epsilon}_d} : \frac{\partial \mathbf{\epsilon}_d}{\partial \mathbf{\epsilon}} + \frac{\partial U_t}{\partial \mathbf{\epsilon}}$$

In order to prove Equation 95, one needs to show that

$$\frac{\partial U_d}{\partial \mathbf{\epsilon}} = \frac{\partial U_d}{\partial \mathbf{\epsilon}_d} : \frac{\partial \mathbf{\epsilon}_d}{\partial \mathbf{\epsilon}} = \text{dev} \left( \frac{\partial U_d}{\partial \mathbf{\epsilon}_d} \right)$$

Using Equation 93, the deviatoric strain tensor can be written as follows:

$$(\mathbf{\epsilon}_d)_{ij} = (\mathbf{\epsilon})_{ij} - \frac{1}{3} \delta_{ij} \epsilon_t$$

where  $\delta_{ij}$  is the Kronecker delta and  $\epsilon_t = \epsilon_{11} + \epsilon_{22} + \epsilon_{33}$ . Note that

$$\left( \frac{\partial \mathbf{\epsilon}_d}{\partial \mathbf{\epsilon}} \right)_{ijkl} = \frac{\partial (\mathbf{\epsilon}_d)_{ij}}{\partial (\mathbf{\epsilon})_{kl}} = \frac{\partial (\mathbf{\epsilon})_{ij}}{\partial (\mathbf{\epsilon})_{kl}} - \delta_{ij} \frac{\partial \epsilon_t}{\partial (\mathbf{\epsilon})_{kl}} = \delta_{ik} \delta_{jl} - \frac{1}{3} \delta_{ij} \delta_{kl}$$

It follows that

$$\left( \frac{\partial U_d}{\partial \mathbf{\epsilon}} \right)_{kl} = \frac{\partial U_d}{\partial (\mathbf{\epsilon})_{kl}} = \frac{\partial U_d}{\partial (\mathbf{\epsilon}_d)_{ij}} \frac{\partial (\mathbf{\epsilon}_d)_{ij}}{\partial (\mathbf{\epsilon})_{kl}} = \frac{\partial U_d}{\partial (\mathbf{\epsilon}_d)_{ij}} \left( \delta_{ik} \delta_{jl} - \frac{1}{3} \delta_{ij} \delta_{kl} \right)$$

Note that

$$\frac{\partial U_d}{\partial (\mathbf{\epsilon}_d)_{ij}} \delta_{ik} \delta_{jl} = \frac{\partial U_d}{\partial (\mathbf{\epsilon}_d)_{kl}}$$

and

$$\frac{\partial U_d}{\partial (\mathbf{\epsilon}_d)_{ij}} \left( \frac{1}{3} \delta_{ij} \delta_{kl} \right) = \frac{1}{3} \left( \left( \frac{\partial U_d}{\partial \mathbf{\epsilon}_d} \right)_{11} + \left( \frac{\partial U_d}{\partial \mathbf{\epsilon}_d} \right)_{22} + \left( \frac{\partial U_d}{\partial \mathbf{\epsilon}_d} \right)_{33} \right) \delta_{kl}$$

The preceding three equations lead to

$$\begin{aligned} \left( \frac{\partial U_d}{\partial \mathbf{\epsilon}} \right)_{kl} &= \frac{\partial U_d}{\partial (\mathbf{\epsilon})_{kl}} = \frac{\partial U_d}{\partial (\mathbf{\epsilon}_d)_{kl}} - \frac{1}{3} \left( \left( \frac{\partial U_d}{\partial \mathbf{\epsilon}_d} \right)_{11} + \left( \frac{\partial U_d}{\partial \mathbf{\epsilon}_d} \right)_{22} + \left( \frac{\partial U_d}{\partial \mathbf{\epsilon}_d} \right)_{33} \right) \delta_{kl} \\ &= \frac{\partial U_d}{\partial (\mathbf{\epsilon}_d)_{kl}} - \frac{1}{3} \text{tr} \left( \frac{\partial U_d}{\partial \mathbf{\epsilon}_d} \right) \delta_{kl} \end{aligned}$$

or in a matrix form

$$\frac{\partial U_d}{\partial \mathbf{\epsilon}} = \text{dev} \left( \frac{\partial U_d}{\partial \mathbf{\epsilon}_d} \right)$$

**Example 4.8**

In order to prove Equation 99, one can integrate Equation 98 by parts. This leads to

$$\begin{aligned} \mathbf{q}_i &= \frac{\gamma_i}{\tau_{ri}} \int_{-\infty}^t e^{-\frac{(t-\tau)}{\tau_{ri}}} \operatorname{dev} \left( \frac{\partial U_d}{\partial \boldsymbol{\epsilon}_d} \right) d\tau \\ &= \frac{\gamma_i}{\tau_{ri}} \left\{ \left[ \tau_{ri} e^{-\frac{(t-\tau)}{\tau_{ri}}} \operatorname{dev} \left( \frac{\partial U_d}{\partial \boldsymbol{\epsilon}_d} \right) \right]_{\tau=-\infty}^{\tau=t} - \int_{-\infty}^t \tau_{ri} e^{-\frac{(t-\tau)}{\tau_{ri}}} \frac{d}{d\tau} \left( \operatorname{dev} \left( \frac{\partial U_d}{\partial \boldsymbol{\epsilon}_d} \right) \right) d\tau \right\} \end{aligned}$$

This equation can be written as

$$\begin{aligned} \mathbf{q}_i &= \frac{\gamma_i}{\tau_{ri}} \int_{-\infty}^t e^{-\frac{(t-\tau)}{\tau_{ri}}} \operatorname{dev} \left( \frac{\partial U_d}{\partial \boldsymbol{\epsilon}_d} \right) d\tau \\ &= \gamma_i \left\{ \operatorname{dev} \left( \frac{\partial U_d}{\partial \boldsymbol{\epsilon}_d} \right) - \int_{-\infty}^t e^{-\frac{(t-\tau)}{\tau_{ri}}} \frac{d}{d\tau} \left( \operatorname{dev} \left( \frac{\partial U_d}{\partial \boldsymbol{\epsilon}_d} \right) \right) d\tau \right\} \end{aligned}$$

Substituting this into Equation 91, one obtains

$$\begin{aligned} \boldsymbol{\sigma} &= \frac{\partial U_v}{\partial \boldsymbol{\epsilon}} - \sum_{i=1}^N \mathbf{q}_i = \operatorname{dev} \left( \frac{\partial U_d}{\partial \boldsymbol{\epsilon}_d} \right) + \frac{\partial U_t}{\partial \boldsymbol{\epsilon}} - \sum_{i=1}^N \mathbf{q}_i \\ &= \operatorname{dev} \left( \frac{\partial U_d}{\partial \boldsymbol{\epsilon}_d} \right) + \frac{\partial U_t}{\partial \boldsymbol{\epsilon}} - \operatorname{dev} \left( \frac{\partial U_d}{\partial \boldsymbol{\epsilon}_d} \right) \sum_{i=1}^N \gamma_i + \sum_{i=1}^N \gamma_i \int_{-\infty}^t e^{-\frac{(t-\tau)}{\tau_{ri}}} \frac{d}{d\tau} \left( \operatorname{dev} \left( \frac{\partial U_d}{\partial \boldsymbol{\epsilon}_d} \right) \right) d\tau \\ &= \frac{\partial U_t}{\partial \boldsymbol{\epsilon}} + \left( 1 - \sum_{i=1}^N \gamma_i \right) \operatorname{dev} \left( \frac{\partial U_d}{\partial \boldsymbol{\epsilon}_d} \right) + \sum_{i=1}^N \gamma_i \int_{-\infty}^t e^{-\frac{(t-\tau)}{\tau_{ri}}} \frac{d}{d\tau} \left( \operatorname{dev} \left( \frac{\partial U_d}{\partial \boldsymbol{\epsilon}_d} \right) \right) d\tau \end{aligned}$$

which can be written as

$$\begin{aligned} \boldsymbol{\sigma} &= \frac{\partial U_v}{\partial \boldsymbol{\epsilon}} - \sum_{i=1}^N \mathbf{q}_i \\ &= \frac{\partial U_t}{\partial \boldsymbol{\epsilon}} + \gamma_p \operatorname{dev} \left( \frac{\partial U_d}{\partial \boldsymbol{\epsilon}_d} \right) + \sum_{i=1}^N \gamma_i \int_{-\infty}^t e^{-\frac{(t-\tau)}{\tau_{ri}}} \frac{d}{d\tau} \left( \operatorname{dev} \left( \frac{\partial U_d}{\partial \boldsymbol{\epsilon}_d} \right) \right) d\tau \end{aligned}$$

One can write

$$\operatorname{dev} \left( \frac{\partial U_d}{\partial \boldsymbol{\epsilon}_d} \right) = \int_{-\infty}^t \frac{d}{d\tau} \left( \operatorname{dev} \left( \frac{\partial U_d}{\partial \boldsymbol{\epsilon}_d} \right) \right) d\tau$$

where the fact that  $\text{dev}(\partial U_d / \partial \epsilon_d) \rightarrow 0$  as  $t \rightarrow -\infty$  has been used. Combining the last two equations one can write

$$\sigma = \frac{\partial U_t}{\partial \epsilon} + \int_{-\infty}^t \left( \gamma_p + \sum_{i=1}^N \gamma_i e^{-\frac{(t-\tau)}{\tau_i}} \right) \frac{d}{d\tau} \left( \text{dev} \left( \frac{\partial U_d}{\partial \epsilon_d} \right) \right) d\tau$$

or

$$\sigma = \frac{\partial U_t}{\partial \epsilon} + \int_{-\infty}^t G(t-\tau) \frac{d}{d\tau} \left( \text{dev} \left( \frac{\partial U_d}{\partial \epsilon_d} \right) \right) d\tau$$

where  $G(t)$  is defined by Equation 100.

## 4.8 NONLINEAR VISCOELASTICITY

In the case of the nonlinear analysis, the principle of superposition employed in the preceding section for the linear analysis does not apply. Furthermore, the infinitesimal strain tensor can no longer be used, appropriate strain and stress measures must be used, and the constitutive equations must be frame-indifferent in order to satisfy the objectivity requirement.

A straightforward generalization of the formulation presented in the preceding section to the case of finite strains is to use a multiplicative decomposition of the matrix of position vector gradients. To this end, one can define the following matrix:

$$\bar{\mathbf{J}} = J^{-\frac{1}{3}} \mathbf{J} \quad (4.104)$$

Using this definition, one has the following simple multiplicative decomposition of  $\mathbf{J}$ :

$$\mathbf{J} = J^{\frac{1}{3}} \bar{\mathbf{J}} \quad (4.105)$$

Because on the right-hand side of Equation 104, every row of  $\mathbf{J}$  is multiplied by  $J^{-\frac{1}{3}}$ , it follows that the determinant of  $\bar{\mathbf{J}}$  is always equal to one, that is

$$\det(\bar{\mathbf{J}}) = 1 \quad (4.106)$$

One can then define the following right Cauchy–Green deformation tensors:

$$\mathbf{C}_r = \mathbf{J}^T \mathbf{J}, \quad \bar{\mathbf{C}}_r = \bar{\mathbf{J}}^T \bar{\mathbf{J}} \quad (4.107)$$

As was previously shown

$$\frac{\partial J}{\partial \mathbf{C}_r} = \frac{1}{2} J \mathbf{C}_r^{-1} \quad (4.108)$$

The stored elastic energy can be written as the sum of two parts as follows:

$$U = U_1(J) + U_2(\bar{\mathbf{C}}_r) \quad (4.109)$$



In this equation,  $U_1$  is the strain energy due to the volumetric change, whereas  $U_2$  is the strain energy due to volume-preserving deformations.

Motivated by the development presented in the preceding section, the second Piola–Kirchhoff stress tensor can be defined for the viscoelastic model using the energy density function and the partial stresses as

$$\boldsymbol{\sigma}_{P2} = \frac{\partial U}{\partial \boldsymbol{\varepsilon}} - J^{-\frac{2}{3}} \left( \sum_{i=1}^N \mathbf{q}_i \right) = 2 \frac{\partial U}{\partial \bar{\mathbf{C}}_r} - J^{-\frac{2}{3}} \left( \sum_{i=1}^N \mathbf{q}_i \right) \quad (4.110)$$

In this equation,  $\mathbf{q}_i$ ,  $i = 1, 2, \dots, N$ , are the partial stresses. Because  $\boldsymbol{\sigma}_{P2}$  does not change under an arbitrary rigid-body motion, as shown in the preceding chapter, the partial stresses  $\mathbf{q}_i$  must remain unchanged under the arbitrary rigid-body motion in order to satisfy the objectivity requirement for the stress. The evolution equations for the partial stresses can be written as

$$\dot{\mathbf{q}}_i + \frac{1}{\tau_{ri}} \mathbf{q}_i = \frac{\gamma_i}{\tau_{ri}} \text{dev} \left( 2 \frac{\partial U_2}{\partial \bar{\mathbf{C}}_r} \right), \quad i = 1, 2, \dots, N \quad (4.111)$$

In this equation, the trace of  $\text{dev}(2\partial U_2/\partial \bar{\mathbf{C}}_r)$  is not in general equal to zero as in the case of the second Piola–Kirchhoff stress tensor. The material parameters must satisfy the following condition:

$$\gamma_p + \sum_{i=1}^N \gamma_i = 1 \quad (4.112)$$

The solutions for the partial stresses must satisfy  $\lim_{t \rightarrow -\infty} \mathbf{q}_i(t) = \mathbf{0}$ . Equation 111 represents a set of  $N$  linear first-order differential equations, which can be solved for the partial stresses. Using the convolution integrals, the solution for the partial stresses can be obtained as

$$\mathbf{q}_i = \frac{\gamma_i}{\tau_{ri}} \int_{-\infty}^t e^{-\frac{(t-\tau)}{\tau_{ri}}} \text{dev} \left( 2 \frac{\partial U_2}{\partial \bar{\mathbf{C}}_r} \right) d\tau, \quad i = 1, 2, \dots, N \quad (4.113)$$

Substituting this equation into the expression for  $\boldsymbol{\sigma}_{P2}$ , one obtains the constitutive equations in the convolution integral form as (Simo and Hughes, 1998)

$$\boldsymbol{\sigma}_{P2} = J \frac{\partial U_1}{\partial J} \mathbf{C}_r^{-1} + J^{-\frac{2}{3}} \int_{-\infty}^t G(t-\tau) \frac{d}{d\tau} \left\{ \text{dev} \left( 2 \frac{\partial U_2}{\partial \bar{\mathbf{C}}_r} \right) \right\} d\tau \quad (4.114)$$

In this equation,

$$G(t) = \gamma_p + \sum_{i=1}^N \gamma_i e^{-\left(\frac{t}{\tau_{ri}}\right)} \quad (4.115)$$

The function  $G(t)$  is the *normalized relaxation function*. As mentioned in the preceding section, other forms of the relaxation function  $G(t)$  can also be considered.

**Example 4.9**

In order to provide a proof of Equation 114, one can use Equation 107 to define the elements of the second-order tensor  $\bar{\mathbf{C}}_r$ , as

$$(\bar{\mathbf{C}}_r)_{ij} = J^{-\frac{2}{3}} (\mathbf{C}_r)_{ij}$$

Therefore, one can write

$$\frac{\partial(\bar{\mathbf{C}}_r)_{kl}}{\partial(\mathbf{C}_r)_{ij}} = J^{-\frac{2}{3}} \frac{\partial(\mathbf{C}_r)_{kl}}{\partial(\mathbf{C}_r)_{ij}} - \frac{2}{3} J^{-\frac{5}{3}} (\mathbf{C}_r)_{kl} \frac{\partial J}{\partial(\mathbf{C}_r)_{ij}}$$

Using Equation 108, this equation can be written as

$$\begin{aligned} \frac{\partial(\bar{\mathbf{C}}_r)_{kl}}{\partial(\mathbf{C}_r)_{ij}} &= J^{-\frac{2}{3}} \frac{\partial(\bar{\mathbf{C}}_r)_{kl}}{\partial(\mathbf{C}_r)_{ij}} - \frac{1}{3} J^{-\frac{2}{3}} (\mathbf{C}_r)_{kl} (\mathbf{C}_r^{-1})_{ij} \\ &= J^{-\frac{2}{3}} \left( \delta_{ki} \delta_{lj} - \frac{1}{3} (\mathbf{C}_r)_{kl} (\mathbf{C}_r^{-1})_{ij} \right) \end{aligned}$$

Because  $\partial U / \partial \boldsymbol{\varepsilon} = 2(\partial U / \partial \mathbf{C}_r)$ , the use of Equations 109 and 110 leads to

$$\boldsymbol{\sigma}_{p2} = 2 \frac{\partial U}{\partial \mathbf{C}_r} - J^{-\frac{2}{3}} \sum_{i=1}^N \mathbf{q}_i = 2 \frac{\partial U_1}{\partial J} \frac{\partial J}{\partial \mathbf{C}_r} + 2 \frac{\partial U_2}{\partial \bar{\mathbf{C}}_r} : \frac{\partial \bar{\mathbf{C}}_r}{\partial \mathbf{C}_r} - J^{-\frac{2}{3}} \sum_{i=1}^N \mathbf{q}_i$$

which, upon the use of Equation 108, can be written in indicial form as

$$\begin{aligned} (\boldsymbol{\sigma}_{p2})_{ij} &= J \frac{\partial U_1}{\partial J} (\mathbf{C}_r^{-1})_{ij} + 2 \sum_{k,l=1}^3 \left\{ \frac{\partial U_2}{\partial(\bar{\mathbf{C}}_r)_{kl}} J^{-\frac{2}{3}} \left( \delta_{ki} \delta_{lj} - \frac{1}{3} (\mathbf{C}_r)_{kl} (\mathbf{C}_r^{-1})_{ij} \right) \right\} - J^{-\frac{2}{3}} \left( \sum_{i=1}^N \mathbf{q}_i \right)_{ij} \\ &= J \frac{\partial U_1}{\partial J} (\mathbf{C}_r^{-1})_{ij} + J^{-\frac{2}{3}} \sum_{k,l=1}^3 \left( 2 \frac{\partial U_2}{\partial(\bar{\mathbf{C}}_r)_{ij}} - \frac{2}{3} \frac{\partial U_2}{\partial(\bar{\mathbf{C}}_r)_{kl}} (\mathbf{C}_r)_{kl} (\mathbf{C}_r^{-1})_{ij} \right) - J^{-\frac{2}{3}} \left( \sum_{i=1}^N \mathbf{q}_i \right)_{ij} \end{aligned}$$

Note that  $\left( 2\partial U_2 / \partial(\bar{\mathbf{C}}_r)_{ij} - \frac{2}{3} (\partial U_2 / \partial(\bar{\mathbf{C}}_r)_{kl}) (\mathbf{C}_r)_{kl} (\mathbf{C}_r^{-1})_{ij} \right)$  gives the notion of “deviatoric” stress tensor in the reference configuration, as  $\mathbf{S}_{p2}$  defines the deviatoric part of the second Piola–Kirchhoff stress tensor  $\boldsymbol{\sigma}_{p2}$ . This can be demonstrated by writing

$$\begin{aligned} \left( 2 \frac{\partial U_2}{\partial \bar{\mathbf{C}}_r} - \frac{1}{3} \left( 2 \frac{\partial U_2}{\partial \bar{\mathbf{C}}_r} : \mathbf{C}_r \right) \mathbf{C}_r^{-1} \right) : \mathbf{C}_r &= 2 \frac{\partial U_2}{\partial \bar{\mathbf{C}}_r} : \mathbf{C}_r - \frac{1}{3} \left( 2 \frac{\partial U_2}{\partial \bar{\mathbf{C}}_r} : \mathbf{C}_r \right) \mathbf{C}_r^{-1} : \mathbf{C}_r \\ &= 2 \frac{\partial U_2}{\partial \bar{\mathbf{C}}_r} : \mathbf{C}_r - \frac{1}{3} \left( 2 \frac{\partial U_2}{\partial \bar{\mathbf{C}}_r} : \mathbf{C}_r \right) (3) = 0 \end{aligned}$$

where the fact that  $\mathbf{C}_r$  and its inverse are symmetric is utilized. Therefore, one can assume that the equation for  $\boldsymbol{\sigma}_{p2}$  can be written as

$$\boldsymbol{\sigma}_{p2} = J \frac{\partial U_1}{\partial J} \mathbf{C}_r^{-1} + J^{-\frac{2}{3}} \text{dev} \left( 2 \frac{\partial U_2}{\partial \bar{\mathbf{C}}_r} \right) - J^{-\frac{2}{3}} \sum_{i=1}^N \mathbf{q}_i$$

Integrating Equation 113 by parts, one obtains

$$\mathbf{q}_i = \gamma_i \left( \text{dev} \left( 2 \frac{\partial U_2}{\partial \bar{\mathbf{C}}_r} \right) - \int_{-\infty}^t e^{-\frac{(t-\tau)}{\tau_{ri}}} \frac{d}{d\tau} \left( \text{dev} \left( 2 \frac{\partial U_2}{\partial \bar{\mathbf{C}}_r} \right) \right) d\tau \right)$$

Substituting this into the equation for  $\boldsymbol{\sigma}_{p2}$ , one obtains

$$\begin{aligned} \boldsymbol{\sigma}_{p2} &= J \frac{\partial U_1}{\partial J} \mathbf{C}_r^{-1} + J^{-\frac{2}{3}} \left( 1 - \sum_{i=1}^N \gamma_i \right) \text{dev} \left( 2 \frac{\partial U_2}{\partial \bar{\mathbf{C}}_r} \right) \\ &\quad + J^{-\frac{2}{3}} \sum_{i=1}^N \int_{-\infty}^t \gamma_i e^{-\frac{(t-\tau)}{\tau_{ri}}} \frac{d}{d\tau} \left( \text{dev} \left( 2 \frac{\partial U_2}{\partial \bar{\mathbf{C}}_r} \right) \right) d\tau \\ &= J \frac{\partial U_1}{\partial J} \mathbf{C}_r^{-1} + J^{-\frac{2}{3}} \left( \gamma_p \text{dev} \left( 2 \frac{\partial U_2}{\partial \bar{\mathbf{C}}_r} \right) + \sum_{i=1}^N \int_{-\infty}^t \gamma_i e^{-\frac{(t-\tau)}{\tau_{ri}}} \frac{d}{d\tau} \left( \text{dev} \left( 2 \frac{\partial U_2}{\partial \bar{\mathbf{C}}_r} \right) \right) d\tau \right) \end{aligned}$$

One can also write

$$\text{dev} \left( 2 \frac{\partial U_2}{\partial \bar{\mathbf{C}}_r} \right) = \int_{-\infty}^t \frac{d}{d\tau} \left( \text{dev} \left( 2 \frac{\partial U_2}{\partial \bar{\mathbf{C}}_r} \right) \right) d\tau$$

Using the preceding two equations, one obtains

$$\boldsymbol{\sigma}_{p2} = J \frac{\partial U_1}{\partial J} \mathbf{C}_r^{-1} + J^{-\frac{2}{3}} \sum_{i=1}^N \int_{-\infty}^t \left( \gamma_p + \gamma_i e^{-\frac{(t-\tau)}{\tau_{ri}}} \right) \frac{d}{d\tau} \left( \text{dev} \left( 2 \frac{\partial U_2}{\partial \bar{\mathbf{C}}_r} \right) \right) d\tau$$

which can be written as

$$\boldsymbol{\sigma}_{p2} = J \frac{\partial U_1}{\partial J} \mathbf{C}_r^{-1} + J^{-\frac{2}{3}} \int_{-\infty}^t G(t-\tau) \frac{d}{d\tau} \left( \text{dev} \left( 2 \frac{\partial U_2}{\partial \bar{\mathbf{C}}_r} \right) \right) d\tau$$

where  $G(t-\tau)$  is defined by Equation 115.

### Another Model

Another formulation that is based on the *Maxwell model* and presented in Belytschko et al. (2000) is discussed in the remainder of this section. In this model, it is assumed that the second Piola–Kirchhoff stresses, in the case of the nonlinear viscoelastic model, are related to the Green–Lagrange strains using the following constitutive model:

$$\boldsymbol{\sigma}_{P2}(t) = \int_{-\infty}^t \mathbf{R}(t, \tau, \boldsymbol{\varepsilon}) : \frac{d\boldsymbol{\varepsilon}(\tau)}{d\tau} d\tau \quad (4.116)$$

where  $\mathbf{R}$  is the tensor of relaxation functions. One form of the tensor  $\mathbf{R}$  motivated by the model presented in the preceding section and is considered as a specialization to the generalized Maxwell model that consists of  $n_v$  Maxwell elements connected in parallel is in terms of *Prony series* given as

$$\mathbf{R}(t, \tau, \boldsymbol{\varepsilon}) = \sum_{k=1}^{n_v} \mathbf{G}_K(\boldsymbol{\varepsilon}(\tau)) \mathbf{e}^{-(t-\tau)/\tau_{rk}} \quad (4.117)$$

The hyperelastic model can be obtained using the constitutive model presented in this section by setting  $\tau_{rk}$  equal to infinity. Note also that by differentiating the constitutive equation presented in this section, one obtains

$$(\dot{\boldsymbol{\sigma}}_{P2})_k + \frac{(\boldsymbol{\sigma}_{P2})_k}{\tau_{rk}} = \mathbf{G}_k : \dot{\boldsymbol{\varepsilon}} \quad (4.118)$$

where  $\boldsymbol{\sigma}_{P2} = \sum_{k=1}^{n_v} (\boldsymbol{\sigma}_{P2})_k$  and  $(\boldsymbol{\sigma}_{P2})_k$  are called the partial stresses. The preceding equation shows that the model presented in this section for nonlinear viscoelasticity can be considered as a series of parallel connections of Maxwell elements.

#### Example 4.10

In order to prove the constitutive relation of Equation 118, the following basic calculus identity is used (Kaplan, 1991):

$$\frac{d}{dt} \int_a^t f(t, \tau) d\tau = \frac{1}{(t-a)} \int_a^t \left[ (t-a) \frac{\partial}{\partial t} f(t, \tau) + (\tau-a) \frac{\partial}{\partial \tau} f(t, \tau) + f(t, \tau) \right] d\tau$$

where  $f(t, \tau)$  is an arbitrary function and  $a$  is a constant. Using Equations 116 and 117, one can write, for each series of the Maxwell elements, which are connected in parallel, the following stress equation:

$$(\boldsymbol{\sigma}_{P2})_k = \int_{-\infty}^t e^{-\frac{(t-\tau)}{\tau_{rk}}} \mathbf{G}_k(\boldsymbol{\varepsilon}(\tau)) : \frac{d\boldsymbol{\varepsilon}(\tau)}{d\tau} d\tau$$

Therefore,

$$(\dot{\mathbf{\sigma}}_{P2})_k = \frac{d}{dt} \int_{-\infty}^t e^{-\frac{(t-\tau)}{\tau_{rk}}} \mathbf{G}_k(\mathbf{\varepsilon}(\tau)) : \frac{d\mathbf{\varepsilon}(\tau)}{d\tau} d\tau$$

Using the calculus identity presented at the beginning of the example,  $(\dot{\mathbf{\sigma}}_{P2})_k$  can be written as

$$\begin{aligned} (\dot{\mathbf{\sigma}}_{P2})_k &= \frac{1}{(t-a)} \int_a^t (t-a) \frac{\partial}{\partial t} \left( e^{-\frac{(t-\tau)}{\tau_{rk}}} \mathbf{G}_k(\mathbf{\varepsilon}(\tau)) : \frac{d\mathbf{\varepsilon}(\tau)}{d\tau} \right) d\tau \\ &\quad + \frac{1}{(t-a)} \int_a^t (\tau-a) \frac{\partial}{\partial \tau} \left( e^{-\frac{(t-\tau)}{\tau_{rk}}} \mathbf{G}_k(\mathbf{\varepsilon}(\tau)) : \frac{d\mathbf{\varepsilon}(\tau)}{d\tau} \right) d\tau \\ &\quad + \frac{1}{(t-a)} \int_a^t \left( e^{-\frac{(t-\tau)}{\tau_{rk}}} \mathbf{G}_k(\mathbf{\varepsilon}(\tau)) : \frac{d\mathbf{\varepsilon}(\tau)}{d\tau} \right) d\tau \end{aligned}$$

where  $a \rightarrow -\infty$ . This equation can be written as

$$\begin{aligned} (\dot{\mathbf{\sigma}}_{P2})_k &= -\frac{1}{\tau_{rk}} \int_a^t \left( e^{-\frac{(t-\tau)}{\tau_{rk}}} \mathbf{G}_k(\mathbf{\varepsilon}(\tau)) : \frac{d\mathbf{\varepsilon}(\tau)}{d\tau} \right) d\tau \\ &\quad + \frac{1}{(t-a)} \int_a^t (\tau-a) \frac{\partial}{\partial \tau} \left( e^{-\frac{(t-\tau)}{\tau_{rk}}} \mathbf{G}_k(\mathbf{\varepsilon}(\tau)) : \frac{d\mathbf{\varepsilon}(\tau)}{d\tau} \right) d\tau \\ &\quad + \frac{1}{(t-a)} \int_a^t \left( e^{-\frac{(t-\tau)}{\tau_{rk}}} \mathbf{G}_k(\mathbf{\varepsilon}(\tau)) : \frac{d\mathbf{\varepsilon}(\tau)}{d\tau} \right) d\tau \end{aligned}$$

or equivalently

$$\begin{aligned} (\dot{\mathbf{\sigma}}_{P2})_k &= -\frac{(\mathbf{\sigma}_{P2})_k}{\tau_{rk}} + \frac{1}{(t-a)} \int_a^t (\tau-a) \frac{\partial}{\partial \tau} \left( e^{-\frac{(t-\tau)}{\tau_{rk}}} \mathbf{G}_k(\mathbf{\varepsilon}(\tau)) : \frac{d\mathbf{\varepsilon}(\tau)}{d\tau} \right) d\tau \\ &\quad + \frac{1}{(t-a)} \int_a^t \left( e^{-\frac{(t-\tau)}{\tau_{rk}}} \mathbf{G}_k(\mathbf{\varepsilon}(\tau)) : \frac{d\mathbf{\varepsilon}(\tau)}{d\tau} \right) d\tau \end{aligned}$$

Because  $a \rightarrow -\infty$ , the last term in the previous equation is equal to zero. Therefore, one can write

$$(\dot{\mathbf{\sigma}}_{P2})_k = -\frac{(\mathbf{\sigma}_{P2})_k}{\tau_{rk}} + \frac{1}{(t-a)} \int_a^t (\tau-a) \frac{\partial}{\partial \tau} \left( e^{-\frac{(t-\tau)}{\tau_{rk}}} \mathbf{G}_k(\mathbf{\varepsilon}(\tau)) : \frac{d\mathbf{\varepsilon}(\tau)}{d\tau} \right) d\tau$$

The limit of last term in this equation when  $a \rightarrow -\infty$  is

$$\begin{aligned} \frac{1}{(t-a)} \int_a^t (\tau-a) \frac{\partial}{\partial \tau} \left( e^{-\frac{(t-\tau)}{\tau_{rk}}} \mathbf{G}_k(\mathbf{e}(\tau)) : \frac{d\mathbf{e}(\tau)}{d\tau} \right) d\tau &= \int_a^t \frac{\partial}{\partial \tau} \left( e^{-\frac{(t-\tau)}{\tau_{rk}}} \mathbf{G}_k(\mathbf{e}(\tau)) : \frac{d\mathbf{e}(\tau)}{d\tau} \right) d\tau \\ &= \left[ e^{-\frac{(t-\tau)}{\tau_{rk}}} \mathbf{G}_k(\mathbf{e}(\tau)) : \frac{d\mathbf{e}(\tau)}{d\tau} \right]_{\tau=-\infty}^{\tau=t} \\ &= \mathbf{G}_k(\mathbf{e}(t)) : \frac{d\mathbf{e}(t)}{dt} = \mathbf{G}_k(\mathbf{e}(t)) : \dot{\mathbf{e}}(t) \end{aligned}$$

Combining the last two equations one can write

$$(\dot{\mathbf{S}}_{P2})_k + \frac{(\mathbf{S}_{P2})_k}{\tau_{rk}} = \mathbf{G}_k : \dot{\mathbf{e}}$$

which is the constitutive equation in the rate form given by Equation 118.

#### 4.9 A SIMPLE VISCOELASTIC MODEL FOR ISOTROPIC MATERIALS

In this section, a simple viscoelastic model for isotropic materials is presented. In this model, for simplicity, the viscoelastic response is restricted to the deviatoric stress and strains, whereas the volume change is assumed to obey linearly elastic relationship. Recall the following form of the Cauchy stress tensor developed in the preceding chapter:

$$\boldsymbol{\sigma} = \mathbf{S} + p\mathbf{I} \quad (4.119)$$

where  $\mathbf{S}$  is the stress deviator tensor and  $p$  is the *hydrostatic pressure* defined as

$$p = \frac{1}{3}(\sigma_{11} + \sigma_{22} + \sigma_{33}) = \frac{1}{3} \sum_{i=1}^3 \sigma_{ii} \quad (4.120)$$

Note that  $\text{tr}(\mathbf{S}) = 0$ , and because Cauchy stress tensor is used, the hydrostatic pressure  $p$  has a physical interpretation. As discussed in the preceding chapter, the decomposition of the Cauchy stress tensor to deviatoric and hydrostatic pressure parts can be used to obtain the following decomposition for the second Piola–Kirchhoff stress tensor:

$$\mathbf{S}_{P2} = J\mathbf{J}^{-1}\boldsymbol{\sigma}\mathbf{J}^{-1^T} = J\mathbf{J}^{-1}(\mathbf{S} + p\mathbf{I})\mathbf{J}^{-1^T} = \mathbf{S}_{P2} + pJ\mathbf{J}^{-1}\mathbf{J}^{-1^T} \quad (4.121)$$

where

$$\mathbf{S}_{P2} = J\mathbf{J}^{-1}\mathbf{S}\mathbf{J}^{-1^T} \quad (4.122)$$

The tensor  $\mathbf{S}_{P2}$  is the deviatoric components of the second Piola–Kirchhoff stress tensor. Recall that the trace of  $\mathbf{S}_{P2}$  is not necessarily equal to zero despite the fact that the trace of  $\mathbf{S}$  is equal to zero.

In a similar manner, the Green–Lagrange strain tensor can be written as follows:

$$\boldsymbol{\varepsilon} = \boldsymbol{\varepsilon}_d + \frac{1}{3}\varepsilon_t \mathbf{I} \quad (4.123)$$

where  $\boldsymbol{\varepsilon}_d$  is the strain deviator tensor and  $\varepsilon_t$  is the dilatation. In the model presented in this section, the pressure–volume relationship is assumed to be linear and is defined as

$$p = K\varepsilon_t \quad (4.124)$$

where  $K$  is the bulk modulus. A more general model than the one presented in this section can be obtained by using, in the relationships developed in the remainder of this section, the components of the Green–Lagrange strain and the second Piola–Kirchhoff stress tensors instead of the deviatoric parts.

Constitutive equations that relate the stress and strain deviators and are based on the differential form and a generalized Maxwell model that consists of  $n_v$  elements connected in series can be written as (Zienkiewicz and Taylor, 2000)

$$\mathbf{S}_{P2} = 2G \left( \mu_0 \boldsymbol{\varepsilon}_d + \sum_{k=1}^{n_v} \mu_k \mathbf{q}_k \right) \quad (4.125)$$

In this equation,  $G$  is a relaxation modulus,  $\mathbf{q}_k$ ,  $k = 1, 2, \dots, n_v$ , are dimensionless deviatoric partial strains, and  $\mu_k$  are dimensionless parameters that satisfy the following condition:

$$\sum_{k=1}^{n_v} \mu_k = 1 \quad (4.126)$$

The deviatoric partial strains are obtained by solving the following system of ordinary first-order differential equations:

$$\dot{\mathbf{q}}_k + \frac{1}{\tau_{rk}} \mathbf{q}_k = \dot{\boldsymbol{\varepsilon}}_d \quad (4.127)$$

in which  $\tau_{rk}$ ,  $k = 1, 2, \dots, n_v$ , are the relaxation times. If the state of strains is known at a given time, a simple single-step method can be used to solve the preceding equation for the partial deviatoric strains  $\mathbf{q}_k$ . The partial strains can then be substituted into the constitutive equations to determine the deviatoric stress tensor  $\mathbf{S}_{P2}$ . Because the hydrostatic pressure can be determined using the linear elastic model of Equation 124, one can obtain the elements of the second Piola–Kirchhoff stress tensor using Equation 121.

If the coefficients that appear in the equations presented in this section are nonlinear and depend on the state of stress and strain, an iterative Newton–Raphson algorithm can be used to solve for the stresses. In this case, the tangent moduli for the viscoelastic model must be determined. The tangent moduli for the viscoelastic isotropic material model discussed in this section can be found in the literature (Zienkiewicz and Taylor, 2000).

## 4.10 FLUID CONSTITUTIVE EQUATIONS

Unlike solids, fluids cannot resist shear stresses because any shear force applied to a fluid produces motion. In the case of fluids, the stress components are expressed as functions of the rate of strains. If the shear stresses are proportional to the rate of strains, one has the case of *Newtonian viscous fluid*. The constant of proportionality is the *viscosity coefficient*. If the

effect of viscosity is neglected, one has the case of *inviscid flow* in which the effect of shear is neglected. In reality, no fluid has viscosity coefficient that is equal to zero. The viscosity coefficient can be a function of the spatial coordinates, pressure, and/or temperature. A flow is called *incompressible* if the density and volume are assumed to remain constant.

Linear constitutive equations of the fluid can be assumed in the following form (Spencer, 1980):

$$\boldsymbol{\sigma} = -p(\rho, T)\mathbf{I} + \mathbf{E} : \mathbf{D} \quad (4.128)$$

In this equation,  $\rho$  is the mass density,  $T$  is the temperature,  $\mathbf{D}$  is the rate of deformation tensor,  $p$  is the hydrostatic pressure, and  $\mathbf{E}$  is the fourth-order tensor of viscosity coefficients. The preceding equation states that in the case of fluid motion, all the stresses are linear functions of the components of the rate of deformation tensor. The normal stresses in particular are equal to the hydrostatic pressure plus terms that depend linearly on the components of the rate of deformation tensor.

If the fluid is assumed to be *isotropic*, one can use an argument similar to the one made in the case of solids to derive the fluid constitutive equations. In this case, one can write the following fluid constitutive equations (Spencer, 1980):

$$\boldsymbol{\sigma} = \{-p(\rho, T) + \lambda(\rho, T)\text{tr}(\mathbf{D})\}\mathbf{I} + 2\mu(\rho, T)\mathbf{D} \quad (4.129)$$

where  $\lambda$  and  $\mu$  are viscosity coefficients that depend on the fluid density and temperature. These viscosity coefficients are different from Lamé's constants previously introduced in this chapter. It is clear from the preceding equation that if the velocity gradients are equal to zero, the shear stresses are equal to zero, and the normal stress components reduce to the hydrostatic pressure  $p$ . In the preceding equation,  $\mu$  is the *coefficient of shear viscosity* and  $(\lambda + (2/3)\mu)$  is called the *coefficient of bulk viscosity*. If  $\lambda + (2/3)\mu = 0$ , one has the *Stokes' relation*.

The relationship between the stress components and the rate of strains must be invariant under coordinate transformations. Recall that the rate of deformation tensor satisfies the objectivity requirement when it is used with a proper stress measure, which in this case is the Cauchy stress tensor  $\boldsymbol{\sigma}$ , because  $\boldsymbol{\sigma} : \mathbf{L} = \boldsymbol{\sigma} : \mathbf{D}$ , as shown in the preceding chapter. Using this fact, one can show that the fluid constitutive equations presented in this section are invariant under an arbitrary rigid-body motion. It can be shown that isotropy follows from Equation 128 and the requirement that the stresses must be selected to satisfy the objectivity requirement. Therefore, one does not need to introduce the isotropy as a separate assumption (Spencer, 1980).

For *incompressible fluids*,  $\text{tr}(\mathbf{D}) = 0$ . In this special case, the mass density  $\rho$  is constant and Equation 129 reduces to

$$\boldsymbol{\sigma} = -p(T)\mathbf{I} + 2\mu(T)\mathbf{D} \quad (4.130)$$

In principle, as previously discussed, the incompressibility condition must be introduced using algebraic constraint equations imposed on the deformation in order to ensure that the volume remains unchanged throughout the fluid motion. The algebraic equations must be solved simultaneously with the dynamic equations of motion of the fluid. Introducing an incompressibility algebraic constraint equation, as previously mentioned, leads to a constraint force (stress reaction) that can be used to determine the hydrostatic pressure, which enters into the formulation of the constitutive equations. This constraint force can be expressed in terms of a Lagrange multiplier. Note that in the preceding equation the hydrostatic pressure and the viscosity coefficient depend only on the temperature  $T$ . A fluid that is incompressible and inviscid is called an *ideal fluid*. In this special case, there are no constitutive equations required and the stresses can be determined by simply using the equations  $\boldsymbol{\sigma} = -p\mathbf{I}$ .



#### 4.11 NAVIER–STOKES EQUATIONS

In order to obtain the fluid equations of motion, the fluid constitutive equations can be used to define the stresses, which in turn can be substituted into the partial differential equations of equilibrium obtained in the preceding chapter. This leads to the well-known *Navier–Stokes equations* (White, 2003). In the case of incompressible fluid, the incompressibility algebraic equations must be added to the Navier–Stokes equations in order to ensure that the fluid volume remains unchanged. In the preceding chapter, it was shown that the dynamic equations of equilibrium in the case of a symmetric stress tensor are given by

$$(\nabla \boldsymbol{\sigma})^T + \mathbf{f}_b - \rho \mathbf{a} = \mathbf{0} \quad (4.131)$$

where  $\boldsymbol{\sigma}$  is the stress tensor,  $\mathbf{f}_b$  is the vector of the body forces,  $\rho$  is the mass density, and  $\mathbf{a}$  is the vector of absolute acceleration of the material points. The variables in the preceding equation are defined in the current configuration. Using the definition of the stress given for *isotropic materials* by Equation 129, one can write

$$\nabla \boldsymbol{\sigma} = -\nabla(p\mathbf{I}) + \nabla(\lambda \text{tr}(\mathbf{D})\mathbf{I}) + \nabla(2\mu\mathbf{D}) \quad (4.132)$$

Substituting this equation into Equation 131, one obtains

$$\rho \mathbf{a} = \mathbf{f}_b + \{-\nabla(p\mathbf{I}) + \nabla(\lambda \text{tr}(\mathbf{D})\mathbf{I}) + \nabla(2\mu\mathbf{D})\}^T \quad (4.133)$$

If the fluid is assumed to be Newtonian, the preceding equation leads to

$$\rho \mathbf{a} = \mathbf{f}_b + \{-\nabla(p\mathbf{I}) + \lambda \nabla(\text{tr}(\mathbf{D})\mathbf{I}) + 2\mu \nabla \mathbf{D}\}^T \quad (4.134)$$

This equation is known as the Navier–Stokes equations.

For an *incompressible fluid*,  $\text{tr}(\mathbf{D}) = 0$ , the preceding equation reduces to

$$\rho \mathbf{a} = \mathbf{f}_b + \{-\nabla(p\mathbf{I}) + \nabla(2\mu\mathbf{D})\}^T \quad (4.135)$$

The ratio  $\alpha_1 = \mu/\rho$  is known as the *kinematic viscosity*. If the Stokes' relation is assumed, one has  $\alpha_1 + \alpha_2 = \alpha_1/3$ , where  $\alpha_1 = \lambda/\rho$ .

In order to solve the Navier–Stokes equations, the boundary conditions must be defined. In general, the viscous fluid is assumed to stick to the boundaries such that the fluid has the boundary velocities in the regions of contact. If the boundary is stationary, the viscous fluid is assumed to have zero velocity at the boundary. In the case of inviscid fluid, the fluid can have a tangential velocity at the boundary, whereas the normal component of the velocity is assumed to be zero.

#### PROBLEMS

1. Write explicitly all the conditions of the material symmetry that lead to Equation 22.
2. In the case of *plane stress*,  $\sigma_{33} = \sigma_{13} = \sigma_{23} = 0$ . Derive the constitutive equation in this plane stress case.
3. In the case of *plane strains*,  $\epsilon_{33} = \epsilon_{13} = \epsilon_{23} = 0$ . Derive the constitutive equation in this case of plane strains.

4. Let  $I_1$ ,  $I_2$ , and  $I_3$  be the invariants of the right Cauchy–Green strain tensor  $\mathbf{C}_r$ . Show that  $\partial I_1 / \partial \mathbf{C}_r = \mathbf{I}$ ,  $\partial I_2 / \partial \mathbf{C}_r = I_1 \mathbf{I} - \mathbf{C}_r^T$ ,  $\partial I_3 / \partial \mathbf{C}_r = I_3 \mathbf{C}_r^{-1T}$ .
5. For the Neo–Hookean material model presented in this chapter, show that the second Piola–Kirchhoff stress tensor is given as  $\boldsymbol{\sigma}_{P2} = \mu(\mathbf{I} - \mathbf{C}_r^{-1}) + \lambda(\ln J)\mathbf{C}_r^{-1}$ , where  $\lambda$  and  $\mu$  are Lamé’s constants and  $\mathbf{C}_r$  is the right Cauchy–Green deformation tensor.
6. For the Neo–Hookean material model presented in this chapter, show that the Kirchhoff stress tensor is given as  $\boldsymbol{\sigma}_K = \mu(\mathbf{C}_l - \mathbf{I}) + \lambda(\ln J)\mathbf{I}$ , where  $\lambda$  and  $\mu$  are Lamé’s constants and  $\mathbf{C}_l$  is the left Cauchy–Green deformation tensor.
7. Show that the fourth-order tensor of the elastic coefficients for the Neo–Hookean material model presented in this chapter is given as  $\mathbf{E} = \lambda_h \mathbf{C}_r^{-1} \otimes \mathbf{C}_r^{-1} - 2\mu_h (\partial \mathbf{C}_r^{-1} / \partial \mathbf{C}_r)$ , where  $\mathbf{C}_r$  is the right Cauchy–Green deformation tensor, and  $\lambda_h$  and  $\mu_h$  are the coefficients defined in this chapter.
8. Show that the creep function for the one-dimensional standard viscoelastic model is given by  $K = (1/E_p)\{1 - (E_s/E_t)e^{-(E_p/\tau_r E_t)t}\}$ , where the coefficients that appear in this equation are defined in Section 7.
9. Obtain the constitutive equations for the simple one-dimensional viscoelastic Maxwell model.
10. Derive a more general viscoelastic model for isotropic materials than the one presented in Section 9 by using, in the relationships developed in Section 9, the components of the Green–Lagrange strain and the second Piola–Kirchhoff stress tensors instead of their deviatoric parts.



# FINITE ELEMENT FORMULATION: LARGE-DEFORMATION, LARGE-ROTATION PROBLEM

---

In the preceding chapters, the general nonlinear continuum mechanics theory was presented. In order to make use of this theory in many practical applications, a finite dimensional model must be developed. In this model, the partial differential equations of equilibrium are written using approximation methods as a finite set of ordinary differential equations. One of the most popular approximation methods that can be used to achieve this goal is the *finite element method*. In this method, the spatial domain of the body is divided into small regions called *elements*. Each element has a set of nodes, called *nodal points*, that are used to connect this element with other elements used in the discretization of the body. The displacement of the material points of an element is approximated using a set of shape functions and the displacements of the nodes and possibly their derivatives with respect to the spatial coordinates. In this case, the dimension of the problem depends on the number of nodes and number and type of the nodal coordinates used.

### Small- and Large-Deformation Problems

In the literature, there are many finite element formulations that are developed for the deformation analysis of mechanical, aerospace, structural, and biological systems. Some of these formulations are developed for small-deformation and small-rotation linear problems, some for large-deformation and large-rotation nonlinear analysis, and the others for large-rotation and small-deformation nonlinear problems. Several numerical solution procedures and computational algorithms are also proposed for solving the resulting system of finite element differential equations.

The following chapter is devoted to the important nonlinear problem of small deformation and large rotation of flexible bodies, which is typical of multibody system (MBS) applications. In the case of small deformations, one can use more efficient formulations that employ smaller number of coordinates. These formulations, as will be discussed in the following chapter, allow for filtering out complex deformation shapes associated with high-frequency modes of oscillations while ensuring correct description of arbitrary rigid-body displacements. To this end, the concept of the *intermediate element coordinate system* will be introduced. The treatment of the more general problem of large deformation and large rotation, on the other hand, does not allow for such an efficient use of the techniques of coordinate reduction because the shape of deformations can be very complex and higher-order models are required in order to be able to capture the details of the deformation shapes. Nonetheless, in many large-deformation applications, one deals with softer materials that do not exhibit high-frequency oscillations, and for this reason, large-deformation formulations can be efficiently used.

### Absolute Nodal Coordinate Formulation (ANCF)

In this chapter, a more general large-rotation and large-deformation finite element formulation is discussed. This formulation, which is called the *absolute nodal coordinate formulation* (ANCF), imposes no restrictions on the amount of rotation or deformation within the finite element. In addition to its simplicity and its consistency with the nonlinear theory of continuum mechanics, the absolute nodal coordinate formulation has several advantages as compared to other large-rotation and large-deformation finite element formulations that exist in the literature. This formulation leads to a constant mass matrix and zero centrifugal and Coriolis forces; allows for the use of general constitutive models in case of beams, plates, and shells; and accounts for the dynamic coupling between the rigid-body motion and the elastic deformation.

There are three conditions that must be met in order to have the absolute nodal coordinate formulation discussed in this chapter. First, the problem under investigation must be a dynamic problem in order to address the formulation of the inertia forces. Second, *consistent mass formulation* must be used because lumped mass formulations do not lead to a correct representation of the rigid-body dynamics (Shabana, 2013). Third, global gradients or slopes obtained by differentiation of absolute position vectors with respect to the spatial coordinates are used as nodal coordinates in order to ensure continuity of rotation parameters. The latter requirement is particularly important when finite elements are assembled. In the assembly process, proper gradient transformation must be used instead of the vector transformation often used in the finite element literature. Gradients are tangent to coordinate lines, and therefore, for two gradient vectors to be equal they must be tangent to the same coordinate line. Understanding the concept of gradients is crucial in the ANCF implementation, particularly when discontinuities or initially curved structures are considered. Using ANCF finite elements one can develop a nonincremental solution procedure for solving large-deformation problems.

### Chapter Organization

This chapter is organized as follows. In Section 1, the displacement field and coordinates of the finite element are defined. In Section 2, the element connectivity conditions are introduced. In Section 3, the finite element inertia and elastic forces are formulated, whereas in Section 4 the virtual work of the inertia and elastic forces of the element is used to formulate the virtual work expression of the equations of motion of the finite element. This virtual work expression

is used to obtain the equations of motion of the deformable body by assembling the equations of its finite elements. Because ANCF finite elements leads to a nonlinear expression of the elastic forces, one must resort in general to evaluate numerically the integrals of these elastic forces, as discussed in Section 5. In Section 6, the basic differential geometry theories of curves and surfaces are briefly reviewed in order to help the reader better understand the modes of deformations of beams, plates, and shells. In Sections 7–13, several examples of two- and three-dimensional finite element shape functions are presented, and the procedures for formulating the elastic forces of these elements are outlined. In Section 14, the performance of the finite elements is discussed, including topics such as the *patch test*, *shear*, *membrane*, and *volumetric locking*; and *reduced* and *selective integrations*. In Section 15, other large-deformation finite element formulations used in the literature are discussed and compared with the ANCF presented in more detail in this chapter. The formulations of the dynamic equations obtained using the *updated Lagrangian* and *Eulerian* approaches are compared in Section 16.

## 5.1 DISPLACEMENT FIELD

In the finite element method, as previously pointed out, the domain of the body is divided into small regions called *elements*. Assuming that these elements are small, one can use low-order polynomials to describe the displacement field of the element. For example, if the deformation of the body is negligible or small, only six coordinates are sufficient to define the rigid-body translation and rotation. In this special case, first-order polynomials can be used to describe exactly the rigid-body motion. For a small finite element on a deformable body, on the other hand, the deformation within the element can be in general much smaller than the overall deformation of the body, and therefore, one can still justify using a lower-order polynomial to describe the displacement of a small region on the body. After introducing the low-order polynomials to define the equations of motion of the finite elements, the body equations of motion can be obtained by assembling the equations of motion of its elements using the connectivity conditions at the finite element boundaries. By using this procedure, one can develop a powerful tool for the computer-aided analysis of structural components that have complex geometric shapes.

### Separation of Variables

Finite element approximations are based on the concept of the *separation of variables* briefly introduced in Chapter 1 and used in the examples presented in several chapters of this book. The displacement of the finite element can be written as the product of two sets of functions: one set depends on the spatial coordinates, whereas the other set depends on time only. The separation of variables can conveniently be achieved by assuming that the position vector of arbitrary material points on the element can be written as polynomials of the spatial local coordinates of the element. The coefficients of these polynomials in the case of dynamics are the time-dependent variables. One can select points on the element, called *nodes*, and assign variables such as displacements, rotations, and slopes as *nodal coordinates*. Knowing the coordinates of these nodes in the reference configuration, one can write a set of algebraic equations using the assumed polynomial displacement field and determine the polynomial coefficients in terms of the nodal variables. In the formulation discussed in this section, all the components of the position vector are interpolated using polynomials that have the same

order. For example, for a given domain defined by the spatial coordinates  $x_1$ ,  $x_2$ , and  $x_3$ , the  $k$ th component of the position vector can be written as

$$r_k = a_{0k} + a_{1k}x_1 + a_{2k}x_2 + a_{3k}x_3 + a_{4k}x_1^2 + a_{5k}x_2^2 + \cdots, \quad k = 1, 2, 3 \quad (5.1)$$

The coefficients  $a_{ik}$ ,  $i = 0, 1, 2, 3, \dots$ , in the case of dynamics, are assumed to depend only on time. In this case, the above assumed displacement field can be written as the product of functions that depend only on the spatial coordinates  $\mathbf{x} = [x_1 \ x_2 \ x_3]^T$  and a vector of time-dependent coordinates. To see this separation of variables, the preceding equation can be written as

$$r_k = \begin{bmatrix} 1 & x_1 & x_2 & x_3 & x_1^2 & x_2^2 & \dots \end{bmatrix} \begin{bmatrix} a_{0k} \\ a_{1k} \\ a_{2k} \\ a_{3k} \\ a_{4k} \\ a_{5k} \\ \vdots \end{bmatrix}, \quad k = 1, 2, 3 \quad (5.2)$$

Denoting the space-dependent row in this equation as  $\mathbf{P}_k(\mathbf{x})$  and the time-dependent vector as  $\mathbf{a}_k(t)$ , the preceding equation can be written as

$$r_k = \mathbf{P}_k(\mathbf{x})\mathbf{a}_k(t), \quad k = 1, 2, 3 \quad (5.3)$$

where

$$\mathbf{P}_k(\mathbf{x}) = \begin{bmatrix} 1 & x_1 & x_2 & x_3 & x_1^2 & x_2^2 & \dots \end{bmatrix}, \quad \mathbf{a}_k(t) = \begin{bmatrix} a_{0k} \\ a_{1k} \\ a_{2k} \\ a_{3k} \\ a_{4k} \\ a_{5k} \\ \vdots \end{bmatrix} \quad (5.4)$$

One can select, as discussed in Chapter 1 and demonstrated by the examples presented at the end of this section, position coordinates and possibly spatial derivatives of the coordinates at selected points and write the coefficients  $\mathbf{a}_k(t)$  in terms of these position coordinates and their derivatives. The number of the selected position coordinates and their derivatives must be equal to the number of the polynomial coefficients in order to have a number of algebraic equations, which can be solved for these coefficients. Let  $\mathbf{e}$  be the vector of coordinates that may include position coordinates and their spatial derivatives at selected points at known local positions on the element. Substituting the values of the spatial coordinates in the preceding equation, one can write the following relationship between the selected coordinates and the coefficients of the polynomial:

$$\mathbf{e}(t) = \mathbf{B}_p \mathbf{a}(t) \quad (5.5)$$

where  $\mathbf{B}_p$  is a constant square nonsingular matrix and  $\mathbf{a}$  is the total vector of the polynomial coefficients. The preceding equation can be solved for the coefficients  $\mathbf{a}$  in terms of the selected

coordinates as  $\mathbf{a}(t) = \mathbf{B}_p^{-1} \mathbf{e}(t)$ . Substituting this equation into the assumed displacement field of Equation 3, one can write the displacement field in terms of the selected coordinates as

$$\begin{aligned} \mathbf{r}(\mathbf{x}, t) &= \begin{bmatrix} r_1 \\ r_2 \\ r_3 \end{bmatrix} = \begin{bmatrix} \mathbf{P}_1 \mathbf{a}_1 \\ \mathbf{P}_2 \mathbf{a}_2 \\ \mathbf{P}_3 \mathbf{a}_3 \end{bmatrix} = \begin{bmatrix} \mathbf{P}_1 & \mathbf{0} & \mathbf{0} \\ \mathbf{0} & \mathbf{P}_2 & \mathbf{0} \\ \mathbf{0} & \mathbf{0} & \mathbf{P}_3 \end{bmatrix} \begin{bmatrix} \mathbf{a}_1 \\ \mathbf{a}_2 \\ \mathbf{a}_3 \end{bmatrix} \\ &= \mathbf{P}(\mathbf{x}) \mathbf{a}(t) = \mathbf{P}(\mathbf{x}) \mathbf{B}_p^{-1} \mathbf{e}(t) \end{aligned} \quad (5.6)$$

In this equation,

$$\mathbf{P}(\mathbf{x}) = \begin{bmatrix} \mathbf{P}_1 & \mathbf{0} & \mathbf{0} \\ \mathbf{0} & \mathbf{P}_2 & \mathbf{0} \\ \mathbf{0} & \mathbf{0} & \mathbf{P}_3 \end{bmatrix}, \quad \mathbf{a}(t) = \begin{bmatrix} \mathbf{a}_1(t) \\ \mathbf{a}_2(t) \\ \mathbf{a}_3(t) \end{bmatrix} \quad (5.7)$$

One, therefore, can write the position vector  $\mathbf{r}$  using Equation 6 as

$$\mathbf{r}(\mathbf{x}, t) = \mathbf{S}(\mathbf{x}) \mathbf{e}(t) \quad (5.8)$$

where  $\mathbf{S}(\mathbf{x}) = \mathbf{P}(\mathbf{x}) \mathbf{B}_p^{-1}$ . In this approach,  $\mathbf{S}(\mathbf{x})$  is called the *shape function matrix*. The position vector field can then be written as the product of the space-dependent matrix  $\mathbf{S}(\mathbf{x})$  and the vector of time-dependent coordinates  $\mathbf{e}(t)$ .

Using this approach of the separation of variables, and assuming that the continuum is divided into a number of  $n_e$  finite elements as shown in Figure 1, the displacement field of a finite element  $j$  can be written as

$$\mathbf{r}^j(\mathbf{x}^j, t) = \mathbf{S}^j \mathbf{e}^j, \quad j = 1, 2, \dots, n_e \quad (5.9)$$

where  $\mathbf{r}^j$  is the global position vector of an arbitrary point on the finite element  $j$  as shown in Figure 1,  $\mathbf{S}^j = \mathbf{S}^j(\mathbf{x}^j)$  is a *shape function matrix* that depends on the element spatial coordinates  $\mathbf{x}^j = [x_1^j \ x_2^j \ x_3^j]^T$  defined in the element reference configuration, and  $\mathbf{e}^j = \mathbf{e}^j(t)$  is the vector of time-dependent nodal coordinates that define the displacements and possibly their spatial derivatives at a set of nodal points selected for the finite element.

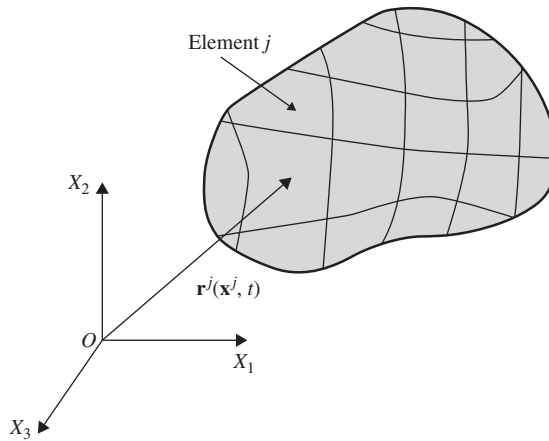


**Figure 5.1** Finite element discretization



## Modes of Displacement

The selection of the number of nodal points and the number of coordinates at each node is one of the important factors that determine the accuracy of the finite element approximation. The general theory of continuum mechanics discussed in this book shows that the matrix of position vector gradients leads to nine independent modes of displacements for an infinitesimal volume at a material point. The polar decomposition theorem shows that the matrix of position vector gradients can be decomposed as the product of an orthogonal matrix and a symmetric matrix. The orthogonal matrix is function of three independent parameters that define the rotation of the infinitesimal volume, whereas the symmetric matrix is a function of six independent deformation parameters that define the strain components. Therefore, if the translation of the infinitesimal volume is considered, one has a total of 12 displacement modes for the infinitesimal volume: 3 translations, 3 rotations, and 6 deformation modes. Motivated by this simple and general continuum mechanics description of the motion of the infinitesimal volume, the vector of nodal coordinates can be selected in the three-dimensional analysis to consist of three translations and nine components of the position vector gradients. The nine components of the position vector gradients account for three rotations and six deformation modes. In this case, the vector of nodal coordinates  $\mathbf{e}^j$  of the finite element at a node  $k$  can be written as

$$\mathbf{e}^{jk} = \left[ \mathbf{r}^{jkT} \quad \mathbf{r}_{x_1}^{jkT} \quad \mathbf{r}_{x_2}^{jkT} \quad \mathbf{r}_{x_3}^{jkT} \right]^T \quad (5.10)$$

where  $\mathbf{r}^{jk}$  is the absolute (global) position vector of the node  $k$  of the finite element  $j$  and  $\mathbf{r}_{x_l}^{jk}$  is the vector of position gradients obtained by differentiation with respect to the spatial coordinate  $x_l$ ,  $l = 1, 2, 3$ . Note that  $\mathbf{r}_x^{jk} = \mathbf{J}^{jk}$  is the matrix of the position vector gradients at node  $k$ , where  $\mathbf{x}^j = \begin{bmatrix} x_1^j & x_2^j & x_3^j \end{bmatrix}^T$ . Note also that the last three vector elements of the vector of nodal coordinates  $\mathbf{e}^{jk}$  in Equation 10 are the columns of the matrix of position vector gradients  $\mathbf{J}^{jk} = \mathbf{r}_x^{jk}$  that enters in the formulation of the strain tensors. It is important that the chosen assumed displacement field and nodal coordinates correctly describe an arbitrary displacement including rigid-body displacement. This is an essential requirement, particularly in problems in the field of MBS dynamics in which the system components may undergo finite rotations.

## Nodal Coordinates

In the finite element literature, one can find a large number of finite elements that have been developed to suit varieties of applications. Some elements take the shape of trusses, some the shape of beams, some the shape of rectangle, triangle or plate, solid (prism), tetrahedral, and many other shapes. These elements employ different numbers and types of nodal coordinates. For example, solid, triangle, rectangle, and tetrahedral elements employ, for the most part, only displacement coordinates. Rotations, slopes, or gradients are not commonly used for these elements. Conventional beam, plate, and shell elements employ, in addition to the displacement coordinates, infinitesimal rotation coordinates. Arbitrary rigid body motion, however, cannot be defined as linear functions of infinitesimal rotations. Some newer beam, plate, and shell elements use finite rotations as nodal coordinates and define a rotation field that is independent from the displacement field. Because in the general theory of continuum mechanics, the rotation field is defined from the displacement field using the matrix of position vector

gradients, the use of an independent finite rotation field can lead to coordinate redundancy, which can be a source of fundamental and numerical problem (Ding et al., 2014). Discussion on other types of finite elements and finite element formulations is presented in a later section.

In the ANCF discussed in this chapter, no infinitesimal or finite rotations are used as nodal coordinates. In this formulation, only absolute position vectors consistent with the general continuum mechanics are interpolated, and the position vector gradient field is obtained by differentiation of the position vector field with respect to the spatial coordinates of the finite element. As will be shown in this chapter, in addition to having a description consistent with the general continuum mechanics theory, the formulation discussed in this chapter has many unique features that make it suited for the analysis of large deformation and large rotation of very flexible structures.

### Example 5.1

An example of a finite element that is based on the motion description presented in this section is the three-dimensional, two-node beam element shown in Figure 2. Each node has 12 coordinates that include the 3 components of the global position vector of the node and the 9 components of the matrix of position vector gradients at the node. The element, therefore, has 24 degrees of freedom (Shabana and Yakoub, 2001; Yakoub and Shabana, 2001). Let  $x_1^j$  be the spatial coordinate along the beam element axis, and  $x_2^j$  and  $x_3^j$  be the other two spatial coordinates. Because there are 24 coordinates and in the ANCF all the components of the position vector must be interpolated using polynomials that have the same order, one can write the following interpolating polynomial for the beam element:

$$\mathbf{r}^j = \begin{bmatrix} r_1^j \\ r_2^j \\ r_3^j \end{bmatrix} = \begin{bmatrix} a_0 + a_1 x_1^j + a_2 x_2^j + a_3 x_3^j + a_4 x_1^j x_2^j + a_5 x_1^j x_3^j + a_6 (x_1^j)^2 + a_7 (x_1^j)^3 \\ b_0 + b_1 x_1^j + b_2 x_2^j + b_3 x_3^j + b_4 x_1^j x_2^j + b_5 x_1^j x_3^j + b_6 (x_1^j)^2 + b_7 (x_1^j)^3 \\ c_0 + c_1 x_1^j + c_2 x_2^j + c_3 x_3^j + c_4 x_1^j x_2^j + c_5 x_1^j x_3^j + c_6 (x_1^j)^2 + c_7 (x_1^j)^3 \end{bmatrix}$$

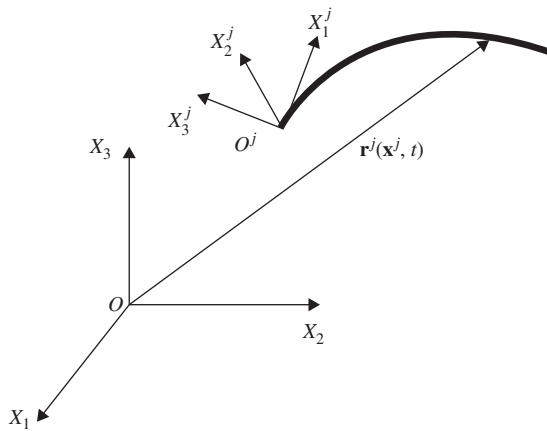


Figure 5.2 Three-dimensional beam element

In this equation,  $a_i, b_i, c_i; i = 0, 1, 2, \dots, 7$ , are the coefficients of the interpolating polynomials. Note that the interpolation in the preceding equation is cubic in  $x_1^j$  and linear in  $x_2^j$  and  $x_3^j$ . As described in this section, the 24 coefficients  $a_i, b_i, c_i; i = 0, 1, 2, \dots, 7$ , can be determined by applying the following conditions. At node 1, one has

$$\begin{aligned} \mathbf{r}^{j1} = \mathbf{r}^j(0, 0, 0) &= \begin{bmatrix} e_1 \\ e_2 \\ e_3 \end{bmatrix}, & \mathbf{r}_{x_1}^{j1} = \mathbf{r}_{x_1}^j(0, 0, 0) &= \begin{bmatrix} e_4 \\ e_5 \\ e_6 \end{bmatrix}, \\ \mathbf{r}_{x_2}^{j1} = \mathbf{r}_{x_2}^j(0, 0, 0) &= \begin{bmatrix} e_7 \\ e_8 \\ e_9 \end{bmatrix}, & \mathbf{r}_{x_3}^{j1} = \mathbf{r}_{x_3}^j(0, 0, 0) &= \begin{bmatrix} e_{10} \\ e_{11} \\ e_{12} \end{bmatrix} \end{aligned}$$

and at node 2, one has

$$\begin{aligned} \mathbf{r}^{j2} = \mathbf{r}^j(l, 0, 0) &= \begin{bmatrix} e_{13} \\ e_{14} \\ e_{15} \end{bmatrix}, & \mathbf{r}_{x_1}^{j2} = \mathbf{r}_{x_1}^j(l, 0, 0) &= \begin{bmatrix} e_{16} \\ e_{17} \\ e_{18} \end{bmatrix}, \\ \mathbf{r}_{x_2}^{j2} = \mathbf{r}_{x_2}^j(l, 0, 0) &= \begin{bmatrix} e_{19} \\ e_{20} \\ e_{21} \end{bmatrix}, & \mathbf{r}_{x_3}^{j2} = \mathbf{r}_{x_3}^j(l, 0, 0) &= \begin{bmatrix} e_{22} \\ e_{23} \\ e_{24} \end{bmatrix} \end{aligned}$$

where  $l$  is the length of the element, and  $\mathbf{r}^j = \partial \mathbf{r}^j / \partial x_i^j, i = 1, 2, 3$ . Using the conditions and the procedure described in this section, one can show that the displacement field of the element can be written as

$$\mathbf{r}^j(\mathbf{x}^j, t) = \mathbf{S}^j(\mathbf{x}^j) \mathbf{e}^j(t)$$

In this equation, the vector  $\mathbf{e}^j = [e_1 \ e_2 \ \dots \ e_{24}]^T$  is the vector of nodal coordinates as defined previously in this example, and  $\mathbf{S}^j$  is the element shape function matrix, which can be written as

$$\mathbf{S}^j = [s_1 \mathbf{I} \ s_2 \mathbf{I} \ s_3 \mathbf{I} \ s_4 \mathbf{I} \ s_5 \mathbf{I} \ s_6 \mathbf{I} \ s_7 \mathbf{I} \ s_8 \mathbf{I}]$$

where the shape functions  $s_i, i = 1, 2, \dots, 8$ , are defined as (Yakoub and Shabana, 2001)

$$\begin{aligned} s_1 &= 1 - 3\xi^2 + 2\xi^3, & s_2 &= l(\xi - 2\xi^2 + \xi^3), \\ s_3 &= l(\eta - \xi\eta), & s_4 &= l(\zeta - \xi\zeta), \\ s_5 &= 3\xi^2 - 2\xi^3, & s_6 &= l(-\xi^2 + \xi^3), \\ s_7 &= l\xi\eta, & s_8 &= l\xi\zeta \end{aligned}$$

where

$$\xi = \frac{x_1^j}{l}, \quad \eta = \frac{x_2^j}{l}, \quad \zeta = \frac{x_3^j}{l}$$

It is left to the reader as an exercise to show that the displacement field used in this example for the three-dimensional two-node beam element can describe an arbitrary rigid-body motion.

**Example 5.2**

A special case of the element presented in the preceding section is the two-dimensional, two-node beam element. In this case, each node has six coordinates: two position coordinates and four gradient components. The total number of element coordinates is then 12. Each component of the position vector field can then be approximated with a polynomial, which has six coefficients. For this planar element, the following interpolating polynomials are assumed (Omar and Shabana, 2001):

$$\mathbf{r} = \begin{bmatrix} r_1 \\ r_2 \end{bmatrix} = \begin{bmatrix} a_0 + a_1 x_1^j + a_2 x_2^j + a_3 x_1^j x_2^j + a_4 (x_1^j)^2 + a_5 (x_1^j)^3 \\ b_0 + b_1 x_1^j + b_2 x_2^j + b_3 x_1^j x_2^j + b_4 (x_1^j)^2 + b_5 (x_1^j)^3 \end{bmatrix}$$

In order to replace the polynomial coefficients with nodal variables that have physical meaning, we impose the following conditions at node 1:

$$\mathbf{r}^{j1} = \mathbf{r}^j(0, 0) = \begin{bmatrix} e_1 \\ e_2 \end{bmatrix}, \quad \mathbf{r}_{x_1}^{j1} = \mathbf{r}_{x_1}^j(0, 0) = \begin{bmatrix} e_3 \\ e_4 \end{bmatrix}, \quad \mathbf{r}_{x_2}^{j1} = \mathbf{r}_{x_2}^j(0, 0) = \begin{bmatrix} e_5 \\ e_6 \end{bmatrix}$$

and the following conditions at node 2:

$$\mathbf{r}^{j2} = \mathbf{r}^j(l, 0) = \begin{bmatrix} e_7 \\ e_8 \end{bmatrix}, \quad \mathbf{r}_{x_1}^{j2} = \mathbf{r}_{x_1}^j(l, 0) = \begin{bmatrix} e_9 \\ e_{10} \end{bmatrix}, \quad \mathbf{r}_{x_2}^{j2} = \mathbf{r}_{x_2}^j(l, 0) = \begin{bmatrix} e_{11} \\ e_{12} \end{bmatrix}$$

where  $l$  is the length of the element, and  $\mathbf{r}_{x_i}^j = \partial \mathbf{r}^j / \partial x_i^j$ ,  $i = 1, 2$ . Using the conditions and the procedure described in this section, one can show that the displacement field of the element can be written as

$$\mathbf{r}^j(\mathbf{x}^j, t) = \mathbf{S}^j(\mathbf{x}^j) \mathbf{e}^j(t)$$

In this equation, the vector  $\mathbf{e}^j = [e_1 \ e_2 \ \dots \ e_{12}]^T$  is the vector of nodal coordinates as defined previously in this example, and  $\mathbf{S}^j$  is the element shape function matrix, which can be written as

$$\mathbf{S}^j = [s_1 \mathbf{I} \quad s_2 \mathbf{I} \quad s_3 \mathbf{I} \quad s_4 \mathbf{I} \quad s_5 \mathbf{I} \quad s_6 \mathbf{I}]$$

where the shape functions  $s_i$ ,  $i = 1, 2, \dots, 6$  are defined as (Omar and Shabana, 2001)

$$\begin{aligned} s_1 &= 1 - 3\xi^2 + 2\xi^3, & s_2 &= l(\xi - 2\xi^2 + \xi^3), \\ s_3 &= l\eta(1 - \xi), & s_4 &= 3\xi^2 - 2\xi^3, \\ s_5 &= l(-\xi^2 + \xi^3), & s_6 &= l\xi\eta \end{aligned}$$

where

$$\xi = \frac{x_1^j}{l}, \quad \eta = \frac{x_2^j}{l}$$

It is also left to the reader to show that the shape function matrix and nodal coordinate vector used for the planar beam element discussed in this example can be used to describe an arbitrary rigid-body motion. Note that the displacement field used in this example is the same as the displacement field used previously in several examples presented in the preceding chapters.

## 5.2 ELEMENT CONNECTIVITY

In order to obtain the equations of motion of the continuum, the finite elements that form the continuum domain must be properly connected at the nodal points. Let the vector of nodal coordinates of all elements before connecting them be denoted as  $\mathbf{e}_b$ . This vector is then given by

$$\mathbf{e}_b = [\mathbf{e}^{1T} \mathbf{e}^{2T} \dots \mathbf{e}^{n_e T}]^T \quad (5.11)$$

where  $\mathbf{e}^j$  is the vector of nodal coordinates of the finite element  $j$  and  $n_e$  is the total number of finite elements. Let  $\mathbf{e}$  be the vector of all nodal coordinates of the continuum after the elements are connected. It is assumed that the finite element coordinates are defined in the same coordinate system as the continuum coordinates. The case in which the element nodal coordinates are defined in a coordinate system different from the continuum reference coordinate system will be also discussed. The vector of the element  $j$  coordinates can be written in terms of the nodal coordinates of the body as

$$\mathbf{e}^j = \mathbf{B}^j \mathbf{e} \quad (5.12)$$

where  $\mathbf{B}^j$  is a Boolean matrix that includes zeros and ones and maps the element coordinates to the body coordinates. If the finite elements have different orientations, which is the case of slope discontinuity, a constant transformation can be defined and can be systematically introduced into the preceding equation (Shabana and Mikkola, 2003; Shabana, 2011). In this case, one can first define the element coordinates by the vector  $\tilde{\mathbf{e}}^j$  and write this vector in terms of element nodal coordinates defined in the same coordinate system as the continuum (body) nodal coordinates, that is,  $\tilde{\mathbf{e}}^j = \mathbf{T}^j \mathbf{e}^j$ , where  $\mathbf{T}^j$  is an element transformation matrix (Shabana and Mikkola, 2003; Shabana, 2011) and  $\mathbf{e}^j$  is a vector of nodal coordinates defined in the same coordinate system as the body nodal coordinates. The Boolean matrix  $\mathbf{B}^j$  can then be used to write the vector of the element nodal coordinates in terms of the body nodal coordinates as  $\tilde{\mathbf{e}}^j = \mathbf{T}^j \mathbf{B}^j \mathbf{e}$ . In the case of using position vector gradients as nodal coordinates, a proper transformation for the gradients must be used. In the remainder of this chapter, for simplicity, we will assume that such a transformation is applied and use Equation 12 with the understanding that the element and the body nodal coordinates  $\mathbf{e}^j$  and  $\mathbf{e}$  are properly defined in the same coordinate system.

Using Equation 12, one can then write

$$\begin{bmatrix} \mathbf{e}^1 \\ \mathbf{e}^2 \\ \vdots \\ \mathbf{e}^{n_e} \end{bmatrix} = \begin{bmatrix} \mathbf{B}^1 \\ \mathbf{B}^2 \\ \vdots \\ \mathbf{B}^{n_e} \end{bmatrix} \mathbf{e} = \mathbf{B} \mathbf{e} \quad (5.13)$$

where  $\mathbf{B}$  is the Boolean matrix formed using the element Boolean matrices as

$$\mathbf{B} = \begin{bmatrix} \mathbf{B}^1 \\ \mathbf{B}^2 \\ \vdots \\ \mathbf{B}^{n_e} \end{bmatrix} \quad (5.14)$$

This matrix has a number of rows equal to the dimension of the vector  $\mathbf{e}_b$  and a number of columns equal to the dimension of the vector  $\mathbf{e}$ . This procedure of assembling the finite elements is demonstrated by the following simple example.

**Example 5.3**

Figure 3 shows two finite elements, each of which has two nodes and four nodal coordinates per node. The nodal coordinates of the two elements can then be written as

$$\mathbf{e}^1 = [e_1^1 \ e_2^1 \ e_3^1 \ e_4^1 \ e_5^1 \ e_6^1 \ e_7^1 \ e_8^1]^T$$

$$\mathbf{e}^2 = [e_1^2 \ e_2^2 \ e_3^2 \ e_4^2 \ e_5^2 \ e_6^2 \ e_7^2 \ e_8^2]^T$$

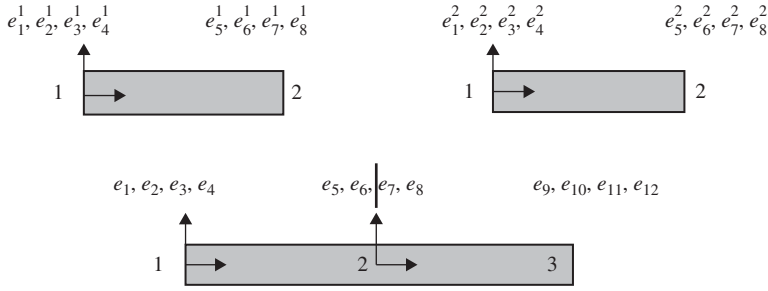


**Figure 5.3** Element connectivity

The vector  $\mathbf{e}_b$  is defined as

$$\mathbf{e}_b = [\mathbf{e}^{1T} \ \mathbf{e}^{2T}]^T$$

When the two elements are assembled as shown in Figure 3, the vector of the body (continuum) nodal coordinates  $\mathbf{e}$  can be written as

$$\mathbf{e} = [e_1 \ e_2 \ \dots \ e_{12}]^T$$

It is clear that the relationships between the element and the body coordinates that define the element connectivity can be written as

$$\mathbf{e}^1 = \mathbf{B}^1 \mathbf{e}, \quad \mathbf{e}^2 = \mathbf{B}^2 \mathbf{e}$$

where the two  $8 \times 12$  Boolean matrices  $\mathbf{B}^1$  and  $\mathbf{B}^2$  are defined as

$$\mathbf{B}^1 = \begin{bmatrix} 1 & 0 & 0 & 0 & 0 & 0 & 0 & 0 & 0 & 0 & 0 & 0 \\ 0 & 1 & 0 & 0 & 0 & 0 & 0 & 0 & 0 & 0 & 0 & 0 \\ 0 & 0 & 1 & 0 & 0 & 0 & 0 & 0 & 0 & 0 & 0 & 0 \\ 0 & 0 & 0 & 1 & 0 & 0 & 0 & 0 & 0 & 0 & 0 & 0 \\ 0 & 0 & 0 & 0 & 1 & 0 & 0 & 0 & 0 & 0 & 0 & 0 \\ 0 & 0 & 0 & 0 & 0 & 1 & 0 & 0 & 0 & 0 & 0 & 0 \\ 0 & 0 & 0 & 0 & 0 & 0 & 1 & 0 & 0 & 0 & 0 & 0 \\ 0 & 0 & 0 & 0 & 0 & 0 & 0 & 1 & 0 & 0 & 0 & 0 \end{bmatrix}$$

and

$$\mathbf{B}^2 = \begin{bmatrix} 0 & 0 & 0 & 0 & 1 & 0 & 0 & 0 & 0 & 0 & 0 & 0 \\ 0 & 0 & 0 & 0 & 0 & 1 & 0 & 0 & 0 & 0 & 0 & 0 \\ 0 & 0 & 0 & 0 & 0 & 0 & 1 & 0 & 0 & 0 & 0 & 0 \\ 0 & 0 & 0 & 0 & 0 & 0 & 0 & 1 & 0 & 0 & 0 & 0 \\ 0 & 0 & 0 & 0 & 0 & 0 & 0 & 0 & 1 & 0 & 0 & 0 \\ 0 & 0 & 0 & 0 & 0 & 0 & 0 & 0 & 0 & 1 & 0 & 0 \\ 0 & 0 & 0 & 0 & 0 & 0 & 0 & 0 & 0 & 0 & 1 & 0 \\ 0 & 0 & 0 & 0 & 0 & 0 & 0 & 0 & 0 & 0 & 0 & 1 \end{bmatrix}$$

Note that the Boolean matrix of the finite element always has a number of rows equal to the number of the finite element nodal coordinates and a number of columns equal to the number of the body nodal coordinates.

### 5.3 INERTIA AND ELASTIC FORCES

In this section, the formulation of the finite element inertia and elastic forces is discussed. It will be shown that the finite element formulation discussed in this chapter leads to a simple expression for the inertia forces and to a more complex expression for the elastic forces. This is in contrast with the floating frame of reference (FFR) formulation discussed in the following chapter and used mainly for the small-deformation, large-rotation analysis. The FFR formulation leads to a complex expression for the inertia forces and to a simple expression for the elastic forces.

#### Inertia Forces

In order to formulate the inertia forces of the finite element, one must obtain an expression for the acceleration vector. Differentiating the global position vector of Equation 9 with respect to time, the absolute velocity vector  $\mathbf{v}^j$  of an arbitrary material point on the element  $j$  can be written as

$$\mathbf{v}^j = \dot{\mathbf{r}}^j = \mathbf{S}^j \dot{\mathbf{e}}^j, \quad j = 1, 2, \dots, n_e \quad (5.15)$$

Differentiating this equation with respect to time, the acceleration vector  $\mathbf{a}^j$  can be written in the case of the ANCF as

$$\mathbf{a}^j = \ddot{\mathbf{r}}^j = \mathbf{S}^j \ddot{\mathbf{e}}^j, \quad j = 1, 2, \dots, n_e \quad (5.16)$$

The virtual work of the inertia forces of the finite element can then be defined as

$$\delta W_i^j = \int_{V^j} \rho^j \mathbf{a}^{jT} \delta \mathbf{r}^j dV^j \quad (5.17)$$

where  $\rho^j$  and  $V^j$  are, respectively, the mass density and volume of the finite element. It is important to point out that because of the principle of conservation of mass,  $\rho^j dV^j = \text{constant}$ ,

the mass density  $\rho^j$ , and the volume  $V^j$  in the reference configuration can be used. For the simplicity of the notation in this chapter, we use  $\rho^j$  instead of  $\rho_o^j$  to denote the density in the reference configuration because in most of the developments presented in this chapter and the following one, the inertia can be formulated using the reference configuration. A specific mention will be made if  $\rho^j$  is the mass density associated with the current configuration, as it is the case when the equations that govern the fluid motion are discussed.

The virtual change in the position vector of the material point can be written as

$$\delta \mathbf{r}^j = \mathbf{S}^j \delta \mathbf{e}^j \quad (5.18)$$

Using the preceding two equations with the expression for the acceleration of Equation 16 and keeping in mind that the time-dependent nodal coordinates do not depend on the spatial coordinates and can be factored out of the integration sign, one obtains the following equation for the virtual work of the inertia forces:

$$\delta W_i^j = \left\{ \ddot{\mathbf{e}}^{jT} \int_{V^j} \rho^j \mathbf{S}^{jT} \mathbf{S}^j dV^j \right\} \delta \mathbf{e}^j \quad (5.19)$$

This equation can be written as

$$\delta W_i^j = \{ \ddot{\mathbf{e}}^{jT} \mathbf{M}^j \} \delta \mathbf{e}^j \quad (5.20)$$

where  $\mathbf{M}^j$  is the symmetric mass matrix of the finite element  $j$  defined as

$$\mathbf{M}^j = \int_{V^j} \rho^j \mathbf{S}^{jT} \mathbf{S}^j dV^j \quad (5.21)$$

This mass matrix is constant in both two- and three-dimensional cases. This is a unique feature of the ANCF because other known three-dimensional finite element formulations that give complete information about the rotation at the nodes and use infinitesimal or finite rotation parameters as nodal coordinates do not lead to a constant mass matrix in the case of three-dimensional analysis. This important property of the formulation simplifies the governing equations significantly since it leads to zero centrifugal and Coriolis forces when the body experiences an arbitrary large deformation and finite rotation.

By using the preceding equations, the virtual work of the inertia forces can be written as

$$\delta W_i^j = \mathbf{Q}_i^{jT} \delta \mathbf{e}^j \quad (5.22)$$

where  $\mathbf{Q}_i^j$  is the vector of the inertia forces that takes the following simple form:

$$\mathbf{Q}_i^j = \mathbf{M}^j \ddot{\mathbf{e}}^j \quad (5.23)$$

One can show that, for many ANCF finite elements, the mass matrix remains the same under an orthogonal coordinate transformation.



## Elastic Forces

An expression for the virtual work of the stresses of the continuum was obtained in Chapter 3 in terms of the Green–Lagrange strain tensor and the second Piola–Kirchhoff stress tensor. For the finite element  $j$ , the virtual work of the stresses can be written as

$$\delta W_s^j = - \int_{V^j} \boldsymbol{\sigma}_{P2}^j : \delta \mathbf{e}^j dV^j \quad (5.24)$$

In this equation,  $\boldsymbol{\sigma}_{P2}^j$  is the second Piola–Kirchhoff stress tensor and  $\mathbf{e}^j$  is the Green–Lagrange strain tensor at an arbitrary material point on the finite element  $j$ . The stress and strain tensors used in Equation 24 are defined in the reference configuration. The virtual strain can be expressed in terms of the virtual changes of the position vector gradients as

$$\delta \mathbf{e}^j = \frac{1}{2} \{ (\delta \mathbf{J}^T) \mathbf{J}^j + \mathbf{J}^{jT} (\delta \mathbf{J}^j) \} \quad (5.25)$$

The second Piola–Kirchhoff stresses are related to the Green–Lagrange strains using the constitutive equations

$$\boldsymbol{\sigma}_{P2}^j = \mathbf{E}^j : \mathbf{e}^j \quad (5.26)$$

where  $\mathbf{E}^j$  is the fourth-order tensor of elastic coefficients. Substituting the preceding two equations into the expression of the virtual work of the stresses, using the definition of the matrix of position vector gradients, and using the expression of the gradients in terms of the finite element nodal coordinates, one can show that the virtual work of the stresses of the finite element  $j$  can be written as

$$\delta W_s^j = - \frac{1}{2} \int_{V^j} (\mathbf{E}^j : \mathbf{e}^j) : \{ (\delta \mathbf{J}^T) \mathbf{J}^j + \mathbf{J}^{jT} (\delta \mathbf{J}^j) \} dV^j = - \mathbf{Q}_s^{jT} \delta \mathbf{e}^j \quad (5.27)$$

In this equation,  $\mathbf{Q}_s^j$  is the vector of the elastic forces associated with the nodal coordinates of the finite element  $j$ . This vector, which is the result of the deformation of the continuum, takes a more complex form as compared to the simple expression of the inertia forces obtained previously in this section. Because the integrals for the stress forces are, in general, highly nonlinear functions in the nodal and spatial coordinates, numerical integration methods are often used for the evaluation of the nonlinear generalized stress forces.

## 5.4 EQUATIONS OF MOTION

The equations of motion of the finite elements that form the body can be developed using the *principle of virtual work in dynamics* (Roberson and Schwertassek, 1988; Shabana, 2001). In the case of unconstrained motion, the principle of virtual work for the continuum can be written as

$$\delta W_i = \delta W_s + \delta W_e \quad (5.28)$$

In this equation,  $\delta W_i$  is the virtual work of the inertia forces of the body,  $\delta W_s$  is the virtual work of the elastic forces due to the deformation, and  $\delta W_e$  is the virtual work of the applied

forces such as gravity, magnetic, and other external forces. For instance, the virtual work of an external force  $\mathbf{F}^j$  acting at a point  $P$  defined by the coordinates  $\mathbf{x}_p^j$  on the finite element  $j$  can be written as

$$\delta W_e^j = \mathbf{F}^{jT} \delta \mathbf{r}_p^j = \mathbf{F}^{jT} \mathbf{S}^j(\mathbf{x}_p^j) \delta \mathbf{e}^j = \mathbf{Q}_e^{jT} \delta \mathbf{e}^j \quad (5.29)$$

where  $\mathbf{S}^j(\mathbf{x}_p^j)$  is a constant matrix that defines the element shape function at point  $\mathbf{x}_p^j$  and  $\mathbf{Q}_e^j$  is the vector of generalized forces associated with the element nodal coordinates  $\mathbf{e}^j$  as the result of the application of the force vector  $\mathbf{F}^j$ . This vector of generalized forces is defined as

$$\mathbf{Q}_e^j = \mathbf{S}^{jT}(\mathbf{x}_p^j) \mathbf{F}^j \quad (5.30)$$

A similar expression can be obtained for all forces acting on the finite elements. One can then write the virtual work of the applied forces acting on the continuum by summing up the virtual work of the forces acting on its finite elements, that is,

$$\delta W_e = \sum_{j=1}^{n_e} \delta W_e^j = \sum_{j=1}^{n_e} \mathbf{Q}_e^{jT} \delta \mathbf{e}^j \quad (5.31)$$

The virtual work of the inertia forces of the body can be obtained by summing up the virtual work of the inertia forces of its finite elements. Using the expression of the virtual work of the finite element inertia forces obtained in the preceding section, one can write

$$\delta W_i = \sum_{j=1}^{n_e} \delta W_i^j = \sum_{j=1}^{n_e} (\mathbf{M}^j \ddot{\mathbf{e}}^j)^T \delta \mathbf{e}^j \quad (5.32)$$

Similarly, the virtual work of the stress forces of the body can be written as

$$\delta W_s = \sum_{j=1}^{n_e} \delta W_s^j = - \sum_{j=1}^{n_e} \mathbf{Q}_s^{jT} \delta \mathbf{e}^j \quad (5.33)$$

Substituting the preceding three equations into the principle of virtual work in dynamics of Equation 28, one obtains

$$\sum_{j=1}^{n_e} (\mathbf{M}^j \ddot{\mathbf{e}}^j + \mathbf{Q}_s^j - \mathbf{Q}_e^j)^T \delta \mathbf{e}^j = 0 \quad (5.34)$$

This equation can also be written as

$$\left\{ \begin{bmatrix} \mathbf{M}^1 & \mathbf{0} & \cdots & \mathbf{0} \\ \mathbf{0} & \mathbf{M}^2 & \cdots & \mathbf{0} \\ \vdots & \vdots & \ddots & \mathbf{0} \\ \mathbf{0} & \mathbf{0} & \cdots & \mathbf{M}^{n_e} \end{bmatrix} \begin{bmatrix} \ddot{\mathbf{e}}^1 \\ \ddot{\mathbf{e}}^2 \\ \vdots \\ \ddot{\mathbf{e}}^{n_e} \end{bmatrix} + \begin{bmatrix} \mathbf{Q}_s^1 \\ \mathbf{Q}_s^2 \\ \vdots \\ \mathbf{Q}_s^{n_e} \end{bmatrix} - \begin{bmatrix} \mathbf{Q}_e^1 \\ \mathbf{Q}_e^2 \\ \vdots \\ \mathbf{Q}_e^{n_e} \end{bmatrix} \right\}^T \begin{bmatrix} \delta \mathbf{e}^1 \\ \delta \mathbf{e}^2 \\ \vdots \\ \delta \mathbf{e}^{n_e} \end{bmatrix} = 0 \quad (5.35)$$

Because  $\delta \mathbf{e}^j = \mathbf{B}^j \delta \mathbf{e}$  and  $\ddot{\mathbf{e}}^j = \mathbf{B}^j \ddot{\mathbf{e}}$ , where  $\mathbf{B}^j$  is a Boolean matrix that defines the element connectivity and  $\mathbf{e}$  is the vector of the body nodal coordinates, Equation 34 can be written in terms of the nodal coordinates of the body as

$$\left\{ \sum_{j=1}^{n_e} (\mathbf{M}^j \mathbf{B}^j \ddot{\mathbf{e}} + \mathbf{Q}_s^j - \mathbf{Q}_e^j)^T \mathbf{B}^j \right\} \delta \mathbf{e} = 0 \quad (5.36)$$

If the body motion is unconstrained, the elements of the vector  $\delta \mathbf{e}$  are independent, and as a consequence, their coefficients in the preceding equation must be equal to zero, that is,

$$\sum_{j=1}^{n_e} \left\{ \mathbf{B}^{jT} \mathbf{M}^j \mathbf{B}^j \ddot{\mathbf{e}} + \mathbf{B}^{jT} \mathbf{Q}_s^j - \mathbf{B}^{jT} \mathbf{Q}_e^j \right\} = \mathbf{0} \quad (5.37)$$

By performing the summation in this equation, one can show that the finite element equation of motion of the body can be written as

$$\mathbf{M} \ddot{\mathbf{e}} + \mathbf{Q}_s - \mathbf{Q}_e = \mathbf{0} \quad (5.38)$$

where  $\mathbf{M}$  is the body symmetric mass matrix,  $\mathbf{Q}_s$  is the vector of body elastic forces, and  $\mathbf{Q}_e$  is the vector of the body applied forces. The mass matrix and force vectors that appear in the preceding equation are obtained from the mass matrices and force vectors of the finite elements as

$$\mathbf{M} = \sum_{j=1}^{n_e} \mathbf{B}^{jT} \mathbf{M}^j \mathbf{B}^j, \quad \mathbf{Q}_s = \sum_{j=1}^{n_e} \mathbf{B}^{jT} \mathbf{Q}_s^j, \quad \mathbf{Q}_e = \sum_{j=1}^{n_e} \mathbf{B}^{jT} \mathbf{Q}_e^j \quad (5.39)$$

In the finite element formulation discussed in this chapter, the body mass matrix is constant, and therefore, the vectors of centrifugal and Coriolis forces are identically equal to zero in this formulation. The vector of the body elastic forces due to the stresses, on the other hand, is a nonlinear function of the nodal coordinates, as discussed in the preceding section. The fact that the mass matrix is constant can be utilized in developing a computational algorithm for solving the finite element equations. In this case, there is no need to iteratively perform the **LU** factorization of this matrix. One can use a transformation based on *Cholesky coordinates* that leads to an identity mass matrix (Shabana, 1998). Such a coordinate transformation leads to an optimum sparse matrix structure when ANCF finite elements are used in MBS algorithms.

#### Example 5.4

The finite element in Example 2 is assumed to be subjected to a sinusoidal force defined by the vector  $\mathbf{F}^j = [F_1 \sin \omega t \quad F_2 \sin \omega t]^T$ , where  $\omega$  is constant and  $t$  is time. The point of application of the force is assumed to be at a point  $\mathbf{x}_p^j$  defined by the dimensionless parameters  $\xi = 0.5$  and  $\eta = 0.5$ . Determine the generalized nodal forces due to the application of this force.

*Solution:* The assumed displacement field of the element is  $\mathbf{r}^j = \mathbf{S}^j \mathbf{e}^j$ . For this element,  $\mathbf{e}^j = [e_1 \ e_2 \ \dots \ e_{12}]^T$  is the vector of nodal coordinates as defined in Example 2, and  $\mathbf{S}^j$  is the

element shape function matrix, which can be written as

$$\mathbf{S}^j = [s_1 \mathbf{I} \quad s_2 \mathbf{I} \quad s_3 \mathbf{I} \quad s_4 \mathbf{I} \quad s_5 \mathbf{I} \quad s_6 \mathbf{I}]$$

where the shape functions  $s_i$ ,  $i = 1, 2, \dots, 6$ , were obtained in Example 2 as (Omar and Shabana, 2001)

$$\begin{aligned} s_1 &= 1 - 3\xi^2 + 2\xi^3, & s_2 &= l(\xi - 2\xi^2 + \xi^3), \\ s_3 &= l\eta(1 - \xi), & s_4 &= 3\xi^2 - 2\xi^3, \\ s_5 &= l(-\xi^2 + \xi^3), & s_6 &= l\xi\eta \end{aligned}$$

where  $\xi = x_1^j/l$ ,  $\eta = x_2^j/l$ , and  $l$  is the length of the finite element. For  $\xi = 0.5$  and  $\eta = 0.5$ , the shape functions take the values

$$s_1 = 0.5, \quad s_2 = 0.125l, \quad s_3 = 0.25l, \quad s_4 = 0.5, \quad s_5 = -0.125l, \quad s_6 = 0.25l$$

Therefore, the shape function defined at the point of application of the force  $\mathbf{x}_p^j$  is

$$\mathbf{S}^j(\mathbf{x}_p^j) = [0.5 \mathbf{I} \quad 0.125 \mathbf{I} \quad 0.25 \mathbf{I} \quad 0.5 \mathbf{I} \quad -0.125 \mathbf{I} \quad 0.25 \mathbf{I}]$$

The virtual work of the force  $\mathbf{F}^j$  can be written as

$$\delta W_e^j = \mathbf{F}^{jT} \delta \mathbf{r}_p^j = \mathbf{F}^{jT} \mathbf{S}^j(\mathbf{x}_p^j) \delta \mathbf{e}^j = \mathbf{Q}_e^{jT} \delta \mathbf{e}^j$$

where

$$\begin{aligned} \mathbf{Q}_e^j &= \mathbf{S}^{jT}(\mathbf{x}_p^j) \mathbf{F}^j \\ &= 0.125 \sin \omega t [4F_1 \quad 4F_2 \quad F_1 l \quad F_2 l \quad 2F_1 l \quad 2F_2 l \quad 4F_1 \quad 4F_2 \quad -F_1 l \quad -F_2 l \quad 2F_1 l \quad 2F_2 l]^T \end{aligned}$$

## Curved Geometry

ANCF finite elements can be used to conveniently describe complex shapes. These shapes can represent curved geometry in the undeformed reference configurations. In these cases, the position vector gradients in the undeformed reference configuration are not orthogonal unit vectors because of the continuum initial geometry. Examples of these applications, which were presented in Chapter 2 and include tires, belt drives, and tank cars, are shown in Figure 4. As discussed in Chapter 2, in these cases, the strains evaluated using the matrix of position vector gradients in the initial configuration must be identically equal to zero. In order to explain how the strains are formulated in these cases of initial curved geometry, the three different configurations shown in Figure 5 were considered in Chapter 2. Because complex geometries can always be obtained by changing the shape of simple objects, the first configuration in Figure 5 depicts the simple geometry, which can represent straight metal sheets described conveniently using ANCF finite elements. In this simple geometry configuration, the location of the material



Figure 5.4 Initial geometry

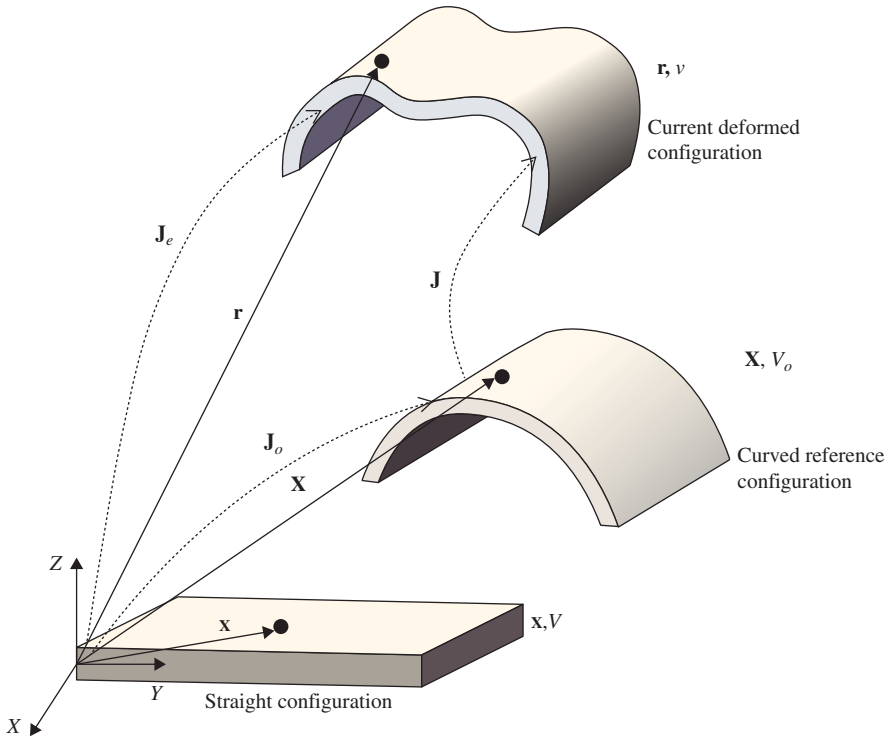


Figure 5.5 ANCF description of curved geometry

points is defined using the position vector  $\mathbf{x}$  of the ANCF element or an assembly of ANCF finite elements. The second configuration is the reference configuration, which defines the initial undeformed geometry. In this undeformed reference configuration, the position of the material points is defined by the vector  $\mathbf{X}$ . One can write  $d\mathbf{X} = \mathbf{J}_o d\mathbf{x}$ , where  $\mathbf{J}_o = \partial\mathbf{X}/\partial\mathbf{x}$ , and the superscript that indicates the finite element number is dropped for simplicity. The third configuration shown in Figure 5 defines the current deformed configuration. In this configuration, the position of the material points is defined by the vector  $\mathbf{r}$ . As discussed in Chapter 2, one can write  $d\mathbf{r} = \mathbf{J} d\mathbf{X}$ , with  $\mathbf{J} = \partial\mathbf{r}/\partial\mathbf{X}$ . It follows that  $\mathbf{J} = \partial\mathbf{r}/\partial\mathbf{X} = (\partial\mathbf{r}/\partial\mathbf{x})(\partial\mathbf{x}/\partial\mathbf{X}) = \mathbf{J}_e \mathbf{J}_o^{-1}$ , where  $\mathbf{J}_e = \partial\mathbf{r}/\partial\mathbf{x}$ .

The volume of the curved structure  $V_o$  is related to the volume of the straight structure  $V$  (Figure 5) using the relationship  $dV_o = J_o dV$ , where  $J_o = |\mathbf{J}_o|$  is the determinant of the matrix of position vector gradients  $\mathbf{J}_o = \partial \mathbf{X} / \partial \mathbf{x}$ . Therefore, integration with respect to the domain  $V_o$  can be converted to integration with respect to the straight domain  $V$  by using the transformation  $dV_o = J_o dV$ . This allows for using the original dimensions of the simpler geometry to carry out the integrations associated with the initially curved configuration. Note that the matrix  $\mathbf{J}_o = \partial \mathbf{X} / \partial \mathbf{x}$  is constant.

The matrix of position vector gradients  $\mathbf{J} = \partial \mathbf{r} / \partial \mathbf{X}$  is the matrix, which is used to determine the Lagrangian strain tensor  $\boldsymbol{\varepsilon}$  as  $\boldsymbol{\varepsilon} = (\mathbf{J}^T \mathbf{J} - \mathbf{I}) / 2$ . This matrix can be defined using the ANCF description as

$$\mathbf{J} = \frac{\partial \mathbf{r}}{\partial \mathbf{X}} = \left( \frac{\partial \mathbf{r}}{\partial \mathbf{x}} \right) \left( \frac{\partial \mathbf{x}}{\partial \mathbf{X}} \right) = \mathbf{J}_e \mathbf{J}_o^{-1} \quad (5.40)$$

where, as previously defined,  $\mathbf{J}_e = \partial \mathbf{r} / \partial \mathbf{x}$ . Therefore, the Lagrangian strain tensor can be written as

$$\boldsymbol{\varepsilon} = \frac{1}{2} (\mathbf{J}^T \mathbf{J} - \mathbf{I}) = \frac{1}{2} (\mathbf{J}_o^{-1T} (\mathbf{J}_e^T \mathbf{J}_e) \mathbf{J}_o^{-1} - \mathbf{I}) \quad (5.41)$$

Note that the relationship between the volume in the current deformed configuration  $v$  and the volume in the curved reference configuration  $V$  can be written as  $dv = J dV_o$ , where  $J = |\mathbf{J}|$  is the determinant of the matrix of position gradients  $\mathbf{J}$ . It follows that  $dv = J dV_o = |\mathbf{J}_e| |\mathbf{J}_o^{-1}| dV_o$ . Using the relationship  $dV_o = J_o dV$ , one has  $dv = |\mathbf{J}_e| dV$ .

As mentioned in Chapter 2, the procedure described in this section to model the initial curvature, which is the same as the one used in the literature for modeling the initially curved configuration of belt drives and rubber chains (Dufva et al., 2007; Maqueda et al., 2010), will lead to zero strains for an arbitrary initially curved geometry. Using the ANCF finite elements discussed later in this chapter, the constant matrix of position vector gradients  $\mathbf{J}_o = \partial \mathbf{X} / \partial \mathbf{x}$  can be determined in a straightforward manner. In the ANCF description, the assumed displacement field can be written as  $\mathbf{r}(\mathbf{x}, t) = \mathbf{S}(\mathbf{x}, t) \mathbf{e}(t)$ , where  $\mathbf{r}$  is the global position vector,  $\mathbf{x} = [x_1 \ x_2 \ x_3]^T$  is the vector of the element spatial coordinates,  $t$  is time,  $\mathbf{S}$  is the element shape function matrix, and  $\mathbf{e}$  is the vector of the element nodal coordinates that include absolute position and gradient coordinates. In the ANCF description, the vector of nodal coordinates  $\mathbf{e}$  can be written as  $\mathbf{e}(t) = \mathbf{e}_o(t) + \mathbf{e}_d(t)$ , where  $\mathbf{e}_o$  is the vector of nodal coordinates in the reference configuration and  $\mathbf{e}_d$  is the vector of nodal displacements. Using this partitioning, the assumed displacement field can be written as  $\mathbf{r}(\mathbf{x}, t) = \mathbf{S}(\mathbf{x}, t) \mathbf{e}(t) = \mathbf{S}(\mathbf{x}, t) (\mathbf{e}_o(t) + \mathbf{e}_d(t))$ . Using the general continuum mechanics description  $\mathbf{r}(\mathbf{X}, t) = \mathbf{X} + \mathbf{u}(\mathbf{X}, t)$ , where  $\mathbf{X}$  is the absolute position vector of an arbitrary point in the reference configuration and  $\mathbf{u}$  is the displacement vector, one can write  $\mathbf{X} = \mathbf{S} \mathbf{e}_o$  and  $\mathbf{u} = \mathbf{S} \mathbf{e}_d$ . By appropriate choice of the elements of the vector  $\mathbf{e}_o$ , initially curved structures can be defined in a straightforward manner using ANCF finite elements.

As previously mentioned, integration with respect to the domain  $V_o$  can be converted to integration with respect to the straight element domain  $V$  by using the transformation  $dV_o = J_o dV$ , where  $J_o = |\mathbf{J}_o|$  is the determinant of the matrix of position vector gradients  $\mathbf{J}_o = \partial \mathbf{X} / \partial \mathbf{x} = \partial (\mathbf{S} \mathbf{e}_o) / \partial \mathbf{x}$ . In the ANCF description, the matrix  $\mathbf{J}_o = \partial (\mathbf{S} \mathbf{e}_o) / \partial \mathbf{x}$  is constant, while  $\mathbf{J}_e = \partial (\mathbf{S} \mathbf{e}) / \partial \mathbf{x}$ . Table 1 explains how the basic continuum mechanics description is implemented using ANCF finite elements.

TABLE 5.1 ANCF Description of Curved Geometry

Issue	Continuum Mechanics	ANCF	Comments
Kinematic description	$\mathbf{r} = \mathbf{X} + \mathbf{u}$	$\mathbf{r}(\mathbf{x}, t) = \mathbf{S}\mathbf{e}_o + \mathbf{S}\mathbf{e}_d = \mathbf{S}(\mathbf{e}_o + \mathbf{e}_d)$	$\mathbf{X} = \mathbf{S}(\mathbf{x})\mathbf{e}_o(t)$ , $\mathbf{u} = \mathbf{S}(\mathbf{x})\mathbf{e}_d(t)$ $\mathbf{X}$ is the body parameters in the initially straight or curved configuration, and $\mathbf{x}$ is the ANCF finite element parameters. Note that $\mathbf{X} = \mathbf{X}(\mathbf{x})$
Lagrangian strains	$\mathbf{J} = \frac{\partial \mathbf{r}}{\partial \mathbf{X}} = \mathbf{r}_{\mathbf{x}}$ $\boldsymbol{\varepsilon} = \frac{1}{2}(\mathbf{J}^T \mathbf{J} - \mathbf{I})$	$\mathbf{J} = \frac{\partial \mathbf{r}}{\partial \mathbf{X}} = \left( \frac{\partial \mathbf{r}}{\partial \mathbf{x}} \right) \left( \frac{\partial \mathbf{x}}{\partial \mathbf{X}} \right) = \mathbf{J}_e \mathbf{J}_o^{-1}$ $\mathbf{J}_o = \frac{\partial \mathbf{X}}{\partial \mathbf{x}} = \mathbf{X}_{\mathbf{x}}, \quad \mathbf{J}_e = \frac{\partial \mathbf{r}}{\partial \mathbf{x}}$ $\boldsymbol{\varepsilon} = \frac{1}{2}(\mathbf{J}^T \mathbf{J} - \mathbf{I})$	The Lagrangian strains are obtained by differentiation with respect to $\mathbf{X}$ . Therefore, the gradients are tangent to these parameters and the strains are defined along these parameters (fibers or coordinate lines)
Strain in the element coordinates	Does not apply	$\mathbf{J} = \frac{\partial \mathbf{r}}{\partial \mathbf{X}} = \left( \frac{\partial \mathbf{r}}{\partial \mathbf{x}} \right) \left( \frac{\partial \mathbf{x}}{\partial \mathbf{X}} \right) = \mathbf{J}_e \mathbf{J}_o^{-1}$ $\boldsymbol{\varepsilon} = \frac{1}{2}(\mathbf{J}^T \mathbf{J} - \mathbf{I})$ $= \frac{1}{2}((\mathbf{J}_e \mathbf{J}_o^{-1})^T \mathbf{J}_e \mathbf{J}_o^{-1} - \mathbf{I})$ $= \frac{1}{2} \mathbf{J}_o^{-1T} (\mathbf{J}_e^T \mathbf{J}_e - \mathbf{J}_o^T \mathbf{J}_o) \mathbf{J}_o^{-1}$ $= \mathbf{J}_o^{-1T} \boldsymbol{\varepsilon}_e \mathbf{J}_o^{-1}$ $\boldsymbol{\varepsilon}_e = \mathbf{J}_o^T \boldsymbol{\varepsilon} \mathbf{J}_o$	These equations show that if the Lagrangian strains $\boldsymbol{\varepsilon}$ along the body coordinate lines $\mathbf{X}$ are given, the strains $\boldsymbol{\varepsilon}_e$ along the element coordinates $\mathbf{x}$ can be obtained in a straightforward manner using the matrix $\mathbf{J}_o$ . Note that $(\boldsymbol{\varepsilon}_e)_{11}$ in the case of fully parameterized elements accounts for both axial and bending strains. Note also that by using the expression for the strain $\boldsymbol{\varepsilon}$ , the initial curvature in undeformed state does not contribute to the stress forces

Displacement gradients	$\mathbf{J} = \frac{\partial \mathbf{r}}{\partial \mathbf{X}} = \mathbf{I} + \frac{\partial \mathbf{u}}{\partial \mathbf{X}}$ $= \mathbf{I} + \mathbf{J}_d, \quad \mathbf{J}_d = \frac{\partial \mathbf{u}}{\partial \mathbf{X}}$ $\boldsymbol{\varepsilon} = \frac{1}{2}(\mathbf{J}_d + \mathbf{J}_d^T + \mathbf{J}_d^T \mathbf{J}_d)$	$\mathbf{u} = \mathbf{S} \mathbf{e}_d$ $\mathbf{J}_d = \frac{\partial \mathbf{u}}{\partial \mathbf{X}} = \left( \frac{\partial \mathbf{u}}{\partial \mathbf{x}} \right) \left( \frac{\partial \mathbf{x}}{\partial \mathbf{X}} \right)$ $= \mathbf{J}_{ed} \mathbf{J}_o^{-1}$ $\boldsymbol{\varepsilon} = \frac{1}{2}(\mathbf{J}_d + \mathbf{J}_d^T + \mathbf{J}_d^T \mathbf{J}_d)$ $\boldsymbol{\varepsilon} = \frac{1}{2} \mathbf{J}_o^{-1T} (\mathbf{J}_o^T \mathbf{J}_{ed} + \mathbf{J}_{ed}^T \mathbf{J}_o + \mathbf{J}_{ed}^T \mathbf{J}_{ed}) \mathbf{J}_o^{-1}$ $= \mathbf{J}_o^{-1T} \boldsymbol{\varepsilon}_e \mathbf{J}_o^{-1}$ $\boldsymbol{\varepsilon}_e = \mathbf{J}_o^T \boldsymbol{\varepsilon} \mathbf{J}_o$	<p>The displacement gradients that are function of the displacement coordinates and do not depend on the initial configuration defined by <math>\mathbf{e}_o</math> can be used to formulate the strains, and this allows for modeling curved structures</p>
Derivatives	Does not apply	$\frac{\partial}{\partial \mathbf{e}} \left( \frac{\partial \mathbf{r}}{\partial \mathbf{X}} \right) = \frac{\partial}{\partial \mathbf{e}} \left( \frac{\partial \mathbf{r}}{\partial \mathbf{x}} \right) \left( \frac{\partial \mathbf{x}}{\partial \mathbf{X}} \right)$ $= \frac{\partial}{\partial \mathbf{e}} \left( \frac{\partial \mathbf{r}}{\partial \mathbf{x}} \right) \mathbf{J}_o^{-1}$ $= \frac{\partial}{\partial \mathbf{e}} \left( [\mathbf{r}_x \ \mathbf{r}_y \ \mathbf{r}_z] \mathbf{J}_o^{-1} \right)$	<p>These equations show how the derivatives can be obtained from the derivatives with respect to the element coordinates in the straight configuration</p>



## 5.5 NUMERICAL EVALUATION OF THE ELASTIC FORCES

As previously pointed out and shown in this chapter, the nonlinear large-deformation finite element absolute nodal coordinate formulation leads to a simple expression for the inertia forces and a nonlinear expression for the stress elastic forces. This is in contrast with the small-deformation finite element FFR formulation presented in the following chapter. The FFR formulation leads to a simple expression for the elastic forces and to a highly nonlinear expression for the inertia forces. Nonetheless, as will be shown in the following chapter, the nonlinear inertia forces obtained using the FFR formulation can be expressed in terms of a unique set of *inertia shape integrals*. These shape integrals can be evaluated in advance of the dynamic simulation using information from existing structural dynamics finite element codes.

Because closed-form expressions for the nonlinear ANCF elastic forces cannot be, in general, obtained, the numerical evaluation of these forces is discussed in this section. The numerical evaluation of integrals of functions is covered in detail in textbooks on numerical methods (Carnahan et al., 1969; Atkinson, 1978). Therefore, in this section, a brief introduction to this subject is presented. To this end, consider the following integral of a single function  $f(x)$  over the interval  $[a, b]$ :

$$I = \int_a^b f(x) dx \quad (5.42)$$

If the function  $f(x)$  is not simple or is given in a tabulated form, analytical evaluation of the preceding integral can be difficult, or even impossible. In these cases, one must resort to numerical methods in order to evaluate the integral. Formulas used for numerical integration are called *quadratures*. One approach is to try to find a polynomial  $P_n(x)$  of order  $n$  that can be a good approximation of  $f(x)$ . One can then obtain the integral of the polynomial in a closed form. Because  $P_n(x)$  is not in general the same as  $f(x)$ , one can define the following error function:

$$\delta(x) = f(x) - P_n(x) \quad (5.43)$$

In general,  $\delta(x)$  can take positive and negative values, and as a consequence, some of the positive errors cancel the effect of the negative errors when the integral  $\int_a^b \delta(x) dx$  is evaluated even in the case when  $P_n(x)$  is not a good approximation of  $f(x)$ . For this reason, integration is known as a smoothing process (Carnahan et al., 1969). Furthermore, if  $f(x)$  is a polynomial or a function, which is described by data representing a polynomial, then one can always find a polynomial  $P_n(x)$  such that the integral  $I$  is exact. If  $f(x)$  is not a polynomial, the numerical integration will give an approximate evaluation of the integral of  $f(x)$ . If the functions used in the approximation of the integrals are evaluated at equally spaced base points, one obtains the *Newton–Cotes formulas*, an example of which is the well-known *Simpson's rule* for numerical integration. If the functions used to approximate the integrals are evaluated using unequally spaced base points, one obtains the *Gauss quadrature formulas*. In the Gauss quadrature formulas, the locations of the base points are selected to achieve the best accuracy. In these formulas, the properties of orthogonal polynomials are used. Examples of orthogonal polynomials are the *Legendre*, *Laquerre*, *Chebyshev*, and *Hermite polynomials*. For example, the first

few Legendre polynomials are defined as (Carnahan et al., 1969)

$$\left. \begin{aligned} L_0(x) &= 1, & L_1(x) &= x, & L_2(x) &= \frac{1}{2}(3x^2 - 1), \\ L_3(x) &= \frac{1}{2}(5x^3 - 3x), & L_4(x) &= \frac{1}{8}(35x^4 - 30x^2 + 3) \end{aligned} \right\} \quad (5.44)$$

In general, the Legendre polynomials are defined by the following general recursion relation:

$$L_n(x) = \left( \frac{2n-1}{n} \right) x L_{n-1}(x) - \left( \frac{n-1}{n} \right) L_{n-2}(x) \quad (5.45)$$

One can show that these polynomials are orthogonal on the interval  $[-1, 1]$ . That is,

$$\left. \begin{aligned} \int_{-1}^1 L_n(x) L_m(x) dx &= 0, \quad n \neq m \\ \int_{-1}^1 [L_n(x)]^2 dx &= c_n \end{aligned} \right\} \quad (5.46)$$

Because the Legendre polynomials are orthogonal, an arbitrary polynomial can be described as a linear combination of the Legendre polynomials.

### Gaussian Quadrature

In the Gaussian quadrature formulas, the integral is evaluated by approximating the function  $f(x)$  by a polynomial  $P_n(x)$  defined at unequally spaced base points. This function approximation can lead to an error  $\delta(x)$ , as previously mentioned. The locations of the base points are determined by developing a set of algebraic equations that make the integral of the error function equal to zero. The solution of these algebraic equations, which are obtained using the properties of the orthogonal polynomials, defines the base points. One can then write the integral  $I$  in the following form:

$$I = \int_a^b f(x) dx = \int_a^b P_n(x) dx + \int_a^b \delta(x) dx \quad (5.47)$$

The domain of integration can be changed from  $x \in [a, b]$  to  $\xi \in [-1, 1]$  by using the substitution

$$x = \frac{1}{2} \{ \xi(b-a) + (a+b) \} \quad (5.48)$$

The steps used to determine the base points are first to employ the Lagrangian interpolating polynomials to approximate  $P_n(x)$  and  $\delta(x)$ . The Lagrangian interpolating polynomials do not require equally spaced base points. The resulting polynomials are then expressed in terms of the orthogonal Legendre polynomials. The Legendre polynomial orthogonality conditions are used to define a set of algebraic equations that make the integral of the error function equal to zero. This set of algebraic equations defines the base points for different orders of the polynomial  $P_n(x)$ . The integral can then be written in terms of the function evaluated at these base points multiplied by *weight factors* or *weight coefficients*. This procedure for determining

the base points is described in detail by Carnahan et al. (1969). The results are weight factors, which depend on the order of the polynomial or the number of base points selected to approximate  $f(x)$ . These weight factors are presented in tables in mathematics handbooks or in textbooks on the subject of numerical analysis. In general, if the integral of the error function becomes zero and the domain of integration is changed to  $[-1, 1]$ , the integral  $I$  can be written in terms of the function at the base points and the weight coefficients as

$$I = \int_{-1}^1 g(\xi) d\xi = w_1 g(\xi_1) + w_2 g(\xi_2) + \cdots + w_n g(\xi_n) = \sum_{i=1}^m w_i g(\xi_i) \quad (5.49)$$

where  $w_i$ ,  $i = 1, 2, \dots, m$ , are the weight factors. These weight factors are called *Gauss–Legendre coefficients*. The weight factors are selected in order to achieve the greatest accuracy. Symmetrically located base points have the same weight coefficients. Note that if  $g(\xi)$  is approximated by one quadrature point, there is only one base point  $\xi_1 = 0$ . In this case, the integral is given by  $I = \int_{-1}^1 g(\xi) d\xi = w_1 g(\xi_1)$ . If  $g(\xi)$  is an arbitrary linear function ( $n = 1$ ), this integration result obtained using one quadrature point is exact. In this case,  $w_1$  represents the length of the domain of integration, that is,  $w_1 = 2$ , and  $g(\xi_1)$  is the height used to determine the area under the curve. In this case, the function  $g(\xi)$  is evaluated at  $\xi_1 = 0$ , which represents the center of the interval. If  $g(\xi)$ , on the other hand, represents a higher-order function, the one-point quadrature integration is an approximation. In general, a polynomial of degree  $n$  requires  $m = (n + 1)/2$  quadrature base points for exact integration, where in this simple rule  $n$  is assumed an odd number.

### Example 5.5

In order to explain the concept used in the Gaussian quadrature, one can write the error associated with the use of a polynomial of order  $n$  as

$$\Delta_n = \int_{-1}^1 g(\xi) d\xi - \sum_{i=1}^m w_i g(\xi_i)$$

The goal here is to determine the weight coefficients  $w_i$  and the base points  $\xi_i$ ,  $i = 1, 2, \dots, m$ , where  $m = (n + 1)/2$ . In the case of approximation based on a polynomial of order  $n$ , one can write

$$g(\xi) \approx a_0 + a_1 \xi + a_2 \xi^2 + \cdots + a_n \xi^n$$

It follows that

$$\Delta_n = \int_{-1}^1 (a_0 + a_1 \xi + a_2 \xi^2 + \cdots + a_n \xi^n) d\xi - \sum_{i=1}^m w_i g(\xi_i)$$

This equation can be written as

$$\Delta_n = \int_{-1}^1 \left( \sum_{i=0}^n a_i \xi^i \right) d\xi - \sum_{i=1}^m w_i g(\xi_i)$$

In the case  $n = 1$  ( $m = 1$ ), one has

$$\Delta_1 = \int_{-1}^1 (a_0 + a_1 \xi) d\xi - w_1 (a_0 + a_1 \xi_1)$$

This equation can be written as

$$\Delta_1 = a_0 \left\{ \int_{-1}^1 (1) d\xi - w_1 \right\} + a_1 \left\{ \int_{-1}^1 \xi d\xi - w_1 \xi_1 \right\}$$

For the error  $\Delta_1$  to be zero, one must have the following two conditions satisfied:

$$\int_{-1}^1 (1) d\xi - w_1 = 0, \quad \int_{-1}^1 \xi d\xi - w_1 \xi_1 = 0$$

These two conditions can be used to define  $w_1$  and  $\xi_1$  as

$$w_1 = 2, \quad \xi_1 = 0$$

The integral of the function  $g$  can then be approximated as

$$I = \sum_{i=1}^m w_i g(\xi_i) = w_1 g(\xi_1) = 2g(0),$$

which is the midpoint rule.

If  $n = 3$  ( $m = 2$ ), one has four unknowns,  $w_1$ ,  $w_2$ ,  $\xi_1$ , and  $\xi_2$ . In this case, one can write the error as

$$\begin{aligned} \Delta_2 = & \int_{-1}^1 (a_0 + a_1 \xi + a_2 \xi^2 + a_3 \xi^3) d\xi \\ & - w_1 (a_0 + a_1 \xi_1 + a_2 \xi_1^2 + a_3 \xi_1^3) - w_2 (a_0 + a_1 \xi_2 + a_2 \xi_2^2 + a_3 \xi_2^3) \end{aligned}$$

This equation can be written as

$$\begin{aligned} \Delta_2 = & a_0 \left\{ \int_{-1}^1 (1) d\xi - w_1 - w_2 \right\} + a_1 \left\{ \int_{-1}^1 \xi d\xi - w_1 \xi_1 - w_2 \xi_2 \right\} \\ & + a_2 \left\{ \int_{-1}^1 \xi^2 d\xi - w_1 \xi_1^2 - w_2 \xi_2^2 \right\} + a_3 \left\{ \int_{-1}^1 \xi^3 d\xi - w_1 \xi_1^3 - w_2 \xi_2^3 \right\} \end{aligned}$$

In order to make  $\Delta_2 = 0$ , one can impose the following four conditions:

$$\begin{aligned} \int_{-1}^1 (1) d\xi - w_1 - w_2 &= 0, & \int_{-1}^1 \xi d\xi - w_1 \xi_1 - w_2 \xi_2 &= 0, \\ \int_{-1}^1 \xi^2 d\xi - w_1 \xi_1^2 - w_2 \xi_2^2 &= 0, & \int_{-1}^1 \xi^3 d\xi - w_1 \xi_1^3 - w_2 \xi_2^3 &= 0, \end{aligned}$$

These conditions lead to the following four algebraic equations:

$$\begin{aligned} w_1 + w_2 &= 2, & w_1\xi_1 + w_2\xi_2 &= 0, \\ w_1\xi_1^2 + w_2\xi_2^2 &= \frac{2}{3}, & w_1\xi_1^3 + w_2\xi_2^3 &= 0 \end{aligned}$$

The solution of these four algebraic equations defines  $w_1$ ,  $w_2$ ,  $\xi_1$ , and  $\xi_2$  as

$$w_1 = w_2 = 1, \quad \xi_1 = -\xi_2 = -\frac{\sqrt{3}}{3}$$

These values can be used to approximate the integral as

$$I = \sum_{i=1}^m w_i g(\xi_i) = w_1 g(\xi_1) + w_2 g(\xi_2) = g\left(-\frac{\sqrt{3}}{3}\right) + g\left(\frac{\sqrt{3}}{3}\right)$$

## Generalization

The procedure used for integrating a function that depends on one variable can be generalized to the case in which the function depends on two or three variables, as it is the case in some finite element assumed displacement fields. In the two-dimensional case, consider the function  $g(\xi, \eta)$ . It is assumed that the domains of integration are changed as discussed before such that  $\xi \in [-1, 1]$ , and  $\eta \in [-1, 1]$ . The integral of the function  $g(\xi, \eta)$  can then be written as

$$\int_{-1}^1 \int_{-1}^1 g(\xi, \eta) d\xi d\eta = \int_{-1}^1 \left[ \sum_i w_i g(\xi_i, \eta) \right] d\eta \quad (5.50)$$

Performing the second integration with respect to  $\eta$ , one obtains

$$\int_{-1}^1 \int_{-1}^1 g(\xi, \eta) d\xi d\eta = \sum_i \sum_j w_i w_j g(\xi_i, \eta_j) \quad (5.51)$$

Following a similar procedure, one can show that in the case of a function that depends on three variables,  $\xi$ ,  $\eta$ , and  $\zeta$ , one has the following Gauss quadrature formula:

$$\int_{-1}^1 \int_{-1}^1 \int_{-1}^1 g(\xi, \eta, \zeta) d\xi d\eta d\zeta = \sum_i \sum_j \sum_k w_i w_j w_k g(\xi_i, \eta_j, \zeta_k) \quad (5.52)$$

If the original function is expressed in terms of the coordinates  $x_1$ ,  $x_2$ , and  $x_3$ , that is,  $f = f(x_1, x_2, x_3)$ , the preceding formula requires using the relationship  $dx_1 dx_2 dx_3 = J d\xi d\eta d\zeta$ , where  $J$  is the determinant of the Jacobian of the coordinate transformation.

Using the Gauss quadrature formulas presented in this section, a systematic procedure for the numerical evaluation of the nonlinear stress elastic forces of the finite elements can be developed. The number of quadrature points used in the numerical integration defines the

accuracy of the integration, and therefore, this number must be carefully selected in order to avoid increasing the computational cost or obtaining inaccurate results. There is no advantage gained from using a number of quadrature points larger than the number that gives exact evaluation of the integral (full integration). In some applications, on the other hand, there is an advantage in selecting a number of points that does not yield exact evaluation of the integrals. This is the case of *reduced integration*, which is commonly adopted in the finite element computational algorithms and will be discussed in a later section.

## 5.6 FINITE ELEMENTS AND GEOMETRY

In the following sections, examples of several finite elements that can be used to study the large deformations in a wide range of applications are presented. These elements have been developed over the last few years, and more details on the formulation of their shape functions, the mass matrices, and the vectors of elastic forces can be found in the literature. Some of these elements have been already used in this book in the examples presented in this chapter and preceding chapters.

### General Continuum Mechanics Approach and Classical Theories

It is important to point out that in all the finite elements that are discussed in this chapter, classical theories can be used by introducing a local element frame. Therefore, for beam elements, one can still use Euler–Bernoulli and Timoshenko beam theories; and, for plate and shell elements, one can still use Kirchhoff and Mindlin plate theories. This can always be accomplished by using the element local frame, which serves the only purpose of measuring the deformation (Shabana, 2013), and such a frame does not enter into the formulation of the inertia forces. Therefore, it is important to distinguish between this local element frame and the *corotational frame* used in the finite element literature. If the general continuum mechanics approach is used instead of the classical theories, one obtains more general formulations that relax the assumptions of Euler–Bernoulli, Timoshenko, Kirchhoff, and Mindlin theories. In these general formulations, the element cross section is allowed to deform.

### Gradient Vectors

Some of the elements presented in this chapter employ a complete set of gradient vectors as nodal coordinates. These elements allow, in a straightforward manner, for the use of a general continuum mechanics approach to formulate the elastic forces. The use of these elements also allows for using more general constitutive relationships. Elements that do not employ a complete set of parameters required to evaluate all the gradient vectors are called in this book, *gradient deficient*. The use of a general continuum mechanics approach with these elements is not as straightforward as compared to elements that have a complete set of parameters (spatial coordinates). The latter elements are called *fully parameterized elements*.

### Locking Problems

ANCF finite elements were introduced to deal with very flexible components. These finite elements perform well in the case of very flexible bodies, and efficient solutions for large

deformations of very flexible bodies can be obtained because a *nonincremental solution* procedure can be used with these ANCF elements. As the element stiffness decreases, ANCF elements become more efficient. Some researchers, however, used ANCF finite elements in the analysis of thin and stiff structures. In this case, some elements exhibit *locking problems* when the general continuum mechanics approach is used to formulate the elastic forces. The general continuum mechanics approach leads to what is called *ANCF-coupled deformation modes* (Hussein et al., 2007). These modes, which couple the deformation of the cross section and other deformations such as bending, can have high frequencies and can be a source of numerical problems (Schwab and Meijaard, 2005). Several techniques were proposed in the literature to solve the locking problems and improve the element performance.

In order to better understand the behavior of the finite elements introduced in the following sections, an understanding of the geometry is necessary. Some basic results from the theories of curves and surfaces, which are covered in the subject of differential geometry, can help the reader better understand and solve the problems encountered when ANCF finite elements are used.

## Theory of Curves

The centerline of a beam element represents a space curve. A curve can be uniquely defined in terms of one parameter. That is, the Cartesian coordinates that define the curve can be determined once this parameter is specified. Let  $\alpha$  be the parameter that defines the curve over the interval  $a \leq \alpha \leq b$ . The curve can then be represented by the following parametric form:

$$\mathbf{r}(\alpha) = [r_1(\alpha) \quad r_2(\alpha) \quad r_3(\alpha)]^T \quad (5.53)$$

The tangent vector to the curve at  $\alpha$  is given by

$$\mathbf{r}_\alpha = \frac{d\mathbf{r}}{d\alpha} = \left[ \frac{dr_1(\alpha)}{d\alpha} \quad \frac{dr_2(\alpha)}{d\alpha} \quad \frac{dr_3(\alpha)}{d\alpha} \right]^T \quad (5.54)$$

If at a given point  $\alpha$ ,  $|d\mathbf{r}(\alpha)/d\alpha| = 0$ , the point is called a *singular point*. The parameter  $\alpha$  can be selected to be the *arc length*  $s$ . If the arc length is used as a parameter, the tangent vector  $\mathbf{r}_s$  is a unit vector. That is,

$$\left| \frac{d\mathbf{r}}{ds} \right| = |\mathbf{r}_s(s)| = 1 \quad (5.55)$$

In order to mathematically prove this important result, let  $\mathbf{r}$  be the vector that defines the position of the points on a space curve. One can write the following equation:

$$\mathbf{r}(\alpha + \Delta\alpha) = \mathbf{r}(\alpha) + \Delta\mathbf{r} \quad (5.56)$$

If  $\Delta\alpha$  is assumed small,  $\Delta\mathbf{r}$  defines the tangent vector. In this case, if  $s$  is assumed to be the arc length of the space curve that defines the centerline of the element, then one has

$$(ds)^2 = \Delta\mathbf{r}^T \Delta\mathbf{r} \quad (5.57)$$

This equation shows that in the limit when  $\Delta s$  approaches zero, one has

$$1 = \left( \frac{d\mathbf{r}}{ds} \right)^T \left( \frac{d\mathbf{r}}{ds} \right) \quad (5.58)$$

That is, the tangent vector obtained by differentiation with respect to the arc length is indeed a unit vector.

If a curve is parameterized by its arc length, the derivative of the unit tangent vector defines the *curvature vector*. That is, the curvature vector is defined as

$$\mathbf{r}_{ss}(s) = \frac{d^2\mathbf{r}}{ds^2} = \frac{d\mathbf{r}_s}{ds} \quad (5.59)$$

The magnitude of the curvature vector at a given  $s$  is called the *curvature* and given as

$$\kappa(s) = |\mathbf{r}_{ss}(s)| \quad (5.60)$$

Because the tangent vector  $\mathbf{r}_s(s)$  is a unit vector, the curvature  $\kappa(s)$  measures the rate of change of orientation of the tangent vector, that is, it measures the amount of bending of the curve. The preceding two equations show that linear displacement fields lead to zero curvature and, therefore, such fields are not appropriate for describing the displacement of components subjected to bending. Although one can approximate a curve by a large number of straight segments, in the finite element implementation the use of linear field will require the use of a very large number of finite elements. This increases the dimensions of the problem and can lead to a very inefficient solution procedure.

Because the tangent and curvature vectors are orthogonal, a unit vector along the curvature vector defines the unit normal to the curve  $\mathbf{n}$  given as

$$\mathbf{n}(s) = \frac{\mathbf{r}_{ss}(s)}{\kappa(s)} \quad (5.61)$$

The unit tangent and normal vectors form a plane called the *osculating plane*. The *radius of curvature* of the curve at  $s$  is defined as  $R = 1/\kappa(s)$ . A vector normal to the osculating plane, called the *binomial vector* at  $s$ , is given by

$$\mathbf{b}(s) = \mathbf{r}_s(s) \times \mathbf{n}(s) \quad (5.62)$$

The three orthogonal unit vectors  $\mathbf{r}_s$ ,  $\mathbf{n}$ , and  $\mathbf{b}$  form a coordinate system called the *Frenet frame*.

Differentiating Equation 62 with respect to  $s$  and keeping in mind that the vectors  $\mathbf{r}_{ss}(s)$  and  $\mathbf{n}(s)$  are parallel, one obtains

$$\mathbf{b}_s(s) = \mathbf{r}_{ss}(s) \times \mathbf{n}(s) + \mathbf{r}_s(s) \times \mathbf{n}_s(s) = \mathbf{r}_s(s) \times \mathbf{n}_s(s) \quad (5.63)$$

This equation shows that  $\mathbf{b}_s(s)$  is normal to  $\mathbf{r}_s$ . Furthermore, because  $\mathbf{b}(s)$  is a unit vector,  $\mathbf{b}_s(s)$  and  $\mathbf{b}(s)$  are two orthogonal vectors, and  $\mathbf{b}_s(s)$  is parallel to  $\mathbf{n}$ . Therefore,  $\mathbf{b}_s(s)$  can be written in the following form:

$$\mathbf{b}_s(s) = -\tau(s)\mathbf{n}(s) \quad (5.64)$$

where  $\tau$  is called the *torsion*. The curvature and torsion uniquely define the space curve.



## Theory of Surfaces

Whereas a general space curve can be defined in terms of one parameter, a surface can be completely described in terms of two parameters  $s_1$  and  $s_2$ . In general, a surface can be described in the following parametric form (Goetz, 1970; Kreyszig, 1991):

$$\mathbf{r}(s_1, s_2) = [r_1(s_1, s_2) \quad r_2(s_1, s_2) \quad r_3(s_1, s_2)]^T \quad (5.65)$$

It is required that the mapping in this equation is one to one, and the Jacobian matrix

$$\mathbf{J} = \begin{bmatrix} \frac{\partial \mathbf{r}}{\partial s_1} & \frac{\partial \mathbf{r}}{\partial s_2} \end{bmatrix} = \begin{bmatrix} \frac{\partial r_1}{\partial s_1} & \frac{\partial r_1}{\partial s_2} \\ \frac{\partial r_2}{\partial s_1} & \frac{\partial r_2}{\partial s_2} \\ \frac{\partial r_3}{\partial s_1} & \frac{\partial r_3}{\partial s_2} \end{bmatrix} \quad (5.66)$$

has a rank equal to two. This condition is satisfied if  $(\partial \mathbf{r} / \partial s_1) \times (\partial \mathbf{r} / \partial s_2) \neq 0$ , which implies that the two columns of the Jacobian matrix in the preceding equation are linearly independent. The two vectors  $\mathbf{r}_{s_1} = \partial \mathbf{r} / \partial s_1$  and  $\mathbf{r}_{s_2} = \partial \mathbf{r} / \partial s_2$  represent the two tangent vectors at the point of intersection of the coordinate lines  $s_1$  and  $s_2$ . The unit vector normal to the surface at this point can then be defined as

$$\mathbf{n} = \frac{(\mathbf{r}_{s_1} \times \mathbf{r}_{s_2})}{|\mathbf{r}_{s_1} \times \mathbf{r}_{s_2}|} \quad (5.67)$$

As in the case of curves, the surface can be defined uniquely using local geometric quantities called the *first* and *second fundamental forms*. The *first fundamental form* of a surface is defined as follows:

$$I = d\mathbf{r} \cdot d\mathbf{r} = d\mathbf{r}^T d\mathbf{r} \quad (5.68)$$

This equation shows that the first fundamental form  $I$  can be used as a measure of distance or length. Using the fact that  $d\mathbf{r} = \mathbf{r}_{s_1} ds_1 + \mathbf{r}_{s_2} ds_2$ , the first fundamental form of the preceding equation can be written as

$$\begin{aligned} I &= (\mathbf{r}_{s_1} ds_1 + \mathbf{r}_{s_2} ds_2)^T (\mathbf{r}_{s_1} ds_1 + \mathbf{r}_{s_2} ds_2) \\ &= E_I (ds_1)^2 + 2F_I ds_1 ds_2 + G_I (ds_2)^2 \end{aligned} \quad (5.69)$$

where

$$E_I = \mathbf{r}_{s_1}^T \mathbf{r}_{s_1}, \quad F_I = \mathbf{r}_{s_1}^T \mathbf{r}_{s_2}, \quad G_I = \mathbf{r}_{s_2}^T \mathbf{r}_{s_2} \quad (5.70)$$

These coefficients are called the *coefficients of the first fundamental form*. One can show that distances, angles, and areas on the surface can be expressed in terms of the first fundamental form (Goetz, 1970; Kreyszig, 1991).

The *second fundamental form* of a surface is defined as

$$\begin{aligned} II &= -d\mathbf{r} \cdot d\mathbf{n} = -(\mathbf{r}_{s_1} ds_1 + \mathbf{r}_{s_2} ds_2)^T (\mathbf{n}_{s_1} ds_1 + \mathbf{n}_{s_2} ds_2) \\ &= L_{II} (ds_1)^2 + 2M_{II} ds_1 ds_2 + N_{II} (ds_2)^2 \end{aligned} \quad (5.71)$$

where  $\mathbf{n}$  is the unit normal and the coefficients of the second fundamental form are defined as

$$L_{II} = -\mathbf{r}_{s_1}^T \mathbf{n}_{s_1}, \quad M_{II} = -\frac{1}{2}(\mathbf{r}_{s_1}^T \mathbf{n}_{s_2} + \mathbf{r}_{s_2}^T \mathbf{n}_{s_1}), \quad N_{II} = -\mathbf{r}_{s_2}^T \mathbf{n}_{s_2} \quad (5.72)$$

Because  $\mathbf{r}_{s_1}$  and  $\mathbf{r}_{s_2}$  are perpendicular to  $\mathbf{n}$  for all values of the parameters  $s_1$  and  $s_2$ , one has the following identities:

$$\left. \begin{aligned} \mathbf{r}_{s_1 s_1}^T \mathbf{n} &= -\mathbf{r}_{s_1}^T \mathbf{n}_{s_1}, & \mathbf{r}_{s_1 s_2}^T \mathbf{n} &= -\mathbf{r}_{s_1}^T \mathbf{n}_{s_2}, \\ \mathbf{r}_{s_2 s_1}^T \mathbf{n} &= -\mathbf{r}_{s_2}^T \mathbf{n}_{s_1}, & \mathbf{r}_{s_2 s_2}^T \mathbf{n} &= -\mathbf{r}_{s_2}^T \mathbf{n}_{s_2} \end{aligned} \right\} \quad (5.73)$$

Using these identities, the coefficients of the second fundamental form can be written in an alternate form as follows:

$$L_{II} = \mathbf{r}_{s_1 s_1}^T \mathbf{n}, \quad M_{II} = \mathbf{r}_{s_1 s_2}^T \mathbf{n}, \quad N_{II} = \mathbf{r}_{s_2 s_2}^T \mathbf{n} \quad (5.74)$$

where  $\mathbf{r}_{s_i s_j} = (\partial^2 \mathbf{r} / \partial s_i \partial s_j)$ . Using the preceding equation, and the fact that

$$d^2 \mathbf{r} = \mathbf{r}_{s_1 s_1} (ds_1)^2 + 2\mathbf{r}_{s_1 s_2} ds_1 ds_2 + \mathbf{r}_{s_2 s_2} (ds_2)^2, \quad (5.75)$$

one can show that the second fundamental form can be written in the following alternate form:

$$II = d^2 \mathbf{r} \cdot \mathbf{n} \quad (5.76)$$

This equation can be used to measure the rate of change of orientation of the tangent plane. The coefficients of the second fundamental form can be used to determine the nature of the surface in the neighborhood of an arbitrary point  $P$ . If  $L_{II}N_{II} - M_{II}^2 > 0$ , the surface is called *elliptic*. If  $L_{II}N_{II} - M_{II}^2 < 0$ , the surface is called *hyperbolic*. If  $L_{II}N_{II} - M_{II}^2 = 0$ , the surface is called *parabolic*. If  $L_{II} = M_{II} = N_{II} = 0$ , the surface is called *planar*. Figure 6 shows examples of such surface geometry

## Surface Curvature

One can always define a curve on a surface if the parameters  $s_1$  and  $s_2$  are expressed in terms of one parameter  $\alpha$ . Let  $\mathbf{c} = \mathbf{c}(s_1(\alpha), s_2(\alpha))$  be a regular curve defined on the surface  $\mathbf{r} = \mathbf{r}(s_1, s_2)$ . The *normal curvature vector* to the curve  $\mathbf{c}$  at point  $P$  denoted by  $\mathbf{K}_n$  is defined as the projection of the curvature vector  $\mathbf{c}_{ss}$  of the curve onto the normal  $\mathbf{n}$  to the surface at point  $P$  and is given by

$$\mathbf{K}_n = (\mathbf{c}_{ss} \cdot \mathbf{n})\mathbf{n} \quad (5.77)$$

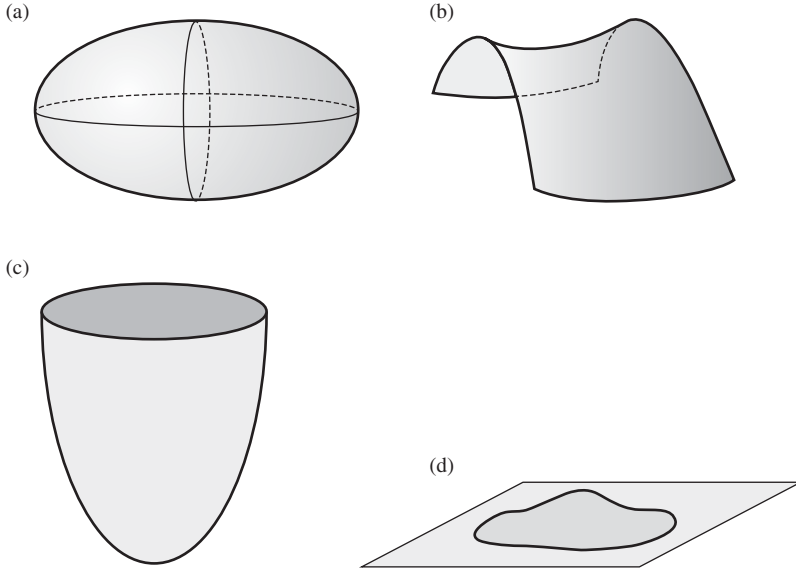


**Figure 5.6** Surface geometry. (a) Elliptic surface, (b) hyperbolic surface, (c) parabolic surface, and (d) planar surface

In this equation,  $s$  is the arc length of the curve. Note that the curve  $\mathbf{c}$  can be defined as the intersection of a plane that contains the tangent to  $\mathbf{c}$  and the normal vector. The norm of the normal curvature vector defined in the preceding equation is called the *normal curvature* and is defined as

$$k_n = \mathbf{c}_{ss} \cdot \mathbf{n} \quad (5.78)$$

Recall that the curvature vector of the curve at a point  $P$  on the surface  $\mathbf{r}$  is given by

$$\mathbf{c}_{ss} = \frac{d\mathbf{r}_s}{ds} = \frac{d\mathbf{r}_s}{d\alpha} \left( \frac{d\alpha}{ds} \right) = \frac{1}{|d\mathbf{r}/d\alpha|} \frac{d\mathbf{r}_s}{d\alpha} \quad (5.79)$$

where  $\mathbf{r}_s$  is the tangent vector to the curve at  $P$  and  $s$  is the curve arc length. In deriving the preceding equation, one utilized the fact that  $|d\mathbf{r}/d\alpha| = |\mathbf{r}_s| (ds/d\alpha) = (ds/d\alpha)$ , which is the consequence of the fact that  $|\mathbf{r}_s| = 1$ . Because  $\mathbf{r}_s$  is orthogonal to  $\mathbf{n}$ , one has  $(d/d\alpha)(\mathbf{r}_s^T \mathbf{n}) = 0$ , which leads to

$$\left( \frac{d\mathbf{r}_s}{d\alpha} \right)^T \mathbf{n} = -\mathbf{r}_s^T \frac{d\mathbf{n}}{d\alpha} \quad (5.80)$$

Substituting Equation 79 into Equation 78 and using Equation 80, one obtains

$$k_n = \frac{L_{II}(ds_1)^2 + 2M_{II}ds_1ds_2 + N_{II}(ds_2)^2}{E_I(ds_1)^2 + 2F_I ds_1ds_2 + G_I(ds_2)^2} = \frac{II}{I}, \quad (ds_1)^2 + (ds_2)^2 \neq 0 \quad (5.81)$$

Because the first fundamental form  $I$  is positive, the sign of  $k_n$  depends on the sign of the second fundamental form  $II$ . Using the preceding equation, one can show that  $k_n = 0$  in all directions

for a planar point. For an elliptic point,  $k_n \neq 0$  and has the same sign as the ratio  $ds_1/ds_2$ . In the case of a hyperbolic point,  $k_n$  can be positive, negative, or zero, depending on the sign and value of  $ds_1/ds_2$ . For a parabolic point,  $k_n$  maintains the same sign and it is zero if the second fundamental form  $II$  is equal to zero.

The directions that define the maximum or minimum values of the normal curvature can be obtained by differentiating Equation 81 with respect to the parameters  $s_1$  and  $s_2$ , and setting the results equal to zero. That is,

$$\frac{\partial k_n}{\partial(ds_1)} = \frac{\partial k_n}{\partial(ds_2)} = 0 \quad (5.82)$$

Substituting Equation 81 into these equations, one obtains

$$\begin{bmatrix} L_{II} - k_n E_I & M_{II} - k_n F_I \\ M_{II} - k_n F_I & N_{II} - k_n G_I \end{bmatrix} \begin{bmatrix} ds_1 \\ ds_2 \end{bmatrix} = \begin{bmatrix} 0 \\ 0 \end{bmatrix} \quad (5.83)$$

This equation has a nontrivial solution if and only if the determinant of the coefficient matrix is equal to zero, that is,

$$(E_I G_I - F_I^2)(k_n)^2 - (E_I N_{II} + G_I L_{II} - 2F_I M_{II})k_n + L_{II} N_{II} - M_{II}^2 = 0 \quad (5.84)$$

The solution of this quadratic equation defines two roots  $k_1$  and  $k_2$ . These two roots, which are called the *principal curvatures*, can be substituted into Equation 83 to determine the *principal directions*. The *mean curvature*  $K_m$  and the *Gaussian curvature*  $k_G$  at a point  $P$  on the surface are defined in terms of the principal curvatures as

$$K_m = \frac{1}{2}(k_1 + k_2), \quad K_G = k_1 k_2 \quad (5.85)$$

These surface definitions as well as the analysis of curve and surface geometry presented in this section are important to understand the behavior of beams, plates, and shells. Some of the obtained geometric results shed light on the order of approximation that must be used when employing the finite element method to solve beam, plate, and shell problems. For example, as previously discussed, the curvature is obtained from the second derivative of the position vector. Therefore, finite elements that employ linear or bilinear approximation cannot be effectively used in bending problems because the curvature will always be equal to zero. When these linear and bilinear elements are employed, one must use a very fine mesh in order to be able to represent a space curve or a shell by straight lines or flat sections, respectively. This approach tends to be very inefficient and, therefore, the use of structural finite elements that are based on higher-order interpolations is recommended. Some of these ANCF elements are discussed in the following sections.

## 5.7 TWO-DIMENSIONAL EULER-BERNOULLI BEAM ELEMENT

The Euler–Bernoulli beam element presented in this section has two nodes. Each node  $k$  for an element  $j$  has four coordinates; two translations  $\mathbf{r}^{jk}$ , and two gradient coordinates  $\mathbf{r}_{x_1}^{jk}$ . Therefore, the vector of nodal coordinates has eight elements and is defined as

$$\mathbf{e}^j = \left[ \mathbf{r}^{jT}(x_1^j = 0) \quad \mathbf{r}_{x_1}^{jT}(x_1^j = 0) \quad \mathbf{r}^{jT}(x_1^j = l) \quad \mathbf{r}_{x_1}^{jT}(x_1^j = l) \right]^T \quad (5.86)$$

The shape function matrix of the element can be defined by using the following interpolation functions:

$$\mathbf{r}^j = \begin{bmatrix} r_1 \\ r_2 \end{bmatrix} = \begin{bmatrix} a_0 + a_1 x_1 + a_2 (x_1)^2 + a_3 (x_1)^3 \\ b_0 + b_1 x_1 + b_2 (x_1)^2 + b_3 (x_1)^3 \end{bmatrix}^j \quad (5.87)$$

where  $a_i$  and  $b_i$ ,  $i=0, 1, 2, 3$ , are the polynomial coefficients. Using this interpolation and the nodal coordinates of Equation 86, one can follow the procedure previously described in this chapter to define the element shape function matrix. For this element, the shape function matrix  $\mathbf{S}^j$  is a  $2 \times 8$  matrix and is defined as

$$\mathbf{S}^j = [s_1 \mathbf{I} \quad s_2 \mathbf{I} \quad s_3 \mathbf{I} \quad s_4 \mathbf{I}] \quad (5.88)$$

In this equation,  $\mathbf{I}$  is a  $2 \times 2$  identity matrix and

$$\left. \begin{aligned} s_1 &= 1 - 3\xi^2 + 2\xi^3, & s_2 &= l(\xi - 2\xi^2 + \xi^3), \\ s_3 &= 3\xi^2 - 2\xi^3, & s_4 &= l(-\xi^2 + \xi^3) \end{aligned} \right\} \quad (5.89)$$

where  $\xi = x_1^j/l$ . This beam element shape function matrix, which does not allow for shear deformations, was also used by Milner (1981) to study static problems.

### Kinematics of the Element

In order to understand the kinematics of the two-dimensional Euler–Bernoulli finite element discussed in this section, some differential geometry results are required. For simplicity, the superscript that indicates the element number is dropped in the following discussion.

The displacement field of the Euler–Bernoulli beam element is function of one spatial coordinate  $x_1$  only. For a given, deformed shape of the element, the element centerline defines a space curve. The *unit tangent* to this space curve is defined by the vector

$$\mathbf{r}_s = \frac{\partial \mathbf{r}}{\partial s} = \frac{\partial \mathbf{r}}{\partial x_1} \left( \frac{\partial x_1}{\partial s} \right) \quad (5.90)$$

In this equation,  $s$  is the arc length. Because  $\mathbf{r}_s$  is a unit vector, that is,  $\mathbf{r}_s^T \mathbf{r}_s = 1$ , it follows by differentiating this equation that  $\mathbf{r}_s^T \mathbf{r}_{ss} = 0$ . This implies that the derivative of the unit tangent with respect to the arc length defines the *curvature vector*  $\mathbf{r}_{ss}$ , which is perpendicular to  $\mathbf{r}_s$ . The magnitude of the curvature vector  $\kappa$ , called the *curvature*, measures the rate of change of the tangent vector  $\mathbf{r}_s$  along the arc length. Therefore, the curvature, as previously defined in this chapter, is

$$\kappa = |\mathbf{r}_{ss}| \quad (5.91)$$

This curvature can be expressed in terms of derivatives with respect to the element spatial coordinate  $x_1$  (Goetz, 1970; Dmitrochenko and Pogorelov, 2003; Gerstmayr and Shabana, 2006). To this end, recall that  $\mathbf{r}_s = \mathbf{r}_{x_1} (dx_1/ds)$ . Because  $\mathbf{r}_{x_1}$  has the same direction as the unit tangent  $\mathbf{r}_s$ , one can write  $\mathbf{r}_s = \mathbf{r}_{x_1}/|\mathbf{r}_{x_1}|$  and  $dx_1/ds = 1/|\mathbf{r}_{x_1}|$ . It follows that

$$\mathbf{r}_{ss} = \frac{d}{ds} \left( \frac{\mathbf{r}_{x_1}}{|\mathbf{r}_{x_1}|} \right) = \frac{\mathbf{r}_{x_1 x_1}}{|\mathbf{r}_{x_1}|} \frac{dx_1}{ds} + \mathbf{r}_{x_1} \frac{d}{ds} \left( \frac{1}{|\mathbf{r}_{x_1}|} \right) = \frac{\mathbf{r}_{x_1 x_1}}{|\mathbf{r}_{x_1}|^2} + \mathbf{r}_{x_1} \frac{d}{ds} \left( \frac{1}{|\mathbf{r}_{x_1}|} \right) \quad (5.92)$$

Because  $\mathbf{r}_s$  is a unit vector perpendicular to  $\mathbf{r}_{ss}$ , the curvature can be written upon utilizing the preceding equation as

$$\kappa = |\mathbf{r}_s \times \mathbf{r}_{ss}| = \left| \frac{\mathbf{r}_{x_1}}{|\mathbf{r}_{x_1}|} \times \left( \frac{\mathbf{r}_{x_1 x_1}}{|\mathbf{r}_{x_1}|^2} + \mathbf{r}_{x_1} \frac{d}{ds} \left( \frac{1}{|\mathbf{r}_{x_1}|} \right) \right) \right| = \frac{|\mathbf{r}_{x_1} \times \mathbf{r}_{x_1 x_1}|}{|\mathbf{r}_{x_1}|^3} \quad (5.93)$$

This definition of the curvature does not imply any linearization or simplifications and can be used to define the bending strain in the large-deformation analysis of the Euler–Bernoulli beam element described in this section.

The discussion on the geometry presented in this section shows that if linear interpolation instead of the cubic interpolation is used for this element, the curvature will be zero everywhere inside the element, as previously pointed out. That is, one cannot bend this element. Therefore, a finite element mesh that employs linear interpolation will require a very large number of elements to achieve convergence in beam-bending problems. If quadratic interpolation is used, one obtains, at most, constant curvature. Elements that employ quadratic interpolations lead to zero shear forces as can be demonstrated using simple equilibrium considerations. It is, therefore, recommended to use cubic interpolation to represent beam bending.

### Formulation of the Element Elastic Forces

In the case of the Euler–Bernoulli beam element, one can define one gradient vector only because the element assumed displacement field is expressed in terms of one spatial coordinate  $x_1$ . That is, this element is gradient deficient. Therefore, for this element, the only nonzero strain component is the axial strain, and the shear strain is assumed to be zero. When one or more gradient vectors are missing, the formulation of the elastic forces using the general continuum mechanics approach is not straightforward. Elements that are not gradient deficient have two gradient vectors in the planar analysis and three gradient vectors in the spatial analysis.

Because one spatial coordinate only is used for the Euler–Bernoulli beam element,  $\mathbf{r}_{x_2}$  cannot be determined using the element assumed displacement field. In this case, the normal to the centerline of the element remains normal, and as a consequence, the shear deformation is assumed to be equal to zero and the cross section of the element is assumed to remain rigid and perpendicular to the element centerline. For this shear nondeformable element, only the strain component  $\varepsilon_{11}$  can have nonzero value, and it measures only the extensional strain. The bending strain can be defined using the curvature. In the case of two-dimensional elements, which are not gradient deficient, the component  $\varepsilon_{11}$  is a function of the spatial coordinate  $x_2$ , and such a component contributes to the bending strain of the finite element, as will be demonstrated in later sections. In this case of shear deformable elements, the use of the curvature definition to define the bending strain energy is not necessary.

The elastic forces of the two-dimensional Euler–Bernoulli beam element can be obtained by using the virtual work or the strain energy. The virtual work of the elastic forces can be written as

$$\delta W_s = \int_0^l EA \varepsilon_{11} \delta \varepsilon_{11} dx_1 + \int_0^l EI \kappa \delta \kappa dx_1 \quad (5.94)$$

In this equation,  $l$  is the length of the element,  $E$  is the modulus of elasticity,  $A$  is the cross-sectional area, and  $I$  is the second moment of area. It is assumed in the preceding equation that the curvature and strain are defined in terms of the reference spatial coordinate  $x_1$ . Therefore, one can use undeformed geometry data in the integrations of the preceding equation.

The strain energy for the Euler–Bernoulli beam element can be written as

$$U = \frac{1}{2} \int_0^l EA(\epsilon_{11})^2 dx_1 + \frac{1}{2} \int_0^l EI\kappa^2 dx_1 \quad (5.95)$$

The first integral in the preceding equation represents the strain energy due to the extension, whereas the second integral is the strain energy due to bending. It is important to note that because this element is gradient deficient, one must resort to the curvature definition in order to account for the bending deformation. The curvature definition requires the evaluation of the second derivatives, which is one of the disadvantages of this element. If the element has a complete set of gradients, as it is the case of the shear deformable beam element discussed in the following section, one can use the Green–Lagrange strain tensor to evaluate the elastic forces. This tensor is a function of only first derivatives of the absolute position vector.

The expression of the total strain energy presented in the preceding equation can be used in the large-deformation analysis because no assumptions are made regarding the amount of axial and bending deformations. The strain and curvature can be expressed in terms of the element nodal coordinates. The vector of the elastic forces can be determined using the virtual work as previously described or by using the strain energy as  $\mathbf{Q}_s = -(\partial U / \partial \mathbf{e})^T$ . Different elastic force models can be developed for the Euler–Bernoulli beam element presented in this section, as discussed in the literature (Berzeri and Shabana, 2000).

### Special Case

As previously mentioned, the expression of the strain energy presented in this section imposes no restrictions on the amount of the axial and bending deformations of the element. The resulting elastic forces are nonlinear functions of the element nodal coordinates. These nonlinear forces include terms that couple the axial and bending deformations. This coupling has a significant effect on the dynamics of rotating beams. The ANCF element automatically accounts for this coupling when nonlinear strain displacement relationships as the ones employed in this section are used (Berzeri and Shabana, 2002).

In many *structural applications*, Euler–Bernoulli beam theory has been used for small-deformation analysis. In these structural applications, the rigid-body motion is eliminated. In this special case, an assumption is made that  $s = x_1$ . Using this assumption, one has  $|\mathbf{r}_{x_1}| \approx 1$ . It follows that the curvature in this special case can be written as

$$\kappa = \frac{|\mathbf{r}_{x_1} \times \mathbf{r}_{x_1 x_1}|}{|\mathbf{r}_{x_1}|^3} \approx |\mathbf{r}_{x_1 x_1}| \quad (5.96)$$

Recall that the curvature vector can be written as

$$\mathbf{r}_{x_1 x_1} = [(r_1)_{x_1 x_1} \ (r_2)_{x_1 x_1}]^T \quad (5.97)$$

For structural systems in which the rigid-body motion is eliminated,  $r_1 = u$  is the axial displacement, and  $r_2 = v$  is the bending displacement. In this case, the strain  $\epsilon_{11}$  is approximated as  $\epsilon_{11} = u_{,x_1}$ . Furthermore, the effect of the derivatives of  $(r_1)_{,x_1x_1}$  on the curvature is neglected. The curvature can then be approximated as  $\kappa = v_{,x_1x_1}$ . Using these assumptions, the strain energy that does not account for the coupling between the axial and bending displacements can be written as

$$U = \frac{1}{2} \int_0^l EA(u_{,x_1})^2 dx_1 + \frac{1}{2} \int_0^l EI(v_{,x_1x_1})^2 dx_1 \quad (5.98)$$

This expression for the strain energy can only be used in the small-deformation analysis of structural systems, and the use of such an expression in the case of rotating beams can lead to significant errors as the result of the neglect of the effect of the coupling between bending and axial deformations.

## 5.8 TWO-DIMENSIONAL SHEAR DEFORMABLE BEAM ELEMENT

The two-dimensional shear deformable beam element, which was used in several examples in this book, has two nodes. Each node  $k$  of element  $j$  has six degrees of freedom: two translational coordinates  $\mathbf{r}^{jk}$  and four gradient coordinates defined by the two vectors  $\mathbf{r}_{x_1}^{jk}$  and  $\mathbf{r}_{x_2}^{jk}$ . The vector of nodal coordinates has 12 elements and is defined at  $\eta = 0$  as

$$\mathbf{e}^j = \begin{bmatrix} \mathbf{r}^{jT} (x_1^j = 0) & \mathbf{r}_{x_1}^{jT} (x_1^j = 0) & \mathbf{r}_{x_2}^{jT} (x_1^j = 0) \\ \mathbf{r}^{jT} (x_1^j = l) & \mathbf{r}_{x_1}^{jT} (x_1^j = l) & \mathbf{r}_{x_2}^{jT} (x_1^j = l) \end{bmatrix}^T \quad (5.99)$$

The shape function matrix for this element is given by

$$\mathbf{S}^j = [s_1 \mathbf{I} \quad s_2 \mathbf{I} \quad s_3 \mathbf{I} \quad s_4 \mathbf{I} \quad s_5 \mathbf{I} \quad s_6 \mathbf{I}] \quad (5.100)$$

where  $\mathbf{I}$  is a  $2 \times 2$  identity matrix and the shape functions  $s_i$ ,  $i = 1, 2, \dots, 6$ , were obtained in Example 2 as (Omar and Shabana, 2001)

$$\left. \begin{aligned} s_1 &= 1 - 3\xi^2 + 2\xi^3, & s_2 &= l(\xi - 2\xi^2 + \xi^3), \\ s_3 &= l(\eta - \xi\eta), & s_4 &= 3\xi^2 - 2\xi^3, \\ s_5 &= l(-\xi^2 + \xi^3), & s_6 &= l\xi\eta \end{aligned} \right\} \quad (5.101)$$

where  $\xi = x_1^j/l$  and  $\eta = x_2^j/l$ . Note that this fully parameterized element has a complete set of gradient vectors and allows for the deformation of the cross section. Therefore, the element relaxes the assumptions of the Euler–Bernoulli beam theory. Because the cross section does not remain rigid when this element is used, one also obtains a model that is more general than the one based on Timoshenko beam theory.



## Formulation of the Elastic Forces

Because the shear deformable beam element used in this section is not gradient deficient, one can use the general continuum mechanics approach to formulate the element elastic forces. For simplicity, superscript  $j$  that indicates the element number will be again dropped in the discussion presented in the remainder of this section. The matrix of position vector gradients of the element can be written in this case as

$$\mathbf{J} = [\mathbf{r}_{x_1} \quad \mathbf{r}_{x_2}] \quad (5.102)$$

The Green–Lagrange strain tensor can then be evaluated to define two normal strain components  $\varepsilon_{11}$  and  $\varepsilon_{22}$ , and one shear strain component  $\varepsilon_{12}$ . The general procedure described previously in this chapter can be employed to define the elastic forces by using the constitutive equations that relate the second Piola–Kirchhoff stress tensor to the Green–Lagrange strain tensor.

The interpolating polynomials used to develop the two-dimensional shear deformable element shape function matrix were introduced in Chapter 1. These polynomials were defined as

$$\mathbf{r} = \begin{bmatrix} r_1 \\ r_2 \end{bmatrix} = \begin{bmatrix} a_0 + a_1 x_1 + a_2 x_2 + a_3 x_1 x_2 + a_4 (x_1)^2 + a_5 (x_1)^3 \\ b_0 + b_1 x_1 + b_2 x_2 + b_3 x_1 x_2 + b_4 (x_1)^2 + b_5 (x_1)^3 \end{bmatrix} \quad (5.103)$$

where  $a_i$  and  $b_i$ ,  $i = 0, 1, \dots, 5$ , are the polynomial coefficients. Note that using this representation, which is cubic in  $x_1$  and linear in  $x_2$ , one can write the vector  $\mathbf{r}$  as

$$\mathbf{r} = \mathbf{r}_0 + x_2 \mathbf{r}_{x_2} \quad (5.104)$$

where  $\mathbf{r}_0 = \mathbf{r}(x_2 = 0)$  defines the global position of the material points on the centerline of the finite element and  $x_2 \mathbf{r}_{x_2}$  defines the location of the points on the cross section with respect to the centerline. Note that if  $\mathbf{r}_{x_2}$  remains a unit vector perpendicular to the tangent to the centerline, one obtains the Euler–Bernoulli beam model. If, on the other hand,  $\mathbf{r}_{x_2}$  remains a unit vector that does not remain perpendicular to the tangent to the centerline, one obtains a model similar to the Timoshenko beam model. Using the preceding equation, the strain components can be written as (Sugiyama et al., 2006)

$$\left. \begin{aligned} \varepsilon_{11} &= \frac{1}{2} (\mathbf{r}_{x_1}^T \mathbf{r}_{x_1} - 1) = \frac{1}{2} (\mathbf{r}_{0x_1}^T \mathbf{r}_{0x_1} - 1) + x_2 \mathbf{r}_{0x_1}^T \mathbf{r}_{x_1 x_2} + \frac{1}{2} (x_2)^2 \mathbf{r}_{x_1 x_2}^T \mathbf{r}_{x_1 x_2} \\ \varepsilon_{22} &= \frac{1}{2} (\mathbf{r}_{x_2}^T \mathbf{r}_{x_2} - 1), \quad \varepsilon_{12} = \frac{1}{2} (\mathbf{r}_{x_2}^T \mathbf{r}_{0x_1} + x_2 \mathbf{r}_{x_2}^T \mathbf{r}_{x_1 x_2}) \end{aligned} \right\} \quad (5.105)$$

In this equation,  $\mathbf{r}_{0x_1}$  is the tangent to the centerline of the element, and  $\mathbf{r}_{x_1 x_2}$  describes the rate of change of the gradient vector  $\mathbf{r}_{x_2}$  with respect to the spatial coordinate  $x_1$ . Because a linear interpolation with respect to  $x_2$  is used, one can show for the finite element described in this section that

$$\mathbf{r}_{x_1 x_2} = \frac{1}{l} (\mathbf{r}_{x_2}^2 - \mathbf{r}_{x_2}^1) \quad (5.106)$$

where  $\mathbf{r}_{x_2}^k$  is the gradient vector  $\mathbf{r}_{x_2}$  defined at node  $k$ ,  $k = 1, 2$ . One can verify that in the case of a rigid-body motion  $\mathbf{r}_{x_1 x_2}$  is identically equal to zero. In general, this vector is constant

everywhere inside the element, that is, this vector does not depend on the spatial coordinate  $x_1$ . The fact that the gradient vector  $\mathbf{r}_{x_2}$  can vary only linearly with respect to  $x_1$  regardless of the load applied can introduce excessive stiffness, leading to the locking problem. This problem becomes more serious when thin and stiff structures are modeled. The use of different orders of spatial coordinate interpolations leads to different orders of interpolations for deformations and strain components. When some strain components are restricted to take certain values as the result of a low-order interpolation, the element tends to have unreasonable high stiffness. Different approaches for solving this problem can be used and these approaches, which are well documented in the finite element literature, are briefly discussed in a later section.

### 5.9 THREE-DIMENSIONAL CABLE ELEMENT

The three-dimensional cable element is a simple element that can be efficiently used for cable and belt applications. The element does not have the degree of freedom of the rigid-body rotation about its own axis. Therefore, this element should not be used in applications subject to arbitrary three-dimensional rigid-body rotations. This element, which does not allow for shear deformation, has two nodes. Each node  $k$  of element  $j$  has six coordinates: three translational coordinates  $\mathbf{r}^{jk}$  and three gradient coordinates defined by the vector  $\mathbf{r}_{x_1}^{jk}$ . Therefore, the vector of nodal coordinates has 12 elements and is defined as

$$\mathbf{e}^j = \left[ \mathbf{r}^{jT} (x_1^j = 0) \quad \mathbf{r}_{x_1}^{jT} (x_1^j = 0) \quad \mathbf{r}^{jT} (x_1^j = l) \quad \mathbf{r}_{x_1}^{jT} (x_1^j = l) \right]^T \quad (5.107)$$

The interpolation used for the cable element is given by

$$\mathbf{r} = \begin{bmatrix} r_1 \\ r_2 \\ r_3 \end{bmatrix} = \begin{bmatrix} a_0 + a_1 x_1 + a_2 (x_1)^2 + a_3 (x_1)^3 \\ b_0 + b_1 x_1 + b_2 (x_1)^2 + b_3 (x_1)^3 \\ c_0 + c_1 x_1 + c_2 (x_1)^2 + c_3 (x_1)^3 \end{bmatrix} \quad (5.108)$$

In this interpolation, only one spatial coordinate,  $x_1$ , is used. The shape function matrix  $\mathbf{S}^j$  is a  $3 \times 12$  matrix defined as (Gerstmayr and Shabana, 2006)

$$\mathbf{S}^j = [s_1 \mathbf{I} \quad s_2 \mathbf{I} \quad s_3 \mathbf{I} \quad s_4 \mathbf{I}] \quad (5.109)$$

In this equation,  $\mathbf{I}$  is a  $3 \times 3$  identity matrix, and

$$\left. \begin{aligned} s_1 &= 1 - 3\xi^2 + 2\xi^3, & s_2 &= l(\xi - 2\xi^2 + \xi^3), \\ s_3 &= 3\xi^2 - 2\xi^3, & s_4 &= l(-\xi^2 + \xi^3) \end{aligned} \right\} \quad (5.110)$$

where  $\xi = x_1^j / l$  and  $l$  is the length of the element.

The cable element is gradient deficient because only one gradient vector is used in the vector of nodal coordinates. In this case, the elastic forces can be formulated using the virtual work or the strain energy. The virtual work of the elastic forces is given as

$$\delta W_s = \int_0^l EA \varepsilon_{11} \delta \varepsilon_{11} dx_1 + \int_0^l EI \kappa \delta \kappa dx_1 \quad (5.111)$$

where  $E$  is the modulus of elasticity,  $A$  is the element cross-sectional area,  $I$  is the second moment of area, and  $\kappa$  is the curvature. The effect of the twist of the cable element can also be accounted for by considering the virtual work or the strain energy due to the torsion of the element space curve. Alternatively, the elastic forces of the cable element can be evaluated using the following expression of the strain energy:

$$U = \frac{1}{2} \int_0^l EA(\epsilon_{11})^2 dx_1 + \frac{1}{2} \int_0^l EI\kappa^2 dx_1 \quad (5.112)$$

Several investigations have shown that the simple cable element discussed in this section can be very efficient in special applications; particularly, in cable and belt drive applications.

### 5.10 THREE-DIMENSIONAL BEAM ELEMENT

This is the fully parameterized element, which was used in Example 1. This element that accounts for shear deformation and rotary inertia has two nodes. Each node  $k$  of element  $j$  has 12 coordinates: 3 translational coordinates  $\mathbf{r}^{jk}$  and 9 gradient coordinates defined by the 3 vectors  $\mathbf{r}_{x_1}^{jk}$ ,  $\mathbf{r}_{x_2}^{jk}$ , and  $\mathbf{r}_{x_3}^{jk}$ . Therefore, the element has 24 nodal coordinates, which can be written in a vector form as

$$\mathbf{e}^j = \begin{bmatrix} \mathbf{e}^{1T} & \mathbf{e}^{2T} \end{bmatrix}^T \quad (5.113)$$

In this equation,

$$\mathbf{e}^{jk} = \begin{bmatrix} \mathbf{r}^{jkT} & \mathbf{r}_{x_1}^{jkT} & \mathbf{r}_{x_2}^{jkT} & \mathbf{r}_{x_3}^{jkT} \end{bmatrix}^T, \quad k = 1, 2 \quad (5.114)$$

For Node 1, the coordinates are defined at  $x_1^j = x_2^j = x_3^j = 0$ , and for Node 2, the coordinates are defined at  $x_1^j = l$  and  $x_2^j = x_3^j = 0$ . The interpolation polynomials used for this element are given in Example 1. Using these interpolating polynomials, the element shape function matrix is defined as (Yakoub and Shabana, 2001)

$$\mathbf{S}^j = \begin{bmatrix} s_1 \mathbf{I} & s_2 \mathbf{I} & s_3 \mathbf{I} & s_4 \mathbf{I} & s_5 \mathbf{I} & s_6 \mathbf{I} & s_7 \mathbf{I} & s_8 \mathbf{I} \end{bmatrix} \quad (5.115)$$

where  $\mathbf{I}$  is the  $3 \times 3$  identity matrix and the shape functions  $s_i$ ,  $i = 1, 2, \dots, 8$ , are defined as

$$\left. \begin{aligned} s_1 &= 1 - 3\xi^2 + 2\xi^3, & s_2 &= l(\xi - 2\xi^2 + \xi^3), \\ s_3 &= l(\eta - \xi\eta), & s_4 &= l(\zeta - \xi\zeta), \\ s_5 &= 3\xi^2 - 2\xi^3, & s_6 &= l(-\xi^2 + \xi^3), \\ s_7 &= l\xi\eta, & s_8 &= l\xi\zeta \end{aligned} \right\} \quad (5.116)$$

where  $\xi = x_1^j/l$ ,  $\eta = x_2^j/l$ ,  $\zeta = x_3^j/l$ .

Two methods can be used to formulate the elastic forces of the three-dimensional beam element presented in this section because such an element is not gradient deficient. The first method is based on the general continuum mechanics approach, as previously described in this chapter. In this case, the nonlinear strain displacement relationships are defined in terms

of the matrix of the position vector gradients. It is recommended to use the general continuum mechanics approach in the case of very flexible structures because the use of this approach leads to coupled deformation modes that can be significant in the case of large-deformation problems (Hussein et al., 2007). In the case of very thin and very stiff structures, the use of the general continuum mechanics approach is not recommended because the coupled deformation modes can have very high frequencies that lead to deterioration in the element performance. In the case of very thin and stiff structures, one can use an alternate approach, called the *elastic line approach* (Schwab and Meijaard, 2005). In the elastic line approach, the following gradient vectors are defined at the element centerline:

$$\mathbf{r}_{0x_1} = \mathbf{r}_{x_1}(x_1, 0, 0), \quad \mathbf{r}_{x_2} = \mathbf{r}_{x_2}(x_1, 0, 0), \quad \mathbf{r}_{x_3} = \mathbf{r}_{x_3}(x_1, 0, 0) \quad (5.117)$$

The following strain and curvature components can also be defined:

$$\left. \begin{aligned} \varepsilon_{011} &= \frac{1}{2} (\mathbf{r}_{0x_1} \cdot \mathbf{r}_{0x_1} - 1), \quad \varepsilon_{22} = \frac{1}{2} (\mathbf{r}_{x_2} \cdot \mathbf{r}_{x_2} - 1), \quad \varepsilon_{33} = \frac{1}{2} (\mathbf{r}_{x_3} \cdot \mathbf{r}_{x_3} - 1), \\ \gamma_{012} &= \mathbf{r}_{0x_1} \cdot \mathbf{r}_{x_2}, \quad \gamma_{013} = \mathbf{r}_{0x_1} \cdot \mathbf{r}_{x_3}, \quad \gamma_{23} = \mathbf{r}_{x_2} \cdot \mathbf{r}_{x_3}, \\ \theta &= \frac{1}{2} (\mathbf{r}_{x_1x_2} \cdot \mathbf{r}_{x_3} - \mathbf{r}_{x_2} \cdot \mathbf{r}_{x_1x_3}), \quad \bar{\kappa}_{0x_2} = \frac{\mathbf{r}_{x_3} \cdot \mathbf{r}_{0x_1x_1}}{|\mathbf{r}_{x_3}| |\mathbf{r}_{0x_1x_1}|}, \quad \bar{\kappa}_{0x_3} = \frac{\mathbf{r}_{x_2} \cdot \mathbf{r}_{0x_1x_1}}{|\mathbf{r}_{x_2}| |\mathbf{r}_{0x_1x_1}|} \end{aligned} \right\} \quad (5.118)$$

where  $\varepsilon_{011}$ ,  $\varepsilon_{22}$ , and  $\varepsilon_{33}$  are the normal strains;  $\gamma_{012}$ ,  $\gamma_{013}$ , and  $\gamma_{23}$  are the shear strains;  $\theta$  is the twist; and  $\bar{\kappa}_{0x_2}$  and  $\bar{\kappa}_{0x_3}$  are the expressions of the bending curvature. The strain energy for the element based on the elastic line approach can be written as

$$U = \frac{1}{2} \int_V \boldsymbol{\varepsilon}_0^T \mathbf{E} \boldsymbol{\varepsilon}_0 dV + U_b + U_t \quad (5.119)$$

In this equation,  $\mathbf{E}$  is an appropriate matrix of elastic coefficients, and

$$\boldsymbol{\varepsilon}_0 = [\varepsilon_{011} \quad \varepsilon_{22} \quad \varepsilon_{33} \quad \gamma_{012} \quad \gamma_{013} \quad \gamma_{23}]^T \quad (5.120)$$

The scalars  $U_b$  and  $U_t$  represent the strain energy due to bending and twist and are defined as

$$U_b = \frac{1}{2} \int_0^l \left\{ EI_{x_2} (\bar{\kappa}_{0x_2})^2 + EI_{x_3} (\bar{\kappa}_{0x_3})^2 \right\} dx_1, \quad U_t = \frac{1}{2} \int_0^l GI_p (\theta)^2 dx_1 \quad (5.121)$$

where  $E$  and  $G$  are, respectively, the modulus of elasticity and modulus of rigidity;  $I_{x_2}$  and  $I_{x_3}$  are the second moments of area about the element  $x_2$  and  $x_3$  axes, respectively; and  $I_p$  is the polar second moment of area. The strain energy  $U$  can be used to evaluate the elastic forces, as previously described.

Studies have shown that the use of the elastic line approach leads to natural frequencies that are in a good agreement with the analytical solutions that are based on small-deformation assumptions (Schwab and Meijaard, 2005). In the elastic line approach, the coupling between the deformation of the cross section and bending is neglected, thereby leading to a model that is more consistent with the assumptions of the linear theory. When the general continuum

mechanics approach is used, the ANCF-coupled deformation modes, as previously mentioned, can introduce high frequencies in the case of thin and stiff structures due to the cross-sectional deformations.

### 5.11 THIN-PLATE ELEMENT

The three-dimensional thin-plate element is based on Kirchhoff's plate theory. The element, as shown in Figure 7, has four nodal points, and its midsurface is defined by the element spatial coordinates  $x_1^j$  and  $x_2^j$ . Each node has nine degrees of freedom: three translational coordinates  $\mathbf{r}^k$ , and six gradient coordinates defined by the two vectors  $\mathbf{r}_{x_1}^{jk}$  and  $\mathbf{r}_{x_2}^{jk}$ . The element, therefore, has a total of 36 nodal coordinates, which can be written as

$$\mathbf{e}^j = \left[ \mathbf{e}^{j1T} \quad \mathbf{e}^{j2T} \quad \mathbf{e}^{j3T} \quad \mathbf{e}^{j4T} \right]^T \quad (5.122)$$

In this equation,

$$\mathbf{e}^{jk} = \left[ \mathbf{r}^{jkT} \quad \mathbf{r}_{x_1}^{jkT} \quad \mathbf{r}_{x_2}^{jkT} \right]^T, \quad j = 1, 2, 3, 4 \quad (5.123)$$

For Node 1 at point A, the coordinates are defined at  $x_1^j = x_2^j = x_3^j = 0$ ; for Node 2 at point B, the coordinates are defined at  $x_1^j = a$ , and  $x_2^j = x_3^j = 0$ ; for Node 3 at point C, the coordinates are defined at  $x_1^j = a$ ,  $x_2^j = b$ , and  $x_3^j = 0$ ; and for Node 4 at point D, the coordinates are defined at  $x_1^j = 0$ ,  $x_2^j = b$ , and  $x_3^j = 0$ ; where  $a$  and  $b$  are the length and width of the element. The element shape function matrix is given by (Dufva and Shabana, 2005)

$$\mathbf{S}^j = [s_1 \mathbf{I} \quad s_2 \mathbf{I} \quad s_3 \mathbf{I} \quad s_4 \mathbf{I} \quad s_5 \mathbf{I} \quad s_6 \mathbf{I} \quad s_7 \mathbf{I} \quad s_8 \mathbf{I} \quad s_9 \mathbf{I} \quad s_{10} \mathbf{I} \quad s_{11} \mathbf{I} \quad s_{12} \mathbf{I}] \quad (5.124)$$

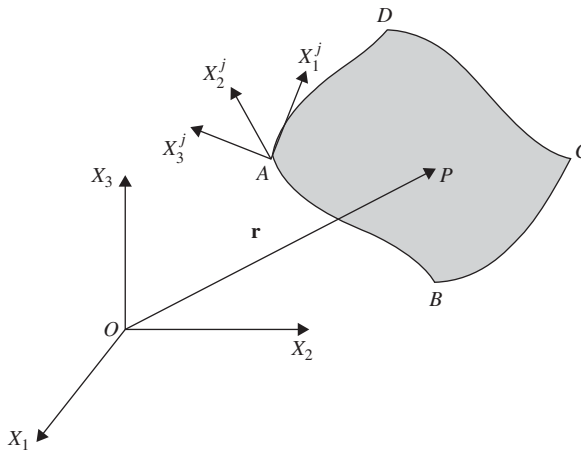


Figure 5.7 Plate element

where  $\mathbf{I}$  is the  $3 \times 3$  identity matrix and the shape functions  $s_i$ ,  $i = 1, 2, \dots, 12$ , are as follows:

$$\left. \begin{aligned} s_1 &= -(\xi - 1)(\eta - 1)(2\eta^2 - \eta + 2\xi^2 - \xi - 1), & s_2 &= -a\xi(\xi - 1)^2(\eta - 1), \\ s_3 &= -b\eta(\eta - 1)^2(\xi - 1), & s_4 &= \xi(2\eta^2 - \eta - 3\xi + 2\xi^2)(\eta - 1), \\ s_5 &= -a\xi^2(\xi - 1)(\eta - 1), & s_6 &= b\xi\eta(\eta - 1)^2, \\ s_7 &= -\xi\eta(1 - 3\xi - 3\eta + 2\eta^2 + 2\xi^2), & s_8 &= a\xi^2\eta(\xi - 1), \\ s_9 &= b\xi\eta^2(\eta - 1), & s_{10} &= \eta(\xi - 1)(2\xi^2 - \xi - 3\eta + 2\eta^2), \\ s_{11} &= a\xi\eta(\xi - 1)^2, & s_{12} &= -b\eta^2(\xi - 1)(\eta - 1) \end{aligned} \right\} \quad (5.125)$$

where  $\xi = x_1^j/a$ ,  $\eta = x_2^j/b$ .

Because for the thin-plate element only the coordinate vector  $\mathbf{r}$  and the gradient vectors  $\mathbf{r}_{x_1}$  and  $\mathbf{r}_{x_2}$  are used as nodal coordinates, the element is gradient deficient. The shape function matrix does not depend on the  $x_3$  element coordinate, and therefore, the gradient vector  $\mathbf{r}_{x_3}$  cannot be used as a coordinate vector. Following Kirchhoff theory, the strain energy of a thin plate can be written as the sum of two terms: one term is due to membrane and shear deformations at the plate midsurface, whereas the other term is due to the plate bending and twist. The strain energy can then be written for a thin plate as follows (Dmitrochenko and Pogorelov, 2003; Dufva and Shabana, 2005):

$$U = \frac{1}{2} \int_V \boldsymbol{\varepsilon}^T \mathbf{E}_\varepsilon \boldsymbol{\varepsilon} dV + \frac{1}{2} \int_V \boldsymbol{\kappa}^T \mathbf{E}_\kappa \boldsymbol{\kappa} dV \quad (5.126)$$

where the curvature vector is  $\boldsymbol{\kappa} = [\bar{\kappa}_1 \quad \bar{\kappa}_2 \quad \bar{\kappa}_{12}]^T$  (subscript “0” is omitted here because the shape function matrix does not depend on the element  $x_3$  coordinate), and in the case of orthotropic plate, one has

$$\boldsymbol{\varepsilon} = \begin{bmatrix} \varepsilon_{11} \\ \varepsilon_{22} \\ \varepsilon_{12} \end{bmatrix}, \quad \mathbf{E}_\kappa = \begin{bmatrix} D_{11} & D_{00} & 0 \\ D_{00} & D_{22} & 0 \\ 0 & 0 & D_{12} \end{bmatrix}, \quad \mathbf{E}_\varepsilon = \frac{6}{h^2} \mathbf{E}_k \quad (5.127)$$

In this equation,  $h$  is the plate thickness,  $D_{ij} = E_{ij}h^3/12(1 - \nu_{12}\nu_{21})$  when  $i = j$ ,  $D_{12} = E_{12}h^3/6$ ,  $D_{00} = (1/2)(D_{11}\nu_{21} + D_{22}\nu_{12})$ ,  $E_{ij}$  are the Young and shear moduli, and  $\nu_{ij}$  are the Poisson ratios. The strain components  $\varepsilon_{11}$ ,  $\varepsilon_{22}$ , and  $\varepsilon_{12}$  can be evaluated using the expression for the Green–Lagrange strain tensor, whereas the curvatures can be evaluated using the following expressions.

$$\bar{\kappa}_1 = \mathbf{r}_{0x_1x_1} \cdot \mathbf{n}, \quad \bar{\kappa}_2 = \mathbf{r}_{0x_2x_2} \cdot \mathbf{n}, \quad \bar{\kappa}_{12} = \mathbf{r}_{0x_1x_2} \cdot \mathbf{n} \quad (5.128)$$

where the normal  $\mathbf{n}$  is defined as

$$\mathbf{n} = (\mathbf{r}_{0x_1} \times \mathbf{r}_{0x_2}) / |\mathbf{r}_{0x_1} \times \mathbf{r}_{0x_2}| \quad (5.129)$$

Using the strain energy, the elastic forces of the thin-plate element can be calculated using numerical integration methods (Dufva and Shabana, 2005).

## 5.12 HIGHER-ORDER PLATE ELEMENT

The higher-dimensional plate element employs the full parameterization  $x_1^j$ ,  $x_2^j$ , and  $x_3^j$ . The element has four nodes. Each node has 12 coordinates: 3 translational coordinates  $\mathbf{r}^{jk}$ , and 9 gradient coordinates defined by the three vectors  $\mathbf{r}_{x_1}^{jk}$ ,  $\mathbf{r}_{x_2}^{jk}$ , and  $\mathbf{r}_{x_3}^{jk}$ . Therefore, the element has 48 nodal coordinates, which can be written in a vector form as

$$\mathbf{e}^j = \left[ \mathbf{e}^{j1T} \quad \mathbf{e}^{j2T} \quad \mathbf{e}^{j3T} \quad \mathbf{e}^{j4T} \right]^T \quad (5.130)$$

In this equation,

$$\mathbf{e}^{jk} = \left[ \mathbf{r}^{jkT} \quad \mathbf{r}_{x_1}^{jkT} \quad \mathbf{r}_{x_2}^{jkT} \quad \mathbf{r}_{x_3}^{jkT} \right]^T \quad (5.131)$$

For Node 1, the coordinates are defined at  $x_1^j = x_2^j = x_3^j = 0$ ; for Node 2, the coordinates are defined at  $x_1^j = a$  and  $x_2^j = x_3^j = 0$ ; for Node 3, the coordinates are defined at  $x_1^j = a$ ,  $x_2^j = b$ , and  $x_3^j = 0$ ; and for Node 4, the coordinates are defined at  $x_1^j = 0$ ,  $x_2^j = b$ , and  $x_3^j = 0$ ; where  $a$  and  $b$  are the length and width of the element. The element shape function matrix is defined as (Mikkola and Shabana, 2003)

$$\mathbf{S}^j = \begin{bmatrix} s_1 \mathbf{I} & s_2 \mathbf{I} & s_3 \mathbf{I} & s_4 \mathbf{I} & s_5 \mathbf{I} & s_6 \mathbf{I} & s_7 \mathbf{I} & s_8 \mathbf{I} \\ s_9 \mathbf{I} & s_{10} \mathbf{I} & s_{11} \mathbf{I} & s_{12} \mathbf{I} & s_{13} \mathbf{I} & s_{14} \mathbf{I} & s_{15} \mathbf{I} & s_{16} \mathbf{I} \end{bmatrix} \quad (5.132)$$

where  $\mathbf{I}$  is the  $3 \times 3$  identity matrix and the shape functions  $s_i$ ,  $i = 1, 2, \dots, 16$ , are as follows:

$$\left. \begin{aligned} s_1 &= -(\xi - 1)(\eta - 1)(2\eta^2 - \eta + 2\xi^2 - \xi - 1), & s_2 &= -a\xi(\xi - 1)^2(\eta - 1), \\ s_3 &= -b\eta(\eta - 1)^2(\xi - 1), & s_4 &= t\xi(\xi - 1)(\eta - 1), \\ s_5 &= \xi(2\eta^2 - \eta - 3\xi + 2\xi^2)(\eta - 1), & s_6 &= -a\xi^2(\xi - 1)(\eta - 1), \\ s_7 &= b\xi\eta(\eta - 1)^2, & s_8 &= -t\xi\xi(\eta - 1), \\ s_9 &= -\xi\eta(1 - 3\xi - 3\eta + 2\eta^2 + 2\xi^2), & s_{10} &= a\xi^2\eta(\xi - 1), \\ s_{11} &= b\xi\eta^2(\eta - 1), & s_{12} &= t\xi\eta\xi, \\ s_{13} &= \eta(\xi - 1)(2\xi^2 - \xi - 3\eta + 2\eta^2), & s_{14} &= a\xi\eta(\xi - 1)^2, \\ s_{15} &= -b\eta^2(\xi - 1)(\eta - 1), & s_{16} &= -t\eta\xi(\xi - 1) \end{aligned} \right\} \quad (5.133)$$

where  $\xi = x_1^j/a$ ,  $\eta = x_2^j/b$ ,  $\varsigma = x_3^j/t$ , and  $t$  is the element thickness. The mass matrix of the element is constant, as it is the case in the elements previously discussed in this chapter. The elastic forces can be formulated using the general continuum mechanics approach or the *elastic midsurface approach* used for the thin-plate element discussed in the preceding section. In the case of thin- and stiff-plate structures, as in the case of other elements, the use of the general continuum mechanics approach introduces high-frequency modes that lead to deterioration of the performance of the element. For such thin and stiff structures, it is recommended to use the elastic midsurface approach, which does not include in the elastic forces coupling between the membrane and bending effects. In the case of very flexible structures, on the other hand, the

use of the general continuum mechanics approach for formulating the elastic forces does not lead to deterioration in the element performance, and the use of this approach captures coupled deformation modes that can be significant in the case of large and/or plastic deformations, as previously mentioned in this chapter.

### 5.13 BRICK ELEMENT

A three-dimensional ANCF brick element, with an incomplete polynomial representation, can be developed. This element, shown in Figure 8, has eight nodes. The nodal coordinates  $\mathbf{e}^{jk}$  at node  $k$  of the finite element  $j$  can be defined as  $\mathbf{e}^{jk} = [\mathbf{r}^{jkT} \mathbf{r}_{x_1}^{jkT} \mathbf{r}_{x_2}^{jkT} \mathbf{r}_{x_3}^{jkT}]^T$ ,  $k = 1, \dots, 8$ , where  $\mathbf{r}^{jk}$  is the absolute position vector at node  $k$  of the finite element  $j$  and  $\mathbf{r}_{x_1}^{jk}$ ,  $\mathbf{r}_{x_2}^{jk}$ , and  $\mathbf{r}_{x_3}^{jk}$  are the position vector gradients obtained by differentiation with respect to the spatial coordinates  $x_1$ ,  $x_2$ , and  $x_3$ , respectively. The displacement field of each coordinate of the brick element can be defined using an incomplete polynomial with 32 coefficients as (Olshevskiy et al., 2013)

$$\begin{aligned} \varphi(x, y, z) = & \alpha_1 + \alpha_2 x_1 + \alpha_3 x_2 + \alpha_4 x_3 + \alpha_5 x_1^2 + \alpha_6 x_2^2 + \alpha_7 x_3^2 + \alpha_8 x_1 x_2 + \alpha_9 x_2 x_3 + \alpha_{10} x_1 x_3 \\ & + \alpha_{11} x_1^3 + \alpha_{12} x_2^3 + \alpha_{13} x_3^3 + \alpha_{14} x_1^2 x_2 + \alpha_{15} x_1^2 x_3 + \alpha_{16} x_2^2 x_3 + \alpha_{17} x_1 x_2^2 + \alpha_{18} x_1 x_3^2 \\ & + \alpha_{19} x_2 x_3^2 + \alpha_{20} x_1 x_2 x_3 + \alpha_{21} x_1^3 x_2 + \alpha_{22} x_1^3 x_3 + \alpha_{23} x_1 x_2^3 + \alpha_{24} x_2^3 x_3 + \alpha_{25} x_1 x_3^3 \\ & + \alpha_{26} x_2 x_3^3 + \alpha_{27} x_1^2 x_2 x_3 + \alpha_{28} x_1 x_2^2 x_3 + \alpha_{29} x_1 x_2 x_3^2 + \alpha_{30} x_1^3 x_2 x_3 + \alpha_{31} x_1 x_1^2 x_3 + \alpha_{32} x_1 x_2 x_3^3 \end{aligned} \quad (5.134)$$

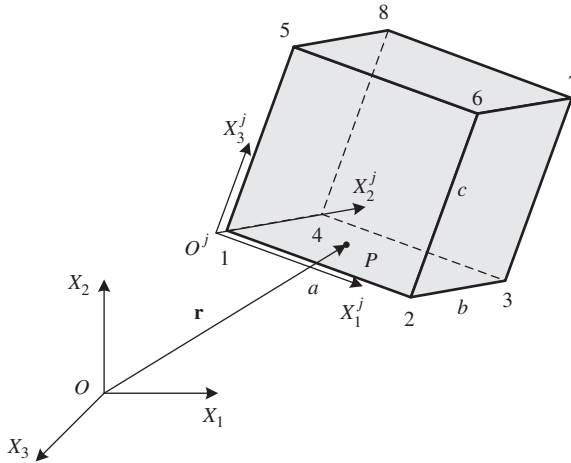


Figure 5.8 ANCF brick element



In this equation,  $\alpha_k$ ,  $k = 1, 2, \dots, 32$ , are the polynomial coefficients. Using this polynomial description, the shape functions of the ANCF brick element can be derived as follows:

$$\left. \begin{aligned} \mathbf{S}^{k,1} &= (-1)^{1+\xi_k+\eta_k+\zeta_k} (\xi + \xi_k - 1) (\eta + \eta_k - 1) (\zeta + \zeta_k - 1) \cdot \\ &\quad (1 + (\xi - \xi_k)(1 - 2\xi) + (\eta - \eta_k)(1 - 2\eta) + (\zeta - \zeta_k)(1 - 2\zeta)) \\ \mathbf{S}^{k,2} &= (-1)^{\eta_k+\zeta_k} a \xi^{\xi_k+1} (\xi - 1)^{2-\xi_k} \eta^{\eta_k} (\eta - 1)^{1-\eta_k} \zeta^{\zeta_k} (\zeta - 1)^{1-\zeta_k} \\ \mathbf{S}^{k,3} &= (-1)^{\xi_k+\zeta_k} b \xi^{\xi_k} (\xi - 1)^{1-\xi_k} \eta^{\eta_k+1} (\eta - 1)^{2-\eta_k} \zeta^{\zeta_k} (\zeta - 1)^{1-\zeta_k} \\ \mathbf{S}^{k,4} &= (-1)^{\xi_k+\eta_k} c \xi^{\xi_k} (\xi - 1)^{1-\xi_k} \eta^{\eta_k} (\eta - 1)^{1-\eta_k} \zeta^{\zeta_k+1} (\zeta - 1)^{2-\zeta_k} \end{aligned} \right\} \quad k = 1, \dots, 8 \quad (5.135)$$

where  $a$ ,  $b$ , and  $c$  are, respectively, the dimensions of the element along the  $x_1$ ,  $x_2$ , and  $x_3$  directions,  $\xi = x_1/a$ ,  $\eta = x_2/b$ ,  $\zeta = x_3/c$ ,  $\xi, \eta, \zeta \in [0, 1]$ , and  $\xi_k, \eta_k, \zeta_k$  are the dimensionless nodal locations for node  $k$ . The position vector of an arbitrary material point on element  $j$  can be written as

$$\mathbf{r}^j = \sum_{k=1}^8 [\mathbf{S}^{k,1} \mathbf{I} \quad \mathbf{S}^{k,2} \mathbf{I} \quad \mathbf{S}^{k,3} \mathbf{I} \quad \mathbf{S}^{k,4} \mathbf{I}] \mathbf{e}^{jk} = \mathbf{S}^j \mathbf{e}^j \quad (5.136)$$

where  $\mathbf{I}$  is the  $3 \times 3$  identity matrix,  $\mathbf{S}^j$  and  $\mathbf{e}^j$  are, respectively, the element shape function matrix and the vector of nodal coordinates, which can be written as

$$\left. \begin{aligned} \mathbf{S}^j &= [\mathbf{S}^{1,1} \mathbf{I} \quad \mathbf{S}^{1,2} \mathbf{I} \quad \mathbf{S}^{1,3} \mathbf{I} \quad \mathbf{S}^{1,4} \mathbf{I} \quad \dots \quad \mathbf{S}^{8,1} \mathbf{I} \quad \mathbf{S}^{8,2} \mathbf{I} \quad \mathbf{S}^{8,3} \mathbf{I} \quad \mathbf{S}^{8,4} \mathbf{I}] \\ \mathbf{e}^j &= [\mathbf{e}^{j1^T} \quad \mathbf{e}^{j2^T} \quad \mathbf{e}^{j3^T} \quad \mathbf{e}^{j4^T} \quad \mathbf{e}^{j5^T} \quad \mathbf{e}^{j6^T} \quad \mathbf{e}^{j7^T} \quad \mathbf{e}^{j8^T}]^T \end{aligned} \right\} \quad (5.137)$$

The ANCF brick element described in this section has 96 degrees of freedom and can assume very complex shapes as demonstrated by Wei et al. (2015) in their study of the fluid sloshing problem. Wei et al. (2015) also presented a higher-order ANCF brick element based on a complete polynomial representation.

## 5.14 ELEMENT PERFORMANCE

All the finite elements presented in this chapter lead to a constant mass matrix and can be used in the large-rotation and large-deformation analysis because nonlinear theory is used with an assumed displacement field that can correctly describe arbitrary large displacements. The use of the two-dimensional Euler–Bernoulli beam and the three-dimensional cable element is restricted to certain applications because they are less general as compared to other elements. Nonetheless, most of the elements described in the preceding sections can be considered as *isoparametric* elements if the centerlines or the midsurfaces are considered. A finite element is said to be isoparametric if the element shape function can be used to describe both positions (geometry) and displacements of the material points. One can verify that the beam and plate elements presented in this chapter are isoparametric if the positions and displacements of the material points on the centerline or the midsurface are considered. For isoparametric elements, it is straightforward to develop curved elements such as *curved beams* and *shells* because

one can always use the same displacement field to define stress-free configuration by giving appropriate values for the nodal coordinates. A finite element is said to be *subparametric* if the order of interpolation used for the positions is lower than the order of interpolation used for the displacement. The element is said to be *superparametric* if the order of interpolation used for the positions is higher than the order of interpolation used for the displacements. Subparametric and superparametric elements will not be discussed further in this book.

In addition to the elements presented in this chapter, several other elements have been proposed in the literature. Among these elements is the three-dimensional beam element proposed by von Dombrowski (2002) who demonstrated the use of his element in interesting large-deformation applications. In von Dombrowski's element, rotation coordinates are used as nodal coordinates in order to develop an Euler–Bernoulli beam element that accounts for the effect of the rotary inertia. Von Dombrowski's element, which is a more general element as compared to the cable element, is obtained at the expense of not having a constant mass matrix. Because the rotation in this element formulation is assumed to be infinitesimal and only represents rotation about the tangent to the element centerline, the nonlinearity arising from introducing this rotation is not severe and the mass matrix is nearly constant.

Other beam and plate elements were introduced by several authors; some of these elements employ curvature vectors as nodal coordinates. The reader who is interested in this subject can learn about these elements and the formulation of their mass and stiffness matrices from the work of Takahashi and Shimizu (1999), Dmitrochenko and Pogorelov (2003), Garcia-Vallejo et al. (2003), Sapanen and Mikkola (2003), Garcia-Vallejo et al. (2004), and Yoo et al. (2004).

## Patch Test

The patch tests are simple tests, which are used to check the convergence of the finite element formulation as well as the computer implementation. These tests can also be used to evaluate the element performance and stability by checking whether or not the element satisfies basic equilibrium requirements. A successful patch test for an element is an indication that if the element is used to model a structure, a refinement of the finite element mesh will produce solutions that converge to the exact solutions. To perform the patch test, one considers a finite element mesh that consists of a small number of elements with at least one node inside the patch. The patch can be subjected to forces or prescribed nodal displacements to develop problems with known exact solutions. For example, boundary nodes can be constrained just enough to eliminate the rigid-body motion of the structure. One can then apply, at the free boundary nodes, loads that correspond to the state of a constant stress. The computed stresses inside the elements are compared with the exact solution to check whether or not the two solutions agree to within the numerical errors. The patch test is repeated to cover all cases of constant stresses relevant to this element. If all the computed stress results agree with the exact solution, the element passes the patch test, and a fine mesh of a structure using this element will produce a solution that converges to the exact one.

One can also examine the strains and displacements to make sure that the computed values are correct. One must also check that in the case of prescribed displacements of the boundary nodes and in the absence of the body forces, the stress and strains must be constant in order for the element to satisfy the partial differential equations of equilibrium. If these conditions are not satisfied, then it is likely that the element assumed displacement field is not correct

and/or there is a problem with the computer implementation. It is also recommended to perform an eigenvalue analysis to check that the element has the correct number of rigid-body modes for a given support condition. The eigenvalue analysis should not produce a zero eigenvalue associated with a deformation mode; otherwise, the element will exhibit unstable behavior.

## Locking Problem

With regard to the finite element performance, one of the important issues that have been discussed in the literature is the *locking problem*. Some finite elements exhibit in some applications overly stiff behavior due to two main reasons. First, the order of the polynomial interpolation used for the element is low such that some important modes of deformations cannot be effectively captured. For example, if a linear interpolation is used for a finite element, the curvature which is necessary to describe bending will be zero everywhere inside the element. The use of such low-order finite elements for bending is therefore not recommended because a very large number of elements will be required to solve a simple bending problem. The use of such a fine finite element mesh can be very inefficient in solving beam and plate problems. The second reason for the poor performance of an element is the existence of high-frequency modes that have no significant effect on the solution but lead to a deterioration of the element performance. Such modes can be consistently eliminated using approximation methods based on coordinate reduction as described in the following chapter, or by using analytical methods by introducing kinematic algebraic constraints to prevent the motion in the direction of such stiff modes. The algebraic constraint equations can be used to systematically eliminate these stiff modes from the formulation or can be used to introduce constraint forces that can be expressed in terms of Lagrange multipliers; a subject that has been extensively covered in the MBS dynamics literature (Roberson and Schwertassek, 1988; Shabana, 2013).

As the result of low-order interpolations and the existence of high-frequency modes of deformations, the element performance deteriorates and serious numerical problems can be encountered. There are several types of locking, including *volumetric*, *membrane*, and *shear locking*. For example, most structural materials are nearly incompressible. Changes of the dilatation can be accompanied by large values of stresses that absorb a significant part of the energy and make the element very stiff or lock. Theoretically, an ideal solution to deal with incompressible or nearly incompressible materials is to impose the incompressibility condition as a constraint by assuming that the determinant of the matrix of position vector gradients remains equal to one and does not change. This condition arises from the relationship between the volumes in the current and reference configurations,  $dv = JdV$ , where  $J$  is the determinant of the matrix of position vector gradients, and  $dv$  and  $dV$  are, respectively, the volumes in the current and reference configurations. As previously mentioned, imposing the incompressibility condition can be accomplished using two approaches: in the first, a *Lagrange multiplier technique* is used, whereas in the second, a penalty method is used. The *penalty method* is easier to use because it is equivalent to adding a force to the equations of motion to guarantee that the incompressibility condition is satisfied. On the other hand, when the Lagrange multiplier technique is used, one must augment the equations of motion with algebraic equations that describe the constraint conditions. This leads to a system of differential and algebraic equations that must be solved simultaneously, making the numerical procedure much more complex as compared to using the penalty method.

The use of the penalty method is equivalent to changing the strain energy of the system by adding another term that enforces the incompressibility condition. Another method used in the finite element literature to solve the locking problems is to use *multifield variational principles*, which are also called *mixed* or *hybrid principles*. In these principles, the stress and strain components that lead to overly stiff behavior are interpolated independently of the displacements. The independent interpolation allows for using higher order for those components that are the source of the locking behavior. Examples of these mixed principles are the *Hellinger–Reissner principle* and the *Hu–Washizu principle*: the first is stress based, whereas the second is strain based. The use of these principles allows using different fields for stresses and strains to avoid the locking problem and improve the element behavior in some problems such as beam and plate bending. For this reason, the resulting elements are also called *assumed strain* or *assumed stress elements* depending on which variables are interpolated. The drawback of using the mixed principles is that the elements can exhibit instabilities in other fields and, therefore, it is important to check the accuracy of the solution obtained for other field variables.

*Shear locking*, which is also a source of numerical problems in beam and plate problems, is the result of excessive shear stresses. For thin elements, the cross section is expected to remain perpendicular to the element centerline or midsurface of the element. This is the basic assumption used in Euler–Bernoulli beam theory. Elements that are based on this theory do not allow for shear deformation, and therefore, such elements do not, in general, suffer from the shear locking problem. Examples of these elements are the two-dimensional Euler–Bernoulli beam element and the three-dimensional cable element discussed previously in this chapter. These elements, as demonstrated in the literature, are efficient in thin-beam applications. Shear deformable elements, on the other hand, can suffer from locking problems if they are used in thin structure applications. When these elements are used, the cross section does not remain perpendicular to the element centerline, leading to shear forces. For thin structures, the resulting shear stresses can be very high leading to numerical problems. This problem can be circumvented by using the elastic line or midsurface approaches, the mixed variational principles, or reduced integration methods.

Similarly, some shell-element formulations produce coupling between membrane and bending deformations. In these formulations, a bending of a plate leads to membrane (extension) displacements. This kinematic coupling can lead to the problem of *membrane locking*, which in turn leads to numerical difficulties when thin shell structures are analyzed. In some applications such as papers and cloths, bending does not produce extension. For these applications, it is recommended to use the thin-plate element formulation, which is based on the elastic midsurface approach. In the formulation of the elastic forces of this element, it is assumed that the bending and extension are not coupled. If, on the other hand, the higher-order fully parameterized plate element is used in thin structural shell applications, it is recommended to use the elastic midsurface approach, the mixed variational principles, and reduced integration methods.

## Reduced Integration

One must be careful when speaking of the order of the interpolation and the performance of an element. Although low-order interpolation may necessitate the use of a larger number of elements in order to be able to capture a certain deformation mode, higher-order terms

in a polynomial introduce more complex shapes that are associated with high-frequency modes of oscillations. These high-frequency modes can also lead to a deterioration of the element performance. Elimination of these modes can enhance the element performance in some applications. One method, which is recommended in the finite element literature, is to use reduced integration instead of full integration. In the reduced integration, fewer quadrature points are used in the numerical integration of the elastic forces. This is equivalent to using lower-order polynomials to approximate the integrands that appear in the elastic force expressions. Lower-order polynomials have simpler shapes, which are associated with lower modes of oscillations. Elimination of the complex shapes is equivalent to eliminating high frequencies and is equivalent to lowering the element stiffness. This can significantly enhance the element performance. Underintegration, which can be used effectively to eliminate shear locking in some applications, leads to additional computational advantage because it reduces the number of calculations by using fewer quadrature points. Reduced integration, however, should not be used if it leads to mesh instabilities or wrong solutions. It is, therefore, important that the integration rule used is tested in order to make sure that an accurate solution is obtained.

Another form of reduced integration is the *selective reduced integration*, which can be used to enhance the element performance in some problems. In this integration method, some terms that are the source of locking can be selected and underintegrated, whereas full integration is used for other terms that appear in the expression of the elastic forces. For example, the terms that define the contribution to the elastic forces from the volumetric strains can be underintegrated, whereas terms associated with the deviatoric strains can have a higher order of integration. This method of selective reduced integration can be effective in dealing with volumetric locking in some applications.

Reduced integration if not carefully performed can lead to instabilities. For example, if the deformations at all the selected quadrature points happen to be zero, one obtains zero strain energy for a nonrigid-body mode. In this case, the stiffness matrix is singular and the element exhibits unstable behavior. These types of modes are called in the finite element literature *hourglass modes*, *zero energy modes*, or *spurious singular modes*. These types of modes can be detected using an eigenvalue analysis. In this case, the number of modes of the finite element that have zero eigenvalue is higher than the number of rigid-body modes of the element because the improper selection of the quadrature points leads to a zero eigenvalue associated with a deformation mode.

## 5.15 OTHER FINITE ELEMENT FORMULATIONS

In this chapter, ANCF finite elements were introduced and discussed. The ANCF approach is suited for the analysis of a general class of problems in which the bodies undergo large rotations including rigid-body rotations. This is a problem that is typical in MBS applications. ANCF finite elements employ absolute position vectors and their gradients as nodal coordinates. There are several reasons, discussed in this section, which motivated introducing this approach and presenting it in this continuum-mechanics-based book. In the finite element literature, there are other types of finite elements that employ different sets of coordinates. In the remainder of this section, we discuss these element formulations in order to further explain the motivation for introducing the formulation presented in this chapter.

## Isoparametric Finite Elements

Some elements such as the two-dimensional *rectangular* and *triangular elements* and the three-dimensional *solid* and *tetrahedral elements* (Zienkiewicz, 1977) employ only position coordinates. These elements can correctly describe rigid-body motion and they are of the *isoparametric* type because the same shape function can be used to describe the displacement and geometry of the element. Nonetheless, the nodal coordinates do not include rotation variables, which make these elements unsuitable for beam, plate, and shell applications and also unsuitable for many MBS applications where joint constraints between bodies are often formulated in terms of rotation coordinates. Because the continuity of the rotation field at the nodal points is not guaranteed when these isoparametric elements are used, imposing MBS connectivity conditions that allow relative motion is not straightforward. Furthermore, the limitations of these conventional isoparametric elements in the analysis of bending, as the result of the low order of interpolation, are well known and have been discussed in the literature.

## Use of Infinitesimal Rotation Coordinates

Another type of finite elements includes elements that employ infinitesimal rotations in addition to translational coordinates as nodal variables. Examples of these conventional finite elements are *beam*, *plate*, and *shell elements*. These elements, which were widely used in many structural applications, cannot correctly describe large rigid-body rotation; they can describe only infinitesimal rigid-body rotation. Because of the use of the infinitesimal rotations as nodal coordinates, one can show that the kinematic equations of these elements employ linearization (Shabana, 1996a). For this reason, these elements have been used in structural dynamics applications in the framework of an incremental solution procedure. It is known, however, that the incremental solutions based on linearized equations eventually diverge from the correct solution of the nonlinear problem. Furthermore, most MBS algorithms that are designed to solve large rigid-body rotation problems are based on nonincremental solution procedure. In order to be able to use these finite elements in MBS algorithms, the *finite element FFR formulation* was proposed in the early 1980s (Shabana and Wehage, 1981; Shabana, 1982). This approach, which is discussed in detail in the following chapter, leads to correct description of the rigid-body motion of the finite elements that employ infinitesimal rotations as nodal coordinates. The FFR formulation has been primarily used for small-deformation problems because the elements are assumed to undergo small displacements with respect to the floating frame, which may experience an arbitrary rigid-body motion including finite rotations. The FFR formulation remains an effective and efficient tool for modeling the small deformation of flexible bodies because it allows reducing systematically the number of deformation degrees of freedom. This formulation, which will be discussed in more detail in the following chapter, is implemented in most general purpose flexible MBS computer programs.

Perhaps, it is also important to point out that, in MBS applications, one cannot use infinitesimal or finite rotations as nodal coordinates in the interpolation of the rigid-body displacement field. Recall, as shown in Chapter 1, that the rigid-body kinematic equations are defined in terms of trigonometric functions and not in terms of angles. Trigonometric functions can be approximated by angles only when these angles are infinitesimal.

## Use of Finite Rotation Coordinates

Another element formulation, which was introduced in the mid-1980s, is based on using two independent fields with finite rotation coordinates as nodal coordinates (Simo and Vu-Quoc, 1986). The resulting elements are capable of correctly describing arbitrary rigid-body displacements. In this formulation, the two independent fields are introduced for the position vector and the finite rotations of the cross section of the finite element. That is, the position and rotations are obtained from independent interpolations. As demonstrated in this book, using the polar decomposition theorem, the rotation field can be defined using the matrix of position vector gradients. That is, the position vector field is sufficient to determine the rotations of infinitesimal volumes. The use of independent displacement and rotation fields, therefore, can lead to a problem of coordinate redundancy and inconsistency in the definition of the rotation variables (Ding et al., 2014). Formulations that suffer from this problem of coordinate redundancy can lead to numerical problems in the analysis of large rotations, particularly large rigid-body rotations. For instance, some of these formulations do not automatically satisfy the principle of work and energy, and special measures must be taken in the numerical integration routines in order to satisfy this principle. On the other hand, because the ANCF position vector field is used to determine the gradients that define the rotation field, such a problem is not encountered, and ANCF finite elements automatically satisfy the principle of work and energy without the need for special measures as demonstrated in the literature (Campanelli et al., 2000).

## 5.16 UPDATED LAGRANGIAN AND EULERIAN FORMULATIONS

In this chapter, a *total Lagrangian* large-deformation finite element formulation was considered. Integrations and differentiations are defined with respect to the Lagrangian coordinates, and stress and strain measures are defined with respect to the reference configuration. The ANCF finite elements presented in this chapter can also be used with an updated Lagrangian formulation. In this case, one uses stress and strain measures defined in the current configuration. Furthermore, the differentiations are defined with respect to the coordinates  $\mathbf{r}$ , whereas the integrations are defined using the current volumes and areas. In principle, as discussed in Chapter 3, the total and updated Lagrangian formulations are equivalent, and one formulation can be obtained from the other using a coordinate transformation. Therefore, the choice of a formulation is a matter of convenience or preference, and in some cases, some variables defined in the current configuration are used with the total Lagrangian formulation and vice versa. For this reason, the updated Lagrangian formulation will not be discussed further in this book. The reader interested in the updated Lagrangian formulation can consult the literature on the nonlinear finite element method.

Whereas in the Lagrangian formulations, the finite element nodal points move as the result of the applied forces, in the *Eulerian formulations* with fixed mesh, the nodes are fixed since the focus is on a region of the continuum that is defined by the vector  $\mathbf{r}$ . One then does not follow the motion of a material point that has coordinates  $\mathbf{x}$  in the reference configuration; instead, the focus is on a point through which the material flows, and the interest is to determine the behavior of the continuum when the material passes by this point, which is fixed in space. The *Eulerian description* is more convenient to use in the case of fluid dynamics, whereas the



Lagrangian description is used more often in solid mechanics. In the Eulerian formulations, three sets of variables are often used; the density  $\rho$ , the stresses  $\boldsymbol{\sigma}$ , and the velocities  $\mathbf{v}$ . In order to solve for these three sets of variables, three sets of equations are used. These equations are the continuity or conservation of mass equation, the constitutive equations, and the equations of motion. The constitutive equations are often expressed in the rate form. These three sets of equations can be written in the following form:

$$\left. \begin{aligned} \frac{\partial \rho}{\partial t} + \nabla \cdot (\rho \mathbf{v}) &= 0 \\ \dot{\boldsymbol{\sigma}} &= \dot{\boldsymbol{\sigma}}(\mathbf{D}) \\ (\nabla \boldsymbol{\sigma}^T)^T + \mathbf{f}_b - \rho \mathbf{a} &= 0 \end{aligned} \right\} \quad (5.138)$$

In this equation,  $\rho$  is the density defined in the current configuration,  $\mathbf{v}$  is the velocity vector,  $\boldsymbol{\sigma}$  is the stress tensor,  $\mathbf{D}$  is the rate of deformation tensor,  $\mathbf{f}_b$  is the vector of body forces, and  $\mathbf{a}$  is the acceleration vector. The continuity equation can also be written in the following alternate form:

$$\frac{\partial \rho}{\partial t} + \frac{\partial \rho}{\partial \mathbf{r}} \mathbf{v} + \rho \sum_{i=1}^3 \frac{\partial v_i}{\partial r_i} = 0 \quad (5.139)$$

In the Eulerian formulations, independent interpolations are used for the density, stresses, and velocities. One can then write for element  $j$  the following finite element description:

$$\mathbf{r}^j = \mathbf{S}^j \mathbf{e}^j, \quad \boldsymbol{\sigma}^j = \mathbf{S}_\sigma^j \mathbf{e}_\sigma^j, \quad \rho^j = \mathbf{S}_\rho^j \mathbf{e}_\rho^j \quad (5.140)$$

In this equation,  $\mathbf{S}^j$  is the element shape function used for the displacement,  $\mathbf{e}^j$  is the vector of element position nodal coordinates,  $\mathbf{S}_\sigma^j$  is the shape function used for the stresses,  $\mathbf{e}_\sigma^j$  is the set of stress nodal variables,  $\mathbf{S}_\rho^j$  is the density shape function, and  $\mathbf{e}_\rho^j$  is the set of density nodal variables. Because  $\mathbf{v}^j = \dot{\mathbf{r}}^j = \dot{\mathbf{S}}^j \mathbf{e}^j$ , Equation 140 can be used to define the following virtual changes:

$$\delta \mathbf{v}^j = \dot{\mathbf{S}}^j \delta \mathbf{e}^j, \quad \delta \boldsymbol{\sigma}^j = \mathbf{S}_\sigma^j \delta \mathbf{e}_\sigma^j, \quad \delta \rho^j = \mathbf{S}_\rho^j \delta \mathbf{e}_\rho^j \quad (5.141)$$

As previously mentioned, in the Eulerian formulation with fixed mesh, the nodal points are assumed to be fixed. On fixed boundaries in fluid applications, the velocities at the boundary nodal points are assumed to be zero.

In order to obtain the discrete equations, one can multiply the first equation in Equation 138 by  $\delta \rho^j$ , the second equation by  $\delta \boldsymbol{\sigma}^j$ , and the third equation by  $\delta \mathbf{v}^j$ ; integrating over the domain of the element and using Equation 141, one can show that the finite element discrete equations in the Eulerian formulation can be written as

$$\left. \begin{aligned} \mathbf{M}_\rho^j \dot{\mathbf{e}}_\rho^j &= \mathbf{Q}_\rho^j \\ \mathbf{M}_\sigma^j \dot{\mathbf{e}}_\sigma^j &= \mathbf{Q}_\sigma^j \\ \mathbf{M}^j \dot{\mathbf{e}}^j &= \mathbf{Q}^j \end{aligned} \right\} \quad (5.142)$$

where  $\mathbf{M}_\rho^j$ ,  $\mathbf{M}_\sigma^j$ , and  $\mathbf{M}^j$  are coefficient matrices; and  $\mathbf{Q}_\rho^j$ ,  $\mathbf{Q}_\sigma^j$ , and  $\mathbf{Q}^j$  are vectors that can depend on the unknown variables. In obtaining Equation 142, the integration is carried out over a



fixed element domain in the case of a fixed mesh. Note that in the ANCF Eulerian formulation discussed in this chapter, the mass matrix  $\mathbf{M}^i$  depends on the density, which is a function of time in the case of compressible materials or fluid. Consequently, this mass matrix is not constant as in the case of the Lagrangian formulations. If the material is incompressible, the density is not a function of time, and the continuity equation is simplified. In this case, ANCF finite elements lead to a constant mass matrix. In general, the three sets of equations given by Equation 142 are solved simultaneously to determine the values of the coupled variables of the continuum at the nodes. In the case of fluid dynamics, there are several simulation scenarios that depend on the fluid conditions. In some of these scenarios, the governing equations given in Equation 139 can be simplified.

It is important, however, to point out that a total Lagrangian formulation that employs ANCF finite element can still be used in some fluid applications such as in the case of sloshing problems (Wei et al., 2015). In such applications, the effect of the fluid motion on vehicle dynamics is the primary concern. When ANCF finite elements are used, the expression for the inertia forces remains as previously discussed in this chapter. Regardless of the magnitude of the fluid displacement, the mass matrix remains constant, and the centrifugal and Coriolis forces are identically zero. The stress forces can be determined using the fluid constitutive equations as discussed in Chapter 4. Figure 9 shows the fluid simulation results obtained by Wei et al. (2015). These results are obtained using the ANCF solid element, which ensures the continuity of the displacement gradients at the nodal points (Olshevskiy et al., 2013). The total Lagrangian nonincremental liquid sloshing solution procedure proposed by Wei et al. (2015) can be used to avoid the difficulties of integrating most of fluid dynamics formulations, which are based on the Eulerian approach, with MBS dynamics formulations, which are based on a total Lagrangian approach. The proposed total Lagrangian FE fluid dynamics formulation, which can be systematically integrated with computational MBS algorithms, differs significantly from the conventional FE or finite volume methods, which are based on an Eulerian representation that employs the velocity field of a fixed control volume in the region of interest. The ANCF fluid equations are expressed in terms of displacement and gradient coordinates of material points, allowing for straightforward implementation of kinematic constraint equations and for the systematic modeling of the interaction of the fluid with the external environment or with rigid and flexible bodies. The fluid incompressibility conditions and surface traction

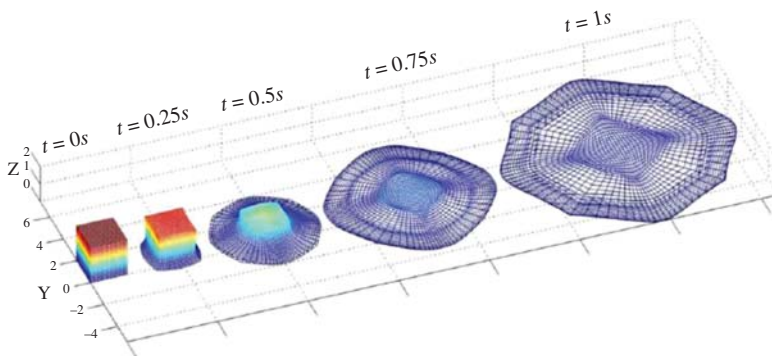


**Figure 5.9** ANCF total Lagrangian fluid simulation (Wei et al., 2015)

forces are considered and derived directly from the Navier Stokes equations. Wei et al. (2015) formulated the fluid problem using two ANCF brick elements, one is obtained using an incomplete polynomial representation and the other is obtained from a B-spline volume representation. The new approach, in addition to ensuring the continuity of the displacement gradients at the nodal points, allows for imposing higher degree of continuity across the element interface by applying algebraic constraint equations that can be used to eliminate dependent variables and reduce the model dimensionality.

## 5.17 CONCLUDING REMARKS

In this chapter, an approach for the large displacement analysis of continuous systems is described. In order to be able to use this approach to develop accurate models for engineering and physics systems, it is necessary to understand some basic geometry and analysis concepts.

### ANCF Finite Elements

The following characteristics define the ANCF solution framework:

1. The problem must be a dynamics problem that requires addressing the formulation of the inertia forces, which are expressed in terms of a constant inertia matrix and, therefore, the Coriolis and centrifugal forces are identically zero.
2. The elements must be of higher order in order to provide the option for imposing continuity on gradient vectors. The vector of nodal coordinates of ANCF finite elements can consist of position and gradient coordinates and the gradients must be interpreted correctly during the entire solution procedure. Conventional  $C^0$  finite elements do not ensure continuity of the gradient or rotation fields. As it is known continuity of the gradients ensures continuity of the rotations. The converse, however, is not, in general, true.
3. The finite elements must correctly describe an arbitrary rigid body motion including arbitrary finite rotations using the assumed displacement field  $\mathbf{r}(\mathbf{x}, t) = \mathbf{S}(\mathbf{x}) \mathbf{e}(t)$ , where  $\mathbf{r}$  is the global position vector of an arbitrary point on the element,  $\mathbf{S}$  is the element shape function matrix,  $\mathbf{e}$  is the vector of nodal coordinates,  $\mathbf{x} = [x_1 \ x_2 \ x_3]^T$  is the vector of the element spatial coordinates, and  $t$  is time.

When using ANCF finite elements, the equations of motion can be solved nonincrementally and, therefore, there is no need for the use of the corotational approach, which was introduced to remedy the problems associated with finite elements that employ infinitesimal rotations. In the FE literature, there has been frequent reference to gradients and slopes. Nonetheless, all the above conditions are not often met as the result of improper treatment of the gradients, the use of incremental procedures, and/or the focus on static procedures without addressing the formulation of the element inertia when the element experiences arbitrary finite rotations (Betsch and Stein, 1995; Milner, 1981).

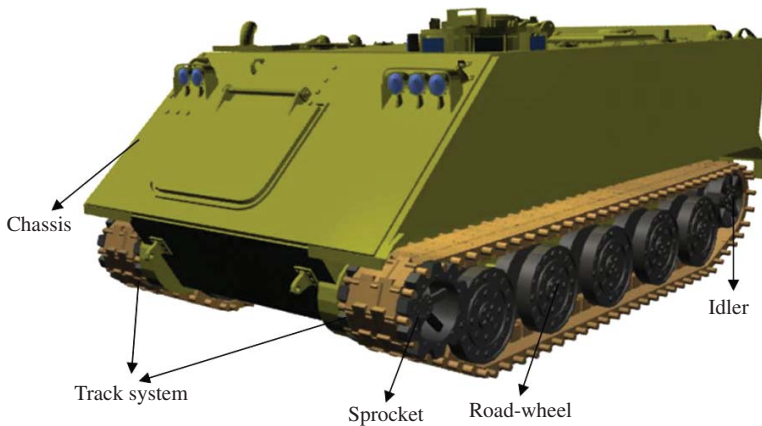


**Figure 5.10** Tracked vehicles

### Constrained Motion

As discussed in this chapter, ANCF finite elements can be used as the basis for a nonincremental solution procedure that allows for developing new computer models with significant details. One example of these models is the tracked vehicle shown in Figure 10. The links of the track chains of this vehicle are modeled as flexible bodies connected by pin (revolute) joints that allow relative rotation as well as relative deformations between the chain links. This detailed vehicle model was successfully developed using ANCF finite elements and computational MBS algorithms (Hamed et al, 2015; Wallin et al., 2013). Using ANCF finite elements, linear connectivity conditions, that define the pin (revolute) joints, were developed, allowing eliminating the dependent variables at a preprocessing stage (Garcia-Vallejo et al, 2003; Hamed et al., 2015). The two tracks of the vehicle can be treated as one ANCF finite element mesh since ANCF finite elements allow for arbitrarily large displacements. The track chains mass matrix remains constant and the centrifugal and Coriolis forces remain equal to zero. The development of such a heavily constrained model, in which the algebraic connectivity conditions are eliminated at a preprocessing stage, using ANCF finite elements is straightforward.

### ANCF Reference Node

Another important concept that has been used effectively in modeling complex system is the *ANCF reference node* (Shabana, 2015a,b). The ANCF reference node is a node that is not associated with a particular ANCF finite element. This node can be used for assembling rigid and structural components. Such a node can also be used to describe a rigid body by imposing six rigidity constraints that eliminate the deformation modes of the reference node. The reference node can be used to develop new tire assembly models and can be used also to develop an MBS submodel at a preprocessing stage as shown in Figure 11 (Shabana, 2015a,b).

### Deformation Modes

As discussed in the literature, and also in this book, fully parameterized ANCF finite elements may exhibit locking behavior, particularly in the case of thin and stiff structures. Nonetheless,

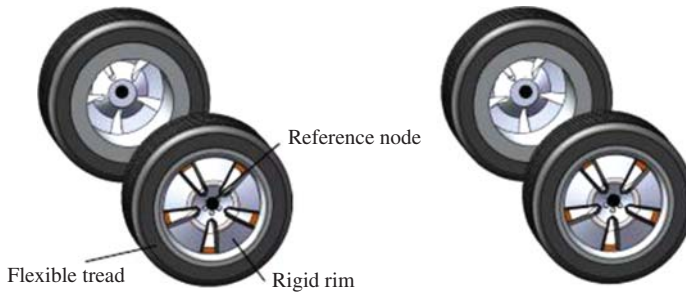


**Figure 5.11** Tire assembly

the use of such fully parameterized ANCF finite elements is necessary in order to be able to capture correct physics in many applications. For example, excessive axial and bending forces lead to change in the cross-sectional dimensions of beam-like structure. Formulations that assume rigid cross section, from the outset, cannot be used to capture this physics behavior. In the finite element literature, many solutions were proposed to solve the locking problem. Some of the locking-solution techniques can be applied in the case of fully parameterized ANCF finite elements, allowing for developing new models that correctly capture the physics of the problem under consideration.

## PROBLEMS

1. Verify the expressions of the shape functions presented in Example 1.
2. Show that the displacement field used in Example 1 can describe an arbitrary rigid-body motion.
3. Verify the expressions of the shape functions presented in Example 2, and show that the displacement field used in Example 2 can describe an arbitrary rigid-body motion.
4. Show that, by using the Cholesky factorization of the symmetric mass matrix, one can define a new set of coordinates that lead to an identity mass matrix.
5. Show that the virtual changes in the Green–Lagrange strains can be written in terms of the virtual changes of the position vector gradients. Show also that the virtual changes in the position vector gradients can be written in terms of the virtual changes of the finite element nodal coordinates.
6. A force vector  $\mathbf{F}(t) = [F_1(t) \ F_2(t)]^T$  applied at a point defined by  $\xi = 0.5$  of the two-dimensional Euler–Bernoulli beam element defined in Section 7. Define the vector of nodal forces due to the application of this force vector. Define also the vector of nodal forces if this force vector is applied at a point defined by  $\xi = 1$ . Discuss the nodal forces associated with the gradient coordinates of this element. Repeat this problem using the two-dimensional shear deformable element.
7. In the two-dimensional case, define the relationship between the virtual change in the rotation and the virtual change of the gradient coordinates at the node for both Euler–Bernoulli

and shear deformable beam elements. Use this relationship to define the relationship between the Cartesian moment and the forces associated with the gradient coordinates of these two elements.

8. Develop the mass matrix of the two-dimensional Euler–Bernoulli beam element discussed in Section 7.
9. A force vector  $\mathbf{F}(t) = [F_1(t) \ F_2(t) \ F_3(t)]^T$  is applied at a point defined by  $\xi = 0.5$  of the cable element presented in Section 9. Define the vector of nodal forces due to the application of this force vector. Define also the vector of nodal forces if this force vector is applied at a point defined by  $\xi = 1$ . Discuss the nodal forces associated with the gradient coordinates of this element. Repeat this problem using the three-dimensional shear deformable element.
10. Obtain the expression for the nodal forces due to gravity in the case of the following finite elements: (1) two-dimensional Euler–Bernoulli beam element, (2) two-dimensional shear deformable beam element, (3) cable element, (4) three-dimensional shear deformable element, and (5) thin-plate element.
11. Obtain the mass matrix of the three-dimensional cable element.

# FINITE ELEMENT FORMULATION: SMALL-DEFORMATION, LARGE-ROTATION PROBLEM

---

In the preceding chapter, a nonlinear finite element formulation for the large-deformation analysis was presented. This formulation, which is consistent with the motion description used in the theory of continuum mechanics and can be used to correctly describe an arbitrary rigid-body motion, leads to a constant mass matrix and nonlinear vector of elastic forces. The formulation imposes no restrictions on the amount of rotation or deformation within the element, except for the restriction imposed by the order of the interpolating polynomials used. In large-deformation problems, in general, the shape of deformation of the bodies can be complex and this, in turn, necessitates the use of a large number of finite element nodal coordinates in order to be able to correctly capture the geometry of deformation. Therefore, in the analysis of the large-deformation problem using the absolute nodal coordinate formulation (ANCF) discussed in the preceding chapter, one simply selects an adequate number of finite elements and formulates the equations of motion in terms of the element nodal coordinates. There is no need to introduce another reference frame or be concerned with the use of coordinate reduction techniques. The ANCF results published in the literature demonstrated that this formulation can be used in modeling very large deformations with relatively small number of finite elements compared to other existing nonlinear finite element formulations.

The use of a full finite element representation to study *small-deformation problems* is not recommended because such a representation is not the most efficient approach to solve for the small deformations. The geometry of the small deformation of the bodies takes simple forms, and one in this case can develop a lower-dimension model that can be efficiently used to solve this class of problems. Furthermore, in the analysis of small deformations, with a proper selection of the coordinate systems, one can use finite elements, which have smaller

number of nodal coordinates. For example, conventional nonisoparametric beam, plate, and shell finite elements, which cannot correctly describe arbitrary rigid-body motion using the element nodal coordinates, can still be used in small-deformation large-displacement formulations. By defining a local linear elasticity problem, linear modes can also be used to further reduce the number of the model degrees of freedom and eliminate high-frequency modes of vibration. The approach that is most widely used to solve the small-deformation, large-rotation problem is called the *floating frame of reference (FFR) formulation*. The finite element FFR formulation, which is discussed in this chapter, was introduced in the early 1980s (Shabana and Wehage, 1981; Shabana, 1982) and was the basis for developing new computational algorithms that led to introducing new generation of codes that became known as *flexible multibody computer codes*, which are widely used in industry, universities, and research institutions.

In this chapter, a brief introduction to the FFR formulation is presented. A crucial step in developing the finite element FFR formulation is the concept of the finite element *intermediate coordinate system*. The use of this intermediate element coordinate system allows modeling flexible bodies with complex geometry, using the finite element method. The concept of the intermediate coordinate system resembles the concept of the *parallel axis theorem* used in rigid-body mechanics. Although the FFR formulation leads to a highly nonlinear system of equations of motion, it is shown that the nonlinear inertia terms developed using this formulation can be expressed in terms of a set of constant *shape integrals* that can be evaluated in advance for the dynamic simulation. More detailed discussion on the FFR formulation can be found on texts on the subject of multibody system dynamics (Shabana, 2013).

## 6.1 BACKGROUND

As pointed out in the preceding chapter, until the mid-1980s, there were two types of finite elements: isoparametric and nonisoparametric finite elements. *Isoparametric finite elements* are elements in which the same shape function is used to describe the geometry and displacements. These elements generally have only translational nodal coordinates and are capable of correctly describing rigid-body motion. Examples of these elements are the two-dimensional rectangular and triangular elements and the three-dimensional solid and tetrahedral elements (Zienkiewicz, 1977). A dynamic formulation of these elements can lead to a constant mass matrix. Nonetheless, these elements do not impose continuity on any rotation parameters at the nodes and are not suitable for modeling many beam-, plate-, and shell-like structures, which are common in engineering applications. The continuity of the rotation field at the nodal point is required in the modeling of many applications such as in the case of multibody systems where mechanical joints between different bodies are defined at the nodal points. Imposing some of these joint constraints requires the continuity of rotation fields.

Other conventional finite elements such as beam, plate, and shell finite elements, which are not of the isoparametric type, employ infinitesimal rotations as nodal coordinates. These finite elements were extensively used in modeling beam-, plate-, and shell-like structures in many engineering applications. Nonetheless, these elements cannot be used to correctly describe an arbitrary rigid-body motion. An arbitrary rigid-body motion of these elements can produce

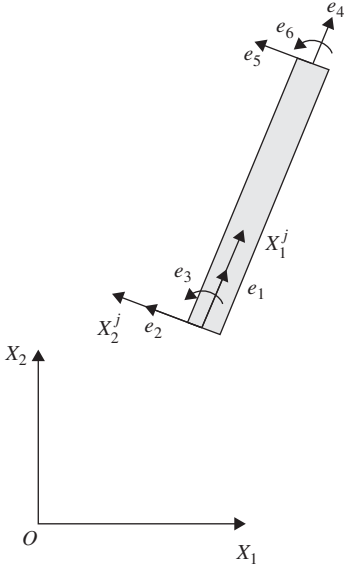


Figure 6.1 Two-dimensional beam element

nonzero strains. An example of these elements is the beam element shown in Figure 1. This element has two nodes, and each of its nodes has three degrees of freedom: two translational coordinates and one infinitesimal rotation coordinate. Therefore, the vector of nodal coordinates of the element can be written as

$$\mathbf{e} = [e_1 \ e_2 \ e_3 \ e_4 \ e_5 \ e_6]^T = [r_1^1 \ r_2^1 \ \theta^1 \ r_1^2 \ r_2^2 \ \theta^2]^T \quad (6.1)$$

The shape function of this element is defined as

$$\mathbf{S} = \begin{bmatrix} 1 - \xi & 0 & 0 & \xi & 0 & 0 \\ 0 & 1 - 3(\xi)^2 + 2(\xi)^3 & l\{\xi - 2(\xi)^2 + (\xi)^3\} & 0 & 3(\xi)^2 - 2(\xi)^3 & l\{(\xi)^3 - (\xi)^2\} \end{bmatrix} \quad (6.2)$$

where  $\xi = x_1/l$  and  $l$  is the length of the finite element. The element shape function presented in the preceding equation uses different interpolations for the displacement components because for this conventional element, the first displacement component is interpreted as the axial displacement, whereas the second component is interpreted as the bending displacement. For this reason, this element shape function cannot be used to define absolute position vectors; and as a consequence, a reference frame that shares the rigid-body motion of the finite element must be used. This motion description is fundamentally different from the ANCF description in which the shape function matrix and the nodal coordinates define the global position vector of the material points on the element, and therefore, the same polynomials are used in the interpolation of the components of the position vector. The derivation of the shape function presented in Equation 2 is outlined in the following example.



**Example 6.1**

For the two-dimensional beam element defined by the nodal coordinates and shape function matrix presented, respectively, in Equations 1 and 2, linear interpolation is used for the axial displacement, whereas cubic interpolation is used for the transverse displacement. A local displacement vector can then be interpolated as follows:

$$\mathbf{r} = \begin{bmatrix} r_1 \\ r_2 \end{bmatrix} = \begin{bmatrix} a_0 + a_1 x_1 \\ b_0 + b_1 x_1 + b_2 x_1^2 + b_3 x_1^3 \end{bmatrix}$$

This interpolation has six coefficients  $a_0, a_1, b_0, b_1, b_2,$  and  $b_3$  that can be expressed in terms of six nodal variables  $e_1, e_2, \dots, e_6$ . The following conditions can be applied at the first node of the element:

$$e_1 = r_1(x_1 = 0), \quad e_2 = r_2(x_1 = 0), \quad e_3 = \left. \frac{\partial r_2}{\partial x_1} \right|_{x_1=0}$$

At the second node, one has the following three conditions:

$$e_4 = r_1(x_1 = l), \quad e_5 = r_2(x_1 = l), \quad e_6 = \left. \frac{\partial r_2}{\partial x_1} \right|_{x_1=l}$$

where  $l$  is the length of the finite element. Substituting the conditions presented in the preceding two equations into the assumed displacement field, one can write the polynomial coefficients  $a_0, a_1, b_0, b_1, b_2,$  and  $b_3$  in terms of the nodal coordinates  $e_1, e_2, \dots, e_6$ . Using this procedure, one can show that the vector  $\mathbf{r}$  can be written as  $\mathbf{r} = \mathbf{S}\mathbf{e}$ , where the vector of nodal coordinates  $\mathbf{e}$  is defined by Equation 1, and the shape function matrix  $\mathbf{S}$  is defined by Equation 2. The resulting finite element cannot be used to account for the shear deformation, and for this reason, it is called an *Euler–Bernoulli beam element*.

**Rigid-Body Motion**

In the case of an arbitrary rigid-body displacement defined by the translation  $\mathbf{r}_O = [r_{O1} \ r_{O2}]^T$  of the first node and the rotation  $\theta$ , the vector of nodal coordinates of Equation 1 is defined as

$$\mathbf{e} = [r_{O1} \ r_{O2} \ \theta \ r_{O1} + l \cos \theta \ r_{O2} + l \sin \theta \ \theta]^T \quad (6.3)$$

Using this vector of nodal coordinates and the element shape function matrix  $\mathbf{S}$ , one can show that the position of the material points on the element centerline in the case of rigid-body motion is given by

$$\mathbf{r} = \mathbf{S}\mathbf{e} = \begin{bmatrix} r_{O1} + x_1 \cos \theta \\ r_{O2} + x_1 \sin \theta + x_1(\sin \theta - \theta)(3\xi - 2\xi^2) \end{bmatrix} \neq \begin{bmatrix} r_{O1} + x_1 \cos \theta \\ r_{O2} + x_1 \sin \theta \end{bmatrix} \quad (6.4)$$

That is, an arbitrary rigid-body motion cannot be correctly described using this element and such an element leads to nonzero strain under an arbitrary rigid-body displacement. It can

be shown, however, that if  $\sin \theta$  instead of the infinitesimal rotation  $\theta$  is used as the nodal coordinate, one obtains exact description of the rigid-body motion (Shabana, 1996a, 2013). In this case, the third and sixth coordinates of the nodal variables should not be interpreted as angles, and the use of different orders of interpolation for the displacement components cannot be justified if the nodal coordinates are used to describe the large displacement of the element. Therefore, for this element,  $\sin \theta$  must remain small, that is  $\sin \theta \approx \theta$ , which amounts to a linearization of the kinematic equations. These limitations become even more severe when three-dimensional elements such as beams, plates, and shells are considered. In the three-dimensional analysis, in addition to the linearization and the fact that finite rotations are not commutative, some of the conventional finite elements do not correctly capture the correct inertia in the case of rigid-body motion.

## Translations

It is clear from Equation 4 that if the rotation angle  $\theta$  is equal to zero, the assumed displacement field of the beam element considered in this section correctly describes an arbitrary rigid-body translation. That is, one can describe correctly the rigid-body translation of the element with respect to any coordinate system that is parallel to the element coordinate system. This property of the finite elements, which is crucial in the nonlinear finite element formulation discussed in this chapter, allows for using a concept, similar to the elementary mechanics concept of the parallel axis theorem, to develop a procedure for correctly accounting for the inertia of bodies with complex geometry and slope discontinuities.

In order to be able to use nonisoparametric elements, such as the conventional beam element discussed in this section, and be able to correctly describe an arbitrary rigid-body displacement, the FFR formulation is used. In this formulation, the gross motion is described using a set of absolute coordinates that define the location and orientation of the floating frame, whereas the deformation of the body with respect to the floating frame is described using the finite element nodal coordinates. The motion of the element, therefore, is not described by only the element nodal coordinates; instead, a coupled set of body reference and elastic element nodal coordinates is used. It is important, however, to point out that the use of such a description does not imply a separation between the rigid-body motion and the elastic deformation. The reference motion, which is the motion of the rigid floating frame, should not be interpreted as the rigid-body motion of the continuum because different floating frames of reference can be used.

## 6.2 ROTATION AND ANGULAR VELOCITY

In the FFR formulation discussed in this section, the kinematic equations are formulated in terms of a set of rotation coordinates that define the orientation of the floating frame with respect to the inertial frame. The concept of the angular velocity becomes important, and for this reason, it is helpful to review and understand the definition of the angular velocity before developing the kinematic equations used in the FFR formulation.

In this section, the general definition of the absolute angular velocity is presented. As will be seen from the development presented in this section, the components of the angular velocity vector are function of a selected set of orientation parameters and their derivatives. Regardless of the set of orientation parameters used, the components of the angular velocity can be written

as linear functions of the derivatives of the orientation coordinates. A sequence of *Euler angles* is used in this section as an example to illustrate how the absolute angular velocity vector can be expressed in terms of the derivatives of the orientation parameters.

### Identities

First, some basic identities that will be used in the definition of the angular velocity are developed. Recall that if  $\mathbf{A}$  is an orthogonal matrix, one has

$$\mathbf{A}^T \mathbf{A} = \mathbf{A} \mathbf{A}^T = \mathbf{I} \quad (6.5)$$

Differentiating  $\mathbf{A}^T \mathbf{A}$  with respect to time and using the preceding equation, one obtains

$$\dot{\mathbf{A}}^T \mathbf{A} + \mathbf{A}^T \dot{\mathbf{A}} = \mathbf{0} \quad (6.6)$$

This equation shows that

$$\mathbf{A}^T \dot{\mathbf{A}} = -(\dot{\mathbf{A}}^T \mathbf{A}) = -(\mathbf{A}^T \dot{\mathbf{A}})^T \quad (6.7)$$

A matrix that is equal to the negative of its transpose is a skew-symmetric matrix. Therefore,  $\mathbf{A}^T \dot{\mathbf{A}}$  is a skew-symmetric matrix denoted as  $\tilde{\bar{\boldsymbol{\omega}}}$ , that is

$$\mathbf{A}^T \dot{\mathbf{A}} = \tilde{\bar{\boldsymbol{\omega}}} = \begin{bmatrix} 0 & -\bar{\omega}_3 & \bar{\omega}_2 \\ \bar{\omega}_3 & 0 & -\bar{\omega}_1 \\ -\bar{\omega}_2 & \bar{\omega}_1 & 0 \end{bmatrix} \quad (6.8)$$

The bar over a vector or a matrix is used in this chapter to indicate a vector or a matrix whose components are defined in a body or local coordinate system.

Similarly, one can differentiate the second part ( $\mathbf{A} \mathbf{A}^T = \mathbf{I}$ ) of Equation 5 with respect to time and follow a procedure similar to the one used to obtain the preceding equation to show that  $\dot{\mathbf{A}} \mathbf{A}^T$  is a skew-symmetric matrix (Shabana, 2001), that is,

$$\dot{\mathbf{A}} \mathbf{A}^T = \tilde{\boldsymbol{\omega}} = \begin{bmatrix} 0 & -\omega_3 & \omega_2 \\ \omega_3 & 0 & -\omega_1 \\ -\omega_2 & \omega_1 & 0 \end{bmatrix} \quad (6.9)$$

Another important identity presented in Chapter 1 is associated with skew-symmetric matrices and the cross product. Recall that the cross product of two vectors  $\mathbf{a} = [a_1 \ a_2 \ a_3]^T$  and  $\mathbf{b} = [b_1 \ b_2 \ b_3]^T$  can always be written as  $\mathbf{a} \times \mathbf{b} = \tilde{\mathbf{a}} \mathbf{b}$ , where  $\tilde{\mathbf{a}}$  is a skew-symmetric matrix defined

$$\tilde{\mathbf{a}} = \begin{bmatrix} 0 & -a_3 & a_2 \\ a_3 & 0 & -a_1 \\ -a_2 & a_1 & 0 \end{bmatrix} \quad (6.10)$$

The simple identities presented in this section will be used to develop the kinematic velocity equations in the FFR formulation.

## General Displacement

In the case of a rigid-body motion, the position vector of an arbitrary point on the body can be defined in the global coordinate system, as shown in Figure 2, as follows (Shabana, 2001):

$$\mathbf{r} = \mathbf{r}_O + \mathbf{A}\bar{\mathbf{u}} \quad (6.11)$$

where  $\mathbf{r}_O$  is the global position vector of the origin of the body coordinate system,  $\mathbf{A}$  is the orthogonal transformation matrix that defines the orientation of the body coordinate system, and  $\bar{\mathbf{u}}$  is the local position vector of the arbitrary point with respect to the body coordinate system. Differentiating the preceding equation with respect to time, the absolute velocity vector of the arbitrary point on the body can be written as

$$\dot{\mathbf{r}} = \dot{\mathbf{r}}_O + \dot{\mathbf{A}}\bar{\mathbf{u}} \quad (6.12)$$

Because the rotation matrix  $\mathbf{A}$  is an orthogonal matrix, using Equations 8 and 9, the preceding equation can be written in the following two equivalent forms:

$$\left. \begin{aligned} \dot{\mathbf{r}} &= \dot{\mathbf{r}}_O + \mathbf{A}(\bar{\boldsymbol{\omega}} \times \bar{\mathbf{u}}) \\ \dot{\mathbf{r}} &= \dot{\mathbf{r}}_O + \boldsymbol{\omega} \times \mathbf{u} \end{aligned} \right\} \quad (6.13)$$

where  $\bar{\boldsymbol{\omega}}$  and  $\boldsymbol{\omega}$  to are called the angular velocity vectors defined, respectively, in the body and the global coordinate systems, and  $\mathbf{u} = \mathbf{A}\bar{\mathbf{u}}$ . Using the FFR motion description, it is

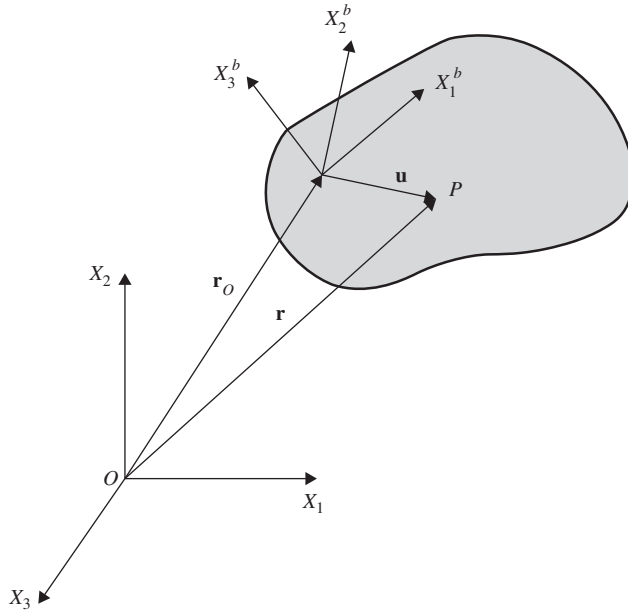


**Figure 6.2** Floating frame of reference

important to note the following:

1. The transformation matrix is, in general, a highly nonlinear function in the parameters used to describe the orientations of the bodies in space. From Equations 8, 9, and 13, it is clear that the angular velocity vector can be a highly nonlinear function of the orientation coordinates in the case of an arbitrary large rotation.
2. Despite the fact that the angular velocity vectors are, in general, highly nonlinear functions of the orientation coordinates, Equations 8 and 9 show that the angular velocity vectors are linear functions of the time derivatives of the orientation coordinates. The reader can demonstrate this fact because the definition of the angular velocity is obtained from the first time derivative of the transformation matrix.

Using these two remarks, it is clear that the angular velocity vector defined in the body and the global coordinate systems can be written, respectively, as

$$\bar{\omega} = \bar{G}\dot{\theta}, \quad \omega = G\dot{\theta} \quad (6.14)$$

where  $\bar{G}$  and  $G$  are two matrices that can be nonlinear functions of the orientation coordinates  $\theta$ .

### Illustrative Example

The preceding equation shows that in the three-dimensional motion, the angular velocity vector is not, in general, equal to the derivatives of the orientation parameters. Nonetheless, the form of the angular velocity vector depends on the orientation parameters used. There are different sets of rotation parameters that can be used to define the body orientation in space. Among these sets are the four *Euler parameters*, the three *Euler angles*, the three *Rodriguez parameters*, and the nine *direction cosines*. If Euler angles are used, the expression of the angular velocity depends on the sequence of rotations used to define the Euler angle transformation matrix (Shabana, 2001, 2013). In vehicle applications, it is convenient to use the following sequence: a rotation  $\psi$  about the body  $X_3^b$  axis, followed by a rotation  $\phi$  about the body  $X_1^b$  axis, followed by a third rotation  $\theta$  about the body  $X_2^b$  axis. These three angles, in the order given, are the *yaw*, *roll*, and *pitch* angles; this is with the assumption that  $X_1^b$  is the longitudinal axis. Note that by using this sequence, the singularity associated with Euler angles can be avoided because in some vehicle applications, the yaw and the roll angles remain small.

Using the sequence of rotations introduced in this section, the simple rotation matrices associated with the three Euler angles are given by

$$\begin{aligned} \mathbf{A}_3 &= \begin{bmatrix} \cos \psi & -\sin \psi & 0 \\ \sin \psi & \cos \psi & 0 \\ 0 & 0 & 1 \end{bmatrix}, \quad \mathbf{A}_1 = \begin{bmatrix} 1 & 0 & 0 \\ 0 & \cos \phi & -\sin \phi \\ 0 & \sin \phi & \cos \phi \end{bmatrix}, \\ \mathbf{A}_2 &= \begin{bmatrix} \cos \theta & 0 & \sin \theta \\ 0 & 1 & 0 \\ -\sin \theta & 0 & \cos \theta \end{bmatrix} \end{aligned} \quad (6.15)$$

If another sequence of rotations is used, one obtains a different set of simple rotation matrices. The product of the three matrices in the preceding equation defines the following body transformation matrix in terms of the three Euler angles:

$$\mathbf{A} = \mathbf{A}_3 \mathbf{A}_1 \mathbf{A}_2$$

$$= \begin{bmatrix} \cos \psi \cos \theta - \sin \psi \sin \phi \sin \theta & -\sin \psi \cos \phi & \cos \psi \sin \theta + \sin \psi \sin \phi \cos \theta \\ \sin \psi \cos \theta + \cos \psi \sin \phi \sin \theta & \cos \psi \cos \phi & \sin \psi \sin \theta - \cos \psi \sin \phi \cos \theta \\ -\cos \phi \sin \theta & \sin \phi & \cos \phi \cos \theta \end{bmatrix} \quad (6.16)$$

It is convenient to write the three Euler angles in the following vector form:

$$\boldsymbol{\theta} = [\psi \ \phi \ \theta]^T \quad (6.17)$$

The matrices  $\tilde{\mathbf{G}}$  and  $\mathbf{G}$  can be determined by differentiation of Equation 16 with respect to time and substituting into Equations 8 and 9, respectively. This approach for determining the matrices  $\tilde{\mathbf{G}}$  and  $\mathbf{G}$  requires manipulation of complex expressions of Euler angles and their derivatives. A second simpler approach that can be used to determine the matrices  $\tilde{\mathbf{G}}$  and  $\mathbf{G}$  is to recognize the columns of these matrices as unit vectors about which the three Euler angle rotations are performed. The columns of the matrix  $\tilde{\mathbf{G}}$  are unit vectors, defined in the body coordinate system, about which the three Euler rotations are performed. The columns of the matrix  $\mathbf{G}$  are the same unit vectors defined in the global coordinate system. This second approach for determining the matrices  $\tilde{\mathbf{G}}$  and  $\mathbf{G}$  is the one that is used in this section because it clearly shows the dependence of the expressions of the angular velocities on the sequence of rotations used in defining Euler angles. Nonetheless, the final results obtained should be the same as the results that can be obtained using Equations 8 and 9. Using this second approach, it can be shown that the matrices  $\tilde{\mathbf{G}}$  and  $\mathbf{G}$  are given by

$$\tilde{\mathbf{G}} = \begin{bmatrix} -\cos \phi \sin \theta & \cos \theta & 0 \\ \sin \phi & 0 & 1 \\ \cos \phi \cos \theta & \sin \theta & 0 \end{bmatrix}, \quad \mathbf{G} = \begin{bmatrix} 0 & \cos \psi & -\sin \psi \cos \phi \\ 0 & \sin \psi & \cos \psi \cos \phi \\ 1 & 0 & \sin \phi \end{bmatrix} \quad (6.18)$$

Using these two matrices, one obtains the following expressions for the absolute angular velocity vector defined, respectively, in the body and the global coordinate systems:

$$\bar{\boldsymbol{\omega}} = \begin{bmatrix} -\dot{\psi} \cos \phi \sin \theta + \dot{\phi} \cos \theta \\ \dot{\psi} \sin \phi + \dot{\theta} \\ \dot{\psi} \cos \phi \cos \theta + \dot{\phi} \sin \theta \end{bmatrix}, \quad \boldsymbol{\omega} = \begin{bmatrix} \dot{\phi} \cos \psi - \dot{\theta} \sin \psi \cos \phi \\ \dot{\phi} \sin \psi + \dot{\theta} \cos \psi \cos \phi \\ \dot{\psi} + \dot{\theta} \sin \phi \end{bmatrix} \quad (6.19)$$

Note that the preceding equation shows, as previously mentioned, that the components of the angular velocity vector are not, in general, the derivatives of Euler angles. Nonetheless, the components of the angular velocity are linear functions of the derivatives of Euler angles.

**Example 6.2**

In the case of infinitesimal rotations,

$$\begin{aligned}\cos \psi &= \cos \theta = \cos \phi \approx 1, \\ \sin \psi &\approx \psi, \quad \sin \theta \approx \theta, \quad \sin \phi \approx \phi\end{aligned}$$

In this case, one can show, using Equation 16, that the transformation matrix expressed in terms of Euler angles reduces to

$$\mathbf{A} = \begin{bmatrix} 1 & -\psi & \theta \\ \psi & 1 & -\phi \\ -\theta & \phi & 1 \end{bmatrix}$$

The angular velocity vectors in the case of infinitesimal rotations reduce to

$$\bar{\boldsymbol{\omega}} = \begin{bmatrix} \dot{\phi} \\ \dot{\theta} \\ \dot{\psi} \end{bmatrix}, \quad \boldsymbol{\omega} = \begin{bmatrix} \dot{\phi} \\ \dot{\theta} \\ \dot{\psi} \end{bmatrix}$$

In obtaining these simplified expressions for the angular velocity, quadratic terms are neglected.

**Euler Angles Singularity**

Euler angles suffer from the problem of singularity. For example, when  $\cos \phi = 0$ , both matrices  $\mathbf{G}$  and  $\bar{\mathbf{G}}$  become singular, and one cannot solve for the time derivatives of Euler angles in terms of the components of the angular velocity. This singularity problem is a characteristic of any method that uses three parameters only to describe the orientation of the rigid body in space. For this reason, the four Euler parameters are often used in computational dynamics in order to avoid this singularity problem. Note that when four parameters are used to describe the orientation of the moving frame of reference in space, a kinematic constraint equation must be introduced because the four parameters are not totally independent (Shabana, 2013).

**6.3 FLOATING FRAME OF REFERENCE (FFR)**

The example of the conventional beam element discussed in Section 1 shows that correct description of an arbitrary rigid-body motion cannot be obtained using the element nodal coordinates that include infinitesimal rotations. Because the nodal coordinates used for this type of elements imply linearization of the kinematic equations, an incremental solution procedure must be used if these elements are used in the analysis of large rotation problems and the element equations are formulated solely in terms of the nodal coordinates. Because the incremental solution of linearized equations eventually diverges from the correct solution and because most multibody system algorithms are based on nonincremental solution procedure (Roberson and Schwertassek, 1988; Shabana, 2013), there was a need to develop a finite element formulation that can utilize the many nonisoparametric elements and at the same time

leads to a correct description of the rigid-body motion. For this reason, the FFR formulation, which correctly describes the rigid-body motion and leads to zero strains under an arbitrary rigid-body displacement, was introduced. It is important, however, to mention that the FFR formulation for flexible bodies has been in existence long before the finite element was introduced. On the other hand, the finite element FFR formulation, as presented in this chapter, was introduced more recently.

It is crucial in the finite element FFR formulation that the element shape functions can describe arbitrary rigid-body translations in all directions. Fortunately, this requirement is met by most nonisoparametric finite elements that employ infinitesimal rotations as nodal coordinates. Using this property, an *intermediate element coordinate system* is used in order to obtain a correct expression for the inertia of bodies that have complex geometry characterized by discontinuities. The concept employed is similar to the concept of the *parallel axis theorem* used in elementary mechanics.

In the FFR formulation, a body coordinate system  $X_1^b X_2^b X_3^b$  that shares the large overall displacement of the body is introduced. The position vector of the origin of the body coordinate system is defined by the three-dimensional vector  $\mathbf{r}_O$ , whereas the orientation of the body coordinate system is defined using the orthogonal transformation matrix  $\mathbf{A}$ . The unconstrained motion of the coordinate system of the body can then be described using six independent coordinates: three translational coordinates defined by the components of the vector  $\mathbf{r}_O = [r_{O1} \ r_{O2} \ r_{O3}]^T$  and three independent rotation parameters  $\boldsymbol{\theta}$  that enter into the definition of the orthogonal matrix  $\mathbf{A}$  (Roberson and Schwertassek, 1988; Shabana, 2013). Note that these six coordinates are sufficient to describe an arbitrary rigid-body displacement. Using these coordinates, the global position of an arbitrary point on the finite element  $j$  of the body as shown in Figure 3 can be written as

$$\mathbf{r}^j = \mathbf{r}_O + \mathbf{A}\bar{\mathbf{u}}^j, \quad j = 1, 2, \dots, n_e \quad (6.20)$$

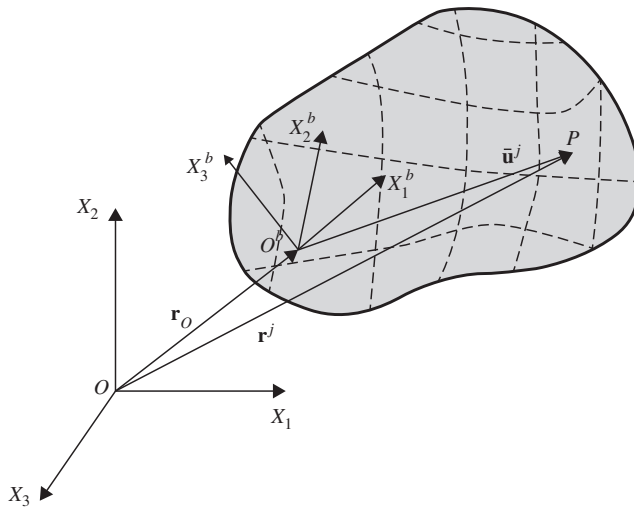


**Figure 6.3** Body kinematics



where  $n_e$  is the total number of finite elements used in the body discretization and  $\bar{\mathbf{u}}^j$  is the location of the arbitrary point on the finite element  $j$  with respect to the origin of the body coordinate system. Note that in the preceding equation,  $\mathbf{r}_O$  and  $\mathbf{A}$  are the same for all elements, and therefore, the body coordinate system represents a common reference for all elements and as such can serve as the basis for defining the connectivity between the finite elements. The goal is to develop linear conditions of connectivity between the finite elements of the body regardless of the element orientations. This requires introducing the concept of the intermediate element coordinate system discussed in the following section.

## 6.4 INTERMEDIATE ELEMENT COORDINATE SYSTEM

Modeling deformable bodies with complex geometries characterized by slope discontinuities require the use of finite elements, which can have different orientations in the undeformed reference configuration. In order to be able to describe the kinematics of these elements, an *intermediate element coordinate system*  $\bar{X}_1^j \bar{X}_2^j \bar{X}_3^j$  is introduced (Shabana, 1982, 2013). The intermediate element coordinate system has an origin, which is rigidly attached to the origin of the body coordinate system and has axes that are initially parallel to the axes of the element coordinate system  $X_1^j X_2^j X_3^j$  as shown in Figure 4. Because it is assumed that the element shape function matrix and the nodal coordinates can describe an arbitrary rigid-body translation, the position vector of the arbitrary point on the finite element  $j$  with respect to the intermediate element coordinate system  $\bar{X}_1^j \bar{X}_2^j \bar{X}_3^j$  can be written as

$$\bar{\mathbf{u}}^j = \mathbf{S}^j \bar{\mathbf{e}}^{ji}, \quad j = 1, 2, \dots, n_e \quad (6.21)$$

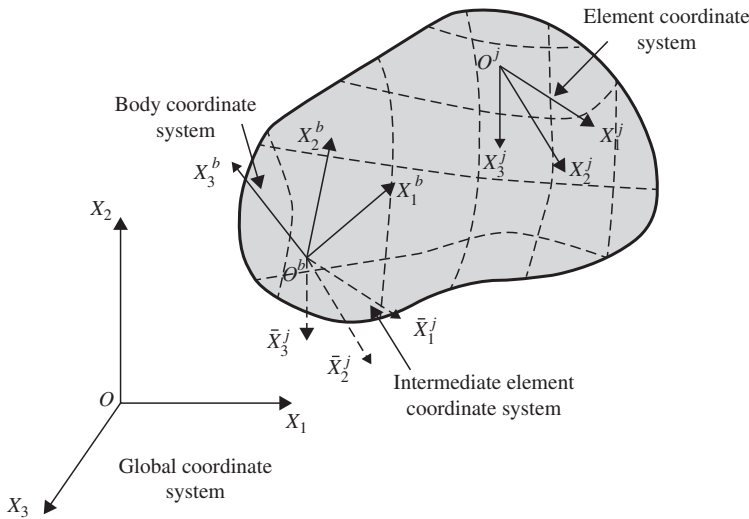


**Figure 6.4** Intermediate element coordinate system

In this equation,  $\mathbf{S}^j$  is the element shape function matrix, and  $\bar{\mathbf{e}}^{ji}$  is the vector of the element nodal coordinates defined in the intermediate element coordinate system. Using the assumption of small deformation and assuming that the elements are initially straight, one can write

$$\bar{\mathbf{e}}^{ji} = \bar{\mathbf{e}}_o^{ji} + \bar{\mathbf{e}}_f^{ji} \quad (6.22)$$

where  $\bar{\mathbf{e}}_o^{ji}$  is the vector of nodal coordinates in the reference configuration, and  $\bar{\mathbf{e}}_f^{ji}$  is the vector of nodal coordinates that define the element small deformation with respect to the intermediate element coordinate system. Because both of these nodal coordinate vectors are defined in the intermediate element coordinate system that has axes initially parallel to the axes of the element coordinate system, the components in the vector  $\bar{\mathbf{e}}_o^{ji}$  that correspond to infinitesimal rotations are identically equal to zero. The vector  $\bar{\mathbf{e}}_o^{ji}$ , therefore, describes the initial location (translation) of the element with respect to the intermediate element coordinate system before displacement. The element nodal coordinates  $\bar{\mathbf{e}}^{ji}$  defined in the intermediate element coordinate system  $\bar{X}_1^j \bar{X}_2^j \bar{X}_3^j$  can be expressed in terms of element coordinates  $\mathbf{e}^j$  defined in the body coordinate system  $X_1^b X_2^b X_3^b$  using the orthogonal transformation  $\bar{\mathbf{T}}_n^{ji}$  as (Shabana, 2013)

$$\bar{\mathbf{e}}^{ji} = \bar{\mathbf{T}}_n^{ji} \mathbf{e}^j \quad (6.23)$$

One can then write the vector  $\bar{\mathbf{u}}^{ji}$  in terms of element nodal coordinates defined in the body coordinate system as

$$\bar{\mathbf{u}}^{ji} = \mathbf{S}^j \bar{\mathbf{T}}_n^{ji} \mathbf{e}^j, \quad j = 1, 2, \dots, n_e \quad (6.24)$$

In this equation,  $\bar{\mathbf{T}}_n^{ji}$  is a constant transformation because the intermediate element coordinate system  $\bar{X}_1^j \bar{X}_2^j \bar{X}_3^j$  is assumed to have a constant orientation with respect to the body coordinate system  $X_1^b X_2^b X_3^b$ . The dimension of this constant transformation matrix is equal to the number of the element nodal coordinates. Furthermore, because infinitesimal nodal rotations due to the deformation with respect to the body coordinate system can be treated as elements of a vector, the transformation  $\bar{\mathbf{T}}_n^{ji}$  can be applied without any loss of generality to the nodal deformation vector  $\bar{\mathbf{e}}_f^{ji}$ . Note that the transformation of Equation 23 cannot be applied if the nodal rotations due to the deformation with respect to the body coordinate system  $X_1^b X_2^b X_3^b$  were assumed to be finite.

Similarly, the components of the vector  $\bar{\mathbf{u}}^{ji}$  can be defined in the body coordinate system as

$$\bar{\mathbf{u}}^j = \bar{\mathbf{T}}_u^{ji} \bar{\mathbf{u}}^{ji} = \bar{\mathbf{T}}_u^{ji} \mathbf{S}^j \bar{\mathbf{T}}_n^{ji} \mathbf{e}^j, \quad j = 1, 2, \dots, n_e \quad (6.25)$$

where  $\bar{\mathbf{T}}_u^{ji}$  is also a constant transformation matrix that has dimension equal to the dimension of the vector  $\bar{\mathbf{u}}^{ji}$  (2 for planar elements and 3 for spatial elements). The preceding equation defines the position vector of an arbitrary material point on the element in the body coordinate system. This equation can be written as

$$\bar{\mathbf{u}}^j = \mathbf{S}_b^j \mathbf{e}^j, \quad j = 1, 2, \dots, n_e \quad (6.26)$$

where

$$\mathbf{S}_b^j = \bar{\mathbf{T}}_u^{ji} \mathbf{S}^j \bar{\mathbf{T}}_n^{ji} \quad (6.27)$$

is the element shape function defined in the body coordinate system.

### Example 6.3

Consider the two-dimensional beam element discussed in Section 1. Assume that a body or a structure is discretized using this finite element. Assume that element  $j$  on the body initially makes an angle  $\alpha^j$  with the selected body coordinate system. In the intermediate element coordinate system  $\bar{X}_1^j \bar{X}_2^j \bar{X}_3^j$ , the vector of initial nodal coordinates  $\bar{\mathbf{e}}_o^{ji}$  is in general given by

$$\begin{aligned} \bar{\mathbf{e}}_o^{ji} &= [\bar{e}_{o1}^{ji} \ \bar{e}_{o2}^{ji} \ \bar{e}_{o3}^{ji} \ \bar{e}_{o4}^{ji} \ \bar{e}_{o5}^{ji} \ \bar{e}_{o6}^{ji}]^T \\ &= [\bar{e}_{o1}^{ji} \ \bar{e}_{o2}^{ji} \ 0 \ \bar{e}_{o1}^{ji} + l^j \ \bar{e}_{o2}^{ji} \ 0]^T \end{aligned}$$

where  $l^j$  is the length of the finite element  $j$ , and  $[\bar{e}_{o1}^{ji} \ \bar{e}_{o2}^{ji}]^T$  is the vector that defines the position of the first node with respect to the origin of the intermediate element coordinate system.

In this case of two-dimensional beam element, the constant transformation matrix  $\bar{\mathbf{T}}_n^{ji}$  used in Equation 23 to define the relationship between the element nodal coordinates in the body and the intermediate element coordinate systems is a  $6 \times 6$  matrix and is given by

$$\bar{\mathbf{T}}_n^{ji} = \begin{bmatrix} \bar{\mathbf{T}}_{n1}^{ji} & \mathbf{0} \\ \mathbf{0} & \bar{\mathbf{T}}_{n1}^{ji} \end{bmatrix}$$

where the matrix  $\bar{\mathbf{T}}_{n1}^{ji}$  is a  $3 \times 3$  constant transformation matrix which can be expressed in terms of the constant angle  $\alpha^j$  that defines the orientation of the finite element in the initial configuration with respect to the body coordinate system. This matrix can be written as

$$\bar{\mathbf{T}}_{n1}^{ji} = \begin{bmatrix} \cos \alpha^j & \sin \alpha^j & 0 \\ -\sin \alpha^j & \cos \alpha^j & 0 \\ 0 & 0 & 1 \end{bmatrix}$$

The  $2 \times 2$  constant transformation matrix  $\bar{\mathbf{T}}_u^{ji}$  used in Equation 25 to define the position vector of the material points on the finite element  $j$  with respect to the body coordinate system can be written in terms of the constant angle  $\alpha^j$  as follows:

$$\bar{\mathbf{T}}_u^{ji} = \begin{bmatrix} \cos \alpha^j & -\sin \alpha^j \\ \sin \alpha^j & \cos \alpha^j \end{bmatrix}$$

## 6.5 CONNECTIVITY AND REFERENCE CONDITIONS

In order to define a unique displacement field and develop the final form of the kinematic equations that will be used to develop the equations of motion of the finite element, it is necessary to impose two sets of conditions: the *connectivity* and the *reference conditions*.

The connectivity conditions lead to the element assembly, whereas the reference conditions eliminate the rigid-body modes of the element shape function matrix, define a unique displacement field, and define the nature of the floating body coordinate system  $X_1^b X_2^b X_3^b$ , which does not have to be rigidly attached to a point on the body.

### Connectivity Conditions

In the preceding section, the position vector of an arbitrary point on the finite element was defined in terms of nodal coordinates defined in the body coordinate system  $X_1^b X_2^b X_3^b$ , which serves as a common standard for all the finite elements that form this body. Using the Boolean matrix approach discussed in the preceding chapter, the element nodal coordinates can be written in terms of the body nodal coordinates as

$$\mathbf{e}^j = \mathbf{B}_c^j \mathbf{e}_b, \quad j = 1, 2, \dots, n_e \quad (6.28)$$

where  $\mathbf{e}_b$  is the vector of the body nodal coordinates, and  $\mathbf{B}_c^j$  is the constant Boolean matrix that defines the connectivity conditions for the finite element  $j$ . Therefore, the position vector of the material points, after substituting Equation 28 into Equation 26, can be defined as

$$\bar{\mathbf{u}}^j = \mathbf{S}_b^j \mathbf{B}_c^j \mathbf{e}_b, \quad j = 1, 2, \dots, n_e \quad (6.29)$$

Another set of conditions, reference conditions, must be imposed before this equation can be used effectively in the motion description of the deformable body that undergoes large reference displacement.

### Reference Conditions

Although the shape functions of conventional beam, plate, and shell elements cannot describe correctly arbitrary rigid-body displacements, these shape functions have rigid-body modes that can describe arbitrary rigid-body translations and infinitesimal rigid-body rotations. In the FFR formulation, however, the reference rigid-body motion is described using the absolute Cartesian coordinates  $\mathbf{r}_O$  and the orientation coordinates  $\boldsymbol{\theta}$ , as previously described. These coordinates that define the location of the origin and the orientation of the body coordinate system can describe an arbitrary rigid-body displacement. In order to define a unique displacement field, the redundant rigid-body modes of the element shape functions must be eliminated. To this end, a set of *reference conditions* imposed on the nodal deformation coordinates must be used (Agrawal and Shabana, 1985; Shabana, 1996b, 2013). These reference conditions also define the nature of the body coordinate system used and how the deformation is measured with respect to the body coordinate system. As in the case of the individual elements, one can write the vector of body nodal coordinates as the sum of two vectors as

$$\mathbf{e}_b = \mathbf{e}_{bo} + \mathbf{e}_{bf} \quad (6.30)$$

where  $\mathbf{e}_{bo}$  is the vector of nodal coordinates in the initial undeformed configuration, and  $\mathbf{e}_{bf}$  is the vector of deformation nodal coordinates. By imposing the reference conditions, one can write  $\mathbf{e}_{bf}$  in terms of a new reduced set of body nodal coordinates  $\mathbf{e}_f$  as

$$\mathbf{e}_{bf} = \mathbf{B}_r \mathbf{e}_f \quad (6.31)$$

where  $\mathbf{B}_r$  is the matrix of reference conditions that eliminates nodal coordinates and defines how the deformation is measured with respect to the body coordinate system. The number

of reference conditions should not be less than the number of the rigid-body modes of the finite element shape function matrix (Agrawal and Shabana, 1985; Shabana, 1996b, 2013). The position vector  $\bar{\mathbf{u}}^j$  of the material point on the finite element can then be defined in the body coordinate system as

$$\bar{\mathbf{u}}^j = \mathbf{S}_b^j \mathbf{B}_c^j (\mathbf{e}_{bo} + \mathbf{B}_r \mathbf{e}_f), \quad j = 1, 2, \dots, n_e \quad (6.32)$$

This position vector can be written as the sum of the position vector in the undeformed state plus the vector of deformation as

$$\bar{\mathbf{u}}^j = \bar{\mathbf{u}}_o^j + \bar{\mathbf{u}}_f^j, \quad j = 1, 2, \dots, n_e \quad (6.33)$$

where

$$\bar{\mathbf{u}}_o^j = \mathbf{S}_b^j \mathbf{B}_c^j \mathbf{e}_{bo}, \quad \bar{\mathbf{u}}_f^j = \mathbf{S}_b^j \mathbf{B}_c^j \mathbf{B}_r \mathbf{e}_f \quad (6.34)$$

This equation shows that  $\bar{\mathbf{u}}_o^j$  does not depend on time, whereas  $\bar{\mathbf{u}}_f^j$  is time dependent. Note that the nodal position vector  $\mathbf{e}_{bo}$  and the nodal deformation vector  $\mathbf{e}_f$  do not have the same dimension because the reference conditions are imposed only on the deformation vector  $\mathbf{e}_f$ .

### Rigid-Body and Reference Motion

Before using the equations developed in this section in formulating the velocity and acceleration equations, it is important to reiterate at this point that the application of the reference conditions to eliminate the rigid-body motion may lead to a coordinate system whose origin is not rigidly attached to a material point on the body. Nonetheless, there must be no rigid-body motion of the body with respect to its reference. This is the reason that the moving frame used in this formulation is called *floating*. It is important also to realize that the use of the floating frame does not imply a separation between the rigid-body motion and the elastic deformation, as previously mentioned. There is a separation between the motion of the rigid reference and the elastic deformation. The reference motion cannot be in general interpreted as the rigid-body motion of the body. Different choices of references can be made, and the use of these different references leads to the same results as demonstrated in the literature (Agrawal and Shabana, 1985; Shabana, 1996b, 2013).

The choice of the floating frame and its relationship with the constraints imposed on the boundary of the deformable bodies is one of the most fundamental problems in the analysis of flexible bodies that experience large displacements. This fundamental problem is also important in developing an efficient computational procedure that integrates existing finite element and multibody system algorithms. Although the choice of the reference frame can be arbitrary, it is important to recognize that some choices of the reference frame can lead to a more efficient and accurate solution. The choice of the reference frame must lead to deformation measures that are consistent with the linear elasticity theory used in some formulations. Recall that the deformations are measured with respect to the floating frame. In one frame, the deformation can be considered small, whereas in another frame, the deformation can be large. If linear strain displacement relations are used, a choice of a reference frame may not be consistent with the theory employed. This is demonstrated by the following example;

**Example 6.4**

Consider the slider crank mechanism shown in Figure 5. The connecting rod of this mechanism is treated as a flexible body. To explain the concept of the reference conditions, we assume that the connecting rod is modeled using one two-dimensional beam finite element only. The finite element used is assumed to be the one presented in Section 1. This finite element has six degrees of freedom, three of which describe the rigid-body motion. Because the reference conditions must be imposed on the deformation coordinates only, the vector of nodal deformations of the beam is defined as

$$\begin{aligned}\mathbf{e}_{bf} &= [e_{bf1} \ e_{bf2} \ e_{bf3} \ e_{bf4} \ e_{bf5} \ e_{bf6}]^T \\ &= [r_{bf1}^1 \ r_{bf2}^1 \ \theta_{bf}^1 \ r_{bf1}^2 \ r_{bf2}^2 \ \theta_{bf}^2]^T\end{aligned}$$

where  $r_{bf1}^1$ ,  $r_{bf2}^1$ , and  $\theta_{bf}^1$  are the two translational coordinates of the first node and the infinitesimal rotation at the first node, respectively; and  $r_{bf1}^2$ ,  $r_{bf2}^2$ , and  $\theta_{bf}^2$  are the two translational coordinates of the second node and the infinitesimal rotation at the second node, respectively.

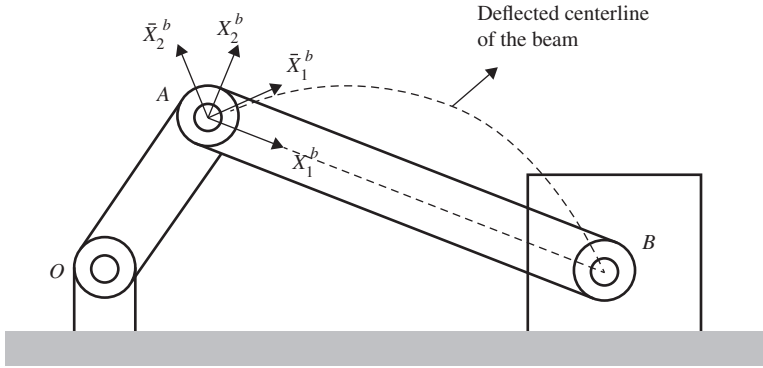


**Figure 6.5** Slider crank mechanism

The connecting rod shown in the figure, when it deforms, assumes a simple shape similar to the one shown in Figure 5. Several FFR choices can be made. In this example, two of these choices are discussed.

**Chord frame** The chord frame  $X_1^b X_2^b$ , shown in Figure 5, can be selected to measure the deformation of the connecting rod. The origin of this frame is assumed to be attached to point A; nonetheless, the material point at point A can experience infinitesimal rotation with respect to the coordinate system  $X_1^b X_2^b$ . Furthermore, it is assumed that the endpoint B is free to deform in the axial direction, whereas no transverse deformation is allowed at this point. One can then assume the following three reference conditions that can be used to eliminate the

rigid-body motion of the beam with respect to its reference and define the nature of the chord frame  $X_1^b X_2^b$ :

$$e_{bf1} = 0, \quad e_{bf2} = 0, \quad e_{bf5} = 0$$

By imposing these three conditions, one can write the total vector of the beam coordinates in terms of the independent coordinates as

$$\begin{bmatrix} e_{bf1} \\ e_{bf2} \\ e_{bf3} \\ e_{bf4} \\ e_{bf5} \\ e_{bf6} \end{bmatrix} = \begin{bmatrix} 0 & 0 & 0 \\ 0 & 0 & 0 \\ 1 & 0 & 0 \\ 0 & 1 & 0 \\ 0 & 0 & 0 \\ 0 & 0 & 1 \end{bmatrix} \begin{bmatrix} e_{bf3} \\ e_{bf4} \\ e_{bf6} \end{bmatrix}$$

which can be written in the form of Equation 31 as

$$\mathbf{e}_{bf} = \mathbf{B}_r \mathbf{e}_f$$

where

$$\mathbf{e}_{bf} = \begin{bmatrix} e_{bf1} \\ e_{bf2} \\ e_{bf3} \\ e_{bf4} \\ e_{bf5} \\ e_{bf6} \end{bmatrix}, \quad \mathbf{B}_r = \begin{bmatrix} 0 & 0 & 0 \\ 0 & 0 & 0 \\ 1 & 0 & 0 \\ 0 & 1 & 0 \\ 0 & 0 & 0 \\ 0 & 0 & 1 \end{bmatrix}, \quad \mathbf{e}_f = \begin{bmatrix} e_{bf3} \\ e_{bf4} \\ e_{bf6} \end{bmatrix}$$

Note that in this case, the  $X_1^b$  axis of the beam coordinate system must always be along the line connecting points  $A$  and  $B$  as the results of the constraints imposed on the deformations by the reference conditions. That is, the nature of the body coordinate system  $X_1^b X_2^b$  is defined by the reference conditions used to eliminate the rigid-body modes of the flexible body.

The reference conditions used to define the coordinate system  $X_1^b X_2^b$  are similar to those boundary conditions used for the simply supported beams. It is important, however, to realize that there is no relationship between the natural frequencies of the simply supported beam and the solution of the nonlinear problem of the rotating constrained connecting rod, as discussed in the literature. Different coordinate systems can be used for the connecting rod, and the solution should not, in principle, depend on the choice of the coordinate system, provided this choice is consistent with the formulation employed. One can also see from Figure 5 that if the midpoint deflection of the connecting rod is small, the deformations of all points measured with respect to the coordinate system  $X_1^b X_2^b$  are small.

**Tangent frame** In the case of the tangent frame  $\bar{X}_1^b \bar{X}_2^b$ , also shown in Figure 5, the origin of the body coordinate system is assumed to be rigidly attached to point  $A$ . In this case, the deformations and slope measured with respect to the coordinate system are assumed to be zero at point  $A$ . Therefore, the reference conditions that define the tangent frame  $\bar{X}_1^b \bar{X}_2^b$  can be written as follows:

$$e_{bf1} = 0, \quad e_{bf2} = 0, \quad e_{bf3} = 0$$

Using these conditions, which also eliminate the rigid-body motion of the beam, one can write the total vector of coordinates in terms of the remaining free coordinates as

$$\begin{bmatrix} e_{bf1} \\ e_{bf2} \\ e_{bf3} \\ e_{bf4} \\ e_{bf5} \\ e_{bf6} \end{bmatrix} = \begin{bmatrix} 0 & 0 & 0 \\ 0 & 0 & 0 \\ 0 & 0 & 0 \\ 1 & 0 & 0 \\ 0 & 1 & 0 \\ 0 & 0 & 1 \end{bmatrix} \begin{bmatrix} e_{bf4} \\ e_{bf5} \\ e_{bf6} \end{bmatrix}$$

which can also be written in the form

$$\mathbf{e}_{bf} = \mathbf{B}_r \mathbf{e}_f$$

where in the case,

$$\mathbf{e}_{bf} = \begin{bmatrix} e_{bf1} \\ e_{bf2} \\ e_{bf3} \\ e_{bf4} \\ e_{bf5} \\ e_{bf6} \end{bmatrix}, \quad \mathbf{B}_r = \begin{bmatrix} 0 & 0 & 0 \\ 0 & 0 & 0 \\ 0 & 0 & 0 \\ 1 & 0 & 0 \\ 0 & 1 & 0 \\ 0 & 0 & 1 \end{bmatrix}, \quad \mathbf{e}_f = \begin{bmatrix} e_{bf4} \\ e_{bf5} \\ e_{bf6} \end{bmatrix}$$

Note that the transverse deformation of point  $B$  with respect to the tangent frame  $\bar{X}_1^b \bar{X}_2^b$  cannot be considered small.

The same procedure described in this example can be applied to bodies discretized using a large number of finite elements. The number of reference conditions should be equal or greater than the number of the rigid-body modes of the flexible body in order to define a unique displacement field.

## 6.6 KINEMATIC EQUATIONS

Using Equations 20 and 33, the global position vector of an arbitrary material point on element  $j$  can be written as

$$\mathbf{r}^j = \mathbf{r}_O + \mathbf{A}(\bar{\mathbf{u}}_o^j + \bar{\mathbf{u}}_f^j), \quad j = 1, 2, \dots, n_e \quad (6.35)$$



where  $\tilde{\mathbf{u}}_o^j$  and  $\tilde{\mathbf{u}}_f^j$  are defined by Equation 34. A virtual change in the position vector  $\mathbf{r}^j$  is given by

$$\delta \mathbf{r}^j = \delta \mathbf{r}_O - \mathbf{A} \tilde{\mathbf{u}}^j \bar{\mathbf{G}} \delta \boldsymbol{\theta} + \mathbf{A} \mathbf{S}_b^j \mathbf{B}_c^j \mathbf{B}_r \delta \mathbf{e}_f \quad (6.36)$$

In this equation,  $\tilde{\mathbf{u}}^j$  is the skew-symmetric matrix associated with the vector  $\tilde{\mathbf{u}}^j$  and  $\bar{\mathbf{G}}$  is the matrix that relates the angular velocity vector to the time derivatives of the orientation parameters as discussed in Section 2. The preceding equation can be written for the finite element  $j$  as

$$\delta \mathbf{r}^j = \begin{bmatrix} \mathbf{I} & -\mathbf{A} \tilde{\mathbf{u}}^j \bar{\mathbf{G}} & \mathbf{A} \mathbf{S}_b^j \mathbf{B}_c^j \mathbf{B}_r \end{bmatrix} \begin{bmatrix} \delta \mathbf{r}_O \\ \delta \boldsymbol{\theta} \\ \delta \mathbf{e}_f \end{bmatrix} \quad (6.37)$$

which can also be written as

$$\delta \mathbf{r}^j = \mathbf{S}_f^j \delta \mathbf{q} \quad (6.38)$$

where

$$\mathbf{S}_f^j = \begin{bmatrix} \mathbf{I} & -\mathbf{A} \tilde{\mathbf{u}}^j \bar{\mathbf{G}} & \mathbf{A} \mathbf{S}_b^j \mathbf{B}_c^j \mathbf{B}_r \end{bmatrix}, \quad \mathbf{q} = \begin{bmatrix} \mathbf{r}_O \\ \boldsymbol{\theta} \\ \mathbf{e}_f \end{bmatrix} \quad (6.39)$$

The vector  $\mathbf{q}$  that contains the reference and elastic nodal coordinates of the body can be written as

$$\mathbf{q} = \begin{bmatrix} \mathbf{q}_r \\ \mathbf{q}_f \end{bmatrix} \quad (6.40)$$

where

$$\mathbf{q}_r = [\mathbf{r}_O^T \ \boldsymbol{\theta}^T]^T, \quad \mathbf{q}_f = \mathbf{e}_f \quad (6.41)$$

In this equation,  $\mathbf{q}_r$  is the vector of *reference coordinates*, and  $\mathbf{q}_f$  is the vector of *elastic coordinates*.

It follows from the development presented in this section that the absolute velocity vector can be written as

$$\dot{\mathbf{r}}^j = \mathbf{S}_f^j \dot{\mathbf{q}} \quad (6.42)$$

and the acceleration vector is

$$\ddot{\mathbf{r}}^j = \dot{\mathbf{S}}_f^j \dot{\mathbf{q}} + \mathbf{S}_f^j \ddot{\mathbf{q}} \quad (6.43)$$

It can be shown that the velocity and acceleration vectors of Equations 42 and 43, respectively, can be expressed in terms of the angular velocity and acceleration vectors of the body reference.

The kinematic equations presented in this section can be used with the principle of virtual work to develop the equations of motion of the deformable body. Note that these kinematic equations are expressed in terms of a coupled set of reference and elastic coordinates. This is one of the fundamental differences between the motion description used in this chapter and the one used in the preceding chapter. The motion description used in this chapter allows for the use of a systematic procedure to reduce the number of elastic degrees of freedom in the case of

small deformations, as discussed in later sections of this chapter. One of the interesting issues that arise when the FFR formulation is used is the study of the dynamic coupling between the reference motion and the elastic deformation. This subject is discussed in more detail after the inertia forces are formulated.

## 6.7 FORMULATION OF THE INERTIA FORCES

Some of the shape functions of the conventional finite elements that employ infinitesimal rotations as nodal coordinates can correctly capture the rigid-body inertia about the axes of their coordinate system. For example, using the shape function matrix of the two-dimensional beam element defined in Equation 2, one can show that this shape function matrix can be used to correctly define the mass moment of inertia about the element  $X_3^j$  axis, as demonstrated by the following example. The FFR formulation can be used to correctly account for the change in the rigid-body inertia of the finite element due to the deformations. In this formulation, each of the inertia coefficients can be written as the sum of two terms: the first term represents the rigid-body inertia, whereas the second term represents the change in the inertia due to deformation (Shabana, 2013). Therefore, if a finite element does not correctly capture the rigid-body inertia, one can always provide the correct inertia since in the FFR approach, the rigid-body inertia terms explicitly appear in the dynamic equations of motion.

### Example 6.5

Using the shape function matrix of Equation 2 and assuming a constant cross-sectional area, one can write the mass moment of inertia of the finite element about its  $X_3^j$  axis as

$$m_{\theta\theta}^j = \int_0^{\ell^j} \rho^j A^j \mathbf{r}^j \mathbf{r}^j dx_1^j$$

where  $\ell^j$  is the length of the finite element,  $\rho^j$  is the mass density,  $A^j$  is the cross-sectional area,  $x_1^j$  is the axial coordinate, and

$$\mathbf{r}^j = \mathbf{S}^j \mathbf{e}^j,$$

In this equation,  $\mathbf{S}^j$  is the element shape function matrix given by Equation 2, and  $\mathbf{e}^j$  is the vector of nodal coordinates defined in this case as

$$\mathbf{e}^j = [0 \quad 0 \quad 0 \quad \ell^j \quad 0 \quad 0]^T$$

Substituting the preceding two equations into the expression for  $m_{\theta\theta}^j$ , one obtains

$$m_{\theta\theta}^j = \int_0^{\ell^j} \rho^j A^j \mathbf{r}^j \mathbf{r}^j dx_1^j = \frac{m^j (\ell^j)^2}{3}$$

which is the correct rigid-body mass moment of inertia.

In general, the virtual work of the inertia forces of the finite element  $j$  can be written as

$$\delta W_i^j = \int_{V^j} \rho^j \ddot{\mathbf{r}}^j \delta \mathbf{r}^j dV^j \quad (6.44)$$

In this equation,  $\rho^j$  is the mass density of the material points of the element, and  $V^j$  is the element volume. Both  $\rho^j$  and  $V^j$  are defined in the reference configuration. For the most part, the FFR formulation is used for small-deformation problems. As such, one can assume that the determinant of the matrix of position vector gradients  $\mathbf{J}$  is equal to one. That is,  $J = |\mathbf{J}| \approx 1$ , and as a consequence, the changes in density and volume are assumed to be small. Using the definitions of  $\delta \mathbf{r}^j$  and  $\ddot{\mathbf{r}}^j$  in Equations 38 and 43 presented in the preceding section, the virtual work of the inertia forces of the finite element can be written as

$$\delta W_i^j = \int_{V^j} \rho^j (\mathbf{S}_f^j \ddot{\mathbf{q}} + \dot{\mathbf{S}}_f^j \dot{\mathbf{q}})^T \mathbf{S}_f^j \delta \mathbf{q} dV^j \quad (6.45)$$

In this equation,  $\mathbf{q}$  is the vector of generalized coordinates of the body. Equation 45 can be written as the sum of two terms: one linear in the accelerations and the other is quadratic in the velocities, that is,

$$\delta W_i^j = \left\{ \ddot{\mathbf{q}}^T \left( \int_{V^j} \rho^j \mathbf{S}_f^{jT} \mathbf{S}_f^j dV^j \right) + \dot{\mathbf{q}}^T \left( \int_{V^j} \rho^j \dot{\mathbf{S}}_f^{jT} \mathbf{S}_f^j dV^j \right) \right\} \delta \mathbf{q} \quad (6.46)$$

or

$$\delta W_i^j = \{ \ddot{\mathbf{q}}^T \mathbf{M}^j - \mathbf{Q}_v^j \} \delta \mathbf{q} \quad (6.47)$$

where  $\mathbf{M}^j$  is the symmetric mass matrix of the finite element  $j$ , and  $\mathbf{Q}_v^j$  is the vector of Coriolis and centrifugal forces. The mass matrix  $\mathbf{M}^j$  and the vector  $\mathbf{Q}_v^j$  are defined as

$$\mathbf{M}^j = \int_{V^j} \rho^j \mathbf{S}_f^{jT} \mathbf{S}_f^j dV^j, \quad \mathbf{Q}_v^j = - \left( \int_{V^j} \rho^j \mathbf{S}_f^{jT} \dot{\mathbf{S}}_f^j dV^j \right) \dot{\mathbf{q}} \quad (6.48)$$

The definition of the matrix  $\mathbf{S}_f^j$  shows that the element mass matrix and the vector of Coriolis and centrifugal forces are highly nonlinear functions of the reference and elastic coordinates. This is another fundamental difference between the FFR formulation and the large deformation ANCF presented in the preceding chapter where the mass matrix is constant and the Coriolis and centrifugal force vector are identically zero. The complexity of the FFR formulation appears in the inertia forces. Nonetheless, one can show that the nonlinear mass matrix and the centrifugal and Coriolis forces can be expressed in terms of a unique set of finite element *inertia shape integrals*. Assuming that the element shape function matrix can describe arbitrary translational motion in all directions, it is left to the reader to show that in the case of three-dimensional analysis, the inertia forces of the finite element can be written in terms of the following unique seven inertia shape integrals:

$$\left. \begin{aligned} \bar{\mathbf{S}}^j &= \int_{V^j} \rho^j \mathbf{S}_b^j dV^j \\ \mathbf{S}_{kl}^j &= \int_{V^j} \rho^j \mathbf{S}_{bk}^{jT} \mathbf{S}_{bl}^j dV^j, \quad k, l = 1, 2, 3 \end{aligned} \right\} \quad (6.49)$$

where  $\mathbf{S}_{bk}^j$  is the  $k$ th row of the element shape function matrix  $\mathbf{S}_b^j$  of Equation 27. Note that  $\tilde{\mathbf{S}}^j$  has the same dimension as the element shape function matrix, whereas  $\mathbf{S}_{kl}^j$  are square matrices that have dimensions equal to the number of nodal coordinates of the finite element.

In the case of the two-dimensional analysis, one can show that the inertia shape integrals reduce to three integrals only defined as

$$\tilde{\mathbf{S}}^j = \int_{V^j} \rho^j \mathbf{S}_b^j dV^j, \quad \tilde{\mathbf{S}}^j = \int_{V^j} \rho^j \mathbf{S}_b^{jT} \tilde{\mathbf{I}} \mathbf{S}_b^j dV^j, \quad \mathbf{S}_{ff}^j = \int_{V^j} \rho^j \mathbf{S}_b^{jT} \mathbf{S}_b^j dV^j \quad (6.50)$$

where  $\tilde{\mathbf{I}}$  is a skew-symmetric matrix defined as

$$\tilde{\mathbf{I}} = \begin{bmatrix} 0 & 1 \\ -1 & 0 \end{bmatrix} \quad (6.51)$$

The first inertia shape integral in Equation 50 has a dimension equal to the dimension of the element shape function matrix, whereas the last two inertia shape integrals are square matrices that have dimension equal to the number of element nodal coordinates. In particular,  $\tilde{\mathbf{S}}^j$  is a skew-symmetric matrix, whereas  $\mathbf{S}_{ff}^j$  is a symmetric matrix.

### Body Inertia Shape Integrals

The virtual work of the inertia forces of the body can be obtained by summing up the expressions of the virtual work of the inertia forces of its finite elements, that is,

$$\delta W_i = \sum_{j=1}^{n_e} \delta W_i^j = \left( \sum_{j=1}^{n_e} \{ \ddot{\mathbf{q}}^T \mathbf{M}^j - \mathbf{Q}_v^{jT} \} \right) \delta \mathbf{q} \quad (6.52)$$

which can also be written as

$$\delta W_i = \left( \ddot{\mathbf{q}}^T \sum_{j=1}^{n_e} \mathbf{M}^j - \sum_{j=1}^{n_e} \mathbf{Q}_v^{jT} \right) \delta \mathbf{q} = (\ddot{\mathbf{q}}^T \mathbf{M} - \mathbf{Q}_v^T) \delta \mathbf{q} \quad (6.53)$$

where  $\mathbf{M}$  is the body mass matrix, and  $\mathbf{Q}_v$  is the vector of body centrifugal and Coriolis forces. The matrix  $\mathbf{M}$  and the vector  $\mathbf{Q}_v$  are defined as

$$\mathbf{M} = \sum_{j=1}^{n_e} \mathbf{M}^j, \quad \mathbf{Q}_v = \sum_{j=1}^{n_e} \mathbf{Q}_v^j \quad (6.54)$$

Note that the body and the element mass matrices are symmetric. It was possible to use summation in the preceding equation because of the use of the Boolean matrix  $\mathbf{B}_c^j$  for the finite element. Using this matrix makes the dimensions of all the element mass matrices and the element vectors of Coriolis and centrifugal forces equal to the dimension of the vector of the body nodal coordinates.

As in the case of a single finite element, one can also show that the inertia forces of the body can be expressed in terms of a unique set of inertia shape integrals obtained by summing

up the inertia shape integrals of its elements. In the case of the three-dimensional analysis, the inertia shape integrals of the body are obtained using Equation 49 as

$$\left. \begin{aligned} \bar{\mathbf{S}} &= \left( \sum_{j=1}^{n_e} \bar{\mathbf{S}}^j \mathbf{B}_c^j \right) \mathbf{B}_r \\ \mathbf{S}_{kl} &= \mathbf{B}_r^T \left( \sum_{j=1}^{n_e} \mathbf{B}_c^{jT} \mathbf{S}_{kl}^j \mathbf{B}_c^j \right) \mathbf{B}_r, \quad k, l = 1, 2, 3 \end{aligned} \right\} \quad (6.55)$$

Similarly, in the two-dimensional analysis, one has the following three body inertia shape integrals obtained by summing up the inertia shape integrals of the finite elements presented in Equation 50:

$$\left. \begin{aligned} \bar{\mathbf{S}} &= \left( \sum_{j=1}^{n_e} \bar{\mathbf{S}}^j \mathbf{B}_c^j \right) \mathbf{B}_r \\ \tilde{\mathbf{S}} &= \mathbf{B}_r^T \left( \sum_{j=1}^{n_e} \mathbf{B}_c^{jT} \tilde{\mathbf{S}}^j \mathbf{B}_c^j \right) \mathbf{B}_r \\ \mathbf{S}_{ff} &= \mathbf{B}_r^T \left( \sum_{j=1}^{n_e} \mathbf{B}_c^{jT} \mathbf{S}_{ff}^j \mathbf{B}_c^j \right) \mathbf{B}_r \end{aligned} \right\} \quad (6.56)$$

The inertia shape integrals play a fundamental role in the computational algorithms developed for the deformation analysis of bodies that undergo large rotation and small deformation. They play a central role in the successful integration of small-deformation finite element and multi-body system algorithms. Change or reduction of the elastic coordinates can be achieved by operating on these inertia shape integrals only. This automatically changes the equations of motion to be expressed in terms of the new set of coordinates. Furthermore, understanding the role of the inertia shape integrals allows one to develop an automated scheme for coupling existing commercial general purpose finite element computer codes and general purpose flexible multibody computer codes.

## 6.8 ELASTIC FORCES

The elastic forces can be formulated using the virtual work as described in Chapter 3. The virtual work of the elastic forces can be written for the finite element  $j$  as

$$\delta W_s^j = - \int_{V^j} \boldsymbol{\sigma}_{p2}^j : \delta \boldsymbol{\epsilon}^j dV^j \quad (6.57)$$

where  $\boldsymbol{\sigma}_{p2}^j$  is the second Piola–Kirchhoff stress tensor and  $\boldsymbol{\epsilon}^j$  is the Green–Lagrange strain tensor. In the case of small deformation, as is often assumed when the FFR formulation is used in MBS applications, no distinction needs to be made between the second Piola–Kirchhoff

stress tensor and Cauchy stress tensor. Using the constitutive equations, the preceding equation can be written in terms of the strains as

$$\delta W_s^j = - \int_{V^j} (\mathbf{E}^j : \boldsymbol{\epsilon}^j) : \delta \boldsymbol{\epsilon}^j dV^j \quad (6.58)$$

where  $\mathbf{E}^j$  is the fourth-order tensor of elastic coefficients. The strain components can be written in terms of the displacement gradients, which can in turn be written in terms of the components of the vector of elastic coordinates. In the FFR formulation, the deformation of the finite element is defined with respect to the body coordinate system using the vector  $\mathbf{u}_f^j$ . In this case, one can use a linear strain–displacement relationship because the rigid-body displacement is correctly described using the reference coordinates  $\mathbf{q}_r = [\mathbf{r}_O^T \ \boldsymbol{\theta}^T]^T$ .

One can show by using the strain–displacement relationship that the virtual work of the elastic forces can be written as

$$\delta W_s^j = \mathbf{Q}_s^{jT} \delta \mathbf{e}_f^j \quad (6.59)$$

where  $\mathbf{Q}_s^j$  is the vector of elastic forces associated with the element nodal coordinates. Because the vector of element nodal deformation coordinates  $\mathbf{e}_f^j$  can be written in terms of the body deformation nodal coordinates as

$$\mathbf{e}_f^j = \mathbf{B}_c^j \mathbf{B}_r \mathbf{e}_f, \quad (6.60)$$

one can write the virtual work of the element elastic forces as

$$\delta W_s^j = \mathbf{Q}_s^{jT} \mathbf{B}_c^j \mathbf{B}_r \delta \mathbf{e}_f \quad (6.61)$$

The virtual work of the elastic forces of the body can be obtained as

$$\delta W_s = \sum_{j=1}^{n_e} \delta W_s^j = \left( \sum_{j=1}^{n_e} \mathbf{Q}_s^{jT} \mathbf{B}_c^j \right) \mathbf{B}_r \delta \mathbf{e}_f \quad (6.62)$$

which can be written as

$$\delta W_s = \mathbf{Q}_{sf}^T \delta \mathbf{e}_f \quad (6.63)$$

where

$$\mathbf{Q}_{sf} = \mathbf{B}_r^T \left( \sum_{j=1}^{n_e} \mathbf{B}_c^{jT} \mathbf{Q}_s^j \right) \quad (6.64)$$

Because in the FFR formulation the rigid-body motion leads to zero strains, the virtual work of the elastic forces can also be written as

$$\delta W_s = \mathbf{Q}_s^T \delta \mathbf{q} \quad (6.65)$$

where

$$\mathbf{Q}_s = \begin{bmatrix} \mathbf{0} \\ (\mathbf{Q}_s)_f \end{bmatrix}, \quad \mathbf{q} = \begin{bmatrix} \mathbf{q}_r \\ \mathbf{q}_f \end{bmatrix} = \begin{bmatrix} \mathbf{r}_O \\ \boldsymbol{\theta} \\ \mathbf{e}_f \end{bmatrix} \quad (6.66)$$

The vector of the elastic forces  $(\mathbf{Q}_s)_f$  can also be written as the product of a body-stiffness matrix  $\mathbf{K}$  multiplied by the vector of body-nodal coordinates  $\mathbf{q}$ . It can be shown that the FFR formulation leads to a constant stiffness matrix when linear strain–displacement relationship is used in the analysis of small deformations. This cannot be achieved when the large-deformation ANCF is used since the stiffness matrix is always a nonlinear function of the nodal coordinates even in the case in which the deformations are assumed small with respect to an element coordinate system. The use of the stiffness matrix expression is useful when coordinate reduction techniques are used as discussed later in this chapter.

## 6.9 EQUATIONS OF MOTION

The equations of motion of the body can be obtained using the principle of virtual work in dynamics, which can be written as

$$\delta W_i = \delta W_s + \delta W_e \quad (6.67)$$

where  $\delta W_i$  is the virtual work of the inertia forces,  $\delta W_s$  is the virtual work of the elastic forces, and  $\delta W_e$  is the virtual work of the applied forces such as gravity, external forces, and magnetic forces. It can be shown that the virtual work of the applied forces can be written as

$$\delta W_e = \mathbf{Q}_e^T \delta \mathbf{q} \quad (6.68)$$

Using this equation and the expressions for the virtual work of the inertia and elastic forces obtained in the preceding two sections, the principle of virtual work in dynamics can be written as

$$\{\ddot{\mathbf{q}}^T \mathbf{M} - \mathbf{Q}_v^T\} \delta \mathbf{q} = \mathbf{Q}_s^T \delta \mathbf{q} + \mathbf{Q}_e^T \delta \mathbf{q} \quad (6.69)$$

In the case of unconstrained motion, the elements of the vector  $\mathbf{q}$  are independent and the preceding equation leads to the equations of motion of the body given by

$$\mathbf{M}\ddot{\mathbf{q}} = \mathbf{Q}_s + \mathbf{Q}_e + \mathbf{Q}_v \quad (6.70)$$

Using the coordinate partitioning  $\mathbf{q} = \begin{bmatrix} \mathbf{q}_r^T & \mathbf{q}_f^T \end{bmatrix}^T$ , the preceding equation can be written as

$$\begin{bmatrix} \mathbf{M}_{rr} & \mathbf{M}_{rf} \\ \mathbf{M}_{fr} & \mathbf{M}_{ff} \end{bmatrix} \begin{bmatrix} \ddot{\mathbf{q}}_r \\ \ddot{\mathbf{q}}_f \end{bmatrix} = \begin{bmatrix} \mathbf{0} \\ (\mathbf{Q}_s)_f \end{bmatrix} + \begin{bmatrix} (\mathbf{Q}_e)_r \\ (\mathbf{Q}_e)_f \end{bmatrix} + \begin{bmatrix} (\mathbf{Q}_v)_r \\ (\mathbf{Q}_v)_f \end{bmatrix} \quad (6.71)$$

In this equation, subscripts  $r$  and  $f$  refer, respectively, to reference and elastic coordinates. The details of the matrices and vectors that appear in the preceding equation can be found in the literature (Shabana, 2013). The dynamic coupling between the reference motion and the elastic deformation is represented by the two matrices  $\mathbf{M}_{rf}$  and  $\mathbf{M}_{fr}$ . The study of this dynamic coupling is one of the interesting problems that have been the subject of several investigations in the multibody system dynamics literature. The dependence of the expressions of the matrices  $\mathbf{M}_{rf}$  and  $\mathbf{M}_{fr}$  on the choice of the body coordinate system has been also investigated.

It is important also to note that the submatrix  $\mathbf{M}_{ff}$ , which is the mass matrix that appears in linear finite element formulations, is a constant symmetric matrix. The reader can prove this fact by using the definition of the element mass matrix and the partitioning of the element coordinates as reference and elastic. The fact that the matrix  $\mathbf{M}_{ff}$  is constant will be utilized when component mode techniques are used to reduce the number of elastic coordinates.

It is clear from the structure of Equation 71 that the equations of motion that govern the dynamics of *rigid bodies* (no deformation) and the equations of motion that govern the dynamics of *structural systems* (no reference motion) can be obtained as special cases from Equation 71. It is left to the reader as an exercise to prove this fact and show how the well-known *Newton–Euler equations* used in rigid-body dynamics can be obtained from the more general development presented in this chapter. In the case of the Newton–Euler equations, a body coordinate system that has an origin rigidly attached to the body center of mass must be used. A set of *generalized Newton–Euler equations* for flexible bodies is presented in the literature (Shabana, 2013).

## 6.10 COORDINATE REDUCTION

The use of the FFR formulation in the analysis of the small deformation of multibody systems has an important advantage because it leads to a local linear problem that can be exploited in reducing systematically the number of elastic degrees of freedom. This number can be very large compared to the number of reference coordinates. A body can have a large number of finite elements and its reference motion is described using only six reference coordinates. Coordinate reduction techniques are not often used with large-deformation formulations because of the complexity of the geometry of the deformation shape. In the small-deformation problems, on the other hand, the bodies take simple shapes that can be described using few simple functions. One can then start with a detailed finite element model for a body whose elements can have arbitrary orientations and use the formulation presented in this chapter to obtain the inertia, elastic, and applied forces. The vector of the body coordinates can then be written in terms of another smaller set of coordinates, thereby significantly reducing the problem dimensionality and eliminating high-frequency modes that do not have significant effect on the solution accuracy.

One way to define the reduced set of coordinates is to use component mode reduction techniques. The use of this approach allows reducing systematically the number of coordinates and at the same time eliminating high-frequency modes that can be a source of problems when the equations of motion are integrated numerically. In order to demonstrate the application of the component mode techniques, the vector of elastic forces  $\mathbf{Q}_s$  can be written as

$$\mathbf{Q}_s = - \begin{bmatrix} \mathbf{0} & \mathbf{0} \\ \mathbf{0} & \mathbf{K}_{ff} \end{bmatrix} \begin{bmatrix} \mathbf{q}_r \\ \mathbf{q}_f \end{bmatrix} \quad (6.72)$$

where in this equation  $\mathbf{K}_{ff}$  is the stiffness matrix associated with the elastic coordinates of the body. This stiffness matrix is positive definite as the result of imposing the reference conditions. Note that in the preceding equation, as a result of using the mixed set of absolute reference and local deformation coordinates, a rigid-body motion does not contribute to the vector of elastic forces and the FFR formulation leads to zero strains under an arbitrary rigid-body motion. Substituting the preceding equation into the equations of motion of



Equation 71, one obtains

$$\begin{bmatrix} \mathbf{M}_{rr} & \mathbf{M}_{rf} \\ \mathbf{M}_{fr} & \mathbf{M}_{ff} \end{bmatrix} \begin{bmatrix} \ddot{\mathbf{q}}_r \\ \ddot{\mathbf{q}}_f \end{bmatrix} + \begin{bmatrix} \mathbf{0} & \mathbf{0} \\ \mathbf{0} & \mathbf{K}_{ff} \end{bmatrix} \begin{bmatrix} \mathbf{q}_r \\ \mathbf{q}_f \end{bmatrix} = \begin{bmatrix} (\mathbf{Q}_e)_r \\ (\mathbf{Q}_e)_f \end{bmatrix} + \begin{bmatrix} (\mathbf{Q}_v)_r \\ (\mathbf{Q}_v)_f \end{bmatrix} \quad (6.73)$$

It is important to point out that by using a consistent mass formulation as described in this chapter and by applying the reference conditions defined by the matrix  $\mathbf{B}_r$ , that eliminates the rigid-body modes, one can always obtain a positive definite mass and stiffness matrices  $\mathbf{M}_{ff}$  and  $\mathbf{K}_{ff}$ , respectively. Furthermore, proper selection of the reference conditions is important in order to have a good approximation of the deformation shape with a small number of coordinates, and also in order to have strain measures that are consistent with the small deformation assumption often used with the FFR formulation.

In order to use the component mode techniques, one first considers the case of free vibration of the body with respect to its reference. This is the special case in which there is no reference motion. In this special case, the preceding equation leads to

$$\mathbf{M}_{ff}\ddot{\mathbf{q}}_f + \mathbf{K}_{ff}\mathbf{q}_f = \mathbf{0} \quad (6.74)$$

If one further assumes linear material behavior and linear strain–displacement relationship, the stiffness matrix  $\mathbf{K}_{ff}$  is constant. Using the fact that the matrix  $\mathbf{M}_{ff}$  is also constant, one can assume a solution for the preceding equation in the form

$$\mathbf{q}_f = \mathbf{a}e^{i\beta t} \quad (6.75)$$

where  $i = \sqrt{-1}$ ,  $\mathbf{a}$  is the vector of amplitude,  $t$  is time, and  $\beta$  is the frequency. Substituting Equation 75 into Equation 74, one obtains the following *generalized eigenvalue problem*:

$$(\mathbf{K}_{ff} - \beta^2\mathbf{M}_{ff})\mathbf{a} = \mathbf{0} \quad (6.76)$$

This equation can be solved for a set of eigenvalues  $\beta_k^2$ ,  $k = 1, 2, \dots, n_f$ , where  $n_f$  is the number of elastic nodal coordinates. The solution of the preceding equation also defines the *eigenvectors* or *mode shapes* associated with the eigenvalues  $\beta_k^2$ . The eigenvectors describe the possible shape of deformation of the body with respect to its reference. In the case of small deformation, the shape of the body deformation is simple and can be described using few eigenvectors called the *fundamental mode shapes*. A reduced-order dynamic model can be obtained by using only  $n_m$  modes where  $n_m$  can be much smaller than  $n_f$ .

A constant coordinate transformation from the physical nodal coordinates  $\mathbf{q}_f$  to the new modal elastic coordinates  $\mathbf{p}_f$  can then be written as follows:

$$\mathbf{q}_f = \mathbf{B}_m\mathbf{p}_f \quad (6.77)$$

where  $\mathbf{B}_m$  is the *modal transformation matrix* whose columns are the low-frequency  $n_m$  mode shapes. The vector  $\mathbf{p}_f$  is the reduced vector of modal coordinates. One can then write the total vector of the body coordinates in terms of the new reduced set of coordinates as

$$\mathbf{q} = \begin{bmatrix} \mathbf{q}_r \\ \mathbf{q}_f \end{bmatrix} = \begin{bmatrix} \mathbf{I} & \mathbf{0} \\ \mathbf{0} & \mathbf{B}_m \end{bmatrix} \begin{bmatrix} \mathbf{p}_r \\ \mathbf{p}_f \end{bmatrix} \quad (6.78)$$

Substituting this transformation into the equations of motion (Equation 73) and premultiplying by the transpose of the coefficient matrix in the coordinate transformation of Equation 78 leads to the following reduced set of the equations of motion expressed in terms of the coupled reference and modal coordinates:

$$\begin{bmatrix} \mathbf{M}_{rr} & \bar{\mathbf{M}}_{rf} \\ \bar{\mathbf{M}}_{fr} & \bar{\mathbf{M}}_{ff} \end{bmatrix} \begin{bmatrix} \ddot{\mathbf{p}}_r \\ \ddot{\mathbf{p}}_f \end{bmatrix} + \begin{bmatrix} \mathbf{0} & \mathbf{0} \\ \mathbf{0} & \bar{\mathbf{K}}_{ff} \end{bmatrix} \begin{bmatrix} \mathbf{p}_r \\ \mathbf{p}_f \end{bmatrix} = \begin{bmatrix} (\mathbf{Q}_e)_r \\ (\bar{\mathbf{Q}}_e)_f \end{bmatrix} + \begin{bmatrix} (\mathbf{Q}_v)_r \\ (\bar{\mathbf{Q}}_v)_f \end{bmatrix} \quad (6.79)$$

In this equation,

$$\left. \begin{aligned} \bar{\mathbf{M}}_{rf} &= \bar{\mathbf{M}}_{fr}^T = \mathbf{M}_{rf} \mathbf{B}_m, & \bar{\mathbf{M}}_{ff} &= \mathbf{B}_m^T \mathbf{M}_{ff} \mathbf{B}_m \\ \bar{\mathbf{K}}_{ff} &= \mathbf{B}_m^T \mathbf{K}_{ff} \mathbf{B}_m, & (\bar{\mathbf{Q}}_e)_f &= \mathbf{B}_m^T (\mathbf{Q}_e)_f, & (\bar{\mathbf{Q}}_v)_f &= \mathbf{B}_m^T (\mathbf{Q}_v)_f \end{aligned} \right\} \quad (6.80)$$

The application of the modal transformation to reduce the number of coordinates can be made at a preprocessing stage before the dynamic simulation starts. In this case, the array space required during the dynamic simulation can be significantly reduced. This important subject and the interface between the finite element and multibody system computer programs are discussed in the following section.

## 6.11 INTEGRATION OF FINITE ELEMENT AND MULTIBODY SYSTEM ALGORITHMS

In the FFR formulation presented in this chapter, the equations of motion of the continuous body that undergoes finite rotations are formulated in terms of a unique set of finite element inertia shape integrals. These inertia shape integrals play a fundamental role in an efficient computational scheme that was developed for solving the dynamic equations of *flexible multi-body systems*. This scheme, which is implemented in several widely used commercial codes, requires the integration of small-deformation finite element and multibody system algorithms. In this scheme, constant vectors and matrices that appear in the nonlinear dynamic equations of motion are identified and evaluated at a preprocessing stage. For example, the constant inertia shape integrals, the stiffness matrix if constant, and the mode shapes can be evaluated in a preprocessor finite element computer program. The inertia shape integrals and the stiffness matrix can be constructed for each finite element. The body inertia shape integrals and stiffness matrix can be obtained by assembling the inertia shape integrals and stiffness matrices of its elements. This means that finite element computer programs in the finite element FFR formulation must be used as preprocessors for flexible multibody system computer programs. This was not the sequence of computations that was in use before 1980s.

### Linear Theory of Elastodynamics

Before introducing the finite element FFR formulation, rigid multibody system computer codes, which were available at that time, were used first to determine the inertia and joint forces. Finite element codes were used at a postprocessing stage in order to determine the deformations and stresses. This procedure is known in the literature as the *linear theory of*

*elastodynamics* (Shabana, 2013). The sequence of using the multibody systems and finite element codes based on the linear theory of elastodynamics was reversed when the finite element FFR formulation presented in this chapter was introduced. Based on this formulation, one obtains a set of data from the finite element code that is considered as a part of the input data to the flexible multibody system code, which is based on a formulation that employs a mixed set of reference and elastic coordinates.

### Nodal and Modal Coordinates

As previously mentioned, understanding the role of the inertia shape integrals is important in developing a general and efficient computational algorithm for the dynamic analysis of flexible bodies that undergo finite rotations. In fact, the main processor flexible multibody computer program can be made independent of the use of physical nodal or modal coordinates. That is, the main processor can be designed to be the same and works with or without coordinate reduction. In the computer implementation, it is not required to consider Equation 79; Equation 73 can work for the two cases of physical nodal and modal coordinates. One only needs to express the inertia shape integrals in their appropriate form. If physical nodal coordinates are used, the inertia shape integrals will have their original dimensions, which depend on the number of nodal coordinates. On the other hand, if modal coordinates are used, the inertia shape integrals are transformed to the modal space and the vector of elastic coordinates has dimension equal to the number of modes used. One can show by using Equation 55 that the modal form of the inertia shape integrals in the three-dimensional analysis is given by

$$\left. \begin{aligned} (\bar{\mathbf{S}})_m &= \bar{\mathbf{S}}\mathbf{B}_m = \left( \sum_{j=1}^{n_e} \bar{\mathbf{S}}^j \mathbf{B}_c^j \right) \mathbf{B}_r \mathbf{B}_m \\ (\mathbf{S}_{kl})_m &= \mathbf{B}_m^T \mathbf{S}_{kl} \mathbf{B}_m = \mathbf{B}_m^T \mathbf{B}_r^T \left( \sum_{j=1}^{n_e} \mathbf{B}_c^{jT} \mathbf{S}_{kl}^j \mathbf{B}_c^j \right) \mathbf{B}_r \mathbf{B}_m, \quad k, l = 1, 2, 3 \end{aligned} \right\} \quad (6.81)$$

Similarly, by using Equation 56 one can show that in the two-dimensional analysis, the modal form of the body inertia shape integrals is given by

$$\left. \begin{aligned} (\bar{\mathbf{S}})_m &= \bar{\mathbf{S}}\mathbf{B}_m = \left( \sum_{j=1}^{n_e} \bar{\mathbf{S}}^j \mathbf{B}_c^j \right) \mathbf{B}_r \mathbf{B}_m \\ (\tilde{\mathbf{S}})_m &= \mathbf{B}_m^T \bar{\mathbf{S}} \mathbf{B}_m = \mathbf{B}_m^T \mathbf{B}_r^T \left( \sum_{j=1}^{n_e} \mathbf{B}_c^{jT} \bar{\mathbf{S}}^j \mathbf{B}_c^j \right) \mathbf{B}_r \mathbf{B}_m \\ (\mathbf{S}_{ff})_m &= \mathbf{B}_m^T \mathbf{S}_{ff} \mathbf{B}_m = \mathbf{B}_m^T \mathbf{B}_r^T \left( \sum_{j=1}^{n_e} \mathbf{B}_c^{jT} \mathbf{S}_{ff}^j \mathbf{B}_c^j \right) \mathbf{B}_r \mathbf{B}_m \end{aligned} \right\} \quad (6.82)$$

where in the preceding two equations, subscript  $m$  refers to modal form.

## Numerical Evaluation of the Inertia Shape Integrals

Coupling commercial finite element codes with flexible multibody codes does not require knowledge of the shape functions in the finite element computer programs in order to evaluate the inertia shape integrals. This was one of the main concerns when the finite element FFR formulation was introduced. This problem, however, was successfully solved by using numerical approximation to evaluate the inertia shape integrals instead of performing the integrations analytically (Shabana, 1985, 2013). After determining the mode shapes in the finite element preprocessor, these mode shapes can be used with numerical integration and a lumped mass scheme to obtain the inertia shape integrals in their modal form. This procedure does not require knowledge of the element shape function matrix used in the finite element computer program. It is important, however, to recognize that the use of the numerical approximation to evaluate the inertia shape integrals based on the mass lumping does not lead to a diagonal body mass matrix. The resulting mass matrix remains nonlinear and nondiagonal.

Because finite element computer programs can solve for the mode shapes for the finite elements that exist in their library, one can utilize the rich library of the finite element computer codes in developing detailed multibody system models for many applications. The finite element codes can produce a standard file that contains the inertia shape integrals and constant-stiffness coefficients. This file can be used, as previously mentioned, as input to general purpose flexible multibody computer programs. This process is now a standard procedure that is implemented in several widely used commercial codes.

## Scaling of the Modal Coordinates

In many MBS applications, the reference coordinates  $\mathbf{q}_r$  can have large absolute values, while the elastic coordinates  $\mathbf{q}_f$  defined in the body coordinate system can have very small values. An example is the tank car shown in Figure 6. A train can travel thousands of miles, while the deformation of the tank car can be relatively small. Having two sets of coordinates that can differ significantly in magnitude can lead to numerical problems, particularly when implementing the FFR formulation. It is, therefore, important to scale the elastic coordinates to make all coordinates have comparable magnitude.

In the case of metals, it is recommended to make the mode shapes orthonormal with respect to the stiffness matrix. In this case, the modal stiffness matrix becomes the identity matrix. This provides a natural scaling of the modal coordinates and can lead to a more efficient implementation of the FFR formulation. If the mode shapes are orthonormal with respect to the stiffness matrix, one has  $\bar{\mathbf{K}}_{ff} = \mathbf{B}_m^T \mathbf{K}_{ff} \mathbf{B}_m = \mathbf{I}$ , where  $\mathbf{I}$  is the identity matrix. Since the strain energy expressed in terms the physical nodal coordinates  $\mathbf{q}_f$  or the modal coordinates  $\mathbf{p}_f$  must be the same, one has

$$U = \frac{1}{2} \mathbf{q}_f^T \mathbf{K}_{ff} \mathbf{q}_f = \frac{1}{2} \mathbf{p}_f^T \mathbf{I} \mathbf{p}_f \quad (6.83)$$

In the case of metals, the elements of the stiffness matrix  $\mathbf{K}_{ff}$  can be very large. Since the stiffness matrix  $\bar{\mathbf{K}}_{ff} = \mathbf{B}_m^T \mathbf{K}_{ff} \mathbf{B}_m$  associated with the modal coordinates is the identity matrix, which has nonzero elements much smaller in magnitude than the elements of  $\mathbf{K}_{ff}$ , the magnitude of the modal coordinates  $\mathbf{p}_f$  associated with modes that are orthonormal with respect to the stiffness matrix will be larger than the magnitude of the physical nodal coordinates  $\mathbf{q}_f$ . The experience with the implementation of the FFR formulation showed that such a scaling



**Figure 6.6** Scaling of the elastic coordinates

of coordinates may be necessary for robust implementation of this formulation that employs two coupled sets of coordinates.

### Limitations of the FFR Formulation

The FFR formulation is used, for the most part, to study small deformation problems. This formulation allows creating a local linear problem that enables applying coordinate reduction techniques. In some applications, however, the FFR formulation can be used to study large deformation problems if the shape of deformation can be described using simple functions. In this case, one can still use linear modes with nonlinear strain–displacement relationships. The constant part of the stiffness matrix can be used to obtain the linear modes, or alternatively other techniques can be used to obtain a set of assumed shapes. In the literature, one can find applications, such as rotor blades, in which the FFR formulation was successfully used to study the large deformation problem and capture the effect of geometric stiffening.

Nonetheless, ANCF finite elements are, in general, more suited for large deformation problems. Figure 7 shows the ANCF results obtained, for a liquid sloshing problem, using higher order ANCF brick elements for three different base excitations,  $y = 0.1 \sin 3t$  m,  $y = 0.1 \sin 8t$  m, and  $y = 0.3 \sin 8t$  m. These results are obtained using only one ANCF brick element. Figure 8 shows the results obtained using the FFR formulation for the same liquid sloshing problem in the case of the first base excitation  $y = 0.1 \sin 3t$  m (Wei et al., 2015; Wang et al., 2015). In the case of the FFR formulation, the conventional brick element that has only translational nodal coordinates is used. This element does not ensure the continuity of the gradients at the nodal points. The comparative numerical study reported by Wei et al. (2015) showed that a larger number of finite elements is required when

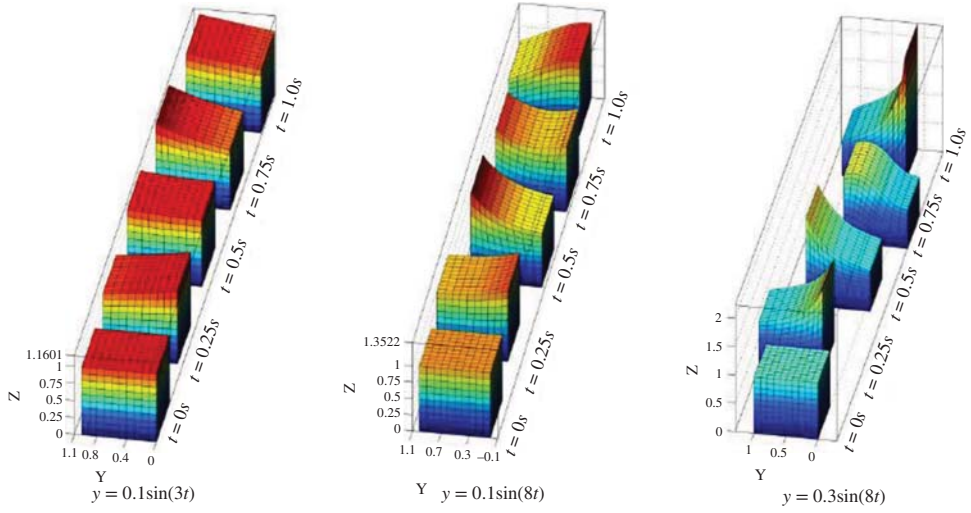


**Figure 6.7** Liquid sloshing results using ANCF finite elements (Wei et al., 2015)

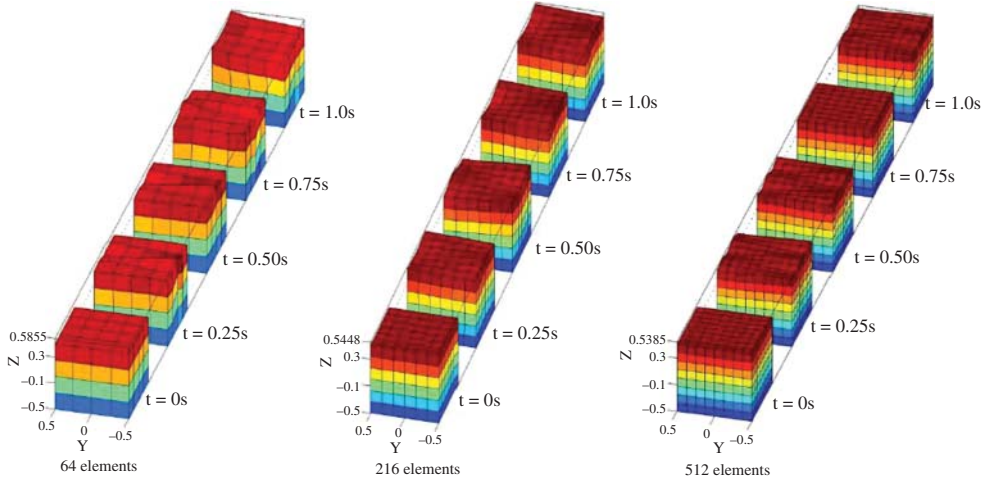


**Figure 6.8** Liquid sloshing results using the FFR formulation (Wei et al., 2015)

using the FFR formulation to study this liquid sloshing problem. In order to impose the fluid incompressibility condition, Wang et al. (2015) formulated the matrix of position vector gradients  $\mathbf{J}^j = \partial \mathbf{r}^j / \partial \mathbf{x} = [\partial \mathbf{r}^j / \partial x_1 \quad \partial \mathbf{r}^j / \partial x_2 \quad \partial \mathbf{r}^j / \partial x_3]$  for an element  $j$  using the FFR kinematic description  $\mathbf{r}^j = \mathbf{r}_O + \mathbf{A}(\bar{\mathbf{u}}_O^j + \bar{\mathbf{S}}_b^j \mathbf{e}_f)$ , where  $\bar{\mathbf{S}}_b^j = \mathbf{S}_b^j \mathbf{B}_c^j \mathbf{B}_r$ . Using this description and the vector  $\mathbf{x} = [x_1 \ x_2 \ x_3]^T$ , the matrix of position vector gradients for element  $j$  can be written as

$$\mathbf{J}^j = \frac{\partial \mathbf{r}^j}{\partial \mathbf{x}} = \mathbf{A} \left( \mathbf{I} + \left[ \left( \frac{\partial \bar{\mathbf{S}}_b^j}{\partial x_1} \right) \mathbf{e}_f \quad \left( \frac{\partial \bar{\mathbf{S}}_b^j}{\partial x_2} \right) \mathbf{e}_f \quad \left( \frac{\partial \bar{\mathbf{S}}_b^j}{\partial x_3} \right) \mathbf{e}_f \right] \right) \quad (6.84)$$

This equation can be written compactly as

$$\mathbf{J}^j = \frac{\partial \mathbf{r}^j}{\partial \mathbf{x}} = \mathbf{A} \left( \mathbf{I} + \frac{\partial \bar{\mathbf{u}}_f^j}{\partial \mathbf{x}} \right) = \mathbf{A}(\mathbf{I} + \bar{\mathbf{J}}_d^j) \quad (6.85)$$

where

$$\bar{\mathbf{J}}_d^j = \frac{\partial \bar{\mathbf{u}}_f^j}{\partial \mathbf{x}} = \left[ \left( \frac{\partial \bar{S}_b^j}{\partial x_1} \right) \mathbf{e}_f \left( \frac{\partial \bar{S}_b^j}{\partial x_2} \right) \mathbf{e}_f \left( \frac{\partial \bar{S}_b^j}{\partial x_3} \right) \mathbf{e}_f \right] \quad (6.86)$$

If the condition  $J^j = 1$  is imposed, one has  $J^j = |\mathbf{J}^j| = |\mathbf{J}_r^j \mathbf{J}_d^j| = |\mathbf{A}| |\mathbf{I} + \bar{\mathbf{J}}_d^j| = |\mathbf{I} + \bar{\mathbf{J}}_d^j| = 1$ , where  $\mathbf{J}_r^j = \mathbf{A}$  is the Jacobian matrix associated with the rigid body rotation and  $\mathbf{J}_d^j = (\mathbf{I} + \bar{\mathbf{J}}_d^j)$  is the Jacobian matrix associated with the body deformation. If the condition  $J^i = 0$  is imposed, the time derivative of  $J^i$  can be evaluated as  $\dot{J}^i = \text{tr}(\mathbf{D}^i) J^i$ , where  $\mathbf{D}^i$  is the rate of deformation tensor. One can also write  $\dot{J}^j = (\bar{\mathbf{J}}^j : (\mathbf{J}^{j-1})^T) J^j$ , where in the FFR formulation,  $\bar{\mathbf{J}}^j = \dot{\mathbf{A}}[\mathbf{I} + \bar{\mathbf{J}}_d^j] + \mathbf{A}\bar{\mathbf{J}}_d^j$ , and  $\dot{\mathbf{A}} = \mathbf{A}\tilde{\boldsymbol{\omega}}$ .

## PROBLEMS

1. Derive the Euler angle transformation matrix if the sequence of rotation used is  $X_1^b, X_2^b$ , and  $X_3^b$ .
2. Derive the Euler angle transformation matrix if the sequence of rotation used is  $X_3^b, X_1^b$ , and  $X_2^b$ .
3. In Problem 1, determine the expressions for the angular velocity vectors  $\tilde{\boldsymbol{\omega}}$  and  $\boldsymbol{\omega}$  in terms of Euler angles. Determine also the singular configurations associated with this sequence of Euler angles.
4. In Problem 2, determine the expressions for the angular velocity vectors  $\tilde{\boldsymbol{\omega}}$  and  $\boldsymbol{\omega}$  in terms of Euler angles. Determine also the singular configurations associated with this sequence of Euler angles.
5. Determine the  $\mathbf{G}$  and  $\bar{\mathbf{G}}$  matrices of Equation 14 in the case of planar motion.
6. Consider the beam element whose nodal coordinates and shape function are defined by Equations 1 and 2, respectively. Assume that the location and orientation of this element with respect to the body coordinate system are defined, respectively, by the translation  $\mathbf{a} = [a_1 \ a_2]^T$  of its first node and a rotation  $\alpha$ . Using the concept of the intermediate element coordinate system, define the vector  $\bar{\mathbf{u}}^j$  of Equation 25 before the deformation takes place. Determine the numerical values of this vector if  $\mathbf{a} = [2 \ 1]^T$  m,  $\alpha = 30^\circ$ , and the length of the element  $l = 1$  m.
7. Consider two beam elements that are rigidly connected. The nodal coordinates and shape functions of the elements are as defined in Equations 1 and 2, respectively. The location and orientation of the two elements with respect to the body coordinate system are defined, respectively, by the translations  $\mathbf{a}^j = [a_1^j \ a_2^j]^T$  of its first node and a rotation  $\alpha^j$ ,  $j = 1, 2$ .

It follows that in the reference undeformed configuration the location of the first node of the second element must be  $[l^1 \sin \alpha^1 \ l^1 \cos \alpha^1]^T$ , where  $l^1$  is the length of the finite element  $j$ . Using the concept of the intermediate element coordinate system, define the matrices  $\bar{\mathbf{T}}_u^j$ ,  $\bar{\mathbf{T}}_n^j$  and  $\mathbf{B}_c^j$  for both elements.

8. Determine the position, velocity, and accelerations of the midpoint of the beam in Problem 6 assuming the following values for the coordinates, velocities, and accelerations:

$$\mathbf{q} = \begin{bmatrix} \mathbf{R}^T & \theta & \mathbf{q}_f^T \end{bmatrix}^T = \begin{bmatrix} 1 & -1 & 45^\circ & 0 & 0 & 0 & 0.001 & 0 & 0 \end{bmatrix}^T$$

$$\dot{\mathbf{q}} = \begin{bmatrix} \dot{\mathbf{R}}^T & \dot{\theta} & \dot{\mathbf{q}}_f^T \end{bmatrix}^T = \begin{bmatrix} 10 & 0 & 0 & 0 & 0 & 0 & 50 & 0 & 0 \end{bmatrix}^T$$

$$\ddot{\mathbf{q}} = \begin{bmatrix} \ddot{\mathbf{R}}^T & \ddot{\theta} & \ddot{\mathbf{q}}_f^T \end{bmatrix}^T = \begin{bmatrix} 0 & 2 & 0 & 0 & 0 & 0 & 0 & 0 & 0 \end{bmatrix}^T$$

where  $\theta$  is the angle that defines the orientation of the body coordinate system.

9. Show that the inertia forces of the flexible body that undergoes finite rotation can be written in terms of the inertia shape integrals of Equation 49 in the case of three-dimensional analysis and in terms of the inertia shape integrals of Equation 50 in the case of planar analysis.
10. Obtain the inertia shape integrals of the finite element that has nodal coordinates and shape function matrix defined by Equations 1 and 2, respectively.
11. Using linear strain–displacement relationship, show that the vector of the elastic forces in the FFR formulation is a linear function of the element nodal coordinates.
12. Based on the results of the preceding problem, explain why the FFR formulation leads to a vector of elastic forces, which is linear in the nodal coordinates when linear strain–displacement relationships are used, whereas the absolute nodal coordinate formulation leads to a vector of elastic forces, which is nonlinear function of the element nodal coordinates.





# COMPUTATIONAL GEOMETRY AND FINITE ELEMENT ANALYSIS

---

Computational geometry methods such as Bezier, B-spline, and Non-Uniform Rational B-Splines (NURBS) are widely used in the design of engineering and physics systems (Dierckx, 1993; Farin, 1999; Piegl and Tiller, 1997; Rogers, 2001). At the design stage, the geometry of the systems is defined using *computer-aided design* (CAD) software. The CAD models then are converted to a finite element (FE) mesh to perform the analysis to determine deformations, stresses, and forces as the result of the applied loads. CAD systems use computational geometry methods that accurately define complex shapes and allow for efficient shape manipulation. These methods have many desirable features and share many of the properties required for the development of accurate analysis methods. Nonetheless, computational geometry methods are used primarily for the system geometric construction.

Because of the limitations of existing FE formulations and the fact that the geometric (i.e., kinematic) descriptions used in them are not equivalent to the geometric description used in CAD systems, there is a recent trend to use computational geometry methods as analysis tools. Although both FE and computational geometry methods are based on polynomial representations, many of the existing FE formulations distort the geometry because of the nature of the nodal coordinates selected. As a result, the geometry of the FE mesh used in the analysis can be different from the geometry defined in the CAD systems. This inconsistency makes the conversion of the CAD model to an analysis model difficult and costly and leads to analysis models that are not consistent with the CAD-geometry models. The two FE formulations discussed in Chapters 5 and 6 were developed to address and remedy this problem. The two formulations can be used as the basis for a successful *integration of computer-aided design and analysis* (I-CAD-A).

Both the FE floating frame of reference (FFR) formulation and the absolute nodal coordinate formulation (ANCF) (see Chapters 5 and 6) use a kinematic description that leads to a deformed shape that is invariant under an arbitrary rigid-body displacement. Because of this important property, both formulations lead to zero strains when the finite elements experience rigid-body displacements. Defining a geometry that is invariant under rigid body displacement is an important requirement for an accurate large-displacement analysis method. The FFR formulation, in particular, allows the use of finite elements that do not preserve the geometry to form an FE mesh that correctly describes rigid-body rotations. Using the concept of the *intermediate element coordinate system*, these finite elements can be assembled to form a mesh with geometry that is invariant under arbitrary rigid-body displacements.

In this chapter, computational geometry methods and their relationship to the FE formulations presented in this book are discussed. The limitations of using computational geometry methods as analysis tools are highlighted for an understanding of the potential use of these methods as alternatives to the FE formulations. As discussed herein, computational geometry methods – although they have many desirable features – have a rigid recurrence structure that can lead to higher-dimensional models, to the loss of flexibility provided by FE formulations in the selection of the basis functions, and to failure to capture certain types of geometric discontinuities that characterize many mechanical and structural systems. Nonetheless, a good grasp of computational geometry methods is important for understanding the limitations of some existing large-displacement FE formulations that have been widely used for decades.

## 7.1 GEOMETRY AND FINITE ELEMENT METHOD

As previously mentioned, computational geometry methods and FE formulations use polynomial representations. Nonetheless, in many structural FE formulations – particularly for beams, plates, and shells – the geometry is distorted because of the way the FE nodal coordinates are selected. Although rigid-body motion can be described in terms of trigonometric functions, as was shown in this book, the use of infinitesimal or finite rotations in the position field as nodal coordinates can lead to shapes that are not invariant under arbitrary rigid-body displacements. Similarly, finite rotations cannot be interpolated independently from the position field as is the case in some large-displacement FE formulations. The matrix of position-vector gradients uniquely defines the rotation and deformation fields. Therefore, independent interpolation of the rotation field leads to coordinate redundancy, as previously discussed. The limitations of existing FE formulations motivated researchers in the FE community to call for abandoning them and adopting computational geometry methods as analysis tools. However, computational geometry methods, as discussed in this chapter, have limitations as analysis tools: they can lead to higher-dimensional models, they do not provide the flexibility offered by the FE approach, and their recurrence formula fails to automatically capture certain types of geometric discontinuities, as previously mentioned.

ANCF description, on the other hand, is compatible with and has many of the desirable features offered by computational geometry methods. ANCF provides the flexibility of choosing the basis functions, does not have a rigid recurrence structure, and captures the geometric discontinuities that cannot be captured by computational geometry methods. For these reasons, ANCF finite elements allow for developing a simple interface between the CAD systems and analysis software.

## Bezier Geometry

Computational geometry methods such as Bezier, B-spline, and NURBS used in CAD systems are based on polynomial representations (Dierckx, 1993; Farin, 1999; Piegl and Tiller, 1997; Rogers, 2001). The coefficients of the polynomials are replaced by coordinates of points, called *control points*, that form what is called a *control polygon*. Not all of the control points must lie on the curve or the surface; therefore, they are not necessarily material points as is the case in the FE representation. The use of control points that are not necessarily material points is a fundamental difference between computational geometry methods and FE formulations that use nodal coordinates to represent material points. Computational geometry methods are rooted in Bezier representation. Bezier representation, however, does not allow for domain discretization and for the use of piecewise polynomials; more complex shapes can be represented in Bezier geometry by increasing the polynomial order. Therefore, Bezier description, which does not allow for efficient shape manipulation, can be considered the counterpart of the Raleigh–Ritz analysis method, which uses modes that describe the deformation of the entire structure.

## B-Spline Geometry

B-spline, in contrast, allows for domain discretization and the use of piecewise polynomials that define shapes over domain intervals (subdomains). B-spline geometry, therefore, is described by segments connected at points called *breakpoints*. For this reason, B-spline geometry description, which uses control points, can be considered the counterpart of the FE method. Being able to describe independently the geometry of segments over subdomains allows for efficient local shape manipulation because geometric changes can be made over small regions without affecting the geometry away from those regions. B-spline also uses the concept of *knot vector* and *knot multiplicity*, which allows for adjusting the degree of continuity at the breakpoints at which B-spline segments are connected. As the knot multiplicity at a given breakpoint decreases, the degree of continuity at that point increases. For example, a cubic B-spline curve representation with knot multiplicity of four at a point makes the curve discontinuous ( $C^{-1}$ ) at this point; knot multiplicity of three is associated with coordinate continuity ( $C^0$ ); knot multiplicity of two is associated with coordinate and gradient continuity ( $C^1$ ); and so on. B-spline representation is based on a recurrence structure that allows for automatically adjusting the degree of continuity by changing the knot multiplicity. Such a representation also allows for *knot insertion* and for adding control points to locally manipulate the geometry.

## NURBS Geometry

There are shapes such as circular and conic segments the geometry of which cannot be described exactly using nonrational polynomials as those used in Bezier and B-splines; these shapes can be described exactly by using only rational functions (Dierckx, 1993; Farin, 1999; Piegl and Tiller, 1997; Rogers, 2001). NURBS geometry uses rational polynomials, allowing for exact geometric representation of circular and conic sections. NURBS geometry is based on a recurrence formula similar to that used in B-spline representation and it uses similar knot-vector and knot-multiplicity concepts. In Bezier, B-spline, and NURBS geometries, rigid-body displacement of a shape can be achieved by simply operating on the control points.

A rigid-body transformation applied to the control points does not distort the geometry that undergoes the same transformation. For this reason, Bezier, B-spline, and NURBS geometry does not have the problems associated with some FE formulations in which the shape is not preserved under arbitrary rigid-body displacements.

## 7.2 ANCF GEOMETRY

As discussed in Chapter 5, the displacement field of ANCF finite elements is expressed in terms of position and gradient coordinates. This displacement field is invariant under arbitrary rigid-body displacements. In this section, it is shown that the ANCF kinematic description can be expressed in terms of the control points used in computational geometry methods. This alternate description can be used to establish the relationship among the ANCF, Bezier, B-spline, and NURBS descriptions. To this end, the three-dimensional ANCF two-node cable element that employs cubic interpolation is used. At each node, the element has six degrees of freedom, including three position coordinates and three components of one vector of position-vector gradients that remains tangent to the element centerline. The procedure developed in this section can be applied to other ANCF finite elements and generalized to the cases of surfaces and solids that are described using more general ANCF fully parameterized finite elements.

### ANCF Element Geometry

In the case of the ANCF Euler–Bernoulli cable element, the global position vector  $\mathbf{r}$  of an arbitrary point on the FE centerline can be defined using the element shape function matrix and the nodal coordinate vector as follows:

$$\mathbf{r}(x, t) = \mathbf{S}(x)\mathbf{e}(t) \quad (7.1)$$

where  $\mathbf{S}$  is the element shape function matrix expressed in terms of the element spatial coordinate  $x$ ;  $\mathbf{e}$  is the vector of nodal coordinates that consist of absolute nodal position coordinates and position coordinate gradients; and  $t$  is time. The element shape function matrix used in Equation 1 for the three-dimensional cable elements can be written as

$$\mathbf{S} = [s_1\mathbf{I} \ s_2\mathbf{I} \ s_3\mathbf{I} \ s_4\mathbf{I}] \quad (7.2)$$

where  $\mathbf{I}$  is the identity matrix and  $s_i$ ,  $i = 1, 2, 3, 4$ , are appropriate shape functions that can be introduced using polynomials or other geometric representations. The vector of the element nodal coordinates can be written as follows:

$$\mathbf{e} = [(\mathbf{e}^A)^T \ (\mathbf{e}^B)^T]^T \quad (7.3)$$

where superscripts  $A$  and  $B$  refer to the first and second nodes of the element, respectively; and the element nodal coordinate vector at node  $N$  is defined as follows:

$$\mathbf{e}^N = \left[ (\mathbf{r}^N)^T \left( \frac{\partial \mathbf{r}^N}{\partial x} \right)^T \right]^T, \quad N = A, B \quad (7.4)$$

The displacement field of this element can be defined using polynomial representation (described previously) as

$$\mathbf{r} = (1 - 3\xi^2 + 2\xi^3)\mathbf{r}^A + l(\xi - 2\xi^2 + \xi^3)\mathbf{r}_x^A + (3\xi^2 - 2\xi^3)\mathbf{r}^B + l(-\xi^2 + \xi^3)\mathbf{r}_x^B \quad (7.5)$$

In this equation,  $l$  is the length of the finite element, and  $\xi = x/l$ .

### Control-Point Representation

Whereas ANCF finite elements use gradients of absolute position vectors as nodal coordinates, a gradient vector always can be expressed in terms of the position vectors of two points divided by a scaling-length factor. Therefore, the ANCF geometric description presented in this section in terms of gradient vectors always can be converted to an equivalent geometric representation expressed solely in terms of position vectors of points that do not have to lie on the beam space curve or the plate and shell midsurface. As the finite element deforms, the location of these points will change with time. To demonstrate this coordinate transformation, the simple cable element defined previously is considered. For the cubic representation of Equation 5, one can define four points whose position vectors are defined by the vectors  $\mathbf{P}_0$ ,  $\mathbf{P}_1$ ,  $\mathbf{P}_2$ , and  $\mathbf{P}_3$ . Using these position vectors, the following coordinate transformation can be defined:

$$\begin{bmatrix} \mathbf{r}^A \\ \mathbf{r}_x^A \\ \mathbf{r}^B \\ \mathbf{r}_x^B \end{bmatrix} = \begin{bmatrix} \mathbf{P}_0 \\ \frac{3}{l}(\mathbf{P}_1 - \mathbf{P}_0) \\ \mathbf{P}_3 \\ \frac{3}{l}(\mathbf{P}_3 - \mathbf{P}_2) \end{bmatrix} \quad (7.6)$$

Substituting the coordinate transformation of this equation into Equation 5, one can show that the displacement field of the ANCF finite element can be written in terms of the point coordinates instead of the gradient coordinates as

$$\mathbf{r} = (1 - \xi)^3\mathbf{P}_0 + 3\xi(1 - \xi)^2\mathbf{P}_1 + 3\xi^2(1 - \xi)\mathbf{P}_2 + \xi^3\mathbf{P}_3 \quad (7.7)$$

The two representations of Equations 5 and 7 are equivalent and each can be used in the description of the geometry as well as the displacement, including deformations and rigid-body motion. Figure 1 is a graphical representation demonstrating the relationship between the *gradient coordinates* and *point coordinates*. In computational geometry, the points  $\mathbf{P}_0$ ,  $\mathbf{P}_1$ ,  $\mathbf{P}_2$ , and  $\mathbf{P}_3$  are called *control points*. These points, which form the control polygon, do not have to represent material points. Equation 7, therefore, demonstrates how the geometric description of the ANCF finite elements can be expressed in terms of control points. The inverse relationship, in which the ANCF position and gradients coordinates are expressed in terms of the control points, can be obtained as explained in the following section. Such a relationship allows for converting CAD models to ANCF analysis meshes without geometry distortion.

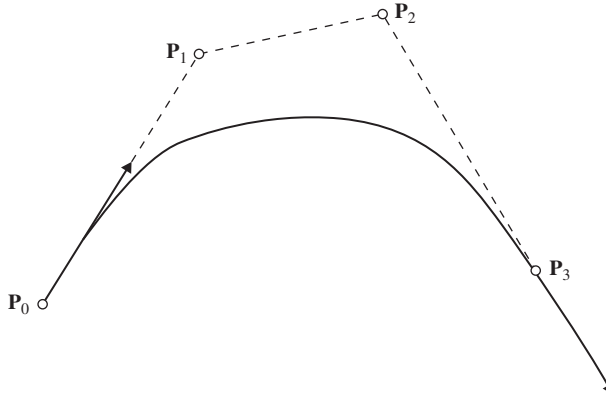


Figure 7.1 Gradients and control points

### 7.3 BEZIER GEOMETRY

Different methods can be used to represent polynomials, including the *power basis* and *Bezier methods* (Piegl and Tiller, 1997). Although the power basis and Bezier methods are equivalent, the Bezier method is more suited for shape manipulations and geometric modeling. In this section, it is shown that the Bezier geometry can be converted to ANCF geometry. This result is used to demonstrate that B-spline geometry can be converted to ANCF geometry, which can be proven because B-spline geometry is considered to consist of several Bezier segments.

A Bezier curve with  $m$ -degree is defined as (Piegl and Tiller, 1997)

$$\mathbf{r}(\xi) = \sum_{i=0}^m S_{i,m}(\xi) \mathbf{P}_i, \quad 0 \leq \xi \leq 1 \quad (7.8)$$

In this equation,  $S_{i,m}(\xi)$  are called the *basis* or *blending functions*, and the coefficients  $\mathbf{P}_i$  are called the *control points*. The basis functions  $S_{i,m}(\xi)$  are the  $m$ -degree *Bernstein polynomials* defined as

$$S_{i,m}(\xi) = \frac{m!}{i!(m-i)!} \xi^i (1-\xi)^{m-i} \quad (7.9)$$

For example, in the case of a cubic curve ( $m=3$ ), one needs to evaluate  $S_{0,3}$ ,  $S_{1,3}$ ,  $S_{2,3}$ , and  $S_{3,3}$ . These four basis functions can be defined using Equation 9 as

$$\left. \begin{aligned} S_{0,3} &= (1-\xi)^3, & S_{1,3} &= 3\xi(1-\xi)^2, \\ S_{2,3} &= 3\xi^2(1-\xi), & S_{3,3} &= \xi^3 \end{aligned} \right\} \quad (7.10)$$

Using these blending cubic functions and Equation 8, one can show that the cubic Bezier curve is defined by

$$\mathbf{r} = (1-\xi)^3 \mathbf{P}_0 + 3\xi(1-\xi)^2 \mathbf{P}_1 + 3\xi^2(1-\xi) \mathbf{P}_2 + \xi^3 \mathbf{P}_3 \quad (7.11)$$

This equation is the same as Equation 7 obtained using the ANCF geometry and the transformation from the gradient coordinates to the point coordinates defined by Equation 6. Equations 7 and 11 clearly demonstrate that the Bezier geometry can be converted to ANCF geometry using a simple linear transformation.

One can show that the Bernstein polynomials of Equation 9 have the following property (Piegl and Tiller, 1997):

$$\frac{\partial S_{i,m}}{\partial \xi} = m(S_{i-1,m-1} - S_{i,m-1}), \quad (7.12)$$

with  $S_{-1,m-1} = S_{m,m-1} = 0$ . Using this property, one can write

$$\frac{\partial \mathbf{r}}{\partial \xi} = m \sum_{i=0}^{m-1} S_{i,m-1}(\mathbf{P}_{i+1} - \mathbf{P}_i) \quad (7.13)$$

The Bernstein polynomials have many other interesting properties that are shared by the shape functions of many of the commonly used finite elements. Some of these properties are

$$S_{i,m}(\xi) \geq 0, \quad \sum_{i=0}^m S_{i,m}(\xi) = 1, \quad S_{0,m}(0) = S_{m,m}(1) = 1 \quad (7.14)$$

Using the properties of the Bernstein polynomials, one can develop efficient algorithms, such as the *deCasteljau algorithm*, for the construction of Bezier curves (Piegl and Tiller, 1997).

The cubic Bezier function can also be expressed in terms of power-basis functions. This provides the following alternate form of Equation 7 or 11:

$$\mathbf{r} = \mathbf{P}_0 + 3\xi(\mathbf{P}_1 - \mathbf{P}_0) + 3\xi^2(\mathbf{P}_0 - 2\mathbf{P}_1 + \mathbf{P}_2) + \xi^3(3\mathbf{P}_1 - \mathbf{P}_0 - 3\mathbf{P}_2 + \mathbf{P}_3) \quad (7.15)$$

In this equation,  $1$ ,  $\xi$ ,  $\xi^2$ , and  $\xi^3$  are the power-basis functions. Bezier geometry also can be generalized to the case of surfaces, as discussed after introducing the B-spline geometry.

## 7.4 B-SPLINE CURVE REPRESENTATION

Bezier representation can be considered a special case of the more general B-spline representation. In the B-spline representation, several polynomial segments can be used, allowing for efficient shape and geometry manipulations. The B-spline geometry method, therefore, can be considered the counterpart of the FE analysis method, which allows geometric description over subdomains. A B-spline curve with  $p$ -degree is defined as (Dierckx, 1993; Farin, 1999; Piegl and Tiller, 1997; Rogers, 2001):

$$\mathbf{r}(u) = N_{0,p}(u)\mathbf{P}_0 + N_{1,p}(u)\mathbf{P}_1 + \cdots + N_{n,p}(u)\mathbf{P}_n = \sum_{i=0}^n N_{i,p}(u)\mathbf{P}_i \quad (7.16)$$



where  $N_{i,p}(u)$  are B-spline basis functions of degree  $p$ ,  $\mathbf{P}_i$  are the control points, and  $n$  is the number of control points. The B-spline basis functions  $N_{i,p}(u)$  are defined as

$$\left. \begin{aligned} N_{i,0}(u) &= \begin{cases} 1 & \text{if } u_i \leq u < u_{i+1} \\ 0 & \text{otherwise} \end{cases} \\ N_{i,j}(u) &= \frac{u - u_i}{u_{i+j} - u_i} N_{i,j-1}(u) + \frac{u_{i+j+1} - u}{u_{i+j+1} - u_{i+1}} N_{i+1,j-1}(u) \end{aligned} \right\} \quad (7.17)$$

where  $u_i = 0, 1, 2, \dots, n + p + 1$  are called the *knots*, which represent a nondecreasing sequence; that is,  $u_i \leq u_{i+1}$ . The vector  $\mathbf{U} = \{u_0, u_1, \dots, u_{n+p+1}\}$  is called the *knot vector*. The knots do not have to be distinct; distinct knots are called *breakpoints* and define segments with nonzero length. Each nonzero knot span corresponds to a segment of the B-spline curve. The number of the nondistinct knots at a point is referred to as the *knot multiplicity*.

### Control Points and Degree of Continuity

For a given polynomial order  $p$ , one can always define at a breakpoint  $p + 1$  vectors. These vectors represent the position vector and its derivatives up to the  $p$ th derivative. For example, in the case of a cubic Bezier curve ( $p = 3$ ), one can define  $\mathbf{r}$ ,  $\partial\mathbf{r}/\partial u$ ,  $\partial^2\mathbf{r}/\partial u^2$ , and  $\partial^3\mathbf{r}/\partial u^3$ . Higher derivatives will be equal to zero. Therefore, in the case of two cubic Bezier segments  $i$  and  $j$ , one can have different conditions. If the two segments are not connected, the number of control points totals eight because each Bezier segment is represented using four ( $p + 1$ ) control points. This is the case of  $C^{-1}$  continuity. In this case, all of the vectors  $\mathbf{r}$ ,  $\partial\mathbf{r}/\partial u$ ,  $\partial^2\mathbf{r}/\partial u^2$ , and  $\partial^3\mathbf{r}/\partial u^3$  that correspond to the first segment at the breakpoint are not related to the vectors  $\mathbf{r}$ ,  $\partial\mathbf{r}/\partial u$ ,  $\partial^2\mathbf{r}/\partial u^2$ , and  $\partial^3\mathbf{r}/\partial u^3$  that correspond to the second segment at this breakpoint. This case of  $C^{-1}$  continuity corresponds to the case of knot multiplicity of four ( $p + 1$ ). If continuity is to be imposed on the position at the breakpoint at which the two segments are connected, one must have at the breakpoint the condition  $\mathbf{r}^i = \mathbf{r}^j$ , where  $i$  and  $j$  are the segment numbers. This algebraic equation, which ensures  $C^0$  continuity, can be used to write a control point of one segment in terms of the remaining control points. This leads to a reduction of the number of control points by one. This case of  $C^0$  continuity corresponds to knot multiplicity of three. Similarly, in the case of  $C^1$  continuity, two conditions are imposed at the breakpoint: the positions must be the same,  $\mathbf{r}^i = \mathbf{r}^j$ ; and the gradients must be the same,  $(\partial\mathbf{r}/\partial u)^i = (\partial\mathbf{r}/\partial u)^j$ . These two vector algebraic equations allow for reducing the number of control points by two. This case corresponds to knot multiplicity of two in the case of cubic polynomials. Using a similar procedure, one can show that in the case of cubic polynomials,  $C^2$  continuity at a breakpoint corresponds to knot multiplicity of one and  $C^3$  continuity corresponds to knot multiplicity of zero. In the latter case of  $C^3$  continuity, the two segments blend together to form one larger cubic segment; four control points are eliminated, thereby reducing the number of control points for the newly created segment to four.

The concept of the knot multiplicity and the B-spline recurrence formula can be used to achieve automatically a higher degree of continuity by reducing the number of independent control points. Understanding the role of the knot multiplicity in B-spline representation is important when relating geometry methods to FE analysis methods that use the concept of nodes and degrees of freedom. If  $r + 1$  is the number of knots in  $\mathbf{U}$ , then in the B-spline

geometry, one must have  $r = n + p + 1$ . This relationship can be verified easily starting with one Bezier segment. It is clear from this relationship that for a given polynomial degree  $p$ , reducing the knot multiplicity, to increase the degree of continuity, leads to a similar reduction in the number of control points, and increasing the knot multiplicity leads to a similar increase in the number of control points.

### Illustrative Example

Figure 2 shows a cubic B-spline curve that has the six control points  $\mathbf{P}_0, \mathbf{P}_1, \mathbf{P}_2, \mathbf{P}_3, \mathbf{P}_4$ , and  $\mathbf{P}_5$  and the knot vector  $\mathbf{U} = \{0 \ 0 \ 0 \ 0 \ 1 \ 2 \ 3 \ 3 \ 3 \ 3\}$  (Lan and Shabana, 2010). The number of segments in this example is  $s = 3$  and the distinct breakpoints are  $\bar{u}_0 = 0$ ,  $\bar{u}_1 = 1$ ,  $\bar{u}_2 = 2$ , and  $\bar{u}_3 = 3$ . Note that if the knot vector has the form  $\mathbf{U} = \{\underbrace{0 \cdots 0}_{p+1} \underbrace{1 \cdots 1}_{p+1}\}$ , the B-spline curve

reduces to a  $p$ -order Bezier curve; therefore, the Bezier curve can be considered a special case of the B-spline curve representation, as previously mentioned. At  $\bar{u}_0 = 0$ , the knot multiplicity is four, which implies that there is no continuity condition imposed at this breakpoint, and  $\mathbf{r}$ ,  $\partial \mathbf{r} / \partial u$ ,  $\partial^2 \mathbf{r} / \partial u^2$ , and  $\partial^3 \mathbf{r} / \partial u^3$  are discontinuous. At the breakpoint  $\bar{u}_1 = 1$ , the knot multiplicity is one and the curve is  $C^2$  continuous at this point. In this case,  $\mathbf{r}$ ,  $\partial \mathbf{r} / \partial u$ , and  $\partial^2 \mathbf{r} / \partial u^2$  are continuous, whereas the continuity of  $\partial^3 \mathbf{r} / \partial u^3$  is not ensured. The B-spline recurrence formula with the knot vector defined previously can be used to demonstrate this fact. The breakpoint  $\bar{u}_2 = 2$  has knot multiplicity of one; therefore, this point has continuity conditions similar to the breakpoint  $\bar{u}_1 = 1$ . The breakpoint  $\bar{u}_3 = 3$  has knot multiplicity of four; therefore, this point has continuity conditions similar to  $\bar{u}_0 = 0$ .

### Knot Insertion

By inserting knots into a B-spline knot vector, one can increase the number of control points as well as the knot multiplicity at selected points. For example, the S-shaped cubic B-spline curve

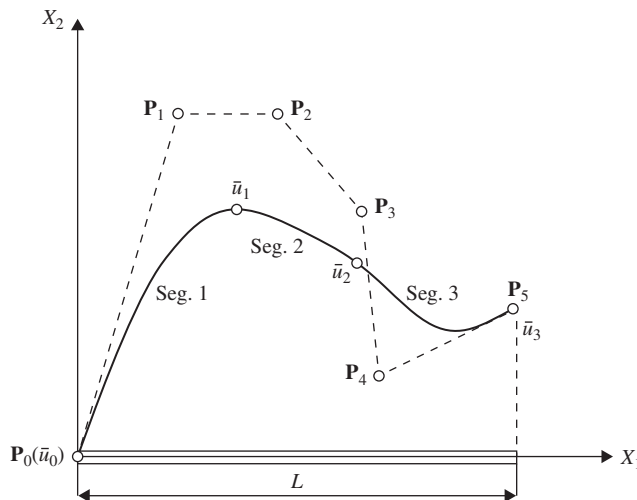


Figure 7.2 B-spline curve

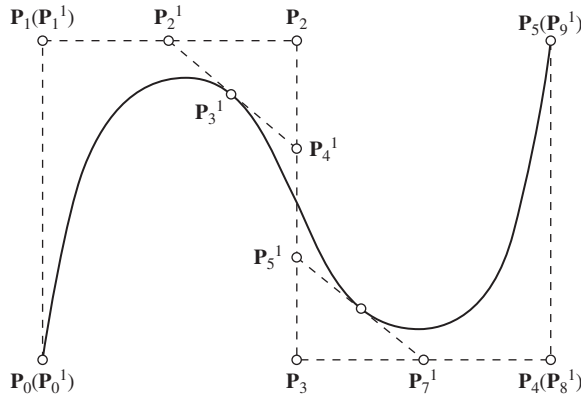


Figure 7.3 Knot insertion

shown in Figure 3, which has three segments, can be described by the knot vector  $\mathbf{U} = \{0\ 0\ 0\ 0\ 1\ 2\ 3\ 3\ 3\ 3\}$  and the control points  $\mathbf{P}_0, \mathbf{P}_1, \mathbf{P}_2, \mathbf{P}_3, \mathbf{P}_4$ , and  $\mathbf{P}_5$ . Changing the knot vector to  $\mathbf{U} = \{0\ 0\ 0\ 0\ 1\ 1\ 1\ 2\ 2\ 2\ 3\ 3\ 3\ 3\}$  by increasing the multiplicity at  $\bar{u}_2 = 1$  and  $\bar{u}_2 = 2$  to three reduces the degree of continuity at these breakpoints. At these points, the B-spline curve has  $C^0$  continuity, which ensures the continuity of the position vector only. Because the knot multiplicity is increased by two at two breakpoints, the number of control points increases by four. The corresponding control points for the new B-spline curve  $\mathbf{P}_0^1, \mathbf{P}_1^1, \mathbf{P}_2^1, \mathbf{P}_3^1, \mathbf{P}_4^1, \mathbf{P}_5^1, \mathbf{P}_6^1, \mathbf{P}_7^1, \mathbf{P}_8^1$ , and  $\mathbf{P}_9^1$  also are shown in Figure 3. This B-spline curve, which ensures only  $C^0$  continuity at the inner breakpoints, is formed from three cubic Bezier curves that have the control points  $(\mathbf{P}_0^1, \mathbf{P}_1^1, \mathbf{P}_2^1, \mathbf{P}_3^1)$ ,  $(\mathbf{P}_3^1, \mathbf{P}_4^1, \mathbf{P}_5^1, \mathbf{P}_6^1)$ , and  $(\mathbf{P}_6^1, \mathbf{P}_7^1, \mathbf{P}_8^1, \mathbf{P}_9^1)$ . In fact, one can verify that any  $p$ -order  $C^0$  B-spline curve can be constructed using Bezier curves if the knot vector takes the form  $\mathbf{U} = \underbrace{\{u_0 \cdots u_0\}}_{p+1} \cdots \underbrace{\{u_i \cdots u_i\}}_p \cdots \underbrace{\{u_s \cdots u_s\}}_{p+1}$ . Decreasing the knot multiplicity at the inner

breakpoints automatically increases the degree of continuity and eliminates the redundant control points. This process is built automatically in the powerful recurrence formula defined by Equations 16 and 17. Using these equations, one can also show that when the multiplicity at a breakpoint reduces to zero, two B-spline segments blend together to define one knot span with a length equal to the sum of the lengths of the two original segments. In addition to this powerful feature of the B-spline representation that provides the flexibility of easily changing the degree of continuity, the B-spline basis functions have unique desirable features such as the local support property, the nonnegativity, and the partition of unity (Dierckx, 1993; Farin, 1999; Piegl and Tiller, 1997; Rogers, 2001).

### Comparison with FE Formulations

Because of the problems associated with the kinematic description of existing FE formulations, computational geometry methods are being adopted as analysis tools. This led to a new research field known as *isogeometric analysis*, which is based on using CAD systems for both geometric modeling and analysis. As discussed in a subsequent section, computational

geometry methods have serious limitations as analysis tools. These methods do not provide the flexibility offered by FE analysis methods and fail to capture certain types of discontinuities that define the geometric shapes of many mechanical and structural components. In the remainder of this section, the focus is on basic differences between the descriptions used by computational geometry and FE methods (Lan and Shabana, 2010).

The concept of nodes that represent material points on a curve or a surface is not used in B-spline geometry and other computational geometry methods; instead, computational geometry methods use control points that do not have to represent material points. The definition of nodes, is fundamental in the FE analysis. Different coordinate types such as positions, angles, gradients, curvatures, and stresses, among others, can be used as the nodal variables. The use of some of these coordinate types can impose restrictions on the geometric shapes that can be assumed by the finite elements. In fact, some of the conventional finite elements do not preserve the shapes of the finite elements under an arbitrary rigid-body transformation, as previously discussed. The kinematic description used for these elements, therefore, is not equivalent to the descriptions used by computational geometry methods such as the B-spline representation. For this reason, the geometry of the FE mesh used in the analysis in the reference configuration is not always identical to the geometry created in CAD systems. B-spline geometry, however, can always be converted to ANCF geometry using simple linear transformation. The converse is not always true, as demonstrated later in this chapter.

Another fundamental difference between the geometric descriptions used in the FE and computational geometry methods is the *domain definition*. Most FE formulations use the domain in the reference configuration such as the undeformed-length or cross-sectional dimensions of a beam to carry out the integrations required to formulate the FE inertia and stiffness forces. The concept of reference configuration or element domain as used in FE analysis is not used in computational geometry methods. Therefore, it is important to address this issue to successfully convert the B-spline geometry to an FE mesh with the exact geometric properties as that developed in a CAD system (Lan and Shabana, 2010).

## 7.5 CONVERSION OF B-SPLINE GEOMETRY TO ANCF GEOMETRY

One method for the integration of CAD and analysis is to establish an efficient interface that can be used to convert the CAD model to an FE mesh that has geometry identical to the model created in the CAD system. This was not possible in the past because conventional structural finite elements such as beams, plates, and shells are based on a kinematic description that is not consistent with the description used by computational geometry methods. This problem, however, can be solved by using ANCF finite elements because B-spline geometry can always be converted to an ANCF representation using simple linear transformation.

How to convert a Bezier curve representation to ANCF representation is shown in this chapter (Sanborn and Shabana, 2009). Because a B-spline curve can be represented as a series of connected Bezier curves, the curves can be converted to ANCF cable elements. This demonstrates that ANCF cable elements can have geometry identical to that of the original B-spline curve representation. In the case of the ANCF cable elements, the global position vector  $\mathbf{r}$  of an arbitrary point on the FE centerline can be defined using the element shape functions and the nodal coordinate vector as  $\mathbf{r}(x, t) = \mathbf{S}(x)\mathbf{e}(t)$ , where  $\mathbf{S}$  is the element shape function matrix expressed in terms of the element spatial coordinate  $x$ ;  $\mathbf{e} = [(\mathbf{r}^A)^T \ (\mathbf{r}_x^A)^T \ (\mathbf{r}^B)^T \ (\mathbf{r}_x^B)^T]^T$

is the vector of nodal coordinates that consist of absolute position and gradient coordinates of the first and second nodes of the element (denoted, respectively, as  $A$  and  $B$ ); and  $t$  is time. For the three-dimensional cable elements, the shape function matrix can be written as  $\mathbf{S} = [s_1 \mathbf{I} \ s_2 \mathbf{I} \ s_3 \mathbf{I} \ s_4 \mathbf{I}]$ , where  $\mathbf{I}$  is the identity matrix and  $s_i$ ,  $i = 1, 2, 3, 4$ , are shape functions defined as

$$\left. \begin{aligned} s_1 &= 1 - 3\xi^2 + 2\xi^3, & s_2 &= l(\xi - 2\xi^2 + \xi^3), \\ s_3 &= 3\xi^2 - 2\xi^3, & s_4 &= l(-\xi^2 + \xi^3) \end{aligned} \right\} \quad (7.18)$$

In this equation,  $l$  is the FE length, and  $\xi = x/l$ .

The cubic Bezier curve control points  $\mathbf{P}_0$ ,  $\mathbf{P}_1$ ,  $\mathbf{P}_2$ , and  $\mathbf{P}_3$  can be written in terms of the ANCF nodal coordinates using the following equation (see also Equation 6):

$$\begin{bmatrix} \mathbf{P}_0 \\ \mathbf{P}_1 \\ \mathbf{P}_2 \\ \mathbf{P}_3 \end{bmatrix} = \begin{bmatrix} \mathbf{I} & \mathbf{0} & \mathbf{0} & \mathbf{0} \\ \mathbf{I} & \frac{l}{3}\mathbf{I} & \mathbf{0} & \mathbf{0} \\ \mathbf{0} & \mathbf{0} & \mathbf{I} & -\frac{l}{3}\mathbf{I} \\ \mathbf{0} & \mathbf{0} & \mathbf{I} & \mathbf{0} \end{bmatrix} \begin{bmatrix} \mathbf{r}^A \\ \mathbf{r}_x^A \\ \mathbf{r}^B \\ \mathbf{r}_x^B \end{bmatrix} \quad (7.19)$$

Substituting this equation into the Bezier curve representation, one can obtain ANCF representation that has identical geometry to that represented by the B-spline recurrence formula. Alternatively, using Equation 6, one can show that the kinematics of the ANCF cable element can be expressed in terms of the cubic Bezier curve control points as (Lan and Shabana, 2010):

$$\mathbf{r}(\xi) = \sum_{i=0}^3 \mathbf{S}_{i,3}(\xi) \mathbf{P}_i, \quad 0 \leq \xi \leq 1 \quad (7.20)$$

where the relationship between the ANCF shape functions and the Bernstein polynomials  $S_{0,3}$ ,  $S_{1,3}$ ,  $S_{2,3}$ , and  $S_{3,3}$  is defined as

$$\left. \begin{aligned} s_1 &= S_{0,3} + S_{1,3}, & s_2 &= \frac{l}{3} S_{1,3}, \\ s_3 &= S_{2,3} + S_{3,3}, & s_4 &= -\frac{l}{3} S_{2,3} \end{aligned} \right\} \quad (7.21)$$

To convert a B-spline curve into an ANCF cable element, an assumed element length  $l$  should be defined first. In this case, the B-spline curve that is represented with a series of ANCF cable elements also has a domain that is the sum of all of the assumed element lengths. This domain is defined as  $L = \sum_{i=1}^s l_i$ , where  $L$  is the assumed domain of the B-spline curve,  $s$  is the number of segments, and  $l_i$  is the length of the  $i$ th ANCF cable element in the reference undeformed configuration. As described by Lan and Shabana (2010), this domain can be used to define consistently the gradients and derivatives when converting B-spline geometry to ANCF FE representation.

## 7.6 ANCF AND B-SPLINE SURFACES

Fully parameterized planar ANCF finite elements and all spatial ANCF finite elements, including gradient-deficient elements, preserve the geometry under an arbitrary rigid-body displacement. This important condition, which also is satisfied by computational geometry methods, ensures that B-spline geometry can always be converted to ANCF FE mesh that has identical geometry. Nonetheless, ANCF geometry cannot always be converted to B-spline geometry because of the structure of the B-spline recurrence formula. In this section, fundamental differences between the ANCF and B-spline geometric representations are discussed. To this end, surface geometry in fully parameterized planar ANCF beam elements and gradient-deficient spatial-plate elements is used.

### B-Spline Surfaces

B-spline surfaces are defined using the product of B-spline base functions, two parameters, and two knot vectors. B-spline surfaces can be defined in the following parametric form (Piegl and Tiller, 1997):

$$\mathbf{r}(u, v) = \sum_{i=0}^n \sum_{j=0}^m N_{i,p}(u) N_{j,q}(v) \mathbf{P}_{i,j} \quad (7.22)$$

where  $u$  and  $v$  are the parameters;  $N_{i,p}(u)$  and  $N_{j,q}(v)$  are B-spline basis functions of degrees  $p$  and  $q$ , respectively; and  $\mathbf{P}_{i,j}$  are a set of bidirectional net of control points. The B-spline basis functions  $N_{i,p}(u)$  are defined as

$$\left. \begin{aligned} N_{i,0}(u) &= \begin{cases} 1 & \text{if } u_i \leq u < u_{i+1} \\ 0 & \text{otherwise} \end{cases} \\ N_{i,j}(u) &= \frac{u - u_i}{u_{i+j} - u_i} N_{i,j-1}(u) + \frac{u_{i+j+1} - u}{u_{i+j+1} - u_{i+1}} N_{i+1,j-1}(u) \end{aligned} \right\} \quad (7.23)$$

where  $u_{i,j} = 0, 1, 2, \dots, n+p+1$  are called the *knots* and  $u_i \leq u_{i+1}$ . The vector  $\mathbf{U} = \{u_0, u_1, \dots, u_{n+p+1}\}$  is called the *knot vector* associated with the  $u$  parameter. Similar definitions can be introduced for  $N_{j,q}(v)$  with another knot vector  $\mathbf{V} = \{v_0, v_1, \dots, v_{m+q+1}\}$ . Note that the orders of the polynomials in the  $u$  and  $v$  directions can be different; for example, a cubic interpolation can be used along  $u$ , whereas a linear interpolation can be used along  $v$ . As in the case of B-spline curves, the knots of B-spline surfaces do not have to be distinct; distinct knots are called *breakpoint* and define surface segments with nonzero dimensions. The number of the nondistinct knots in  $\mathbf{U}$  and  $\mathbf{V}$  at a point is referred to as the knot multiplicity associated, respectively, with the parameters  $u$  and  $v$  at this point. At a given breakpoint, the multiplicity associated with  $u$  can be different from the multiplicity associated with  $v$ , allowing for different degrees of continuity for the derivatives with respect to  $u$  and  $v$ . For cubic  $N_{i,p}$  ( $p=3$ ),  $C^0$ ,  $C^1$ , or  $C^2$  conditions correspond, respectively, to knot multiplicity of three, two, and one; whereas in the case of linear interpolation of  $N_{j,q}$ , the highest continuity degree that can be demanded is continuity of the gradients. When zero multiplicity is used at a breakpoint, the segments blend together at this point.

In B-spline surface representation, there is a relationship among the polynomial degree, the number of knots, and the number of control points. This relationship must be fully understood if B-spline geometry is used as an analysis tool. If  $r + 1$  is the number of knots in  $\mathbf{U}$  and  $s + 1$  is the number of knots in  $\mathbf{V}$ , then in B-spline geometry, one must have

$$r = n + p + 1, \quad s = m + q + 1 \quad (7.24)$$

As in the case of B-spline curves, these formulas imply that for a given polynomial order, if the number of knots decreases, the number of control points that defines the number of degrees of freedom used in the analysis must also decrease. This also can be equivalent to increasing the degree of continuity because eliminating a control point can be the result of imposing algebraic equations that relate the derivatives at a certain breakpoint.

From the bidirectional structure used in Equation 22, a surface segment that has cubic interpolation along  $u$  ( $p = 3$ ,  $n = 3$ ,  $r + 1 = 8$ ) and a linear interpolation along  $v$  ( $q = 1$ ,  $m = 1$ ,  $s + 1 = 4$ ) should have  $(n + 1) \times (m + 1) = 8$  control points; this is true regardless of whether the surface is two- or three-dimensional. Manipulation of the B-spline surface defined by Equation 22 shows that these eight control points are the result of using the alternate basis set  $1, u, v, uv, (u)^2, (u)^2v, (u)^3, (u)^3v$ . That is, B-spline representation and the formulas of Equation 24 do not allow for the use of the basis set  $1, u, v, uv, (u)^2, (u)^3$ , which can be used effectively to develop a shear deformable beam model. If a cubic interpolation is used for both  $u$  and  $v$  (case of thin plate), the B-spline representation will require 16 control points because the expansion must include all terms  $(u)^k (v)^l$ ;  $k, l = 0, 1, 2, 3$ , regardless of whether the shape of deformation of the plate is simple or complex; one must follow strictly the B-spline rigid structure. This can be a disadvantage in the analysis because such a geometric representation can increase unnecessarily the dimensions of the model and lead to the loss of flexibility offered by the FE method or modal analysis techniques. Another important and interesting issue regarding the use of B-spline as an analysis tool is capturing discontinuities, which is discussed later in this chapter.

## ANCF Surfaces

Whereas B-spline geometry always can be converted to ANCF geometry, the converse is not true. ANCF geometry does not impose restrictions on the basis functions that must be included in the interpolating polynomials. This allows for developing finite elements that have a small number of nodal coordinates as compared to those developed using the B-spline representation. Furthermore, ANCF geometry can be used to model both structural and nonstructural discontinuities, whereas the rigid B-spline recurrence representation cannot be used to model structural discontinuities in a straightforward manner, as discussed in the following section.

A basic difference between ANCF and B-spline geometries is demonstrated in this section using a planar-beam example. The displacement field of the shear deformable beam used can be written as  $\mathbf{r}(x_1, x_2) = \mathbf{S}(x_1, x_2) \mathbf{e}(t)$ , where  $x_1$  and  $x_2$  are the element spatial coordinates,  $t$  is time,  $\mathbf{S}$  is the element shape function matrix, and  $\mathbf{e}$  is the vector of the element nodal coordinates. The shape function matrix for the element considered in this section is defined as

$$\mathbf{S}^j = [s_1 \mathbf{I} \ s_2 \mathbf{I} \ s_3 \mathbf{I} \ s_4 \mathbf{I} \ s_5 \mathbf{I} \ s_6 \mathbf{I}] \quad (7.25)$$

where the shape functions  $s_i$ ,  $i = 1, 2, \dots, 6$ , are defined as (Omar and Shabana, 2001):

$$\left. \begin{aligned} s_1 &= 1 - 3\xi^2 + 2\xi^3, & s_2 &= l(\xi - 2\xi^2 + \xi^3), & s_3 &= l\eta(1 - \xi), \\ s_4 &= 3\xi^2 - 2\xi^3, & s_5 &= l(-\xi^2 + \xi^3), & s_6 &= l\xi\eta \end{aligned} \right\} \quad (7.26)$$

In this equation,  $\xi = x_1/l$ , and  $\eta = x_2/l$ . ANCF finite elements use gradient vectors as nodal coordinates. For the element used in this section, the vector of nodal coordinates is defined as

$$\mathbf{e} = [(\mathbf{r}^1)^T \quad (\partial \mathbf{r}^1 / \partial x_1)^T \quad (\partial \mathbf{r}^1 / \partial x_2)^T \quad (\mathbf{r}^2)^T \quad (\partial \mathbf{r}^2 / \partial x_1)^T \quad (\partial \mathbf{r}^2 / \partial x_2)^T]^T \quad (7.27)$$

where superscript  $k$ ,  $k = 1, 2$ , indicates variables evaluated at node  $k$  of the element. The element defined by the preceding equations is based on a cubic interpolation for  $x_1$  and a linear interpolation for  $x_2$ .

The finite element described in this section is an example of ANCF elements that cannot be converted to B-spline representation. This element is based on a polynomial expansion that does not have the two basis functions  $(x_1)^2 x_2$  and  $(x_1)^3 x_2$ . These terms can be systematically included in ANCF geometry by adding nodal coordinates, which allows for converting B-spline representation to ANCF representation. Similar comments apply to ANCF thin-plate elements that do not require including all of the basis functions  $(x_1)^k (x_2)^l$ ;  $k, l = 0, 1, 2, 3$ . This flexibility offered by ANCF geometry allows for developing finite elements that have a smaller number of nodal coordinates compared to those elements developed by B-spline geometry.

## 7.7 STRUCTURAL AND NONSTRUCTURAL DISCONTINUITIES

In this section, two types of discontinuities explain another fundamental difference between ANCF and B-spline geometries: *structural* and *nonstructural discontinuities*. In the case of structural discontinuity, there is no relative rigid-body motion at the discontinuity node; all of the relative degrees of freedom are deformation degrees of freedom. An example of structural discontinuity is at point  $C$  in Figure 4. At the structural-discontinuity node, in the case of the planar system shown in Figure 4, there is only one state of strains. Nonstructural discontinuity, conversely, allows for relative rigid-body rotation. At points  $O$  and  $B$  in Figure 4, there can be two different states of strains because of the rigid-body mode. Although both structural and

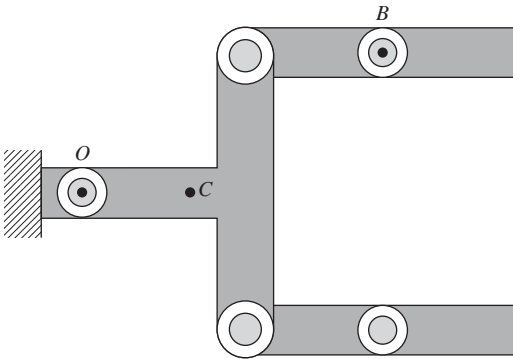


**Figure 7.4** Structural and nonstructural discontinuities



nonstructural discontinuities can be classified as  $C^0$ , they are fundamentally different from the analysis perspective because they lead to two completely different joint models that have different degrees of freedom. Only one of these types of discontinuities can be captured by the B-spline recurrence formula, whereas the other cannot be captured. Both, however, can be captured by ANCF finite elements.

### B-Spline Model

As previously mentioned, reducing the knot multiplicity by one at a curve breakpoint leads to  $C^0$  continuity and to the elimination of one control point. This is equivalent to the multibody system (MBS) pin-joint-constraint definition in planar analysis and to the MBS spherical-joint definition in spatial analysis. This type of  $C^0$  continuity captured by B-spline is of the nonstructural-discontinuity type that leads to a rigid-body mode and to a nonunique state of the strain at the discontinuity node. The B-spline recurrence formula structure leads automatically to this type of discontinuity. The structural discontinuity, although it is also of the  $C^0$  type, requires additional algebraic equations to define a unique strain state by eliminating the relative rotation at the joint definition point. These algebraic equations can be used to eliminate other control points and such elimination is not embedded in the rigid B-spline geometry representation. Only one type of  $C^0$  continuity can be described using B-spline formula; reducing the knot multiplicity by one in B-spline representation does not capture structural discontinuity. More fundamental problems are encountered when B-spline surfaces are considered in MBS applications as explained in the literature (Yu and Shabana, 2015).

### ANCF Model

One can show that ANCF finite elements describe both structural and nonstructural discontinuities. Nonstructural discontinuities that allow for large rigid-body rotations can be described using a  $C^0$  model obtained by imposing constraints only on the position coordinates. For example, if two elements  $i$  and  $j$  are connected by a pin joint at a node, one can apply the algebraic equations  $\mathbf{r}^i = \mathbf{r}^j$  at this node. These algebraic equations can be imposed at a pre-processing stage to eliminate the dependent variables and to define an FE mesh that has a constant mass matrix and zero Coriolis and centrifugal forces, despite the finite rotations allowed between the finite elements of the mesh. As previously mentioned, nonstructural discontinuities also can be described using B-spline geometry by reducing the knot multiplicity by one at the joint node. In the case of nonstructural discontinuities, no constraints are imposed on the gradient vectors; therefore, the state of strain is not unique at the joint node. Each of the Lagrangian strains  $\epsilon_{11} = (\mathbf{r}_{x_1}^T \mathbf{r}_{x_1} - 1)/2$ ,  $\epsilon_{22} = (\mathbf{r}_{x_2}^T \mathbf{r}_{x_2} - 1)/2$ , and  $\epsilon_{12} = \mathbf{r}_{x_1}^T \mathbf{r}_{x_2}/2$  has two values at the joint node: one defined on element  $i$  and the other on element  $j$ . Here,  $\mathbf{r}_{x_1} = \partial \mathbf{r} / \partial x_1$ ,  $\mathbf{r}_{x_2} = \partial \mathbf{r} / \partial x_2$ .

The concept of degrees of freedom widely used in mechanics is not considered in developing the recurrence relationships on which B-spline and NURBS geometry are based. This represents another serious limitation when these computational geometry methods are used as analysis tools, which is evident by the fact that B-spline geometry cannot describe structural discontinuities. As previously mentioned, this type, although it is of the  $C^0$  continuity type, requires imposing additional gradients constraints, which cannot be captured by the B-spline

recurrence formula because they require the elimination of additional vectors. In the case of B-spline,  $C^0$  continuity is achieved by reducing the knot multiplicity by one, which eliminates one control point leading to the definition of a pin joint (nonstructural discontinuity). ANCF geometry, conversely, allows for imposing constraints on the gradients using the tensor transformation  $(\partial \mathbf{r} / \partial \mathbf{x}) = (\partial \mathbf{r} / \partial \mathbf{y}) \mathbf{A}$ , where  $\mathbf{x} = [x_1 \ x_2]^T$  and  $\mathbf{y} = [y_1 \ y_2]^T$  are two sets of coordinate lines and  $\mathbf{A}$  is the matrix of coordinate-line transformation. Using this tensor-gradient transformation, the structural discontinuities can be modeled systematically using ANCF finite elements, as described in the literature (Shabana and Mikkola, 2003; Shabana, 2011).

## PROBLEMS

1. Explain the differences between Bezier and B-spline geometry representations.
2. Discuss the similarities and differences between the B-spline and NURBS representations.
3. Starting with a cubic polynomial, derive the cubic Bezier curve in terms of the control points and define the basis functions of Equation 10.
4. Explain the basic differences between the B-spline and finite element representations.
5. For a cubic Bezier curve, derive the relationship between the control points and the nodal coordinates of the ANCF cable element.
6. Explain how the degree of continuity can be adjusted when using the B-spline geometry. In B-spline geometry, can continuity be imposed on the gradients without having position continuity? Provide an explanation.
7. Explain the meaning of the knot multiplicity. In the case of cubic B-spline curve, explain the meaning of knot multiplicity of 1, 2, 3, and 4. Give examples to show the relationship between the knot multiplicity and the number of the B-spline control points.
8. Explain why B-spline geometry can always be converted to ANCF geometry, while the converse is not true. Give an example to support the argument made.
9. Give an example of a cubic B-spline surface and explain how this surface can be converted to an ANCF finite element.
10. Explain the differences between structural and nonstructural discontinuities. Give examples to explain these differences.



# PLASTICITY FORMULATIONS

---

The analysis of plastic deformation is important in many engineering applications including crashworthiness, impact analysis, manufacturing problems, among many others. When materials undergo plastic deformations, permanent strains are developed when the load is removed. Many materials exhibit elastic–plastic behaviors, that is, the material exhibits elastic behavior up to a certain stress limit called the *yield strength* after which plastic deformation occurs. If the stress of elastic–plastic materials depends on the strain rate, one has a *rate-dependent material*; otherwise, the material is called *rate independent*. In the classical plasticity analysis of solids, a nonunique stress–strain relationship that is independent of the rate of loading but does depend on the loading sequence is used (Zienkiewicz and Taylor, 2000). In rate-dependent plasticity, on the other hand, the stress–strain relationship depends on the rate of the loading.

The yield strength of elastic–plastic materials can increase after the initial yield. This phenomenon is known as *strain hardening*. In the theory of plasticity, there are two types of strain hardening: *isotropic* and *kinematic hardening*. In the case of isotropic hardening, the yield strength changes as the result of the plastic deformation. In the case of kinematic hardening, on the other hand, the center of the yield surface experiences a motion in the direction of the plastic flow. The kinematic hardening behavior is closely related to a phenomenon known as the *Bauschinger effect*, which is the result of a reduction in the compressive yield strength following an initial tensile yield. The kinematic hardening effect is important in the case of cyclic loading.

The assumptions on which the theory of plasticity is based can be summarized as follows (Belytschko et al., 2000):

1. The assumption of the *strain additive decomposition* by which the strain increment can be decomposed as a reversible elastic part  $d\epsilon^e$  and irreversible plastic part  $d\epsilon^p$  is used. The assumption of the additive decomposition is used in the case of small deformation. In the case of large deformation, the *multiplicative decomposition* of the matrix of the position vector gradients is used instead of the additive decomposition.
2. A *yield function*  $f$  that depends on some internal variables defined later in this chapter is used to determine whether the behavior is elastic or plastic. This yield function can be expressed in terms of the stresses or strains. If the plasticity equations are formulated in terms of the stresses, one has a *stress space formulation*. If, on the other hand, the equations are formulated in terms of the strains, one has a *strain space formulation*. There are different yield functions that are used in the plasticity formulations; the most common one is the von *Mises yield function*. The yield criterion based on the von Mises function assumes that plastic yield occurs when the second invariant of the deviatoric stress tensor reaches a critical value. Another yield criterion is based on the *Tresca yield function*. When this criterion is used, it is assumed that plastic yield occurs when the maximum shear stress reaches a certain critical value.
3. A *flow rule* that defines the plastic flow is used to determine the strain increment. This flow rule, which defines the plastic strain rate, introduces additional differential equations required to determine the unknown variables in the plasticity formulation. Depending on the form of the flow rule, different plasticity models can be developed.
4. A set of *evolution equations* are introduced for the internal variables and strain-hardening relation. The internal variables and hardening parameters enter into the definition of the yield function. As in the case of the flow rule, additional first-order differential equations are introduced in order to be able to determine the internal variables.

It is important to note that part of the work done during the plastic deformation is converted to other forms of energy such as heat. Therefore, elastic–plastic behavior is path dependent, and such a behavior leads to energy dissipation.

In this chapter, following the sequence of presentation adopted by Simo and Hughes (1998), the one-dimensional small-strain plasticity problem is first considered in order to explain the concepts and solution procedure of the plasticity equations without delving into the details of the three-dimensional theory. The basic plasticity equations are first presented followed by the loading and unloading conditions, which are introduced in Section 2. In Section 3, the solution procedure for the plasticity equations is summarized including the *return mapping algorithm*. In Section 4, the general three-dimensional theory that includes both isotropic and kinematic hardening is summarized. This theory can be applied only in the case of small strains because the additive decomposition of the strain is used. In this case of small strains, there is no need to distinguish between different stress and strain measures. The concepts and solution procedures introduced for the small-strain plasticity can be generalized and used in more general plasticity formulations. In Section 5, the special case of the  $J_2$  flow theory, which is applicable to metal plasticity, is discussed. Both isotropic and kinematic hardenings are considered in developing this theory. In Section 6, a plasticity finite displacement formulation for hyperelastic materials based on the multiplicative decomposition of the matrix of position vector gradients is

presented. This formulation is specialized in Section 7 to obtain the  $J_2$  flow theory that can be used in the large displacement analysis of metals.

## 8.1 ONE-DIMENSIONAL PROBLEM

In order to develop the small deformation plasticity model, the following assumption of the *strain additive decomposition* is used:

$$\varepsilon = \varepsilon^e + \varepsilon^p \quad (8.1)$$

In this equation,  $\varepsilon$  is the total strain,  $\varepsilon^e$  is the elastic strain, and  $\varepsilon^p$  is the plastic strain. The stress  $\sigma$  can be written in terms of the total strain as

$$\sigma = E\varepsilon^e = E(\varepsilon - \varepsilon^p) \quad (8.2)$$

In this equation,  $E$  is the modulus of elasticity.

In the theory of plasticity, it is assumed that the plastic deformation occurs when the stress (alternatively strain in the strain space formulation) exceeds a certain limit defined by the *yield criterion* or the *yield condition*. In the case of *isotropic* and *kinematic hardening*, the yield condition for the one-dimensional problem can be written as

$$f(\sigma, q, \alpha) = |\sigma - q| - (\sigma_y + H_i \alpha) \leq 0 \quad (8.3)$$

In this equation,  $q$  is a parameter, called the *back stress*, that accounts for the kinematic hardening,  $\sigma_y$  is the *yield stress* or *flow stress*,  $H_i$  is the *isotropic plastic modulus* that accounts for the isotropic hardening, and  $\alpha$  is a nonnegative function of the amount of plastic flow (slip) called *internal isotropic hardening variable*. If  $H_i < 0$ , one has the case of strain-softening. The change in the yield strength as the result of the plastic deformation can be a function, for example, in the rate of plastic work or in the accumulated plastic strain  $\varepsilon^p$ . In the case of isotropic hardening only (no kinematic hardening),  $q = 0$ . If there is no hardening, then  $q = 0$  and  $H_i = 0$ , and one has the case of *perfect plasticity*. Note also that in the preceding equation, if  $H_i$  is constant, one has a linear isotropic hardening law because  $\sigma_y$  is replaced in the yield condition by  $\sigma_y + H_i \alpha$ .

In order to be able to determine the new plasticity variables  $\varepsilon^p$ ,  $q$ , and  $\alpha$ , additional relationships must be introduced. The evolution of the back stress can be defined by *Ziegler's rule* as

$$\dot{q} = H_k \dot{\varepsilon}^p \quad (8.4)$$

In this equation,  $H_k$  is called the *kinematic hardening modulus*. The internal hardening variable  $\alpha$  is assumed to be a function of the plastic flow. One can write the evolutionary equation for  $\alpha$  in the following form:

$$\dot{\alpha} = \gamma \quad (8.5)$$

where  $\gamma$  is called the *slip rate* or the *consistency parameter*. If  $\dot{\varepsilon}^p$  can be written as

$$\dot{\varepsilon}^p = \gamma \frac{\partial f}{\partial \sigma}, \quad (8.6)$$

one has the case of *associative plasticity* or *associative flow rule*. In this case, the back stress  $q$  can be written as

$$\dot{q} = H_k \dot{\epsilon}^p = \gamma H_k \text{sign}(\sigma - q) \quad (8.7)$$

Note that in the case of associative plasticity, the plastic flow is in a direction normal to the yield surface (see Equation 6).

The distinction between associative and nonassociative plasticity is important, particularly when three-dimensional models are considered. In the case of nonassociative plasticity, the restriction of defining the flow rule in terms of the yield function is relaxed by introducing a *plastic flow rule potential*  $Q$  such that

$$Q = Q(\sigma, q, \alpha) \quad (8.8)$$

In this more general case of nonassociative plasticity,  $\dot{\epsilon}^p$  can be written as

$$\dot{\epsilon}^p = \gamma \frac{\partial Q}{\partial \sigma} \quad (8.9)$$

Therefore, the plastic-strain-rate components in the case of nonassociative plasticity are not required to be normal to the yield surface. The definitions of associative and nonassociative plasticity are not limited to the one-dimensional theory but can also be generalized to include three-dimensional plasticity problems.

The analysis presented in this section shows that, in addition to the constitutive equation (Equation 2), several other relationships must be introduced in order to be able to determine the new variables that enter into the formulation of the plasticity equations. In Section 3, the procedure for determining the stress  $\sigma$ , the back stress  $q$ , the plastic strain  $\epsilon^p$ , and the isotropic hardening internal variable  $\alpha$  will be discussed.

## 8.2 LOADING AND UNLOADING CONDITIONS

In this section, the conditions that can be used to define the state of deformation or the change between the elastic and plastic states are discussed. In the plasticity theory, it is assumed that  $\gamma$  is greater than or equal to zero, and  $f(\sigma, q, \alpha)$  is less than or equal to zero. That is,  $\gamma \geq 0$ , and  $f(\sigma, q, \alpha) \leq 0$ . These conditions imply that a plastic deformation occurs only when  $f(\sigma, q, \alpha) = 0$ . If  $f(\sigma, q, \alpha) < 0$ , the deformation is elastic. It follows that one has the following *Kuhn–Tucker complementarity condition*:

$$\gamma f(\sigma, q, \alpha) = 0 \quad (8.10)$$

This equation shows that if  $\gamma > 0$  (plastic deformation),  $f(\sigma, q, \alpha) = 0$  and  $f(\sigma, q, \alpha) \leq 0$  in order to avoid having  $f(\sigma, q, \alpha) > 0$ . Therefore, one must also have the following *consistency* or *persistency condition* (Simo and Hughes, 1998):

$$\gamma \dot{f}(\sigma, q, \alpha) = 0 \quad (8.11)$$

This consistency condition can be used to determine the consistency parameter  $\gamma$ , as will be demonstrated in the following section.

In the case of plasticity, there are different loading and unloading mechanisms that depend on the state of deformation, whether it is elastic or plastic. One can then summarize the possible loading and unloading scenarios as follows:

1. *Elastic Deformation*: In this case, one has an elastic state. That is,  $f(\sigma, q, \alpha) < 0$ ,  $\gamma = 0$ .
2. *Elastic Loading*: This is the case in which the plastic state is changing to an elastic state. In this case, one has  $f(\sigma, q, \alpha) = 0$ ,  $\gamma = 0$ , and  $\dot{f}(\sigma, q, \alpha) < 0$ .
3. *Plastic Loading*: In this case, one has a plastic state. That is,  $f(\sigma, q, \alpha) = 0$ ,  $\gamma > 0$ , and  $\dot{f}(\sigma, q, \alpha) = 0$ .
4. *Neutral Loading*: In this case,  $f(\sigma, q, \alpha) = 0$ ,  $\gamma = 0$ , and  $\dot{f}(\sigma, q, \alpha) = 0$ .

These loading and unloading scenarios must be considered in the computational algorithms used to solve the plasticity equations. One must check the state of deformation, whether it is elastic or plastic, in order to be able to use the appropriate constitutive model. Depending on the loading conditions, the behavior of the material at a given point can change from elastic to plastic or vice versa. Examples of the computational algorithms and solution procedures used to solve the plasticity problems are presented in later sections of this chapter. It is important also to point out that the loading and unloading scenarios discussed in this section can also be applied to the more general case of three-dimensional plasticity problems.

### 8.3 SOLUTION OF THE PLASTICITY EQUATIONS

For a given material, it is assumed that  $\sigma_y$ ,  $H_i$ , and  $H_k$  are known. It is also assumed that at a given time-step, the total strain can be determined from the solution of the dynamic equilibrium equations, that is,  $\epsilon$  is known. The unknowns in the plasticity formulation are  $\sigma$ ,  $\epsilon^p$ ,  $q$ , and  $\alpha$ . One, however, has a number of equations that can be used to solve for these unknowns if the material exhibits plastic deformation at a given point. These are Equations 2 and 4–6. The consistency parameter  $\gamma$  can be determined from the consistency condition of Equation 11 as will be demonstrated in this section. Note that if  $\gamma$  can be determined,  $\dot{\epsilon}^p$ ,  $\dot{q}$ , and  $\dot{\alpha}$  can be determined and integrated to determine  $\epsilon^p$ ,  $q$ , and  $\alpha$ . In this case, one can evaluate the yield function  $f(\sigma, q, \alpha)$  and determine the state of deformation and the loading scenario.

The consistency parameter  $\gamma$ , as previously mentioned, can be determined from the consistency condition of Equation 11. This procedure can be demonstrated using the simple one-dimensional case of associative plasticity. Note that in the case of associative plasticity, if the yield function of Equation 3 is used, one has  $(\partial f / \partial \sigma) = \text{sign}(\sigma - q)$  and  $(\partial f / \partial q) = -\text{sign}(\sigma - q)$ . Based on the discussion presented in the preceding section, in the case of plastic deformation,  $\gamma > 0$  and  $\dot{f}(\sigma, q, \alpha) = 0$ . These conditions lead to

$$\begin{aligned}
 \dot{f} &= \frac{\partial f}{\partial \sigma} \dot{\sigma} + \frac{\partial f}{\partial q} \dot{q} + \frac{\partial f}{\partial \alpha} \dot{\alpha} \\
 &= \text{sign}(\sigma - q) \{ E(\dot{\epsilon} - \dot{\epsilon}^p) - \dot{q} \} - H_i \dot{\alpha} \\
 &= \text{sign}(\sigma - q) E \dot{\epsilon} - \gamma (E + (H_k + H_i)) = 0
 \end{aligned} \tag{8.12}$$



This equation can be used to define  $\gamma$  as

$$\gamma = \frac{\text{sign}(\sigma - q)E\dot{\epsilon}}{E + (H_k + H_i)} \quad (8.13)$$

Because in the case of *associative flow rule*,  $\dot{\epsilon}^p = \gamma \text{sign}(\sigma - q)$ , the stress in this special case can be written using Equation 2 as follows:

$$\begin{aligned} \dot{\sigma} &= E(\dot{\epsilon} - \dot{\epsilon}^p) = E\dot{\epsilon} - \frac{E^2\dot{\epsilon}}{E + (H_k + H_i)} \\ &= E \left( 1 - \frac{E}{E + (H_k + H_i)} \right) \dot{\epsilon} \\ &= \frac{E(H_k + H_i)}{E + (H_k + H_i)} \dot{\epsilon} = E^{ep} \dot{\epsilon} \end{aligned} \quad (8.14)$$

in which

$$E^{ep} = \frac{E(H_k + H_i)}{E + (H_k + H_i)} \quad (8.15)$$

is called the *elastoplastic tangent modulus*. This modulus defines the plasticity constitutive equation in its rate form. Note that the simple constant elastoplastic tangent modulus could be obtained in a closed form because of the use of the assumption of the associative flow rule. Because  $\epsilon$  and  $\dot{\epsilon}$  are assumed to be known, the preceding equations can be used to determine  $\dot{\sigma}$ , and  $\dot{\epsilon}^p$ , which can be used to determine  $\dot{q}$  and  $\dot{\alpha}$  using Equations 4 and 5, respectively.

## Numerical Solution

For the simple one-dimensional case of associative plasticity with constant hardening coefficients, one can obtain, as demonstrated in this section, a closed-form solution for the stress rate. In a more general case of nonlinear coefficients, one must resort to numerical techniques. The main idea underlying many of the solution procedures developed for the plasticity analysis is to use a simple numerical integration method to transform the differential equations to a set of nonlinear algebraic equations that can be solved using iterative methods such as the Newton–Raphson method. In this section, the use of the numerical procedure is demonstrated using the simple one-dimensional model introduced in this chapter.

Recall that  $\dot{\alpha} = \gamma$ , and if the strain  $\epsilon$  and its rate  $\dot{\epsilon}$  are known, then one has the following plasticity equations:

$$\left. \begin{aligned} \dot{\sigma} + E\dot{\epsilon}^p &= E\dot{\epsilon} \\ \dot{q} - H_k\dot{\epsilon}^p &= 0 \\ \dot{\epsilon}^p - \dot{\alpha}f_\sigma &= 0 \\ \dot{f} &= f_\sigma\dot{\sigma} + f_q\dot{q} + f_\alpha\dot{\alpha} = 0 \end{aligned} \right\} \quad (8.16a)$$

In this equation, a subscript  $a$  is used to indicate partial differentiation with respect to  $a$ . Given  $\dot{\epsilon}$ , Equation 16a can be considered as a system of four first-order differential equations in the four unknown  $\sigma$ ,  $\epsilon^p$ ,  $q$ , and  $\alpha$ . This system can be written in the following matrix form:

$$\begin{bmatrix} 1 & E & 0 & 0 \\ 0 & -H_k & 1 & 0 \\ 0 & 1 & 0 & f_\sigma \\ f_\sigma & 0 & f_q & f_\alpha \end{bmatrix} \begin{bmatrix} \dot{\sigma} \\ \dot{\epsilon}^p \\ \dot{q} \\ \dot{\alpha} \end{bmatrix} = \begin{bmatrix} E\dot{\epsilon} \\ 0 \\ 0 \\ 0 \end{bmatrix} \quad (8.16b)$$

This system of differential equations can be solved using standard explicit or implicit numerical integration methods. In practical applications, it was found that explicit integration methods do not always lead to an accurate solution. For this reason, implicit integration methods are often used to solve the resulting plasticity first-order differential equations. When implicit methods are used, one converts the first-order differential equations to a system of nonlinear algebraic equations, which can be solved using an iterative Newton–Raphson algorithm. Several integration methods such as the trapezoidal rule or the implicit Euler methods can be used to obtain the nonlinear algebraic equations.

In order to demonstrate the procedure of converting the first-order differential equations to a set of nonlinear algebraic equations, the *backward implicit Euler* method can be used as an example. In the backward implicit Euler integration method, an unknown variable  $x$  is approximated using the following recurrence formula:

$$x_{n+1} = x_n + \Delta t g(x_{n+1}) = x_n + \Delta x, \quad \dot{x} = g(x) \quad (8.17)$$

In this equation,  $x_n$  is the known value of  $x$  at the beginning of the integration step,  $x_{n+1}$  is the unknown value of  $x$  at the end of the time-step,  $g = \dot{x} = dx/dt$ ,  $t$  is time, and  $\Delta t$  is the time-step. The preceding formula is called implicit because  $x_{n+1}$  appears in the right-hand side of the equation. If the function  $g$  is determined using  $x_n$  instead of  $x_{n+1}$ , one obtains an explicit formula that leads to a linear system of algebraic equations. It can be shown that if the implicit formula of Equation 17 is used to approximate the unknowns in Equation 16, one obtains a nonlinear system of algebraic equations that can be solved iteratively using a Newton–Raphson algorithm. This can be seen by evaluating  $\dot{x}$  using  $x_{n+1}$  and the governing plasticity equation. One can then substitute  $\dot{x}$  into Equation 17, leading to a nonlinear equation in  $x_{n+1}$ . This equation can be iteratively solved to determine  $x_{n+1}$  and advance the integration. For example, Equation 16b can be written as  $\mathbf{C}_c \dot{\mathbf{p}} = \boldsymbol{\epsilon}_R$ , where  $\mathbf{C}_c$  is the coefficient matrix,  $\mathbf{p} = [\sigma \quad \epsilon^p \quad q \quad \alpha]^T$  and  $\boldsymbol{\epsilon}_R = [E\dot{\epsilon} \quad 0 \quad 0 \quad 0]^T$ . Using Equation 17, one can then write  $\mathbf{p}_{n+1} = \mathbf{p}_n + \dot{\mathbf{p}}(\mathbf{p}_{n+1})\Delta t$  or  $\mathbf{p}_{n+1} = \mathbf{p}_n + (\mathbf{C}_c^{-1} \boldsymbol{\epsilon}_R)\Delta t$ . This procedure transforms the first-order differential equations to a set of nonlinear algebraic equations. If the yield function  $f$  and/or the hardening coefficients are nonlinear functions of the unknown variables, the equation  $\mathbf{p}_{n+1} = \mathbf{p}_n + (\mathbf{C}_c^{-1} \boldsymbol{\epsilon}_R)\Delta t$  must be solved iteratively using a Newton–Raphson algorithm in order to determine  $\mathbf{p}_{n+1}$ .

The integration procedure described in this section is general and can be applied to three-dimensional plasticity problems. In the case of one-dimensional plasticity problems or in the case of some special three-dimensional plasticity formulations, there are special features that can be exploited in order to obtain an efficient solution of the plasticity equations.

In the remainder of this section, it is demonstrated, using the one-dimensional problem, how one can take advantage of the special structure of some of the plasticity formulations.

### Plasticity Equations

There are special features of the plasticity equations that can be exploited in the process of the numerical integration. In order to discuss these special features, which can be used to avoid the iterative procedure and obtain an efficient solution, we use the backward implicit Euler method as an example. Using the implicit formula of Equation 17, the first-order differential equations associated with  $\sigma$ ,  $\epsilon^p$ ,  $\alpha$ , and  $q$  can be written as follows:

$$\left. \begin{aligned} \sigma_{n+1} &= \sigma_n + E\Delta(\epsilon - \epsilon^p) \\ \epsilon_{n+1}^p &= \epsilon_n^p + \Delta\alpha f_\sigma \\ \alpha_{n+1} &= \alpha_n + \Delta\alpha \\ q_{n+1} &= q_n + \Delta\alpha H_k f_\sigma \end{aligned} \right\} \quad (8.18)$$

In this equation, it is assumed that  $\Delta\alpha = \dot{\alpha}_n \Delta t = \gamma_n \Delta t$  and  $\Delta\epsilon^p = \Delta\alpha f_\sigma$ . As previously mentioned, the preceding algebraic equations in their most general form can be solved numerically using an iterative Newton–Raphson algorithm. The solution of these equations defines  $\sigma_{n+1}$ ,  $\epsilon_{n+1}^p$ ,  $\alpha_{n+1}$ , and  $q_{n+1}$ . Alternatively, by using the *return mapping algorithm*, one can obtain a more efficient algorithm as compared to the algorithm based on the direct application of the iterative Newton–Raphson method.

In order to demonstrate the use of the return mapping algorithm, the stress at time  $t_{n+1}$  can also be written in a different form as

$$\begin{aligned} \sigma_{n+1} &= E(\epsilon_{n+1} - \epsilon_{n+1}^p) = E(\epsilon_{n+1} - \epsilon_n^p) - E(\epsilon_{n+1}^p - \epsilon_n^p) \\ &= E(\epsilon_{n+1} - \epsilon_n^p + \epsilon_n - \epsilon_n) - E(\epsilon_{n+1}^p - \epsilon_n^p) \\ &= E(\epsilon_n - \epsilon_n^p) + E(\epsilon_{n+1} - \epsilon_n - \epsilon_{n+1}^p + \epsilon_n^p) \\ &= \sigma_n + E\Delta\epsilon - E\Delta\alpha f_\sigma \end{aligned} \quad (8.19)$$

For the return mapping algorithm that will be discussed in this section, the preceding equation can be written in the following form:

$$\sigma_{n+1} = \sigma_{n+1}^{trial} - E\Delta\alpha f_\sigma \quad (8.20)$$

In this equation,

$$\sigma_{n+1}^{trial} = \sigma_n + E\Delta\epsilon \quad (8.21)$$

It is clear that  $\sigma_{n+1}^{trial}$  is an elastic update of the stress, which does not take into account the change in the strain due to the plastic deformation. Because  $\epsilon_{n+1}$  is assumed to be known,  $\sigma_{n+1}^{trial}$  can be evaluated. The elastic update  $\sigma_{n+1}^{trial}$  represents a departure away from the yield surface and is known as the *elastic predictor*. The term  $-E\Delta\alpha f_\sigma$ , known as the *plastic corrector*, returns the stress to the yield surface in the stress space formulations. The use of the implicit *backward*

*Euler method*, as previously mentioned, leads to a system of algebraic equations that can be solved for  $\sigma_{n+1}$ ,  $q_{n+1}$ ,  $\epsilon_{n+1}^p$ , and  $\gamma_{n+1}$ . For the one-dimensional simple system discussed in this chapter, the use of this method can lead to a closed-form set of algebraic equations that can be solved for the unknown parameters. To this end, two steps are used: in the first step, a trial solution is assumed, whereas in the second step, the *return mapping algorithm* is used. These two steps are discussed in the following paragraphs in more detail.

### Trial Step

The interest is to advance the integration from time  $t_n$  to  $t_{n+1}$  to determine the unknown plasticity variables  $\sigma_{n+1}$ ,  $q_{n+1}$ ,  $\epsilon_{n+1}^p$ , and  $\gamma_{n+1}$ . It is assumed that all the parameters and variables are known at time  $t_n$  and  $\epsilon_{n+1}$  is also known at time  $t_{n+1}$ . An iterative procedure for solving the resulting nonlinear algebraic equations that define the unknown plasticity variables at time  $t_{n+1}$  requires making an initial guess of the solution. In the return mapping algorithm, one can make an initial guess that leads to a closed-form solution without the need for using an iterative procedure as demonstrated by the analysis presented in this section. In some other cases, the use of such an initial guess significantly simplifies the numerical plasticity problem in many formulations.

In the return mapping algorithm, one can assume the following trial solution for the algebraic system of Equation 18:

$$\left. \begin{aligned} \sigma_{n+1}^{trial} &= E(\epsilon_{n+1} - \epsilon_n^p) = \sigma_n + E\Delta\epsilon \\ \epsilon_{n+1}^{p\, trial} &= \epsilon_n^p \\ \alpha_{n+1}^{trial} &= \alpha_n \\ q_{n+1}^{trial} &= q_n \end{aligned} \right\} \quad (8.22)$$

Associated with this trial solution, the yield function is defined as

$$f_{n+1}^{trial} = |\sigma_{n+1}^{trial} - q_n| - (\sigma_y + H_i \alpha_n) \quad (8.23)$$

The trial variables on the left-hand side of Equations 22 and 23 can be computed because they are expressed in terms of known variables. In order to determine the state of deformation whether it is elastic or plastic, the following condition can be used:

$$f_{n+1}^{trial} \begin{cases} \leq 0 & \text{elastic step, } \gamma = 0 \\ > 0 & \text{plastic step, } \gamma > 0 \end{cases} \quad (8.24)$$

If the step is plastic, one can apply the return mapping algorithm summarized as follows.

### The Return Mapping Algorithm

As previously pointed out, the algebraic equations used in the return mapping algorithm can be obtained from the continuum model by applying the implicit backward Euler difference

scheme. Using Equations 18 and 20, the yield function of Equation 3, and the assumption of associative plasticity of Equation 6, one obtains the following system of algebraic equations (Simo and Hughes, 1998):

$$\left. \begin{aligned} \sigma_{n+1} &= \sigma_{n+1}^{trial} - \Delta\alpha E \text{sign}(\sigma_{n+1} - q_{n+1}) \\ \epsilon_{n+1}^p &= \epsilon_n^p + \Delta\alpha \text{sign}(\sigma_{n+1} - q_{n+1}) \\ \alpha_{n+1} &= \alpha_n + \Delta\alpha \\ q_{n+1} &= q_n + \Delta\alpha H_k \text{sign}(\sigma_{n+1} - q_{n+1}) \\ f_{n+1} &= |\sigma_{n+1} - q_{n+1}| - (\sigma_y + H_i \alpha_{n+1}) = 0 \end{aligned} \right\} \quad (8.25)$$

It is important to note, in this simple one-dimensional problem, that all the unknowns in the preceding equation can be determined if  $\Delta\alpha$  and  $\text{sign}(\sigma_{n+1} - q_{n+1})$  are determined. The procedure for determining  $\Delta\alpha$  and  $\text{sign}(\sigma_{n+1} - q_{n+1})$  is described as follows.

Note that by subtracting the fourth equation from the first equation in Equation 25, one obtains

$$\xi_{n+1} = \sigma_{n+1} - q_{n+1} = (\sigma_{n+1}^{trial} - q_n) - \Delta\alpha(E + H_k) \text{sign}(\xi_{n+1}) \quad (8.26)$$

By using the definitions  $\xi_{n+1}^{trial} = \sigma_{n+1}^{trial} - q_n$ ,  $\xi_{n+1} = \text{sign}(\xi_{n+1})|\xi_{n+1}|$ ,  $\xi_{n+1}^{trial} = \text{sign}(\xi_{n+1}^{trial})|\xi_{n+1}^{trial}|$ , and rearranging the terms in the preceding equation, one obtains

$$\{|\xi_{n+1}| + \Delta\alpha(E + H_k)\} \text{sign}(\xi_{n+1}) = |\xi_{n+1}^{trial}| \text{sign}(\xi_{n+1}^{trial}) \quad (8.27)$$

Because  $\Delta\alpha = \gamma \Delta t > 0$  and  $(H_k + E) > 0$ , one concludes from the preceding equation that

$$\text{sign}(\xi_{n+1}) = \text{sign}(\xi_{n+1}^{trial}) \quad (8.28)$$

and

$$|\xi_{n+1}| + \Delta\alpha(E + H_k) = |\xi_{n+1}^{trial}| \quad (8.29)$$

Using the preceding equation and the third and fifth equations in Equation 25, the incremental variable  $\Delta\alpha > 0$  can be determined from the fifth equation of Equation 25 as follows:

$$\begin{aligned} f_{n+1} &= |\xi_{n+1}^{trial}| - (E + H_k)\Delta\alpha - (\sigma_y + H_i \alpha_{n+1}) \\ &= |\xi_{n+1}^{trial}| - (E + H_k)\Delta\alpha - (\sigma_y + H_i \alpha_n) - H_i(\alpha_{n+1} - \alpha_n) \\ &= f_{n+1}^{trial} - \Delta\alpha\{E + (H_i + H_k)\} = 0 \end{aligned} \quad (8.30)$$

In this equation,  $f_{n+1}^{trial} = |\xi_{n+1}^{trial}| - (\sigma_y + H_i \alpha_n)$ , which can be evaluated based on the information known from the previous step. The preceding equation then yields

$$\Delta\alpha = \frac{f_{n+1}^{trial}}{E + (H_i + H_k)} > 0 \quad (8.31)$$

Using Equations 29 and 31, all the unknowns in Equation 25,  $\sigma_{n+1}$ ,  $\epsilon_{n+1}^p$ ,  $\alpha_{n+1}$ , and  $q_{n+1}$ , can be determined. That is, the use of the return mapping algorithm in this simple case allows determining all the unknowns in a closed form.

For von Mises plasticity, the yield surface is circular, and as a result, the normal to the yield surface is radial. In this special case, the general return mapping algorithm reduces to the popular *radial return mapping algorithm*.

### Example 8.1

In the case of *isotropic hardening* (no kinematic hardening),  $q = 0$ . It follows that  $q_{n+1} = q_n = 0$ , and  $H_k = 0$ . In this special case of isotropic hardening only, the yield function can be written as

$$f = |\sigma| - (\sigma_y + H_i \alpha)$$

It is assumed that the material properties  $E$ ,  $\sigma_y$ , and  $H_i$  are known, and the values of the variables  $\epsilon_n$ ,  $\dot{\epsilon}_n$ ,  $\sigma_n$ ,  $\epsilon_n^p$ , and  $\alpha_n$  are known at time  $t_n$ . Furthermore, the total strain  $\epsilon_{n+1}$  is assumed to be known at time  $t_{n+1}$ . One can then choose a time-step  $\Delta t = t_{n+1} - t_n$  and write

$$\Delta \epsilon = \epsilon_{n+1} - \epsilon_n$$

The value of  $\sigma_{n+1}^{trial}$  can be calculated as follows.

$$\sigma_{n+1}^{trial} = E(\epsilon_n - \epsilon_n^p) + E\Delta \epsilon$$

Furthermore, because  $q_n = 0$ , one has

$$\xi_{n+1}^{trial} = \sigma_{n+1}^{trial} - q_n = \sigma_{n+1}^{trial}$$

It follows that  $f_{n+1}^{trial}$  is obtained from the equation

$$f_{n+1}^{trial} = |\xi_{n+1}^{trial}| - (\sigma_y + H_i \alpha_n) = |\sigma_{n+1}^{trial}| - (\sigma_y + H_i \alpha_n)$$

Substituting into Equation 31, one obtains

$$\Delta \alpha = \frac{f_{n+1}^{trial}}{E + H_i}$$

Because  $f_{n+1}^{trial}$  can be evaluated from the information available at time  $t_n$ , the preceding equation can be used to determine  $\Delta \alpha$ . One can also show that

$$\text{sign}(\xi_{n+1}) = \text{sign}(\xi_{n+1}^{trial}) = \text{sign}(\sigma_{n+1}^{trial})$$

The preceding equations and Equation 25 can be used to determine the solution at time  $t_{n+1}$ , where  $t_{n+1} = t_n + \Delta t$ , as follows:

$$\sigma_{n+1} = \sigma_{n+1}^{trial} - \Delta \alpha E \text{sign}(\xi_{n+1}^{trial})$$

$$\begin{aligned}\epsilon_{n+1}^p &= \epsilon_n^p + \Delta\alpha \operatorname{sign}(\xi_{n+1}^{trial}) \\ \alpha_{n+1} &= \alpha_n + \Delta\alpha\end{aligned}$$

Because  $\operatorname{sign}(\xi_{n+1}^{trial})$  is known since it can be evaluated based on the continuum state at time  $t_n$ , the preceding three equations can be used to determine  $\sigma_{n+1}$ ,  $\epsilon_{n+1}^p$ , and  $\alpha_{n+1}$ .

### Example 8.2

In the case of *perfect plasticity*, there is no hardening. In this case, one can use the same procedure as the one used in Example 1 and set the value of  $H_i$  to be zero. In this case, the yield function can be written as

$$f = |\sigma| - \sigma_y$$

In the case of perfect associative plasticity, one then has the following four equations:

$$\begin{aligned}\dot{\sigma} &= E(\dot{\epsilon} - \dot{\epsilon}^p), \quad \dot{\epsilon}^p = \gamma f_{\sigma}, \\ \dot{\alpha} &= \gamma, \quad f = |\sigma| - \sigma_y\end{aligned}$$

Using the constitutive equation, one can write

$$\dot{\sigma} = E(\dot{\epsilon} - \dot{\epsilon}^p) = E(\dot{\epsilon} - \gamma f_{\sigma}) = E(\dot{\epsilon} - \gamma \operatorname{sign}(\sigma))$$

In this case, one has

$$\sigma_{n+1}^{trial} = \sigma_n + E\Delta\epsilon$$

Using the preceding two equations, one has

$$\sigma_{n+1} = \sigma_{n+1}^{trial} - \Delta\alpha E \operatorname{sign}(\sigma_{n+1})$$

In this equation,  $\Delta\alpha = \gamma \Delta t$ . The preceding equation can be written as

$$(|\sigma_{n+1}| + \Delta\alpha E) \operatorname{sign}(\sigma_{n+1}) = |\sigma_{n+1}^{trial}| \operatorname{sign}(\sigma_{n+1}^{trial})$$

which leads to the following two identities

$$\begin{aligned}\operatorname{sign}(\sigma_{n+1}) &= \operatorname{sign}(\sigma_{n+1}^{trial}) \\ |\sigma_{n+1}| + \Delta\alpha E &= |\sigma_{n+1}^{trial}|\end{aligned}$$

Using a procedure similar to the one used to obtain Equation 31, one can show that

$$\Delta\alpha = \frac{f_{n+1}^{trial}}{E}$$

where in this case

$$f_{n+1}^{trial} = |\sigma_{n+1}^{trial}| - \sigma_y = |\sigma_n + E\Delta\epsilon| - \sigma_y$$

The new state at time  $t_{n+1}$  can be obtained by using Equation 25 as follows:

$$\begin{aligned}\sigma_{n+1} &= \sigma_{n+1}^{trial} - \Delta\alpha E \operatorname{sign}(\xi_{n+1}) \\ \epsilon_{n+1}^p &= \epsilon_n^p + \Delta\alpha \operatorname{sign}(\xi_{n+1}) \\ \alpha_{n+1} &= \alpha_n + \Delta\alpha\end{aligned}$$

## 8.4 GENERALIZATION OF THE PLASTICITY THEORY: SMALL STRAINS

The one-dimensional plasticity theory presented in the preceding sections can be generalized and used in the three-dimensional analysis (Simo and Hughes, 1998). To this end, the same notation previously used will be used in this section, except bold letters are used to denote vectors, matrices, and tensors that replace the scalar variables used in the one-dimensional theory. Because in this section, the additive decomposition of the strain rate is used, strains are assumed small and there is no distinction made between different stress measures. For this reason, Cauchy stress tensor is used in this section with the Green–Lagrange strain tensor. Furthermore, the objectivity requirement is not an issue in the small-strain formulation. The formulation presented in this section can be used with hypoelastic material models and does not require that the stress–strain relationships are obtained from a potential function as in the case of hyperelastic material models.

The stress–strain relationship can be written as

$$\boldsymbol{\sigma} = \mathbf{E} : \boldsymbol{\epsilon}^e = \mathbf{E} : (\boldsymbol{\epsilon} - \boldsymbol{\epsilon}^p) \quad (8.32)$$

In this equation,  $\mathbf{E}$  is the fourth-order tensor of elastic coefficients,  $\boldsymbol{\sigma}$  is the second-order stress tensor,  $\boldsymbol{\epsilon}$  is the second-order total strain tensor,  $\boldsymbol{\epsilon}^e$  is the second-order tensor of elastic strains, and  $\boldsymbol{\epsilon}^p$  is the second-order tensor of plastic strains. The elastic domain is defined by

$$f(\boldsymbol{\sigma}, \mathbf{q}) \leq 0 \quad (8.33)$$

where  $\mathbf{q}$  is the vector of the internal variables that depend on the plastic strains and a set of hardening parameters  $\boldsymbol{\alpha}$ . These internal variables account in this case for both the kinematic and isotropic hardening. The general *nonassociative model flow rule* and *hardening law* are defined as

$$\left. \begin{aligned} \dot{\boldsymbol{\epsilon}}^p &= \gamma \mathbf{g}(\boldsymbol{\sigma}, \mathbf{q}) \\ \dot{\mathbf{q}} &= -\gamma \mathbf{h}(\boldsymbol{\sigma}, \mathbf{q}) \end{aligned} \right\} \quad (8.34)$$

where  $\mathbf{g}$  and  $\mathbf{h}$  are prescribed second-order tensor functions of  $\boldsymbol{\sigma}$  and  $\mathbf{q}$ , and  $\gamma$  is the consistency parameter.

Based on the analysis used in the case of the one-dimensional model, the *Kuhn–Tucker loading and unloading complementarity condition* for the more general three-dimensional case can be written as

$$\gamma \geq 0, \quad f(\boldsymbol{\sigma}, \mathbf{q}) \leq 0, \quad \gamma f(\boldsymbol{\sigma}, \mathbf{q}) = 0 \quad (8.35)$$



The *consistency condition* is

$$\gamma \dot{f}(\boldsymbol{\sigma}, \mathbf{q}) = 0 \quad (8.36)$$

This consistency condition,  $\dot{f} = 0$ , can be used to determine the consistency parameter. This condition defines  $\gamma$ , as shown in the following example, as

$$\gamma = \frac{f_{\boldsymbol{\sigma}} : \mathbf{E} : \dot{\boldsymbol{\varepsilon}}}{f_{\boldsymbol{\sigma}} : \mathbf{E} : \mathbf{g} + f_{\mathbf{q}} : \mathbf{h}} \quad (8.37)$$

In this equation,  $f_{\boldsymbol{\sigma}}$  and  $f_{\mathbf{q}}$  are second-order tensors that result from the differentiation of the yield function  $\dot{f}$  with respect to  $\boldsymbol{\sigma}$  and  $\mathbf{q}$ , respectively. It is assumed that the denominator in the preceding equation is always greater than zero, an assumption that always holds for associative plasticity.

Because of the assumption of small deformation, the stress rate can be written as

$$\dot{\boldsymbol{\sigma}} = \mathbf{E} : (\dot{\boldsymbol{\varepsilon}} - \dot{\boldsymbol{\varepsilon}}^p) = \mathbf{E} : (\dot{\boldsymbol{\varepsilon}} - \gamma \mathbf{g}) \quad (8.38)$$

Substituting Equation 37 into this equation, one obtains

$$\dot{\boldsymbol{\sigma}} = \mathbf{E}^{ep} : \dot{\boldsymbol{\varepsilon}} \quad (8.39)$$

where  $\mathbf{E}^{ep}$  is the tensor of *tangent elastoplastic moduli* given by

$$\mathbf{E}^{ep} = \begin{cases} \mathbf{E} & \gamma = 0 \\ \mathbf{E} - \frac{(\mathbf{E} : \mathbf{g}) \otimes (f_{\boldsymbol{\sigma}} : \mathbf{E})}{f_{\boldsymbol{\sigma}} : \mathbf{E} : \mathbf{g} + f_{\mathbf{q}} : \mathbf{h}} & \gamma > 0 \end{cases} \quad (8.40)$$

Note the incremental nature of the plasticity formulation because of the rate form of Equation 39. Note also that in the general case of nonassociative plasticity, the tangent elastoplastic moduli tensor is not necessarily symmetric. In the actual implementation, if there is no need to evaluate the tensor of Equation 40, one can simply determine the stress rate by substituting the scalar  $\gamma$  of Equation 37 into Equation 38. In this case, the use of the tensor multiplication given in Equation 40 can be avoided.

### Example 8.3

In order to prove Equations 37 and 40, one can differentiate the yield function with respect to time to obtain

$$\dot{f} = f_{\boldsymbol{\sigma}} : \dot{\boldsymbol{\sigma}} + f_{\mathbf{q}} : \dot{\mathbf{q}} = 0$$

The constitutive equation is given by

$$\boldsymbol{\sigma} = \mathbf{E} : (\boldsymbol{\varepsilon} - \boldsymbol{\varepsilon}^p)$$

This equation can be written in the rate form as

$$\dot{\boldsymbol{\sigma}} = \mathbf{E} : \dot{\boldsymbol{\varepsilon}} - \mathbf{E} : \dot{\boldsymbol{\varepsilon}}^p = \mathbf{E} : \dot{\boldsymbol{\varepsilon}} - \gamma \mathbf{E} : \mathbf{g}$$

The differential equation for the hardening variables is given by

$$\dot{\mathbf{q}} = -\gamma \mathbf{h}$$

By substituting for  $\dot{\boldsymbol{\sigma}}$  and  $\dot{\mathbf{q}}$  in  $\dot{f}$ , one obtains

$$f_{\boldsymbol{\sigma}} : \mathbf{E} : \dot{\boldsymbol{\varepsilon}} - \gamma f_{\boldsymbol{\sigma}} : \mathbf{E} : \mathbf{g} - \gamma f_{\mathbf{q}} : \mathbf{h} = 0$$

or

$$f_{\boldsymbol{\sigma}} : \mathbf{E} : \dot{\boldsymbol{\varepsilon}} = \gamma (f_{\boldsymbol{\sigma}} : \mathbf{E} : \mathbf{g} + f_{\mathbf{q}} : \mathbf{h})$$

This equation defines the consistency parameter of Equation 37 as

$$\gamma = \frac{f_{\boldsymbol{\sigma}} : \mathbf{E} : \dot{\boldsymbol{\varepsilon}}}{f_{\boldsymbol{\sigma}} : \mathbf{E} : \mathbf{g} + f_{\mathbf{q}} : \mathbf{h}}$$

Substituting the expression for  $\gamma$  into the constitutive equation in its rate form  $\dot{\boldsymbol{\sigma}} = \mathbf{E} : \dot{\boldsymbol{\varepsilon}} - \gamma \mathbf{E} : \mathbf{g}$ , one obtains  $\dot{\boldsymbol{\sigma}} = \mathbf{E} : \dot{\boldsymbol{\varepsilon}} = \mathbf{E}^{ep} : \dot{\boldsymbol{\varepsilon}}$  if  $\gamma > 0$ . That is,  $\mathbf{E}^{ep} = \mathbf{E}$ . If  $\gamma < 0$ , one has

$$\dot{\boldsymbol{\sigma}} = \mathbf{E} : \dot{\boldsymbol{\varepsilon}} - \left( \frac{f_{\boldsymbol{\sigma}} : \mathbf{E} : \dot{\boldsymbol{\varepsilon}}}{f_{\boldsymbol{\sigma}} : \mathbf{E} : \mathbf{g} + f_{\mathbf{q}} : \mathbf{h}} \right) \mathbf{E} : \mathbf{g}$$

The components of this tensor can be written as

$$\dot{\sigma}_{ij} = \sum_{k,l=1}^3 \varepsilon_{ijkl} \dot{\varepsilon}_{kl} - \sum_{\substack{k,l,w, \\ x,u,v=1}}^3 \frac{(f_{\boldsymbol{\sigma}})_{wx} e_{wxkl} \dot{\varepsilon}_{kl}}{f_{\boldsymbol{\sigma}} : \mathbf{E} : \mathbf{g} + f_{\mathbf{q}} : \mathbf{h}} e_{ijuv} g_{uv}$$

This equation can be written as

$$\dot{\sigma}_{ij} = \sum_{k,l=1}^3 \left( e_{ijkl} - \frac{\left( \sum_{u,v=1}^3 e_{ijuv} g_{uv} \right) \left( \sum_{w,x=1}^3 (f_{\boldsymbol{\sigma}})_{wx} e_{wxkl} \right)}{f_{\boldsymbol{\sigma}} : \mathbf{E} : \mathbf{g} + f_{\mathbf{q}} : \mathbf{h}} \right) \dot{\varepsilon}_{kl}$$

which defines  $\dot{\boldsymbol{\sigma}}$  as

$$\dot{\boldsymbol{\sigma}} = \left( \mathbf{E} - \frac{(\mathbf{E} : \mathbf{g}) \otimes (f_{\boldsymbol{\sigma}} : \mathbf{E})}{f_{\boldsymbol{\sigma}} : \mathbf{E} : \mathbf{g} + f_{\mathbf{q}} : \mathbf{h}} \right) \dot{\boldsymbol{\varepsilon}} = \mathbf{E}^{ep} : \dot{\boldsymbol{\varepsilon}}$$

where

$$\mathbf{E}^{ep} = \left( \mathbf{E} - \frac{(\mathbf{E} : \mathbf{g}) \otimes (f_{\boldsymbol{\sigma}} : \mathbf{E})}{f_{\boldsymbol{\sigma}} : \mathbf{E} : \mathbf{g} + f_{\mathbf{q}} : \mathbf{h}} \right)$$

### Associative Plasticity

In the special case of associative plasticity, one has the following assumptions:

$$\dot{\epsilon}^p = \gamma \frac{\partial f}{\partial \boldsymbol{\sigma}}, \quad \dot{\mathbf{q}} = -\gamma \mathbf{D}_p \frac{\partial f}{\partial \mathbf{q}} \quad (8.41)$$

where in this equation  $\mathbf{D}_p$  is the matrix of generalized plastic moduli. The preceding equation implies that  $\mathbf{g} = \partial f / \partial \boldsymbol{\sigma}$  and the plastic flow is in the direction of the normal to the yield surface. Using the assumptions of associative plasticity, it can be shown that the denominator in the right-hand side of Equation 37 that also appears in Equation 40 is greater than zero, as previously mentioned. It is also clear from Equation 40 that in the case of associative plasticity, the tangent elastoplastic moduli tensor is symmetric.

#### Example 8.4

One can show that in the case of associative plasticity, the tensor of the tangent elastoplastic moduli is symmetric. To this end, the following result obtained in the preceding example is used:

$$\mathbf{E}^{ep} = \left( \mathbf{E} - \frac{(\mathbf{E} : \mathbf{g}) \otimes (f_{\boldsymbol{\sigma}} : \mathbf{E})}{f_{\boldsymbol{\sigma}} : \mathbf{E} : \mathbf{g} + f_{\mathbf{q}} : \mathbf{h}} \right)$$

In order to prove the symmetry of  $\mathbf{E}^{ep}$  in the case of associative plasticity, recall that in this special case,  $\mathbf{g} = f_{\boldsymbol{\sigma}}$  and  $\mathbf{h} = \mathbf{D}_p f_{\mathbf{q}}$ . It follows upon substituting into  $\mathbf{E}^{ep}$  that

$$\mathbf{E}^{ep} = \left( \mathbf{E} - \frac{(\mathbf{E} : f_{\boldsymbol{\sigma}}) \otimes (f_{\boldsymbol{\sigma}} : \mathbf{E})}{f_{\boldsymbol{\sigma}} : \mathbf{E} : f_{\boldsymbol{\sigma}} + f_{\mathbf{q}} : (\mathbf{D}_p f_{\mathbf{q}})} \right)$$

The components of this fourth-order tensor can be written as

$$e_{ijkl}^{ep} = \left( e_{ijkl} - \frac{\left( \sum_{u,v=1}^3 e_{ijuv} (f_{\boldsymbol{\sigma}})_{uv} \right) \left( \sum_{w,x=1}^3 (f_{\boldsymbol{\sigma}})_{wx} e_{wxkl} \right)}{f_{\boldsymbol{\sigma}} : \mathbf{E} : f_{\boldsymbol{\sigma}} + f_{\mathbf{q}} : (\mathbf{D}_p f_{\mathbf{q}})} \right)$$

Because  $\mathbf{E}$  is symmetric, one has  $e_{ijkl} = e_{jikl} = e_{ijlk}$ , and as a consequence, one has

$$\begin{aligned} e_{jikl}^{ep} &= \left( e_{jikl} - \frac{\left( \sum_{u,v=1}^3 e_{jiuv} (f_{\boldsymbol{\sigma}})_{uv} \right) \left( \sum_{w,x=1}^3 (f_{\boldsymbol{\sigma}})_{wx} e_{wxkl} \right)}{f_{\boldsymbol{\sigma}} : \mathbf{E} : f_{\boldsymbol{\sigma}} + f_{\mathbf{q}} : (\mathbf{D}_p f_{\mathbf{q}})} \right) \\ &= \left( e_{ijkl} - \frac{\left( \sum_{u,v=1}^3 e_{ijuv} (f_{\boldsymbol{\sigma}})_{uv} \right) \left( \sum_{w,x=1}^3 (f_{\boldsymbol{\sigma}})_{wx} e_{wxkl} \right)}{f_{\boldsymbol{\sigma}} : \mathbf{E} : f_{\boldsymbol{\sigma}} + f_{\mathbf{q}} : (\mathbf{D}_p f_{\mathbf{q}})} \right) = e_{ijkl}^{ep} \end{aligned}$$

A similar relationship can be obtained by interchanging  $k$  and  $l$ . From the symmetry properties one also has  $e_{ijkl}^{ep} = e_{klij}^{ep}$  because

$$e_{klij}^{ep} = \left( e_{klij} - \frac{\left( \sum_{u,v=1}^3 e_{kluv}(f_{\sigma})_{uv} \right) \left( \sum_{w,x=1}^3 (f_{\sigma})_{wx} e_{wxij} \right)}{f_{\sigma} : \mathbf{E} : f_{\sigma} + f_{\mathbf{q}} : (\mathbf{D}_p f_{\mathbf{q}})} \right) \\ = \left( e_{ijkl} - \frac{\left( \sum_{u,v=1}^3 e_{uvkl}(f_{\sigma})_{uv} \right) \left( \sum_{w,x=1}^3 (f_{\sigma})_{wx} e_{ijwx} \right)}{f_{\sigma} : \mathbf{E} : f_{\sigma} + f_{\mathbf{q}} : (\mathbf{D}_p f_{\mathbf{q}})} \right) = e_{ijkl}^{ep}$$

### Numerical Solution of the Plasticity Equations

In the remainder of this section, the procedure used to solve the nonassociative plasticity equations presented in this section is described. The numerical procedure for integrating the plasticity equations is called the *constitutive integration algorithm* or the *stress update algorithm*. A class of solution algorithms that are widely used in the solution of the plasticity equations is the *return mapping* algorithms that are discussed in this section. It is, however, important to point out that in the case of the large-deformation plasticity formulations discussed in later sections of this chapter, the objectivity requirements need to be satisfied by the rate constitutive equations.

For nonassociative plasticity, the equations for small-strain elastoplasticity can be summarized as follows:

$$\left. \begin{aligned} \dot{\boldsymbol{\sigma}} &= \mathbf{E} : \dot{\boldsymbol{\varepsilon}}^e = \mathbf{E} : (\dot{\boldsymbol{\varepsilon}} - \dot{\boldsymbol{\varepsilon}}^p) \\ \dot{\boldsymbol{\varepsilon}}^p &= \gamma \mathbf{g}(\boldsymbol{\sigma}, \mathbf{q}) \\ \dot{\mathbf{q}} &= -\gamma \mathbf{h}(\boldsymbol{\sigma}, \mathbf{q}) \\ \dot{f} &= f_{\sigma} : \dot{\boldsymbol{\sigma}} + f_{\mathbf{q}} : \dot{\mathbf{q}} = 0 \\ \gamma &\geq 0, \quad f(\boldsymbol{\sigma}, \mathbf{q}) \leq 0, \quad \gamma f(\boldsymbol{\sigma}, \mathbf{q}) = 0 \end{aligned} \right\} \quad (8.42)$$

Assume that at time  $t_n$ ,  $\boldsymbol{\sigma}_n$ ,  $\boldsymbol{\varepsilon}_n$ ,  $\boldsymbol{\varepsilon}_n^p$ , and  $\mathbf{q}_n$  are known, where subscript  $n$  refers to the time-step. The goal is to use the preceding equations to determine the states of stresses and strains at time  $t_{n+1}$  that satisfy the loading and unloading conditions. From the solution of the dynamic equations,  $\boldsymbol{\varepsilon}_{n+1}$  and  $\Delta \boldsymbol{\varepsilon} = \boldsymbol{\varepsilon}_{n+1} - \boldsymbol{\varepsilon}_n$  are known.

### Explicit Solution

Let the plasticity parameter  $\gamma = \dot{\alpha}$ , with  $\Delta \alpha = \gamma \Delta t$ . It was shown previously that the use of the consistency condition leads to (Equation 37)

$$\gamma = \dot{\alpha} = \frac{f_{\sigma} : \mathbf{E} : \dot{\boldsymbol{\varepsilon}}}{f_{\sigma} : \mathbf{E} : \mathbf{g} + f_{\mathbf{q}} : \mathbf{h}} \quad (8.43)$$

One may consider, as it was the case in some of the early work on computational plasticity, to use this value of the plasticity parameter to update the plastic strains, internal variables, and stresses using a simple explicit one-step Euler method as follows:

$$\left. \begin{aligned} \boldsymbol{\varepsilon}_{n+1}^p &= \boldsymbol{\varepsilon}_n^p + \Delta\alpha \mathbf{g}_n \\ \mathbf{q}_{n+1} &= \mathbf{q}_n - \Delta\alpha \mathbf{h}_n \\ \boldsymbol{\sigma}_{n+1} &= \mathbf{E} : (\boldsymbol{\varepsilon}_{n+1} - \boldsymbol{\varepsilon}_{n+1}^p) = \boldsymbol{\sigma}_n + \mathbf{E}^{ep} : \Delta\boldsymbol{\varepsilon} \end{aligned} \right\} \quad (8.44)$$

There is no guarantee, however, that this explicit updating scheme, sometimes referred to as *tangent modulus update scheme*, will satisfy the yield condition. Therefore, the use of the explicit scheme as defined by Equation 44 is not recommended. Instead, one can use the implicit method described in the following paragraph to obtain a more accurate solution.

### Implicit Solution

Using an implicit integration method, the first four equations in Equation 42 can be converted to a set of nonlinear algebraic equations. These algebraic equations, in principle, can be solved iteratively using a Newton–Raphson algorithm, as in the one-dimensional case, to determine  $\boldsymbol{\sigma}$ ,  $\boldsymbol{\varepsilon}^p$ ,  $\mathbf{q}$ , and  $\gamma$ . Nonetheless, one can try to take advantage of the structure of the plasticity equations in order to develop an effective and more efficient algorithm for the three-dimensional plasticity problems. In order to ensure that the yield condition is satisfied, the return mapping algorithms are used. In the return mapping algorithms, as in the case of the one-dimensional model, an initial *elastic predictor step* that may give a solution away from the yield surface is first used. A *plastic corrector step* is then used to bring the solution to the updated yield surface. In the return mapping algorithms, as previously mentioned, a simple numerical integration method such as the trapezoidal rule, Runge–Kutta method, or the midpoint method is first used to transform the plasticity differential equations into a set of nonlinear algebraic equations that can be solved using a Newton–Raphson algorithm to determine the stresses, strains, and internal variables at time  $t_{n+1}$ . For example, if the *fully implicit backward Euler method* is used as the numerical integrator, the equations are written in terms of variables defined at the end of the time-step. This leads to

$$\left. \begin{aligned} \boldsymbol{\varepsilon}_{n+1}^p &= \boldsymbol{\varepsilon}_n^p + \Delta\alpha \mathbf{g}_{n+1} \\ \mathbf{q}_{n+1} &= \mathbf{q}_n - \Delta\alpha \mathbf{h}_{n+1} \\ \boldsymbol{\sigma}_{n+1} &= \mathbf{E} : (\boldsymbol{\varepsilon}_{n+1} - \boldsymbol{\varepsilon}_{n+1}^p) \\ f_{n+1} &= f(\boldsymbol{\sigma}_{n+1}, \mathbf{q}_{n+1}) \end{aligned} \right\} \quad (8.45)$$

where again  $\gamma \Delta t = \Delta\alpha$ . One may choose to work directly with these four sets of equations, or eliminate some unknowns before starting the numerical procedure. For example, the plastic strains can be eliminated by using the constitutive equations. In this case, one can write the plastic strain tensor  $\boldsymbol{\varepsilon}_{n+1}^p$  in terms of the stress tensor  $\boldsymbol{\sigma}_{n+1}$  as

$$\boldsymbol{\varepsilon}_{n+1}^p = -(\mathbf{E}^{-1} : \boldsymbol{\sigma}_{n+1} - \boldsymbol{\varepsilon}_{n+1}) \quad (8.46)$$

This equation can be used to eliminate  $\epsilon_{n+1}^p$  from Equation 45 and obtain the following reduced system of nonlinear algebraic equations

$$\left. \begin{aligned} \mathbf{a}_1 &= \mathbf{E}_i : \boldsymbol{\sigma}_{n+1} - \boldsymbol{\epsilon}_{n+1} + \boldsymbol{\epsilon}_n^p + \Delta\alpha \mathbf{g}_{n+1} = \mathbf{0} \\ \mathbf{a}_2 &= -\mathbf{q}_{n+1} + \mathbf{q}_n - \Delta\alpha \mathbf{h}_{n+1} = \mathbf{0} \\ f_{n+1} &= f(\boldsymbol{\sigma}_{n+1}, \mathbf{q}_{n+1}) = 0 \end{aligned} \right\} \quad (8.47)$$

where  $\mathbf{E}_i$  is the fourth-order tensor used to write the strain components in terms of the stress components (inverse relationship). This system of nonlinear algebraic equations can be solved using the iterative Newton–Raphson method in order to determine  $\boldsymbol{\sigma}_{n+1}$ ,  $\mathbf{q}_{n+1}$ , and  $\Delta\alpha$ . This requires constructing and iteratively solving the following system:

$$\begin{bmatrix} \mathbf{E}_i + \Delta\alpha(\mathbf{g}_{n+1})_{\boldsymbol{\sigma}} & \Delta\alpha(\mathbf{g}_{n+1})_{\mathbf{q}} & \mathbf{g}_{n+1} \\ -\Delta\alpha(\mathbf{h}_{n+1})_{\boldsymbol{\sigma}} & -\mathbf{I} - \Delta\alpha(\mathbf{h}_{n+1})_{\mathbf{q}} & -\mathbf{h}_{n+1} \\ f_{\boldsymbol{\sigma}} & f_{\mathbf{q}} & 0 \end{bmatrix} \begin{bmatrix} \bar{\Delta}\boldsymbol{\sigma}_{n+1} \\ \bar{\Delta}\mathbf{q}_{n+1} \\ \bar{\Delta}(\Delta\alpha) \end{bmatrix} = \begin{bmatrix} -\mathbf{a}_1 \\ -\mathbf{a}_2 \\ -f_{n+1} \end{bmatrix} \quad (8.48)$$

In this equation,  $\bar{\Delta}$  is used to denote Newton differences. Note that the increment of the plastic strains can be written as

$$\Delta\epsilon^p = \epsilon_{n+1}^p - \epsilon_n^p = \Delta\alpha \mathbf{g}_{n+1} \quad (8.49)$$

which upon substituting into the stress equation yields

$$\begin{aligned} \boldsymbol{\sigma}_{n+1} &= \mathbf{E} : (\boldsymbol{\epsilon}_{n+1} - \epsilon_{n+1}^p) = \mathbf{E} : (\boldsymbol{\epsilon}_{n+1} - \epsilon_n^p - \Delta\epsilon^p) \\ &= \mathbf{E} : (\boldsymbol{\epsilon}_n + \Delta\boldsymbol{\epsilon} - \epsilon_n^p - \Delta\epsilon^p) = \mathbf{E} : (\boldsymbol{\epsilon}_n - \epsilon_n^p) + \mathbf{E} : \Delta\boldsymbol{\epsilon} - \mathbf{E} : \Delta\epsilon^p \\ &= (\boldsymbol{\sigma}_n + \mathbf{E} : \Delta\boldsymbol{\epsilon}) - \mathbf{E} : \Delta\epsilon^p \end{aligned} \quad (8.50)$$

The *trial stress* of the *elastic predictor step* is defined as

$$\boldsymbol{\sigma}_{n+1}^{\text{trial}} = \boldsymbol{\sigma}_n + \mathbf{E} : \Delta\boldsymbol{\epsilon} \quad (8.51)$$

which upon substituting into Equation 50, one obtains

$$\boldsymbol{\sigma}_{n+1} = \boldsymbol{\sigma}_{n+1}^{\text{trial}} - \mathbf{E} : \Delta\epsilon^p = \boldsymbol{\sigma}_{n+1}^{\text{trial}} - \Delta\alpha \mathbf{E} : \mathbf{g}_{n+1} \quad (8.52)$$

In this equation

$$(\Delta\boldsymbol{\sigma}_{n+1})_p = \Delta\alpha \mathbf{E} : \mathbf{g}_{n+1} = -\mathbf{E} : \Delta\epsilon^p \quad (8.53)$$

is the *plastic corrector* that brings the trial stress to the yield surface along a direction specified by the plastic flow direction. During the elastic predictor step, the plastic strains and the internal variables remain fixed, whereas during the plastic corrector step, the total strain is fixed (Belytschko et al., 2000). It follows from the preceding equation that

$$\Delta\epsilon^p = -\mathbf{E}_i : (\Delta\boldsymbol{\sigma})_p \quad (8.54)$$

In the solution procedure described in this section, the total strain is assumed to be fixed while the plasticity equations are solved for stresses, plastic strains, internal hardening variables, and consistency parameter. Consequently, the values of the elastic strains will depend on the values of the plastic strains obtained using the plasticity equations. The elastic strains can be determined using the strain additive decomposition as  $\boldsymbol{\varepsilon}^e = \boldsymbol{\varepsilon} - \boldsymbol{\varepsilon}^p$ . In the large deformation theory, this additive decomposition is not used. Before introducing the large deformation theory, a  $J_2$  flow theory based on the small-strain assumptions is first discussed.

## 8.5 $J_2$ FLOW THEORY WITH ISOTROPIC/KINEMATIC HARDENING

A special case of the small-strain three-dimensional formulation presented in the preceding sections is the  $J_2$  flow theory. This theory that is based on the von Mises yield surface is useful, particularly in the plasticity analysis of metals. The main assumption used in this theory is that the plastic flow is not affected by the hydrostatic pressure as was experimentally demonstrated (Bridgman, 1949). Using this assumption, the yield condition and the plastic flow are formulated in terms of the deviatoric stresses. The yield function in this case becomes a function of only the second invariant of the deviatoric stresses  $J_2$ .

In the  $J_2$  flow theory with isotropic and kinematic hardening, the set of *internal variables* ( $\alpha, \bar{\mathbf{q}}$ ) is introduced (Simo and Hughes, 1998). Here,  $\alpha$  is the *equivalent plastic strain* that defines the isotropic hardening of the von Mises yield surface and  $\bar{\mathbf{q}}$  defines the kinematic hardening variables in the stress deviator space in the case of the von Mises yield surface. Let

$$\boldsymbol{\eta} = \mathbf{S} - \bar{\mathbf{q}}, \quad \text{tr}(\bar{\mathbf{q}}) = 0 \quad (8.55)$$

In this equation,  $\mathbf{S}$  is the stress deviator. Note that the trace of the tensor  $\bar{\mathbf{q}}$  is assumed to be equal to zero. The resulting  $J_2$  plasticity model is governed by the following equations (Zienkiewicz and Taylor, 2000):

$$\left. \begin{aligned} f(\mathbf{S}, \bar{\mathbf{q}}, \alpha) &= \|\boldsymbol{\eta}\| - \sqrt{\frac{2}{3}} H_i(\alpha) \\ \dot{\boldsymbol{\varepsilon}}_d^p &= \gamma \frac{\boldsymbol{\eta}}{\|\boldsymbol{\eta}\|} \\ \dot{\bar{\mathbf{q}}} &= \frac{2}{3} \gamma H_k(\alpha) \frac{\boldsymbol{\eta}}{\|\boldsymbol{\eta}\|} \\ \dot{\alpha} &= \sqrt{\frac{2}{3}} \gamma \end{aligned} \right\} \quad (8.56)$$

where  $\|\boldsymbol{\eta}\| = \sqrt{\text{tr}(\boldsymbol{\eta}^T \boldsymbol{\eta})} = \sqrt{\text{tr}(\boldsymbol{\eta}^2)}$ . In this equation,  $\gamma$  is the consistency parameter; the functions  $H_i(\alpha)$  and  $H_k(\alpha)$  are, respectively, the *isotropic* and *kinematic hardening moduli*; and  $\boldsymbol{\varepsilon}_d^p$  is the plastic strain tensor deviator. The yield function defined by the first equation in Equation 56 is called the *Huber–von Mises yield function*. In many applications, particularly in the case of metals, the isotropic hardening modulus  $H_i(\alpha)$  is assumed to be the linear function of  $\alpha$ . In this

special case,  $H_i(\alpha)$  can be written as  $H_i(\alpha) = \sigma_y + \bar{H}_i \alpha$ , where  $\sigma_y$  is the yield stress and  $\bar{H}_i$  is a constant. On the other hand, if the kinematic hardening modulus  $H_k(\alpha)$  is assumed to be constant, one has the *Prager–Ziegler rule*. The reader may also notice the similarity between the third equation in Equations 56 and 7 in the simple case of the one-dimensional theory. The factor  $\sqrt{2/3}$  is introduced in Equation 56 in order to match the behavior of the metals in the case of uniaxial testing (Zienkiewicz and Taylor, 2000).

It is clear from the second equation in Equation 56 that  $|\dot{\epsilon}_d^p| = \gamma$ . Using this fact, the last equation in Equation 56 yields

$$\alpha(t) = \sqrt{\frac{2}{3}} \int_0^t |\dot{\epsilon}_d^p(\tau)| d\tau \quad (8.57)$$

This equation defines the relationship between  $\alpha$  and the norm of the plastic-strain-rate deviator (Simo and Hughes, 1998).

As discussed in the general small deformation plasticity theory, the differential equations associated with  $\dot{\epsilon}_d^p$ ,  $\dot{\mathbf{q}}$ , and  $\dot{\alpha}$  can be augmented with a constitutive equation in a rate form. In the case of the  $J_2$  plasticity, the constitutive equations for the stress deviator are used. The elastic deviatoric stress–strain relation can be written as

$$\mathbf{S} = 2\mu \mathbf{e}_d^e = 2\mu (\mathbf{e}_d - \mathbf{e}_d^p) \quad (8.58)$$

where  $\mu$  is the shear modulus (Lame’s constant),  $\mathbf{e}_d$  is the strain deviator,  $\mathbf{e}_d^e$  is the elastic strain deviator, and  $\mathbf{e}_d^p$  is the plastic strain deviator. Note that the strain additive decomposition is used in the preceding equation, and consequently, the development presented in this section can be used for small-strain problems only. Differentiating the preceding equation, and using Equation 56, one obtains

$$\dot{\mathbf{S}} = 2\mu (\dot{\mathbf{e}}_d - \dot{\mathbf{e}}_d^p) = 2\mu (\dot{\mathbf{e}}_d - \gamma \mathbf{n}) \quad (8.59)$$

and

$$\mathbf{n} = \frac{\boldsymbol{\eta}}{\|\boldsymbol{\eta}\|} \quad (8.60)$$

Because the  $\text{tr}(\mathbf{n}) = 0$ , one has  $\mathbf{n} : \dot{\mathbf{e}} = \mathbf{n} : \dot{\mathbf{e}}_d$ . In Equation 59,  $\dot{\mathbf{e}}_d$  is assumed to be known because the strain and strain rate are assumed to be known. On the other hand, the stress and plastic strain deviators are unknowns, and they are to be determined by solving the plasticity equations.

Equation 59 with the last three equations of Equation 56 defines four sets of first-order differential equations that can be, in principle, solved for the unknowns  $\mathbf{S}$ ,  $\mathbf{e}_d^p$ ,  $\mathbf{q}$ , and  $\alpha$ . In the most general  $J_2$  plasticity formulations, an integration method can be used to transform these differential equations into a set of nonlinear algebraic equations, which can be solved simultaneously for the unknowns as previously discussed in this chapter. The first equation in Equation 56 can be used to determine the consistency parameter  $\gamma$ , as will be discussed later in this section.

It is important, however, before presenting the form of the consistency parameter to realize that the  $J_2$  plasticity theory can be formulated also in terms of the stress tensor instead of the



deviatoric stress tensor. Recall that  $\boldsymbol{\sigma} = \mathbf{S} + p\mathbf{I}$ , where  $p$  is the hydrostatic pressure. Therefore, if the deviatoric stress  $\mathbf{S}$  and the hydrostatic pressure  $p$  are known, the stress tensor  $\boldsymbol{\sigma}$  can be determined. The hydrostatic pressure can be obtained using an elastic relationship between the volumetric strain, which is assumed to be known, and bulk modulus. Furthermore, if the rate of the stress deviator is known, one can obtain the rate of the stress tensor using the following equation:

$$\dot{\boldsymbol{\sigma}} = \dot{\mathbf{S}} + \dot{p}\mathbf{I} = 2\mu (\dot{\boldsymbol{\epsilon}}_d - \gamma \mathbf{n}) + \dot{p}\mathbf{I} \quad (8.61)$$

The general form of the consistency parameter given by Equation 37 reduces the case of  $J_2$  plasticity, as demonstrated in the following example, to

$$\gamma = \frac{\mathbf{n} : \dot{\boldsymbol{\epsilon}}_d}{\left(1 + \frac{H_k + (H_i)_a}{3\mu}\right)} \quad (8.62)$$

Finally, for  $\gamma \geq 0$ , one can show that the elastoplastic tangent moduli in the case of plastic loading can be obtained from the use of the preceding equation or alternatively by using Equation 40 as

$$\mathbf{E}^{ep} = K(\mathbf{I}_2 \otimes \mathbf{I}_2) + 2\mu \left( \mathbf{I}_4 - \frac{1}{3}\mathbf{I}_2 \otimes \mathbf{I}_2 - \frac{\mathbf{n} \otimes \mathbf{n}}{\left(1 + \frac{H_k + (H_i)_a}{3\mu}\right)} \right) \quad (8.63)$$

In this equation,  $K$  is bulk modulus, and  $\mathbf{I}_k$  is the  $k$ th-order identity tensor. Equation 63 is obtained assuming that the hydrostatic pressure  $p$  is related to the volumetric strain  $\epsilon_t$  using the linear elastic relation  $p = K\epsilon_t$ .

### Example 8.5

In the case of the  $J_2$  plasticity theory discussed in this section, show that the consistency parameter  $\gamma$  can be determined using the equation

$$\gamma = \frac{\mathbf{n} : \dot{\boldsymbol{\epsilon}}_d}{\left(1 + \frac{H_k + (H_i)_a}{3\mu}\right)}$$

Also show that the elastoplastic tangent moduli can be obtained as

$$\mathbf{E}^{ep} = K(\mathbf{I}_2 \otimes \mathbf{I}_2) + 2\mu \left( \mathbf{I}_4 - \frac{1}{3}\mathbf{I}_2 \otimes \mathbf{I}_2 - \frac{\mathbf{n} \otimes \mathbf{n}}{\left(1 + \frac{H_k + (H_i)_a}{3\mu}\right)} \right)$$

*Solution:* In the case of plastic deformation, one has

$$f = \|\boldsymbol{\eta}\| - \sqrt{\frac{2}{3}}H_i(\alpha) = 0$$

It follows that

$$f_{\eta} : \dot{\boldsymbol{\eta}} + f_{\alpha} \dot{\alpha} = 0$$

where

$$\dot{\boldsymbol{\eta}} = \dot{\mathbf{S}} - \dot{\mathbf{q}}$$

Note that by using the identity  $\|\boldsymbol{\eta}\| = \sqrt{\text{tr}(\boldsymbol{\eta}^2)}$ , the yield function  $f$  can be written as

$$f = \sqrt{\text{tr}(\boldsymbol{\eta}^2)} - \sqrt{\frac{2}{3}} H_i(\alpha)$$

One can show that

$$\begin{aligned} \frac{\partial(\text{tr}(\boldsymbol{\eta}^2))}{\partial \eta_{ij}} &= \sum_{k,l=1}^3 \frac{\partial(\eta_{kl} \eta_{kl})}{\partial \eta_{ij}} \\ &= \sum_{k,l=1}^3 \left( \frac{\partial(\eta_{kl})}{\partial \eta_{ij}} \eta_{kl} + \eta_{kl} \frac{\partial(\eta_{kl})}{\partial \eta_{ij}} \right) = \sum_{k,l=1}^3 2\eta_{kl} \delta_{ki} \delta_{lj} = 2\eta_{ij} \end{aligned}$$

which shows that

$$\frac{\partial(\text{tr}(\boldsymbol{\eta}^2))}{\partial \boldsymbol{\eta}} = 2\boldsymbol{\eta}$$

It follows that

$$\frac{\partial f}{\partial \boldsymbol{\eta}} = \frac{\partial \sqrt{\text{tr}(\boldsymbol{\eta}^2)}}{\partial \boldsymbol{\eta}} = \mathbf{n}$$

From Equation 59, one can write

$$\dot{\mathbf{S}} = 2\mu(\dot{\epsilon}_d - \gamma \mathbf{n})$$

From Equation 56, one has

$$\dot{\mathbf{q}} = \frac{2}{3} \gamma H_k \mathbf{n}$$

Using the preceding two equations, one can write

$$\dot{\boldsymbol{\eta}} = 2\mu(\dot{\epsilon}_d - \gamma \mathbf{n}) - \frac{2}{3} \gamma H_k \mathbf{n} = 2\mu \dot{\epsilon}_d - 2\gamma \mathbf{n} \left( \mu + \frac{1}{3} H_k \right)$$

One also has from Equation 56

$$\dot{\alpha} = \sqrt{\frac{2}{3}} \gamma$$

If  $(H_i)_{\alpha} = \partial H_i / \partial \alpha$ , one has

$$f_{\alpha} = -\sqrt{\frac{2}{3}} (H_i)_{\alpha}$$

Using these definitions, one can write

$$f_{\mathbf{n}} : \dot{\mathbf{n}} + f_a \dot{\alpha} = \mathbf{n} : \left( 2\mu \dot{\mathbf{e}}_d - 2\gamma \mathbf{n} \left( \mu + \frac{1}{3} H_k \right) \right) - \sqrt{\frac{2}{3}} (H_i)_a \left( \sqrt{\frac{2}{3}} \gamma \right) = 0$$

Because  $\mathbf{n} : \mathbf{n} = 1$ , the preceding equation yields

$$2\mu \mathbf{n} : \dot{\mathbf{e}}_d - 2\gamma \left( \mu + \frac{1}{3} H_k \right) - \frac{2}{3} \gamma (H_i)_a = 0$$

This equation can be used to determine the consistency parameter  $\gamma$  as

$$\gamma = \frac{\mu \mathbf{n} : \dot{\mathbf{e}}_d}{\mu + \frac{1}{3} H_k + \frac{1}{3} (H_i)_a} = \frac{\mathbf{n} : \dot{\mathbf{e}}_d}{1 + \frac{H_k + (H_i)_a}{3\mu}}$$

In order to obtain the elastoplastic tangent moduli, one can differentiate  $\boldsymbol{\sigma} = \mathbf{S} + p\mathbf{I}$  with respect to time. This leads to

$$\dot{\boldsymbol{\sigma}} = \dot{\mathbf{S}} + \dot{p}\mathbf{I}$$

Because  $\dot{\mathbf{S}} = 2\mu(\dot{\mathbf{e}}_d - \gamma \mathbf{n})$ , the use of the expression of the consistency parameter  $\gamma$  leads to

$$\dot{\mathbf{S}} = 2\mu(\dot{\mathbf{e}}_d - \gamma \mathbf{n}) = 2\mu \left( \dot{\mathbf{e}}_d - \frac{\mathbf{n} : \dot{\mathbf{e}}_d}{1 + \frac{H_k + (H_i)_a}{3\mu}} \mathbf{n} \right)$$

Recall that in the case of linear elasticity, the stress components and the hydrostatic pressure are, respectively, given by

$$\begin{aligned} \sigma_{ij} &= 2\mu \varepsilon_{ij}^e + \lambda \varepsilon_t^e \\ p &= \frac{1}{3} \sum_{k=1}^3 \sigma_{kk} = \frac{1}{3} (2\mu + 3\lambda) \varepsilon_t^e = K \varepsilon_t^e \end{aligned}$$

where

$$K = \lambda + \frac{2}{3}\mu, \quad \varepsilon_t^e = \sum_{k=1}^3 \varepsilon_{kk}^e$$

In this equation,  $\lambda$  and  $\mu$  are Lamé's constants. It follows that

$$\dot{p} = K \dot{\varepsilon}_t^e$$

In the  $J_2$  flow theory, it is assumed that  $\varepsilon_t^p = 0$ , and as a consequence,  $\varepsilon_t = \varepsilon_t^e + \varepsilon_t^p = \varepsilon_t^e$ . It follows that

$$\dot{p} = K \dot{\varepsilon}_t$$

and

$$\dot{\boldsymbol{\sigma}} = 2\mu \left( \dot{\boldsymbol{\epsilon}}_d - \frac{\mathbf{n} : \dot{\boldsymbol{\epsilon}}_d}{1 + \frac{H_k + (H_l)_a}{3\mu}} \mathbf{n} \right) + K \dot{\boldsymbol{\epsilon}}_t \mathbf{I} = \mathbf{E}^{ep} : \dot{\boldsymbol{\epsilon}}$$

where  $e_{ijkl}^{ep}$  are the elements of the fourth-order tensor  $\mathbf{E}^{ep}$ . The components of the second-order tensor  $\dot{\boldsymbol{\sigma}}$  can then be written as

$$\dot{\sigma}_{ij} = 2\mu \left( \dot{\epsilon}_{dij} - \frac{\sum_{k,l=1}^3 n_{kl} \dot{\epsilon}_{dkl}}{1 + \frac{H_k + (H_l)_a}{3\mu}} n_{ij} \right) + K \dot{\epsilon}_t \delta_{ij} = \sum_{k,l=1}^3 e_{ijkl}^{ep} \dot{\epsilon}_{kl}$$

From the definition of the deviatoric strain, one has

$$\dot{\epsilon}_{dij} = \dot{\epsilon}_{ij} - \frac{1}{3} \delta_{ij} \dot{\epsilon}_t$$

One can also write

$$\dot{\epsilon}_{ij} = \sum_{k,l=1}^3 \delta_{ki} \delta_{lj} \dot{\epsilon}_{kl}, \quad \delta_{ij} \dot{\epsilon}_t = \sum_{k,l=1}^3 \delta_{ij} \delta_{kl} \dot{\epsilon}_{kl}$$

Therefore,

$$\dot{\epsilon}_{dij} = \sum_{k,l=1}^3 \left( \delta_{ki} \delta_{lj} \dot{\epsilon}_{kl} - \frac{1}{3} \delta_{ij} \delta_{kl} \dot{\epsilon}_{kl} \right)$$

and

$$\sum_{k,l=1}^3 n_{kl} \dot{\epsilon}_{dkl} = \sum_{k,l=1}^3 n_{kl} \left( \dot{\epsilon}_{kl} - \frac{1}{3} \delta_{kl} \dot{\epsilon}_t \right) = \sum_{k,l=1}^3 n_{kl} \dot{\epsilon}_{kl} - \frac{1}{3} \sum_{k=1}^3 n_{kk} \dot{\epsilon}_t$$

Because  $\sum_{k=1}^3 n_{kk} = \sum_{k=1}^3 n_{kk} / \|\boldsymbol{\eta}\| = 0$ , one has

$$\sum_{k,l=1}^3 n_{kl} \dot{\epsilon}_{dkl} = \sum_{k,l=1}^3 n_{kl} \dot{\epsilon}_{kl}$$

By substituting into the stress-rate equation, one obtains

$$\begin{aligned} \dot{\sigma}_{ij} &= 2\mu \sum_{k,l=1}^3 \left( \delta_{ki} \delta_{lj} \dot{\epsilon}_{kl} - \frac{1}{3} \delta_{ij} \delta_{kl} \dot{\epsilon}_{kl} - \frac{n_{kl} \dot{\epsilon}_{kl}}{1 + \frac{H_k + (H_l)_a}{3\mu}} n_{ij} \right) + \sum_{k,l=1}^3 K \delta_{ij} \delta_{kl} \dot{\epsilon}_{kl} \\ &= \sum_{k,l=1}^3 \left( 2\mu \left( \delta_{ki} \delta_{lj} - \frac{1}{3} \delta_{ij} \delta_{kl} - \frac{n_{ij} n_{kl}}{1 + \frac{H_k + (H_l)_a}{3\mu}} \right) + K \delta_{ij} \delta_{kl} \right) \dot{\epsilon}_{kl} = \sum_{k,l=1}^3 e_{ijkl}^{ep} \dot{\epsilon}_{kl} \end{aligned}$$

where

$$e_{ijkl}^{ep} = 2\mu \left( \delta_{ki}\delta_{lj} - \frac{1}{3}\delta_{ij}\delta_{kl} - \frac{n_{ij}n_{kl}}{1 + \frac{H_k + (H_l)_a}{3\mu}} \right) + K\delta_{ij}\delta_{kl}$$

which defines the fourth-order elastoplastic tangent moduli tensor as

$$\mathbf{E}^{ep} = 2\mu \left( \mathbf{I}_4 - \frac{1}{3}\mathbf{I}_2 \otimes \mathbf{I}_2 - \frac{\mathbf{n} \otimes \mathbf{n}}{1 + \frac{H_k + (H_l)_a}{3\mu}} \right) + K(\mathbf{I}_2 \otimes \mathbf{I}_2)$$

### Example 8.6

The  $J_2$  plane stress plasticity theory can be considered as a special case of the development presented in this section. In the case of plane stress,

$$\sigma_{13} = \sigma_{31} = \sigma_{23} = \sigma_{32} = \sigma_{33} = 0$$

which leads to

$$\eta_{13} = \eta_{31} = \eta_{23} = \eta_{32} = 0, \quad \eta_{33} = -\eta_{11} - \eta_{22}$$

One can evaluate  $\|\boldsymbol{\eta}\|$  in the case of plane stress as follows:

$$\begin{aligned} \|\boldsymbol{\eta}\| &= \sqrt{\eta_{11}\eta_{11} + \eta_{12}\eta_{12} + \eta_{21}\eta_{21} + \eta_{22}\eta_{22} + \eta_{33}\eta_{33}} \\ &= \sqrt{2(\eta_{11}^2 + \eta_{12}^2 + \eta_{22}^2 + \eta_{11}\eta_{22})} \end{aligned}$$

The stress–strain relation in general case is defined by

$$\dot{\sigma}_{ij} = \sum_{k, l=1}^3 \left( 2\mu \left( \delta_{ki}\delta_{lj} - \frac{1}{3}\delta_{ij}\delta_{kl} - \frac{n_{ij}n_{kl}}{1 + \frac{H_k + (H_l)_a}{3\mu}} \right) + K\delta_{ij}\delta_{kl} \right) \dot{\epsilon}_{kl}$$

Because  $K = \lambda + (2/3)\mu$ , one has

$$\begin{aligned} \dot{\sigma}_{ij} &= \sum_{k, l=1}^3 \left( 2\mu \left( \delta_{ki}\delta_{lj} - \frac{1}{3}\delta_{ij}\delta_{kl} - \frac{n_{ij}n_{kl}}{1 + \frac{H_k + (H_l)_a}{3\mu}} \right) + \left( \lambda + \frac{2}{3}\mu \right) \delta_{ij}\delta_{kl} \right) \dot{\epsilon}_{kl} \\ &= \sum_{k, l=1}^3 \left( 2\mu \left( \delta_{ki}\delta_{lj} - \frac{n_{ij}n_{kl}}{1 + \frac{H_k + (H_l)_a}{3\mu}} \right) + \lambda\delta_{ij}\delta_{kl} \right) \dot{\epsilon}_{kl} \end{aligned}$$

$$= 2\mu \left( \dot{\epsilon}_{ij} - \frac{n_{ij} \sum_{k,l=1}^3 n_{kl} \dot{\epsilon}_{kl}}{1 + \frac{H_k + (H_i)_\alpha}{3\mu}} \right) + \sum_{k=1}^3 \lambda \delta_{ij} \dot{\epsilon}_{kk}$$

Because in the case of plane stress,  $\eta_{13} = \eta_{31} = \eta_{23} = \eta_{32} = 0$ , one has  $n_{13} = n_{31} = n_{23} = n_{32} = 0$ . It follows that

$$\dot{\sigma}_{13} = 2\mu \dot{\epsilon}_{13}, \quad \dot{\sigma}_{23} = 2\mu \dot{\epsilon}_{23}$$

which leads to

$$\dot{\epsilon}_{13} = \dot{\epsilon}_{23} = 0$$

Therefore, one can write the plane stress constitutive relationships as follows:

$$\begin{bmatrix} \dot{\sigma}_{11} \\ \dot{\sigma}_{22} \\ \dot{\sigma}_{12} \end{bmatrix} = \begin{bmatrix} \lambda + 2\mu - 2\mu \frac{n_{11}n_{11}}{H} & \lambda - 2\mu \frac{n_{11}n_{22}}{H} & \lambda - 2\mu \frac{n_{11}n_{33}}{H} & -2\mu \frac{n_{11}n_{12}}{H} \\ \lambda - 2\mu \frac{n_{22}n_{11}}{H} & \lambda + 2\mu - 2\mu \frac{n_{22}n_{22}}{H} & \lambda - 2\mu \frac{n_{22}n_{33}}{H} & -2\mu \frac{n_{22}n_{12}}{H} \\ -2\mu \frac{n_{12}n_{11}}{H} & -2\mu \frac{n_{12}n_{22}}{H} & -2\mu \frac{n_{12}n_{33}}{H} & 2\mu - 2\mu \frac{n_{12}n_{12}}{H} \end{bmatrix} \times \begin{bmatrix} \dot{\epsilon}_{11} \\ \dot{\epsilon}_{22} \\ \dot{\epsilon}_{33} \\ \dot{\epsilon}_{12} \end{bmatrix} = \mathbf{E}_1 \begin{bmatrix} \dot{\epsilon}_{11} \\ \dot{\epsilon}_{22} \\ \dot{\epsilon}_{33} \\ \dot{\epsilon}_{12} \end{bmatrix}$$

where

$$H = 1 + \frac{H_k + (H_i)_\alpha}{3\mu}$$

and

$$\mathbf{E}_1 = \begin{bmatrix} \lambda + 2\mu - 2\mu \frac{n_{11}n_{11}}{H} & \lambda - 2\mu \frac{n_{11}n_{22}}{H} & \lambda - 2\mu \frac{n_{11}n_{33}}{H} & -2\mu \frac{n_{11}n_{12}}{H} \\ \lambda - 2\mu \frac{n_{22}n_{11}}{H} & \lambda + 2\mu - 2\mu \frac{n_{22}n_{22}}{H} & \lambda - 2\mu \frac{n_{22}n_{33}}{H} & -2\mu \frac{n_{22}n_{12}}{H} \\ -2\mu \frac{n_{12}n_{11}}{H} & -2\mu \frac{n_{12}n_{22}}{H} & -2\mu \frac{n_{12}n_{33}}{H} & 2\mu - 2\mu \frac{n_{12}n_{12}}{H} \end{bmatrix}$$

Because  $\dot{\sigma}_{33} = 0$ , one has

$$2\mu \dot{\epsilon}_{33} + \lambda(\dot{\epsilon}_{11} + \dot{\epsilon}_{22} + \dot{\epsilon}_{33}) - 2\mu \frac{n_{33}}{H}(n_{11}\dot{\epsilon}_{11} + n_{22}\dot{\epsilon}_{22} + n_{33}\dot{\epsilon}_{33} + n_{12}\dot{\epsilon}_{12}) = 0$$

Using this equation, one can write

$$\begin{bmatrix} \dot{\epsilon}_{11} \\ \dot{\epsilon}_{22} \\ \dot{\epsilon}_{33} \\ \dot{\epsilon}_{12} \end{bmatrix} = \begin{bmatrix} 1 & 0 & 0 \\ 0 & 1 & 0 \\ \frac{2\mu n_{33}n_{11} - \lambda H}{2\mu H + \lambda H - 2\mu n_{33}n_{33}} & \frac{2\mu n_{33}n_{22} - \lambda H}{2\mu H + \lambda H - 2\mu n_{33}n_{33}} & \frac{2\mu n_{33}n_{12}}{2\mu H + \lambda H - 2\mu n_{33}n_{33}} \\ 0 & 0 & 1 \end{bmatrix} \times \begin{bmatrix} \dot{\epsilon}_{11} \\ \dot{\epsilon}_{22} \\ \dot{\epsilon}_{12} \end{bmatrix} = \mathbf{E}_2 \begin{bmatrix} \dot{\epsilon}_{11} \\ \dot{\epsilon}_{22} \\ \dot{\epsilon}_{12} \end{bmatrix}$$

This equation can be substituted into the rate constitutive equations in the plane stress case to obtain

$$\begin{bmatrix} \dot{\sigma}_{11} \\ \dot{\sigma}_{22} \\ \dot{\sigma}_{12} \end{bmatrix} = \mathbf{E}^{ep} \begin{bmatrix} \dot{\epsilon}_{11} \\ \dot{\epsilon}_{22} \\ \dot{\epsilon}_{12} \end{bmatrix}$$

where  $\mathbf{E}^{ep} = \mathbf{E}_1 \mathbf{E}_2$ , and

$$\mathbf{E}_2 = \begin{bmatrix} 1 & 0 & 0 \\ 0 & 1 & 0 \\ \frac{2\mu n_{33}n_{11} - \lambda H}{2\mu H + \lambda H - 2\mu n_{33}n_{33}} & \frac{2\mu n_{33}n_{22} - \lambda H}{2\mu H + \lambda H - 2\mu n_{33}n_{33}} & \frac{2\mu n_{33}n_{12}}{2\mu H + \lambda H - 2\mu n_{33}n_{33}} \\ 0 & 0 & 1 \end{bmatrix}$$

### Nonlinear Isotropic/Kinematic Hardening

The procedure used to solve the  $J_2$  plasticity equations in the general case of isotropic and kinematic hardening is first outlined. The special case of linear isotropic and kinematic hardening is also discussed before concluding this section.

Using the  $J_2$  flow theory presented in this section, one can use the implicit backward Euler method to transform the first-order differential equations to a set of algebraic equations that are similar to Equations 47 and 48. It can be, however, shown that one only needs to solve one scalar nonlinear equation in order to determine the state of stress and strains at time  $t_{n+1}$ . To this end, the implicit backward Euler method can be used with Equations 55 and 56 to obtain

$$\left. \begin{aligned} \mathbf{S}_{n+1} &= \mathbf{S}_n + 2\mu \Delta \epsilon_d - 2\mu \Delta \gamma \mathbf{n}_{n+1} \\ (\epsilon_d^p)_{n+1} &= (\epsilon_d^p)_n + \Delta \gamma \mathbf{n}_{n+1} \\ \alpha_{n+1} &= \alpha_n + \Delta \alpha = \alpha_n + \sqrt{\frac{2}{3}} \Delta \gamma \\ \bar{\mathbf{q}}_{n+1} &= \bar{\mathbf{q}}_n + \frac{2}{3} \Delta \gamma H_k(\alpha_{n+1}) \mathbf{n}_{n+1} \end{aligned} \right\} \quad (8.64)$$

where  $\Delta\alpha = (2/3)^{\frac{1}{2}}(\Delta t)\gamma = (2/3)^{\frac{1}{2}}\Delta\gamma$ . In Equation 64,  $\Delta\epsilon_d = (\epsilon_d)_{n+1} - (\epsilon_d)_n$  is assumed to be known because the total strain at time  $t_{n+1}$  is assumed to be known. Note also that the unknowns on the left-hand side of Equation 64 can be determined if  $\mathbf{n}_{n+1}$  and  $\Delta\gamma$  are determined. To this end, the trial stress state can be defined by the following equations:

$$\left. \begin{aligned} \mathbf{S}_{n+1}^{trial} &= \mathbf{S}_n + 2\mu \Delta\epsilon_d \\ \boldsymbol{\eta}_{n+1}^{trial} &= \mathbf{S}_{n+1}^{trial} - \bar{\mathbf{q}}_n \end{aligned} \right\} \quad (8.65)$$

These trial solutions are function of known variables defined at time  $t_n$ .

In the following, it is shown that, if  $\mathbf{n}_{n+1}$  can be determined, the solution of Equation 64 reduces to the solution of a nonlinear scalar equation for the consistency parameter  $\Delta\gamma$ . Because  $\mathbf{S}_{n+1} = \mathbf{S}_{n+1}^{trial} - 2\mu(\Delta\gamma \mathbf{n}_{n+1})$ , where  $2\mu(\Delta\gamma \mathbf{n}_{n+1})$  is the plastic corrector,  $\boldsymbol{\eta}_{n+1}$  can be expressed in terms of  $\boldsymbol{\eta}_{n+1}^{trial}$  using the following equation:

$$\begin{aligned} \boldsymbol{\eta}_{n+1} &= \mathbf{S}_{n+1} - \bar{\mathbf{q}}_{n+1} \\ &= \boldsymbol{\eta}_{n+1}^{trial} - \left\{ 2\mu\Delta\gamma + \frac{2}{3}\Delta\gamma H_k(\alpha_{n+1}) \right\} \mathbf{n}_{n+1} \end{aligned} \quad (8.66)$$

Substituting  $\boldsymbol{\eta}_{n+1} = \|\boldsymbol{\eta}_{n+1}\| \mathbf{n}_{n+1}$  in the preceding equation shows that  $\boldsymbol{\eta}_{n+1}^{trial}$  and  $\mathbf{n}_{n+1}$  are in the same direction and, therefore,  $\mathbf{n}_{n+1}$  can be written in terms of the trial elastic stress  $\boldsymbol{\eta}_{n+1}^{trial}$  as

$$\mathbf{n}_{n+1} = \frac{\boldsymbol{\eta}_{n+1}^{trial}}{\|\boldsymbol{\eta}_{n+1}^{trial}\|} \quad (8.67)$$

This equation shows that  $\mathbf{n}_{n+1}$  can be evaluated using information available at time  $t_n$ . Therefore, the only remaining unknown on the left-hand side of Equation 64 is  $\Delta\gamma$ . If  $\Delta\gamma$  is determined, the state of stresses and strains at time  $t_{n+1}$  can be determined using Equation 64. To this end, one can take the double contraction of Equation 66 with  $\mathbf{n}_{n+1}$  and recall in the plastic state that  $\|\boldsymbol{\eta}_{n+1}\| - (\sqrt{2/3})H_i(\alpha_{n+1}) = 0$ , which is the result of the yield condition (see the first equation in Equation 56). One can then obtain the following scalar equation in  $\Delta\gamma$ :

$$\begin{aligned} g(\Delta\gamma) &= -\sqrt{\frac{2}{3}}H_i(\alpha_{n+1}) + \|\boldsymbol{\eta}_{n+1}^{trial}\| \\ &\quad - \left\{ 2\mu\Delta\gamma + \frac{2}{3}\Delta\gamma H_k(\alpha_{n+1}) \right\} = 0 \end{aligned} \quad (8.68)$$

The first term on the right-hand side of this equation is the result of the fact that  $\mathbf{n}_{n+1}$  and  $\boldsymbol{\eta}_{n+1}$  are in the same direction and the following identity:  $\mathbf{n}_{n+1} : \boldsymbol{\eta}_{n+1} = \|\boldsymbol{\eta}_{n+1}\| = (\sqrt{2/3})H_i(\alpha_{n+1})$ . The nonlinear equation of Equation 68 can be solved using a local Newton–Raphson iterative procedure. The convergence is guaranteed because the function is convex as the result of using the associative plasticity model (Simo and Hughes, 1998). Knowing  $\Delta\gamma$  and using Equation 67, all the unknowns in Equation 64 as well as the stress at time  $t_{n+1}$  can be determined.



**Example 8.7**

Show that  $\mathbf{n}_{n+1}^{trial}$  and  $\mathbf{n}_{n+1}$  that appear in Equation 66 are in the same direction. Use this result to derive Equation 68.

*Solution:* From Equation 66, one has

$$\mathbf{n}_{n+1} = \mathbf{n}_{n+1}^{trial} - \left\{ 2\mu\Delta\gamma + \frac{2}{3}\Delta\gamma(H_k)_{n+1} \right\} \mathbf{n}_{n+1}$$

The definition of  $\mathbf{n}$  is

$$\mathbf{n}_{n+1} = \frac{\mathbf{n}_{n+1}}{\|\mathbf{n}_{n+1}\|}$$

which yields  $\mathbf{n}_{n+1} = \|\mathbf{n}_{n+1}\| \mathbf{n}_{n+1}$ . It follows that

$$\|\mathbf{n}_{n+1}\| \mathbf{n}_{n+1} = \mathbf{n}_{n+1}^{trial} - \left\{ 2\mu\Delta\gamma + \frac{2}{3}\Delta\gamma(H_k)_{n+1} \right\} \mathbf{n}_{n+1}$$

This equation can be rewritten as

$$\mathbf{n}_{n+1}^{trial} = \left\{ 2\mu\Delta\gamma + \frac{2}{3}\Delta\gamma(H_k)_{n+1} + \|\mathbf{n}_{n+1}\| \right\} \mathbf{n}_{n+1}$$

This equation indicates that  $\mathbf{n}_{n+1}^{trial}$  and  $\mathbf{n}_{n+1}$  are in the same direction. By taking the square on both sides of the preceding equation and taking the trace of the resulting tensors, one obtains

$$\text{tr}((\mathbf{n}_{n+1}^{trial})^2) = \left\{ 2\mu\Delta\gamma + \frac{2}{3}\Delta\gamma(H_k)_{n+1} + \|\mathbf{n}_{n+1}\| \right\}^2 \text{tr}((\mathbf{n}_{n+1})^2)$$

Recall that

$$\begin{aligned} \text{tr}((\mathbf{n}_{n+1}^{trial})^2) &= \mathbf{n}_{n+1}^{trial} : \mathbf{n}_{n+1}^{trial} = (\|\mathbf{n}_{n+1}^{trial}\|)^2, \\ \text{tr}((\mathbf{n}_{n+1})^2) &= \mathbf{n}_{n+1} : \mathbf{n}_{n+1} = 1 \end{aligned}$$

Therefore,

$$\left\{ 2\mu\Delta\gamma + \frac{2}{3}\Delta\gamma(H_k)_{n+1} + \|\mathbf{n}_{n+1}\| \right\} = \|\mathbf{n}_{n+1}^{trial}\|$$

In the plastic state at time  $t_{n+1}$ , the yield function is

$$f = \|\mathbf{n}_{n+1}\| - \sqrt{\frac{2}{3}}H_i(\alpha_{n+1}) = 0$$

Therefore,

$$\|\mathbf{n}_{n+1}^{trial}\| - \left\{ 2\mu\Delta\gamma + \frac{2}{3}\Delta\gamma(H_k)_{n+1} \right\} - \sqrt{\frac{2}{3}}H_i(\alpha_{n+1}) = 0$$

which is the same as Equation 68.

The relationship between the stresses and strains in the plasticity formulation discussed in this section can be written as follows:

$$\boldsymbol{\sigma}_{n+1} = K(\text{tr}(\boldsymbol{\epsilon}_{n+1}))\mathbf{I}_2 + 2\mu\{(\boldsymbol{\epsilon}_d)_{n+1} - \Delta\gamma\mathbf{n}_{n+1}\} \quad (8.69)$$

The incremental form of this equation can be written as

$$\begin{aligned} d\boldsymbol{\sigma}_{n+1} &= \mathbf{E} : d\boldsymbol{\epsilon}_{n+1} - 2\mu(d\Delta\gamma\mathbf{n}_{n+1} + \Delta\gamma d\mathbf{n}_{n+1}) \\ &= \left\{ \mathbf{E} - 2\mu\mathbf{n}_{n+1} \otimes \frac{\partial\Delta\gamma}{\partial\boldsymbol{\epsilon}_{n+1}} - 2\mu\Delta\gamma \frac{\partial\mathbf{n}_{n+1}}{\partial\boldsymbol{\epsilon}_{n+1}} \right\} : d\boldsymbol{\epsilon}_{n+1} \end{aligned} \quad (8.70)$$

where  $\mathbf{E} = K(\mathbf{I}_2 \otimes \mathbf{I}_2) + 2\mu\{\mathbf{I}_4 - (1/3)\mathbf{I}_2 \otimes \mathbf{I}_2\}$  is the elasticity tensor. Note that

$$\frac{\partial\mathbf{n}}{\partial\boldsymbol{\eta}} = \frac{1}{\|\boldsymbol{\eta}\|}(\mathbf{I}_4 - \mathbf{n} \otimes \mathbf{n}) \quad (8.71)$$

In the general case, the term  $\partial(\Delta\gamma)/\partial\boldsymbol{\epsilon}_{n+1}$  in Equation 70 can be obtained from the differentiation of Equation 68. The incremental form of Equation 70 can be used to determine the consistent tangent moduli that define the relationship between the stresses and the total strains.

### Return Mapping Algorithm for Nonlinear Isotropic/Kinematic Hardening

Based on the discussion presented in this section, the following algorithm can be summarized in the case of the  $J_2$  plasticity theory that accounts for nonlinear isotropic and kinematic hardening (Simo and Hughes, 1998):

1. Using the fact that the strain is known at time  $t_{n+1}$  and using the information at time  $t_n$  compute the deviatoric strain tensor and the trial elastic stresses using the following equations:

$$\left. \begin{aligned} (\boldsymbol{\epsilon}_d)_{n+1} &= \boldsymbol{\epsilon}_{n+1} - \frac{1}{3}(\text{tr}(\boldsymbol{\epsilon}_{n+1}))\mathbf{I}_2 \\ \mathbf{S}_{n+1}^{trial} &= 2\mu\{(\boldsymbol{\epsilon}_d)_{n+1} - (\boldsymbol{\epsilon}_d^n)\} \\ \boldsymbol{\eta}_{n+1}^{trial} &= \mathbf{S}_{n+1}^{trial} - \bar{\mathbf{q}}_n \end{aligned} \right\} \quad (8.72)$$

2. Check the yield condition by evaluating the following Huber–von Mises function:

$$f_{n+1}^{trial} = \|\boldsymbol{\eta}_{n+1}^{trial}\| - \sqrt{\frac{2}{3}}H_i(\alpha_n) \quad (8.73)$$

If  $f_{n+1}^{trial} \leq 0$ , an elastic state is assumed. In this case, set the plasticity variables at  $t_{n+1}$  equal to the plasticity variables at  $t_n$ , determine the stresses using the elastic relationships, and exit.

3. If  $f_{n+1}^{trial} > 0$ , solve the plasticity equations. Compute  $\mathbf{n}_{n+1}$  and find  $\Delta\gamma$  from the solution of Equation 68. In this case, one has

$$\mathbf{n}_{n+1} = \frac{\boldsymbol{\eta}_{n+1}^{trial}}{\|\boldsymbol{\eta}_{n+1}^{trial}\|} \quad (8.74)$$

and

$$\alpha_{n+1} = \alpha_n + \sqrt{\frac{2}{3}} \Delta\gamma \quad (8.75)$$

4. Update the back stress, plastic strain, and stress tensors using the following equations:

$$\left. \begin{aligned} \bar{\mathbf{q}}_{n+1} &= \bar{\mathbf{q}}_n + \frac{2}{3} \Delta\gamma H_k(\alpha_{n+1}) \mathbf{n}_{n+1} \\ (\boldsymbol{\epsilon}_d^p)_{n+1} &= (\boldsymbol{\epsilon}_d^p)_n + \Delta\gamma \mathbf{n}_{n+1} \\ \boldsymbol{\sigma}_{n+1} &= K \operatorname{tr}(\boldsymbol{\epsilon}_{n+1}) \mathbf{I}_2 + \mathbf{S}_{n+1}^{trial} - 2\mu \Delta\gamma \mathbf{n}_{n+1} \end{aligned} \right\} \quad (8.76)$$

5. The consistent elastoplastic tangent moduli can be computed using the formula (Simo and Hughes, 1998)

$$\mathbf{E}_{n+1} = K(\mathbf{I}_2 \otimes \mathbf{I}_2) + 2\mu\theta_{n+1} \left[ \mathbf{I}_4 - \frac{1}{3} \mathbf{I}_2 \otimes \mathbf{I}_2 \right] - 2\mu\bar{\theta}_{n+1} (\mathbf{n}_{n+1} \otimes \mathbf{n}_{n+1}) \quad (8.77)$$

where

$$\theta_{n+1} = 1 - \frac{2\mu\Delta\gamma}{\|\boldsymbol{\eta}_{n+1}^{trial}\|}, \quad \bar{\theta}_{n+1} = \frac{1}{\left(1 + \frac{((H_l)_a + H_k)_{n+1}}{3\mu}\right)} - (1 - \theta_{n+1}) \quad (8.78)$$

This algorithm requires the solution of one nonlinear algebraic equation (Equation 68). In the finite element implementation, this equation needs to be solved at the integration points.

There are important considerations that must be taken into account when implementing the algorithm presented in this section. The following important remarks can be made regarding the proposed algorithm (Simo and Hughes, 1998):

1. In the analysis presented in this section, the backward Euler method was used as an example to obtain the nonlinear plasticity algebraic equations. Nonetheless, other implicit integration methods can be used to transform the first-order differential equations into a set of nonlinear algebraic equations. In particular, the backward Euler method can be replaced by the generalized midpoint rule in the derivation of the discrete equations as proposed by Ortiz and Popov (1985) or Simo and Taylor (1986). For the  $J_2$  flow theory, this results in the return map proposed by Rice and Tracey (1973).
2. Note that the values of the variables at step  $n+1$  are calculated based solely on the converged values at step  $n$ . Use of an iterative scheme based on intermediate nonconverged values is questionable for a problem that is physically path dependent.
3. In the computer implementation, the expression for the consistent tangent moduli should be compared with the “continuum” elastoplastic tangent moduli in order to estimate the errors. For large time-steps, the consistent tangent moduli may differ significantly from the “continuum” elastoplastic tangent moduli.

### Linear Kinematic/Isotropic Hardening

In metal plasticity applications, it is often assumed that the isotropic hardening is linear of the form  $H_i(\alpha) = \sigma_y + \bar{H}_i(\alpha)$  where  $\bar{H}_i$  is a constant. Alternatively, one can use the following form of combined kinematic/isotropic hardening laws (Hughes, 1984):

$$H_k(\alpha) = (1 - \beta)\bar{H}_k, \quad H_i(\alpha) = (\sigma_y + \beta\bar{H}_i\alpha), \quad \beta \in [0, 1] \quad (8.79)$$

where  $\bar{H}_k$  is a constant. As previously mentioned, the assumption of a constant kinematic hardening modulus is known as *Prager–Ziegler rule*. More general isotropic hardening models can also be used (Hughes, 1984).

In the special case of linear kinematic/isotropic hardening, one has

$$f_{n+1}^{trial} = \|\mathbf{n}_{n+1}^{trial}\| - \sqrt{\frac{2}{3}}(\sigma_y + \beta\bar{H}_i\alpha_n) \quad (8.80)$$

where  $\beta \in [0, 1]$  and  $\bar{H}_i > 0$  is a given material hardening parameter. In this special case, a closed-form solution for  $\Delta\gamma$  can be obtained by substituting the preceding equation into Equation 68 and assuming that  $\bar{H}_k = \bar{H}_i$ . This leads to

$$2\mu\Delta\gamma = \frac{f_{n+1}^{trial}}{\left(1 + \frac{\bar{H}_i}{3\mu}\right)} \quad (8.81)$$

Using this result, the update procedure is completed by substituting Equation 81 into Equation 64.

#### Example 8.8

In order to prove Equation 81, one can use Equation 68 to write

$$\|\mathbf{n}_{n+1}^{trial}\| - \left\{2\mu\Delta\gamma + \frac{2}{3}\Delta\gamma(H_k)_{n+1}\right\} - \sqrt{\frac{2}{3}}H_i(\alpha_{n+1}) = 0$$

Recall that

$$f_{n+1}^{trial} = \|\mathbf{n}_{n+1}^{trial}\| - \sqrt{\frac{2}{3}}H_i(\alpha_n)$$

Therefore,

$$f_{n+1}^{trial} + \sqrt{\frac{2}{3}}H_i(\alpha_n) - \left\{2\mu\Delta\gamma + \frac{2}{3}\Delta\gamma(H_k)_{n+1}\right\} - \sqrt{\frac{2}{3}}H_i(\alpha_{n+1}) = 0$$

In the case of linear kinematic/isotropic hardening, one has from Equation 79

$$H_k = (1 - \beta)\bar{H}_k, \quad H_i(\alpha_{n+1}) = \sigma_y + \beta\bar{H}_i\alpha_{n+1}$$

In this equation,  $\bar{H}_k$  and  $\bar{H}_i$  are constants. Using Equation 64, one can write

$$\alpha_{n+1} = \alpha_n + \sqrt{\frac{2}{3}} \Delta\gamma$$

It follows that

$$H_i(\alpha_n) - H_i(\alpha_{n+1}) = \sigma_y + \beta \bar{H}_i \alpha_n - \sigma_y - \beta \bar{H}_i \alpha_{n+1} = -\beta \bar{H}_i \sqrt{\frac{2}{3}} \Delta\gamma$$

Therefore,

$$f_{n+1}^{trial} - \Delta\gamma \left\{ 2\mu + \frac{2}{3} \beta \bar{H}_i + \frac{2}{3} (1 - \beta) \bar{H}_k \right\} = 0$$

In the special case in which  $\bar{H}_i = \bar{H}_k$  the preceding equation leads to

$$2\mu \Delta\gamma = \frac{f_{n+1}^{trial}}{\left( 1 + \frac{\bar{H}_i}{3\mu} \right)}$$

## 8.6 NONLINEAR FORMULATION FOR HYPERELASTIC-PLASTIC MATERIALS

The elastic response of *hyperelastic materials* is derived from a potential function and, therefore, the work done in a deformation process is path independent. This is not the case when hypoelastic models are used. For *hypoelastic materials*, the elastic response is not derived from a potential function and the work done in a deformation process is path dependent. For all *inelastic materials*, the constitutive equations depend on the path followed in a deformation process. It is, therefore, important to follow this path in order to be able to accurately determine the current state of stresses. This is also clear from the mathematical fact that the solution of algebraic equations does not require knowledge of the history, whereas the solution of differential equations requires knowledge of variable history. Similarly, the evaluation of an integral requires one to define the limits of integration. The numerical evaluation of an integral, for example, requires information at several past points, and not only information at the current point.

When hypoelastic-plastic models are used, the yield function is required to be an isotropic function of the stress, and the objectivity requirements restrict the elastic moduli to be isotropic if these moduli are assumed to be constant (Belytschko et al., 2000). Furthermore, the numerical solution of the plasticity equations based on the hypoelastic-plastic formulations requires the use of incrementally objective integration schemes. There are in the literature formulations of hypoelastic materials for large strains based on the additive decomposition of the rate of deformation tensor (Belytschko et al., 2000). It is assumed in these formulations, however, that the elastic strains are small compared to the plastic strains. Furthermore, energy is not conserved in a closed deformation cycle. Such an energy violation, however, can be insignificant if the assumption of small elastic strains is observed. The use

of a hyperelastic–plastic formulation, on the other hand, relaxes these requirements. In this section, the formulation of the constitutive equations for hyperelastic–plastic materials in the case of large strains is presented.

### Multiplicative Decomposition

The multiplicative decomposition of the matrix of the position vector gradients, instead of the additive form assumed for small strains, is the basis for the theory developed in this section for hyperelastic–plastic materials (Bonet and Wood, 1997). Recall that a line element  $d\mathbf{x}$  in the reference configuration corresponds to a line element  $d\mathbf{r}$  in the current configuration. If the material is elastic and the load is removed,  $d\mathbf{x}$  and  $d\mathbf{r}$  differ only by a rigid-body rotation. If the material, on the other hand, experiences a plastic deformation, a certain amount of permanent deformation remains upon the removal of the load, and  $d\mathbf{r}$  will correspond to the vector  $d\mathbf{r}^p$  in a stress-free intermediate configuration called in this book the *intermediate plastic configuration* as shown in Figure 1. The relationship between  $d\mathbf{x}$  and  $d\mathbf{r}$  is given by the matrix of the position vector gradients  $\mathbf{J}$ , whereas the relationship between  $d\mathbf{x}$  and  $d\mathbf{r}^p$  is given by the matrix of the position vector gradients  $\mathbf{J}^p$ . The relationship between  $d\mathbf{r}^p$  and  $d\mathbf{r}$  is given by the matrix of the position vector gradients  $\mathbf{J}^e$ . These kinematic relationships are defined for an arbitrary element  $d\mathbf{x}$  as

$$d\mathbf{r} = \mathbf{J}d\mathbf{x}, \quad d\mathbf{r} = \mathbf{J}^e d\mathbf{r}^p, \quad d\mathbf{r}^p = \mathbf{J}^p d\mathbf{x} \quad (8.82)$$

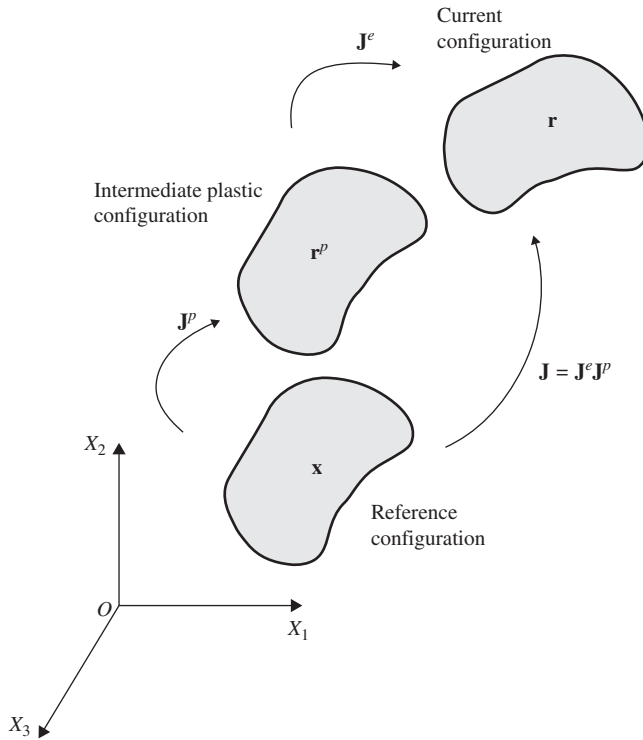


**Figure 8.1** Intermediate plastic configuration

From these equations, it is clear that

$$\mathbf{J} = \mathbf{J}^e \mathbf{J}^p \quad (8.83)$$

This equation is the *multiplicative decomposition of the matrix of position vector gradients* into an elastic part  $\mathbf{J}^e$  and a plastic part  $\mathbf{J}^p$ .

Using the multiplicative decomposition, strain measures that are independent of the rigid-body displacements can be defined. For example, the following right Cauchy–Green strain tensors for the total, elastic, and plastic deformations can be defined as

$$\mathbf{C}_r = \mathbf{J}^T \mathbf{J}, \quad \mathbf{C}_r^e = \mathbf{J}^{eT} \mathbf{J}^e, \quad \mathbf{C}_r^p = \mathbf{J}^{pT} \mathbf{J}^p \quad (8.84)$$

These tensors are often used in the formulation of the constitutive equations of plastic materials. Because  $\mathbf{C}_r$  measures the total strains and  $\mathbf{C}_r^p$  measures the plastic strains, both tensors are required in order to completely describe the current state of the material. Using the preceding equation, an elastic Green–Lagrange strain tensor that measures the elastic deformation from the stress-free intermediate plastic configuration to the current configuration can be defined as

$$\boldsymbol{\varepsilon}^e = \frac{1}{2}(\mathbf{C}_r^e - \mathbf{I}) \quad (8.85)$$

Under a superimposed rigid-body rotation from the current configuration, the final matrix of the position vector gradients from the stress-free intermediate plastic configuration is  $\tilde{\mathbf{J}}^e = \mathbf{A} \mathbf{J}^e$ , where  $\mathbf{A}$  is the rotation matrix. It follows that  $\boldsymbol{\varepsilon}^e$  is invariant under and is not affected by the rigid-body rotation, a property similar to that of the second Piola–Kirchhoff stress tensor as discussed in Chapter 3.

For isotropic materials, it is sometimes simpler to develop the constitutive equations in the current configuration using the elastic left Cauchy–Green tensor given as

$$\mathbf{C}_l^e = \mathbf{J}^e \mathbf{J}^{eT} = \mathbf{J}(\mathbf{J}^p)^{-1} (\mathbf{J}^p)^{-1T} \mathbf{J}^T = \mathbf{J}(\mathbf{C}_r^p)^{-1} \mathbf{J}^T \quad (8.86)$$

It can be shown that the potential function used in a hyperelastic model can be written in terms of the invariants of  $\mathbf{C}_l^e$ .

### Hyperelastic Potential

In the case of large deformations, it is important to distinguish between different stress and strain measures. Associated with the elastic strain tensor  $\boldsymbol{\varepsilon}^e$ , one can define the second Piola–Kirchhoff stress tensor  $\boldsymbol{\sigma}_{p2}^e$  as the pullback of the Kirchhoff stress tensor  $\boldsymbol{\sigma}_K$  as

$$\boldsymbol{\sigma}_{p2}^e = \mathbf{J}^{e^{-1}} \boldsymbol{\sigma}_K \mathbf{J}^{e^{-1T}} \quad (8.87)$$

Kirchhoff stress is used here instead of Cauchy stress because Truesdell rate of Kirchhoff stress is the push-forward of the rate of the second Piola–Kirchhoff stress as demonstrated in Chapter 3. Recall that Kirchhoff stress tensor differs from Cauchy stress tensor by a scalar multiplier, which is the determinant of the matrix of the position vector gradients.

For the hyperelastic material plasticity model discussed in this section, it is assumed that the stress–strain relationships can be obtained from a strain-energy function formulated relative to the intermediate plastic configuration. Using this assumption, the second Piola – Kirchhoff stress tensor can be derived from an energy potential function  $U^e$  as

$$\sigma_{P2}^e = \frac{\partial U^e(\epsilon^e)}{\partial \epsilon^e} = 2 \frac{\partial U^e(C_r^e)}{\partial C_r^e} \quad (8.88)$$

Taking the derivatives of this equation with respect to time, one obtains

$$\dot{\sigma}_{P2}^e = \frac{\partial^2 U^e(\epsilon^e)}{\partial \epsilon^e \partial \epsilon^e} : \dot{\epsilon}^e = \mathbf{E}^e : \dot{\epsilon}^e \quad (8.89)$$

where  $\mathbf{E}^e$  is the matrix of elastic coefficients that relates the rate of the second Piola – Kirchhoff stress tensor  $\sigma_{P2}^e$  to the rate of the elastic Green–Lagrange strain tensor  $\epsilon^e$ . Note that both  $\sigma_{P2}^e$  and  $\epsilon^e$  are invariant under a superimposed rigid-body motion. Therefore, using these two tensors ensures that the elastic response is objective. The preceding equation also shows that  $\mathbf{E}^e$  does not change under a rigid-body rotation and, therefore, the elastic moduli can be anisotropic, unlike the case of hypoelastic models.

### Rate of Deformation Tensors

In the hyperelastic – plastic formulation discussed in this section, the plasticity equations are expressed in terms of the rate of deformation tensors defined in the intermediate plastic configuration (Simo and Hughes, 1998; Belytschko et al., 2000). In order to determine expressions for these tensors, the matrix of velocity gradients is written as

$$\mathbf{L} = \dot{\mathbf{J}}\mathbf{J}^{-1} = \left\{ \frac{d}{dt}(\mathbf{J}^e \mathbf{J}^p) \right\} (\mathbf{J}^e \mathbf{J}^p)^{-1} = \dot{\mathbf{J}}^e \mathbf{J}^{e-1} + \mathbf{J}^e \dot{\mathbf{J}}^p \mathbf{J}^{p-1} \mathbf{J}^{e-1} \quad (8.90)$$

This equation can be written as the sum of elastic and plastic parts as

$$\mathbf{L} = \mathbf{L}^e + \mathbf{L}^p \quad (8.91)$$

where

$$\mathbf{L}^e = \dot{\mathbf{J}}^e \mathbf{J}^{e-1}, \quad \mathbf{L}^p = \mathbf{J}^e \dot{\mathbf{J}}^p \mathbf{J}^{p-1} \mathbf{J}^{e-1} \quad (8.92)$$

This equation shows that the elastic part  $\mathbf{L}^e$  has the usual form of the matrix of the velocity gradients expressed in terms of  $\mathbf{J}^e$  instead of  $\mathbf{J}$ , whereas the plastic part  $\mathbf{L}^p$  is pushed forward by  $\mathbf{J}^e$ . One can define the symmetric and the skew-symmetric parts of  $\mathbf{L}^e$  and  $\mathbf{L}^p$  as follows:

$$\left. \begin{aligned} \mathbf{D}^e &= \frac{1}{2} (\mathbf{L}^e + \mathbf{L}^{eT}), & \mathbf{W}^e &= \frac{1}{2} (\mathbf{L}^e - \mathbf{L}^{eT}) \\ \mathbf{D}^p &= \frac{1}{2} (\mathbf{L}^p + \mathbf{L}^{pT}), & \mathbf{W}^p &= \frac{1}{2} (\mathbf{L}^p - \mathbf{L}^{pT}) \end{aligned} \right\} \quad (8.93)$$



The velocity gradient  $\mathbf{L}$  can be pulled back by  $\mathbf{J}^e$  to the intermediate plastic configuration defining the velocity gradient  $\bar{\mathbf{L}}$  as follows:

$$\bar{\mathbf{L}} = \mathbf{J}^{e^{-1}} \mathbf{L} \mathbf{J}^e = \mathbf{J}^{e^{-1}} \dot{\mathbf{J}}^e + \dot{\mathbf{J}}^p \mathbf{J}^{p^{-1}} = \bar{\mathbf{L}}^e + \bar{\mathbf{L}}^p \quad (8.94)$$

In this equation,

$$\bar{\mathbf{L}}^e = \mathbf{J}^{e^{-1}} \dot{\mathbf{J}}^e, \quad \bar{\mathbf{L}}^p = \dot{\mathbf{J}}^p \mathbf{J}^{p^{-1}} \quad (8.95)$$

are the elastic and plastic parts of  $\bar{\mathbf{L}}$ . One can also obtain  $\bar{\mathbf{L}}^p$  using the elementary definition of Equation 82 as  $\bar{\mathbf{L}}^p = \partial \mathbf{v}^p / \partial \mathbf{r}^p = (\partial \mathbf{v}^p / \partial \mathbf{x})(\partial \mathbf{x} / \partial \mathbf{r}^p) = \dot{\mathbf{J}}^p \mathbf{J}^{p^{-1}}$ , where  $\mathbf{v}^p = d\mathbf{r}^p/dt$ .

Similarly, the following symmetric rate of deformation tensors can be defined as the pullback of  $\mathbf{D}$ ,  $\mathbf{D}^e$ , and  $\mathbf{D}^p$  by  $\mathbf{J}^e$  to the intermediate plastic configuration (Belytschko et al., 2000):

$$\left. \begin{aligned} \bar{\mathbf{D}} &= \mathbf{J}^{e^T} \mathbf{D} \mathbf{J}^e = \frac{1}{2} \left( \mathbf{C}_r^e \bar{\mathbf{L}} + \bar{\mathbf{L}}^T \mathbf{C}_r^e \right) \\ \bar{\mathbf{D}}^e &= \mathbf{J}^{e^T} \mathbf{D}^e \mathbf{J}^e = \frac{1}{2} \left( \mathbf{C}_r^e \bar{\mathbf{L}}^e + \bar{\mathbf{L}}^{e^T} \mathbf{C}_r^e \right) \\ \bar{\mathbf{D}}^p &= \mathbf{J}^{e^T} \mathbf{D}^p \mathbf{J}^e = \frac{1}{2} \left( \mathbf{C}_r^e \bar{\mathbf{L}}^p + \bar{\mathbf{L}}^{p^T} \mathbf{C}_r^e \right) \end{aligned} \right\} \quad (8.96)$$

Note that by using these definitions, one has  $\bar{\mathbf{D}} = \bar{\mathbf{D}}^e + \bar{\mathbf{D}}^p$ . Because  $\boldsymbol{\varepsilon}^e = (1/2)(\mathbf{C}_r^e - \mathbf{I})$ , one has

$$\dot{\boldsymbol{\varepsilon}}^e = \frac{1}{2} \dot{\mathbf{C}}_r^e = \frac{1}{2} \left( \dot{\mathbf{J}}^{e^T} \mathbf{J}^e + \mathbf{J}^{e^T} \dot{\mathbf{J}}^e \right) \quad (8.97)$$

This equation, upon using the previously given definitions of  $\bar{\mathbf{D}}^e$  (Equation 96),  $\mathbf{C}_r^e$  (Equation 84), and  $\bar{\mathbf{L}}^e$  (Equation 95), leads to

$$\dot{\boldsymbol{\varepsilon}}^e = \frac{1}{2} \dot{\mathbf{C}}_r^e = \bar{\mathbf{D}}^e \quad (8.98)$$

Therefore, the stress rate  $\dot{\boldsymbol{\sigma}}_{p2}^e$  can be written using the relationship  $\dot{\boldsymbol{\sigma}}_p^e = \mathbf{E}^e : \dot{\boldsymbol{\varepsilon}}^e$  presented previously in this section for hyperelastic materials (Equation 89) as

$$\dot{\boldsymbol{\sigma}}_{p2}^e = \mathbf{E}^e : \bar{\mathbf{D}}^e = \mathbf{E}^e : (\bar{\mathbf{D}} - \bar{\mathbf{D}}^p) \quad (8.99)$$

This equation, which takes a simple form as the result of using the definitions of Equation 96, will be used to define the elastic–plastic tangent moduli. It is important, however, to point out that the use of the additive decomposition of rates of deformation measures does not impose a restriction on the applicability of the formulation presented in this section to large deformation problems. This argument is similar to the one used when dealing with rotations. Although finite rotations cannot be added, the angular velocities can be added. Recall that the angular velocities are not in general the time derivatives of orientation parameters. Similarly, some of the rates of the deformation measures are also not in general exact differentials.

## Flow Rule and Hardening Law

In the case of the large deformations, the elastic domain can be defined in terms of the stresses and the internal plasticity variables as

$$f(\boldsymbol{\sigma}_{p2}^e, \mathbf{q}) \leq 0 \quad (8.100)$$

In this equation,  $\mathbf{q}$  is a set of internal variables. Because  $\boldsymbol{\sigma}_{p2}^e$  is invariant under a superimposed rigid-body rotation, objectivity imposes no restrictions on the yield function allowing for the use of anisotropic plastic model.

The general *nonassociative model flow rule and hardening law* are defined as

$$\left. \begin{aligned} \bar{\mathbf{L}}^p &= \gamma \mathbf{g}(\boldsymbol{\sigma}_{p2}^e, \mathbf{q}) \\ \dot{\mathbf{q}} &= -\gamma \mathbf{h}(\boldsymbol{\sigma}_{p2}^e, \mathbf{q}) \end{aligned} \right\} \quad (8.101)$$

where  $\mathbf{g}$  and  $\mathbf{h}$  are prescribed functions. Note that, because of the definition of  $\bar{\mathbf{L}}^p$ ,  $\mathbf{g}$  is a tensor defined in the intermediate plastic configuration. In the flow rule,  $\bar{\mathbf{L}}^p$  is used instead of the plastic part of the rate of deformation tensor  $\mathbf{D}^p$  as it is the case in some hypoelastic–plastic models.

The *Kuhn–Tucker loading and unloading complementarity condition* can be written as

$$\gamma \geq 0, \quad f(\boldsymbol{\sigma}_{p2}^e, \mathbf{q}) \leq 0, \quad \gamma f(\boldsymbol{\sigma}_{p2}^e, \mathbf{q}) = 0 \quad (8.102)$$

The *consistency condition* is

$$\gamma \dot{f}(\boldsymbol{\sigma}_{p2}^e, \mathbf{q}) = 0 \quad (8.103)$$

The consistency condition  $\dot{f} = 0$  can be used to determine the consistency parameter as follows:

$$\gamma = \frac{f_{\boldsymbol{\sigma}_{p2}^e} : \mathbf{E}^e : \bar{\mathbf{D}}}{f_{\boldsymbol{\sigma}_{p2}^e} : \mathbf{E}^e : \mathbf{g}_s + f_{\mathbf{q}} : \mathbf{h}} \quad (8.104)$$

In this equation,

$$\mathbf{g}_s = \frac{1}{2}(\mathbf{C}_r^e \mathbf{g} + \mathbf{g}^T \mathbf{C}_r^e) \quad (8.105)$$

is obtained from the definition of  $\bar{\mathbf{L}}^p$  in the flow rule. Note also that

$$\bar{\mathbf{D}}^p = \gamma \mathbf{g}_s \quad (8.106)$$

Substituting these results into the constitutive equations (Equation 99), one obtains

$$\boldsymbol{\sigma}_{p2}^e = \mathbf{E}^e : (\bar{\mathbf{D}} - \bar{\mathbf{D}}^p) = \mathbf{E}^e : (\bar{\mathbf{D}} - \gamma \mathbf{g}_s) \quad (8.107)$$

This equation can be written as

$$\boldsymbol{\sigma}_{p2}^e = \mathbf{E}^{ep} : \bar{\mathbf{D}} \quad (8.108)$$

where  $\mathbf{E}^{ep}$  is the tensor of *tangent elastoplastic moduli* given by

$$\mathbf{E}^{ep} = \begin{cases} \mathbf{E}^e & \gamma = 0 \\ \mathbf{E}^e - \frac{(\mathbf{E}^e : \mathbf{g}_s) \otimes (\mathbf{E}^e : f_{\sigma_{p2}}^e)}{f_{\sigma_{p2}}^e : \mathbf{E}^e : \mathbf{g}_s + f_q : \mathbf{h}} & \gamma > 0 \end{cases} \quad (8.109)$$

In the general case of nonassociative plasticity, the tangent elastic–plastic moduli tensor is not necessarily symmetric. It is symmetric in the case of associative plasticity. It is important to reiterate that the objectivity requirements are automatically satisfied for hyperelastic–plastic formulations because the elastic strains and stresses used in this formulation are invariant under a superimposed rigid-body motion. In order to demonstrate this fact, one follows a procedure similar to the procedure used in the preceding chapter by assuming  $\mathbf{A}$  to be a time-dependent rigid-body rotation from the current configuration. Note that the reference and intermediate plastic configurations are not affected by this rotation. It follows that the new matrix of position vector gradients is given by  $\mathbf{A}\mathbf{J}$ , whereas the elastic part will be  $\mathbf{A}\mathbf{J}^e$  and the plastic part will remain  $\mathbf{J}^p$ . Consequently, the elastic Lagrangian strain  $\boldsymbol{\epsilon}^e$  will remain the same. Consequently, the stresses are not affected by the rotation because they can be directly evaluated using Equation 88 and no integration of stress rate is required.

### Example 8.9

Show that the consistency parameter of Equation 14 can be written as

$$\gamma = \frac{f_{\sigma_{p2}}^e : \mathbf{E}^e : \bar{\mathbf{D}}}{f_{\sigma_{p2}}^e : \mathbf{E}^e : \mathbf{g}_s + f_q : \mathbf{h}}$$

*Solution:* In the case of plastic deformation

$$f(\sigma_{p2}^e, \mathbf{q}) = 0$$

Differentiating this equation with respect to time, one obtains

$$f_{\sigma_{p2}}^e : \dot{\sigma}_{p2}^e + f_q : \dot{\mathbf{q}} = 0$$

From Equation 17, one has

$$\dot{\sigma}_{p2}^e = \mathbf{E}^e : \bar{\mathbf{D}} - \gamma \mathbf{E}^e : \mathbf{g}_s$$

where  $\mathbf{g}_s$  is defined by Equation 105. Using Equation 101, one can write

$$\dot{\mathbf{q}} = -\gamma \mathbf{h}$$

By substituting the values of  $\dot{\boldsymbol{\sigma}}_{p2}^e$  and  $\dot{\mathbf{q}}$  into the differentiated form of the yield function one obtains

$$f_{\boldsymbol{\sigma}_{p2}^e} : \mathbf{E}^e : \bar{\mathbf{D}} - \gamma f_{\boldsymbol{\sigma}_{p2}^e} : \mathbf{E}^e : \mathbf{g}_s - \gamma f_{\mathbf{q}} : \mathbf{h} = 0$$

This equation defines the consistency parameter as

$$\gamma = \frac{f_{\boldsymbol{\sigma}_{p2}^e} : \mathbf{E}^e : \bar{\mathbf{D}}}{f_{\boldsymbol{\sigma}_{p2}^e} : \mathbf{E}^e : \mathbf{g}_s + f_{\mathbf{q}} : \mathbf{h}}$$

### Example 8.10

Show that the tensor of tangent elastoplastic moduli in the case of the plasticity formulation discussed in this section can be written as

$$\mathbf{E}^{ep} = \begin{cases} \mathbf{E}^e & \gamma = 0 \\ \mathbf{E}^e - \frac{(\mathbf{E}^e : \mathbf{g}_s) \otimes (\mathbf{E}^e : f_{\boldsymbol{\sigma}_{p2}^e})}{f_{\boldsymbol{\sigma}_{p2}^e} : \mathbf{E}^e : \mathbf{g}_s + f_{\mathbf{q}} : \mathbf{h}} & \gamma > 0 \end{cases}$$

*Solution:* From Equation 107, one has

$$\dot{\boldsymbol{\sigma}}_{p2}^e = \mathbf{E}^e : \bar{\mathbf{D}} - \gamma \mathbf{E}^e : \mathbf{g}_s$$

If  $\gamma = 0$ , one has the elastic stress–strain relationship, which can be written in the rate form as

$$\dot{\boldsymbol{\sigma}}_{p2}^e = \mathbf{E}^e : \bar{\mathbf{D}}$$

On the other hand, if  $\gamma > 0$ , one can use the value of  $\gamma$  calculated from Equation 104, which leads to the following equation:

$$\dot{\boldsymbol{\sigma}}_{p2}^e = \mathbf{E}^e : \bar{\mathbf{D}} - \left( \frac{f_{\boldsymbol{\sigma}_{p2}^e} : \mathbf{E}^e : \bar{\mathbf{D}}}{f_{\boldsymbol{\sigma}_{p2}^e} : \mathbf{E}^e : \mathbf{g}_s + f_{\mathbf{q}} : \mathbf{h}} \right) \mathbf{E}^e : \mathbf{g}_s$$

This defines the components of the second-order tensor  $\dot{\boldsymbol{\sigma}}_{p2}^e$  as

$$(\dot{\boldsymbol{\sigma}}_{p2}^e)_{ij} = \sum_{k,l=1}^3 e_{ijkl}^e \bar{D}_{kl} - \sum_{k,l,w,x,u,v=1}^3 \left( \frac{(f_{\boldsymbol{\sigma}_{p2}^e})_{wx} e_{wxkl}^e \bar{D}_{kl}}{f_{\boldsymbol{\sigma}_{p2}^e} : \mathbf{E}^e : \mathbf{g}_s + f_{\mathbf{q}} : \mathbf{h}} \right) (e_{ijuv}^e (\mathbf{g}_s)_{uv})$$

This equation can be written as

$$(\dot{\boldsymbol{\sigma}}_{p2}^e)_{ij} = \sum_{k,l=1}^3 \left( e_{ijkl}^e - \frac{\left( \sum_{u,v=1}^3 e_{ijuv}^e (\mathbf{g}_s)_{uv} \right) \left( \sum_{w,x=1}^3 (f_{\boldsymbol{\sigma}_{p2}^e})_{wx} e_{wxkl}^e \right)}{f_{\boldsymbol{\sigma}_{p2}^e} : \mathbf{E}^e : \mathbf{g}_s + f_{\mathbf{q}} : \mathbf{h}} \right) \bar{D}_{kl}$$

which defines the second-order tensor  $\dot{\boldsymbol{\sigma}}_{p2}^e$  as

$$\dot{\boldsymbol{\sigma}}_{p2}^e = \left( \mathbf{E}^e - \frac{(\mathbf{E}^e : \mathbf{g}_s) \otimes (f_{\boldsymbol{\sigma}_{p2}^e} : \mathbf{E}^e)}{f_{\boldsymbol{\sigma}_{p2}^e} : \mathbf{E}^e : \mathbf{g}_s + f_{\mathbf{q}} : \mathbf{h}} \right) : \bar{\mathbf{D}} = \mathbf{E}^{ep} : \bar{\mathbf{D}}$$

From this equation, one can define

$$\mathbf{E}^{ep} = \left( \mathbf{E}^e - \frac{(\mathbf{E}^e : \mathbf{g}_s) \otimes (f_{\boldsymbol{\sigma}_{p2}^e} : \mathbf{E}^e)}{f_{\boldsymbol{\sigma}_{p2}^e} : \mathbf{E}^e : \mathbf{g}_s + f_{\mathbf{q}} : \mathbf{h}} \right)$$

## Numerical Solution

It is assumed that the matrix of position vector gradients  $\mathbf{J}$  and the Green–Lagrange strain tensor  $\boldsymbol{\varepsilon}$  are known. It follows then that the matrix  $\mathbf{J}^e$  can be expressed in terms of the matrix  $\mathbf{J}^p$  as  $\mathbf{J}^e = \mathbf{J}\mathbf{J}^{p-1}$ . Therefore, it can be shown that  $\bar{\mathbf{L}}^p$ ,  $\bar{\mathbf{D}}$ , and  $\bar{\mathbf{D}}^p$  in Equations 99 and 101 can be expressed in terms of  $\mathbf{J}^p$ . As a result, Equations 99–101 represent a set of four systems of equations that can be solved for the unknowns  $\boldsymbol{\sigma}_{p2}^e$ ,  $\mathbf{J}^p$ ,  $\mathbf{q}$ , and  $\gamma$ . To this end, the implicit backward Euler method can be used to convert the system of differential equations to a set of nonlinear algebraic equations that can be solved using the iterative Newton–Raphson method as described previously in this chapter. It is important to point out, however, that  $\mathbf{J}^p$  is not necessarily symmetric, and  $\bar{\mathbf{L}}^p$ ,  $\bar{\mathbf{D}}$ , and  $\bar{\mathbf{D}}^p$  in the general theory presented in this section are not simple functions of  $\mathbf{J}^p$ . For this reason, the numerical solution of the general equations of the hyperelastic–plastic model can be less efficient compared with cases in which a closed-form solution can be obtained.

### Example 8.11

Show that  $\bar{\mathbf{L}}^p$ ,  $\bar{\mathbf{D}}$ , and  $\bar{\mathbf{D}}^p$  in Equations 99 and 101 can be expressed in terms of  $\mathbf{J}^p$ .

*Solution:* From Equation 95, one can write  $\bar{\mathbf{L}}^p$  in terms of  $\mathbf{J}^p$  as follows:

$$\bar{\mathbf{L}}^p = \mathbf{j}^p \mathbf{J}^{p-1}$$

This equation shows that  $\bar{\mathbf{L}}^p$  can be written in terms of  $\mathbf{J}^p$ .

From Equation 96, one can write  $\bar{\mathbf{D}}$  as follows:

$$\bar{\mathbf{D}} = \mathbf{J}^{eT} \mathbf{D} \mathbf{J}^e$$

Note that one can write  $\mathbf{J}^e$  in terms of  $\mathbf{J}^p$  as follows:

$$\mathbf{J}^e = \mathbf{J} \mathbf{J}^{p-1}$$

It follows that

$$\mathbf{J}^{eT} = (\mathbf{J}^{p-1})^T \mathbf{J}^T$$

The rate of deformation tensor is given by the equation

$$\mathbf{D} = \frac{1}{2}(\mathbf{L} + \mathbf{L}^T)$$

From Equation 90, one has  $\mathbf{L} = \dot{\mathbf{J}} \mathbf{J}^{-1}$ . It follows that

$$\mathbf{L}^T = (\mathbf{J}^{-1})^T \dot{\mathbf{J}}^T$$

One can then write  $\bar{\mathbf{D}}$  in terms of  $\mathbf{J}^p$  as follows:

$$\bar{\mathbf{D}} = \mathbf{J}^{eT} \mathbf{D} \mathbf{J}^e = \frac{1}{2} \mathbf{J}^{eT} (\mathbf{L} + \mathbf{L}^T) \mathbf{J}^e = \frac{1}{2} (\mathbf{J}^{p-1})^T \mathbf{J}^T (\dot{\mathbf{J}} \mathbf{J}^{-1} + (\mathbf{J}^{-1})^T \dot{\mathbf{J}}^T) \mathbf{J} \mathbf{J}^{p-1}$$

This equation can be simplified and written as follows:

$$\bar{\mathbf{D}} = \frac{1}{2} ((\mathbf{J}^{p-1})^T \mathbf{J}^T \dot{\mathbf{J}} \mathbf{J}^{p-1} + (\mathbf{J}^{p-1})^T \mathbf{J}^T \dot{\mathbf{J}}^T \mathbf{J} \mathbf{J}^{p-1}) = \frac{1}{2} (\mathbf{J}^{p-1})^T (\mathbf{J}^T \dot{\mathbf{J}} + \dot{\mathbf{J}}^T \mathbf{J}) \mathbf{J}^{p-1}$$

This equation shows that  $\bar{\mathbf{D}}$  can be expressed in terms of  $\mathbf{J}^p$ .

From Equation 96, one has

$$\bar{\mathbf{D}}^p = \frac{1}{2} (\mathbf{C}_r^e \bar{\mathbf{L}}^p + \bar{\mathbf{L}}^{pT} \mathbf{C}_r^e)$$

Using the definition of  $\mathbf{C}_r^e$ , one can write

$$\mathbf{C}_r^e = \mathbf{J}^{eT} \mathbf{J}^e = (\mathbf{J}^{p-1})^T \mathbf{J}^T \mathbf{J} \mathbf{J}^{p-1}$$

From Equation 95, one also has

$$\bar{\mathbf{L}}^{pT} = (\dot{\mathbf{J}}^p \mathbf{J}^{p-1})^T = (\mathbf{J}^{p-1})^T \dot{\mathbf{J}}^{pT}$$

Using the preceding three equations, one can then write  $\bar{\mathbf{D}}^p$  in terms of  $\mathbf{J}^p$  as follows:

$$\bar{\mathbf{D}}^p = \frac{1}{2} ((\mathbf{J}^{p-1})^T \mathbf{J}^T \mathbf{J} \mathbf{J}^{p-1} \dot{\mathbf{J}}^p \mathbf{J}^{p-1} + (\mathbf{J}^{p-1})^T \dot{\mathbf{J}}^{pT} (\mathbf{J}^{p-1})^T \mathbf{J}^T \mathbf{J} \mathbf{J}^{p-1})$$

### Rate-Dependent Plasticity

In the case of *rate-dependent plasticity*,  $\gamma$  is defined as

$$\gamma = \frac{\phi(\boldsymbol{\sigma}_{P2}^e, \mathbf{q})}{\eta} \quad (8.110)$$

In this equation,  $\eta$  is the viscosity and  $\phi$  is an *overstress function*. The relationship between the stress and rate of deformation tensor can be written as

$$\dot{\boldsymbol{\sigma}}_{P2}^e = \mathbf{E}^e : (\bar{\mathbf{D}} - \gamma \mathbf{g}_s) = \mathbf{E}^e : \left( \bar{\mathbf{D}} - \frac{\phi}{\eta} \mathbf{g}_s \right) \quad (8.111)$$

More discussion on the rate-dependent plasticity formulations can be found in the reference by Simo and Hughes (1998).

## 8.7 HYPERELASTIC-PLASTIC $J_2$ FLOW THEORY

In this section, the hyperelastic-plastic formulation based on the  $J_2$  flow theory is discussed. The use of this theory leads to a simple integration algorithm, which can be considered as an extension of the radial return mapping algorithm used for the infinitesimal  $J_2$  flow theory. The development of the formulation is illustrated using a model based on the Neo-Hookean material that is suited for the analysis of large deformation. The main assumptions used in the  $J_2$  flow theory as compared to the general theory presented in the preceding section are that plastic spin is zero and the yield condition is a function of the deviatoric part of the stress only and does not depend on the hydrostatic pressure. Using these two assumptions, the formulation presented in the preceding section can be systematically specialized to the case of the  $J_2$  flow theory.

For the Neo-Hookean material, the energy potential function can be written in the intermediate plastic configuration as

$$U^e = \frac{\mu}{2}(I_1^e - 3) - \mu \ln J^e + \frac{\lambda^e}{2}(\ln J^e)^2 \quad (8.112)$$

where  $I_1^e$  is the first principal invariant of the tensor  $\mathbf{C}_r^e$ ,  $J^e = |\mathbf{J}^e| = \det(\mathbf{J}^e)$ , and  $\lambda^e$  and  $\mu$  are Lamé's constants. The second Piola-Kirchhoff stress tensor is obtained as described in Chapter 4 as

$$\boldsymbol{\sigma}_{P2}^e = \mu(\mathbf{I} - \mathbf{C}_r^{e-1}) + \lambda^e(\ln J^e)\mathbf{C}_r^{e-1} \quad (8.113)$$

This equation can be used to obtain the following rate form of hyperelasticity:

$$\dot{\boldsymbol{\sigma}}_{P2}^e = \mathbf{E}^e : \bar{\mathbf{D}}^e = \mathbf{E}^e : (\bar{\mathbf{D}} - \bar{\mathbf{D}}^p) \quad (8.114)$$

The deviatoric stress tensor associated with the intermediate plastic configuration can also be defined as described in Chapter 4 as

$$\mathbf{S}_{P2}^e = \boldsymbol{\sigma}_{P2}^e - \frac{1}{3}(\boldsymbol{\sigma}_{P2}^e : \mathbf{C}_r^e)\mathbf{C}_r^{e-1} \quad (8.115)$$

The elastic domain is defined by the von Mises yield surface

$$f(\mathbf{S}_{p2}^e, \mathbf{q}) \leq 0 \quad (8.116)$$

In the  $J_2$  flow theory presented in this section, it is assumed that the plastic spin  $\bar{\mathbf{W}}^p$  is identically equal to zero. Therefore, the flow rule can be written in terms of the symmetric part  $\bar{\mathbf{D}}^p$ , instead of  $\bar{\mathbf{L}}^p$ , using the assumptions of associative plasticity as (Belytschko et al., 2000)

$$\bar{\mathbf{D}}^p = \gamma \mathbf{g}_s = \gamma \left( \frac{3}{2\sigma_e} \mathbf{C}_r^e \mathbf{S}_{p2}^e \mathbf{C}_r^e \right) \quad (8.117)$$

In this equation,  $\mathbf{g}_s$  is obtained using Equation 105 where  $\mathbf{g}$  is defined in the intermediate plastic configuration, and  $\sigma_e$  is the *von Mises effective stress* defined as

$$\sigma_e = \sqrt{\frac{3}{2} (\mathbf{S}_{p2}^e \mathbf{C}_r^e) : (\mathbf{S}_{p2}^e \mathbf{C}_r^e)^T} \quad (8.118)$$

Using the equations presented in this section, the elastoplastic tangent moduli can be obtained by substituting in the form presented in the preceding section.

### Example 8.12

Determine the tensor of the tangent elastoplastic moduli in the case of the  $J_2$  flow theory discussed in this section.

*Solution:* In the case of plastic deformation, one has

$$f(\mathbf{S}_{p2}^e, \mathbf{q}) = 0$$

One can use Equation 115 to write  $\mathbf{S}_{p2}^e$  in terms of  $\boldsymbol{\sigma}_{p2}^e$  and  $\mathbf{C}_r^e$ . In this case, the yield function can be written as

$$f(\boldsymbol{\sigma}_{p2}^e, \mathbf{C}_r^e, \mathbf{q}) = 0$$

By differentiating this equation with respect to time, one obtains

$$f_{\boldsymbol{\sigma}_{p2}^e} : \dot{\boldsymbol{\sigma}}_{p2}^e + f_{\mathbf{C}_r^e} : \dot{\mathbf{C}}_r^e + f_{\mathbf{q}} : \dot{\mathbf{q}} = 0$$

From Equations 114 and 106, one has

$$\dot{\boldsymbol{\sigma}}_{p2}^e = \mathbf{E}^e : \bar{\mathbf{D}} - \mathbf{E}^e : \bar{\mathbf{D}}^p = \mathbf{E}^e : \bar{\mathbf{D}} - \gamma \mathbf{E}^e : \mathbf{g}_s$$

Using Equations 98 and 106, one has

$$\dot{\mathbf{C}}_r^e = 2\bar{\mathbf{D}}^e = 2(\bar{\mathbf{D}} - \bar{\mathbf{D}}^p) = 2\bar{\mathbf{D}} - 2\gamma \mathbf{g}_s$$

From Equation 101, one has

$$\dot{\mathbf{q}} = -\gamma \mathbf{h}$$



Substituting the preceding three equations for  $\dot{\boldsymbol{\sigma}}_{p2}^e$ ,  $\dot{\mathbf{C}}_r^e$ , and  $\dot{\mathbf{q}}$  into the differentiated form of the yield function, one obtains

$$f_{\boldsymbol{\sigma}_{p2}^e} : \mathbf{E}^e : \bar{\mathbf{D}} - \gamma f_{\boldsymbol{\sigma}_{p2}^e} : \mathbf{E}^e : \mathbf{g}_s + 2f_{\mathbf{C}_r^e} : \bar{\mathbf{D}} - 2\gamma f_{\mathbf{C}_r^e} : \mathbf{g}_s - \gamma f_{\mathbf{q}} : \mathbf{h} = 0$$

One can then write

$$\gamma = \frac{(f_{\boldsymbol{\sigma}_{p2}^e} : \mathbf{E}^e + 2f_{\mathbf{C}_r^e}) : \bar{\mathbf{D}}}{(f_{\boldsymbol{\sigma}_{p2}^e} : \mathbf{E}^e + 2f_{\mathbf{C}_r^e}) : \mathbf{g}_s + f_{\mathbf{q}} : \mathbf{h}}$$

If  $\gamma = 0$ , one has an elastic state and Equation 114 leads to

$$\dot{\boldsymbol{\sigma}}_{p2}^e = \mathbf{E}^e : \bar{\mathbf{D}}$$

On the other hand, if  $\gamma > 0$ , one has a plastic state. In this case, the stress–strain relationship can be written as follows:

$$\dot{\boldsymbol{\sigma}}_{p2}^e = \mathbf{E}^e : \bar{\mathbf{D}} - \left\{ \frac{(f_{\boldsymbol{\sigma}_{p2}^e} : \mathbf{E}^e + 2f_{\mathbf{C}_r^e}) : \bar{\mathbf{D}}}{(f_{\boldsymbol{\sigma}_{p2}^e} : \mathbf{E}^e + 2f_{\mathbf{C}_r^e}) : \mathbf{g}_s + f_{\mathbf{q}} : \mathbf{h}} \right\} (\mathbf{E}^e : \mathbf{g}_s)$$

The components of this tensor can be written as

$$(\dot{\boldsymbol{\sigma}}_{p2}^e)_{ij} = \sum_{k,l=1}^3 e_{ijkl}^e \bar{D}_{kl} - \frac{\sum_{k,l=1}^3 (f_{\boldsymbol{\sigma}_{p2}^e} : \mathbf{E}^e + 2f_{\mathbf{C}_r^e})_{kl} \bar{D}_{kl}}{(f_{\boldsymbol{\sigma}_{p2}^e} : \mathbf{E}^e + 2f_{\mathbf{C}_r^e}) : \mathbf{g}_s + f_{\mathbf{q}} : \mathbf{h}} \sum_{w,x=1}^3 e_{ijwx}^e (\mathbf{g}_s)_{wx}$$

By factoring out  $\bar{D}_{kl}$ , one obtains

$$(\dot{\boldsymbol{\sigma}}_{p2}^e)_{ij} = \sum_{k,l=1}^3 \left( e_{ijkl}^e - \frac{\left( \sum_{w,x=1}^3 e_{ijwx}^e (\mathbf{g}_s)_{wx} \right) (f_{\boldsymbol{\sigma}_{p2}^e} : \mathbf{E}^e + 2f_{\mathbf{C}_r^e})_{kl}}{(f_{\boldsymbol{\sigma}_{p2}^e} : \mathbf{E}^e + 2f_{\mathbf{C}_r^e}) : \mathbf{g}_s + f_{\mathbf{q}} : \mathbf{h}} \right) \bar{D}_{kl}$$

This equation leads to

$$\dot{\boldsymbol{\sigma}}_{p2}^e = \left( \mathbf{E}^e - \frac{(\mathbf{E}^e : \mathbf{g}_s) \otimes (f_{\boldsymbol{\sigma}_{p2}^e} : \mathbf{E}^e + 2f_{\mathbf{C}_r^e})}{(f_{\boldsymbol{\sigma}_{p2}^e} : \mathbf{E}^e + 2f_{\mathbf{C}_r^e}) : \mathbf{g}_s + f_{\mathbf{q}} : \mathbf{h}} \right) : \bar{\mathbf{D}} = \mathbf{E}^{ep} : \bar{\mathbf{D}}$$

where

$$\mathbf{E}^{ep} = \left( \mathbf{E}^e - \frac{(\mathbf{E}^e : \mathbf{g}_s) \otimes (f_{\boldsymbol{\sigma}_{p2}^e} : \mathbf{E}^e + 2f_{\mathbf{C}_r^e})}{(f_{\boldsymbol{\sigma}_{p2}^e} : \mathbf{E}^e + 2f_{\mathbf{C}_r^e}) : \mathbf{g}_s + f_{\mathbf{q}} : \mathbf{h}} \right)$$

**Example 8.13**

In this example, a proof of Equation 117 is provided. To this end, the von Mises yield function can be written in the following form:

$$f = \sqrt{\frac{3}{2} \text{tr}(\boldsymbol{\eta}^2)} - H_i(\alpha)$$

In case of no kinematic hardening, one has

$$\boldsymbol{\eta} = \text{dev}(\boldsymbol{\sigma}_K) = \mathbf{S}_K$$

where  $\mathbf{S}_K$  is the deviatoric part of the Kirchhoff stress tensor. The derivative of the yield function with respect to the Kirchhoff stress can be calculated as follows:

$$f_{\mathbf{S}_K} = \frac{1}{2\sqrt{\frac{3}{2} \text{tr}(\mathbf{S}_K^2)}} \frac{\partial \left( \frac{3}{2} \text{tr}(\mathbf{S}_K^2) \right)}{\partial \mathbf{S}_K} = \frac{\frac{3}{2} \mathbf{S}_K}{\sqrt{\frac{3}{2} \text{tr}(\mathbf{S}_K^2)}}$$

In order to write  $f_{\mathbf{S}_K}$  in terms of  $\mathbf{S}_{p2}^e$ , one can use the following relation:

$$\mathbf{S}_K = \mathbf{J}^e \mathbf{S}_{p2}^e \mathbf{J}^{eT}$$

Therefore, one can write

$$\begin{aligned} \sqrt{\frac{3}{2} \text{tr}(\mathbf{S}_K^2)} &= \sqrt{\frac{3}{2} \text{tr}((\mathbf{J}^e \mathbf{S}_{p2}^e \mathbf{J}^{eT})(\mathbf{J}^e \mathbf{S}_{p2}^e \mathbf{J}^{eT})^T)} \\ &= \sqrt{\frac{3}{2} \text{tr}(\mathbf{J}^e \mathbf{S}_{p2}^e \mathbf{J}^{eT} \mathbf{J}^e \mathbf{S}_{p2}^{eT} \mathbf{J}^{eT})} \end{aligned}$$

Recall that  $\text{tr}(\mathbf{AB}) = \text{tr}(\mathbf{BA})$ . It then follows that

$$\sqrt{\frac{3}{2} \text{tr}(\mathbf{S}_K^2)} = \sqrt{\frac{3}{2} \text{tr}(\mathbf{S}_{p2}^e \mathbf{J}^{eT} \mathbf{J}^e \mathbf{S}_{p2}^{eT} \mathbf{J}^{eT} \mathbf{J}^e)}$$

By using the definition  $\mathbf{C}_r^e = \mathbf{J}^{eT} \mathbf{J}^e$  in the preceding equation, one obtains

$$\sqrt{\frac{3}{2} \text{tr}(\mathbf{S}_K^2)} = \sqrt{\frac{3}{2} \text{tr}(\mathbf{S}_{p2}^e \mathbf{C}_r^e \mathbf{S}_{p2}^{eT} \mathbf{C}_r^e)}$$

The second-order tensor  $\mathbf{S}_{p2}^e$  is symmetric because

$$\mathbf{S}_{p2}^{eT} = (\mathbf{J}^e \mathbf{J}^{e-1} \mathbf{S} \mathbf{J}^{eT-1})^T = \mathbf{J}^e \mathbf{J}^{e-1} \mathbf{S}^T \mathbf{J}^{eT-1} = \mathbf{J}^e \mathbf{J}^{e-1} \mathbf{S} \mathbf{J}^{eT-1} = \mathbf{S}_{p2}^e$$

It follows that

$$\sqrt{\frac{3}{2}\text{tr}(\mathbf{S}_K^2)} = \sqrt{\frac{3}{2}\text{tr}(\mathbf{S}_{p2}^e \mathbf{C}_r^e \mathbf{S}_{p2}^e \mathbf{C}_r^e)} = \sqrt{\frac{3}{2}(\mathbf{S}_{p2}^e \mathbf{C}_r^e) : (\mathbf{S}_{p2}^e \mathbf{C}_r^e)^T}$$

The second-order tensor  $f_{S_K}$  can then be written as

$$f_{S_K} = \frac{\frac{3}{2} \mathbf{J}^e \mathbf{S}_{p2}^e \mathbf{J}^{eT}}{\sqrt{\frac{3}{2}(\mathbf{S}_{p2}^e \mathbf{C}_r^e) : (\mathbf{S}_{p2}^e \mathbf{C}_r^e)^T}} = \frac{3}{2\sigma^e} \mathbf{J}^e \mathbf{S}_{p2}^e \mathbf{J}^{eT}$$

where

$$\sigma^e = \sqrt{\frac{3}{2}(\mathbf{S}_{p2}^e \mathbf{C}_r^e) : (\mathbf{S}_{p2}^e \mathbf{C}_r^e)^T}$$

If the case of associative plasticity is assumed, one has

$$\mathbf{g} = \mathbf{J}^{e-1} f_{S_K} \mathbf{J}^e$$

It follows that

$$\mathbf{g} = \frac{3}{2\sigma^e} \mathbf{S}_{p2}^e \mathbf{C}_r^e$$

From the flow rule,

$$\bar{\mathbf{L}}^p = \gamma \mathbf{g}$$

Using Equation 96, one can write

$$\bar{\mathbf{D}}^p = \frac{1}{2}(\mathbf{C}_r^e \bar{\mathbf{L}}^p + \bar{\mathbf{L}}^{pT} \mathbf{C}_r^e) = \gamma \left( \frac{3}{2\sigma^e} \mathbf{C}_r^e \mathbf{S}_{p2}^e \mathbf{C}_r^e \right)$$

which is the same as Equation 117.

## PROBLEMS

1. Explain the Bauschinger Phenomenon.
2. Define the basic hypotheses on which the theory of plasticity is based.
3. Define the isotropic and kinematic hardening.
4. What is the difference between associative and nonassociative plasticity?
5. What is the difference between the return mapping algorithm and the radial return mapping algorithm?
6. What are the drawbacks of using explicit integration instead of implicit integration to solve the plasticity equations?

7. Outline in detail the steps of a numerical solution of the plasticity equations of the hyperelastic material model discussed in Section 6.
8. Discuss the main assumptions used in the  $J_2$  flow theory for the hyperelastic model presented in Section 7 as compared to the more general model presented in Section 6.
9. Outline in detail the steps of a numerical solution that can be used for the  $J_2$  flow theory for the hyperelastic model presented in Section 7.



## REFERENCES

---

- Abbas, L.K., Rui, X., and Hammoudi, Z.S. (2010) Plate/shell element of variable thickness based on the absolute nodal coordinate formulation. *IMechE Journal of Multibody Dynamics*, **224** (Part K), 127–141.
- Agrawal, O.P. and Shabana, A. (1985) Dynamic analysis of multi-body systems using component modes. *Computers and Structures*, **21** (6), 1303–1312.
- Aris, R. (1962) *Vectors, Tensors, and the Basic Equations of Fluid Mechanics*, Dover Publications, New York.
- Atkinson, K.E. (1978) *An Introduction to Numerical Analysis*, John Wiley & Sons.
- Bathe, K.J. (1996) *Finite Element Procedures*, Prentice Hall, Inc., Englewood Cliffs, New Jersey.
- Bauchau, O.A., Damilano, G., and Theron, N.J. (1995) Numerical integration of nonlinear elastic multi-body systems. *International Journal for Numerical Methods in Engineering*, **38**, 2727–2751.
- Bauchau, O.A. (1998) Computational schemes for flexible, nonlinear multi-body systems. *Multibody System Dynamics*, **2** (2), 169–225.
- Bauchau, O.A., Bottasso, C.L., and Trainelli, L. (2003) Robust integration schemes for flexible multibody systems. *Computer Methods in Applied Mechanics and Engineering*, **192** (3–4), 395–420.

- Bayo, E., García de Jalón, J., and Serna, M.A. (1988) A modified lagrangian formulation for the dynamic analysis of constrained mechanical systems. *Computer Methods in Applied Mechanics and Engineering*, **71**, 183–195.
- Belytschko, T., Liu, W.K., and Moran, B. (2000) *Nonlinear Finite Elements for Continua and Structures*, John Wiley & Sons, New York.
- Berzeri, M. and Shabana, A.A. (2000) Development of simple models for the elastic forces in the absolute nodal coordinate formulation. *Sound and Vibration*, **235** (4), 539–565.
- Berzeri, M. and Shabana, A.A. (2002) Study of the centrifugal stiffening effect using the finite element absolute nodal coordinate formulation. *Multibody System Dynamics*, **7**, 357–387.
- Betsch, P. and Steinmann, E. (2001) Constrained integration of rigid body dynamics. *Computer Methods in Applied Mechanics and Engineering*, **191**, 467–488.
- Betsch, P. and Steinmann, P. (2002a) A DAE approach to flexible multibody dynamics. *Multibody System Dynamics*, **8**, 367–391.
- Betsch, P. and Steinmann, P. (2002b) Frame-indifferent beam finite element based upon the geometrically exact beam theory. *International Journal of Numerical Methods in Engineering*, **54**, 1775–1788.
- Bonet, J. and Wood, R.D. (1997) *Nonlinear Continuum Mechanics for Finite Element Analysis*, Cambridge University Press.
- Boresi, A.P. and Chong, K.P. (2000) *Elasticity in Engineering Mechanics*, Second edn, John Wiley & Sons.
- Bottasso, C.L. and Borri, M. (1997) Energy preserving/decaying schemes for non-linear beam dynamics using the helicoidal approximation. *Computer Methods in Applied Mechanics and Engineering*, **143**, 393–415.
- Bottasso, C.L., Borri, M., and Trainelli, L. (2001a) Integration of elastic multibody systems by invariant conserving/dissipating algorithms. Part I: formulation. *Computer Methods in Applied Mechanics and Engineering*, **190**, 3669–3699.
- Bottasso, C.L., Borri, M., and Trainelli, L. (2001b) Integration of elastic multibody systems by invariant conserving/dissipating algorithms. Part II: numerical schemes and applications. *Computer Methods in Applied Mechanics and Engineering*, **190**, 3701–3733.
- Bridgman, P. (1949) *The Physics of High Pressure*, Bell and Sons, London.
- Campanelli, M., Berzeri, M., and Shabana, A.A. (2000) Performance of the incremental and non-incremental finite element formulations in flexible multibody problems. *ASME Journal of Mechanical Design*, **122** (4), 498–507.
- Cardona, A. and Géradin, M. (1988) A beam finite element non-linear theory with finite rotation. *International Journal for Numerical Methods in Engineering*, **26**, 2403–2438.
- Cardona, A. and Géradin, M. (1989) Time integration of the equations of motion in mechanism analysis. *Computers and Structures*, **33** (3), 801–820.
- Cardona, A. and Géradin, M. (1992) A superelement formulation for mechanism analysis. *Computer Methods in Applied Mechanics and Engineering*, **100**, 1–29.

- Carnahan, B., Luther, H.A., and Wilkes, J.O. (1969) *Applied Numerical Methods*, John Wiley & Sons.
- Cesnik, C.E.S., Hodges, D.H., and Sutyry, V.G. (1996) Cross-sectional analysis of composite beams including large initial twist and curvature effects. *AIAA Journal*, **34** (9), 1913–1920.
- Chung, J. and Hulbert, G.M. (1993) A time integration algorithm for structural dynamics with improved numerical dissipation: the generalized- $\alpha$  method. *Journal of Applied Mechanics*, **60**, 371–375.
- Cook, R.D., Malkus, D.S., and Plesha, M.E. (1989) *Concepts and Applications of Finite Element Analysis*, 3rd edn, John Wiley & Sons.
- Cottrell, J.A., Hughes, T.J.R., and Reali, A. (2007) Studies of refinement and continuity in the isogeometric analysis. *Computational Methods in Applied Mechanical Engineering*, **196**, 4160–4183.
- Crisfield, M.A. (1991) *Nonlinear Finite Element Analysis of Solids and Structures, Vol 1: Essentials*, John Wiley & Sons.
- Crisfield, M.A. and Jelenic, G. (1999) Objectivity of strain measures in the geometrically exact three-dimensional beam theory and its finite element implementation. *Proceedings of the Royal Society of London A*, **455**, 1125–1147.
- Dierckx, P. (1993) *Curve and Surface Fitting with Splines*, Oxford University Press, NY.
- Dmitrochenko, O.N. and Pogorelov, D.Y. (2003) Generalization of plate finite elements for absolute nodal coordinate formulation. *Multibody System Dynamics*, **10** (1), 17–43.
- Dufva, K. and Shabana, A.A. (2005) Analysis of thin plate structure using the absolute nodal coordinate formulation. *IMechE Journal of Multi-body Dynamics*, **219**, 345–355.
- Farhat, C., Crivelli, L., and G radin, M. (1995) Implicit time integration of a class of constrained hybrid formulations. Part I: spectral stability theory. *Computer Methods in Applied Mechanics and Engineering*, **125**, 71–107.
- Farhat, C.H. and Roux, F.X. (1991) A method of finite element tearing and interconnecting and its parallel solution algorithm. *International Journal for Numerical Methods in Engineering*, **32**, 1205–1227.
- Farhat, C.H. and Roux, F.X. (1994) Implicit parallel processing in structural mechanics. *Computational Mechanics Advances*, **2**, 1–124.
- Farhat, C.H. and Wilson, E. (1988) A parallel active column equation solver. *Computers and Structures*, **28**, 289–304.
- Farin, G. (1999) *Curves and Surfaces for CAGD, A Practical Guide*, Fifth edn, Morgan Kaufmann Publishers, , San Francisco.
- Garc a de Jal n, J., Unda, J., Avello, A., and Jim nez, J.M. (1987) Dynamic analysis of three-dimensional mechanisms in ‘Natural’ coordinates. *Journal of Mechanisms, Transmissions, and Automation in Design*, **109**, 460–465.
- Garcia-Vallejo, D., Escalona, J.L., Mayo, J., and Dominguez, J. (2003) Describing rigid-flexible multibody systems using absolute coordinates. *Nonlinear Dynamics*, **34** (1–2), 75–94.



- Garcia-Vallejo, D., Mayo, J., Escalona, J.L., and Dominguez, J. (2004) Efficient evaluation of the elastic forces and the jacobian in the absolute nodal coordinate formulation. *Nonlinear Dynamics*, **35** (4), 313–329.
- Garcia-Vallejo, D., Valverde, J., and Dominguez, J. (2005) An internal damping model for the absolute nodal coordinate formulation. *Nonlinear Dynamics*, **42** (4), 347–369.
- Geradin, M. and Cardona, A. (2001) *Flexible Multibody Dynamics*, John Wiley & Sons.
- Gerstmayr, J. and Shabana, A.A. (2006) Analysis of thin beams and cables using the absolute nodal coordinate formulation. *Nonlinear Dynamics*, **45**, 109–130.
- Goetz, A. (1970) *Introduction to Differential Geometry*, Addison Wesley.
- Goldenweizer, A. (1961) *Theory of Thin Elastic Shells*, Pergamon Press, Oxford, United Kingdom.
- Goldstein, H. (1950) *Classical Mechanics*, Addison-Wesley.
- Greenwood, D.T. (1988) *Principles of Dynamics*, Prentice Hall.
- Hamed, A.M., Shabana, A.A., Jayakumar, P., and Letherwood, M.D. (2011) Non-structural geometric discontinuities in finite element/multibody system analysis. *Nonlinear Dynamics*, **66**, 809–824.
- Hilber, H.M., Hughes, T.J.R., and Taylor, R.L. (1977) Improved numerical dissipation for time integration algorithms in structural dynamics. *Earthquake Engineering and Structural Dynamics*, **5**, 282–292.
- Holzappel, G.A. (2000) *Nonlinear Solid Mechanics: A Continuum Approach for Engineering*, John Wiley & Sons.
- Hughes, T.J.R. (1984) Numerical implementation of constitutive models: rate independent deviatoric plasticity, in *Theoretical Foundation for Large Scale Computations of Nonlinear Material Behavior* (eds S. Nemat-Nasser, R. Asaro, and G. Hegemier), Martinus Nijhoff Publishers, Dordrecht, The Netherlands, pp. 29–57.
- Hughes, T.J.R., Cottrell, J.A., and Bazilevs, Y. (2005) Isogeometric analysis: CAD, finite elements, NURBS, exact geometry and mesh refinement. *Computational Methods in Applied Mechanical Engineering*, **194**, 4135–4195.
- Hulbert, G.M. (2004) Computational Structural Dynamics, in *Encyclopedia of Computational Mechanics*, vol. **2** (eds E. Stein, R. de Borst, and T.J.R. Hughes), pp. 169–193. John Wiley & Sons.
- Hussein, B.A., Sugiyama, H., and Shabana, A.A. (2007) Coupled deformation modes in the large deformation finite element analysis: problem definition. *ASME Journal of Computational and Nonlinear Dynamics*, **2**, 146–154.
- Ibrahimbegovic, A. and Mamouri, S. (1998) Finite rotations in dynamics of beams and implicit time-stepping schemes. *International Journal of Numerical Methods in Engineering*, **41**, 781–814.
- Ibrahimbegovic, A., Mamour, S., Taylor, R.L., and Chen, A.J. (2000) Finite element method in dynamics of flexible multibody systems: modeling of holonomic constraints and energy

- conserving integration schemes. *Multibody System Dynamics*, **4**, 195–223.
- Jelenic, G. and Crisfield, M.A. (1998) Interpolation of rotational variables in non-linear dynamics of 3D beams. *International Journal of Numerical Methods in Engineering*, **43**, 1193–1222.
- Jelenic, G. and Crisfield, M.A. (2001) Dynamic analysis of 3D beams with joints in presence of large rotations. *Computer Methods in Applied Mechanics and Engineering*, **190**, 4195–4230.
- Kaplan, W. (1991) *Advanced Calculus*, 4th edn, Addison-Wesley, Reading, MA.
- Khan, A.S. and Huang, S. (1995) *Continuum Theory of Plasticity*, John Wiley & Sons.
- Kim, S.S. and Vanderploeg, M.J. (1986) QR decomposition for state space representation of constrained mechanical dynamic systems. *ASME Journal of Mechanisms, Transmissions, and Automation in Design*, **108**, 183–188.
- Kreyszig, E. (1991) *Differential Geometry*, Dover Publications.
- Lan, P. and Shabana, A.A. (2010) Integration of B-spline geometry and ANCF finite element analysis. *Nonlinear Dynamics*, **61**, 193–206.
- Leyendecker, S., Betsch, P., and Steinmann, P. (2004) Energy-conserving integration of constrained hamiltonian systems: a comparison of approaches. *Computational Mechanics*, **33**, 174–185.
- Leyendecker, S., Betsch, P., and Steinmann, P. (2006) Objective energy-momentum conserving integration for constrained dynamics of geometrically exact beams. *Computer Methods in Applied Mechanics and Engineering*, **195**, 2313–2333.
- Mikkola, A.M. and Matikainen, M.K. (2006) Development of elastic forces for the large deformation plate element based on the absolute nodal coordinate formulation. *ASME Journal of Computational and Nonlinear Dynamics*, **1** (2), 103–108.
- Mikkola, A.M. and Shabana, A.A. (2003) A non-incremental finite element procedure for the analysis of large deformation of plates and shells in mechanical system applications. *Multibody System Dynamics*, **9** (3), 283–309.
- Milner, H.R. (1981) Accurate finite element analysis of large displacements in skeletal frames. *Computers & Structures*, **14** (3–4), 205–210.
- Naghdi, P.M. (1972) The theory of shells and plates. *Handbuch der Physik*, **6** (a/2), 425–640, Springer-Verlag, Berlin.
- Ogden, R.W. (1984) *Non-Linear Elastic Deformations*, Dover Publications.
- Omar, M.A. and Shabana, A.A. (2001) A two-dimensional shear deformable beam for large rotation and deformation problems. *Journal of Sound and Vibration*, **243** (3), 565–576.
- Ortiz, M. and Popov, E.P. (1985) Accuracy and stability of integration algorithms for elastoplastic constitutive equations. *International Journal for Numerical Methods in Engineering*, **21**, 1561–1576.
- Piegl, L. and Tiller, W. (1997) *The NURBS Book*, Second edn, Springer-Verlag, New York.

- Rice, J.R. and Tracey, D.M. (1973) Computational fracture mechanics, in *Proceedings of the Symposium on Numerical Methods in Structural Mechanics* (ed. S.J. Fenves), Academic Press, Urbana, IL.
- Roberson, R.E. and Schwertassek, R. (1988) *Dynamics of Multibody Systems*, Springer-Verlag.
- Rogers, D.F. (2001) *An Introduction to NURBS with Historical Perspective*, Academic Press, San Diego, CA.
- Romero, I. (2006) *A Study of Nonlinear Rod Models for Flexible Multibody Dynamics*. Proceedings of the Seventh World Congress on Computational Mechanics, Los Angeles, CA, July 16–22.
- Romero, I. and Armero, F. (2002) Numerical integration of the stiff dynamics of geometrically exact shells: an energy-dissipative momentum-conserving scheme. *International Journal of Numerical Methods in Engineering*, **54**, 1043–1086.
- Romero, I. and Armero, F. (2002) An objective finite element approximation of the kinematics of geometrically exact rods and its use in the formulation of an energy-momentum scheme in dynamics. *International Journal of Numerical Methods in Engineering*, **54**, 1683–1716.
- Schwab, A.L. and Meijaard, J.P. (2005) *Comparison of Three-Dimensional Beam Elements for Dynamic Analysis: Finite Element Method and Absolute Nodal Coordinate Formulation*. Proceedings of the ASME 2005 International Design Engineering Technical Conferences & Computer and Information in Engineering Conference (DETC2005–85104), September 24–28, Long Beach, CA.
- Sanborn, G.G. and Shabana, A.A. (2009) On the integration of computer-aided design and analysis using the finite element absolute nodal coordinate formulation. *Multibody System Dynamics*, **22**, 181–197.
- Shabana, A. (1985) Automated analysis of constrained inertia-variant flexible systems. *ASME Journal of Vibration, Acoustics, Stress, and Reliability in Design*, **107** (4), 431–440.
- Shabana, A.A. (1982) Dynamics of large scale flexible mechanical systems. Ph.D. Dissertation, University of Iowa, Iowa City.
- Shabana, A.A. (1996a) Finite element incremental approach and exact rigid body inertia. *ASME Journal of Mechanical Design*, **118** (2), 171–178.
- Shabana, A.A. (1996b) Resonance conditions and deformable body coordinate systems. *Journal of Sound and Vibration*, **92** (1), 389–398.
- Shabana, A.A. (1996c) *Theory of Vibration: An Introduction*, Springer Verlag, New York.
- Shabana, A.A. (1998) Computer implementation of the absolute nodal coordinate formulation for flexible multibody dynamics. *Nonlinear Dynamics*, **16** (3), 293–306.
- Shabana, A.A. (2001) *Computational Dynamics*, 2nd edn, John Wiley & Sons.
- Shabana, A.A. (2013) *Dynamics of Multibody Systems*, Fourth edn, Cambridge University Press.

- Shabana, A.A. (2011) General method for modeling slope discontinuities and T-sections using ANCF gradient deficient finite elements. *ASME Journal of Computational and Nonlinear Dynamics*, **6**, 024502-1–024502-6.
- Shabana, A.A., Hamed, A.M., Mohamed, A.A., Jayakumar, P. and Lether-wood, M.D. (2011) *Development of New Three-Dimensional Flexible-Link Chain Model Using ANCF Geometry*. Technical Report # MBS2011-1-UIC, Department of Mechanical Engineering, The University of Illinois at Chicago, January.
- Shabana, A.A. and Mikkola, A.M. (2003) Use of the finite element absolute nodal coordinate formulation in modeling slope discontinuity. *ASME Journal of Mechanical Design*, **125** (2), 342–350.
- Shabana, A.A. and Wehage, R. (1981) *Variable Degree of Freedom Component Mode Analysis of Inertia-Variant Flexible Mechanical Systems*. TR No, 81–12, Center for Computer Aided Design, University of Iowa, December.
- Shabana, A.A. and Yakoub, R.Y. (2001) Three dimensional absolute nodal coordinate formulation for beam elements: theory. *ASME Journal of Mechanical Design*, **123** (4), 606–613.
- Simo, J.C. and Hughes, T.J.R. (1998) *Computational Inelasticity*, Springer, New York.
- Simo, J.C. and Taylor, T.J.R. (1986) Return mapping algorithm for plane stress elastoplasticity. *International Journal for Numerical Methods in Engineering*, **22**, 649–670.
- Simo, J.C. and Vu-Quoc, L. (1986) On the dynamics of flexible beams under large overall motions-the plane case: parts I and II. *ASME Journal of Applied Mechanics*, **53**, 849–863.
- Sopanen, J.T. and Mikkola, A.M. (2003) Description of elastic forces in absolute nodal coordinate formulation. *Nonlinear Dynamics*, **34** (1–2), 53–74.
- Stolarski, H., Belytschko, T., and Lee, S.H. (1995) A Review of shell finite elements and corotational theories. *Computational Mechanics Advances*, **2** (2), 125–212.
- Sugiyama, H., Gerstmayr, J., and Shabana, A.A. (2006) Deformation modes in the finite element absolute nodal coordinate formulation. *Sound and Vibration*, **298**, 1129–1149.
- Sugiyama, H., Mikkola, A.M., and Shabana, A.A. (2003) A non-incremental nonlinear finite element solution for cable problems. *ASME Journal of Mechanical Design*, **125**, 746–756.
- Takahashi, Y. and Shimizu, N. (1999) *Study on Elastic Forces of the Absolute Nodal Coordinate Formulation for Deformable Beams*, *Proceedings of the ASME International Design Engineering Technical Conferences and Computer and Information in Engineering Conference*, Las Vegas, NV.
- Tian, Q., Chen, L.P., Zhang, Y.Q., and Yang, J.Z. (2009) An efficient hybrid method for multi-body dynamics simulation based on absolute nodal coordinate formulation. *ASME Journal of Computational and Nonlinear Dynamics*, **4**, 021009-1–021009-14.
- Tian, Q., Zhang, Y., Chen, L., and Yang, J. (2010) Simulation of planar flexible multibody systems with clearance and lubricated revolute joints. *Nonlinear Dynamics*, **60**, 489–511.
- Tseng, F.C. and Hulbert, G.M. (2001) A gluing algorithm for network-distributed dynamics simulation. *Multibody System Dynamics*, **6**, 377–396.

- Tseng, F.C., Ma, Z.D., and Hulbert, G.M. (2003) Efficient numerical solution of constrained multibody dynamics systems. *Computer Methods in Applied Mechanics and Engineering*, **192**, 439–472.
- Ugural, A.C. and Fenster, K. (1979) *Advanced Strength and Applied Elasticity*, Elsevier.
- Von Dombrowski, S. (2002) Analysis of large flexible body deformation in multibody systems using absolute coordinates. *Multibody System Dynamics*, **8** (4), 409–432.
- Wang, J.Z., Ma, Z.D., and Hulbert, G.M. (2003) A gluing algorithm for distributed simulation of multibody systems. *Nonlinear Dynamics*, **34**, 159–188.
- Weaver, W., Timoshenko, S.P., and Young, D.H. (1990) *Vibration Problems in Engineering*, Wiley & Sons, New York.
- White, F.M. (2003) *Fluid Mechanics*, 5th edn, McGraw Hill, New York.
- Yakoub, R.Y. and Shabana, A.A. (2001) Three dimensional absolute nodal coordinate formulation for beam elements: implementation and applications. *ASME Journal of Mechanical Design*, **123** (4), 614–621.
- Yoo, W.S., Lee, J.H., Park, S.J. *et al.* (2004) Large deflection analysis of a thin plate: computer simulation and experiment. *Multibody System Dynamics*, **11** (2), 185–208.
- Zienkiewicz, O.C. (1977) *The Finite Element Method*, 3rd edn, McGraw Hill, New York.
- Zienkiewicz, O.C. and Taylor, R.L. (2000) *The Finite Element Method, Vol. 2: Solid Mechanics*, Fifth edn, Butterworth Heinemann.
- Betsch, P. and Stein, E. (1995) An assumed strain approach avoiding artificial thickness straining for a non-linear 4-node shell element. *Communications in Numerical Methods in Engineering*, **11**, 899–909.
- Betsch, P. and Stein, E. (1996) A nonlinear extensible 4-node shell element based on continuum theory and assumed strain interpolations. *Nonlinear Science*, **6**, 169–199.
- Ding, J., Wallin, M., Wei, C. *et al.* (2014) Use of independent rotation field in the large displacement analysis of beams. *Nonlinear Dynamics*, **76**, 1829–1843.
- Dufva, K., Kerkanen, K., Maqueda, L.G., and Shabana, A.A. (2007) Nonlinear dynamics of three-dimensional belt drives using the finite element method. *Nonlinear Dynamics*, **48**, 449–466.
- Hamed, A.M., Jayakumar, P., Letherwood, M.D. *et al.* (2015) Ideal compliant joints and integration of computer aided design and analysis. *ASME Journal of Computational and Nonlinear Dynamics*, **10**, 021015-1–021015-14.
- Irschik, H., Nader, M., Stangl, M., von Garssen, H.G. (2009) *A Floating Frame-of-Reference Formulation for Deformable Rotors using the Properties of Free Elastic Vibration Modes*. Proceedings of the ASME 2009 International Design Engineering Technical Conferences and Computers and Information in Engineering Conference, ASME, San Diego, CA, US, DETC2009-86660.

- Maqueda, L.G., Mohamed, A.A., and Shabana, A.A. (2010) Use of general nonlinear material models in beam problems: application to belts and rubber chains. *ASME Journal of Computational and Nonlinear Dynamics*, **5**, 021003-1–021003-10.
- Nachbagaer, K. (2012) Development of shear and cross section deformable beam finite elements applied to large deformation and dynamics problems. Ph.D. Dissertation, Johannes Kepler University, Linz, Austria.
- Sherif, K., Irschik, H., and Witteveen, W. (2012) Transformation of arbitrary elastic mode shapes into pseudo-free-surface and rigid body modes for multibody dynamic systems. *ASME Journal of Computational and Nonlinear Dynamics*, **7** (2), 021008 (10 pages).
- Sherif, K., Witteveen, W., Irschik, H. *et al.* (2011) On the extension of global vibration modes with Ritz-vectors needed for local effects, in *Linking Models and Experiments, Volume 2, Proceedings of the 29th IMAC, A Conference on Structural Dynamics 2011, Vol. 4* (ed. T. Proulx), Society of Experimental Mechanics Inc. & Springer, New York, Jacksonville, FL, USA, pp. 37–46.
- Sherif, K., Witteveen, W., and Mayrhofer, K. (2012) Quasi-static consideration of high frequency modes for more efficient flexible multibody simulations. *Acta Mechanica*, **223**, 1285–1305. doi: 10.1007/s00707-012-0624-1
- Olshevskiy, A., Dmitrochenko, O., and Kim, C.W. (2013) Three-dimensional solid brick element using slopes in the absolute nodal coordinate formulation. *ASME Journal of Computational and Nonlinear Dynamics*, **9** (2), 021001. doi: 10.1115/1.4024910
- Shabana, A.A. (2015a) ANCF reference node for multibody system analysis. *IMechE Journal of Multibody Dynamics*, **229** (1), 109–112. doi: 10.1177/1464419314546342
- Shabana, A.A. (2015b) ANCF tire assembly model for multibody system applications. *ASME Journal of Computational and Nonlinear Dynamics*, **10**, 024504-1–024504-4.
- von Dombrowski, S. (1997) Modellierung von Balken bei grossen Verformungen für ein kraftreflektierendes Eingabegerät. Diploma Thesis, University Stuttgart and DLR.
- Wallin, M., Aboubakr, A.K., Jayakumar, P. *et al.* (2013) A comparative study of joint formulations: application to multibody system tracked vehicles. *Nonlinear Dynamics*, **74** (3), 783–800.
- Wang, L., Octavio, J.R.J., Wei, C., and Shabana, A.A. (2015) Low order continuum-based liquid sloshing formulation for vehicle system dynamics. *ASME Journal of Computational and Nonlinear Dynamics*, **10**, 021022-1–021022-10.
- Wei, C., Wang, L., and Shabana, A.A. (2015) A total lagrangian ANCF liquid sloshing approach for multibody system applications. *ASME Journal of Computational and Nonlinear Dynamics*, **10**, 051014-1–051014-10.
- Yu, Z. and Shabana, A.A. (2015) Mixed-coordinate ANCF rectangular plate finite element. *ASME Journal of Computational and Nonlinear Dynamics*, **10** (6), 061003-1–061003-14.
- Fung, Y. (1977) *A First Course in Continuum Mechanics*, Prentice Hall.
- Spencer, A.J.M. (1980) *Continuum Mechanics*, Longman, London.



# INDEX

---

- Absolute coordinates, 52, 229
- Absolute nodal coordinate formulation, 34, 84, 86, 88, 168, 188, 225, 259, 262
  - coupled deformation modes, 194, 207, 208, 211
- Acceleration, 24, 26, 27, 29, 31, 32, 35, 36, 37, 38, 64, 68, 98, 101, 109, 164, 178, 179, 219, 240, 244, 246
- Air pressure, 110–111
- Almansi strains, 47, 59, 60, 67
- ANCF geometry, 264–266, 267, 271, 273, 274, 275, 277
- ANCF surfaces, 274–275
- ANCF-coupled deformation modes, 194, 207, 208, 211
- Angular acceleration, 26, 27
- Angular momentum, 37, 38
- Angular velocity, 26, 27, 229–234, 244
- Anisotropic linearly elastic material, 126–127
- Approximation methods, 1, 32–34, 104, 105, 109, 110, 134, 167, 214
  - classical, finite–element method, Rayleigh–Ritz method
  - Finite element method *see* Finite element method
  - Rayleigh–Ritz method *see* Rayleigh–Ritz method
- Arc length, 40, 88, 194, 195, 198, 200
- Area change, 77–81
- Associative flow rule *see* Associative plasticity
- Associative plasticity, 282, 283, 284, 288, 290, 292, 294, 295, 307, 318, 323, 326
- Assumed displacement field, 81, 84, 134, 170, 171, 172, 182, 185, 192, 201, 212, 213, 221, 228, 229
- Assumed strain element, 215
- Assumed stress element, 215
- Axis of rotation, 62
- Back stress, 281, 282, 310
- Backward implicit Euler method, 285, 286
- Basis functions, 262, 266, 267, 268, 270, 273, 274, 275, 277
- Bauschinger effect, 279, 326
- Beam elements
  - three-dimensional, 173–174, 206–208, 213



Beam elements (*Continued*)

two-dimensional, 32, 49, 54, 175, 227, 228, 238, 241, 245

Beam theory, 202, 203, 215

Bernstein polynomials, 266, 267, 272

Bezier geometry, 263, 266–267

Bezier method, 266

Binomial vector, 195

Biot stress, 107

Blending functions *see* Basis functions

## Body(s)

coordinate system, 24, 25, 27, 28, 38, 43, 51, 52, 64, 101, 102, 231, 233, 235–240, 242, 243, 249–251, 255

force, 27, 29, 98, 100, 101, 109, 110, 112, 134, 164, 213, 219

reference, 52, 64, 229, 244

rigid, 14, 23, 24–29, 31, 34, 35, 36, 38, 39, 42, 43–44, 47, 51–54, 56, 60–62, 65, 66, 74–78, 85, 94, 101, 102, 106, 110, 115–121, 123, 125, 135, 138, 141, 156, 163, 168–169, 172, 174–175, 202–205, 213, 214, 216–218, 221–223, 225–229, 231, 234–236, 239–243, 245, 249–252, 258, 262–265, 271, 273–276, 313–315, 317, 318

Boolean matrix, 176, 178, 182, 239, 247

Breakpoints, 263, 268–270

B-spline, 221, 261, 263, 264, 266, 267–271, 272, 276, 277

surfaces, 273–275

Bulk modulus, 130, 152, 162, 300

Bulk viscosity coefficient, 163

Cable element, 205–206, 212, 213, 215, 224, 264, 265, 271, 272, 277

CAD, 261, 262, 263, 265, 271

Cartesian tensor, 12–21

## Cauchy

elastic material, 124

first law of motion, 101

second law of motion, 103

strain, 59

stress

97, 99, 100, 102–104, 106, 108, 111–121, 137, 141, 161, 163, 249, 291, 314

Cauchy stress formula, 97, 99, 115

Cauchy–Green deformation tensor, 61, 72

left, 61, 79, 80, 95, 137

right, 61, 115, 136, 138, 155, 165

Cayley–Hamilton theorem, 18

Center of mass, 27, 28, 31, 38, 46, 102, 251

Change of parameters, 2, 13, 39–44

Characteristic equation, 15, 18, 71, 73

Characteristic values *see* Eigenvalues

Chebyshev polynomials, 188

Cholesky coordinates, 182

Chord frame, 241, 242

Classical theories, 193

Component mode techniques, 251–252

Computational geometry, 261–277

Computer Aided Design *see* CAD

Connectivity conditions, 169, 217, 222, 239

Conservation of mass, 29, 48, 81, 82, 84, 105, 113, 119, 178, 219

Consistency condition *see* Persistence condition

Consistency parameter, 281–283, 291–293, 298–300, 302, 307, 317–319

Consistent mass, 36, 110, 168, 252

Constitutive equations, 18, 21, 74, 82, 86, 88, 102, 113, 115, 118, 123–165, 180, 204, 219, 220, 249, 295, 296, 299, 306, 312–314, 317

Constitutive integration algorithm, 295

Continuity equation, 48, 81–82, 112, 113, 123, 219, 220

Continuum forces, 29

Control points, 263–266, 268–274, 276, 277

Control polygon, 263, 265

Control volume, 82, 220

Convective stress rate, 117, 118, 121

Convective term, 65

Convolution integral *see* Duhamel integral

Coordinate reduction, 110, 168, 214, 225, 250, 251–253, 254, 256

Coordinate transformation, 13, 15, 17, 39–44, 68–74, 75, 86, 89, 111, 124, 127, 163, 179, 182, 192, 218, 252, 253, 265

Co-rotational frame, 53, 193, 221

Coupled deformation modes *see*

ANCF-coupled deformation modes

Creep function, 145, 148, 165

Curvature, 94, 185, 186, 195, 199–203, 206–207, 209, 213, 214, 271

- Gaussian, 199
  - mean, 199
  - normal, 197, 198, 199
  - principal, 199
  - radius of, 195
  - surface, 197
  - vector, 195, 198, 200, 209, 213
- Curved beams, 212
- Curved configuration, 92–94
- Curved geometry, 92–94, 183–187, 212
- Curved structure, 92–94, 168
- Curves, 40–42, 69, 92–94, 169, 190, 194,
  - 194–200, 206, 263, 265, 266–274, 276, 277
- theory, 194–195
- D'Alembert's principle, 1, 23–29, 31, 32, 38,
  - 46, 104
- deCasteljau algorithm, 267
- Decomposition of displacement, 62–64
- Deformation examples, 84–92
- Deformation measures, 69, 117, 124, 131, 240,
  - 316
- Deviatoric stresses, 103, 113–115, 298
- Dilatation, 72, 84, 85, 86, 129, 130, 131, 152,
  - 162, 214
- Direction cosines, 51, 232
- Discontinuities, 168, 176, 229, 235, 236, 262,
  - 271, 274, 275–277
  - non-structural, 274, 275–277
  - structural, 274, 275–277
- Discrete equations, 1, 34–37, 104, 219, 310
- Displacement, 24, 29, 32, 35, 39, 43, 44, 47,
  - 48, 50, 51, 53, 74–75
  - axial, 59, 203, 227, 228
  - bending, 203, 227
  - decomposition, 62–64
  - field, 23, 29, 54, 57, 59, 80–81, 84, 86, 87,
    - 89, 134, 168, 169–175, 185
  - fluid, 220
  - general, 47, 52, 53, 54, 231–234
  - gradients, 54–56, 59, 61, 116, 220, 221, 249
  - homogeneous, 63, 135–136
  - isochoric, 54, 78
  - modes, 34, 47, 88, 131
  - nodal, 185, 213
  - planar, 84–85
  - reference, 239
  - rigid-body, 29, 34, 52, 53, 61, 168, 217, 218,
    - 228, 229, 235, 239, 262–264, 273, 314
  - transverse, 228
    - 228
  - virtual, 30, 35, 112
- Dissipation, 76, 124, 149–150, 152, 280
- Divergence operator, 101
- Divergence theorem, 82, 83, 100, 112, 119
- Double product, 13–14, 19, 21, 104, 106, 107,
  - 108, 115, 120
- Duhamel integral, 143, 144
- Dummy index, 11–12
- Dyadic product *see* Outer product
- Dynamic coupling *see* Inertia coupling
- Eigenvalue analysis, 91, 92, 214, 216
- Eigenvalue problem, 15–18, 71, 103, 252
- Eigenvalues, 15–18, 22, 71, 73, 103, 136, 252
- Eigenvectors, 15–18, 22, 71, 72, 73, 90, 103,
  - 252
- Elastic coefficients, 125–130, 136, 138, 139,
  - 180, 207, 249, 291, 315
- Elastic coordinates, 244, 246, 248–252, 254,
  - 255, 256
- Elastic energy, 149–150, 155
- Elastic force, 14, 29, 59, 74, 75, 77, 104–106,
  - 109, 115–117, 124, 126, 134, 135, 168,
    - 169, 178–180, 182, 188–194, 201–202,
      - 204–207, 209, 210, 211, 215, 216, 225,
        - 248–251
  - power, 119
- Elastic limit, 125, 137
- Elastic line approach, 207
- Elastic loading, 283
- Elastic mid-surface approach, 210, 215
- Elastic predictor, 286, 296, 297
- Elasto-plastic tangent modulus, 284, 300, 302,
  - 304, 310, 323
- Embedding technique, 37
- Energy, 1, 3, 37–39, 120, 123, 124, 137–140,
  - 214, 218, 280, 312, 315, 322
  - balance, 97, 119–120
  - elastic, 149–150, 155
  - kinetic, 29, 39, 119
  - strain, 29, 74–76, 116, 117, 126, 131, 134,
    - 139, 140, 151, 156, 201–207, 209,
      - 215, 216, 255, 315
- Engineering strain, 56, 58

- Equations of equilibrium, 97, 100–102
- Equations of motion, 1, 23, 30, 37, 39
  - for deformable bodies, 29, 102, 111–113, 168, 180–182, 214, 219, 221, 225, 250–251, 253
  - for fluids, 163–164
  - for particles, 30
  - for rigid bodies, 27–29, 31–32
- Equilibrium
  - equations of, 97, 100–102
  - force, 97–100
- Equivalent plastic strain, 298
- Euler angles, 230, 232, 258
  - singularity, 234
  - transformation matrix in terms of, 233
- Euler equation, 28, 32, 34, 46, 101, 120, 251
- Euler parameters, 232, 234
- Euler–Bernoulli beam, 69, 199–203, 204, 212, 213, 215, 223, 224, 228
- Eulerian coordinates, 48, 65, 67, 111
- Eulerian description, 48, 65, 218
- Eulerian formulation, 112, 113, 218–221
- Eulerian strain, 58–62, 95
- Evolution equations, 151, 156, 280
- Extension, 56–57, 84, 85–88, 201, 202, 215
  
- Finite difference method, 32
- Finite dimensional model, 1, 28–29, 81, 104, 109, 110, 134–135, 167
- Finite element, 1, 22, 23, 29, 32, 34, 36, 37, 39, 42, 44, 48, 53, 69, 70, 84, 86, 94, 102, 104, 105, 109–110, 112, 115, 130, 135, 167–224, 188, 225–259, 246–248, 253–255, 259, 261–277
  - assumed displacement, 81, 84, 94, 134, 170–172, 182, 185, 192, 201, 212, 213, 221, 228, 229
  - assumed strain, 215
  - assumed stress, 215
  - beam, 173–175, 193, 194, 199–205, 206–208, 213, 215, 223, 224, 227–228, 229, 234, 238, 241, 245, 258, 273
  - Boolean matrix, 176, 178, 182, 239, 247
  - brick, 211–212
  - cable, 205–206, 212, 213, 215, 224, 264, 265, 271, 272, 277, 280
  - connectivity conditions, 169, 217, 222, 239
  - formulation, 22, 23, 29, 36, 37, 39, 48, 109, 110, 130, 167–169, 173, 179, 216–218, 225, 251
  - generalized forces, 109, 135, 181
  - gradient deficient, 70, 193, 201, 202, 204, 205, 206, 209, 273
  - inertia shape integrals, 188, 246, 247–248, 253, 254, 255, 259
  - intermediate coordinate system, 168, 226, 235–238, 258, 259, 262
  - isoparametric, 212, 217, 226, 229, 234, 235
  - large deformation, 42, 88, 111, 112, 130, 167–224, 225, 246, 250, 251, 256
  - mass matrix, 110, 168, 179, 182, 210, 212, 213, 220, 222, 223, 224, 225, 226, 246–247, 251, 255, 276
  - method, 1, 32, 37, 102, 104, 105, 167, 169, 199, 218, 226, 262–264
  - nodal coordinates, 44, 53, 95, 167–169, 171–177, 179–182, 185, 193, 199, 200, 202, 203, 205, 206, 208–213, 216, 217, 218, 219, 221, 223, 225–229, 234–239, 244, 245, 247, 249, 250, 252, 254–256, 258, 259, 261–265, 272, 274, 275, 277
  - performance, 194, 207, 211–216
  - plate, 208–211, 212, 213, 215, 224, 273, 275
  - rectangular, 217, 226
  - reference conditions, 238–243, 251, 252
  - shape function, 34, 46, 57, 87, 94, 109, 110, 112, 167, 169, 171, 174, 175, 181, 183, 185, 193, 200, 203–206, 208–210, 212, 217, 219, 221, 223, 226–228, 235–240, 245–247, 255, 258, 259, 264, 267, 271, 272, 274, 275
  - shear deformable, 201–205, 215, 223, 224, 274
  - solid, 172, 211–212, 217, 220, 226
  - stiffness matrix, 216, 250–253, 255, 256
  - subparametric, 213
  - superparametric, 213
  - tetrahedral, 172, 217, 226
  - triangular, 217, 226
- Finite rotation, 28, 172, 173, 179, 217, 218, 221, 229–234, 253, 254, 259, 262, 276, 316
- First fundamental form of surfaces, 196, 198
  - coefficients of, 196

- First Piola-Kirchhoff stress tensor, 106, 107, 112, 114, 115, 120, 121
- Floating frame of reference, 34, 52–54, 64, 110, 178, 225–259, 262
- Flow rule, 280, 282, 284, 291, 317–320, 323, 326
- Flow stress, 281
- Fluid, 32, 48, 64, 82, 101, 112, 113, 123, 124, 163, 164, 212, 218, 219, 220, 221, 257
  - constitutive equations, 162–164
  - ideal, 163
  - incompressible, 163, 164
  - inviscid, 163, 164
  - isotropic, 163, 164
  - Newtonian, 162, 164
- Force, 29, 97–121
  - body, 27, 29, 98, 100, 101, 109, 110, 112, 134, 164, 213, 219
  - continuum, 29
  - elastic, 14, 29, 59, 74, 75, 77, 104–106, 109, 115–117, 119, 121, 124, 126, 134, 135, 168, 169, 178–180, 182, 188–193, 194, 201–207, 209–211, 215, 216, 225, 248–251, 259
  - gravitational, 98, 100
  - inertia, 27–31, 35, 36, 38, 100, 102, 105, 109, 110, 112, 168, 178–181, 188, 193, 220, 221, 245–248, 250, 259
  - magnetic, 98, 100
  - pressure, 110, 111
  - surface, 29, 98–100, 110–111, 119
- Frame indifference, 48, 141
- Free index, 11, 12
- Frenet frame, 195
- Fundamental forms
  - first, 196, 198
  - second, 196–199
- Gauss quadrature, 188, 192
- Gauss theorem, 105
- Gaussian curvature, 199
- Gauss-Legendre coefficients, 190
- General displacement, 47, 52–54, 74, 231–232
- Generalized forces, 37, 109, 135, 181
- Generalized Newton–Euler equations, 251
- Geometric interpretation of strains, 56–58
- Geometry *see* Computational geometry
- Gradient coordinates, 33, 34, 185, 199, 203, 205, 206, 208, 210, 220, 221, 223, 224, 264, 265, 267, 272
- Gradient deficient finite element, 70, 193, 201, 202, 204–206, 209, 273
- Gradient of the displacement vector, 54–55, 61
- Gravitational force, 98, 100
- Green elastic material, 123
- Green-Lagrange strain tensor, 47, 55, 70, 86, 100, 104, 108, 159, 180, 223
- Green–Naghdi stress rate, 117, 118, 121
- Hardening, 279
  - isotropic, 279, 281, 282, 289, 291, 298–312
  - kinematic, 279, 280, 281, 289, 298–312
  - linear, 306
  - nonlinear, 306–312
  - strain, 279, 280
- Hellinger-Reissner principle, 215
- Hermite polynomials, 188
- Homogeneous displacement, 63, 135, 136
- Homogeneous material, 129–136
- Homogeneous motion, 63, 135
- Hookean material, 124
- Hooke’s law, 124–125, 137
- Hourglass modes, 216
- Householder transformation, 23
- Huber-von Mises yield function, 298, 309
- Hu-Washizu principle, 215
- Hybrid principles *see* Multifield variational principles
- Hydrostatic pressure, 100, 113–115, 121, 130, 152, 161–163, 298, 300, 302, 322
- Hyperelastic material, 123, 124, 126, 127, 141, 150, 159, 280, 291, 312, 314, 315, 316, 322, 327
- Hyperelastic potential, 314–315
- Hyperelastic-plastic material, 118, 312–322, 322–326
- Hypoelastic material, 291, 312, 315, 317
- I-CAD-A, 261
- Ideal fluid, 163
- Impulse response function, 143, 144
- Incompressibility, 82, 139–141, 151, 163, 164, 214, 215, 220, 257
- Inelastic material, 86, 124, 142, 312

## Inertia

- coupling, 28, 102, 110, 168, 245, 250
- force, 27–31, 35, 36, 38, 100, 102, 105, 109, 110, 112, 168, 178–181, 188, 193, 220, 221, 245–248, 250, 259
- mass moment of, 28, 31, 46, 245
- shape integrals, 188, 226, 246–248, 253–255, 259
- tensor, 28

Infinitesimal rotation, 53, 62, 172, 217, 221, 226, 227, 229, 234, 235, 237, 241, 245

Infinitesimal strains, 59, 61–62, 155

Intermediate element coordinate system, 168, 226, 235–238, 258, 259, 262

Intermediate plastic configuration, 313–318, 322, 323

Internal variables, 280, 291, 296–298, 317

Interpolating polynomial, 173–175, 189, 206, 225, 274

## Invariants

- strain, 72–74, 95, 131–132, 136–137
- stress, 103, 120, 131–132
- tensor, 14–18

Inviscid flow, 163, 164

Irrotational flow, 64

Isochoric displacement, 54, 78

Isoparametric property, 212, 217, 226, 229, 234, 235

Isotropic fluid, 163, 164

Isotropic hardening, 279, 281, 282, 289, 291, 298–312

Isotropic material, 124, 129–136, 161–162, 164, 165, 314

Isotropic plastic modulus, 281

J2 flow theory, 280, 298–312

isotropic/kinematic hardening, 298–312

Jacobian matrix, 50, 51, 66, 69, 82, 196, 258

Jaumann stress rate, 117, 119, 121

Kelvin viscoelastic model, 148, 152

Kinematic analysis, 47–95

Kinematic equations, 43, 47, 53, 217, 229, 234, 238, 243–245

Kinematic hardening, 279, 280, 281, 289, 298–312

modulus, 281, 298, 299, 311

Kinematic viscosity, 164

Kinematics, 47–95, 243–245

of deformable bodies, 47–95, 243–245

of rigid bodies, 24–27, 43–44, 217

Kirchhoff stress, 75, 106, 115, 118, 137, 138, 165, 314, 325

Knot insertion, 263, 269–270

Knot multiplicity, 263, 268–270, 273, 276, 277

Knot vector, 263, 268–270, 273

Kronecker delta, 7, 153

Kuhn-Tucker complementarity condition, 282, 291, 317

Lagrange multipliers, 37, 140, 141, 163, 214

Lagrange-D'Alembert equation, 30

Lagrangian coordinates, 48, 50, 67, 111, 218

Lagrangian description, 48, 51, 219

Lagrangian formulation

total, 111–113, 218, 220

updated, 111–113, 169, 218–221

Lagrangian strain tensor *see* Green-Lagrange strain tensor

Lame's constants, 124, 129, 130, 131, 134, 138, 139, 163, 165, 299, 302, 322

Laquerre polynomials, 188

Large deformation problem, 104, 137, 167–224, 225, 256, 316

Large rotation, 110, 167–224, 225–259

Leaf spring, (AU: Not found)

Left Cauchy-Green strain tensor, 61, 62, 64, 79, 80, 95, 137, 165, 314

Left stretch tensor, 62

## Legendre

coefficients, 190

polynomials, 188, 189

Linear momentum, 37–38

Linear structural systems, 203, 251

Linear theory of elastodynamics, 253–254

Liquid sloshing, 212, 220, 256–257

Loading and unloading conditions, 280, 282–283, 295

Locking, 115, 130–131, 169, 193–194, 205, 214–216, 222, 223

membrane, 130, 169, 214, 215

shear, 130, 169, 214, 215, 216

volumetric, 130, 169, 214, 216

Logarithmic strain, 56

Lumped mass, 36, 110, 168, 255

Magnetic force, 98, 100

## Mass

- center of, 27, 28, 31, 38, 46, 102, 251
- conservation of, 29, 48, 81, 82, 84, 105, 113, 119, 178, 219
- consistent, 36, 110, 168, 252
- lumped, 36, 110, 168, 255
- matrix, 36, 110, 168, 179, 182, 210, 212, 213, 220, 222, 223, 224, 225, 226, 246, 247, 251, 255, 276
- moment of inertia, 28, 31, 46, 245

## Material

- anisotropic, 126–127
- Cauchy elastic, 124
- coordinates, 75
- Green elastic, 123
- homogeneous, 129–136
- Hookean, 124
- hyperelastic, 123, 124, 126, 127, 141, 150, 159, 280, 291, 312, 314, 315, 316, 322, 327
- hypoelastic, 291, 312, 315, 317
- incompressible, 82, 139–141, 151, 163, 164, 214, 215, 220, 257
- inelastic, 86, 124, 142, 312
- isotropic, 124, 129–136, 161–162, 164, 165, 314
- Mooney-Rivlin, 124, 137, 139–141
- Neo-Hookean, 124, 137–139, 165, 322
- symmetry, 127–129, 164
- viscoelastic, 115, 119, 124, 125, 132, 141–162, 165

## Matrix, 2–6

- addition, 6
- adjoint, 5
- associative law, 6
- cofactor, 3
- determinant, 3
- diagonal, 2
- displacement vector gradients, 61
- elastic coefficients, 125, 126, 128, 207, 315
- identity, 2
- inverse, 5
- mass, 36, 110, 168, 179, 182, 210, 212, 213, 220, 222, 223, 224, 225, 226, 246, 247, 251, 255, 276
- minor, 3

multiplication, 6

null, 2

orthogonal, 5

position vector gradients, 3, 5, 22, 23, 50, 53, 54, 55, 58, 59, 60, 62, 63, 67, 74, 75, 76, 77, 79, 81, 84, 85, 88–95, 104, 106, 107, 109, 110, 116, 121, 133, 134, 135, 137, 138, 140, 141, 155, 172, 173, 180, 183, 185, 204, 214, 218, 246, 257, 262, 280, 314, 318, 320

product, 6

projection, 10

rectangular, 2

singular, 3

skew symmetric, 2

square, 2

stiffness, 216, 250–253, 255, 256

symmetric, 2

trace, 2

transpose, 2

unit, 2

zero, 2

Maxwell viscoelastic model, 148, 159, 162, 165

Mean curvature, 199

Mean surface traction, 98

## Mechanics

particles, 24

rigid bodies, 24–27

Membrane locking, 130, 169, 214, 215

Mixed principles *see* Multi-field variational principles

Modal coordinates, 252–254, 255–256

Modal transformation, 252, 253

Mode shapes, 252, 253, 255

Modulus of elasticity *see* Young's modulus

Modulus of rigidity, 130, 152, 207

Mohr's circle, 91

Moment of inertia, 28, 31, 46, 245

Momentum, 1, 24, 37–39

Mooney-Rivlin material, 124, 137, 139–141

Motion description, 48–54, 64, 101, 112, 173, 225, 227, 231, 239, 244

Multibody computer programs, 253

flexible, 226, 248, 253, 254, 255

Multibody system, 37, 44, 53, 168, 226, 234,

240, 248, 250, 251, 253–258, 276

Multi-field variational principles, 215

- Multiplicative decomposition, 155, 280, 313–314
- Nanson's formula, 79, 80, 106, 110, 111
- Natural strain, 56
- Navier-Stokes equations, 164
- Neo-Hookean material, 124, 137–139, 165, 322
- Neutral loading, 283
- Newton equation, 27, 38
- Newton-Cotes formulas, 188
- Newton–Euler equations, 28, 32, 34, 101, 120, 251
- Newton-Euler formulation, 27, 102
- Newtonian fluid, 162, 164
- Newtonian viscous fluid, 162–163
- Newton's second law, 24, 27, 28, 30, 37, 98
- Nodal
  - coordinates, 44, 53, 95, 167–169, 171–182, 185, 193, 199, 200, 202, 203, 205, 206, 208–213, 216–219, 221, 223, 225–229, 234–239, 244, 245, 247, 249, 250, 252, 254, 255, 256, 258, 259, 261–265, 272, 274, 275, 277
  - points, 167, 171, 172, 176, 208, 217–221, 226, 256
- Nonconservative system, 119
- Nonhomogeneous motion, 63
- Non-incremental solution, 44, 168, 194, 217, 220, 221, 222, 234
- Nonstructural discontinuities, 274, 275–277
- Normal curvature, 197–199
- Normal strain, 56, 58, 70, 72, 74, 86, 89, 91, 92, 130, 131, 204, 207
- Normal stress, 58, 86, 98, 99, 100, 130, 163
- Numerical Solution, 167
  - plasticity equations, 284–286, 295–298, 312, 320–322, 327
- NURBS, 261, 263, 264, 276, 277
- Objectivity, 29, 48, 74–77, 97, 115–119, 125, 141, 155, 156, 163, 291, 295, 312, 317, 318
- Oldroyd stress rate, 117, 118, 121
- Orthogonal matrix, 5
- Orthogonal transformation
  - improper, 6
  - proper, 6
- Osculating plane, 195
- Outer product, 7, 8
- Overstress function, 322
- Parallel axis theorem, 226, 229, 235
- Partial differential equations of equilibrium, 97, 100–102, 104, 109, 112, 115, 119, 120, 123, 164, 167, 213
- Partial stress, 150–152, 156, 159
- Particle mechanics, 24
- Patch test, 169, 213–214
- Penalty method, 140, 141, 214, 215
- Perfect plasticity, 281, 290
- Persistency condition, 282
- Physical stress *see* True stress
- Piola transformation, 117
- Piola-Kirchhoff stress, 75, 104, 106–109, 112–118, 120, 121, 124–126, 133–138, 140, 141, 156, 157, 159, 161, 162, 165, 180, 204, 248, 314, 315, 322
- Pitch angle, 232
- Planar analysis, 24, 201, 259, 276
- Planar motion, 24, 26–28, 43, 85, 120, 258
- Plane strain, 132, 133, 164
- Plane stress, 132, 164, 304–306
- Plastic corrector, 286, 296, 297, 307
- Plastic flow rule, 282
- Plastic loading, 283, 300
- Plastic strain, 280–282, 291, 296–299, 310, 312, 314
- Plasticity, 279–327
  - associative, 282–284, 288, 290, 292, 294, 307, 318, 323, 326
  - equations, 280, 282, 283–291, 295–296, 298, 299, 306, 310, 312, 315, 326, 327
  - explicit solution, 295–296
  - formulations, 115, 279–327
  - implicit solution, 296–298
  - nonassociative, 282, 291, 292, 295, 317, 318, 326
  - perfect, 281, 290
  - rate dependent, 279, 322
  - small strain, 280, 291–298, 299
- Plate element, 208–210, 212, 213
  - thin, 208–209, 215, 224, 273, 275
- Point coordinates, 265, 267
- Poisson effect, 58, 86, 88, 130–131
- Poisson's ratio, 130, 134, 152, 209



- Polar decomposition theorem, 1, 21–23, 45, 47, 62, 63, 95, 107, 172, 218
- Position vector gradients, 43–44, 92, 109, 134, 135, 138, 172, 176, 180, 183, 211, 223, 264 *see also* Matrix of position vector gradients
- Power basis, 266, 267
- Prager-Ziegler rule, 299, 311
- Principal axes, 72
- Principal curvatures, 199
- Principal directions, 71–74, 86, 90, 91, 95, 100, 103, 120, 199
- Principal strain, 71–74, 91
- Principal stress, 103, 120
- Principal values, 23, 71–74, 86, 90, 95, 103, 113, 114, 121
- Principle of conservation of mass, 29, 81, 84, 105, 119, 178
- Principle of virtual work, 27, 30–32, 34, 36, 46, 102, 104, 105, 109, 113, 116, 120, 180, 181, 244, 250
- Projection
  - Matrix, 10–11
- Prony series, 159
- Proportional limit, 137
- Pullback, 59, 66, 67, 118, 314, 316
- Push-forward, 59, 66, 67, 118, 314
  
- QR decomposition, 23
- Quadrature, 188–193, 216
  
- Radius of curvature, 195
- Rate independent material, 279
- Rate of deformation, 47, 65–68, 76, 82, 85, 86, 88, 90, 95, 112, 116, 117, 119, 120, 124, 163, 219, 258, 312, 315–317, 321, 322
- Rate-dependent
  - material, 279
  - plasticity, 279, 322
- Rayleigh–Ritz method, 32
- Rectangular element, 217, 226
- Reduced integration, 169, 193, 215–216
  - selective, 169, 216
- Redundant coordinates, 37
- Reference conditions, 238–243, 251, 252
- Reference coordinate system, 51, 53, 72, 76, 77, 95, 176
- Reference coordinates, 63, 74, 76, 109, 244, 249, 251, 255
  
- Reference motion, 52, 53, 110, 229, 240–243, 245, 250–252
- Reflection, 6, 127–129
- Relaxation function, 143, 145, 149, 152, 156, 159
- Relaxation time, 142, 162
- Return mapping algorithm, 280, 286, 287, 289, 295, 296, 309–312, 326
  - radial, 322
- Reynolds’ transport theorem, 48, 82–84
- Right Cauchy–Green strain tensor, 61, 115, 136, 138, 155, 165
- Right stretch tensor, 62
- Rigid body
  - dynamics, 24–32, 34, 36, 101, 168, 251
  - inertia, 28, 245
  - kinematics, 24–27, 43–44, 51–52, 217
  - mass matrix, 28
  - motion, 51–52, 54, 56, 60–62, 65, 66, 74, 75, 78, 85, 94, 106, 115, 117, 119, 121, 123, 125, 135, 138, 156, 163, 168, 169, 172, 174, 175, 202, 203, 204, 213, 217, 221, 223, 225, 226, 227, 228–229, 231, 234, 235, 239, 240–243, 249, 251, 262, 265, 275, 315, 318
  - planar motion, 24–27
  - translation, 47, 169, 229, 235, 236, 239
- Rodriguez formula, 62
- Rodriguez parameters, 232
- Roll angle, 232
- Rotation, 128–129
  - field, 23, 29, 37, 172, 173, 217, 218, 221, 226, 262
  - finite, 28, 172, 173, 179, 217, 218, 221, 229–234, 253, 254, 259, 262, 276, 316
  - infinitesimal, 53, 62, 172, 217, 221, 226, 227, 229, 234, 235, 237, 241, 245
  - large, 110, 167–224, 225–259
  - matrix, 62, 117, 231, 314
  
- Scalar triple product, 77
- Second fundamental form of surfaces, 196, 197
  - coefficients of, 197
- Second Piola–Kirchhoff stress tensor, 75, 104, 106–109, 112–118, 120, 124–126, 133–138, 140, 141, 156, 157, 159, 161, 162, 165, 180, 204, 248, 314, 315, 322
- Selective reduced integration, 169, 216



- Separation of variables, 169–171
- Shape function, 46, 57, 87, 167, 169, 193, 203, 204, 209, 210, 212, 217, 219, 223, 226, 227, 235, 239, 245, 255, 258, 264, 267, 271, 272, 275
- matrix, 34, 94, 109, 110, 112, 171, 174, 175, 181, 183, 185, 200, 203, 205, 206, 208, 209, 210, 212, 221, 227, 228, 236–240, 245, 246, 247, 255, 258, 259, 264, 271, 272, 274
- Shear
- deformation, 47, 84, 89–92, 200, 201, 205, 206, 209, 215, 228
  - locking, 130, 169, 214, 215, 216
  - modulus, 130, 152, 299
  - strain, 56–58, 70–72, 74, 86, 88, 89, 91, 92, 131, 201, 204, 207
  - stress, 86, 98, 100, 103, 132, 162, 163, 215, 280
  - viscosity coefficient, 163
- Shells, 53, 131, 168, 169, 172, 193, 199, 212, 215, 217, 226, 229, 239, 262, 265, 271
- Simpson's rule, 188
- Singular point, 194
- Slider crank mechanism, 42, 241
- Slip rate, 281
- Sloshing, 212, 220, 256, 257
- Small deformation, 34, 35, 78, 86, 106, 111, 124, 130, 141, 167, 168, 178, 188, 202, 203, 207, 217, 225–259, 280, 281, 292, 299
- Small strains *see* Infinitesimal strains
- Solid element, 172, 211–212, 217, 220, 226
- Spatial coordinates, 27, 32, 34, 43, 65, 74, 109, 135, 163, 167–171, 173, 179, 180, 185, 193, 208, 211, 221, 274
- Spectral decomposition, 17, 72
- Spin
- tensor, 65–66, 68, 85, 90, 117, 119, 322, 323
- Spurious singular modes, 216
- Standard viscoelastic model, 165
- Stiffness matrix, 216, 250–253, 255, 256
- Stokes' relation, 163, 164
- Strain
- Almansi, 47, 59, 60, 67
  - auxiliary strain energy density function, 151
  - Cauchy, 59
  - components, 2, 14, 23, 29, 39, 42, 47, 55–60, 69, 70, 86, 91, 97, 105, 124, 125, 126, 131, 135, 136, 172, 204, 205, 209, 215, 249, 297
  - energy, 29, 74–76, 116, 117, 126, 131, 134, 139, 140, 151, 156, 201–207, 209, 215, 216, 255, 315
  - engineering, 56, 58
  - Eulerian, 58–62, 95
  - Geometric interpretation, 56–58
  - Green–Lagrange, 47, 55, 70, 86, 100, 104, 108, 159, 180, 223
  - hardening, 279, 280
  - infinitesimal, 59, 61–62, 155
  - invariants, 72–74, 95, 131–132, 136–137
  - logarithmic, 56
  - natural, 56
  - normal, 56, 58, 70, 72, 74, 86, 89, 91, 92, 130, 131, 204, 207
  - plane, 132, 133, 164
  - principal, 71–74, 91
  - shear, 56–58, 70–72, 74, 86, 88, 89, 91, 92, 131, 201, 204, 207
  - small *see* Infinitesimal strains
  - space formulation, 280, 281
  - transformation, 70, 76, 91
  - vector, 14, 55, 125
  - volumetric, 72, 151, 152, 216, 300
- Strain additive decomposition, 142, 280, 281, 298, 299
- Strain-displacement relationships *see* Constitutive equations
- Stress, 97–121
- back, 281, 282, 310
  - Biot, 107
  - Cauchy
    - 97, 99, 100, 102–104, 106, 108, 111–121, 137, 141, 161, 163, 249, 291, 314  - components, 14, 29, 100, 113, 125, 128, 162, 163, 297, 302
  - deviatoric, 103, 113–115, 298
  - invariants, 103, 120, 131–132
  - Kirchhoff, 75, 106, 115, 118, 137, 138, 165, 314, 325
  - measures, 29, 75, 76, 97, 105–106, 108, 111, 115, 120, 124, 155, 163, 291
  - normal, 58, 86, 98, 99, 100, 130, 163
  - physical interpretation, 113, 161

- Piola-Kirchhoff, 75, 104, 106–109, 112–118, 120, 121, 124–126, 133–138, 140, 141, 156, 157, 159, 161, 162, 165, 180, 204, 248, 314, 315, 322
- plane, 132, 164, 304–306
- principal, 103, 120
- rate, 97, 117–119, 121, 284, 292, 303, 316, 318
- shear, 86, 98, 100, 103, 132, 162, 163, 215, 280
- space formulation, 280, 286
- symmetry, 102–103
- transformation, 100
- true, 103, 106, 113, 115
- update algorithm, 295
- vector, 14, 125
- Stress–strain relationships *see* Constitutive equations
- Stretch, 42, 51, 85–88, 95, 107, 130, 131, 132
  - Left, 62
  - Right, 62
  - tensor, 62, 63, 118
- Structural applications, 202, 217
- Structural discontinuities, 274, 275–277
- Structural systems, 167, 203, 251, 262
- Subparametric finite element, 213
- Summation convention, 11–12
- Superparametric finite element, 213
- Surface
  - curvature, 197–199
  - elliptic, 197
  - hyperbolic, 197
  - parabolic, 197
  - planar, 197
  - theory, 196–199
- Surface force, 29, 98–100, 110–111, 119
- Surface traction, 98, 105, 120, 220
- Symmetry of the stress tensor, 102–103
- Tangent elastoplastic modulus, 292, 294, 318, 319, 323
- Tangent frame, 23, 243
- Tank car, 92, 183, 255
- Tensor
  - Almansi strain, 47, 59, 60, 67
  - alternating, 20, 45
  - antisymmetric, 18
  - Cartesian, 12–21
  - Cauchy strain, 59
  - contraction, 13–14, 18–21, 104, 125, 307
  - double product, 13–14, 18–21, 104, 125, 307
  - Eulerian strain, 58–62, 95
  - Fourth-order, 18–21, 45, 125, 138, 163, 165, 180, 249, 291, 294, 297, 303, 304
  - Green-Lagrange strain, 47, 55, 70, 86, 100, 104, 108, 159, 180, 223
  - higher order, 18–21
  - identity, 12, 13, 300
  - infinitesimal strain, 59, 61–62, 155
  - invariants, 14–16
  - isotropic, 13
  - left Cauchy-Green strain, 61, 62, 64, 79, 80, 95, 137, 165, 314
  - rate of deformation, 47, 65–68, 76, 82, 85, 86, 88, 90, 95, 112, 116, 117, 119, 120, 124, 163, 219, 258, 312, 315–317, 321, 322
  - right Cauchy-Green strain, 61, 115, 136, 138, 155, 165
  - second order, 12
  - skew symmetric, 18
  - spherical, 13
  - spin, 65–66, 68, 85, 90, 117, 119, 322, 323
  - symmetric, 16–18
  - third order, 18–19
  - unit *see* Identity tensor
  - velocity gradient, 47, 65–66, 75, 76, 82, 85, 90, 116, 117, 119, 120, 121, 163, 315, 316
- Theory of curves, 194–195
- Theory of surfaces, 196–199
- Thin plate element, 208–209, 215, 224, 273, 275
- Tire, 92, 110, 111, 183, 222, 223
- Torsion, 195, 206
- Total Lagrangian formulation, 111–113, 218, 220
- Trace of matrix, 2
- Traction, 98, 105, 120, 220
- Transformation matrix, 6, 17, 43, 52, 64, 69, 74–77, 100, 101, 116, 117, 141, 176, 231, 232, 235, 237, 238, 252
- planar, 25–27, 43, 71, 91, 129
- spatial, 232–233, 234
- in terms of Euler angles, 232–233, 258

- Translation, 24, 28, 47, 51, 102, 169, 172, 199, 203, 205, 206, 208, 210, 217, 226, 227, 228, 229, 235–237, 239, 241, 246, 256, 258
- Transport term, 65
- Transpose of matrix, 2
- Tresca yield function, 280
- Triadic product, 12
- Trial stress, 297, 307
- Triangular element, 217, 226
- Triple product, 77
- True stress, 103, 106, 113, 115
- Truesdell stress rate, 117–118
- Unit dyads, 12
- Updated Lagrangian formulation, 111–113, 169, 218–221
- Vector, 6–11
  - cross product, 7–8
  - dot product, 7
  - dyadic product, 7, 8–9
  - inner product, 7
  - length of, 7
  - norm of, 7
  - orthogonal, 7
  - outer product, 7, 8–9
  - scalar product, 7
  - unit, 7
- Velocity, 24–26, 32, 35, 64–68, 82, 113, 119, 164, 178, 219, 230, 231, 240, 244, 259
  - angular, 26–27, 229–234, 244, 258
  - field, 220
  - gradient, 47, 65–66, 75–76, 82, 85, 90, 116–117, 119–121, 163, 315, 316
  - strain, 65
  - transformation, 36
  - virtual, 112
- Virtual displacement, 30, 35, 112
- Virtual power principle, 112
- Virtual velocity, 112
- Virtual work
  - of applied forces, 36, 180–181, 183, 250
  - of elastic forces, 97, 103–113, 116, 121, 134, 135, 168, 180, 181, 201, 205, 248–250
  - of inertia forces, 35, 168, 178–181, 246–247, 250
  - principle, 1, 27, 29–32, 34, 36, 46, 102, 116, 120, 180, 181, 244, 250
- Viscoelastic material, 115, 119, 124, 125, 132, 141–162, 165
  - Kelvin model, 148, 152
  - linear, 141–155
  - Maxwell model, 148, 159, 162, 165
  - nonlinear, 155–161
  - one-dimensional model, 141–155
  - standard model, 142, 143, 145, 148, 149, 165
  - strain additive decomposition, 142
  - Voigt model, 148, 152
- Viscosity coefficient, 162, 163
- Voigt viscoelastic model, 148, 152
- Volume change, 29, 77–81, 104, 131
- Volumetric locking, 130, 169, 214, 216
- Volumetric strain, 72, 151, 152, 216, 300
- von Mises effective stress, 323
- von Mises yield function, 280, 289, 298, 309, 323, 325
- Vorticity, 64
- Weak form, 105
- Weight
  - coefficients, 189, 190
  - factors, 189, 190
- Work and energy, 1, 37–39, 123, 124
  - principle, 39, 218
- Yaw angle, 232
- Yield condition, 281, 296, 298, 307, 309, 322
- Yield criterion, 280, 281
- Yield function, 113, 280, 282, 283, 285, 287–290, 292, 298, 301, 308, 312, 317, 319, 323–325
  - Huber-von Mises, 298, 309
  - Tresca, 280
  - von Mises, 280, 289, 298, 309, 323, 325
- Yield stress, 137, 281, 299
- Young's modulus, 130
- Zero energy modes, 216
- Ziegler's rule, 281